

# **Green Synthesis, Biodegradation and Antimicrobial Studies of Ionic Liquids and Their Applications in Surfactant Technology**

**By Andrew Jordan BSc. (Hons)**

Under the supervision of Prof. Nicholas Gathergood and  
Dr. Andrew Kellett

School of Chemical Sciences  
Dublin City University

Doctor of Philosophy (Ph.D.)

July 2016

*Dedicated to Mam, Dad and Hannah*  
*For your unwavering support*

## **Declaration**

I hereby certify that this material, which I now submit for assessment on the programme of study leading to the award of Ph.D. is entirely my own work, and that I have exercised reasonable care to ensure that the work is original, and does not to the best of my knowledge breach any law of copyright, and has not been taken from the work of others save and to the extent that such work has been cited and acknowledged within the text of my work.

Signed: \_\_\_\_\_

ID No.: \_\_\_\_\_

Date: \_\_\_\_\_

## **Abstract**

### **Green Synthesis, Biodegradation and Antimicrobial Studies of Ionic Liquids and Their Applications in Surfactant Technology**

**By Andrew Jordan BSc. (Hons)**

A series of L-phenylalanine and L-tyrosine ionic liquids (ILs) and tertiary amino analogues have been synthesised according to the 12 principles of green chemistry and a benign by design concept. The series of ILs are derived from amino acid ethyl esters and a variety of different quaternary nitrogen headgroups have been used to give the series of ILs disclosed within. The green chemistry metrics have been calculated for a number of the compounds within and give insight into the chosen synthetic methodologies potential environmental footprint and how improvements to the synthesis pathways may be conducted in the future.

The ILs and tertiary amino compounds have been evaluated for their antimicrobial toxicity in collaboration with Dr. Marcel Špulák in Charles University, Czech Republic. A panel of 12 fungi, 4 gram positive bacteria and 4 gram negative bacteria were used to investigate the antimicrobial toxicity of the ILs. The ILs examined showed generally a low antimicrobial toxicity whilst the tertiary amino compounds derived from proline appeared overall to be more toxic towards both bacteria and fungi.

The biodegradability of the L-phenylalanine and tertiary amino compounds was examined in collaboration with Prof. Klaus Kümmerer in Leuphana University of Lüneberg, Germany. The test employed was the closed bottle test and a mineralisable pyridinium derived IL was discovered. Furthermore the metabolic products produced from the biodegradation test were identified by LCMS/MS and the potential breakdown pathways of the ILs has been proposed. Synthesis of the metabolic products was undertaken and further biodegradation and antimicrobial evaluation of these metabolites is ongoing.

The information derived from these studies has led to the synthesis of a second generation of linear alkyl and bolaform ILs. The 2<sup>nd</sup> generation of ILs have been assessed for their green chemistry metrics, surfactant properties as well as their antimicrobial toxicity and biodegradability. The 2<sup>nd</sup> generation of ILs synthesised were found to possess favourable surface active properties and a broad spectrum antimicrobial activity and moderate to poor biodegradability.



## Acknowledgements

I would like to thank Prof. Nick Gathergood for giving me the opportunity to carry out this research as part of his group at Dublin City University. I would also like to acknowledge the opportunities that Nick's sabbatical and subsequent departure from DCU to Tallinn, Estonia gave me including the attendance in his stead of a number of international COST action conferences as the substitute representative for Ireland and a chance to visit a number of beautiful European cities. A massive thanks goes to Dr. Kieran Nolan and especially to Dr. Andrew Kellett for their support during Nicks absence and for helping me to carry the torch home.

Special thanks goes to all the friends in the Gathergood group that I have made along the way especially Hannah, Alan, Adam, Dong, Bo and Natasha. Legends all of you. Above all else, thank you Hannah for being the best friend I could ever hope for and being there for me through thick and thin. To Rohit and Mukund, take a bow, you set me on the right track all those years ago and made a chemist of me. Your advice and training in my undergraduate and first months of my Ph.D. were some of the best lessons I have ever learned and ever will.

To all the friends that I have made in DCU along the way during my undergraduate and postgraduate, thank you all for being such a big part of my life. In no particular order Brian, Nicky, Orla, Rachel, Declan, Seán, Nichola, Sarah, Orla II, Andrew, Kae 🙌, Saorla, Gill, Hazel, Leanne, Laura, Stephen, Liam, Finn, Zara, Creina, Tadhg, Nicolo, Teresa, Seán, Catherine, Siobháin, Ciarán, Natalie, Fiona and Miriam.

To the unsung heroes of DCU: the technical staff. Without you guys the place would fall to pieces. Thank you Ambrose, John, Vinnie, Damien, Catherine, Mary and Veronica. Thank you John for helping me out with so much NMR time and the PC game suggestions! Special thanks to Damien, you taught me that a PhD isn't a sprint, it's a marathon, and to slow down and put myself before the research. I owe you one.

Thanks to Dr. Florence Mc Carthy in University College Cork, Ireland and Ivar Järving in Tallinn University of Technology, Estonia for mass spectrometry analysis.

To the collaborators Dr. Marcel Špulák, Charles University, Hradec Králové, Czech Republic for the work performed on the antimicrobial studies and to Prof. Klaus Kümmerer, Leuphana University, Lüneburg, Germany for their biodegradation screening.

Massive thanks to Dr. Lourdes Pérez for hosting me not once but twice in Barcelona. The months I spent in your lab were some of the best and Barcelona will always be a special place for me. Big shout out to all the friends I made over there, especially Marta and Laia.

I'd also like to thank the EPA for funding this research and allowing me to travel to South Korea to present at COIL-6 and to the COST action for allowing me to travel across Europe presenting my work.

Finally, to my family and grandfather Eddie and godmother Margaret, though you may not know what an ionic liquid is (or ever need to), you do know the journey that I have taken, the hardships, failures, successes and eventual victories. Thank you for being there for me and supporting me for over seven years in DCU. To Mary and Tony (nannagwanga), though you will never read this, know that I am eternally grateful to you both for encouraging me and nurturing my curiosity from a young age; I know you would both be proud.

# Table of Contents

Abstract.....	iv
Acknowledgements .....	v
Table of Contents.....	vii
List of Figures.....	xi
List of Tables .....	xviii
List of Schemes .....	xx
List of Abbreviations .....	xxii
1.0 Chapter 1 - Biodegradation – The 10 <sup>th</sup> principle of green chemistry .....	1
1.1 Introduction.....	2
1.2 Biodegradation - The 10th principle of green chemistry .....	4
1.2.1 Biodegradation – standardised tests .....	5
1.2.2 Biodegradation in soil, compost and other matrices .....	11
1.2.3 Biodegradation of ILs under denitrifying conditions.....	14
1.2.4 Biotreating ILs for enhanced biodegradation – axenic cultures.....	17
1.2.5 Suitability of biodegradation tests to IL classes – toxicity vs. biodegradability .	23
1.3 Biodegradation data on classes .....	24
1.3.1 Ionic liquids: anion and cation effects with regards to biodegradation.....	24
1.3.2 Anions .....	25
1.3.3 Cations .....	30
1.3.4 Aromatic Cations – imidazolium, thiazolium, pyridinium .....	30
1.3.5 Non aromatic cations – morpholinium, DABCO, piperidinium, cholinium, quaternary ammonium - quaternary ammonium cations (QAC's).....	40
1.3.6 C <sub>2</sub> symmetric and dicationic ILs – a new class of ILs .....	51
1.4 Metabolite studies .....	54
1.4.1 Aerobic degradation metabolite studies .....	57
1.4.2 Pyridinium.....	58
1.4.3 Sidechain studies.....	59
1.4.4 Anaerobic degradation metabolite studies .....	60

1.5	Computer modelling and predictability and databases available containing IL biodegradation data.....	61
1.6	Abiotic Degradation - Chemically induced degradation in advanced systems .....	63
1.7	Biodegradable Surfactants: An IL by another name. ....	69
1.8	Outlook and recommendations .....	73
1.9	Conclusion .....	75
1.10	References.....	76
2.0	Chapter 2 - Synthesis of 1 <sup>st</sup> Generation Amino Acid Ionic Liquids .....	81
2.1	Aim .....	82
2.2	Introduction.....	83
2.2.1	The twelve principles of green chemistry and green chemistry metrics .....	84
2.2.2	Synthesis .....	87
2.3	Antimicrobial screening and biodegradation studies of 1 <sup>st</sup> generation amino acid ILs and 3° amino analogues .....	113
2.3.1	Antimicrobial screening aim .....	113
2.3.2	Antibacterial screening .....	114
2.3.3	Antifungal screening .....	120
2.3.4	Antimicrobial screening conclusions .....	125
2.4	Biodegradation studies of amino acid ILs and 3° amino analogues .....	125
2.4.1	Biodegradation screening of L-phenylalanine ILs .....	126
2.4.2	Biodegradation screening of 3° amino analogues .....	128
2.4.3	Biodegradation screening of L-tyrosine analogues .....	129
2.4.4	Summary of IL and tertiary amino biodegradation.....	130
2.4.5	LCMS/MS analysis of transformation products .....	131
2.4.6	Synthesis of transformation products.....	135
2.4.7	Biodegradation screening conclusions.....	147
2.5	Antimicrobial screening of transformation products .....	147
2.6	Conclusions to 1st generation IL synthesis, biodegradation and antimicrobial toxicity screening.....	151
2.7	References.....	152

3.0	Chapter 3 - Synthesis of 2 <sup>nd</sup> Generation Amino Acid ILs.....	155
3.1	Aim .....	156
3.2	Introduction.....	156
3.3	Classes of surfactants .....	160
3.3.1	Non-Ionic .....	161
3.3.2	Zwitter-Ionic .....	161
3.3.3	Anionic.....	162
3.3.4	Cationic .....	162
3.4	Subclasses of surfactants.....	164
3.4.1	Linear alkyl .....	165
3.4.2	Bolaform .....	169
3.4.3	Gemini.....	170
3.5	Synthesis, antimicrobial toxicity and biodegradation studies of 2 <sup>nd</sup> generation amino acid ILs .....	171
3.5.1	Synthesis of 2 <sup>nd</sup> generation L-phenylalanine linear alkyl ILs.....	173
3.5.2	Synthesis of 2 <sup>nd</sup> generation L-phenylalanine bolaform (dicationic) ILs.....	181
3.6	Antimicrobial screening and biodegradation studies of 2 <sup>nd</sup> generation amino acid ILs.. .....	189
3.6.1	Antibacterial screening of the 2 <sup>nd</sup> generation linear alkyl amino acid ILs .....	189
3.6.2	Antifungal screening of the 2 <sup>nd</sup> generation linear alkyl amino acid ILs .....	193
3.6.3	Antibacterial screening of the 2 <sup>nd</sup> generation bolaform amino acid ILs .....	195
3.6.4	Antifungal screening of the 2 <sup>nd</sup> generation bolaform amino acid ILs .....	198
3.6.5	Antimicrobial Screening Conclusions.....	200
3.7	Biodegradation Studies of 2 <sup>nd</sup> Generation ILs .....	201
3.7.1	Biodegradation Studies of Linear Alkyl ILs .....	201
3.7.2	Biodegradation Studies of Bolaform ILs .....	209
3.8	Conclusions to 2nd generation IL synthesis, biodegradation and antimicrobial toxicity screening.....	212
3.9	References.....	215

4.0	Chapter 4 - Self-assembly and Surface Active Properties of 2nd Generation L-Phenylalanine Ionic Liquids .....	217
4.1	Aim .....	218
4.2	Introduction.....	218
4.3	Self-Aggregation and physicochemical properties of linear alkyl L-phenylalanine ILs . .....	219
4.3.1	Conductivity measurements .....	219
4.3.2	Tensiometry measurements.....	226
4.3.3	HPLC Models .....	230
4.3.4	Optical Microscopy.....	235
4.3.5	Aqueous stability measurements.....	246
4.4	Self-Aggregation and physico-chemical properties of bolaform L-phenylalanine ILs ( <b>444-452</b> ).....	255
4.4.1	Conductivity measurements .....	255
4.4.2	Tensiometry measurements.....	258
4.4.3	HPLC Models .....	262
4.5	Conclusion .....	267
4.6	References.....	269
5.0	Chapter 5 - Experimental .....	270
5.1	Experimental.....	271
5.1.1	Chemicals.....	271
5.1.2	NMR .....	271
5.1.3	IR analysis.....	271
5.1.4	Melting point.....	271
5.1.5	Optical Rotation .....	271
5.1.6	ESI-MS .....	272
5.2	Experimental preparation of Chapter 2 L-phenylalanine ILs .....	272
5.3	Experimental preparation of Chapter 2 L-phenylalanine tertiary amino compounds	283
5.4	Experimental preparation of Chapter 2 L-tyrosine ILs .....	287
5.5	Experimental preparation of Chapter 2 IL and tertiary amino metabolites.....	292

5.6	Experimental preparation of Chapter 3 linear alkyl amino acid surfactant ILs .....	309
5.7	Experimental preparation of Chapter 3 bolaform amino acid surfactant ILs.....	320
5.8	Antimicrobial Screening .....	329
5.8.1	Antibacterial Screening.....	329
5.8.2	Antifungal Screening .....	330
5.9	Biodegradation Screening .....	331
5.9.1	Closed Bottle Test Method .....	331
5.9.2	LCMS Metabolite Study .....	332
5.10	Self assembly and physico-chemical surfactant property investigations .....	333
5.10.1	Aqueous sample preparation .....	333
5.10.2	Conductivity measurements .....	333
5.10.3	Surface tension measurements .....	333
5.10.4	Optical Microscopy.....	333
5.10.5	HPLC-UV analysis .....	334
5.10.6	Aqueous stability measurements.....	334
5.11	References.....	334
6.0	Chapter 6 - Conclusions and future work .....	336
6.1	Conclusions and future work .....	337
6.2	References.....	342
	Appendix I.....	A1
	Appendix II.....	B1

## List of Figures

Figure 1.1. One of the first ILs, ethylammonium nitrate. ....	3
Figure 1.2. 1-Methyl-3-methylimidazolium iodide .....	3
Figure 1.3. [bmim] ILs.....	5
Figure 1.4. Imidazolium ILs examined by Modelli <i>et al.</i> <sup>41</sup> .....	11
Figure 1.5. Sorption coefficients ( $K_d$ mL g <sup>-1</sup> ) for first layer $K_{d1}$ and final concentration $K_{d2}$ for given soil types. <sup>48</sup> .....	13

Figure 1.6. Imidazolium compounds (8-14) examined for soil adsorption.....	13
Figure 1.7. Sorption isotherms for a, [bmim][Cl], and b, [hmim][Cl] on soil type R3. <sup>48</sup> .....	13
Figure 1.8. Soil elution profiles (breakthrough curves) of ILs [omim][Cl], [bmim][Cl], [mbpy][Cl], [emimOH][Cl] and [emim][Cl] in the three different soil types, CA3, R3 and L2. <sup>48</sup> .....	14
Figure 1.9. Metabolite detected at the end of the study. ....	15
Figure 1.10. [PyBu] derivatives ( <b>52</b> and <b>53</b> ) found to degrade and recalcitrant [bmim][PF <sub>6</sub> ] derivative ( <b>4</b> ). ....	22
Figure 1.11. Some of the most commonly employed halide/pseudohalide anions as their [bmim] ILs. ....	25
Figure 1.12. Sulphate anion core, R = C <sub>n</sub> H <sub>2n+1</sub> , n = 8-12. ....	25
Figure 1.13. [bmim] paired with the biodegradable, octyl sulphate anion failed the CBT and CO <sub>2</sub> Headspace test. <sup>63</sup> .....	26
Figure 1.14. Formate and carboxylate anions. ....	26
Figure 1.15. Two readily biodegradable protic ethanolaminium carboxylate ILs. <sup>70</sup> Biodegradation values assessed by Manometric Respirometry (OECD 301F). ....	26
Figure 1.16. Biodegradable organic acids that have been employed as anions in ILs. <sup>71</sup> .....	27
Figure 1.17. TBA carboxylate ILs. <sup>71</sup> .....	27
Figure 1.18. A readily biodegradable lactate DMDBA IL. <sup>71, 73</sup> .....	28
Figure 1.19. Biodegradable cholinium amino carboxylate ILs. <sup>74</sup> .....	28
Figure 1.20. TBA L-prolinate IL. <sup>71</sup> .....	29
Figure 1.21. Biodegradation data for some 2 <sup>nd</sup> and 3 <sup>rd</sup> generation ILs. <sup>62, 63, 77</sup> .....	30
Figure 1.22. The imidazolium cation and potential sites for derivatisation. ....	31
Figure 1.23. Biodegradation data for imidazole ILs synthesised by Stolte <i>et al.</i> <sup>79</sup> .....	31
Figure 1.24. Aryl imidazolium IL and potential degradation product. <sup>79</sup> .....	32
Figure 1.25. <i>N</i> -Benzyl imidazolium ILs. <sup>18</sup> .....	32
Figure 1.26. Imidazolium ILs classified as Amber. <sup>18-20</sup> .....	34
Figure 1.27. Imidazolium ILs classified as Red by Gathergood <i>et al.</i> <sup>18-20</sup> .....	34
Figure 1.28. Biodegradation data for C-2,4/5 modified imidazolium ILs. <sup>45</sup> .....	35
Figure 1.29. Biodegradation data for C-4/5 modified imidazolium ILs. <sup>45</sup> Biodegradation values assessed by CBT (OECD 301D) .....	35
Figure 1.30. Biodegradation data for amino acid derived imidazolium ILs. <sup>81</sup> .....	36
Figure 1.31. Biodegradation data for thiazolium ILs synthesised by Scammells <i>et al.</i> <sup>69</sup> .....	36
Figure 1.32. Alkyl pyridinium ILs classified as not readily biodegradable. <sup>18, 82</sup> .....	37
Figure 1.33. Pyridinium ILs ( <b>109-112</b> ). <sup>69, 82</sup> .....	38
Figure 1.34. ( <b>113-119</b> ) Pyridinium ILs ether substituted at the 3-position. <sup>69</sup> .....	38
Figure 1.35. Nicotinium derived ILs. <sup>18,83</sup> .....	39



Figure 1.36. A carbamate functionalised pyridinium IL. <sup>69</sup>	40
Figure 1.37. Biodegradation data for morpholinium ILs. <sup>82, 84, 85</sup>	41
Figure 1.38. Morpholinium ILs screened for primary degradation only. <sup>82</sup>	42
Figure 1.39. Biodegradation data for DABCO ILs ( <b>137-141</b> ). <sup>82, 84</sup>	42
Figure 1.40. Biodegradation data for Piperidinium ILs ( <b>142-148</b> ). <sup>82, 84</sup>	43
Figure 1.41. Biodegradation data for pyrrolidinium ILs. <sup>82, 86</sup>	44
Figure 1.42. Readily biodegradable cholinium mesylate ( <b>157</b> ). <sup>86</sup>	45
Figure 1.43. Quaternary ammonium ILs ( <b>158, 159</b> ). <sup>86</sup>	45
Figure 1.44. Biodegradation data for protic aminodiol derived ILs ( <b>160-165</b> ). <sup>70, 86</sup>	46
Figure 1.45. Biodegradation data for protic aminotriol derived ILs ( <b>166-167</b> ). <sup>70</sup>	46
Figure 1.46. Tetrabutylammonium cation and [DMDBA] cation.	47
Figure 1.47. Biodegradation data for selected tetrabutylammonium ILs. <sup>71, 72</sup>	47
Figure 1.48. Triethylmethylammonium IL. <sup>86</sup>	48
Figure 1.49. Biodegradation data for selected DMDBA ILs. <sup>73</sup>	49
Figure 1.50. General structure of phosphonium cations, studied by Scammells. <sup>93</sup>	50
Figure 1.51. Biodegradation data for tricyclohexylphosphonium ILs. <sup>93</sup>	50
Figure 1.52. Biodegradation data for trihexylphosphonium ILs. <sup>93</sup>	51
Figure 1.53. Bis-pyridinium ILs ( <b>214-216</b> ). <sup>69</sup>	52
Figure 1.54. Biodegradation data for dicationic imidazolium and pyrrolidinium ILs ( <b>217-226</b> ) examined by Manometric Respirometry (OECD 301F), Stoltz <i>et al.</i> <sup>94</sup>	53
Figure 1.55. Biodegradation of pyrrolidinium headgroup.	56
Figure 1.56. Inherently biodegradable ILs; effect of cations by Stoltz. <sup>82</sup>	57
Figure 1.57. Commercially available ILs tested under UV/H <sub>2</sub> O <sub>2</sub> oxidation conditions. <sup>37</sup>	64
Figure 1.58. Structures of the commercially available ILs screened. <sup>40</sup>	65
Figure 1.59. Radical oxidation of [bmim][BF <sub>4</sub> ] under various oxidising environments. Adapted from Li <i>et al</i> 2007. <sup>40</sup>	65
Figure 1.60. Example of a pyridinium salt synthesised by Pernak <i>et al.</i> <sup>111</sup> and examined for degradation in an AOP.	67
Figure 1.61. Degree of destruction (%) vs time (min.) for a pyridinium salt ( <b>284</b> ), examined by Pernak <i>et al.</i> <sup>111</sup>	67
Figure 1.62. Observed rate of degradation for [bmim][Cl] is slower than [bmim][CF <sub>3</sub> SO <sub>3</sub> ] or [bmim][C(CN) <sub>3</sub> ]. <sup>112</sup>	68
Figure 1.63. [bmim][BF <sub>4</sub> ] ( <b>3</b> ) and [bmpyrrol][NTf <sub>2</sub> ] ( <b>47</b> ).	68
Figure 1.64. Tris- and tetrakis-imidazolium and benzimidazolium IL surfactants examine for their biodegradability.	73
Figure 2.1. IL design strategy	82
Figure 2.2. General structure of L-phenylalanine (left) and L-tyrosine (right) ILs synthesised.	83

Figure 2.3. Target L-phenylalanine ILs synthesised. ....	88
Figure 2.4. <sup>1</sup> H-NMR of alkylating reagent ( <b>337</b> ) in CDCl <sub>3</sub> after aqueous workup and drying... 91	91
Figure 2.5. <sup>1</sup> H-NMR of Imidazolium IL ( <b>324</b> ) in CDCl <sub>3</sub> .....	95
Figure 2.6. Proposed hydrogen bonding interaction between the imidazolium headgroup, amide linker and bromide counterion. ....	96
Figure 2.7. X-ray crystal structure and CH-Br contacts for [bmim][Br]. ....	96
Figure 2.8. <sup>1</sup> H-NMR of C <sub>2</sub> Symmetric IL ( <b>331</b> ). ....	97
Figure 2.9. Doublets and the roofing effect. ....	98
Figure 2.10. Proposed possible counter ion binding of C <sub>2</sub> symmetric IL ( <b>331</b> ).....	98
Figure 2.11. H to CH <sub>3</sub> NOESY rationale. ....	99
Figure 2.12. Example of a full NOESY spectra of ( <b>332</b> ).....	100
Figure 2.13. Close up of NOESY spectra of ( <b>332</b> ), note there is no NOESY signal correlating to the <i>N</i> -CH <sub>3</sub> and the H alpha to the carbonyl on the prolinium headgroup. ....	101
Figure 2.14. NOESY spectra of ( <b>333</b> ), note the NOESY signal produce at the intersection of the two green lines. ....	102
Figure 2.15. Absolute stereochemistry for ( <b>332-333</b> ) as determined by NOESY. ....	102
Figure 2.16. Absolute stereochemistry of ILs ( <b>334-335</b> ) as confirmed by NOESY experiments. ....	103
Figure 2.17: Tertiary amino derivatives synthesised. ....	103
Figure 2.18. <sup>1</sup> H-NMR of neutral imidazole analogue ( <b>344</b> ) in CDCl <sub>3</sub> .....	105
Figure 2.19. L-Tyrosine ILs ( <b>349-353</b> ) synthesised. ....	106
Figure 2.20. L-Tyrosine alkylating reagents synthesised. ....	107
Figure 2.21. L-Phenylalanine ILs screened for antimicrobial activity. ....	115
Figure 2.22. Diastereomeric pairs of <i>N</i> -methyl-prolinium ILs ( <b>332-335</b> ). ....	117
Figure 2.23. 3° Amino compounds screened for antimicrobial activity. ....	117
Figure 2.24. L-tyrosine ILs screened for antimicrobial activity. ....	119
Figure 2.25. ILs ( <b>329, 331, 332</b> ) were the only ILs to have any discernible toxic effect. ....	121
Figure 2.26. Comparison of stereochemistry and toxicity for tertiary amino derivatives (347, 348). ....	124
Figure 2.27. L-phenylalanine ILs with the highest levels of biodegradability. ....	127
Figure 2.28. Carbon atom distribution of amino acid IL ( <b>324</b> ).....	127
Figure 2.29. Comparison of IL biodegradation to tertiary amino biodegradation. ....	129
Figure 2.30. L-tyrosine IL biodegradation compared to L-phenylalanine for ILs. ....	130
Figure 2.31. <sup>1</sup> H-NMR spectra of benzyl ester ( <b>373</b> ) in red and crude material recovered after hydrogenolysis reaction in blue. ....	138
Figure 2.32. Transesterified product produced from the hydrogenolysis reaction of ( <b>376</b> ). ....	139
Figure 2.33. IL ( <b>382</b> ).....	148

Figure 2.34. ILs ( <b>359</b> , <b>361</b> ). .....	148
Figure 3.1. Structural similarities between ILs and surfactants. ....	156
Figure 3.2. Surfactant orientation at an oil-water interface. ....	158
Figure 3.3. Micelles and some of the different forms that they can take. ....	159
Figure 3.4. Detergent application of a surfactant. ....	159
Figure 3.5. Consumption of surfactants by class. <sup>10</sup> .....	160
Figure 3.6. Uses of surfactants by sector/ application. <sup>10</sup> .....	161
Figure 3.7. Cocamide monoethanolamine ( <b>390</b> ). ....	161
Figure 3.8. Cocamidopropyl betaine ( <b>391</b> ). ....	162
Figure 3.9. Sodium dodecyl sulphate ( <b>392</b> ). ....	162
Figure 3.10. Distearyltrimethylammonium chloride .....	163
Figure 3.11. Alkyl pyridinium surfactants (n = 10-16, 18) reported by Rosen <i>et al.</i> <sup>14</sup> and Skerjanc <i>et al.</i> <sup>15</sup> .....	163
Figure 3.12. Alkyl ester and amide surfactants reported by Pérez <i>et al.</i> <sup>16, 17</sup> Imidazolium ILs ( <b>412-414</b> ) originally reported by Gathergood and Morrissey. <sup>3, 18</sup> .....	163
Figure 3.13. Subclasses of surfactants. ....	164
Figure 3.14. General structure of a polymeric surfactant. <sup>21</sup> .....	165
Figure 3.15. Different classes of alkyl chains. ....	167
Figure 3.16. Linear alkyl pyridinium surfactants of general structure and formula (n= 10-16). <sup>15</sup> .....	167
Figure 3.17. MIC of alkylquinolinium ILs (Figure 3.18) screened by Gilmore <i>et al.</i> <sup>32</sup> .....	168
Figure 3.18. General structure of alkylquinolinium ILs screened by Gilmore <i>et al.</i> <sup>32</sup> .....	168
Figure 3.19. Comparison for bolaform surfactant C <sub>12</sub> Me <sub>6</sub> ( <b>427</b> ) and a C <sub>12</sub> linear alkyl ammonium surfactant ( <b>428</b> ). <sup>34</sup> .....	169
Figure 3.20. Potential bolaform conformations. <sup>33</sup> .....	170
Figure 3.21. Gemini surfactant C <sub>6</sub> H <sub>4</sub> -1,4-bis-[CH <sub>2</sub> N <sup>+</sup> (CH <sub>3</sub> ) <sub>2</sub> C <sub>12</sub> H <sub>25</sub> ].2Br <sup>-</sup> .....	171
Figure 3.22. Comparison of CMC for linear alkyl surfactant (430) to gemini surfactant ( <b>431</b> ). <sup>37</sup> .....	171
Figure 3.23. Surfactant targets ( <b>432-452</b> ). ....	173
Figure 3.24. <sup>1</sup> H-NMR of imidazolium IL ( <b>435</b> ) in CDCl <sub>3</sub> . ....	177
Figure 3.25. <sup>1</sup> H-NMR of imidazolium IL ( <b>447</b> ) in D <sub>2</sub> O. ....	185
Figure 3.26. Aromatic region. ....	186
Figure 3.27. Linear Alkyl ILs ( <b>432-440</b> ) screened for their biodegradability. ....	201
Figure 3.28. Potential breakdown sites on pyridinium IL ( <b>432</b> ). ....	202
Figure 3.29. Comparison of biodegradability for pyridinium ILs ( <b>325</b> , <b>432-434</b> ) .....	205
Figure 3.30. Linear Alkyl ILs ( <b>444-452</b> ) screened for their biodegradability .....	209
Figure 3.31. Potential biodegradation initiation points for IL ( <b>444</b> ). ....	210

Figure 3.32. Proposed carboxylic acid ILs. ....	213
Figure 3.33. Proposed intermediate length ILs ( <b>101, 467-471</b> ). ....	214
Figure 4.1. Linear alkyl ILs examined ( <b>432-440</b> ). ....	219
Figure 4.2. Plot of conductivity vs. concentration for imidazolium C <sub>10</sub> IL surfactant ( <b>436</b> ). ....	220
Figure 4.3. Alkyl pyridinium surfactants (R = C <sub>n</sub> H <sub>2n+1</sub> , n = 10-16, 18) reported by Rosen <i>et al.</i> <sup>9</sup> and Skerjanc <i>et al.</i> <sup>10</sup> ....	222
Figure 4.4. Alkyl ester and amide surfactants reported by Pérez <i>et al.</i> <sup>8, 11</sup> Imidazolium IL ( <b>412-414</b> ) originally reported by Gathergood and Morrissey. <sup>12, 13</sup> ....	222
Figure 4.5. Comparison of literature CMC values to predicted CMC values for linear alkyl pyridinium surfactants previously reported in the literature ( <b>394-401</b> ). ....	224
Figure 4.6. Plot of Surface Tension vs. Log <sub>10</sub> Concentration for C <sub>8</sub> pyridinium IL surfactant ( <b>432</b> ). ....	227
Figure 4.7. HPLC/UV trace for IL C <sub>10</sub> Pyridinium IL ( <b>433</b> ). ....	231
Figure 4.8. Retention time vs CMC for linear alkyl surfactants ( <b>432-440</b> ) examined by conductivity. ....	232
Figure 4.9. No of Carbon atoms in the linear alkyl chain vs CMC (conductivity). ....	233
Figure 4.10. Potential C <sub>4</sub> and C <sub>6</sub> surfactants ( <b>101, 467-471</b> ). ....	233
Figure 4.11. Typical phase diagram for a non-ionic poly-ethoxylated surfactant. ....	236
Figure 4.12. A selection of phases and mesophases that surfactants can form. ....	237
Figure 4.13. C <sub>8</sub> Pyr IL ( <b>432</b> ). 25 °C, x10 magnification. ....	238
Figure 4.14. C <sub>8</sub> Pyr IL ( <b>432</b> ) “Maltese Crosses” visibly forming. 35°C, x10 magnification. ....	238
Figure 4.15. C <sub>8</sub> Pyr IL ( <b>432</b> ), Lamellar phase crystals. 35°C, x10 magnification ....	239
Figure 4.16. C <sub>8</sub> Pyr IL ( <b>432</b> ) Hexagonal phase liquid crystals. 55°C, x10 magnification ....	239
Figure 4.17. C <sub>10</sub> Pyr IL ( <b>433</b> ), an abundance of lamellar phase liquid crystals are visible. 30 °C, x10 magnification. ....	240
Figure 4.18. C <sub>10</sub> Pyr IL ( <b>433</b> ), an abundance of lamellar phase liquid crystals are visible. 30 °C, x10 magnification. ....	240
Figure 4.19. C <sub>12</sub> Pyr IL ( <b>434</b> ), lamellar phase crystals visible as streaks and Maltese crosses. 45 °C, x10 magnification. ....	241
Figure 4.20. C <sub>12</sub> Pyr IL ( <b>434</b> ) Hexagonal phase liquid crystals. 70 °C, x10 magnification. ....	241
Figure 4.21. C <sub>12</sub> Pyr IL ( <b>434</b> ). Cubic liquid crystals observed under a polarised light source..	242
Figure 4.22. The same frame as Figure 4.21, cubic phase observed under non-polarised light. ....	242
Figure 4.23. Lamellar phase liquid crystals observed for imidazolium C <sub>12</sub> IL ( <b>437</b> ). 40 °C, x10 magnification. ....	243
Figure 4.24. Hexagonal phase liquid crystals observed for IL ( <b>437</b> ). 60 °C, x10 magnification. ....	243

Figure 4.25. A forest of Maltese crosses observed for C <sub>12</sub> imidazolium IL ( <b>437</b> ).70 °C, x10 magnification. ....	244
Figure 4.26. Needles growing upon cooling back to room temperature. ....	244
Figure 4.27. Cholinium C <sub>12</sub> ( <b>440</b> ), mosaic and hexagonal phase 20 °C, x10 magnification. ...	245
Figure 4.28. Lamellar phase liquid crystals observed for C <sub>12</sub> cholinium IL ( <b>440</b> ). 60 °C, x10 magnification. ....	245
Figure 4.29. Lamellar phase liquid crystals observed for C <sub>12</sub> cholinium IL ( <b>440</b> ). 60 °C, x10 magnification. ....	246
Figure 4.30. Pyridinium C <sub>10</sub> ( <b>433</b> ) concentration = 2.5 mM, pH = 7, 50°C, at t = 0 h. ....	247
Figure 4.31. Pyridinium C <sub>10</sub> ( <b>433</b> ), pH = 7, 50°C, t = 168 h. ....	248
Figure 4.32. Imidazole C <sub>10</sub> ( <b>436</b> ), concentration = 2.5 mM, pH = 7, 50°C, t = 0 h. Parent peak eluting at 9.5 minutes .....	248
Figure 4.33. Imidazole C <sub>10</sub> ( <b>436</b> ), pH = 7, 50°C, t = 24 h. Parent peak eluting at 9.5 minutes. Hydrolysis product eluting at 3.5 minutes. ....	249
Figure 4.34. Imidazole C <sub>10</sub> ( <b>436</b> ),pH = 7, 50°C, t = 168 h.....	249
Figure 4.35. HPLC/UV trace of cholinium C <sub>10</sub> ( <b>439</b> ), concentration 2.5 mM, 50°C pH = 7, t = 0 h. ....	250
Figure 4.36. HPLC/UV trace of cholinium C <sub>10</sub> ( <b>439</b> ), 50°C pH = 7, t =168 h displaying shoulder to main peak and rapidly eluting hydrolysis product at 3-5 minutes. ....	250
Figure 4.37. Pyridinium C <sub>10</sub> ( <b>433</b> ) at pH 2, concentration 2.5 mM, 25°C, t = 168 h.....	251
Figure 4.38. Imidazolium C <sub>10</sub> ( <b>436</b> ) at pH2, initial concentration 2.5 mM, 25°C, t = 168 h. ...	252
Figure 4.39. Cholinium C <sub>10</sub> ( <b>439</b> ) at pH2, initial concentration 2.5 mM, 25°C, t = 168 h. ....	252
Figure 4.40. Pyridinium C <sub>10</sub> ( <b>433</b> ) at pH 10, initial concentration 2.5 mM, 25°C, t = 24 h. ....	253
Figure 4.41. Imidazolium C <sub>10</sub> ( <b>436</b> ) at pH 10, initial concentration 2.5 mM, 25°C, t = 24 h. ..	254
Figure 4.42. Cholinium C <sub>10</sub> ( <b>439</b> ) at pH10, initial concentration 2.5 mM, 25°C, t = 24 h. ....	254
Figure 4.43. Bolaform ILs ( <b>444- 452</b> ) examined for their surfactant properties. ....	255
Figure 4.44. CMC as determined by conductimetry for C <sub>12</sub> linked pyridinium bolaform ( <b>446</b> ). ....	257
Figure 4.45. Tensiometry curve for C <sub>8</sub> pyridinium bolaform ( <b>444</b> ).....	260
Figure 4.46. Surface tension plot of C <sub>8</sub> cholinium bolaform ( <b>450</b> ).....	261
Figure 4.47. HPLC/UV trace for IL C <sub>8</sub> pyridinium bolaform ( <b>444</b> ).....	263
Figure 4.48. Retention time vs CMC for bolaform surfactants ( <b>444-452</b> ) examined by conductivity.....	264
Figure 4.49. No of Carbon atoms in the linear alkyl chain vs CMC (conductivity). ....	264
Figure 4.50. Bolaform ILs with C <sub>6</sub> , C <sub>14</sub> and C <sub>16</sub> spacers.....	265
Figure 4.51. Intermediate length C <sub>4</sub> and C <sub>6</sub> linear alkyl ILs. ....	267
Figure 6.1: Future intermediate ester chain ILs. ....	340

Figure 6.2. Amino acid carboxylic acid ILs.....	340
Figure 6.3. L-DOPA derived IL .....	340
Figure 6.4. Potential future generation L-phenylalanine and L-tyrosine derived surfactants....	348
Figure 6.5. PEG and PPG L-phenylalanine derived surfactant ILs.....	341
Figure 6.6. NHC ligand derived from IL ( <b>331</b> ).....	342

## List of Tables

Table 1.1. OECD testing guidelines No. 301.....	6
Table 1.2. OECD testing guidelines No. 310.....	7
Table 1.3. OECD testing guidelines No. 302.....	7
Table 1.4. OECD testing guidelines No. 303.....	7
Table 1.5. OECD testing guidelines No. 306.....	8
Table 1.6. OECD testing guidelines No. 307-309 .....	8
Table 1.7. Other non-OECD test guidelines for aerobic biodegradability of plastics in soil.....	9
Table 1.8. OECD testing guidelines No. 311.....	9
Table 1.9. Anaerobic degradation of imidazolium and pyridinium ILs reported by Stolte <i>et al.</i> <sup>53</sup> .....	15
Table 1.10. Biodegradation results for <i>Sphingomonas paucimobilis</i> at 45°C.....	17
Table 1.11. Suitability of organic compounds to biodegradation screening method. <sup>22, 35</sup> Adapted from Coleman <i>et al</i> 2010. <sup>22</sup> .....	23
Table 1.12. Oxidative degradation of alkyl imidazolium ILs assisted by acetic acid and ultrasonic irradiation. Adapted from Li <i>et al</i> 2007. <sup>40</sup> .....	66
Table 1.13. Biodegradation of surfactants and mixtures of surfactants. <sup>118</sup> .....	72
Table 2.1. Summary of yields obtained for compound ( <b>337</b> ) acylation reaction optimisation...	90
Table 2.2. Yields under different conditions for L-phenylalanine ILs ( <b>324-335</b> ). .....	94
Table 2.3. Melting points (uncorrected) obtained for L-phenylalanine ILs ( <b>324-335</b> ). .....	94
Table 2.4. Percentage yields obtained for for L-phenylalanine tertiary amino analogues. ....	104
Table 2.5. Percentage yields and melting points for L-tyrosine ILs synthesised. ....	107
Table 2.6. Summary of green chemistry metrics for compounds synthesised in Section 2.2.2. ....	110
Table 2.7. Antibacterial results obtained for L-phenylalanine ILs.....	116
Table 2.8. Antibacterial results obtained for 3° amino compounds. ....	118
Table 2.9. Antibacterial results obtained for L-tyrosine ILs. ....	119
Table 2.10. L-Phenylalanine ILs screened for antifungal activity. * IC <sub>50</sub> values were assessed for AF, AC and TM and IC <sub>80</sub> for all other strains.....	122

Table 2.11. Antifungal results obtained for L-phenylalanine tertiary amino derivatives.....	123
Table 2.12. Antifungal results obtained for L-tyrosine ILs. ....	124
Table 2.13. Biodegradability and carbon distribution of examined L-phenylalanine IL compounds, colour coded according to the traffic light classification. <sup>51</sup> .....	127
Table 2.14. Biodegradability and carbon distribution of examined tertiary amino compounds. ....	128
Table 2.15. Biodegradability and carbon distribution of examined L-tyrosine compounds. ....	129
Table 2.16. Percentage yields for intermediates synthesised. ....	145
Table 2.17. Synthetic routes and final yields for TPs synthesised. ....	146
Table 2.18. Melting points for IL TPs and intermediates. ....	146
Table 2.19. Antibacterial results obtained for TPs. ....	149
Table 2.20. L-Phenylalanine ILs screened for antifungal activity. * IC <sub>50</sub> values were assessed for AF, AC and TM and IC <sub>80</sub> for all other strains.....	150
Table 3.1. CMC values for a homologous series of pyridinium bromide linear alkyl surfactants. <sup>15</sup> .....	167
Table 3.2: Percentage yields for L-phenylalanine esterification reactions.....	174
Table 3.3. Percentage yields for alkylating reagents ( <b>456-458</b> ).....	175
Table 3.4. Percentage yields and melting points for ILs ( <b>432-441</b> ).....	176
Table 3.5. Green Chemistry metrics calculated for linear alkyl amino acid ILs and precursors. ....	180
Table 3.6. Percentage yields for L-phenylalanine diol esterification reactions, step 1. ....	182
Table 3.7. Percentage yields for bis alkylating reagents ( <b>435-437</b> ).....	183
Table 3.8. Percentage yields and melting points for dicationic ILs synthesised.....	184
Table 3.9. Green Chemistry metrics calculated for dicationic (bolaform) amino acid ILs ( <b>417-425</b> ) and precursors ( <b>432-437</b> ).....	188
Table 3.10. Antibacterial results obtained for L-phenylalanine ILs.....	191
Table 3.11. Antifungal results obtained for the linear alkyl ILs ( <b>432-441</b> ).....	194
Table 3.12. Antibacterial results obtained for bolaform L-phenylalanine ILs. ....	197
Table 3.13. Antifungal results obtained for bolaform L-phenylalanine ILs. ( <b>444-452</b> ).....	199
Table 3.14. Biodegradability and carbon distribution of examined L-phenylalanine ILs ( <b>432-440</b> ), colour coded according to the traffic light classification. <sup>57</sup> .....	205
Table 3.15. Biodegradability and carbon distribution of examined L-phenylalanine ILs ( <b>444-452</b> ), colour coded according to the traffic light classification. <sup>57</sup> .....	210
Table 4.1. Results obtained by conductimetry. ....	220
Table 4.2. Comparison of pyridinium surfactants reported by Rosen <i>et al.</i> ( <b>394-401</b> ), pyridinium ester ( <b>402-406</b> ) and amide ( <b>407-411</b> ) reported by Pérez <i>et al.</i> <sup>8, 11</sup> with new amino acid pyridinium IL surfactants ( <b>432-434</b> ). All surfactants were measured at 25 °C. ....	223

Table 4.3. Predicted CMC vs actual CMC for alkylpyridinium surfactants ( <b>394-400</b> ) and the new amino acid pyridinium ILs ( <b>432-434</b> ) reported in this chapter. ....	224
Table 4.4. Comparison of degree of binding, $\beta$ , in linear alkyl pyridinium surfactants from the literature ( <b>394-400</b> ) and the new amino acid pyridinium ILs ( <b>432-434</b> ) reported in this chapter. ....	225
Table 4.5. Surfactant properties for ILs ( <b>432-440</b> ) determined by tensiometry. ....	228
Table 4.6. Comparison of surface tension properties of new pyridinium surfactants to those reported in the literature. ....	229
Table 4.7. Comparison of CMC by conductivity and by tensiometry. ....	230
Table 4.8. HPLC/UV retention time results. ....	231
Table 4.9. Predicted CMC values for C <sub>4</sub> and C <sub>6</sub> surfactants. ....	234
Table 4.10. Comparison of actual CMC and predicted CMC values using linear regression from Figure 4.9. ....	235
Table 4.11. Results obtained by conductimetry for bolaform ILs ( <b>444-452</b> ). ....	256
Table 4.12. Comparison of CMC for bolaform and linear alkyl ILs. ....	258
Table 4.13. Tensiometry results obtained for bolaform ILs. ....	259
Table 4.14. Comparison of CMC results by tensiometry and conductimetry. ....	262
Table 4.15. HPLC/UV retention time results. ....	263
Table 4.16. Calculated CMC and actual CMC values for bolaform surfactant ILs. ....	266

## List of Schemes

Scheme 1.1. Potential $\beta$ -oxidation pathway of an alkyl imidazolium IL. ....	55
Scheme 1.2. Potential $\beta$ -oxidation pathway of an ester derived imidazolium IL. ....	56
Scheme 1.3. Breakdown pathway of [EtPy][BF <sub>4</sub> ] by an axenic culture of <i>Corynebacterium</i> ....	58
Scheme 1.4. Metabolism of [EtPy][BF <sub>4</sub> ] by an axenic culture of <i>P. fluorescens</i> . <sup>99</sup> ....	59
Scheme 1.5. Breakdown pathway of a poly ethoxylated sidechain. ....	60
Scheme 1.6. Anaerobic biodegradation of an imidazolium IL. <sup>53</sup> ....	61
Scheme 1.7. Possible breakdown products detected by HPLC/MS for [emim][Cl] IL. Further fragmentation was analysed by MS/MS. ....	64
Scheme 1.8. Proposed degradation scheme by Li <i>et al.</i> <sup>40</sup> ....	66
Scheme 1.9. Example of electrochemical decomposition of a pyrrolidinium IL. ....	69
Scheme 1.10. Electrochemical decomposition of a choline chloride ( <b>285</b> ). <sup>39</sup> ....	69
Scheme 2.1. General synthetic route employed for L-phenylalanine bromide ILs ( <b>324-335</b> ). ....	89
Scheme 2.2. General scheme for the synthesis of D- and L-Proline heterocycles ( <b>338-343</b> ). ....	92



Scheme 2.3. Reaction mechanism for the reductive alkylation of L-proline. ....	93
Scheme 2.4. Alkylation of tertiary amines with (337) to give ILs (324-335). ....	93
Scheme 2.5. Alkylation of secondary amines with (337) to give ILs (344-348). ....	104
Scheme 2.6. Synthetic route employed for the synthesis of L-tyrosine ILs. ....	107
Scheme 2.7. Transformation products detected by LCMS for L-phenylalanine ILs. ....	133
Scheme 2.8. Potential biodegradation pathway for IL (325). ....	133
Scheme 2.9. Potential biodegradation pathway of IL (326). ....	134
Scheme 2.10. Transformation products detected for L-phenylalanine tertiary amino derivatives. ....	135
Scheme 2.11. Acid hydrolysis - Route A. ....	136
Scheme 2.12. Base hydrolysis, Route B. ....	137
Scheme 2.13. Benzyl ester hydrogenolysis pathway for prolinium TP (359). ....	137
Scheme 2.14. Benzyl ester hydrogenolysis pathway for prolinium TPs (360). ....	139
Scheme 2.15. Benzyl ester hydrogenolysis pathway for prolinium TP (364/380). ....	140
Scheme 2.16. Benzyl ester hydrogenolysis pathway for prolinium TP (365/382). ....	141
Scheme 2.17. Synthesis of TP (363). ....	142
Scheme 2.18. Synthesis of TP (387). ....	142
Scheme 2.19. Failed benzyl deprotection reaction. ....	143
Scheme 2.20. Redesigned synthesis for TPs (359, 360). ....	143
Scheme 2.21. Formation of TP (367). ....	144
Scheme 3.1. General synthetic route employed for step 1, synthesis of esters (453-455) and step 2, synthesis of alkylating reagents (456-458). ....	174
Scheme 3.2. General scheme for step 3, the synthesis of linear alkyl ILs from alkylating reagents. ....	176
Scheme 3.3. Synthesis of ethyl nicotinium IL (441). ....	177
Scheme 3.4. General synthetic route employed for step 1, the synthesis of bis-amino acid esters (459-461) and step 2, the synthesis of alkylating reagents (462-464). ....	182
Scheme 3.5. General scheme for the synthesis of dicationic ILs (444-452). ....	184
Scheme 3.6. Proposed breakdown pathways of linear alkyl pyridinium IL (432) by ester oxidation. ....	202
Scheme 3.7. Proposed breakdown pathways of linear alkyl pyridinium IL (432) by ester oxidation. ....	203
Scheme 3.8. Proposed breakdown pathways of linear alkyl pyridinium IL (432) by amide hydrolysis. ....	204
Scheme 3.9. Unsuitable amide cleavage after ester cleavage. ....	206
Scheme 3.10. Unsuitable amide cleavage before ester cleavage. ....	206
Scheme 3.11. Slow rates of biodegradation for amino acid octyl ester. ....	207

Scheme 3.12. Cholinium C <sub>8</sub> biodegradation compared to Cholinium C <sub>2</sub> biodegradation. ....	207
Scheme 3.13. Potential amide cleavage pathway for IL ( <b>444</b> ). ....	211

## List of Abbreviations

### A

ADMET	Adsorption distribution metabolism excretion and toxicity
AE	Atom economy
AOP	Advanced oxidation processes
API	Active pharmaceutical ingredient
ASTM	American society for testing and materials
ATCC	American type culture collection
ATR	Attenuated total reflectance

### B

BAC	Benzalkonium chloride
BASIL	Biphasic acid scavenging utilizing ionic liquids
BF <sub>4</sub>	Tetrafluoroborate
BOD	Biochemical oxygen demand

### C

CBT	Closed bottle test
CMC	Critical micelle concentration
COD	Chemical oxygen demand
COSY	Correlation spectroscopy

### D

DABCO	1,4-diazabicyclo[2.2.2]octane
DCN	Dicyanamide
DDMAC	Didecyldimethylammonium chloride
DEEDMAC	Ditalowdimethylammonium chloride
DHTDMAC	Dihydrogenated tallow alkyl dimethyl ammonium chloride
DLS	Dynamic light scattering
DMAP	Dimethylaminopyridine
DMDBA	Dimethyldibutylammonium
DMF	Dimethylformamide
DMSO	Dimethylsulfoxide
DOC	Dissolved organic carbon

DSC	Differential scanning calorimetry
<b>E</b>	
EPA	Environmental protection agency
ESI	Electrospray ionization
<b>G</b>	
GCMS	Gas chromatography-mass spectrometry
<b>H</b>	
HILIC	Hydrophilic interaction chromatography
HPLC	High-performance liquid chromatography
HRMS	High resolution mass spectrometry
<b>I</b>	
IC	Inhibitory concentration
IR	Infrared
ISO	International organization for standardization
<b>L</b>	
LAS	Linear alkylbenzene sulfonates
LC	Liquid chromatography
LCMS	Liquid chromatography-mass spectrometry
<b>M</b>	
MALDI	Matrix-assisted laser desorption ionization
MIC	Minimal inhibitory concentration
MITI	Ministry of international trade and industry (japan)
MS/MS	Tandem mass spectrometry
<b>N</b>	
NCCLS	National committee for clinical laboratory standards
NHC	<i>N</i> -Heterocyclic carbene
NMR	Nuclear magnetic resonance
NOESY	Nuclear overhauser effect spectrometry
NTf <sub>2</sub>	Bistriflimide
<b>O</b>	
OctOSO <sub>3</sub>	Octylsulphate
OECD	Organization for economic cooperation and development
<b>P</b>	
PCR	Polymerase chain reaction
PEG	Polyethylene glycol
PF <sub>6</sub>	Hexafluorophosphate

PPG	Polypropylene glycol
PTSA	<i>p</i> -Toluenesulphonic acid
<b>Q</b>	
QAC	Quaternary ammonium compound
QSABR	Quantitative structure-activity biodegradation relationship
QSAR	Quantitative structure-activity relationship
<b>R</b>	
REACH	Registration, evaluation, authorisation and restriction of chemicals
RT	Room temperature
<b>S</b>	
SABR	Structure-activity biodegradation relationship
SAR	Structure-activity relationship
SDS	Sodium dodecylsulfate
<b>T</b>	
TBA	Tetrabutyl ammonium
TEA	Triethylamine
TFA	Trifluoroacetic acid
ThCO <sub>2</sub>	Theoretical carbon dioxide
THF	Tetrahydrofuran
ThOD	Theoretical oxygen demand
TLC	Thin-layer chromatography
TMS	Trimethylsilyl
TOC	Total organic carbon
TP	Transformation Product
TSAR	Thinking in structure activity relationships
<b>U</b>	
UV	Ultraviolet
<b>V</b>	
VOC	Volatile organic compound
<b>W</b>	
WWTP	Wastewater treatment plant

# **Chapter 1**

## *Biodegradation of Ionic Liquids – A Critical Review*

Chapter 1 - Published in Chemical Society Reviews in its entirety.<sup>1</sup>

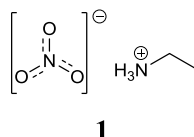
Reproduced by permission of The Royal Society of Chemistry

A. Jordan and N. Gathergood, *Chem. Soc. Rev.*, 2015, 44, 8200-8237.

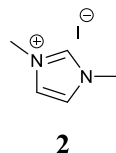
## 1.1 Introduction

Are ionic liquids (ILs) green? Do IL based technologies offer an advantage over current best practice? What performance and green chemistry metrics are used to substantiate these claims? These are questions frequently asked to research groups that promote ILs as a preferred solution to existing problems. Indeed, any new methodology which considers green chemistry principles as core values, should undergo the same rigorous critique and debate. This chapter does not assess the merits of using ILs but rather focuses on one property, biodegradability. The use of persistent or non-biodegradable chemicals, especially as solvents, should be avoided, where suitable biodegradable alternatives exist. This chapter details the progress made by the IL community in their endeavours to invent biodegradable compounds. In the field of ILs, substantial efforts to evaluate the biodegradation properties of a wide range of derivatives has been expended. This data can be included in the overall evaluation and selection of a specific IL for an application. Over the last 15 years various terms have been used to define ILs and their properties; <100 °C m.p., non-volatile, robust, inert, stable to a wide electrochemical window are just a few. Of concern is the apparent ‘desirable’ stability, or resistance to breakdown, especially when initiating a research program to develop biodegradable ILs. However, as we delve more deeply into this fascinating research area, exceptions to these previously widely adopted “classifications” have been found, for example, the negligible vapour pressure has been challenged by Rebelo *et al.* (2005)<sup>2</sup>, and Earle and Seddon *et al.* (2006)<sup>3</sup> in which distillation of ILs with minimal decomposition was demonstrated. The non-flammability property has also been questioned as some ILs have been reported by Rogers *et al.* (2006) as being Class IIIB combustible materials.<sup>4</sup> The question must be asked: ‘Is it possible to design an IL which is stable to a wide range of thermal and chemical conditions yet also biodegrades?’ Can this, at first inspection, apparently mutually exclusive conundrum be solved?

Although ILs have been known for over 100 years, it has only been in recent times that chemists have studied their biodegradation in detail. Many papers credit Walden (1914)<sup>5</sup> or some go even further back to Gabriel and Weiner (1888)<sup>6</sup> with their reported synthesis of ethylammonium nitrate (**1**), Figure 1.1. However the first conventional example the author could find of an imidazolium IL goes back even further to 1881 with the synthesis of 1-methyl-3-methylimidazolium iodide (**2**) by Goldschmidt,<sup>7</sup> see Figure 1.2. Biodegradation studies as part of the characterisation of these ILs would have been unheard of in those times.



**Figure 1.1.** One of the first ILs, ethylammonium nitrate.



**Figure 1.2.** 1-Methyl-3-methylimidazolium iodide

It is our ability to update the definitions, to reclassify and to reinvent design strategy that will underpin continuing success in the field of IL research. Guidelines that have steered the field of IL research over the past two decades have been defined by landmark works such as the creation of the twelve principles of green chemistry by Anastas and Warner.<sup>8</sup> Other examples of concepts that promote cleaner synthesis are atom economy (AE) by Trost,<sup>9</sup> Sheldon's E-Factor,<sup>10</sup> and the Andraos reaction mass efficiency (RME).<sup>11</sup> It is by implementing these principles that green chemists strive to develop their target molecules, monitoring their progress using green chemistry metrics. However, clean synthesis is not the only area that needs stringent protocols in the green chemistry research process. What happens to the molecules when they are ultimately released into the environment is also of paramount importance. The parameters of biodegradability, toxicity – and recently mutagenicity<sup>12</sup> - are becoming more significant.

Wider adoption of ILs by industry and in academia, e.g. BASIL process (Biphasic Acid Scavenging utilising Ionic Liquids), biomass dissolution,<sup>13</sup> metal salt dissolution,<sup>14</sup> lubrication,<sup>15</sup> surfactants,<sup>16, 17</sup> catalysts,<sup>18-20</sup> reaction solvent,<sup>21</sup> has been observed. Over the past decade the potential for (large scale?) accidental release of ILs has become a possibility, thus environmental impact studies, including biodegradation are of increasing importance.

The aim of this chapter is to illustrate the advances, successes and problems encountered in the field of biodegradation of IL research since the preceding publication by Coleman and Gathergood which covered the literature up to 2010.<sup>22</sup>

## 1.2 Biodegradation - The 10th principle of green chemistry

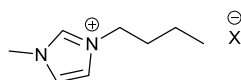
Are biodegradation studies important in the context of green chemistry and ILs? Biodegradation is one method of analysis to determine and predict how a molecule (e.g. IL) interacts with the environment. The overarching aim is to avoid the introduction of persistent molecules including persistent organic pollutants (POPs) into the environment. The issue of environmental persistence of chemicals (including surfactants, antibiotics and solvents), once they have fulfilled their desired application, has been widely studied with detrimental effects on ecosystems observed.<sup>23</sup> Environmental damage ranges from endocrine disruptors against fish<sup>24</sup> to proliferation of bacterial resistance towards important active pharmaceutical ingredients (APIs).<sup>25</sup> Biodegradation is an essential parameter to investigate in ILs, enabling the design of safer analogues where required and reducing environmentally persistent molecules in ecosystems. In 1998, Anastas and Warner highlighted the importance of biodegradation studies for chemists, selecting this as their 10th Principle of Green Chemistry - Design for Degradation.<sup>8</sup>

Design strategies to improve the biodegradability of compounds predate Anastas and Warner's green chemistry principles. Seminal work by Boethling *et al.*<sup>26, 27</sup> includes the highly cited "rules of thumb" which relates structural features and functional groups to biodegradation properties. These rules have been adopted and applied to IL research over the last decade.<sup>22</sup> Boethling's "rules of thumb" propose that a number of factors affect the percentage of mineralisation of chemical compounds by microbial degradation. Beneficial factors include: the presence of aromatic rings, long unbranched alkyl chains, and hydrolysable groups such as alcohols, aldehydes and carboxylic acids.<sup>26, 27</sup> Factors that are detrimental to biodegradation include the presence of halides in the molecule, alkyl chain branching, quaternary carbon atoms, tertiary nitrogen atoms, heterocycles and aliphatic ethers. These "rules of thumb" are not absolutes, indeed caution must be exercised when applying these rules in the absence of biodegradation data of closely related structures and they only suggest general trends in biodegradation pathways, as clearly stated by Boethling in his work.<sup>26, 27</sup>

Early generations of ILs, such as the frequently quoted second generation ILs, the butyl-methylimidazolium [bmim] class, Figure 1.3, were designed to be robust, liquid at room temperature (RT) and inert to a range of chemical conditions thus enabling a broad applicability. For example, the [bmim] series was envisaged as a replacement for VOC electrolytes due to their inherent electrostability, large electrochemical window,<sup>28</sup> thermal stability,<sup>29</sup> low vapour pressure and low/non-flammability.<sup>30</sup> Applications of these stable and low vapour pressure



replacements for electrolytes have been demonstrated in batteries and capacitors.<sup>31</sup> However, it is this lack of reactivity that lead to concern that the molecules could be recalcitrant to biodegradation, with limited breakdown in the environment.<sup>22</sup> Consideration of Boethling's "rules of thumb" also suggests poor biodegradability for these classes of ILs and biodegradation data to confirm the suspicions about this class of compounds was lacking as we entered the new millennium. As biodegradation data for [bmim] ILs began to be experimentally determined, it was found to be in agreement with predictions based on Boethling's work. [Bmim][BF<sub>4</sub>] (**3**), amongst other early examples of 1-methylimidazolium ILs, did not pass readily biodegradable tests, demonstrating the urgent requirement for further work and advances in this area.<sup>21, 32, 33</sup>



**3**, X = BF<sub>4</sub>

**4**, X = PF<sub>6</sub>

**Figure 1.3.** [bmim] ILs

Recent studies conducted by Mao *et al.* further highlight the importance of environmental studies associated with the second generation of ILs, when [bmim][PF<sub>6</sub>], Figure 1.3, (**4**) was shown to proliferate and disseminate antibacterial resistance genes in environmental bacteria, emphasising the need for biodegradability to be a key requirement in future IL generations.<sup>34</sup>

### 1.2.1 Biodegradation – standardised tests

The following section provides an overview of the biodegradation tests which are of interest and available to IL researchers. The research area of biodegradation is categorised into the following terms:

1. **Primary biodegradation** – the loss of a specific structural moiety, example hydrolysis of an ester bond
2. **Inherently biodegradable** - if a compound biodegrades ~20%, then the possibility of further degradation is assumed
3. **Readily biodegradable** - biodegrades a specific % within a given time frame
4. **Ultimately biodegradable** - complete breakdown of a compound
5. **Mineralisation** - decomposition of a compound into molecules available to plants<sup>35</sup>

According to the Organisation of Economic Co-Operation and Development (OECD) and the International Organisation for Standardisation (ISO), there are a number of accepted methods that, if implemented correctly, will provide definitive biodegradation data.<sup>35</sup>

The testing strategy suggested by the OECD is thus:

1. Examine the aerobic biodegradation to assess if a chemical is readily biodegradable.
2. If a test for readily biodegradable is failed, then the chemical of interest can be examined by other simulation tests (optimised aerobic conditions representing conditions potentially found in a sewage treatment plant) to determine biodegradability. An inherent biodegradability test can also be performed.
3. Finally, potential biodegradability can be determined under anaerobic conditions.<sup>35</sup>

The test methods currently supported by the OECD and are as follows:<sup>35, 36</sup>

#### 1.2.1.1 Fresh water

**Table 1.1.** OECD testing guidelines No. 301

Test	Pass Level after 28 Days
Dissolved Organic Carbon (DOC) Die-Away Test (TG 301A)	70% DOC removal
CO <sub>2</sub> Evolution Test (TG 301B)	60% ThCO <sub>2</sub>
Modified MITI Test (I) (TG 301 C)	60% ThOD
Closed Bottle Test (CBT) (TG 301D)	60% ThOD
ISO 10708*	
Modified OECD Screening Test (TG 301E)	70% DOC removal
Manometric Respirometry Test (TG 301F)	60% ThOD

Note: These pass levels must be achieved within a ten day window within the 28 day test limit. The ten day window begins once 10% DOC (Dissolved Organic Carbon), ThCO<sub>2</sub> (Theoretical CO<sub>2</sub>) or ThOD (Theoretical Oxygen Demand) has been achieved.

\*The ten day window is not applied for ISO 10708.

Due to the increased size of the oxygen reservoir in the setup of the ISO 10708 bottle compared to the method described by the OECD 301D, Table 1.1, a higher test substance concentration can be used in the ISO 10708 test as the amount of oxygen in the bottle is less of a limiting factor.

**Table 1.2.** OECD testing guidelines No. 310

Test	Pass Level after 28 Days
CO <sub>2</sub> headspace test (OECD 310) ISO 14593*	60% ThCO <sub>2</sub> evolution

\*The ten day window is not applied for ISO 14593.

### 1.2.1.2 Inherent biodegradation

**Table 1.3.** OECD testing guidelines No. 302

Test	Pass Level
Modified Semi-Continuous Activated Sludge (SCAS) Test (TG 302A)	BOD, DOC and/or COD; No pass levels assigned
Zahn-Wellens/EMPA* Test (TG 302B),	BOD, DOC and/or COD; No pass levels assigned
Modified MITI** Test (II) (TG 302C)	BOD, DOC and/or COD; No pass levels assigned
Concawe Test (draft TG 302D)	BOD, DOC and/or COD; No pass levels assigned

Unlike the readily biodegradable tests described previously in Table 1.1, (OECD 301A-D), the inherent biodegradation test has no pass/fail parameters, Table 1.3. If biodegradation is measured to be above 20% biochemical oxygen demand (BOD) or chemical oxygen demand (COD) or dissolved organic carbon (DOC) then it can be assumed that a chemical can inherently undergo primary biodegradation. If biodegradation of more than 70% is achieved, then it is possible that a chemical is inherently capable of undergoing ultimate biodegradation.

\*EMPA: Swiss Federal Laboratories for Materials Testing and Research.

\*\*MITI: Ministry of International Trade and Industry, Japan

### 1.2.1.3 Aerobic sewage - simulation tests

**Table 1.4.** OECD testing guidelines No. 303

Test	Pass Level after 28 Days
Aerobic Sewage Treatment: Activated Sludge Units (TG 303A) and Biofilms (TG 303B).	DOC and/or COD No pass levels assigned

Similar to OECD 302, using a sewage treatment plant simulation test OECD 303, Table 1.4, no specific limits for pass/fail have been prescribed. This is because the specific operating conditions of every treatment plant are different. The test does however provide an estimate for potential removal of a chemical compound in a sewage treatment plant, thus the quantity of compound that can be released into the environment post treatment can be assessed.

#### 1.2.1.4 Seawater

**Table 1.5.** OECD testing guidelines No. 306

Test	Pass Level after 28 Days
Biodegradability in Seawater (TG 306) Shake flask and closed bottle variants	>70% DOC removal >60% ThOD

The biodegradation in seawater test OECD 306, Table 1.5, differs from the standard 301 tests in that the only microorganisms present are those found naturally in the seawater test media. The flask is not charged with additional inocula, although it is supplemented with nutrients. This test is not intended to represent a marine environment, but rather assess biodegradation in seawater media.

#### 1.2.1.5 Soil, sediment and water

**Table 1.6.** OECD testing guidelines No. 307-309

Test	Test duration and parameters
Aerobic and Anaerobic Transformation in Soil (TG 307)	>120 days testing period - Radio labelled and unlabelled compounds can be used
Aerobic and Anaerobic Transformation in Aquatic Sediment Systems (TG 308)	<100 days testing period - Radio labelled and unlabelled compounds can be used
Aerobic Mineralisation in Surface Water – Simulation Biodegradation Test (TG 309)	<60 days testing period - Radio labelled and unlabelled compounds can be used

Due to the inherent complexities of using a solid medium for biodegradation and the use of radio labelled atoms there are a number of parameters suggested by the OECD that can be used to monitor the fate of chemical compounds in a soil or sedimentary environment.

- First order or pseudo-first order rate constant for biodegradation kinetics
- Degradation half-life ( $DT_{50}$ )
- Half-saturation constant

- Maximum specific growth rate
- Fraction of mineralised  $^{14}\text{C}$ , and, if specific analyses are used, the final level of primary degradation
- Identification and concentration of major transformation products - if radio labelled compounds are used

**Table 1.7.** Other non-OECD test guidelines for aerobic biodegradability of plastics in soil

Test	Test Parameters
ASTM D 5988-96 Standard Test Method for Determining Aerobic Biodegradation of Plastic Materials in Soil	No pass or fail mark assigned - test method only. Degradation measured by $\text{CO}_2$ present in a trapping solution by titration, over a 6 month period.
ISO 17556: Determination of the Ultimate Aerobic Biodegradability of Plastic Materials in Soil by Measuring the Oxygen Demand in a Respirometer or the Amount of Carbon Dioxide Evolved	Biodegradation can be determined by $\text{CO}_2$ evolution or $\text{O}_2$ demand

One other prescribed test for inherent biodegradation of chemical compounds in soil exists and this is the OECD TG 304A. The test however, requires the use of  $^{14}\text{C}$  labelled compounds. A sample of  $^{14}\text{C}$  treated compound is introduced into the test medium. The evolution of  $^{14}\text{CO}_2$  is then monitored using alkali absorption and a liquid scintillation counter.

#### 1.2.1.6 Anaerobic biodegradation

**Table 1.8.** OECD testing guidelines No. 311

Test	Pass Level after 60 Days
Anaerobic Biodegradability of Organic Compounds in Digested Sludge/Method by Measurement of Gas Production (TG 311).	75-80% Theoretical gas evolution = complete anaerobic biodegradation

The TG 311 test, Table 1.8, outlines a method of measuring biodegradability in an aerobic environment. However, TG311 is limited as it only assesses biodegradability in anaerobic

digesters and does not take into account other anaerobic biodegradation pathways possible in different environmental compartments. The test measures gas evolution with a band of 75-80% of theoretical gas production being used as a sign of complete anaerobic biodegradation.

As can be seen from Tables 1.1-1.8, there exists a number of techniques for determining biodegradability with a wide breadth of conditions and scenarios covered. The test methods aforementioned are only approximations of the conditions that exist in the extremely complex and dynamic conditions present in WWTP's and the greater environment and can never truly simulate these conditions. However, if they are treated as tools with which to gain insight into the potential environmental breakdown of chemicals, then this information can be used as part of an environmental impact assessment as well as assisting in the rational design of future generations of chemicals.

Currently a number of different methods have been employed to induce degradation (biotically and abiotically) in molecules, these include altering the temperature of the degradation vessel, inoculating the test media with a specific bacteria, degradation in an advanced oxidation system,<sup>37</sup> degradation in an electrochemical system,<sup>38, 39</sup> and ultrasonic degradation.<sup>40</sup> The overall aim is to possibly develop a system for treating wastewater before release into the environment.

#### **1.2.1.7 Biodegradation metrics**

Currently biodegradation data is categorised by whether a compound passes or fails a test but more recently a visual traffic light metric system has been applied by Gathergood *et al.*<sup>18</sup> to give a colour coded representation of how biodegradation levels compare.<sup>18</sup> The levels of biodegradation are assigned a colour based on the following criteria:

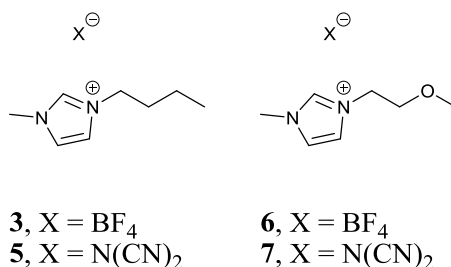
- Green:  $\geq 60\%$  readily biodegradable
- Amber: 20–59%
- Red: 0–19%

This colour coding system allows for libraries of compounds to be compared and categorised visually and with ease. Examples of the system in use will be discussed later in this chapter.

## 1.2.2 Biodegradation in soil, compost and other matrices

### 1.2.2.1 Biodegradation in soil

Biodegradation of imidazolium-based ILs in soil has been previously reported by Modelli *et al.*<sup>41</sup> Four ILs [bmim][BF<sub>4</sub>] (**3**), [bmim][N(CN)<sub>2</sub>] (**5**), [MeOCH<sub>2</sub>CH<sub>2</sub>mim][BF<sub>4</sub>] (**6**) and [MeOCH<sub>2</sub>CH<sub>2</sub>mim][N(CN)<sub>2</sub>] (**7**), Figure 1.4, were examined for their biodegradability according to the ASTM D 5988-96 protocol. In this protocol a pass/fail mark is not assigned and biodegradation is merely observed. Under the test conditions the test compound is mixed with soil and placed in a large glass vessel with CO<sub>2</sub> evolution regularly measured. Soil can be a species rich mixture, but it is expected that the activity will be less than an activated sludge so the test is run over a 6 month period. In this particular study it was found that the linear alkyl [bmim][BF<sub>4</sub>] example, underwent degradation of  $52.1 \pm 6.6\%$  with the N(CN)<sub>2</sub> derivative being less biodegradable than the halide, producing  $17.0 \pm 4.2\%$  degradation. The oxygenated [MeOCH<sub>2</sub>CH<sub>2</sub>mim] derivatives both failed to degrade, producing negligible biodegradation results of  $0.1 \pm 4.0\%$ .



**Figure 1.4.** Imidazolium ILs examined by Modelli *et al.*<sup>41</sup>

### 1.2.2.2 Interactions with soil, compost and other matrices

It is of concern that ILs could reach concentrations high enough in industrial waste water treatment plants (WWTPs) to affect their operating conditions. As outlined in a publication by Stolte *et al.* in 2013, it is believed that ILs will never reach a concentration significant enough to inhibit the bacteria in a domestic WWTP, however due to the toxic effects of some ILs, inhibitory effects on a WWTPs efficacy could be foreseen.<sup>42</sup> Some ILs possess the ability to adsorb onto sewage flocs. This can actually be beneficial in a WWTP environment as it can potentially reduce the concentration of ILs in "solution" and therefore reduce the toxic inhibitory effects, if indeed the ILs are toxic.<sup>43</sup> The ILs partition coefficient and adsorption coefficients however plays a further role in the ILs interaction with soil *vide infra*. Whether WWTPs treatments are enough to remove residual ionic compounds is also questionable as demonstrated by Gomez *et al.* in 2011 where ionic and non-ionic surfactant molecules in  $\mu\text{g l}^{-1}$  concentrations were detected in drinking-water treatment plants, including plants with advanced

tertiary treatment plans.<sup>44</sup> This observation poses the question of whether ILs will behave similarly due to their comparable structural features to ionic surfactants and further justifies the research employed in designing for degradation. Recent evidence for some 1-methylimidazolium IL derivatives provided by Gendaszewska *et al.*<sup>45</sup> demonstrated, using the OECD 302B test, the degree of adsorption of a number of ILs in an inoculum. It was observed that more lipophilic derivatives adsorbed to the inoculum (~3.5%) whereas the highly polar derivatives did not. SDS was adsorbed at a ~35% level.

The interactions of ILs in soils have been examined in a number of recent publications.<sup>41, 46-49</sup> The ability of ILs to interact with a soil and adsorb to this matrix poses a number of problems. If the ILs are not biodegradable, will they adsorb to the soil indefinitely and if so what are the potential consequences and outcomes of these interactions? Furthermore, if the ILs adsorption profile allows it to eventually elute from the soil can the IL then enter the aquifer?

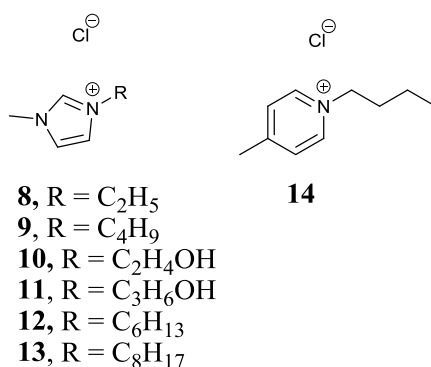
A number of studies have been conducted on ILs and their interactions with soil, bacteria and plant life, with some generalisations reported:

- The lower the lipophilicity the more mobile the IL
- Hydrophobic ILs will only migrate a few centimetres into soil<sup>48</sup>
- IL cations bind more weakly to soils that contain less organic matter<sup>48</sup>
- The mineral content of the soil greatly affects the mechanism of sorption<sup>50</sup>
- The more mobile the IL the greater the ability to pass through soil into ground water
- Sorption of ILs is greatest with strongly exchangeable cations and a high organic content
- The longer the alkyl chain the higher the sorption coefficient and *vice versa*, see Figure 1.5<sup>48</sup>
- Desorption can be inversely correlated to sorption<sup>48</sup>
- Hydroxylated analogues adsorb more weakly<sup>43</sup>
- The higher the hydrophobicity of an IL, the greater the phytotoxic effect<sup>51</sup>
- Bacteria from a high salt environment or a high hydrocarbon environment are far better able to survive in higher concentrations of ILs<sup>52</sup>

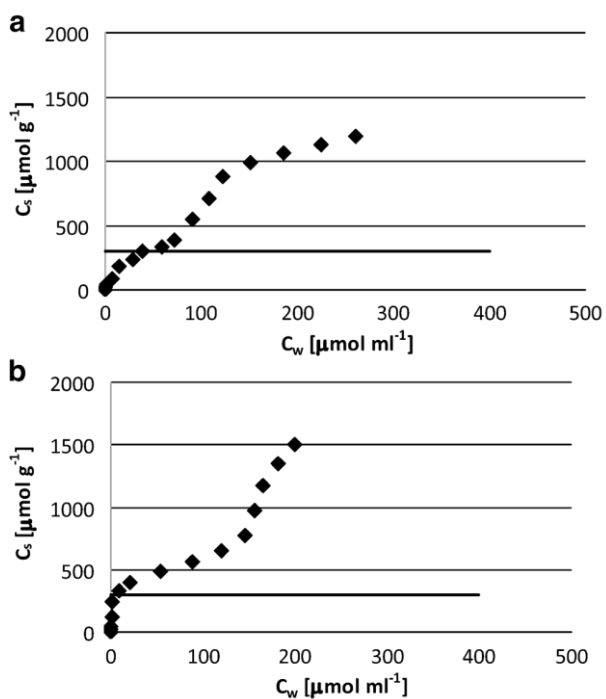


Ionic liquids	R3		L2		CA-1		CA-2		CA-3	
	$K_{d1}$	$K_{d2}$	$K_{d1}$	$K_{d2}$	$K_{d1}$	$K_{d2}$	$K_{d1}$	$K_{d2}$	$K_{d1}$	$K_{d2}$
[EMIM][Cl]	3.3	2.3	1.7	0.7	2.5	1.3	2.8	2	1.2	0.5
[EMIMOH][Cl]	2.1	2.5	1.5	0.9	2.6	0.4	2.3	2	1.7	1
[PMIMOH][Cl]	4.1	2.9	1.9	0.7	3.7	2.1	2.6	2	2	1.1
[BMIM][Cl]	8.7	4.6	2.5	1	15.7	6.8	2.7	2.7	4	0.9
[HMIM][Cl]	22	7.5	3.6	2.2	15.5	9	4.6	3.6	9	2
[OMIM][Cl]	34.2	12.1	4.5	1.7	26.4	8.6	8.7	5.1	10	3.7
[MBPy][Cl]	22	6.4	4.1	1.2	16.8	3.1	5.4	1.5	1.6	1.3

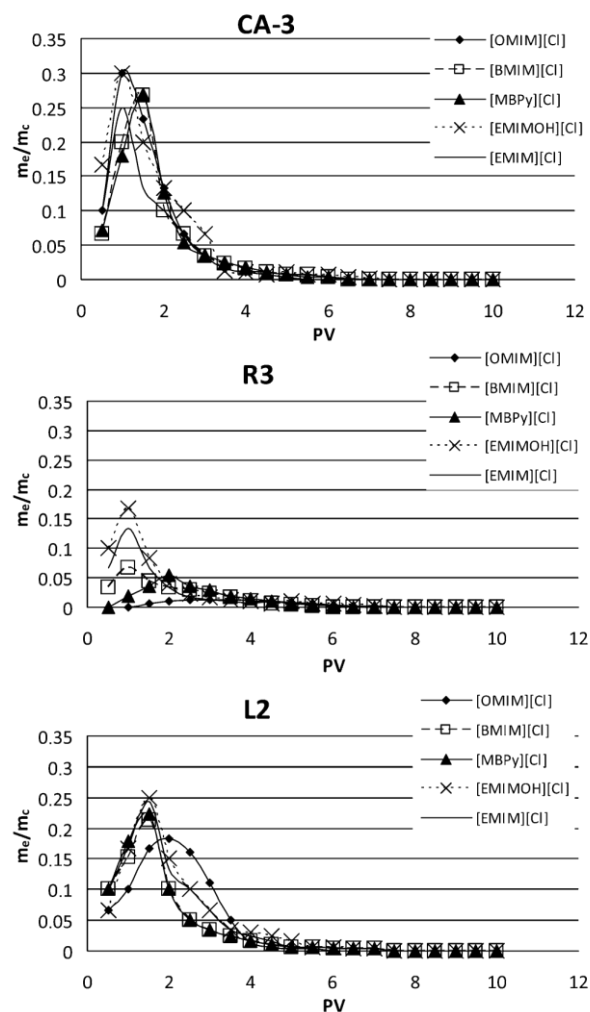
**Figure 1.5.** Sorption coefficients ( $K_d$  mL  $g^{-1}$ ) for first layer  $K_{d1}$  and final concentration  $K_{d2}$  for given soil types.<sup>48</sup>



**Figure 1.6.** Imidazolium compounds (**8-14**) examined for soil adsorption.



**Figure 1.7.** Sorption isotherms for a, [bmim][Cl], and b, [hmim][Cl] on soil type R3.<sup>48</sup>



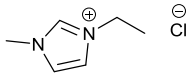
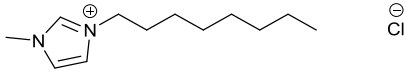
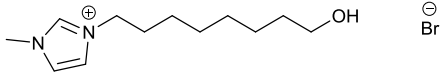
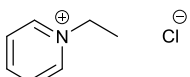
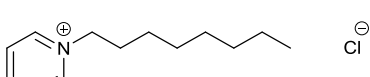
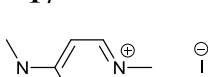
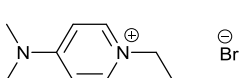
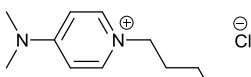
**Figure 1.8.** Soil elution profiles (breakthrough curves) of ILs [omim][Cl], [bmim][Cl], [mbpy][Cl], [emimOH][Cl] and [emim][Cl] in the three different soil types, CA3, R3 and L2.<sup>48</sup>

### 1.2.3 Biodegradation of ILs under denitrifying conditions

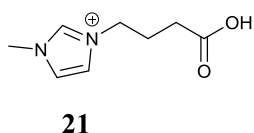
Biodegradation of ILs under denitrifying conditions remains a largely undocumented pathway and has only been reported in one paper.<sup>53</sup> Anaerobic biodegradation conditions are prevalent in nature in soils, aquatic environments and in wastewater treatment plants and are considered of potential significance as IL biodegradation pathways.

#### 1.2.3.1 Anaerobic biodegradation

In the study carried out by Stolte *et al.* in 2010, nine ILs (**8**, **13**, **15-20**) were examined for their anaerobic biodegradability including a metabolite study with compound identification by HPLC-UV.<sup>53</sup> The ILs were subjected to the denitrifying conditions for 11 months.

IL Screened	Primary biodegradation as determined by HPLC/MS
 <b>8</b>	0%
 <b>13</b>	0%
 <b>15</b>	100% Metabolite detected - See Fig. 9
 <b>16</b>	0%
 <b>17</b>	0%
 <b>18</b>	0%
 <b>19</b>	0%
 <b>20</b>	0%

**Table 1.9.** Anaerobic degradation of imidazolium and pyridinium ILs reported by Stolte *et al.*<sup>53</sup>



**Figure 1.9.** Metabolite detected at the end of the study.

The results of the anaerobic study, Table 1.9, showed no reduction in concentration for the ILs studied except for the octyl alcohol derivative (**15**) which broke down completely, within 30-40 days, to the carboxylic acid metabolite (**21**), Figure 1.9, after a period of three months. The

biodegradation pathway and associated metabolite study are further discussed later in this review in Section 1.4.2, *vide infra*. Attempts to induce biodegradation by co-metabolism through the addition of an acetate salt failed.<sup>51</sup> Alkyl substituted imidazolium (**8**, **13**), pyridinium (**16**, **17**) and dimethylaminopyridinium (**18-20**) ILs were not found to be readily biodegradable compounds under the anaerobic test conditions (Table 1.9).

### 1.2.3.2 Anaerobic dehalogenation

Another benefit of investigating the anaerobic biodegradation of ILs is the potential for biodegradation of halogenated compounds. Organohalides make up a large proportion of compounds used as solvents, biocides, pesticides, refrigerants etc. and many can be classed as persistent organic pollutants.<sup>23,54</sup> With the introduction of halogenated ILs into industrial applications, the question of how these compounds will respond to release into the environment must be asked. Under the Stockholm Convention on Persistent Organic Pollutants 2004, bans and reductions on some of the world's most hazardous organic pollutants were put into effect.<sup>55</sup> With a legal and political framework established for the reduction of halogenated and persistent organic pollutants in place, the need to provide readily biodegradable organohalide compounds is imperative. Halo-respiring bacteria are known and the reductive dechlorination of common chlorinated solvents has been reported including trichloroethane, tetrachlorethene and aromatic halides.<sup>56-58</sup> Examination of ILs for anaerobic biodegradation therefore is of importance, especially if the IL is not readily biodegradable under aerobic conditions or if a metabolite study shows that a halogenated moiety remains after degradation has plateaued. Inorganic halide counterions can breakdown with no release of CO<sub>2</sub>, for example BF<sub>4</sub> hydrolysis.<sup>59</sup> In a 2012 study conducted by Stolte *et al.* the biodegradability of fluoro and cyano derived anions was assessed.<sup>60</sup>

Under the aerobic and anaerobic degradation test conditions a number of metal salts of the anions were examined:

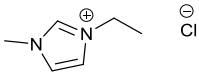
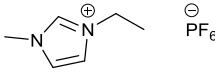
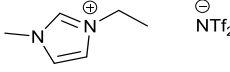
- NaN(CN)<sub>2</sub> -sodium *N*-cyanocyanamide,
- LiNTf<sub>2</sub> – lithium bis(trifluoromethylsulphonyl)amide
- KC(CN)<sub>3</sub> - potassium tricyanomethanide
- KB(CN)<sub>4</sub> - potassium tetracyanoborate
- K(C<sub>2</sub>F<sub>5</sub>)<sub>3</sub>PF<sub>3</sub> – potassium trifluoridotris(pentafluoroethyl)phosphate

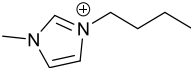
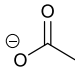
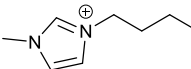
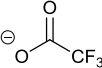
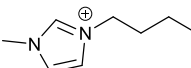
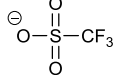
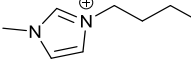
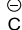
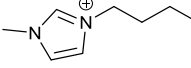
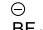
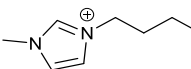
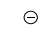
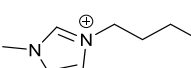
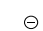
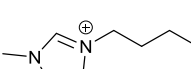
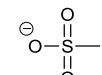
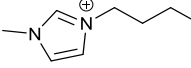

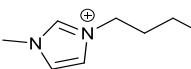
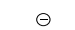
Under both aerobic and anaerobic test conditions it was noted that the metal salts of these anions did not possess any biodegradation potential and were not toxic to the microorganisms in the test sludge (at the concentrations used in the test). It was suggested that the ability for the anions to undergo de-fluorination was also unlikely.<sup>60</sup>

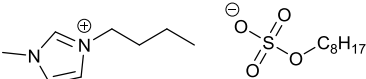
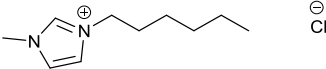
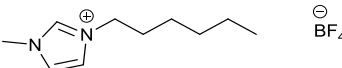
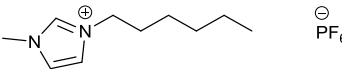
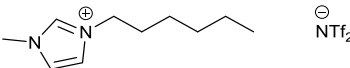
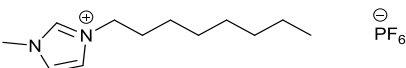
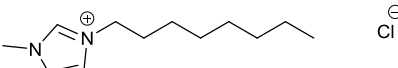
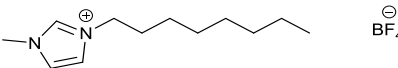
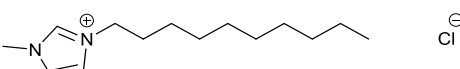
#### 1.2.4 Biotreating ILs for enhanced biodegradation – axenic cultures

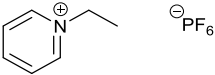
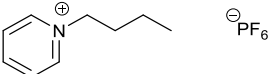
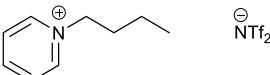
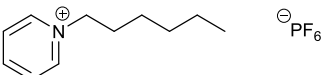
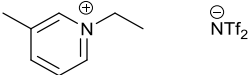
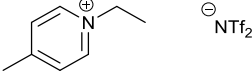
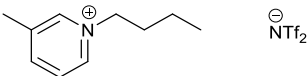
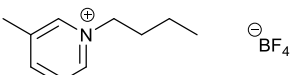
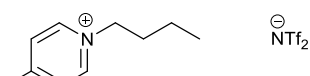
An investigation into the use of axenic bacterial cultures - cultures of bacteria containing only one organism/strain - in enhancing biodegradation was performed by Catalina *et al.* in 2011.<sup>61</sup> The use of judiciously selected bacteria, specifically a *Sphingomonas paucimobilis* (*S. Paucomobilis*) strain, has demonstrated that modifying the test conditions from the prescribed OECD guidelines can heighten biodegradation. The results of these tests are not recognised under the OECD or ISO guidelines; however they do give insight into alternate bio-based treatment options for ILs. Previously recalcitrant compounds were observed undergoing biodegradation under optimised test conditions of 45°C and IL concentrations of 0.5-3.0 g l<sup>-1</sup>. Out of 37 commercially available ILs tested, 20 were found to undergo ≥60% biodegradation in less than 28 days, (3-5, 22, 23, 27-32, 36-41, 45, 46, 49, 50) see Table 1.10, with the choice of anion playing a significant factor in % degradation. Shortening the length of substituted alkyl chains increased biodegradability, e.g. for the chloride series of 1-methylimidazole series (8, 9, 12, 13, 35). The successful application of a specific bacterial strain capable of adapting to higher concentrations of ILs shows that a potential wastewater pre-treatment of non-biodegradable ILs is possible. It is also important that the concentration of IL used in each test played a major role in % biodegradation values, with ~2 mmol l<sup>-1</sup> giving optimum results. It is stated by Catalina *et al.*<sup>61</sup> that no clear relationship between toxicity and biodegradation results were observed for the compounds tested.

**Table 1.10.** Biodegradation results for *Sphingomonas paucimobilis* at 45°C.

Name	Structure	Biodegradation <sup>a</sup>
[emim][Cl]	 8	53*
[emim][PF <sub>6</sub> ]	 22	87
[emim][NTf <sub>2</sub> ]	 23	67

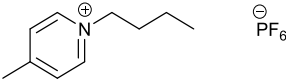
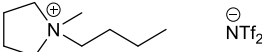
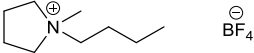
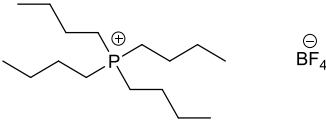
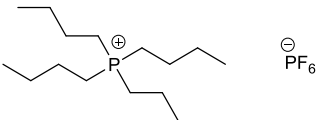
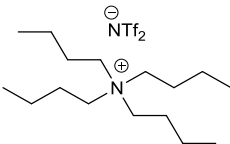
<b>[bmim][CH<sub>3</sub>CO<sub>2</sub>]</b>			<b>51</b>
	<b>24</b>		
<b>[bmim][CF<sub>3</sub>CO<sub>2</sub>]</b>			<b>20</b>
	<b>25</b>		
<b>[bmim][CF<sub>3</sub>SO<sub>3</sub>]</b>			<b>34</b>
	<b>26</b>		
<b>[bmim][Cl]</b>			<b>39*</b>
	<b>9</b>		
<b>[bmim][BF<sub>4</sub>]</b>			<b>80*</b>
	<b>3</b>		
<b>[bmim][PF<sub>6</sub>]</b>			<b>65*</b>
	<b>4</b>		
<b>[bmim][Br]</b>			<b>75*</b>
	<b>27</b>		
<b>[bmim][CH<sub>3</sub>SO<sub>3</sub>]</b>			<b>75*</b>
	<b>28</b>		
<b>[bmim][DCN]</b>			<b>77</b>
	<b>5</b>		
<b>[bmim][NTf<sub>2</sub>]</b>			<b>90*</b>
	<b>29</b>		

<b>[bmim][C<sub>8</sub>H<sub>17</sub>SO<sub>4</sub>]</b>		<b>&gt;95*</b>
<b>30</b>		
<b>[hxmim][Cl]</b>		<b>37</b>
<b>12</b>		
<b>[hxmim][BF<sub>4</sub>]</b>		<b>40</b>
<b>31</b>		
<b>[hxmim][PF<sub>6</sub>]</b>		<b>70</b>
<b>32</b>		
<b>[hxmim][NTf<sub>2</sub>]</b>		<b>73</b>
<b>33</b>		
<b>[omim][PF<sub>6</sub>]</b>		<b>54</b>
<b>34</b>		
<b>[omim][Cl]</b>		<b>32</b>
<b>13</b>		
<b>[omim][BF<sub>4</sub>]</b>		<b>33</b>
<b>35</b>		
<b>[dcmmim][Cl]</b>		<b>12</b>
<b>36</b>		

[1EtPy][PF <sub>6</sub> ]		>95
	37	
[1BuPy][PF <sub>6</sub> ]		80
	38	
[1BuPy][NTf <sub>2</sub> ]		86
	39	
[1HxPy][PF <sub>6</sub> ]		62
	40	
[1Et3MePy][NTf <sub>2</sub> ]		>95
	41	
[1Et4MePy][NTf <sub>2</sub> ]		>95
	42	
[1Bu3MePy][NTf <sub>2</sub> ]		17
	43	
[1Bu3MePy][BF <sub>4</sub> ]		35
	44	
[1Bu4MePy][NTf <sub>2</sub> ]		30
	45	



---

<b>[1Bu4MePy][PF<sub>6</sub>]</b>		<b>78</b>
	<b>46</b>	
<b>[1Bu1MePyrr][NTf<sub>2</sub>]</b>		<b>&gt;95</b>
	<b>47</b>	
<b>[1Bu1MePyrr][BF<sub>4</sub>]</b>		<b>49</b>
	<b>48</b>	
<b>[PBu<sub>4</sub>][BF<sub>4</sub>]</b>		<b>41</b>
	<b>49</b>	
<b>[PBu<sub>4</sub>][PF<sub>6</sub>]</b>		<b>66</b>
	<b>50</b>	
<b>[NBu<sub>4</sub>][NTf<sub>2</sub>]</b>		<b>64</b>
	<b>51</b>	

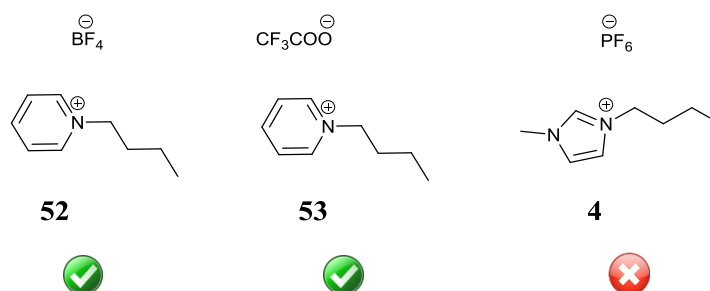
---

a. Colour Coded to traffic light metric system (see Section 1.2.1.7).

\* Compounds previously reported as recalcitrant.<sup>62-63</sup>

Similar success in the use of axenic cultures was observed in the work by Zhang *et al.* in 2010, where it was demonstrated that a *Corynebacteria* species could effectively metabolise the butylpyridinium ILs (**52** and **53**), Figure 1.10 but not [bmim] PF<sub>6</sub> (**4**).<sup>64</sup>

A proposed degradation pathway determined by ESI/MS/MS is presented in Section 1.4.2, *vide infra*. The potential capabilities of judiciously selected bacterial cultures have shown that biodegradation of previously determined recalcitrant IL compounds is possible, subject to optimised conditions.



**Figure 1.10.** [PyBu] derivatives (**52** and **53**) found to degrade and recalcitrant [bmim][PF<sub>6</sub>] derivative (**4**).

Jungnickel *et al.* examined the use of axenic cultures of bacteria in the biodegradation of [omim][Cl] (**13**) in 2014 using the manometric respirometry method (OECD 301F).<sup>65</sup> Under their biodegradation tests, nine bacteria were isolated from an activated sludge and identified by 16S rDNA PCR (polymerase chain reaction) and compared to genetic data available on Genbank. The bacteria were then examined for their biodegradation potential. The bacteria isolated were as follows:

- *Flavobacterium* sp. WB3.2-27
- *Shewanella putrefaciens* CN-32
- *Moraxellaceae* bacterium MAG
- *Flavobacterium* sp. FB7
- *Microbacterium keratanolyticum* AO17b
- *Flavobacterium* sp. WB 4.4-116
- *Arthrobacter* sp. SPC 26
- *Rhodococcus* sp. PN8
- *Arthrobacter protophormiae* strain DSM 20168

It was found that the individual axenic cultures were inefficient at biodegrading the [omim][Cl] exhibiting only  $\leq 8\%$  biodegradation. When all 9 bacteria strains were combined into a mixed culture biodegradation experiment, only 30% biodegradation could be achieved. Under the same experimental conditions, using an activated sludge, degradation of  $\sim 60\%$  was observed for [omim][Cl] (determined by the manometric respirometry method (OECD 301F)).<sup>65</sup> Thus it was proposed by Jungnickel *et al.* that isolated organisms may not facilitate biodegradation as efficiently as they would in an activated sludge of far greater complexity where the possibility of symbiotic relationships of multiple strains of bacteria are present. Another possibility

suggested was that not all of the bacteria required for IL metabolism were isolated for the individual and combined culture experiments.<sup>65</sup>

### 1.2.5 Suitability of biodegradation tests to IL classes – toxicity vs. biodegradability

Not every IL tested for biodegradation by one of the standard OECD methods will be compatible with the test procedure and it has been previously reported that a number of issues exist including sorption and kinetic parameters of ILs in activated sludge as previously described and toxicity of IL to the inoculum.<sup>66</sup> Other issues then arise such as concentration effects of toxic ILs and biodegradation inhibition that may ensue. See Table 1.11 for a general compound suitability to biodegradation test methods.

Test	Analytical method	Suitability for compounds which are:		
		Poorly soluble	Volatile	Adsorbing
DOC Die-Away (301 A)	Dissolved organic carbon	–	–	±
CO <sub>2</sub> evolution (301 B)	Respirometry: CO <sub>2</sub> evolution	+	–	+
MITI (I) (301 C)	Respirometry: oxygen consumption	–	±	+
Closed bottle (301 D)	Respirometry: dissolved oxygen	±	+	+
Modified OECD screening (301 E)	Dissolved organic carbon	–	–	±
Manometric respirometry (301 F)	Oxygen consumption	+	±	+
CO <sub>2</sub> headspace test (ISO 14593)	CO <sub>2</sub> evolution	+	+	+
OECD 309	<sup>14</sup> C labelling	±	+	+
ASTM 5988	CO <sub>2</sub> production/BOD	–	–	±

Suitable method to screen compound: +; unsuitable method to screen compound: –.

**Table 1.11.** Suitability of organic compounds to biodegradation screening method. <sup>22, 35</sup>  
Adapted from Coleman *et al* 2010.<sup>22</sup>

According to current trends from reported biodegradation data, the increase of alkyl side chains has shown to directly lead to an increase in biodegradation due to the extra oxidisable carbons in the chain. However a design conflict is present and an increase in alkyl chain length has been shown to increase antimicrobial toxicity especially around the C<sub>12</sub>-C<sub>14</sub> chain length. Chains of C<sub>16</sub> and C<sub>18</sub> exhibit very poor water solubility and hence have a lower bioavailability.<sup>67</sup> A design optimisation in the addition of ether oxygen in alkyl chains has shown to reduce toxicity but maintain levels of biodegradability.<sup>68</sup>

Validation of biodegradation results is of the utmost importance. For example when carrying out the CBT sodium acetate is often used as a control. The high biodegradability of sodium acetate is known and by comparing biodegradation results to the control it can be determined whether the inoculum chosen for the test is effective.

Further validation is required regarding the toxicity of ILs and the sorption characteristics. Removal of ILs by sorption can be calculated using the guidelines in OECD 302B Zahn-

Wellens test.<sup>35</sup> Toxicity of ILs to the inoculum can be assessed by including a toxicity control series in tandem to the biodegradation test series and a blank sodium acetate + inoculum series. The toxicity reference vessel contains IL + sodium acetate + inoculum, the sodium acetate control contains sodium acetate + inoculum. Any significant differences in oxygen demand between the toxicity control, when compared to the sodium acetate control, can be attributed to toxic effects.

While different research groups may prefer to perform one biodegradation test over another, in particular with the CO<sub>2</sub> headspace test (OECD 310 or ISO 14593), or even primary vs. readily biodegradation tests, it is key to note that this data is just a starting point for a more detailed investigation about chemical fate in the environment. Regardless of where you start the assessment program, the aim is to ultimately complete a thorough (eco)toxicity and biodegradation study of chemicals likely to be used on a large scale and where contamination of the environment is a possibility.

### **1.3 Biodegradation data on classes**

#### **1.3.1 Ionic liquids: anion and cation effects with regards to biodegradation**

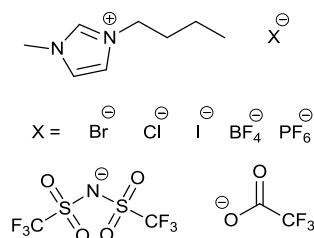
There are a number of different perspectives to consider when interpreting biodegradation data of ILs. All ILs consist of an anion and cation thus two parts must be considered, albeit as a pair. Another consideration is whether the anion or cation is organic or inorganic. For instance if an inorganic ion is used, such as a halide or pseudohalide (or positively charged metal halide cation), then it does not contribute directly as a carbon source for biodegradation determination. Conversely, if an IL contains an anion of high carbon content which is known to have excellent biodegradation characteristics (e.g. octyl sulphate anion, Figure 1.12), then one must be careful not to assume high biodegradability for the ion pair, and thus infer good biodegradability for the other less degradable ion present in the IL.

Within the OECD test regulations a biodegradation level of 60% is usually required within 28 days. The test treats the IL as a single chemical compound and therefore the outcome is that the IL ion pair either passes or fails the biodegradation test. While caution must be exercised when utilising this pass or fail result for biodegradation tests to design future biodegradable ILs, the pass or fail result for each IL is valid as defined by the regulations of the OECD test criteria. It is our expectation that this review will assist researchers to design and develop ILs which pass

ultimate biodegradation and mineralisation assays, which is only possible if both ions biodegrade or are mineralised.

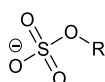
### 1.3.2 Anions

A popular and widespread class of anions are the halides, Figure 1.11. The halide anions and pseudohalides (e.g.  $\text{BF}_4^-$  and  $\text{PF}_6^-$ ) are not a carbon source for biodegradation and thus biodegradation values are dependent on the organic cation. IL [bmim] derivatives have been reported to give poor biodegradability, with values in the, 0-5% range.<sup>22</sup> Anion choice is usually directed by function and application (e.g. in many cases,  $\text{NTf}_2^-$  for hydrophobic ILs). In this section organic anions in ILs are reviewed and their progress towards the development of biodegradable ILs is discussed.

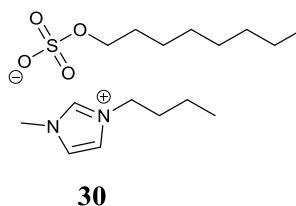


**Figure 1.11.** Some of the most commonly employed halide/pseudohalide anions as their [bmim] ILs.

Organic anions offer a myriad of possibilities when selecting suitable structures to incorporate into ILs. Many natural products (e.g. carboxylic acids, amino acids, and carbohydrates) have been tested as feedstocks for anions. Other examples have been adopted from the surfactant industry, such as the sulphate anions, Figure 1.12. The alkylsulphate anions exhibit good rates of biodegradation. Of note, sodium dodecyl sulphate is used frequently as the positive test control for activated sludge activity.<sup>18</sup> Studies by Scammells *et al.* showed that [bmim][C<sub>8</sub>H<sub>17</sub>SO<sub>4</sub>], (**30**), Figure 1.13, biodegrades 25% in the CBT (OECD 301D),<sup>63</sup> or up to 40% in the CO<sub>2</sub> headspace test (ISO 14593).<sup>69</sup> A reasonable assumption is that the anion is converted to CO<sub>2</sub> with high efficiency and the [bmim] cation is not transformed, however this was not confirmed at the time due to the absence of LCMS data and metabolite identification.

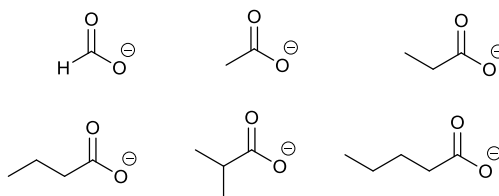


**Figure 1.12.** Sulphate anion core, R = C<sub>n</sub>H<sub>2n+1</sub>, n = 8-12.

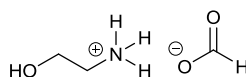


**Figure 1.13.** [bmim] paired with the biodegradable, octyl sulphate anion failed the CBT and CO<sub>2</sub> Headspace test.<sup>63</sup>

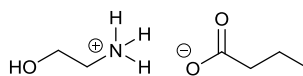
Formates, acetates and other simple carboxylates, Figure 1.14, have been employed as IL anions with very good biodegradation results found when paired with the cholinium cation, Figure 1.15. Cation modification can lead to significant changes in biodegradability which is discussed later in Section 1.3.3, *vide infra*.



**Figure 1.14.** Formate and carboxylate anions.



**54**, 86%

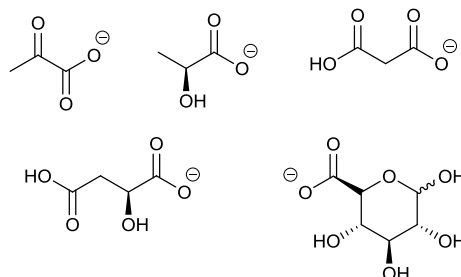


**55**, 95%

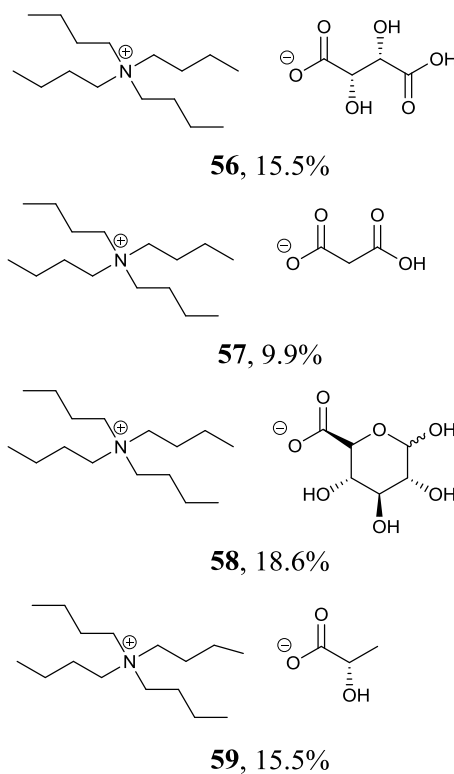
**Figure 1.15.** Two readily biodegradable protic ethanolaminium carboxylate ILs.<sup>70</sup>  
Biodegradation values assessed by Manometric Respirometry (OECD 301F).

Similar success has been demonstrated in the use of malonates, succinates, tartrates and other natural organic acids and sugars, Figure 1.16. However, pairing with an appropriate cation is crucial. In the following examples tetrabutylammonium (TBA) cations have been employed where only the organic anion is degraded, Figure 1.17. Replacing the TBA cation with a dibutyl-dimethyl ammonium cation (DMDBA), Figure 1.18, promotes biodegradation for the

lactate derivative (**59**). The biodegradation values of the TBA derivatives are in good agreement with the percentage carbon equivalent of the anion and it is assumed that the cation is persisting with only the anion undergoing biodegradation, CBT (OECD 301D).<sup>71, 72</sup> See Section 1.3.5.5 on tetraalkylammonium ILs for more information on TBA and DMDBA ILs.

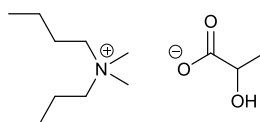


**Figure 1.16.** Biodegradable organic acids that have been employed as anions in ILs.<sup>71</sup>



**Figure 1.17.** TBA carboxylate ILs.<sup>71</sup>

Biodegradation values assessed by CBT (OECD 301 D).

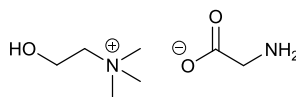


**60**, 72%

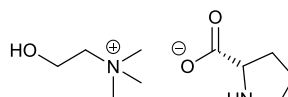
**Figure 1.18.** A readily biodegradable lactate DMDBA IL.<sup>71, 73</sup>

Biodegradation values assessed by Manometric Respirometry (OECD 301F)

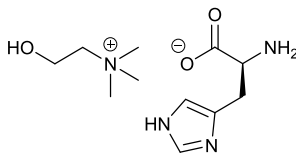
In addition to organic acids and sugar acids, amino acids have been investigated as the anion in ILs, Figure 1.19. There are 23 proteinogenic amino acids for prokaryotic organisms and 21 for eukaryotes. A recent publication by Zong *et al.*<sup>74</sup> showed the successful combination of 18 amino acids (Gly, Ala, Val, Leu, Ile, Ser, Thr, Met, Asp, Glu, Asn, Gln, Lys, His, Arg, Pro, Phe, Trp) with a cholinium cation. All of the ILs passed the CBT (OECD 301D) (65.3 – 87.1%) and the CO<sub>2</sub> headspace test (OECD 310), (62.1 – 85.2%) and can be classed as readily biodegradable. Selected examples are shown in Figure 1.19, for full list see Appendix 1, compounds (**310-322**).



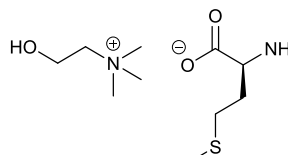
**61**, 76.4%



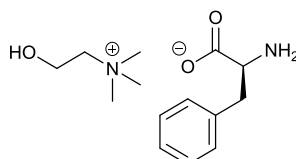
**62**, 70.5%



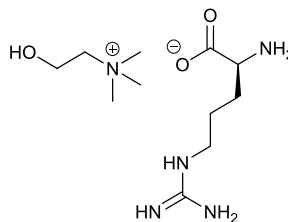
**63**, 63.3%



**64**, 63.6%



**65**, 72.5%



**66**, 65.5%

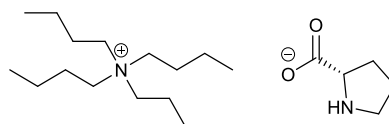
**Figure 1.19.** Biodegradable cholinium amino carboxylate ILs.<sup>74</sup>

Biodegradation values assessed by CO<sub>2</sub> Headspace test (OECD 310).

A common structural feature of all these anions is the free carboxylate which, as suggested by Boethling, can promote biodegradability.<sup>75</sup> It was also noted that the amino acids with branched side chains were more resistant to biodegradability (69-72% in OECD 301D and OECD 310)



compared to >80% biodegradation for unbranched sidechains. The choice of cation will inevitably have a determining factor on the overall biodegradability of the organic anions as can be seen when comparing cholinium prolinates (**62**) to the TBA derivative (**67**), Figure 1.20. TBA L-prolinate (**67**) undergoes levels of 15-20% biodegradation whereas >70% biodegradation was observed for the cholinium analogue (**62**).



**67**, 15-20%

**Figure 1.20.** TBA L-prolinate IL.<sup>71</sup>

Biodegradation values assessed by CO<sub>2</sub> Headspace test (OECD 310).

As an overarching design principal, the authors suggest that a halide anion such as chloride or bromide can provide the foundation for potentially biodegradable ILs as the halide counterion cannot undergo further degradation as it is already in a mineralised form. Thus, an IL formed from a Br or Cl anion will only biodegrade according to the carbon content of the cation. Perfluorinated anions should be avoided as they have been shown to be recalcitrant or their degradation products are more harmful than their parents, e.g. BF<sub>4</sub> degrading to HF.<sup>59</sup>

Overall the organic acid anions appear to be the best selection for promoting biodegradability. Biodegradation information provided by the choices of amino acids screened by Zong *et al.*<sup>74</sup> ILs (**61-66**, **310-322** Appendix I) suggest that the amino acids all undergo high levels of biodegradation in both the CBT (OECD 301D) and the CO<sub>2</sub> headspace test (OECD 310) and will not persist under the test conditions.

The natural organic acids (succinic, tartaric, lactic, malonic, malic, pyruvic, glucuronic, galacturonic etc.) such as those employed by Ferlin *et al.*<sup>70</sup> and Jérôme *et al.*<sup>71</sup> can be shown to promote biodegradability. In these examples, the tetrabutyl ammonium (TBA) ILs (**56-59**) and (**168-172**), it is assumed that the TBA cation is recalcitrant to biodegradation (OECD 301D), and that the organic acid anion is solely breaking down, this is discussed in more detail under Section 1.3.5.5 on tetra alkylammonium cations.

The DMDBA examples (**60**, **175-180**) also displayed great success in the choice of organic acid anions.<sup>73</sup> Finally the amino diol and triol examples (**161-167**)<sup>70</sup> also have high levels of

biodegradability (OECD 301F) when simple carboxylic acid anions such as formate, acetate, propanoate, isopropanoate, butanoate and pentanoate feature.

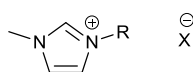
### 1.3.3 Cations

The choice of cation is as large and developed as the choice of anion, with the most common cations including the heterocycles 1-methylimidazolium, pyridinium and the non-aromatic cholinium and tetrabutylammonium. For the majority of ILs synthesised to date, the cation has had a higher carbon content than the anion. This higher carbon content can equate to a larger contribution towards the overall CO<sub>2</sub> evolution/ O<sub>2</sub> demand of the IL within biodegradation screening methods and potentially higher levels of biodegradation. While a shift from inorganic anions to organic anions has been observed, the research conducted towards cation biodegradability has seen many investigations carried out on different organic scaffolds and the effect of various functional groups that may facilitate biodegradation.

### 1.3.4 Aromatic Cations – imidazolium, thiazolium, pyridinium

#### 1.3.4.1 Imidazolium

Derivatives of 1-methylimidazole have long been a choice of cation in IL based technologies with considerable research in the past two decades focussed on 2<sup>nd</sup> and 3<sup>rd</sup> generation ILs (**4**, **8**, **9**, **12**, **29**, **68**) see Figure 1.21.<sup>76</sup> Commercial availability of [bmim] and other alkyl derivatives has facilitated the popularity of ILs as replacement solvents but as previously discussed, identifying readily biodegradable examples has proven difficult.



- 4**, R = C<sub>4</sub>H<sub>9</sub>, X = PF<sub>6</sub>, 0% \*
- 8**, R = C<sub>2</sub>H<sub>5</sub>, X = Cl, 0% \*\*
- 9**, R = C<sub>4</sub>H<sub>9</sub>, X = Cl, 0% \*
- 12**, R = C<sub>6</sub>H<sub>13</sub>, X = Cl, 2%\*\*\*
- 29**, R = C<sub>4</sub>H<sub>9</sub>, X = NTf<sub>2</sub>, <5%\*\*
- 68**, R = C<sub>2</sub>H<sub>5</sub>, X = CH<sub>3</sub>SO<sub>4</sub>, 10%\*\*\*

**Figure 1.21.** Biodegradation data for some 2<sup>nd</sup> and 3<sup>rd</sup> generation ILs.<sup>62, 63, 77</sup>

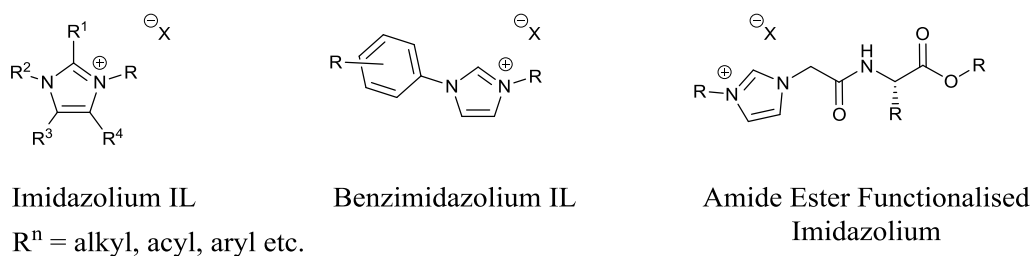
\* Biodegradation values assessed by Manometric Respirometry (OECD 301F)

\*\*Biodegradation values assessed by CBT (OECD 301D)

\*\*\*Biodegradation values assessed by BOD measurement using an OxiDirect kit

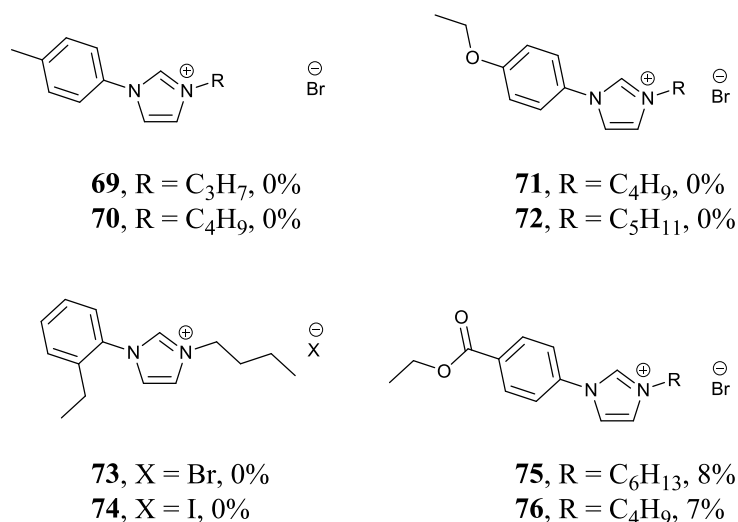
Since the previous IL biodegradation reviews published by Gathergood *et al.* 2010<sup>22</sup> and Stolte *et al.* 2011<sup>78</sup> a number of substituted imidazolium derivatives have been screened for their biodegradability. The imidazolium cation has been functionalised in two ways in efforts to improve biodegradation:

- 1) modification of the *N*-substituents  
and/or
- 2) substitution at the C2 and C4/5 positions of the imidazolium ring, Figure 1.22.



**Figure 1.22.** The imidazolium cation and potential sites for derivatisation.

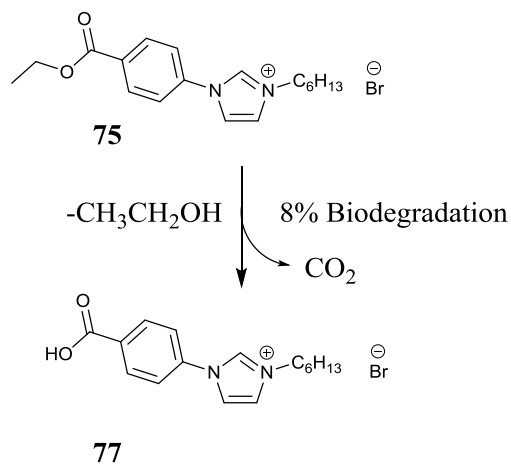
Aryl derivatives (**69-76**) screened by Stolte *et al.* 2013<sup>79</sup> (Figure 1.23) show that aryl imidazolium derivatives are recalcitrant to biodegradation (OECD 301F) with no greater than 8% biodegradation achieved for (**75**) and (**76**), most likely undergoing primary biodegradation via ethyl ester hydrolysis to the carboxylic acid (**77**), Figure 1.24. The introduction of an oxygen atom in the form of the ethyl ether in (**71**) and (**72**) did not initiate biodegradation.



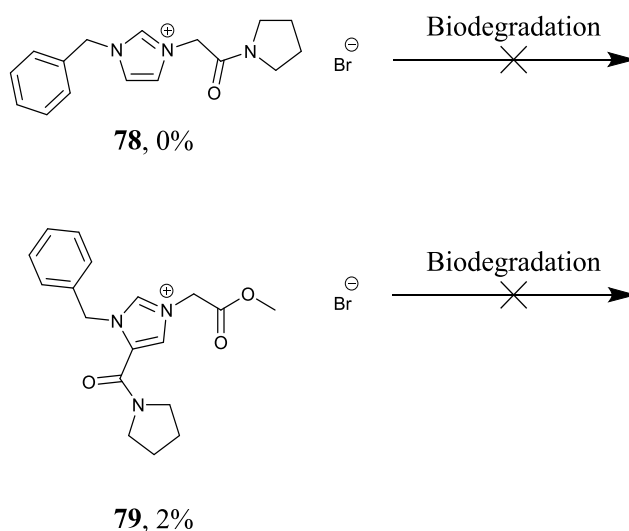
**Figure 1.23.** Biodegradation data for imidazole ILs synthesised by Stolte *et al.*<sup>79</sup>

Biodegradation values assessed by Manometric Respirometry (OECD 301F)

Similar poor levels of biodegradation (0-2% in the CO<sub>2</sub> Headspace Test) for ILs containing phenyl rings were obtained for the *N*-benzyl derivatives (**78**, **79**) screened by Gathergood *et al.* 2013<sup>18</sup> Figure 1.25.



**Figure 1.24.** Aryl imidazolium IL and potential degradation product.<sup>79</sup>



**Figure 1.25.** *N*-Benzyl imidazolium ILs.<sup>18</sup>

Biodegradation values assessed by the CO<sub>2</sub> Headspace Test (ISO 14593)

Modifications by Gathergood *et al.* 2013<sup>18</sup> of the imidazolium cation to introduce ester groups and amide groups at the C2, C4 and C5 positions ILs (**80-96**) did not succeed in raising biodegradation levels (ISO 14593) beyond that which could be explained by ester degradation, Figure 1.26 and 1.27. The imidazolium ILs were categorised by the authors according to the

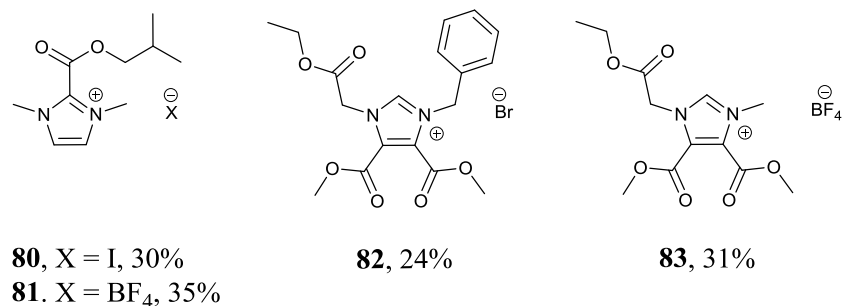
aforementioned traffic light metric and are organised according to amber classified ILs, Figure 1.26 and red classified ILs, Figure 1.27.<sup>18</sup>

Examples of ester modifications at the imidazolium C2 position, ILs (**80, 81**), Figure 1.26 show a moderate amount of biodegradation (30-35%), however this can be attributed to only the degradation of the ester, with the imidazolium ring presumably remaining intact. Imidazolium ILs disubstituted at C4,5 (**82, 83, 86-88**) with ester groups lead to observed biodegradation in the CBT in the range of 3-31% and did not pass the test. Low biodegradation for the C4 substituted analogues (**85, 92**) was also observed. There is no evidence that the introduction of an ester group to the imidazolium ring leads to breakdown of the charged heterocycle. This observation is in contrast to the increase in biodegradability observed when modifying some pyridinium ILs to nicotinium ILs. Possible reasons for this lack of reactivity for the C4 and C4,5 is that after hydrolysis the carboxylic acid or carboxylate salt stabilises the ring making breakdown difficult. For C<sub>2</sub> ester derivatives, hydrolysis forms an unstable intermediate, with facile evolution of CO<sub>2</sub>, and the imidazolium ring intact.<sup>18</sup> Thus the more stable to hydrolysis amide group was examined to investigate the effect of a stable EWG on the imidazolium ring to promote breakdown. However, the authors report that with the amide in the C2 (**89, 90, 91**), C4 (**79**) or C4,5 (**92**) low biodegradation in the range 2-17% was observed.

Amide functionalisation at the nitrogen position to give ILs (**78, 95, 96, 90, 91**), Figure 1.25 and 1.27, also show a resistance to biodegradation. This is best exemplified by (**95**) and (**96**) with levels of 3% biodegradation recorded.

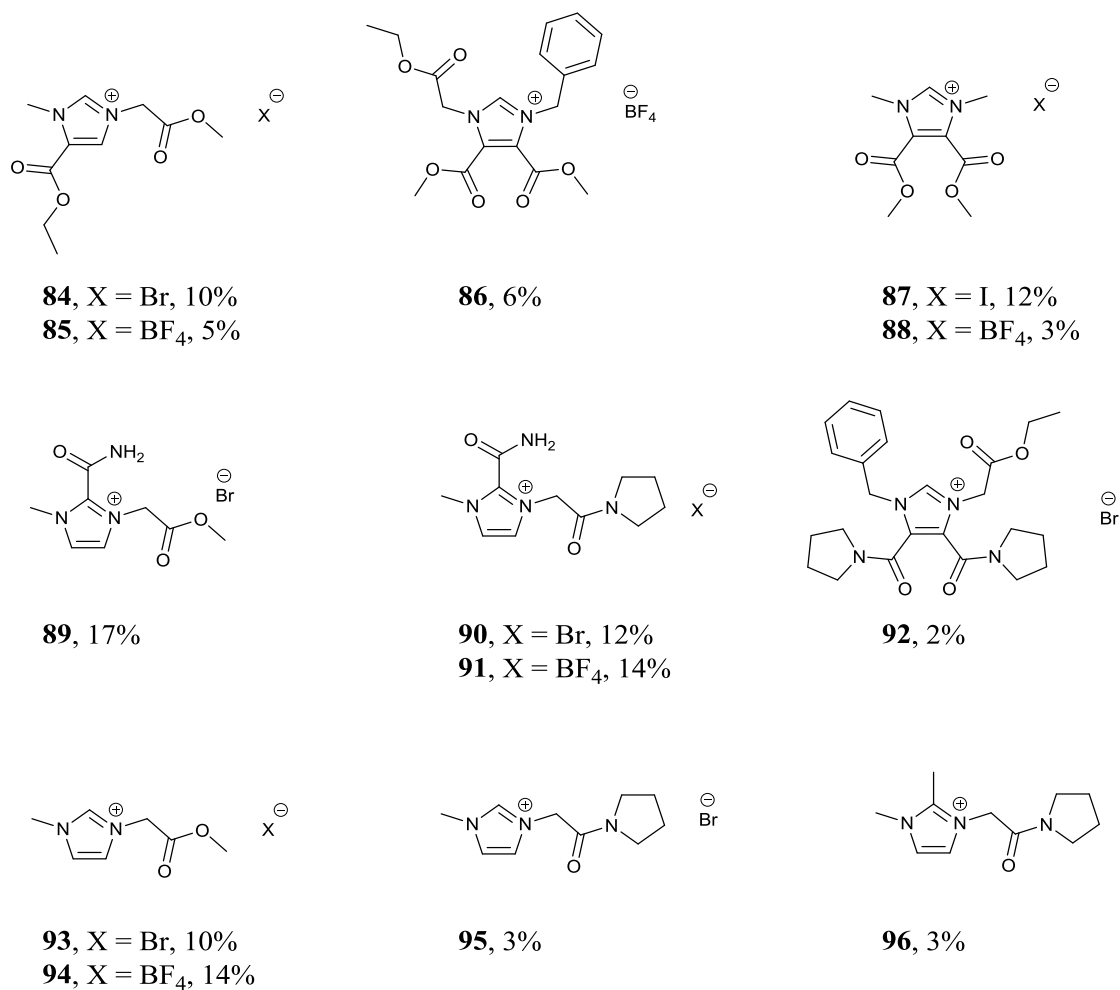
Ester functionalisation at the nitrogen positions (**82-86, 89, 92-94**), again followed the trend of poor biodegradability with levels attributed solely to ester hydrolysis, derivatives (**82**) and (**83**) undergoing ester hydrolysis at all three ester positions to give Amber classified ILs Figure 1.26 while the remaining ILs were classified as Red with <20% biodegradation. The monoester derivatives (**93**) and (**94**) only attained 10-14% biodegradation in the CBT.

The effect of methylation of the C2 position of the imidazolium ring can also be determined from compounds (**95**) and (**96**), with no difference in biodegradation (3%) observed. This is in agreement with previous studies by Scammells *et al.*<sup>80</sup>



**Figure 1.26.** Imidazolium ILs classified as Amber.<sup>18-20</sup>

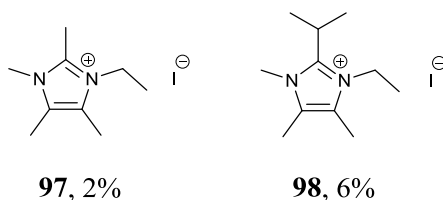
Biodegradation values assessed by the CO<sub>2</sub> Headspace Test (ISO 14593).



**Figure 1.27.** Imidazolium ILs classified as Red by Gathergood *et al.*<sup>18-20</sup>

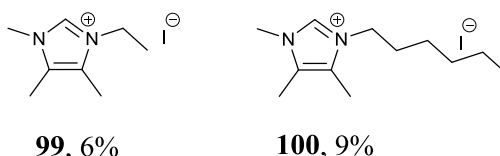
Biodegradation values assessed by the CO<sub>2</sub> Headspace Test (ISO 14593).

The poor biodegradability (OECD 301D) of C2, C4 and C4/5 modified imidazolium ILs was further demonstrated by the work carried out by Gendaszewska *et al.* in 2014 which established the poor biodegradability of four peralkylated imidazolium ILs (**97-100**), Figure 1.28-29.



**Figure 1.28.** Biodegradation data for C-2,4/5 modified imidazolium ILs.<sup>45</sup>

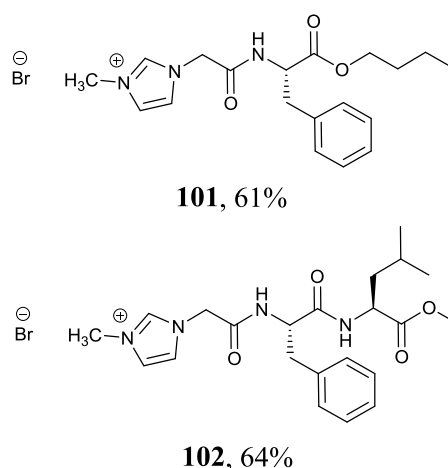
Biodegradation values assessed by CBT (OECD 301D)



**Figure 1.29.** Biodegradation data for C-4/5 modified imidazolium ILs.<sup>45</sup> Biodegradation values assessed by CBT (OECD 301D)

To tackle the problem of poor biodegradability of imidazolium based ionic liquids containing amides, Gathergood *et al.* designed examples in which the amide bond was more ‘peptide like’ than the ‘synthetic’ examples previously screened.<sup>81</sup> The rationale was that an amidase enzyme would be more likely to accept the former substrate than the latter. Thus, modification of the imidazolium core by the incorporation of an amino acid residue into the side chain of the cation has been investigated. In 2012 Gathergood *et al.* disclosed two readily biodegradable amino acid derived imidazolium ILs bromides, Figure 1.30. The two ILs, (**101**, **102**) were screened in the CO<sub>2</sub> headspace test and achieved >60% biodegradation after 28 days and can hence be classed as readily biodegradable. Compound (**101**) an IL based on a butyl ester of L-phenylalanine provided biodegradation of 61% and compound (**102**) a dipeptidyl IL based on L-phenylalanine-L-leucine methyl ester biodegraded 64% under the test conditions. The high levels of biodegradation are beyond that which can be explained by ester hydrolysis and alcohol oxidation.

The selection of compounds screened has shown that the majority of imidazolium based ILs screened are not readily biodegradable with ≤35% biodegradation observed. The rule of thumb regarding imidazolium compounds still stands that *N*-substitution leads to a significant reduction on biodegradability, whereas imidazole and neutral C-substituted imidazole derivatives (i.e. not charged ILs) are readily biodegradable under the OECD 301D (100%)<sup>62</sup> and 302B (83%)<sup>71</sup> test conditions. While progress has been made to develop readily biodegradable imidazolium halide ILs which contain amide groups in the side chain,<sup>81</sup> no evidence of breakdown of the charged core has been presented in a standardized test.

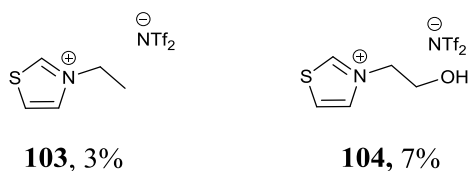


**Figure 1.30.** Biodegradation data for amino acid derived imidazolium ILs.<sup>81</sup>

Biodegradation values assessed by the CO<sub>2</sub> headspace test ISO 14593

#### 1.3.4.2 Thiazolium

A heterocyclic thiazole derivative of the methyl imidazole core has also been screened by Scammells *et al.* in 2010,<sup>69</sup> however the inclusion of a sulphur atom in the aromatic ring did not give any promising biodegradation results with  $\leq 7\%$  biodegradation being achieved in the CO<sub>2</sub> headspace test (ISO 14593), Figure 1.31.



**Figure 1.31.** Biodegradation data for thiazolium ILs synthesised by Scammells *et al.*<sup>69</sup>

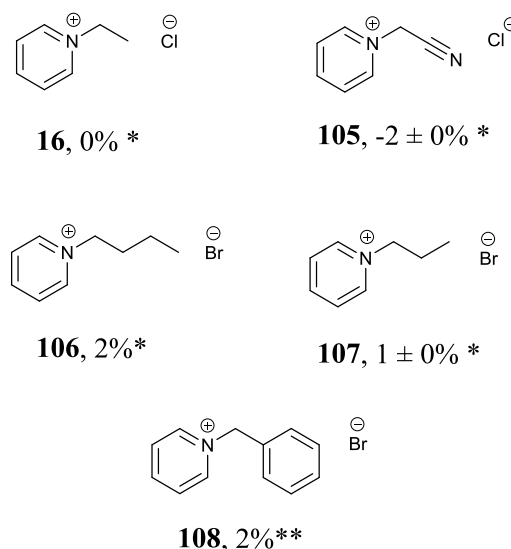
Biodegradation values assessed by the CO<sub>2</sub> Headspace test (ISO 14593)

#### 1.3.4.3 Pyridinium

The popularity of pyridinium and pyridinium based cations from methoxypyridinium and nicotinium acids/esters is high with a larger number screened for their biodegradability. Early generations of pyridinium ILs showed similar inertness to biodegradation (OECD 301F) as imidazolium ILs, with several compounds classified as not readily biodegradable (e.g. **16**, **105-108**), Figure 1.32.<sup>62, 82</sup>



Seminal work by Scammells *et al.* 2010<sup>69</sup> and Stolte *et al.* 2014<sup>82</sup> demonstrated that pyridinium derivatives can pass the CO<sub>2</sub> headspace test (OECD 310) and Manometric Respirometry test (OECD 301F). The primary ethyl alcohol pyridinium derivatives, compound (**109-111**), Figure 1.33, have biodegradation levels of 65% and 62%, respectively, in the CO<sub>2</sub> headspace test whilst the iodide (**111**) example screened in the Manometric Respirometry test gave 65%. Increasing the length of the alcohol substituent from an ethyl alcohol to a propyl alcohol giving derivative (**112**) displayed a reduction in the biodegradability to 51%.



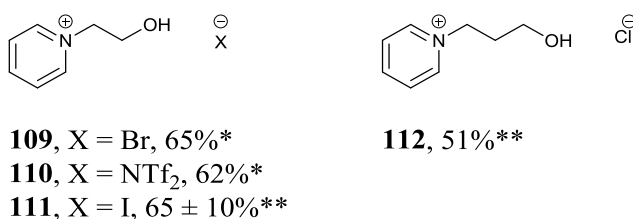
**Figure 1.32.** Alkyl pyridinium ILs classified as not readily biodegradable.<sup>18, 82</sup>

\* Biodegradation values assessed by Manometric Respirometry (OECD 301F)

\*\*Biodegradation values assessed by the CO<sub>2</sub> Headspace test (ISO 14593)

The elevated biodegradation levels can be attributed to the primary alcohol on the alkyl chain promoting biodegradation as a potential site for oxidation. The carbon count of compound (**109**) is 7 x C. The biodegradation levels of 65% would therefore suggest that approximately between 4 and 5 carbon atoms are being mineralised from this compound. With the side chain only supplying 2 x C and the inorganic anion not contributing to CO<sub>2</sub> values, it may be inferred that the pyridinium core is undergoing breakdown under the CO<sub>2</sub> headspace test conditions.

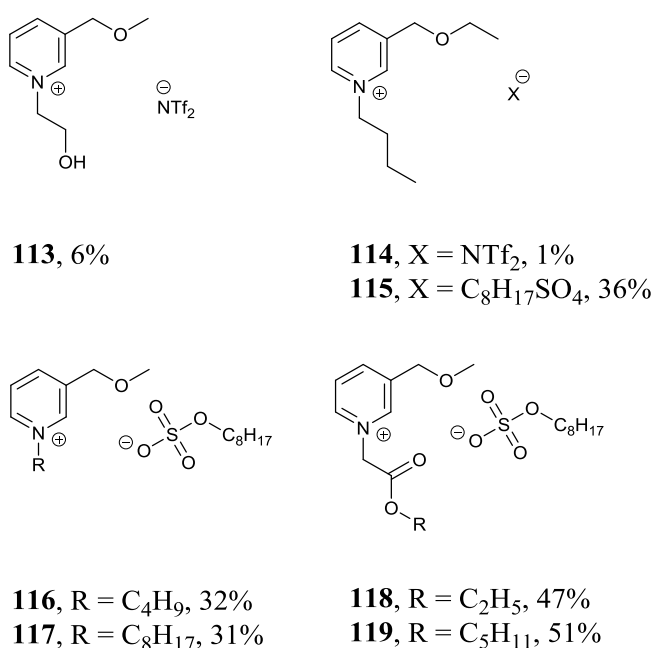
Derivatisation of the pyridinium core can have dramatic effects on the biodegradability of the ILs produced. The addition of a methoxymethyl or a methoxyethyl group at the 3-position to give compounds (**113-119**), Figure 1.34, showed a reduction of biodegradability. For the NTf<sub>2</sub> derivative (**113**) a substantial reduction in biodegradation 6% was observed.



**Figure 1.33.** Pyridinium ILs (**109-112**).<sup>69, 82</sup>

\*Biodegradation values assessed by the CO<sub>2</sub> Headspace test (ISO 14593)

\*\* Biodegradation values assessed by Manometric Respirometry (OECD 301F)



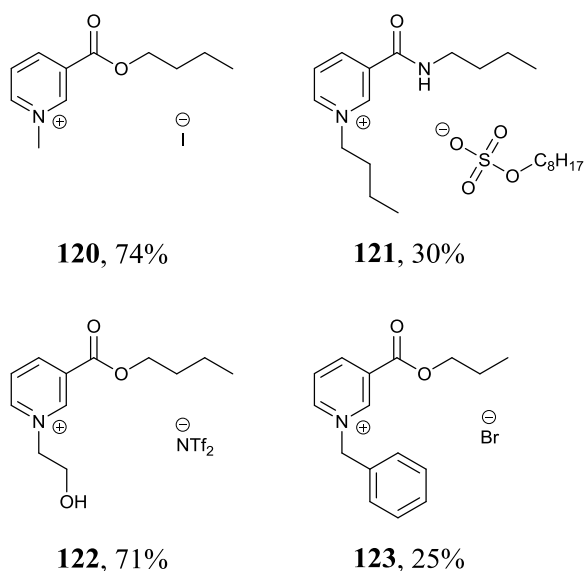
**Figure 1.34.** (**113-119**) Pyridinium ILs ether substituted at the 3-position.<sup>69</sup>

Biodegradation values assessed by the CO<sub>2</sub> Headspace test (ISO 14593).

The 3-position on the pyridinium core appears to be particularly sensitive to its substituent. When comparing methoxymethyl IL (**113**), Figure 1.34, to its pyridinium counterpart (**110**), Figure 1.33, a reduction in biodegradation (ISO 14593) from 62% to just 6% is observed, directly attributable to the addition of a methoxymethyl group on the 3-position. The ethoxymethyl derivative of *N*-butyl pyridinium again highlights the recalcitrance of 3-substituted ILs, with biodegradation of 1% observed for the NTf<sub>2</sub> derivative, IL (**114**) and 36% for the octyl sulphate derivative (**115**), the elevated levels of biodegradation for the latter example are attributable to biodegradation of the anion. For derivatives (**116**, **117**) there is no evidence of biodegradation of the *N*-butyl or methoxymethyl sidechain as levels of biodegradation of 32% and 31%, respectively, once again implies biodegradation of the anion

solely. With the addition of an ester at the *N*-position to give ILs (**118**, **119**) the elevated levels of biodegradation (47-51%) can be attributed to ester hydrolysis plus the degradation of the octyl sulphate anion with the methoxymethyl pyridinium core remaining intact.

With 3-position ethers giving such poor results, a progressive examination of sidechain functionalities logically leads to inspection of ester and amide functionalities at the 3-position, Figure 1.35.

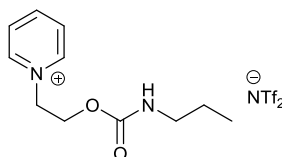


**Figure 1.35.** Nicotinium derived ILs.<sup>18,83</sup>

Biodegradation values assessed by the CO<sub>2</sub> Headspace test (ISO 14593).

Ester functionalities on the 3-position, Figure 1.35, to give nicotinium derivatives, appear to have moderate to good biodegradability with derivative (**120**) being considered readily biodegradable (ISO 14593). Changing the ester to an amide (**121**) produced a considerable decrease in biodegradation to almost nothing that could be attributed to the cation, as derivative (**121**) is mostly likely undergoing anion degradation. Further substitution of the pyridinium core, compound (**122**), to give an ester at the 3 position and a primary alcohol on the *N*-position has shown to elevate the biodegradability back up to 71%. Modification of the ester derived pyridinium ILs with a group other than a terminal alcohol at the *N*-position, compound (**123**), leads to a reduction in biodegradation to 25%.

The rule of thumb observable for increased pyridinium biodegradation appears to be the presence of a primary alcohol attached at the *N*-position with careful introduction of other functionality on the aromatic ring, as required by application.



**124**, 3%

**Figure 1.36.** A carbamate functionalised pyridinium IL.<sup>69</sup>

Biodegradation values assessed by the CO<sub>2</sub> Headspace test (ISO 14593).

The last functional transformation attempted was the introduction of a carbamate group with the aim that the carbamate would undergo hydrolysis at this site. This synthetic transformation leading to compound (**124**), Figure 1.36, proved to be recalcitrant to biodegradation at 3%.<sup>69</sup>

### 1.3.5 Non aromatic cations – morpholinium, DABCO, piperidinium, cholinium, quaternary ammonium - quaternary ammonium cations (QAC's)

#### 1.3.5.1 Morpholinium, DABCO

The non-aromatic headgroups can be further broken down into two subsets, cyclic and acyclic. The former set includes data from the morpholinium and DABCO (1,4-diazabicyclo[2.2.2]octane) series of ILs presented by Pretti *et al.* 2011, Stepnowski *et al.* 2011 and Neumann *et al.* 2014, see Figure 1.37.<sup>82, 84, 85</sup> A series of ILs was prepared using morpholine and DABCO as headgroups with various extensions of alkyl chains substituted at the *N*-position, Figure 1.37, (**125-133**). The shortest alkyl chain morpholinium IL prepared by Pretti *et al.* IL (**125**) displayed biodegradation (ISO 14593) of 30% after 28 days. If the carbon content of the alkyl chain is taken into account, 2 x C, and the overall carbon count of the molecule is 7 then the 30% biodegradation infers mineralisation of just two carbon atoms, perhaps the alkyl chain, however a metabolite study will only tell if any other portion of the molecule is being metabolised. The original postulation that with an increase in alkyl chain length there is an increase in biodegradation is not observed for this series of ILs. This is an example of how one of Boethling's rules of thumb did not apply to this subset of ILs, as biodegradation is seen to decrease with increasing alkyl chain length, *N*-butyl (**126**), *N*-hexyl (**127**), *N*-octyl (**128**) and *N*-decyl (**129**), Figure 1.37. The decreasing biodegradability is in direct correlation with the toxicity results published by the same author demonstrating the increase in toxicity with increase in alkyl chain.<sup>84</sup>



**125**, R = C<sub>2</sub>H<sub>5</sub>, 30%\*      **130**, R = C<sub>2</sub>H<sub>4</sub>OH, X = I, 4 ± 1%\*\*  
**126**, R = C<sub>4</sub>H<sub>9</sub>, 10%\*      **131**, R = C<sub>3</sub>H<sub>6</sub>OH, X = Cl, 31 ± 16\*\*  
**127**, R = C<sub>6</sub>H<sub>13</sub>, 4%\*  
**128**, R = C<sub>8</sub>H<sub>17</sub>, 6%\*  
**129**, R = C<sub>10</sub>H<sub>21</sub>, 7%\*



**132**, 0%\*\*

**133**, 0%\*\*\*

**Figure 1.37.** Biodegradation data for morpholinium ILs.<sup>82, 84, 85</sup>

\*Biodegradation values assessed by CO<sub>2</sub> Headspace test (ISO 14593).

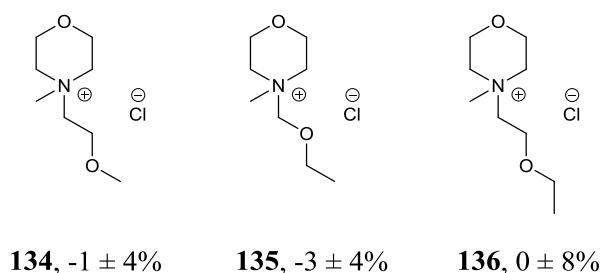
\*\* Biodegradation values assessed by Manometric Respirometry (OECD 301F).

\*\*\* Biodegradation values assessed by CBT (OECD 301D).

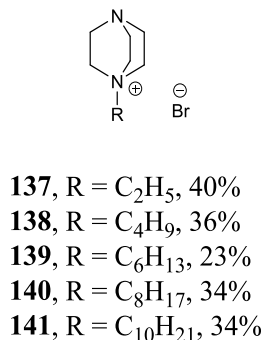
Further addition of primary ethyl alcohol to the morpholinium headgroup to give IL (**130**), gave very poor biodegradability results (OECD 301F).<sup>82</sup> This compound, though analogous to the readily biodegradable pyridinium derivative, Figure 1.33, (**109**), only provided ~1% biodegradation. Increasing the length of the alcohol from C<sub>2</sub> to C<sub>3</sub> increased the biodegradability by up to 30% (**131**). This suggests that the rule of thumb of including primary alcohol groups on the head group to increase biodegradation is questionable for morpholinium derivatives and may be sensitive to chain length.

For the cyano (**132**) and benzyl (**133**) derivatives examined, 0% biodegradability (OECD 301F) was observed. Biotic hydrolysis of the cyano group was detected for IL (**132**).<sup>82</sup>

The *N*-ether derivatives (**134-136**), Figure 1.38, did not undergo primary biodegradation when examined and agree with the rule of thumb that introducing ether groups can reduce biodegradation. Readily biodegradable screening was not carried out on these derivatives.



**Figure 1.38.** Morpholinium ILs screened for primary degradation only.<sup>82</sup>



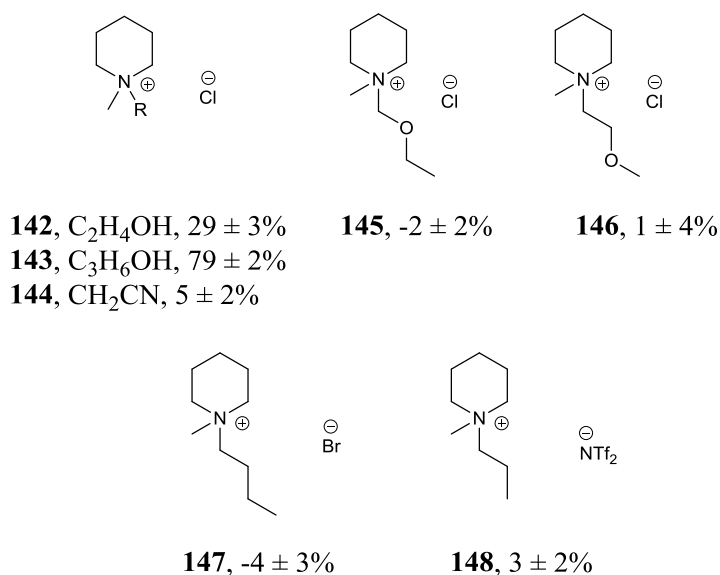
**Figure 1.39.** Biodegradation data for DABCO ILs (**137-141**).<sup>82, 84</sup>

Biodegradation values assessed by Manometric Respirometry (OECD 301F).

Similar results to those observed for the morpholinium ILs were found for the DABCO series of ILs synthesised by Pretti *et al.*, Figure 1.39. Decreasing levels of biodegradation (OECD 301F) were observed when alkyl chain lengths longer than ethyl (**137**) were studied for the series (**137-141**) Figure 1.39. Similarly, toxicity increase as chain length increased was attributed to the reduced levels of biodegradability for these DABCO ILs. As with the ethyl morpholinium IL (**125**), the ethyl substituted DABCO IL (**137**), showed the highest level of biodegradation within its class, with biodegradation of 40% observed for IL (**137**) after 28 days. However, unlike the morpholinium ILs, in this case there exists a possibility that a portion of the DABCO ring is undergoing biodegradation. The ethyl side chain of (**137**) can only contribute 25% of the theoretical carbon for biodegradation, and 40% is observed, thus some portion of the ring must be undergoing biodegradation. In general, the DABCO derivatives biodegraded to a greater extent than the morpholinium derivatives. However, the lowest value observed for DABCO IL biodegradation was 23%, for the hexyl derivative (**139**). In general the range of values for the analogues (**137-141**) is narrow (23-40%).

### 1.3.5.2 Piperidinium ILs

The piperidinium ILs (**142-148**) screened for biodegradability (OECD 301F) by Stolte *et al.* 2014, Figure 1.40, show a similar recalcitrance to biodegradation.<sup>82, 84</sup> The *N*-substituted propyl alcohol IL, (**143**), was the only derivative from this group to be classified as readily biodegradable. The shorter ethanol substituted piperidinium derivative, (**142**) proved to biodegrade to a lower extent and cannot be classed as readily biodegradable. Although when the test time was extended to 60 days (**142**) had undergone ~85% biodegradation.<sup>82, 84</sup> As previously observed, ILs substituted with a single ether group can reduce biodegradability and this was observed for ILs (**145**) and (**146**). Removing the oxygen atom from the *N*-substituted alkyl chains, (**147**) and (**148**) also gave ILs which exhibited poor biodegradation (<5%) in the manometric respirometry test.



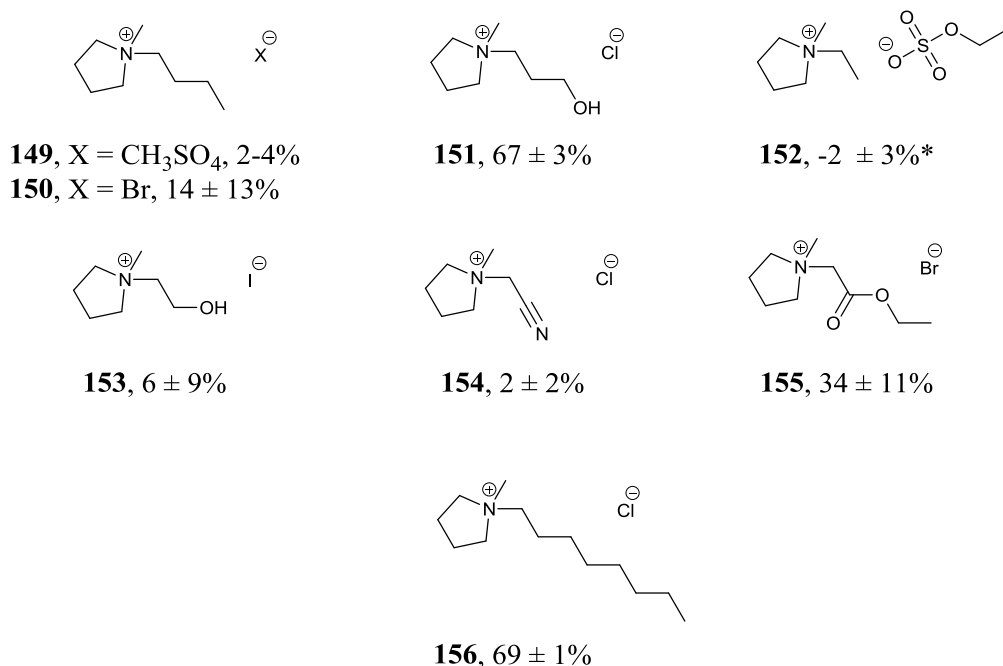
**Figure 1.40.** Biodegradation data for Piperidinium ILs (**142-148**).<sup>82, 84</sup>

Biodegradation values assessed by Manometric Respirometry (OECD 301F).

### 1.3.5.3 Pyrrolidinium

Pyrrolidinium IL biodegradation has rarely been examined except for the work carried out by Stolte *et al.* in 2012 and 2014, Figure 1.41.<sup>82, 86</sup> *N*-alkyl substituted pyrrolidinium ILs (**149**, **150**, **152**) were observed to be recalcitrant to biodegradation (OECD 301F). Cyano derivative (**154**) also did not undergo biodegradation >2% though the cyano group was observed to undergo biotic hydrolysis.<sup>82</sup> An *N*-substituted propyl alcohol IL (**151**) was observed to be readily biodegradable  $67 \pm 3\%$  whereas the ethyl alcohol IL (**153**) biodegraded <10%. The continuing

trend of much greater levels of biodegradation for *N*-substituted C<sub>3</sub> alcohols over C<sub>2</sub> alcohols is observed here. Ethyl ester derivative (**155**) only provided 34 ± 11% biodegradation. Upon extension of the alkyl substituent to C<sub>8</sub>, IL (**156**), a readily biodegradable IL was discovered, with 69% biodegradation observed. This ILs structural features are in agreement with the rules of thumb regarding longer chain lengths being able to provide greater levels of biodegradability, in this case the IL did not inhibit the bacteria of the test medium. The study shows that several of the rules of thumb can be accurately applied for the pyrrolidinium derivatives and is a significant success for the design for degradation concept.



**Figure 1.41.** Biodegradation data for pyrrolidinium ILs.<sup>82, 86</sup>

Biodegradation values assessed by Manometric Respirometry (OECD 301F)

\*Examined for primary biodegradation only

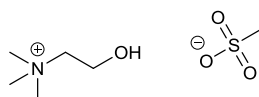
#### 1.3.5.4 Linear ammonium cations

Among the acyclic ammonium cation class are the quaternary ammonium compounds (QAC), such as cholinium and tetrabutylammonium and ILs.

The cholinium cation has been selected as a promising choice for the synthesis of biodegradable ILs, due to the high biodegradability (OECD 301D) and low toxicity of cholinium halide salts.<sup>87, 88</sup> Thus, providing the cation is appropriately paired with an anion that is biodegradable (**157**, Figure 1.42), or an inorganic anion that does not inhibit metabolism, readily biodegradable ILs are a reasonable outcome. Anions derived from organic acids, (see Figures 1.14, 1.16) and the



amino acids, (see Figure 1.19) have all proven successful. See Section 1.3.2 on anions for more cholinium IL biodegradation data and Appendix I structures (**310-322**). Similar protic derivatives synthesised from aminoethanol, to give protic ILs (**54, 55**) Figure 1.15, can also be classified as readily biodegradable, see Section 1.3.2 for anion choices.



**157**, 88-90%

**Figure 1.42.** Readily biodegradable cholinium mesylate (**157**).<sup>86</sup>

Biodegradation values assessed by Manometric Respirometry (OECD 301F).

Biodegradation of the cholinium cation, however, is very sensitive to structural modification. The linear alkyl chain derivative trimethylbutylammonium TMBA (**158**), Figure 1.43, maintains high levels of biodegradability (OECD 301F) at ~87-88%. However, once the free alcohol is converted to a methyl ether (**159**) a large decrease in biodegradation is observed from 88-90% to 27-29%. No inhibitory toxic effects for ILs (**157-159**) were observed.



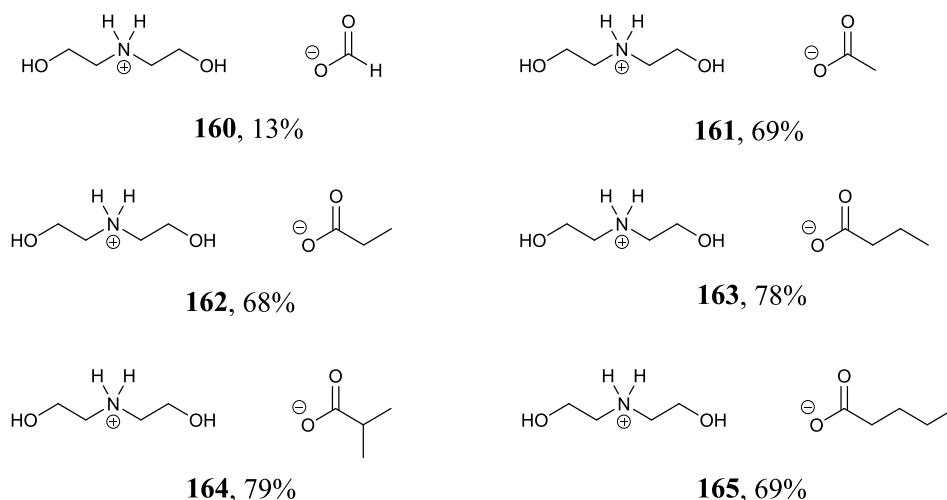
**158**, 87-88%

**159**, 27-29%

**Figure 1.43.** Quaternary ammonium ILs (**158, 159**).<sup>86</sup>

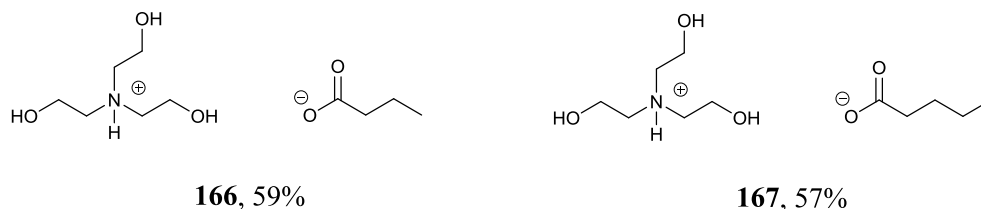
Biodegradation values assessed by Manometric Respirometry (OECD 301F)

Protic IL analogies of cholinium salts, with two ethyl alcohol groups (**160-165**), Figure 1.44 or three ethyl alcohol groups (**166-167**) Figure 1.45, gave favourable biodegradation results (see compounds (**160-167**)) except when the anion employed was a formate anion as in the case of IL (**160**). Carboxylate examples (acetate **161** to pentanoate **165**) pass the manometric respirometry test, and (**166-167**) the triol derivatives (despite failing the test) achieve biodegradation levels very close to a pass (57-59%). In the study carried out by Peric *et al.* 2013 it was shown by LC analysis that the cations had entirely degraded after the 28 day period and anion choice was of more concern, with 7 out of 10 compounds (**54-55, 161-165**) being classed as readily biodegradable.<sup>70</sup>



**Figure 1.44.** Biodegradation data for protic aminodiols derived ILs (**160-165**).<sup>70, 86</sup>

Biodegradation values assessed by Manometric Respirometry (OECD 301F)



**Figure 1.45.** Biodegradation data for protic aminotriols derived ILs (**166-167**).<sup>70</sup>

Biodegradation values assessed by Manometric Respirometry (OECD 301F).

Overall the cholinium and the protic quaternary aminoethanol based ILs with methylsulphonates, methylsulphates, amino acid carboxylates and some organic carboxylate anions have high biodegradability (OECD 301F).

Choline ILs have also been successfully employed as co-substrates in the effective biodegradation of azo dyes.<sup>89</sup> A number of choline salts (lactate, tartrate, saccharinate, dihydrogen phosphate, citrate), were used in conjunction with the bacteria *S. lentus* under optimised conditions to efficiently biodegrade acid blue 113 (92% degradation in 72 h) with choline lactate being the most effective. The degradation products were found to be less toxic than glucose mediated co-degradation.<sup>89</sup>

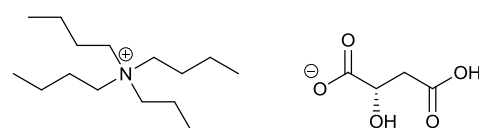
#### 1.3.5.5 Tetraalkylammonium

One of the popular alkylammonium cations is the tetraalkylammonium cation, Figure 1.46, with widespread use in the surfactant industry,<sup>90</sup> as antimicrobials,<sup>91</sup> and other applications including

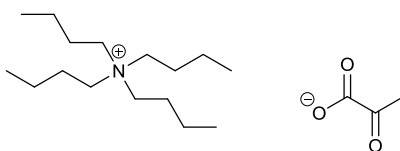
phase transfer catalysis.<sup>92</sup> Amongst the QAC's employed in IL research the tetrabutylammonium (TBA) cation stands out as being one of the most widely used. Recently investigations have also been carried out with the dimethyldibutylammonium (DMDBA) cation, Figure 1.46.



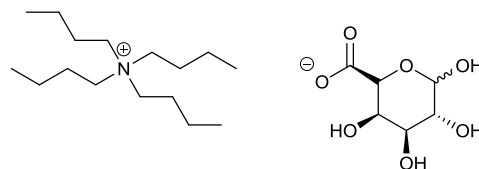
**Figure 1.46.** Tetrabutylammonium cation and [DMDBA] cation.



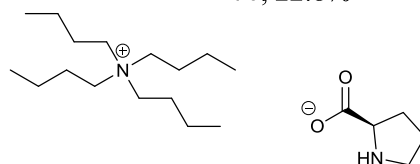
**168**, 14.2%\*



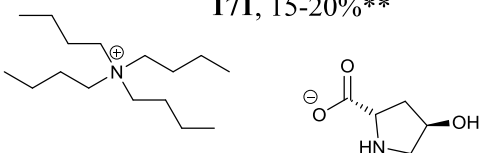
**169**, 12.2%\*



**170**, 22.8%\*



**171**, 15-20%\*\*



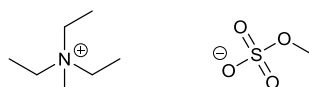
**172**, 20-25%\*\*

**Figure 1.47.** Biodegradation data for selected tetrabutylammonium ILs.<sup>71, 72</sup>

\* Biodegradation values assessed by CBT (OECD 301 D).

\*\*Biodegradation values assessed by CO<sub>2</sub> Headspace test (OECD 310).

Biodegradation data (OECD 301D and OECD 310) of TBA ILs has provided no evidence that the TBA biodegrades, Figure 1.17, (**56-59**) and Figure 1.47, (**168-172**). As can be seen in Figure 1.47, TBA ILs with anions synthesised from organic acids and amino acids achieve levels of biodegradation that can be attributed to anion degradation only, with the TBA cation remaining intact. A more detailed metabolite analysis of the breakdown products would be required to confirm this assumption. Similarly, the triethylmethylammonium IL (**173**) examined by Stolte *et al.*<sup>86</sup> Figure 1.48, did not undergo levels of biodegradation >5% in the manometric respirometry test.



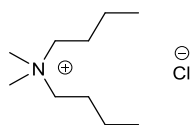
**173**, 4-5%

**Figure 1.48.** Triethylmethylammonium IL.<sup>86</sup>

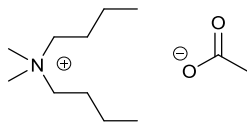
Biodegradation values assessed by Manometric Respirometry (OECD 301F).

A slight modification to the TBA cation produces the DMDBA family of QAC's. This modification, in stark contrast to other tetraalkylammonium salts, significantly increases the biodegradability (OECD 301F) of the QAC's, but only when paired with a biodegradable organic anion. In the study conducted by Jérôme *et al.* 2014 it was shown that the [DMDBA][Cl] (**174**) Figure 1.49, gave 5% biodegradation after 28 days, however changing to the acetate (**175**) lead to 77% biodegradation after 28 days, a dramatic overall increase. It is also important to note that the acetate anion can contribute only 28% to the overall carbon content of the IL. This strongly suggests that the anion has a crucial effect on the cations biodegradation and could be occurring through a co-metabolic pathway; the cation and anion biodegrading concomitantly.<sup>73</sup> The presence or absence of an organic anion appears to promote (**60**, **175-180**) or prohibit (**173**), respectively, biodegradability for this series of compounds. The ILs studied in this work also showed excellent ability at dissolving cellulose with high recyclability.<sup>73</sup>

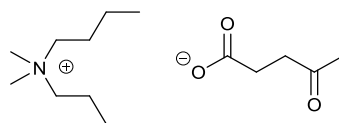
Unfortunately the same effect of promoting biodegradation (OECD 301D) through the use of an organic anion is not apparent for the symmetrical tetraalkylammonium cations (**56-59**) Figure 1.17, (**168-172**) Figure 1.47 as the results published by Bouquillon *et al.* demonstrates the robustness of the tetrabutylammonium cation, even when paired with a biodegradable carboxylate.<sup>71, 72</sup>



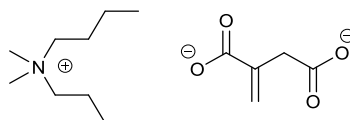
**174, 5%**



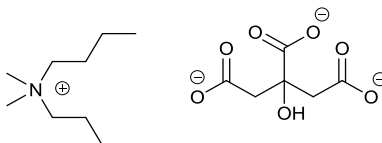
**175, 77%**



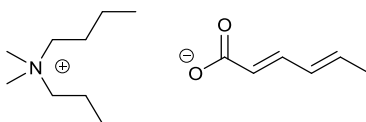
**176, 66%**



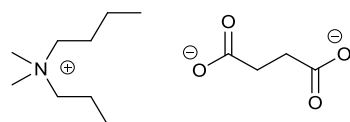
**177, 45%**



**178, 69%**



**179, 54%**



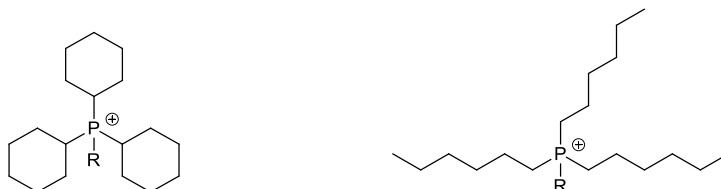
**180, 69%**

**Figure 1.49.** Biodegradation data for selected DMDBA ILs.<sup>73</sup>

Biodegradation values assessed by Manometric Respirometry (OECD 301F).

### 1.3.5.6 Phosphonium ILS

In 2009 Scammells *et al.*<sup>93</sup> screened a range of phosphonium ILS for their biodegradability (ISO 14593) and, to the authors knowledge, represents the only phosphonium ILS to be examined for their biodegradability to date. The two cations screened were tricyclohexyl- and trihexyl-phosphonium, Figure 1.50.<sup>93</sup>



**Figure 1.50.** General structure of phosphonium cations, studied by Scammells.<sup>93</sup>



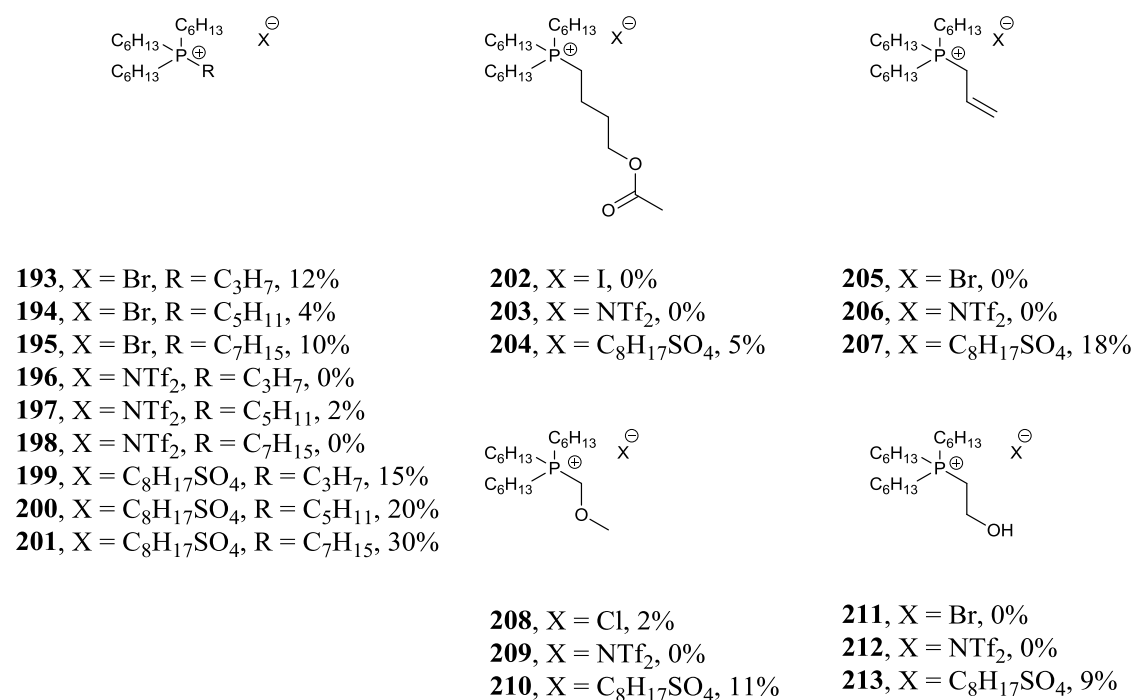
<b>181</b> , X = Br, R = C <sub>3</sub> H <sub>7</sub> , 4%	<b>190</b> , X = I, 9%
<b>182</b> , X = Br, R = C <sub>5</sub> H <sub>11</sub> , 3%	<b>191</b> , X = NTf <sub>2</sub> , 9%
<b>183</b> , X = Br, R = C <sub>7</sub> H <sub>15</sub> , 2%	<b>192</b> , X = C <sub>8</sub> H <sub>17</sub> SO <sub>4</sub> , 22%
<b>184</b> , X = NTf <sub>2</sub> , R = C <sub>3</sub> H <sub>7</sub> , 7%	
<b>185</b> , X = NTf <sub>2</sub> , R = C <sub>5</sub> H <sub>11</sub> , 2%	
<b>186</b> , X = NTf <sub>2</sub> , R = C <sub>7</sub> H <sub>15</sub> , 3%	
<b>187</b> , X = C <sub>8</sub> H <sub>17</sub> SO <sub>4</sub> , R = C <sub>3</sub> H <sub>7</sub> , 18%	
<b>188</b> , X = C <sub>8</sub> H <sub>17</sub> SO <sub>4</sub> , R = C <sub>5</sub> H <sub>11</sub> , 22%	
<b>189</b> , X = C <sub>8</sub> H <sub>17</sub> SO <sub>4</sub> , R = C <sub>7</sub> H <sub>15</sub> , 21%	

**Figure 1.51.** Biodegradation data for tricyclohexylphosphonium ILS.<sup>93</sup>

Biodegradation values assessed by CO<sub>2</sub> Headspace test (ISO 14593).

The general trend observed from the tricyclohexyl derived ILS, Figure 1.51, was a high resistance to biodegradation even though hydrolysable esters were included as one of the side chains. For example, compounds (**181-183**) gave between 2-4% biodegradation. Similarly with the ester bond in a different orientation (**190**), only a slight improvement in biodegradation to 9% was observed. It is believed that the steric bulk of the tricyclohexyl rings inhibits access of esterase enzymes to the labile ester bond. Further altering the cation to NTf<sub>2</sub> did not improve on biodegradability 2-9%, (**184-186**, **191**). When the anion was exchanged to octyl sulphate, (**187-**

**189, 192**), the expected increase in biodegradation (up to 22%) was observed, but can be solely attributed to the biodegradation of the anion and not the cation.



**Figure 1.52.** Biodegradation data for trihexylphosphonium ILs.<sup>93</sup>

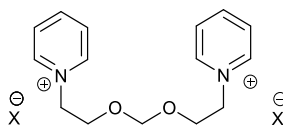
Biodegradation values assessed by CO<sub>2</sub> Headspace test (ISO 14593).

When examining the analogous trihexyl phosphonium derivatives, Figure 1.52, a similar recalcitrance to biodegradation (ISO 14593) was observed. Long alkyl chain ester bromide derivatives, (**193-195**), exhibited poor biodegradation of 4-12%. The reverse orientated ester (**202**), allyl (**205**), ether (**208**) and primary alcohol (**211**) halide analogues did not biodegrade (0-2%). The NTf<sub>2</sub> derivatives (**196-198, 203, 206, 209, 212**) and octyl sulphate derivatives (**199-201, 204, 207, 210, 213**) were also screened. In agreement with the tricyclohexyl derivatives results, exchanging the halide for NTf<sub>2</sub> lead to no improvement while the octyl sulphate derivatives gave a range of biodegradation values between 5 and 30%.

### 1.3.6 C<sub>2</sub> symmetric and dicationic ILs – a new class of ILs

Biodegradation studies of pyridinium cations tethered together using acetal linkers was initially examined by Scammells *et al.*,<sup>69</sup> Figure 1.53 (**214-216**). The design rationale behind this series of *bis*-pyridinium compounds was based on the hypothesis that under biodegradation test conditions the acetal could be hydrolysed to a free alcohol, generating the biodegradable

compound (**109**), Figure 1.33. Upon investigation, however poor biodegradation was observed, <5% in the CO<sub>2</sub> headspace test, for the chloride, bistriflimide and PF<sub>6</sub> ILs (**214-216**).



**214**, X = Cl, 5%  
**215**, X = NTf<sub>2</sub>, 4%  
**216**, X = PF<sub>6</sub>, 3%

**Figure 1.53.** Bis-pyridinium ILs (**214-216**).<sup>69</sup>

Biodegradation values assessed by CO<sub>2</sub> Headspace test (ISO 14593)

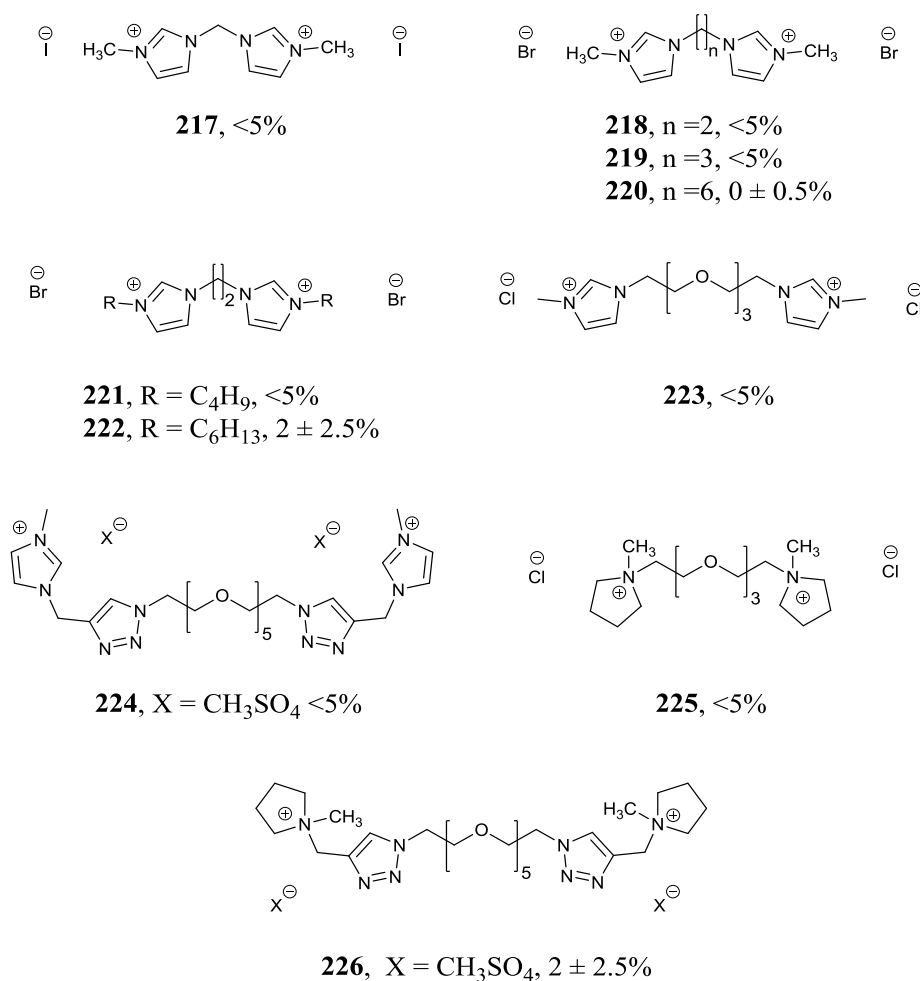
Other bis or dicationic ILs that have been tested for biodegradability include those synthesised and reported by Stolte *et al.* 2014, Figure 1.54. The C<sub>2</sub> symmetrical imidazolium structures (**217-224**) and the pyrrolidinium structures (**225**, **226**) encompass a great diversity and complexity in structure; from bis-ILs linked by an alkyl chain (**217-222**) to less lipophilic poly-ether moieties bridging the two cations (**223-226**). Unfortunately, the trend for biodegradability (OECD 301F) for these dicationic ILs is the same as for the pyridinium species (**214-216**). A characteristic strong resistance to biodegradation is observed for these species, including examples containing butyl or hexyl alkyl chains (**221-222**).<sup>94</sup> Biodegradation for this series of compounds by Stolte *et al.* was observed to be <5%.

A number of trends have been observed when reviewing the biodegradation results for all of the ILs encompassed by this review. The trends can be summarised as follows:

- Terminal cyano groups are readily hydrolysable
- Terminal alcohol groups can lead to an increase in biodegradation and are necessary for anaerobic degradation of alkyl chains
- Length of alcohol substituent is important, some ethanol substituted compounds won't degrade yet the propyl derivative undergoes a disproportionate increase in biodegradability.
- Ester bonds are readily hydrolysable but can slow down the rate of degradation
- Amide bonds are far more robust than esters



- Long alkyl chains help to increase biodegradation except for morpholinium derivatives where it actually decreases
- Amino acid cations are generally readily biodegradable
- Organic acid anions are generally readily biodegradable
- Colonial cations are generally readily biodegradable, but modification leads to a rapid drop off in biodegradation
- Tetrabutylammonium cations are not readily biodegradable, yet the DMDBA cations are when paired with an organic anion
- Hexyl and cyclohexyl substituted phosphonium ILs are too sterically hindered to undergo biodegradation
- Non-aromatic cycles can be classed as readily biodegradable, but only if an *N*-substituted alcohol of appropriate length is used or an alkyl chain of >8 carbons (however long chains can increase toxicity)
- Dicationic ILs examined did not undergo biodegradation of >5%



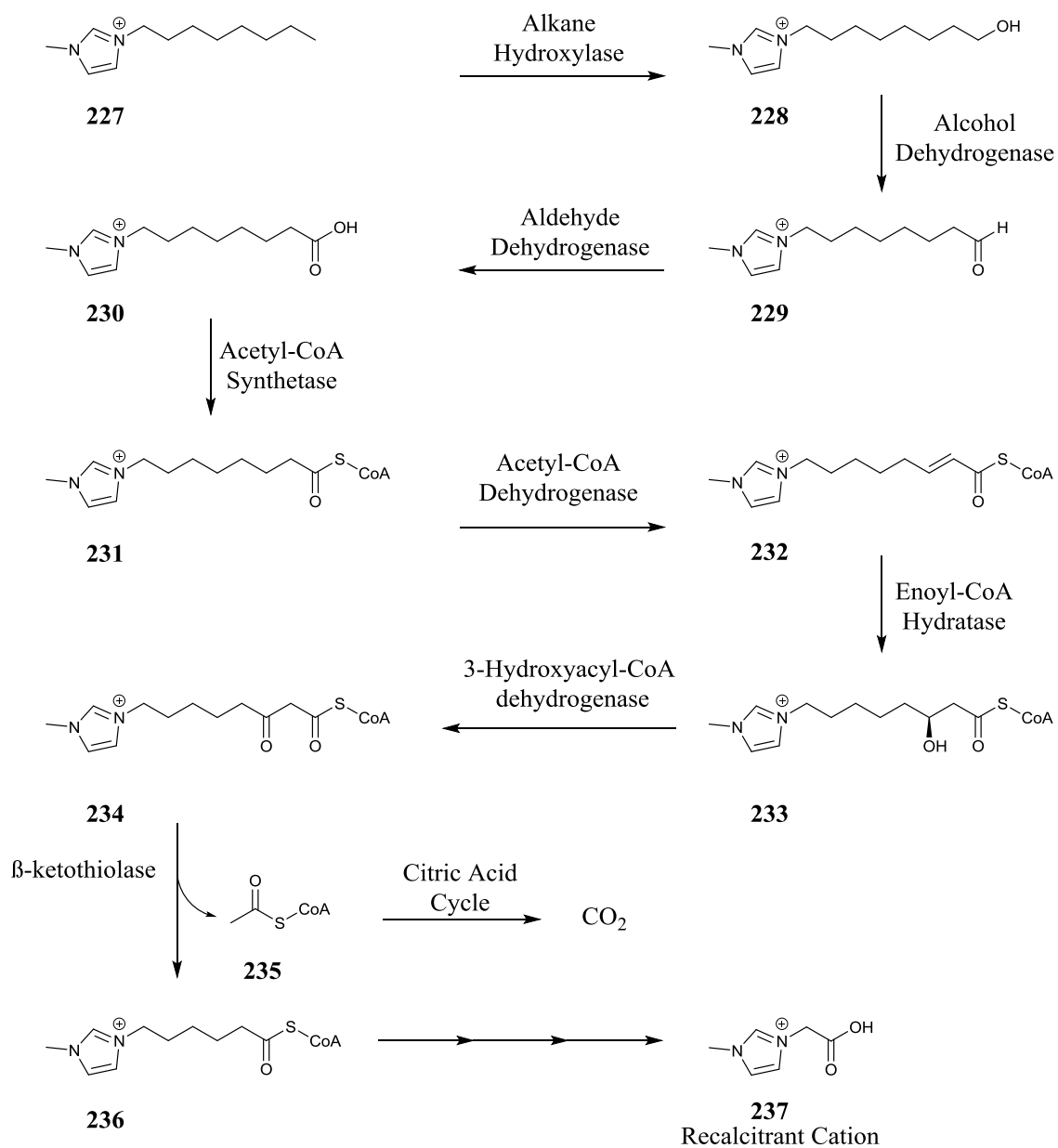
**Figure 1.54.** Biodegradation data for dicationic imidazolium and pyrrolidinium ILs (**217-226**) examined by Manometric Respirometry (OECD 301F), Stolte *et al.*<sup>94</sup>

## 1.4 Metabolite studies

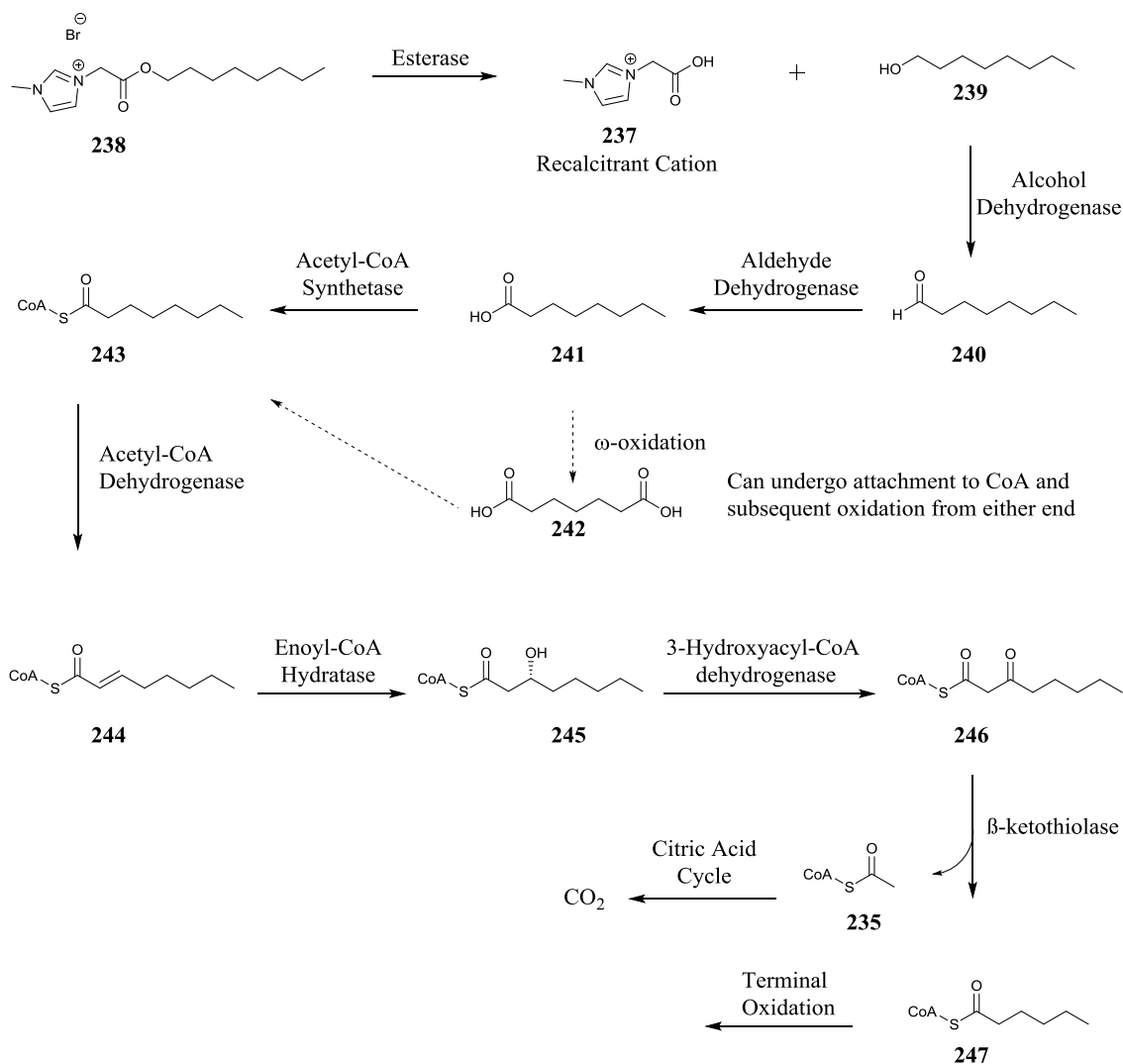
An active area in IL biodegradation research has been metabolite studies. It has been acknowledged that a molecule can pass the readily biodegradable threshold, but a portion may remain indefinitely in the environment. If a non-biodegradable metabolite (or even a metabolite that degrades at a slower pace) is toxic then its release into the environment through biodegradation pathways is a detrimental effect in what would otherwise seem to be a green process. The 4th Principle of Green Chemistry tells us that chemicals should be designed to be both functional with minimal toxicity; therefore examining the toxicity of metabolites is a parameter of consequence.<sup>8</sup>

Multiple methods of metabolite detection have been successfully employed including LC/MS techniques<sup>95</sup>, MALDI <sup>96</sup>, GC/MS <sup>37</sup> etc. In the previous review published by Coleman and Gathergood in 2008, the metabolite studies of 1-butyl-3-methylpyridinium bromide <sup>97</sup> and 1-octyl-3-methylimidazolium chloride <sup>62</sup> were discussed in detail. Since then a number of metabolite studies have been performed analysing the breakdown paths of ILs in OECD approved biodegradation tests and in more complex systems. Forays into predicting breakdown pathways have also been made using computer modelling.

Two of the most common pathways examined in biodegradation and metabolism prediction are  $\beta$ -oxidation and/or  $\omega$ -oxidation of fatty acid or long alkyl chain residues, Scheme 1.1 (**227** to **237**) or the hydrolysis of susceptible bonds such as esters and amides followed by the  $\beta$ -oxidation and/or  $\omega$ -oxidation of any fatty acid residues, Scheme 1.2 (**238-247**).  $\omega$ -Oxidation occurs with oxidation occurring on both ends of the alkane residue to form a dicarboxylic acid (**242**).<sup>98</sup>

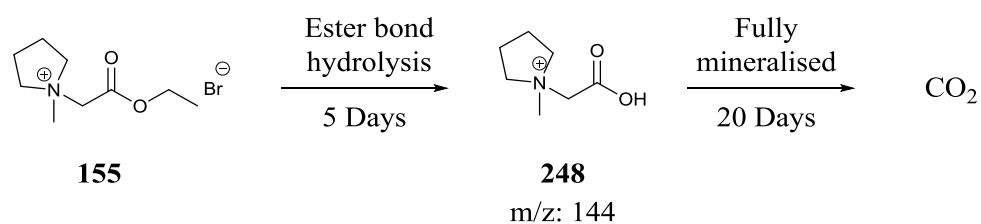


**Scheme 1.1.** Potential  $\beta$ -oxidation pathway of an alkyl imidazolium IL.



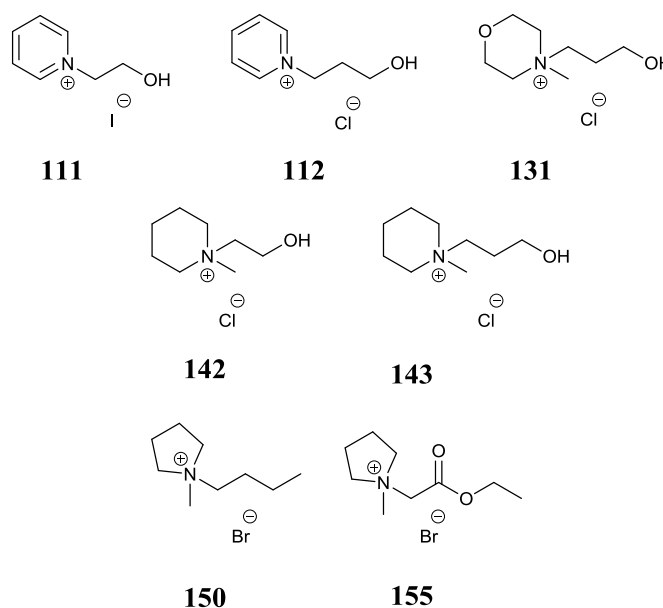
**Scheme 1.2.** Potential  $\beta$ -oxidation pathway of an ester derived imidazolium IL.

Using a combination of IC and LC-MS, pyrrolidinium, morpholinium, piperidinium and imidazolium ILs were examined for headgroup biodegradation, by Stolte *et al.* in 2014.<sup>82</sup> The biodegradation and metabolites are shown in Figure 1.55 for the pyrrolidinium headgroup.



**Figure 1.55.** Biodegradation of pyrrolidinium headgroup.

Stolte also showed that a number of cations (pyrrolidinium **1**, **154**; morpholinium (**131**); piperidinium (**142**, **143**) and pyridinium (**111**, **112**)) could be classified as inherently biodegradable after extended periods of time, >28 days, Figure 1.56. For piperidinium (**142**, **143**) up to 80% biodegradation after 60 days was observed, again classifying these compounds as inherently biodegradable. Supporting other aforementioned data on the imidazolium headgroup, no biodegradation was observed for these compounds.



**Figure 1.56.** Inherently biodegradable ILs; effect of cations by Stolte.<sup>82</sup>

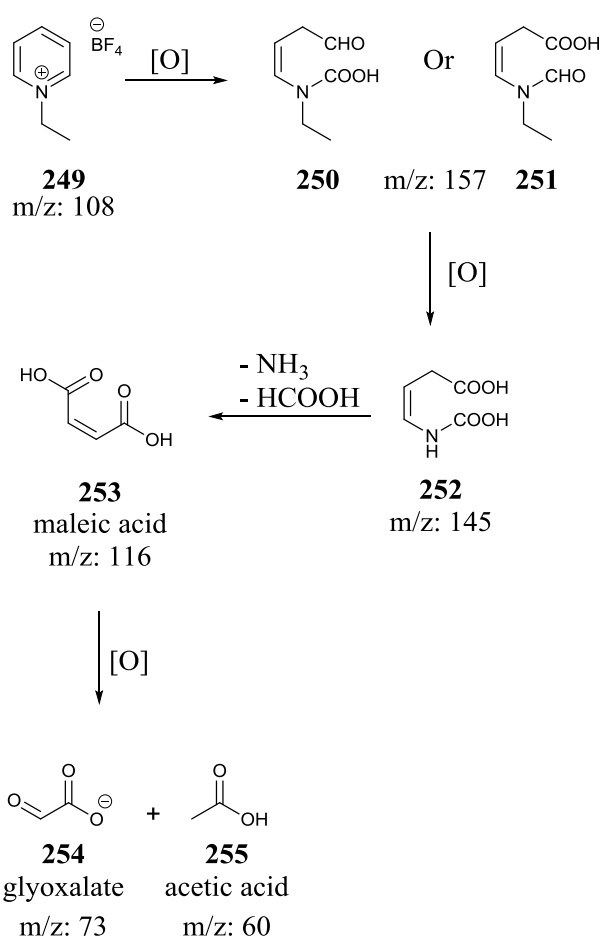
For more robust ILs the aerobic degradation process is much longer, as was observed by Gendazewska *et al.* 2014.<sup>45</sup> After 28 days, limited aerobic oxidation of the 1-methylimidazolium hexyl side chain (**100**), Figure 1.29, to an aldehyde had been detected and a greater proportion of the hexyl substituted methyl imidazolium IL was detected by MS-MS showing that the biodegradation had progressed along the  $\beta$ -pathway very little (total biodegradation of ~ 9%).

#### 1.4.1 Aerobic degradation metabolite studies

Docherty *et al.* 2010 reported the breakdown of three pyridinium ILs, [bmpyr][Br], [hmpyr][Br], [ompyr][Br] into their respective metabolites by GC-MS analysis. The degradation pathways were investigated and in this seminal work, metabolites were screened for their toxicity against *daphnia magna*. The conclusion of this study on IL metabolites showed that the metabolites of these particular pyridinium ILs were less toxic than the parent ILs.<sup>95</sup> The results were discussed in the previous review published by Gathergood *et al.*<sup>22</sup>

### 1.4.2 Pyridinium

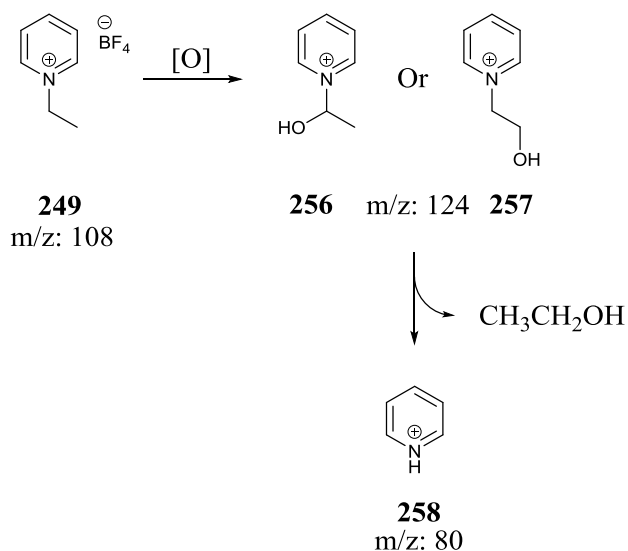
The total metabolism of a pyridinium IL [EtPy][BF<sub>4</sub>] and [EtPy][CF<sub>3</sub>COO] was successfully demonstrated by Zhang *et al.* in 2010 when an axenic culture of bacteria (*Corynebacterium* sp) demonstrated ring opening of the pyridinium cation (**250** or **251**) before the ethyl chain underwent oxidation to (**252**), Scheme 1.3. The study also demonstrated that the same bacteria could not successfully breakdown a methyl imidazolium IL [bmim][PF<sub>6</sub>] and would suggest that different cultures of bacteria are involved in degrading different classes of ILs.<sup>64</sup>



**Scheme 1.3.** Breakdown pathway of [EtPy][BF<sub>4</sub>] by an axenic culture of *Corynebacterium*

The metabolic breakdown of [EtPy][BF<sub>4</sub>] by an axenic culture of *Pseudomonas fluorescens* (*P. fluorescens*) was successfully analysed by Zhang *et al.* in 2011, Scheme 1.4, when the following breakdown pathway was published (Scheme 1.4). The study suggests that *N*-ethyl pyridinium (**249**) degrades by oxidation of the ethyl side chain (**256** or **257**) followed by the elimination of a molecule of ethanol and the formation of a pyridinium salt (**258**).<sup>99</sup> The choice of bacteria for

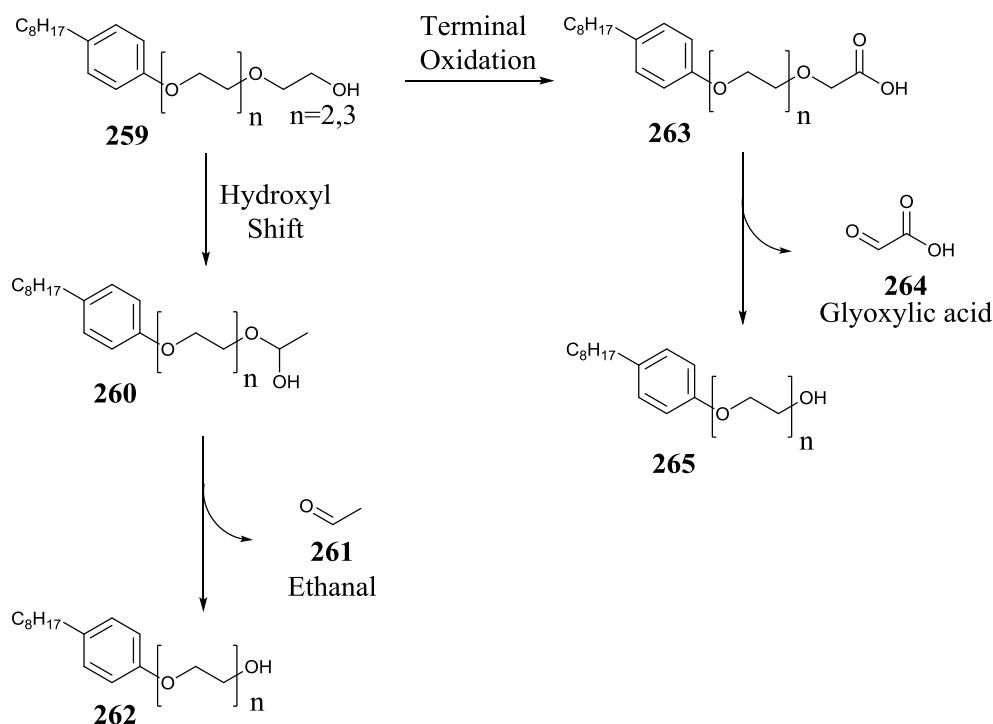
this biodegradation test appears to have altered the metabolic breakdown pathway. In the first test described in Scheme 3, the pyridinium ring is completely mineralised by the *Corynebacterium* strain, yet *P. fluorescens* cannot completely mineralise the ring within the 48 hours of the test described in Scheme 1.4.



**Scheme 1.4.** Metabolism of [EtPy][BF<sub>4</sub>] by an axenic culture of *P. fluorescens*.<sup>99</sup>

### 1.4.3 Sidechain studies

Other metabolic pathways for ethoxylated molecules include terminal oxidation and hydroxyl shift metabolism, Scheme 1.5. Sato *et al.* 2001 demonstrated with the surfactant octylphenol polyethoxylate that the chain could be broken down by two possible pathways. Though these molecules are not ILs, a lot can be learned from potential biodegradation pathways of ethoxylated chains which have been previously employed in IL synthesis.<sup>68</sup> The metabolites were analysed by MALDI-MS.<sup>96</sup>

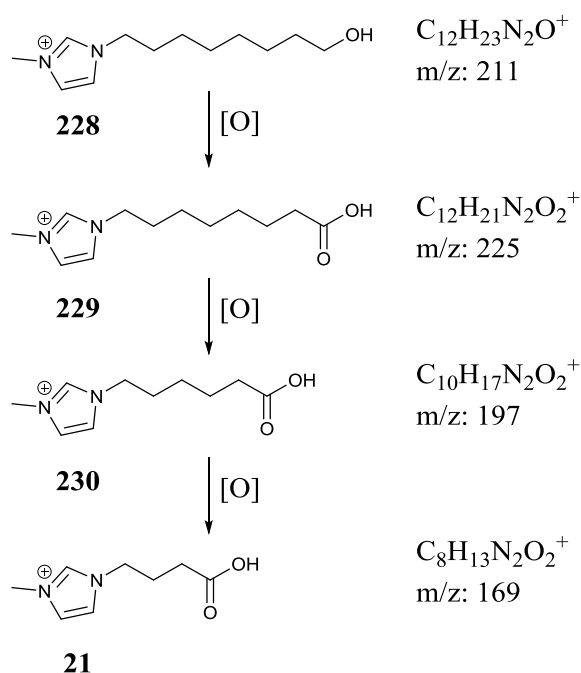


**Scheme 1.5.** Breakdown pathway of a poly ethoxylated sidechain.

#### 1.4.4 Anaerobic degradation metabolite studies

The 2010 investigation carried out by Neumann *et al.* on the anaerobic biodegradation of ILs, included a GC-MS analysis of an imidazolium IL (**228**), see anaerobic breakdown pathway Scheme 1.6. It is important to note, that under the anaerobic denitrifying conditions, biodegradation does not initiate without the presence of the free alcohol site on the alkyl chain. The anaerobic degradation pathways differ to the aerobic pathways in that oxygenase enzymes cannot insert oxygen into the terminus of alkyl chains under anaerobic conditions. The addition of a terminal alcohol could therefore allow some methyl imidazolium ILs an alternate biodegradation pathway, however 318 days were required for the last metabolite identified (**21**) to be detected.<sup>53</sup> Anaerobic degradation can also take place by a fumarate addition mechanism.





**Scheme 1.6.** Anaerobic biodegradation of an imidazolium IL.<sup>53</sup>

## 1.5 Computer modelling and predictability and databases available containing IL biodegradation data

**ADMET - Absorption, Distribution, Metabolism, Excretion, Toxicity**

**TSAR – Thinking in Structure-Activity Relationships**

**SBR – Structure Biodegradation Relationships**

Aside from the physical aspects of measuring biodegradability of ILs there has emerged a drive to predict biodegradation using *in silico* techniques. Modelling software has been successfully used during drug development to screen drug activity and ADMET parameters and it is this ideology and technology that has been adapted for use in IL and surfactant biodegradation prediction. Current software that is available includes TOPKAT,<sup>101</sup> META,<sup>102</sup> BIOWIN,<sup>103</sup> VEGA,<sup>104</sup> START,<sup>105</sup> (also part of ToxTree) and CATABOL.<sup>106</sup> The software suites can have mixed results in predicting biodegradation pathways, in part due to the lack of available biodegradation data sets. In 2013, Benfenati *et al.* conducted an in-depth study of a number of the most popular biodegradation prediction suites (VEGA, TOPKAT, BIOWIN 5 and 6 and START) for the potential use in regulation under the EU REACH legislation or the “Registration Evaluation Authorization and Restriction of Chemicals”. A dataset of 722

compounds was chosen and the software packages were examined under the following headings: accuracy, sensitivity, specificity and Matthew's correlation coefficient (MCC). BIOWIN, TOPKAT and VEGA performed the best out of the examined software. VEGA and TOPKAT gave 88 and 87% accuracy in biodegradation prediction with BIOWIN 6 and 5 performing slightly lower at 83 and 82% and START following up with 70%. Overall it was concluded that BIOWIN, TOPKAT and VEGA could be employed for legislative purposes.<sup>107</sup> However in a critical review by Rucker *et al.* 2012 it was demonstrated that there were issues present with using prediction software. The major downfalls being the difficulty in reproducing biodegradation data due to the inherent issues associated with bacteria and the variability they introduce into a system. Other issues include the secrecy behind some of the datasets used due to their sensitive nature in industry. Other biodegradation data never sees the light of day and remains under industry redaction permanently.<sup>108</sup>

Currently a centralised database of some IL biodegradation data has been established by MERCK in association with UFT Bremen. There currently resides an ever growing library of data on IL - and other associated materials such as starting materials – biodegradation. With the ever increasing datasets available in "UFT / Merck ILs Biological Effects Database" more information about potential eco-persistence posed by ILs can potentially be determined before their synthesis even begins.<sup>109</sup>

The SBR approach in conjunction with Boethling's rules of thumb for designing biodegradable compounds<sup>75</sup> has led to successfully producing some of the first biodegradable ILs. Inspired by design strategies successfully implemented by the surfactant industry, the incorporation of ester linkages was demonstrated to promote biodegradability in a range of previously recalcitrant imidazolium ILs.<sup>80</sup> Similar design strategies include adding susceptible hydroxyl groups such as aldehydes, carboxylic acids and alcohols have all shown to promote biodegradation. Hydrolysable amides, although more stable to chemical hydrolysis than esters, can also potentially promote biodegradation. By considering how these molecules and their functional groups will interact in the environment and especially in WWTP's will allow for a more streamlined synthesis that promotes increased biodegradability. Will a particular bond interact with an enzyme to enhance breakdown? Or can this particular anion be used as a carbon source for aerobic digestion? Will a particular cation adsorb to a sewage floc or into soil and therefore be removed from aerobic degradation pathways altogether? These are the types of design questions that need to be considered when discussing an ILs structure and its potential interactions in the environment.

Combining the SBR approach with computer modelling will be the ultimate goal for rational design of sustainable and biodegradable green ILs. A well informed and designed synthesis, under the 10<sup>th</sup> principle of green chemistry “Design for Degradation”, in conjunction with computer modelling of biodegradation can and will aid the design of the next generation of ILs.

The greatest challenge with using *in silico* methods to predict biodegradation of ILs is that in many cases charged compounds, especially QAC's, are not suitable candidates for these models, (e.g. BIOWIN). In addition, as the majority of ILs screened up to 2010 did not pass readily biodegradable tests, despite the diversity of structures present, they collectively formed a biased training set for the model. However, as this review illustrates, the number of readily biodegradable ILs is increasing, and more balanced training sets are now potentially available.

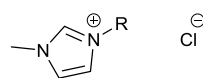
## 1.6 Abiotic Degradation - Chemically induced degradation in advanced systems

Currently there is interest in the area of abiotic degradation of ILs due to the relatively low numbers of ILs passing readily biodegradable tests.<sup>22</sup> Thus, solving the problem of poor biodegradability by investigating alternative methods to biological degradation has been examined including: advanced oxidation systems,<sup>37</sup> peroxide,<sup>40</sup> UV degradation,<sup>110</sup> electrochemical,<sup>38,39</sup> and ultrasonic degradation.<sup>40</sup>

With the increasing use of ILs in technological applications, the chance of release into the environment has grown. Environmental persistence of these compounds has already been postulated and current advanced oxidation process (AOP) technology has demonstrated that where ILs have failed biodegradation tests, AOP's can offer an alternative method of degradation. One of the most common AOP's that can potentially be used in WWTP's is the photolysis of hydrogen peroxide. This process involves irradiating H<sub>2</sub>O<sub>2</sub> with 400 nm UV light causing rapid generation of hydroxyl radicals.

Stepnowski *et al.*<sup>35</sup> showed, by examining the degradation products formed under an advanced oxidation system (hydrogen peroxide 0.2% treatment time 2 hrs UV Lamp 254/366 nm), that the imidazolium core of ILs (**8**, **9**, **12**, **13**), Figure 1.57, is the first part of the molecule to be affected and not the alkyl chain. It was also shown that the imidazolium ring was cleaved and lost its aromatic properties under the test conditions. Other observations include various hydroxyl groups inserted on the alkyl chains and carbonyl insertion into the cleaved

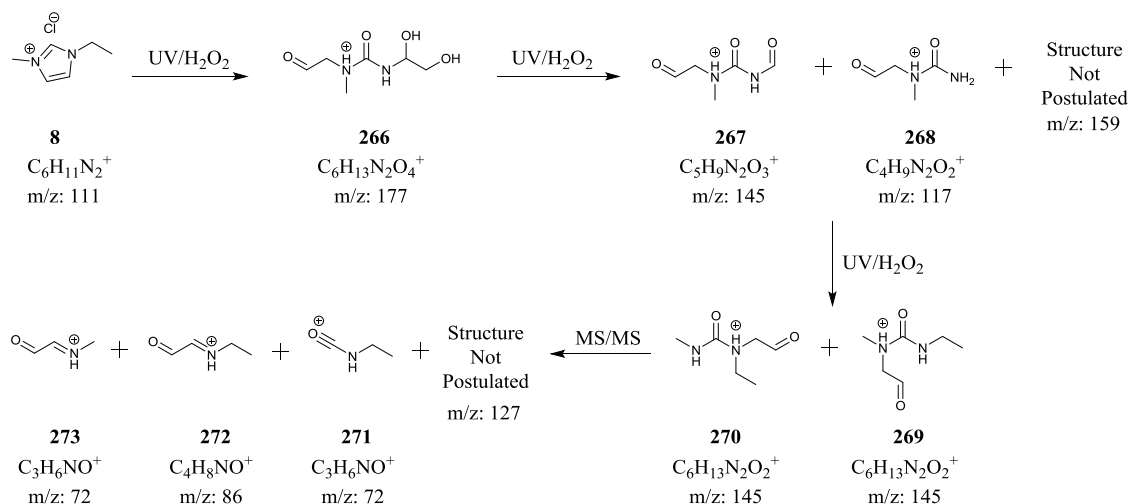
imidazolium ring, some of the observed degradation products (**266-273**) for [emim][Cl] are illustrated in Scheme 1.7.<sup>37</sup>



- 8**, R = C<sub>2</sub>H<sub>5</sub>  
**9**, R = C<sub>4</sub>H<sub>9</sub>  
**12**, R = C<sub>6</sub>H<sub>13</sub>  
**13**, R = C<sub>8</sub>H<sub>17</sub>

**Figure 1.57.** Commercially available ILs tested under UV/H<sub>2</sub>O<sub>2</sub> oxidation conditions.<sup>37</sup>

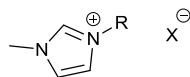
A real, applicable, benefit of an oxidative pre-treatment is that the imidazolium core, which has been shown not to break down under standard aerobic biodegradation conditions, has ring opened (**266**), Scheme 1.7. The insertion of carbonyl groups and hydroxyl functionalities also potentially allows for more rapid biodegradation as free hydroxyl groups have previously shown to enhance biodegradation of alkyl chains.<sup>22</sup>



**Scheme 1.7.** Possible breakdown products detected by HPLC/MS for [emim][Cl] IL. Further fragmentation was analysed by MS/MS.

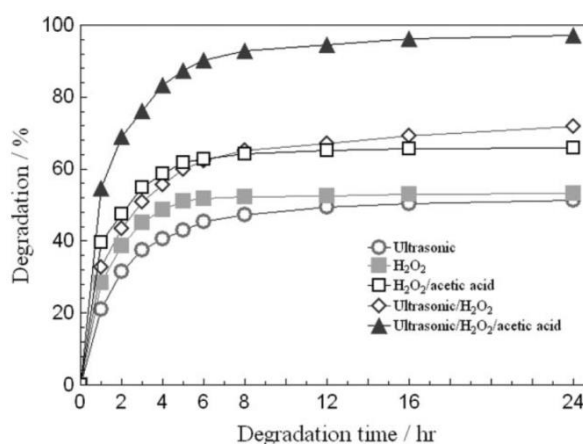
Apart from UV/H<sub>2</sub>O<sub>2</sub> oxidation, a number of other methods have been successful in the area of abiotic degradation. Ultrasonic breakdown of ILs in solution was demonstrated by Tsang *et al.* when they showed that a number of [Rmim] ILs (R = C<sub>2</sub>H<sub>5</sub>, C<sub>3</sub>H<sub>7</sub>, C<sub>4</sub>H<sub>9</sub>, C<sub>5</sub>H<sub>11</sub>, C<sub>6</sub>H<sub>13</sub>), Figure 1.58, could be broken down in a H<sub>2</sub>O<sub>2</sub>/acetic acid/ultrasonic system at a temperature of 50° C.

This system performed to a much higher degree than systems based on the individual components used in the final degradation experiment, see Figure 1.59. Under the optimised test conditions >74% degradation was achieved for all compounds examined after 3 hours and after 12 hours of test time >93% degradation of all ILs examined had been reached. >98% degradation of all 8 of the commercially available ILs was achieved within 72 h, Table 1.12.<sup>40</sup>



- 3**, R = C<sub>4</sub>H<sub>8</sub>, X = BF<sub>4</sub>  
**4**, R = C<sub>4</sub>H<sub>8</sub>, X = PF<sub>6</sub>  
**8**, R = C<sub>2</sub>H<sub>5</sub>, X = Cl  
**27**, R = C<sub>4</sub>H<sub>8</sub>, X = Br  
**31**, R = C<sub>6</sub>H<sub>13</sub>, X = BF<sub>4</sub>  
**274**, R = C<sub>3</sub>H<sub>7</sub>, X = Cl  
**275**, R = C<sub>5</sub>H<sub>11</sub>, X = Cl

**Figure 1.58.** Structures of the commercially available ILs screened.<sup>40</sup>

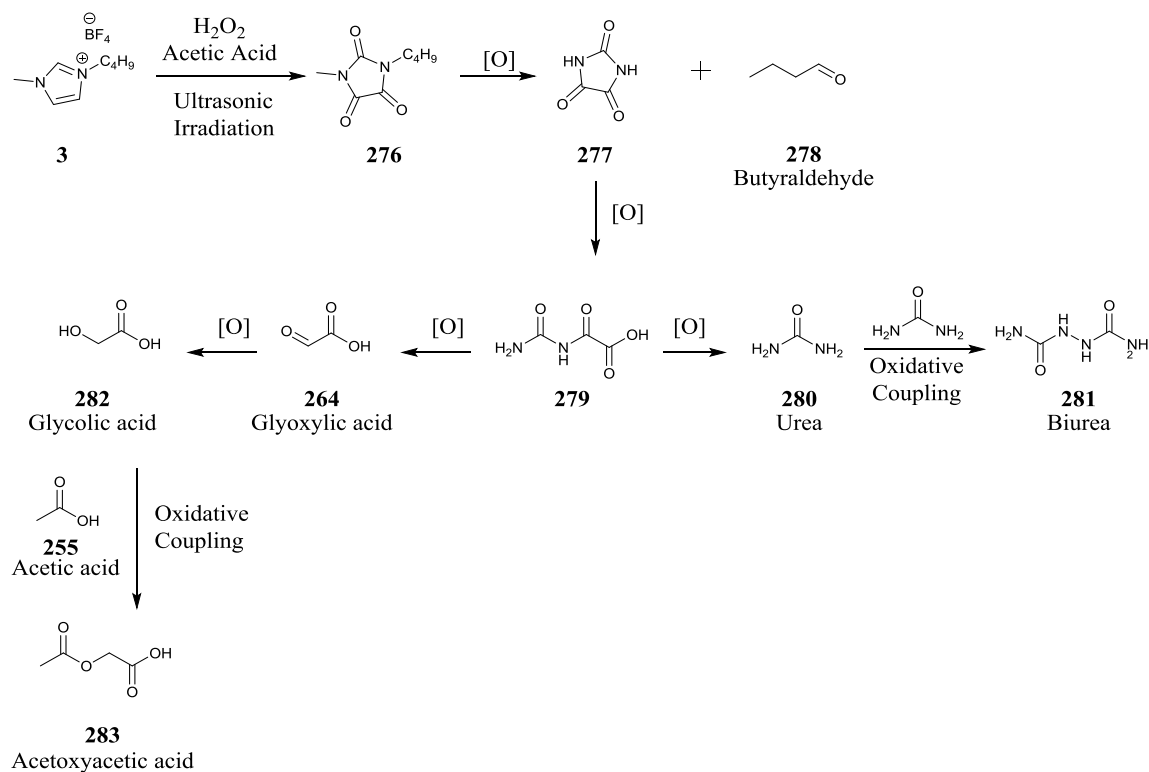


**Figure 1.59.** Radical oxidation of [bmim][BF<sub>4</sub>] under various oxidising environments. Adapted from Li *et al* 2007.<sup>40</sup>

**Table 1.12.** Oxidative degradation of alkyl imidazolium ILs assisted by acetic acid and ultrasonic irradiation. Adapted from Li *et al* 2007.<sup>40</sup>

Degradation %						
ILs	1 h	3 h	5 h	12 h	24 h	72 h
<b>C<sub>2</sub>mim Cl</b>	53.49	76.55	86.62	95.09	96.27	98.35
<b>C<sub>3</sub>mim Cl</b>	52.65	74.26	85.71	93.08	96.22	98.13
<b>C<sub>4</sub>mim Cl</b>	54.60	76.07	87.45	94.58	97.25	99.16
<b>C<sub>4</sub>mim Br</b>	55.35	76.91	87.33	93.66	96.47	98.75
<b>C<sub>4</sub>mim BF<sub>4</sub></b>	54.78	75.25	86.29	94.18	96.87	98.89
<b>C<sub>4</sub>mim PF<sub>6</sub></b>	53.26	77.47	87.63	95.38	97.76	98.47
<b>C<sub>5</sub>mim Cl</b>	55.11	75.63	86.71	93.54	97.18	99.31
<b>C<sub>6</sub>mim BF<sub>4</sub></b>	54.38	76.25	87.32	94.61	96.55	98.68

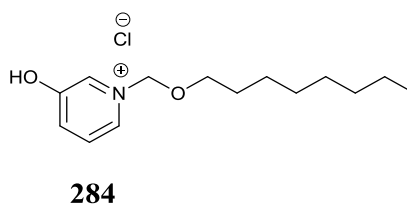
25 ml solution, ILs: 2.5 mM, H<sub>2</sub>O<sub>2</sub>: 21 mM. CH<sub>3</sub>COOH: 10 mM at 50 °C.



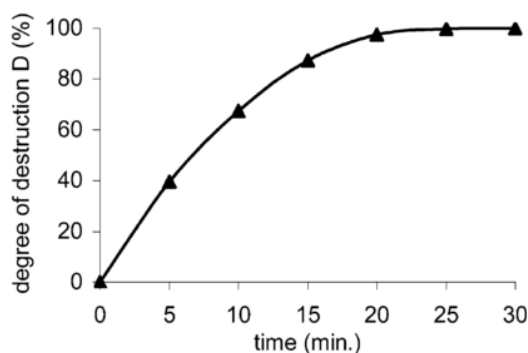
**Scheme 1.8.** Proposed degradation scheme by Li *et al.*<sup>40</sup>

The degradation pathways were also examined using GC-MS, Scheme 1.8. The proposed degradation products (**276-283**) were similar to a number of those reported by Stepnowski *et al.*, Scheme 7.<sup>37</sup> Two of the end products were determined to be biurea and acetoxyacetic acid, both “low-toxicity” molecules.<sup>40</sup>

Further methods of IL degradation in AOP's include ozonolysis<sup>111</sup> or employing the Fenton reaction.<sup>112</sup> Ozonolysis results published by Pernak *et al.* in 2004 demonstrated the effective degradation of 98 pyridinium salts by ozonation within 30 minutes, examples of which include IL (**284**) Figure 1.60 and 1.61. The destruction of the IL is rapid and complete (100% degradation).

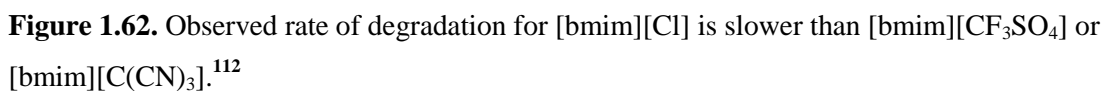




**Figure 1.60.** Example of a pyridinium salt synthesised by Pernak *et al.*<sup>111</sup> and examined for degradation in an AOP.



**Figure 1.61.** Degree of destruction (%) vs time (min.) for a pyridinium salt (**284**), examined by Pernak *et al.*<sup>111</sup>

In the Fenton reaction,  $\text{H}_2\text{O}_2$  in combination with an iron catalyst, are used to produce hydroxyl radicals. However, a strong anion effect was observed on reaction time with the ability of  $[\text{Cl}^-]$  ions from the IL to form  $\text{Fe}^{3+}$  chloride complexes and reduce the rate of radical production, Figure 1.62.  $[\text{bmim}][\text{CF}_3\text{SO}_4]$  was completely degraded after 45 minutes and its tricyanomethide analogue within one hour.<sup>112</sup>

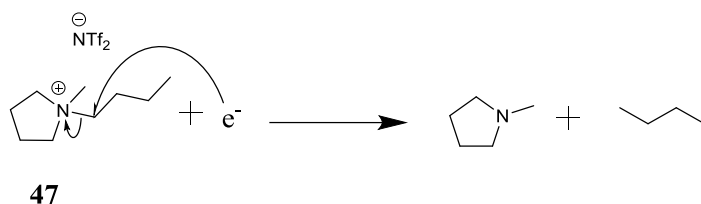


**3**
**47**

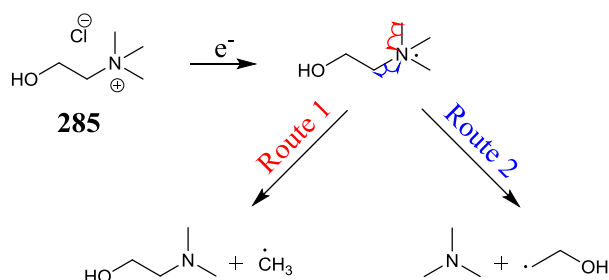
Pyrrolidinium derivative (**47**) was observed to break down into a range of products including methylpyrrolidine, octanes, octenes, 2-butanol, dibutylmethylamine and butylpyrrolidine, Scheme 1.9, whereas with the 1-methylimidazole derivative (**3**), radicals are formed that react with each other in a radical–radical coupling reaction and in a disproportionation reaction.<sup>38</sup> The successful application of quantum calculations in decomposition products shows the potential for predicting IL suitability for task and how the decompositions will affect their usefulness.





**Scheme 1.9.** Example of electrochemical decomposition of a pyrrolidinium IL.

Similarly Van der Bruggen *et al.* demonstrated the breakdown of choline based ILs in a range of electrochemical applications, Scheme 1.10.<sup>39</sup>



**Scheme 1.10.** Electrochemical decomposition of a choline chloride (285).<sup>39</sup>

## 1.7 Biodegradable Surfactants: An IL by another name.

Current designs of biodegradable ILs are based on mid-20<sup>th</sup> century successes in the field of biodegradable surfactants.<sup>113</sup> The drive to replace persistent and low biodegradability surfactants and fabric softeners has seen some great advances in the past 50 years. For instance, the replacement of "DHTDMAC" (di-hydrogenated tallow dimethylammonium chloride) with derivatives incorporating hydrolysable amide or ester linkages, example DEEDMAC,<sup>114</sup> demonstrated increased biodegradability and reducing foaming in sewage treatment plants. There are four major classes of surfactant: non-ionic, anionic, cationic and zwitterionic. ILs hold much in common with the ionic derivatives as the cationic surfactants usually are derived from quaternised nitrogen salts and the anionic derivatives derive their charge often from sulphonate salts. The drive to produce biodegradable surfactants is now cemented by the European Detergents Regulation (Regulation (EC) No 648/2004) which came into law on October 8 2005 and states that "*all surfactants used for domestic detergents have to be ultimately biodegradable*". An exception is also made for some surfactants for use in the industrial and institutional sector "*which are primarily but not ultimately biodegradable only for very special purposes and after having obtained a derogation based on risk assessment and benefits evaluations*".<sup>113</sup> With this regulation in place, designing surfactants for use in the European market requires that they are biodegradable by law.

Since the implementation of the law a number of biocompatible surfactant designs have been published. In 2010 Perez *et al.* published results on arginine based surfactants synthesised using enzymatic catalysis.<sup>115</sup> Three candidates were screened for their ready biodegradability and all three passed the CBT with 79-90% biodegradation values being recorded. All three surfactants contain amide and ester bonds and none showed recalcitrance to biodegradation. It is postulated that the use of natural building blocks in surfactants and ILs, such as amino acids, allow for easier recognition by enzymes and accessibility to a wider range of amino acid specific degradation pathways.

Further work carried out on bis-arginine gemini surfactants by Lozano *et al.* 2011 further demonstrated the effectiveness of using natural building blocks in synthesising biocompatible surfactants. It was suggested that the high levels of biodegradation may be attributed to the formation of biodegradable intermediates during the biodegradation process such as arginine and glycerol.<sup>116</sup>

A number of key points regarding surfactants were illustrated in the review published by Ranke *et al.* 2007<sup>117</sup> and are summarised as follows:

**Cations:**

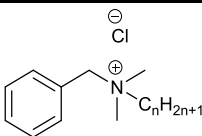
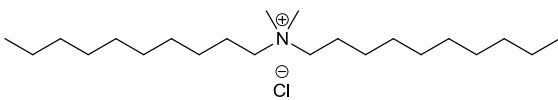
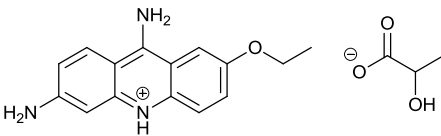
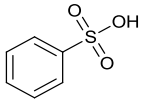
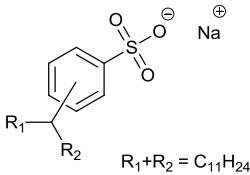
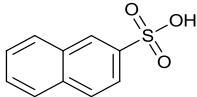
- Medium alkyl chain length pyridinium cations are potential candidates for producing readily biodegradable surfactants
- Alkylpyridinium surfactants are poorly biodegradable
- Dialkyldimethyl-ammonium and alkyldimethylbenzyl-ammonium quaternary compounds are less biodegradable than monoalkyltrimethyl-ammonium quaternaries but more biodegradable than alkyl pyridinium surfactants

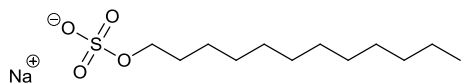
**Biodegradability:** monoalkyltrimethyl-ammonium > dialkyldimethyl-ammonium and alkyldimethylbenzyl-ammonium > alkylpyridinium

**Anions:**

- Linear alkylsulphates exhibit excellent biodegradability
- Linear alkyl sulphonates and alkylbenzene sulphonates show good biodegradability

Surfactants are screened for biodegradation in the same tests that can be employed for ILs, *vide supra*. When released to the environment or indeed to a WWTP, surfactants are not treated as single compounds but as complex mixtures. In 2008 Kümmerer *et al.*<sup>119</sup> screened mixtures of surfactants for their biodegradability and compared the mixtures to the single compound results, Table 1.13. It was found that ion pair formation between organic anions and quaternary ammonium cations, e.g. between LAS (linear alkylbenzene sulphonate) and BAC (benzalkonium chloride) caused a decrease in biodegradation. It was suggested that compounds above 500 Da render the molecule impossible to biodegrade and indeed mixtures of BAC:SDS or DDMAC (didecyldimethylammonium chloride):LAS are all above this molecular weight.

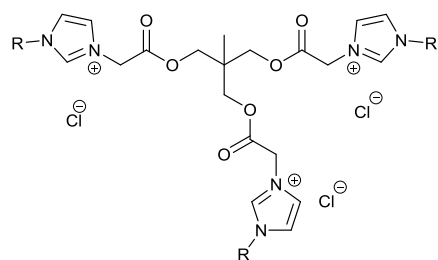
Substance	% Biodegradability CBT <sup>a</sup>
 $n = 8, 10, 12, 14, 16, 18$ <b>BAC - benzalkonium chloride</b>	-8
 <b>DDMAC - didecyldimethylammonium chloride</b>	4
 <b>EL - Ethacridine lactate</b>	13
 <b>BSA – Benzene sulfonic acid</b>	25
 <b>LAS – Linear alkylbenzene sulfonate</b>	50
 	12

<b>NSA – Naphthalene sulfonic acid</b>	
	69
<b>SDS – Sodium dodecyl sulfate</b>	
<b>BAC:BSA 1:1</b>	45
<b>BAC:LAS 1:1</b>	13
<b>BAC:NSA 1:1</b>	45
<b>BAC: SDS 1:1</b>	39
<b>DDMAC:LAS 1:1</b>	11
<b>DDMAC:NSA 1:1</b>	-2
<b>DDMAC:SDS 1:1</b>	15
<b>EL:BSA 1:1</b>	1
<b>EL:LAS 1:1</b>	23
<b>EL:NSA 1:1</b>	16
<b>EL:SDS 1:1</b>	36

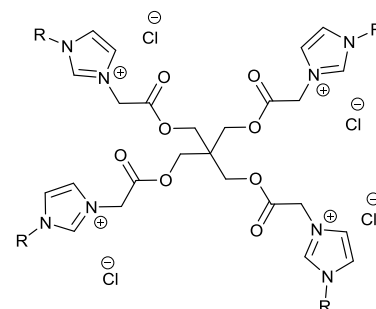
**Table 1.13.** Biodegradation of surfactants and mixtures of surfactants.<sup>118</sup>

<sup>a</sup>Biodegradation values assessed by the CBT OECD (TG 301D)

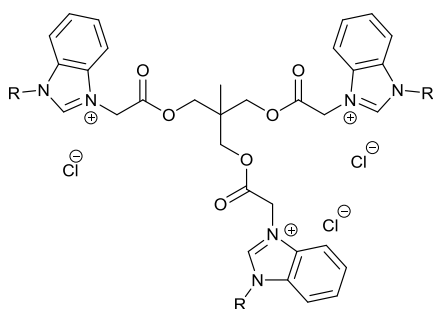
The biodegradability of tris (**286-297**) and tetrakis (**298-309**) imidazolium and benzimidazolium IL surfactants, Figure 1.64, using the CBT (OECD 301D) was reported in 2015 by Al-Mohammed *et al.*<sup>16,17</sup> As can be seen from Figure 1.64, a number of tris and tetrakis imidazolium and benzimidazolium ILs with various alkyl chain lengths, from C<sub>4</sub> to C<sub>12</sub> and benzyl, were synthesised and evaluated for their surfactant properties and their biodegradability. The same trend of increased biodegradation with increased chain length can be observed for these series of IL surfactants with C<sub>12</sub> (**290, 296, 302, 308**) degrading the most (45-56%) and C<sub>4</sub> (**286, 292, 298, 304**) the least (22-35%) and the non-linear *N*-benzyl derivatives (**291, 297, 303, 309**) degrading even less than the C<sub>4</sub> derivatives (16-22%). The tetrakis family (**298-309**) in general appeared to have slightly elevated levels of biodegradability, ~5-10%, when compared to the tris family (**286-297**). The benzimidazolium tris (**292-297**) and tetrakis (**304-309**) families in turn were observed to have lower levels of biodegradability throughout the homologous series of alkyl chains than their respective imidazolium families (**286-291, 298-303**). A plateau in the levels of biodegradability was reached after 16 days and the tests were not run for the full 28 day period.



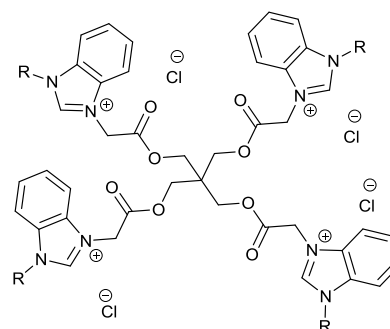
- 286**, R = C<sub>4</sub>H<sub>9</sub>, 27%  
**287**, R = C<sub>6</sub>H<sub>13</sub>, 36%  
**288**, R = C<sub>8</sub>H<sub>17</sub>, 47%  
**289**, R = C<sub>10</sub>H<sub>21</sub>, 45%  
**290**, R = C<sub>12</sub>H<sub>25</sub>, 51%  
**291**, R = CH<sub>2</sub>C<sub>6</sub>H<sub>5</sub>, 20%



- 298**, R = C<sub>4</sub>H<sub>9</sub>, 35%  
**299**, R = C<sub>6</sub>H<sub>13</sub>, 39%  
**300**, R = C<sub>8</sub>H<sub>17</sub>, 49%  
**301**, R = C<sub>10</sub>H<sub>21</sub>, 51.5%  
**302**, R = C<sub>12</sub>H<sub>25</sub>, 56%  
**303**, R = CH<sub>2</sub>C<sub>6</sub>H<sub>5</sub>, 22%



- 292**, R = C<sub>4</sub>H<sub>9</sub>, 22%  
**293**, R = C<sub>6</sub>H<sub>13</sub>, 27%  
**294**, R = C<sub>8</sub>H<sub>17</sub>, 35.5%  
**295**, R = C<sub>10</sub>H<sub>21</sub>, 40%  
**296**, R = C<sub>12</sub>H<sub>25</sub>, 45%  
**297**, R = CH<sub>2</sub>C<sub>6</sub>H<sub>5</sub>, 16%



- 304**, R = C<sub>4</sub>H<sub>9</sub>, 28%  
**305**, R = C<sub>6</sub>H<sub>13</sub>, 33.5%  
**306**, R = C<sub>8</sub>H<sub>17</sub>, 42%  
**307**, R = C<sub>10</sub>H<sub>21</sub>, 44%  
**308**, R = C<sub>12</sub>H<sub>25</sub>, 47%  
**309**, R = CH<sub>2</sub>C<sub>6</sub>H<sub>5</sub>, 21.5%

**Figure 1.64.** Tris- and tetrakis-imidazolium and benzimidazolium IL surfactants examine for their biodegradability.

The scope of this review does not include an in depth discussion on biodegradable surfactants, however the author wishes to acknowledge the overlap between IL biodegradation and the lessons that can be learned from biodegradable surfactant research.

## 1.8 Outlook and recommendations

To date a number of readily biodegradable ILs have been synthesised, ILs (**54**, **55**, **60-66**, **101**, **102**, **109**, **110**, **120**, **122**, **151**, **156-158**, **161-165**, **175**, **176**, **178**, **180**, **310-322**). Nearly 50%, of the readily biodegradable ILs have been comprised of a cholinium cation and organic acid

anion. (**61-66**, **157**, **310-322**). The cholinium cation was shown to be highly sensitive to modification, with most modifications reducing biodegradability. The cholinium family of ILs present the most effective route to readily biodegradable compounds examined to date.

Protic analogues of the cholinium core also proved to be good candidates for synthesising biodegradable ILs with seven considered readily biodegradable (**54**, **55**, **161-165**)

Efforts to prepare a readily biodegradable imidazolium IL have demonstrated that the imidazolium core does not degrade under standardised ISO or OECD test conditions. Chemical oxidation is the most effective method to degrade these compounds. Substitution at the imidazolium rings C2 and C4/5 positions with electron withdrawing groups and readily hydrolysable groups such as esters and amides did not significantly improve biodegradation. It is the recommendation of this review that further studies into imidazolium ILs biodegradation are required.

Biodegradable pyridinium ILs have been synthesised (**109**, **110**, **120**, **122**). Three examples (**109**, **110**, **122**) critically include a primary alcohol terminated chain on the *N*-position. Pyridinium ILs are very sensitive to modification on the ring with many derivatives which fail the CBT and CO<sub>2</sub> headspace test known including 3-position and *N*-substituted ethers .

Most tetra alkylammonium cations do not undergo high levels of biodegradation with the exceptions of TMBA IL (**158**) and 5 DMDBA examples (**60**, **175**, **176**, **178**, **180**). The DMDBA ILs all required a carboxylate counterion for biodegradation to be high enough to pass readily biodegradation tests. The chloride DMDBA derivative (**174**) was found to undergo just 5% biodegradation.

Hexyl and cyclohexyl phosphonium cations appear to sterically hinder enzymatic degradation and further studies in this area are required. It is proposed that shorter, less bulky, alkyl chain substituted phosphonium cations or an asymmetrically substituted cation paired with an organic acid anion may undergo a higher level of biodegradation similar to the DMDBA series.

Non-aromatic 6 membered cyclic compounds examined, such as the morpholinium, DABCO and piperidinium ILs are in general not readily biodegradable. One exception is the derivative (**143**), which degraded 79%. The primary structural feature of (**143**) enabling biodegradation was the presence of an *N*-substituted propyl alcohol terminated chain. The chain length was also of importance, with an ethyl derivative (**142**) undergoing a considerably lower 29% biodegradation.

The 5 membered non-aromatic pyrrolidinium heterocycles underwent similar levels of biodegradation to the 6 membered cycles with the exception of derivatives (**151**) and (**156**), both achieving greater than 60% biodegradation. The key structural feature of (**156**) was an N-substituted octyl chain while the critical feature of (**151**) was the presence of an N-substituted propyl alcohol. Once more it was observed that the shorter ethyl alcohol substituted IL (**153**) did not undergo biodegradation >6%.

Biodegradation screening of symmetrical ILs has been undertaken since Coleman and Gathergood's review in 2010 with a number of imidazolium, pyridinium, pyrrolidinium ILs studied. The dicationic ILs screened all failed to achieve > 5% biodegradation under their respective test conditions and it has been surmised that the compounds are resistant to biodegrading due to inability of enzymes to access hydrolysable sites, whether this is due to steric effects or electronic considerations is unknown.

Metabolite identification as part of biodegradation studies provides useful data to allow researchers to design ILs which can not only pass readily biodegradable tests but reduce the build-up of persistent breakdown products.

## 1.9 Conclusion

To conclude this IL biodegradation review it is necessary to examine the guidelines with which potentially biodegradable ILs are designed. Often, Boethling's rules of thumb are quoted for designing biodegradable ILs but just how compatible are these rules with the ILs that have been synthesised in the past decade?

When the trends in IL biodegradation are taken as a whole it can be observed that a number of the rules of thumb hold true. Longer unbranched alkyl chains promote biodegradability and the presence of hydrolysable groups (i.e. esters) and groups easily oxidised (i.e. alcohols) and carboxylic acids are noted as being amongst the prominent features of the readily biodegradable ILs in this chapter. The use of natural building blocks for instance, choline and nicotinic acid for the cation can lead to biodegradable derivatives. However, even modest changes to the structure can in some cases greatly inhibit access to biodegradation pathways. Detrimental factors that have been observed, that are in agreement with the rules of thumb, include the presence of aliphatic ethers. It is stated in the rules of thumb that heterocycles are best avoided, making the task of producing heterocyclic ILs a challenge from the very beginning, although every compound is unique and requires careful consideration of all structural features.

The goal of making task specific yet biodegradable low toxicity ILs is a daunting one. Can ILs which are robust under a wide range of applications (e.g. chemical reactions, thermal, biocatalysis etc.), yet are suitable substrates for breakdown pathways in the environment, leading to ultimate biodegradation be designed? While this task is challenging, from the data collated in this review the author believes that great progress is being made towards this goal.

To undergo a full eco(toxicity) life cycle assessment is the ultimate goal for any IL that has potential industrial application. The hazard of using the IL versus the benefits must be carefully reviewed as ILs move from academic curiosities to large scale industrial applications. Further studies on metabolic pathways and breakdown products for ILs will be required to stimulate advances that are required in producing readily biodegradable ILs. Ultimately (eco)toxicity analysis of these metabolites will also be required, for after all, what is the benefit of nowadays producing a readily biodegradable IL if its persistent breakdown products are more toxic than the parent compound? Intense debate, of this very issue, at green chemistry, IL and environmental toxicology meetings, conferences and in research papers has raised awareness of the limitations of standardised biodegradation tests. It is proposed that the outcome from this process is that current biodegradation studies of ILs are now at the forefront of new initiatives in biodegradation assays and reinterpretation of results. Chemists working together with experts in environmental science and (eco)toxicology can work towards the common interest of the design of safer chemicals. Indeed, although the number of possible cation and anion combinations which lead to salts classed as ILs seems mindbogglingly large (frequently  $>10^{18}$ ), this is a small subset of possible simple organic molecules. The journey which scientists who study biodegradation of ILs have travelled is a roadmap to enable other researchers to reduce the potential problems of emergence of persistent chemicals in the environment.

## 1.10 References

1. A. Jordan and N. Gathergood, *Chem. Soc. Rev.*, 2015, 44, 8200-8237.
2. L. P. N. Rebelo, J. N. C. Lopes, J. Esperanca and E. Filipe, *J. Phys. Chem. B*, 2005, 109, 6040-6043.
3. M. J. Earle, J. Esperanca, M. A. Gilea, J. N. C. Lopes, L. P. N. Rebelo, J. W. Magee, K. R. Seddon and J. A. Widegren, *Nature*, 2006, 439, 831-834.
4. M. Smiglak, W. M. Reichert, J. D. Holbrey, J. S. Wilkes, L. Sun, J. S. Thrasher, K. Kirichenko, S. Singh, A. R. Katritzky and R. D. Rogers, *Chem. Commun.*, 2006, 2554-2556.
5. P. Walden, *Bull. Acad. Imp. Sci. St. Petersburg*, 1914, 8, 405-422.
6. J. W. S. Gabriel, *Ber. Dtsch. Chem. Ges.*, 1888, 21, 2669-2679.
7. H. Goldschmidt, *Ber. Dtsch. Chem. Ges.*, 1881, 14, 1844-1848.



8. P. T. W. Anastas, J. C. , *Green Chemistry: Theory and Practice*, Oxford University Press: New York, 1998.
9. B. M. Trost, *Angew. Chem., Int. Ed. Engl.*, 1995, 34, 259-281.
10. R. A. Sheldon, *Chemistry & Industry*, 1992, 903-906.
11. J. Andraos, *Org. Process Res. Dev.*, 2005, 9, 149-163.
12. K. M. Docherty, S. Z. Hebbeler and C. F. Kulpa, *Green Chem.*, 2006, 8, 560-567.
13. N. Sun, H. Rodriguez, M. Rahman and R. D. Rogers, *Chem. Commun.*, 2011, 47, 1405-1421.
14. D. Parmentier, S. J. Metz and M. C. Kroon, *Green Chem.*, 2013, 15, 205-209.
15. M. Mahrova, F. Pagano, V. Pejakovic, A. Valea, M. Kalin, A. Igartua and E. Tojo, *Tribol. Int.*, 2015, 82, Part A, 245-254.
16. N. N. Al-Mohammed, R. S. Duali Hussien, T. H. Ali, Y. Alias and Z. Abdullah, *RSC Adv.*, 2015, 5, 21865-21876.
17. N. N. Al-Mohammed, R. S. Duali Hussien, Y. Alias and Z. Abdullah, *RSC Adv.*, 2015, 5, 2869-2881.
18. R. G. Gore, L. Myles, M. Spulak, I. Beadham, T. M. Garcia, S. J. Connon and N. Gathergood, *Green Chem.*, 2013, 15, 2747-2760.
19. L. Myles, R. Gore, M. Spulak, N. Gathergood and S. J. Connon, *Green Chem.*, 2010, 12, 1157-1162.
20. L. Myles, R. G. Gore, N. Gathergood and S. J. Connon, *Green Chem.*, 2013, 15, 2740-2746.
21. R. G. Gore, T.-K.-T. Truong, M. Pour, L. Myles, S. J. Connon and N. Gathergood, *Green Chem.*, 2013, 15, 2727-2739.
22. D. Coleman and N. Gathergood, *Chem. Soc. Rev.*, 2010, 39, 600-637.
23. S. Harrad, *Beyond the Stockholm Convention: An Introduction to Current Issues and Future Challenges in POPs Research*, John Wiley & Sons, Ltd, 2009.
24. S. Milla, S. Depiereux and P. Kestemont, *Ecotoxicology*, 2011, 20, 305-319.
25. R. P. Herwig, J. P. Gray and D. P. Weston, *Aquaculture*, 1997, 149, 263-283.
26. P. H. Howard, R. S. Boethling, W. Stiteler, W. Meylan and J. Beauman, *Sci. Total Environ.*, 1991, 109, 635-641.
27. R. S. Boethling, P. H. Howard, W. Meylan, W. Stiteler, J. Beauman and N. Tirado, *Environ. Sci. Technol.*, 1994, 28, 459-465.
28. M. Galinski, A. Lewandowski and I. Stepniak, *Electrochim. Acta*, 2006, 51, 5567-5580.
29. J. G. Huddleston, A. E. Visser, W. M. Reichert, H. D. Willauer, G. A. Broker and R. D. Rogers, *Green Chem.*, 2001, 3, 156-164.
30. D. M. Fox, W. H. Awad, J. W. Gilman, P. H. Maupin, H. C. De Long and P. C. Trulove, *Green Chem.*, 2003, 5, 724-727.
31. M. Armand, F. Endres, D. R. MacFarlane, H. Ohno and B. Scrosati, *Nat. Mater.*, 2009, 8, 621-629.
32. K. M. Docherty, J. K. Dixon and C. F. Kulpa, *Biodegradation*, 2007, 18, 481-493.
33. G. Quijano, A. Couvert, A. Amrane, G. Darracq, C. Couriol, P. Le Cloirec, L. Paquin and D. Carrié, *Chem. Eng. J.*, 2011, 174, 27-32.
34. Y. Luo, Q. Wang, Q. Lu, Q. Mu and D. Mao, *Environ. Sci. Technol. Lett.*, 2014, 1, 266-270.
35. OECD, *Revised Introduction to the OECD Guidelines for Testing of Chemicals, Section 3*, OECD Publishing, 2006.
36. P. Anastas and N. Eghbali, *Chem. Soc. Rev.*, 2010, 39, 301-312.
37. M. Czerwicka, S. Stolte, A. Muller, E. M. Siedlecka, M. Golebiowski, J. Kumirska and P. Stepnowski, *J. Hazard. Mater.*, 2009, 171, 478-483.
38. M. C. Kroon, W. Buijs, C. J. Peters and G. J. Witkamp, *Green Chem.*, 2006, 8, 241-245.
39. K. Haerens, E. Matthijs, K. Binnemans and B. Van der Bruggen, *Green Chem.*, 2009, 11, 1357-1365.
40. X. H. Li, J. G. Zhao, Q. H. Li, L. F. Wang and S. C. Tsang, *Dalton Trans.*, 2007, 1875-1880.
41. A. Modelli, A. Sali, P. Galletti and C. Samori, *Chemosphere*, 2008, 73, 1322-1327.

42. M. Markiewicz, M. Piszora, N. Caicedo, C. Jungnickel and S. Stolte, *Water Res.*, 2013, 47, 2921-2928.
43. M. Markiewicz, C. Jungnickel, A. Markowska, U. Szczepaniak, M. Paszkiewicz and J. Hupka, *Molecules*, 2009, 14, 4396-4405.
44. V. Gomez, L. Ferreres, E. Pocurull and F. Borrull, *Talanta*, 2011, 84, 859-866.
45. E. Liwarska-Bizukojc, C. Maton, C. V. Stevens and D. Gendaszewska, *J. Chem. Technol. Biotechnol.*, 2014, 89, 763-768.
46. W. Mroziak, A. Kotłowska, W. Kamysz and P. Stepnowski, *Chemosphere*, 2012, 88, 1202-1207.
47. C. Jungnickel, W. Mroziak, M. Markiewicz and J. Luczak, *Curr. Org. Chem.*, 2011, 15, 1928-1945.
48. W. Mroziak, C. Jungnickel, T. Ciborowski, W. R. Pitner, J. Kumirska, Z. Kaczynski and P. Stepnowski, *J. Soils Sed.*, 2009, 9, 237-245.
49. M. Matzke, S. Stolte, J. Arning, U. Uebers and J. Filser, *Ecotoxicology*, 2009, 18, 197-203.
50. P. T. P. Thi, C. W. Cho and Y. S. Yun, *Water Res.*, 2010, 44, 352-372.
51. S. Studzinska and B. Buszewski, *Anal. Bioanal. Chem.*, 2009, 393, 983-990.
52. F. J. Deive, A. Rodriguez, A. Varela, C. Rodrigues, M. C. Leitao, J. Houbraken, A. B. Pereiro, M. A. Longo, M. A. Sanroman, R. A. Samson, L. P. N. Rebelo and C. S. Pereira, *Green Chem.*, 2011, 13, 687-696.
53. J. Neumann, O. Grundmann, J. Thoming, M. Schulte and S. Stolte, *Green Chem.*, 2010, 12, 620-627.
54. M. M. Häggblom, Bossert, Ingeborg D., *Microbial Processes and Environmental Applications*, Kluwer Academic Publishers, Dordrecht, 2003.
55. Ridding the world of pops: A guide to the Stockholm convention on persistent organic pollutants, [http://www.pops.int/documents/guidance/beg\\_guide.pdf](http://www.pops.int/documents/guidance/beg_guide.pdf), Accessed 25/11/2013, 2013.
56. E. Meszaros, R. Sipos, R. Pal, C. Romsics and K. Marialigeti, *Int. Biodeterior. Biodegrad.*, 2013, 84, 126-133.
57. I. Kranzioch, C. Stoll, A. Holbach, H. Chen, L. J. Wang, B. H. Zheng, S. Norra, Y. H. Bi, K. W. Schramm and A. Tiehm, *Environ. Sci. Pollut. Res.*, 2013, 20, 7046-7056.
58. B. Kuipers, W. R. Cullen and W. W. Mohn, *Environ. Sci. Technol.*, 1999, 33, 3579-3585.
59. M. G. Freire, C. M. S. S. Neves, I. M. Marrucho, J. o. A. P. Coutinho and A. M. Fernandes, *J. Phys. Chem. A*, 2009, 114, 3744-3749.
60. J. Neumann, C.-W. Cho, S. Steudte, J. Koser, M. Uerdingen, J. Thoming and S. Stolte, *Green Chem.*, 2012, 14, 410-418.
61. C. Abrusci, J. Palomar, J. L. Pablos, F. Rodriguez and F. Catalina, *Green Chem.*, 2011, 13, 709-717.
62. S. Stolte, S. Abdulkarim, J. Arning, A. K. Blomeyer-Nienstedt, U. Bottin-Weber, M. Matzke, J. Ranke, B. Jastorff and J. Thoming, *Green Chem.*, 2008, 10, 214-224.
63. M. T. Garcia, N. Gathergood and P. J. Scammells, *Green Chem.*, 2005, 7, 9-14.
64. C. Zhang, H. Wang, S. V. Malhotra, C. J. Dodge and A. J. Francis, *Green Chem.*, 2010, 12, 851-858.
65. M. Markiewicz, J. Henke, A. Brillowska-Dabrowska, S. Stolte, J. Luczak and C. Jungnickel, *Int. J. Environ. Sci. Technol.*, 2014, 11, 1919-1926.
66. E. Liwarska-Bizukojc and D. Gendaszewska, *J. Biosci. Bioeng.*, 2013, 115, 71-75.
67. L. Carson, P. K. W. Chau, M. J. Earle, M. A. Gilea, B. F. Gilmore, S. P. Gorman, M. T. McCann and K. R. Seddon, *Green Chem.*, 2009, 11, 492-497.
68. S. Morrissey, B. Pegot, D. Coleman, M. T. Garcia, D. Ferguson, B. Quilty and N. Gathergood, *Green Chem.*, 2009, 11, 475-483.
69. L. Ford, J. R. Harjani, F. Atefi, M. T. Garcia, R. D. Singer and P. J. Scammells, *Green Chem.*, 2010, 12, 1783-1789.
70. B. Peric, J. Sierra, E. Martí, R. Cruañas, M. A. Garau, J. Arning, U. Bottin-Weber and S. Stolte, *J. Hazard. Mater.*, 2013, 261, 99-105.

71. N. Ferlin, M. Courty, S. Gatard, M. Spulak, B. Quilty, I. Beadham, M. Ghavre, A. Haiß, K. Kümmerer, N. Gathergood and S. Bouquillon, *Tetrahedron*, 2013, 69, 6150-6161.
72. N. Ferlin, M. Courty, A. N. Van Nhien, S. Gatard, M. Pour, B. Quilty, M. Ghavre, A. Haiß, K. Kümmerer, N. Gathergood and S. Bouquillon, *RSC Adv.*, 2013, 3, 26241-26251.
73. F. Boissou, A. Muhlbauer, K. De Oliveira Vigier, L. Leclercq, W. Kunz, S. Marinkovic, B. Estrine, V. Nardello-Rataj and F. Jerome, *Green Chem.*, 2014, 16, 2463-2471.
74. X. D. Hou, Q. P. Liu, T. J. Smith, N. Li and M. H. Zong, *PLoS One*, 2013, 8.
75. R. S. Boethling, E. Sommer and D. DiFiore, *Chem. Rev.*, 2007, 107, 2207-2227.
76. N. V. Plechkova and K. R. Seddon, *Chem. Soc. Rev.*, 2008, 37, 123-150.
77. A. Romero, A. Santos, J. Tojo and A. Rodríguez, *J. Hazard. Mater.*, 2008, 151, 268-273.
78. S. Stolte, S. Steudte, A. Igartua and P. Stepnowski, *Curr. Org. Chem.*, 2011, 15, 1946-1973.
79. S. Stolte, T. Schulz, C.-W. Cho, J. Arning and T. Strassner, *ACS Sustainable Chem. Eng.*, 2013, 1, 410-418.
80. N. Gathergood, P. J. Scammells and M. T. Garcia, *Green Chem.*, 2006, 8, 156-160.
81. D. Coleman, M. Spulak, M. T. Garcia and N. Gathergood, *Green Chem.*, 2012, 14, 1350-1356.
82. J. Neumann, S. Steudte, C.-W. Cho, J. Thoming and S. Stolte, *Green Chem.*, 2014, 16, 2174-2184.
83. J. R. Harjani, R. D. Singer, M. T. Garcia and P. J. Scammells, *Green Chem.*, 2009, 11, 83-90.
84. C. Pretti, M. Renzi, S. E. Focardi, A. Giovani, G. Monni, B. Melai, S. Rajamani and C. Chiappe, *Ecotoxicol. Environ. Saf.*, 2011, 74, 748-753.
85. J. Pernak, N. Borucka, F. Walkiewicz, B. Markiewicz, P. Fochtman, S. Stolte, S. Steudte and P. Stepnowski, *Green Chem.*, 2011, 13, 2901-2910.
86. S. Stolte, S. Steudte, O. Areitioaurtena, F. Pagano, J. Thöming, P. Stepnowski and A. Igartua, *Chemosphere*, 2012, 89, 1135-1141.
87. OECD, *SIDS Initial Assessment Report For SIAM 19*, OECD Publishing, Berlin, Germany, 2004
88. K. Radosevic, M. C. Bubalo, V. G. Sreck, D. Grgas, T. L. Dragicevic and I. R. Redovnikovic, *Ecotoxicol. Environ. Saf.*, 2015, 112, 46-53.
89. S. Sekar, M. Surianarayanan, V. Ranganathan, D. R. MacFarlane and A. B. Mandal, *Environ. Sci. Technol.*, 2012, 46, 4902-4908.
90. R. Zana, J. Schmidt and Y. Talmon, *Langmuir*, 2005, 21, 11628-11636.
91. M. L. Ingalsbe, J. D. S. Denis, M. E. McGahan, W. W. Steiner and R. Priefer, *Bioorg. Med. Chem. Lett.*, 2009, 19, 4984-4987.
92. V. I. Pârvolescu and C. Hardacre, *Chem. Rev.*, 2007, 107, 2615-2665.
93. F. Atefi, M. T. Garcia, R. D. Singer and P. J. Scammells, *Green Chem.*, 2009, 11, 1595-1604.
94. S. Steudte, S. Bemowsky, M. Mahrova, U. Bottin-Weber, E. Tojo-Suarez, P. Stepnowski and S. Stolte, *RSC Adv.*, 2014, 4, 5198-5205.
95. K. M. Docherty, M. V. Joyce, K. J. Kulacki and C. F. Kulpa, *Green Chem.*, 2010, 12, 701-712.
96. H. Sato, A. Shibata, Y. Wang, H. Yoshikawa and H. Tamura, *Polym. Degrad. Stab.*, 2001, 74, 69-75.
97. T. P. T. Pham, C. W. Cho, C. O. Jeon, Y. J. Chung, M. W. Lee and Y. S. Yun, *Environ. Sci. Technol.*, 2009, 43, 516-521.
98. F. Rojo, *Environ. Microbiol.*, 2009, 11, 2477-2490.
99. C. Zhang, S. V. Malhotra and A. J. Francis, *Chemosphere*, 2011, 82, 1690-1695.
100. B. K. S. N. Singh, S. Mishra, *Microbial Degradation of Xenobiotics*, Springer, 2012.
101. TOPKAT, <http://accelrys.com/products/discovery-studio/predictive-toxicology.html>, Accessed 09/08/13.
102. META, <http://www.multicase.com/products/prod05.htm>, Accessed 09/08/13.

103. BIOWIN, <http://www.epa.gov/oppt/exposure/pubs/episuitdl.htm>, Accessed 09/08/13.
104. VEGA, <http://www.vega-qsar.eu/download.html>, Accessed 14/01/2014.
105. START, <http://toxtree.sourceforge.net/start.html>, Accessed 14/01/2014.
106. CATABOL, <http://oasis-lmc.org/?section=software&swid=1>, Accessed 09/08/13.
107. F. Pizzo, A. Lombardo, A. Manganaro and E. Benfenati, *Sci. Total Environ.*, 2013, 463–464, 161-168.
108. C. Rucker and K. Kummerer, *Green Chem.*, 2012, 14, 875-887.
109. The UFT / Merck Ionic Liquids Biological Effects Database, [http://www.il-eco.uft.uni-bremen.de/index.php?page=substance&chent\\_id=IM0&view=degradation&lang=en#14013](http://www.il-eco.uft.uni-bremen.de/index.php?page=substance&chent_id=IM0&view=degradation&lang=en#14013), Accessed 24/10/14.
110. P. Stepnowski and A. Zaleska, *J. Photochem. Photobiol., A*, 2005, 170, 45-50.
111. J. Pernak and M. Branicka, *Ind. Eng. Chem. Res.*, 2004, 43, 1966-1974.
112. E. M. Siedlecka, M. Golebiowski, Z. Kaczynski, J. Czupryniak, T. Ossowski and P. Stepnowski, *Appl. Catal., B*, 2009, 91, 573-579.
113. M. J. Scott and M. N. Jones, *Biochim. Biophys. Acta, Biomembr.*, 2000, 1508, 235-251.
114. S. T. Giolando, R. A. Rapaport, R. J. Larson, T. W. Federle, M. Stalmans and P. Masscheleyn, *Chemosphere*, 1995, 30, 1067-1083.
115. M. R. Infante, L. Perez, M. C. Moran, R. Pons, M. Mitjans, M. P. Vinardell, M. T. Garcia and A. Pinazo, *Eur. J. Lipid Sci. Technol.*, 2010, 112, 110-121.
116. A. Pinazo, N. Lozano, L. Perez, M. C. Moran, M. R. Infante and R. Pons, *C. R. Chim.*, 2011, 14, 726-735.
117. J. Ranke, S. Stolte, R. Stormann, J. Arning and B. Jastorff, *Chem. Rev.*, 2007, 107, 2183-2206.
118. H. Sütterlin, R. Alexy, A. Coker and K. Kümmerer, *Chemosphere*, 2008, 72, 479-484.

## Chapter 2

### *Synthesis of 1<sup>st</sup> Generation Amino Acid Ionic Liquids*

Sections of Chapter 2 have been published in Green Chemistry as part of two back to back publications in collaboration with Prof. Klaus Kümmerer and are as follows:

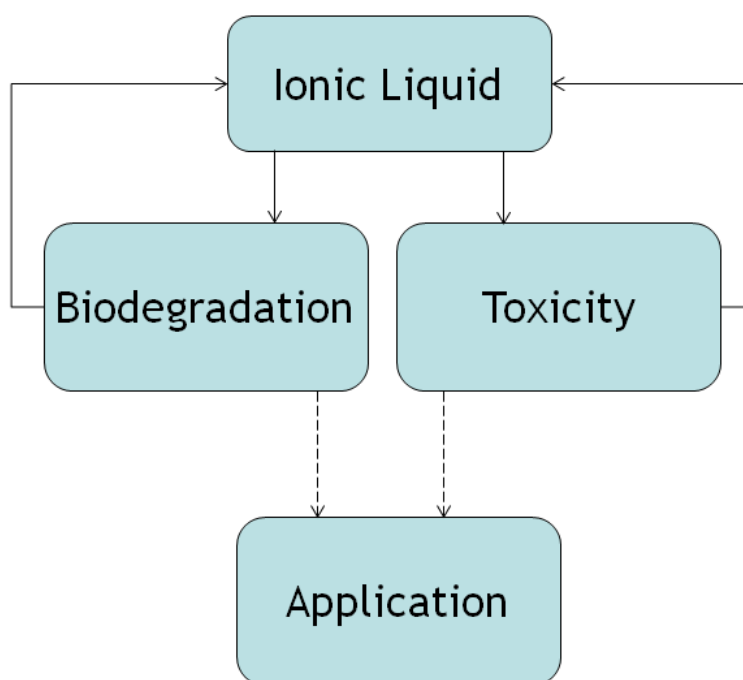
Synthesis of a Series of Amino Acid Derived Ionic Liquids and Tertiary Amines: Green chemistry metrics including microbial toxicity and preliminary biodegradation data analysis. A. Jordan, Haiß, M. Spulak, Y. Karpichev, K. Kummerer and N. Gathergood, *Green Chem.*, 2016, DOI: 10.1039/C6GC00415F.<sup>1</sup>

On the way to greener ionic liquids. Identification of a fully mineralizable phenylalanine-based ionic liquid. Hai, A. Jordan, J. Westphal, E. Logunova, N. Gathergood and K. Kummerer, *Green Chem.*, 2016, DOI: 10.1039/C6GC00417B.<sup>2</sup>

Reproduced by permission of The Royal Society of Chemistry

## 2.1 Aim

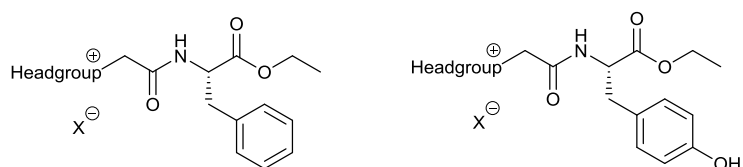
The aim of this investigation was to synthesise a series of amino acid derived ILs, henceforth referred to as the 1st generation amino acid ILs, with respect to the principles of green chemistry and Boethling's rules of thumb for designing biodegradable compounds,<sup>3</sup> the 12 principles of green chemistry,<sup>4</sup> and preceding generations of research conducted within the Gathergood research group.<sup>5-10</sup> Antimicrobial toxicity and biodegradability of the compounds was also to be investigated as part of the assessment of the ILs potential "greenness". Data provided by such studies can contribute to defining structure activity relationships (SAR) and structure activity biodegradation relationships (SABR) of the series of ILs and aid in rationally designing subsequent generations of ILs. Searching for applications suited to the ILs that are designed within the Gathergood group is not the foremost concern, (although model studies for future surfactant compounds is a long term research theme). The primary goal is to synthesise low toxicity, biodegradable ILs and then search for suitable applications after this assessment has been carried out. This design strategy ensures that even if no useful application can be found then the data collected on the toxicity and biodegradability can be utilised in rationally designing next generation ILs. Toxicity and biodegradability assessments are completely independent of application. This design strategy can be visually summarised in Figure 2.1.



**Figure 2.1.** IL design strategy

## 2.2 Introduction

A series of L-phenylalanine ILs, L-tyrosine ILs and L-phenylalanine tertiary amines was synthesised to investigate their antimicrobial toxicity and biodegradability. The general structure of the ILs consisted of an ethyl ester of an amino acid as a backbone (Figure 2.2). An ethyl chain length for the ester moiety was chosen as ethanol is available as a bio-renewable starting material for the esterification and will not contribute disproportionate amounts of carbon towards the overall biodegradability of the molecule, see Chapter 1 for ester biodegradation of ILs (e.g. **75**, **76**, **82**, **83**). Additional carbon in the alkyl sidechain can increase biodegradability but may not accurately represent whether the entire molecule is degrading or whether the ester is only degrading. A short ester chain length should also help in avoiding the associated toxicity that comes with longer alkyl chain cationic molecules.<sup>11, 12</sup> Phenylalanine was chosen as the amino acid backbone as this is also available from potentially bio-renewable sources<sup>13</sup> and results in the introduction of an amide functionality into the IL with the aim of inducing biodegradation by enzyme recognition by amidase enzymes.<sup>14</sup> Phenylalanine's aromatic side chain also allows for additional lipophilicity in the molecule without extending the ester chain length, significantly increasing the melting point and enhancing stability. The headgroup is linked to the amino acid using an amide linker. Ester chain length and counter-ion were not varied in this study and only the headgroup chosen was alternated allowing this study to demonstrate the effect of headgroup on biodegradability and toxicity. A subseries of tertiary amino derived compounds was synthesised to investigate the effect of the presence of a quaternary nitrogen atom on the toxicity and biodegradability and if the presence or absence of a positive charge would promote or retard biodegradability and toxicity. Furthermore the enzyme phenylalanine hydroxylase (PheOH) can convert phenylalanine into tyrosine by an oxidative insertion mechanism<sup>15</sup> and there exists the possibility that phenylalanine ILs could be converted *in vivo* to the tyrosine derivatives before undergoing biodegradation thus a number of L-tyrosine derived ILs were synthesised to investigate whether the presence of a phenolic OH group would affect the toxicity and biodegradability.



**Figure 2.2.** General structure of L-phenylalanine (left) and L-tyrosine (right) ILs synthesised.

### 2.2.1 The twelve principles of green chemistry and green chemistry metrics

ILs presented within this chapter were synthesised according to the 12 Principles of Green Chemistry. The following is an excerpt from a review published by Gathergood and Jordan (2013) entitled *Designing Safer and Greener Antibiotics* in which the 12 Principles are discussed.<sup>16</sup>

The twelve principles of green chemistry are a set of guidelines which “*have directed green chemists in their research endeavours since the late 1990's and were proposed by Anastas and Warner. The principles provide a framework that when adhered to can lead to synthetically useful molecules that are conceived, used, and disposed of, in a more environmentally friendly manner*”<sup>17</sup>.<sup>16</sup> ILs discussed within this chapter, and subsequently Chapter 3, were synthesised according to the following principles outlined by Anastas and Warner:

#### The twelve principles defined are as follows:

##### 1. Prevention

It is better to prevent waste than treating waste after it is produced.<sup>18</sup>

##### 2. Atom Economy

Synthetic methods should be employed so as to maximise incorporation of all reagents used, in the final product.<sup>19</sup>

##### 3. Less Hazardous Chemical Syntheses

When possible, reagents and synthetic methods less toxic to human health and the environment should be used.<sup>20</sup>

##### 4. Designing Safer Chemicals

Chemicals should be designed, fit for purpose, with minimum toxicity to humans and the environment.<sup>21</sup>

##### 5. Safer Solvents and Auxiliaries

The use of auxiliary substances such as solvents, drying agents etc. should be reduced when possible.<sup>22</sup>

##### 6. Design for Energy Efficiency

The energy required to perform a chemical process should be kept to a minimum, e.g. temperature and pressure conditions of reactions.<sup>23</sup>

##### 7. Use of Renewable Feedstocks



Raw materials should be from a renewable source if possible.<sup>24</sup>

#### 8. Reduce Derivatives

Unnecessary use of protecting groups and structural modifications should be avoided to minimise waste production and energy consumption.<sup>25</sup>

#### 9. Catalysis

Employing catalysts reduces waste and energy requirements and should be used when possible and appropriate, i.e. selectivity.<sup>26</sup>

#### 10. Design for Degradation

Synthetic molecules should be designed to breakdown in the environment after use to avoid chronic build-up effects. Eventual fate in the environment must be considered.<sup>27</sup>

#### 11. Real-time analysis for Pollution Prevention

Real-time process monitoring to control and prevent the production of potentially hazardous materials should be employed.<sup>28</sup>

#### 12. Inherently Safer Chemistry for Accident Prevention

Safer reagents, procedures and processes should be employed to reduce the chance of accidents and exposure of chemicals to the environment and people.<sup>29</sup>

*“By incorporating the design principles outlined above, chemists from academia and industry can effectively produce molecules that are fit for purpose and pose far less of a risk to the environment. By including biodegradation, toxicity, sustainability and life cycle assessment in design criteria, ranges of safer compounds can be effectively produced with reduced impact on ecosystems.”<sup>16</sup>*

*“To analyse a pharmaceutical process or a research project one must first produce a set of standards, tests or a scale with which to measure the projects “greenness”. Pioneers of green chemistry metrics in the early 1990s established concepts such as “Atom Economy (Trost)”<sup>19</sup>, “E-factor(Sheldon)”<sup>18</sup>, “Andraos Reaction Mass Efficiency”<sup>30</sup>, “GSK Reaction Mass Efficiency”, “Process Mass Intensity”, “Solvent Intensity”<sup>31-33</sup>. The concept is that every chemical process can be analysed and its greenness determined, compared and improved.*

*In recent years, there has been a drive in the pharmaceutical industry to produce an API with a minimum amount of waste. There is often an economic incentive as well as benefit to the environment. The largest materials usage in the pharmaceutical industry is solvents, which make*

up to 90% of material usage producing bulk API<sup>34</sup>. This makes solvent choice of paramount importance. Pharmaceutical companies have reported solvent selection guides, which illustrate pros and cons of common solvents used in their processes, including common chlorinated solvents and their alternatives.<sup>25</sup>

The atom economy of a reaction represents the percentage incorporation of starting materials into the final product, so a reaction with 100% atom economy will have complete incorporation of all starting materials into the product. For example, a Diels-Alder reaction can have up to 100% atom economy, whereas a Wittig reaction in general is rated with a very low value. However, percentage yield is not a consideration when calculating the atom economy. In addition, atom economy, which can be very easily calculated from a reaction scheme, does not take into account solvent and bulk materials used in the process (e.g., product isolation). The Sheldon “Environmental Factor”, or E-factor, does include solvents and waste parameters and is a simple calculation of waste quantity divided by product quantity; the lower the number the more environmentally acceptable the process.”

The equations associated with the green chemistry metrics are outlined as follows:

Atom Economy<sup>19</sup>, E-factor<sup>18</sup>, Andraos Reaction Mass Efficiency<sup>30</sup>, GSK Reaction Mass Efficiency<sup>35</sup>, Mass Intensity<sup>36</sup>, Solvent Intensity<sup>36</sup>, Stoichiometric Factor<sup>30</sup> and Material Recovery Parameter.<sup>33</sup>

$$\text{E factor} = \frac{\text{Total mass of waste}}{\text{Mass of product}}$$

$$\text{Solvent Intensity} = \frac{\text{Total mass of solvent (excluding water)}}{\text{Mass of Product}}$$

$$\text{Mass Intensity} = \frac{\text{Mass of all materials used (excluding water)}}{\text{Mass of product recovered}}$$

$$\text{GSK Reaction Mass Efficiency} = \frac{\text{Mass of product recovered}}{\text{Mass of all reactants}} \times 100\%$$

$$\text{Atom Economy} = \frac{\text{Molecular weight of desired product}}{\sum \text{Molecular weights of all reagents}}$$

$$\text{Andraos Reaction Mass Efficiency (RME)} = \frac{1}{1 + \text{E Factor}}$$

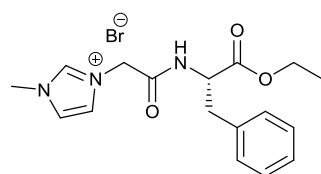
$$\text{Stoichiometric Factor} = 1 + \frac{\sum \text{mass of excess reagents}}{\sum \text{mass of stoichiometric reagents}}$$

Two variations of atom economy (AE) are reported in the literature. The outlined AE above includes the molecular weights of all reagents. This inclusion means that auxiliary bases and acids etc. that take part in the reaction but are not incorporated into the final product are considered in the calculation. The other reported AE calculation only takes the sum of the molecular weights of all reactants i.e. chemicals in the reaction that some portion of which are incorporated into the final product.<sup>37</sup> The AE calculation that is employed in this chapter includes all reagents as it was felt that this equation better represents the synthetic methodologies employed. The replacement of a high molecular weight auxiliary base with a lower molecular weight auxiliary base could reduce the overall mass of the reaction and can lead to greener synthesis and lower mass intensive processes.

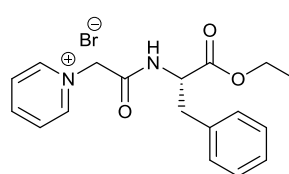
## **2.2.2 Synthesis**

### **2.2.2.1 Targets**

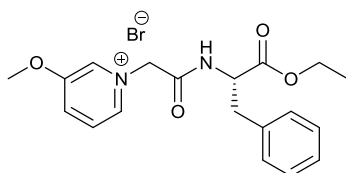
As previously stated in Section 2.1 and 2.2 the series of ILs (Figure 2.3) were designed with respect to Boethling's rules of thumb for designing biodegradable compounds,<sup>36</sup> the 12 principles of green chemistry,<sup>17</sup> and the preceding generations of research conducted within the Gathergood research group.<sup>5-10</sup> Ester group substituent was maintained as an ethyl ester for all compounds synthesised in this chapter to allow this study to demonstrate the effect of the headgroup on biodegradability and toxicity. Scope of headgroups includes cationic aromatic heterocycles, non-aromatic heterocycles and linear quaternary amines.



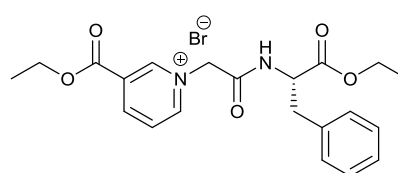
**324**



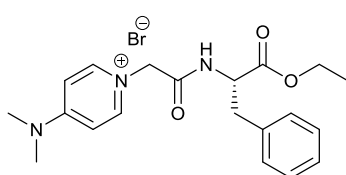
**325**



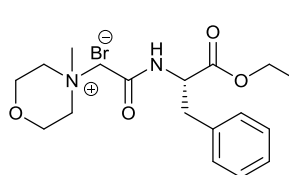
**326**



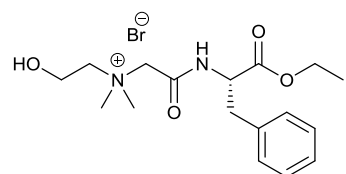
**327**



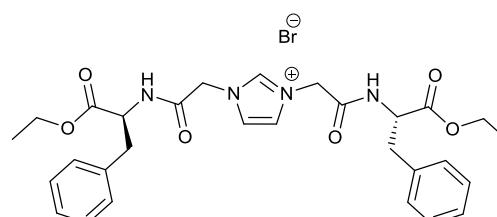
**328**



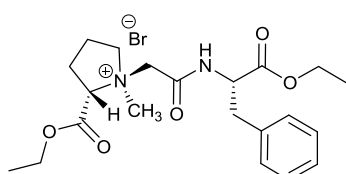
**329**



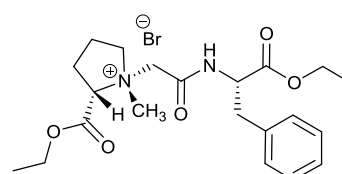
**330**



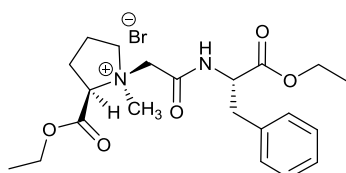
**331**



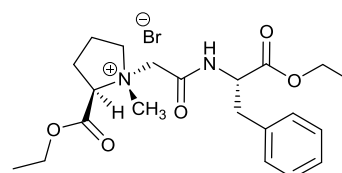
**332**



**333**



**334**

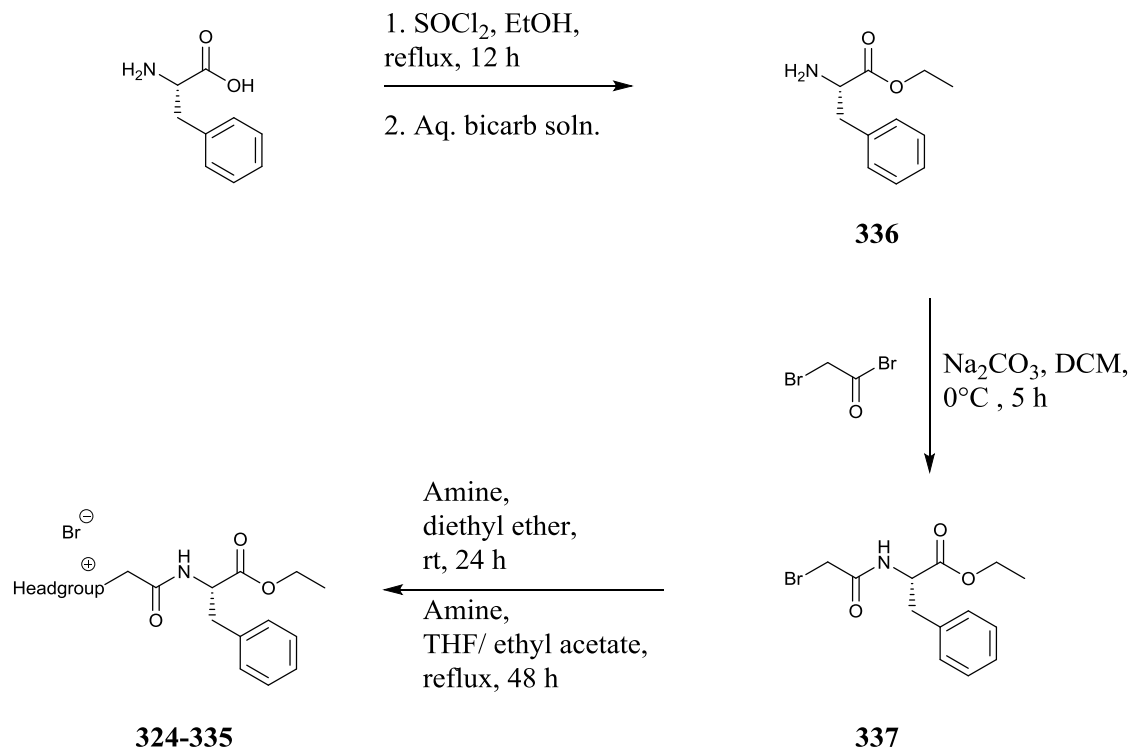


**335**

**Figure 2.3.** Target L-phenylalanine ILs synthesised.

### 2.2.2.2 Synthesis of L-phenylalanine ILs

A series of L-phenylalanine ILs (**324-335**) (Figure 2.3), were synthesised in a high yielding, three step synthesis outlined below in Scheme 2.1



**Scheme 2.1.** General synthetic route employed for L-phenylalanine bromide ILs (**324-335**).

**Step 1:** Fischer-Speier esterification of L-phenylalanine was carried out using thionyl chloride (to produce dry HCl *in situ*) and an excess of ethanol to furnish (**336**) as a HCl salt which was then subsequently neutralised to the free base amine (**336**).

**Step 2:** L-Phenylalanine derivative (**336**) from **step 1** was acylated to form the α-bromoamide (**337**). No column chromatography was required for purification at this stage.

**Step 3:** α-Bromoamide alkylating reagent (**337**) was reacted with the nitrogen heterocycle/tertiary amine of choice, usually in diethyl ether at room temperature for 24 hours, to yield ILs (**324-326**, **328-330**). IL (**327**) required reflux conditions in THF for 48 hours and ILs (**332-335**) required reflux conditions in ethyl acetate to achieve satisfactory yields. Alkylating reagent (**337**) is the key to this series of compounds as it represents a modular building block that acts as a platform to numerous other targets.

The synthesis outlined in Scheme 2.1 is a modification of that employed by Coleman and Gathergood<sup>5</sup> and presents an overall improvement in the formation of the alkylating reagent

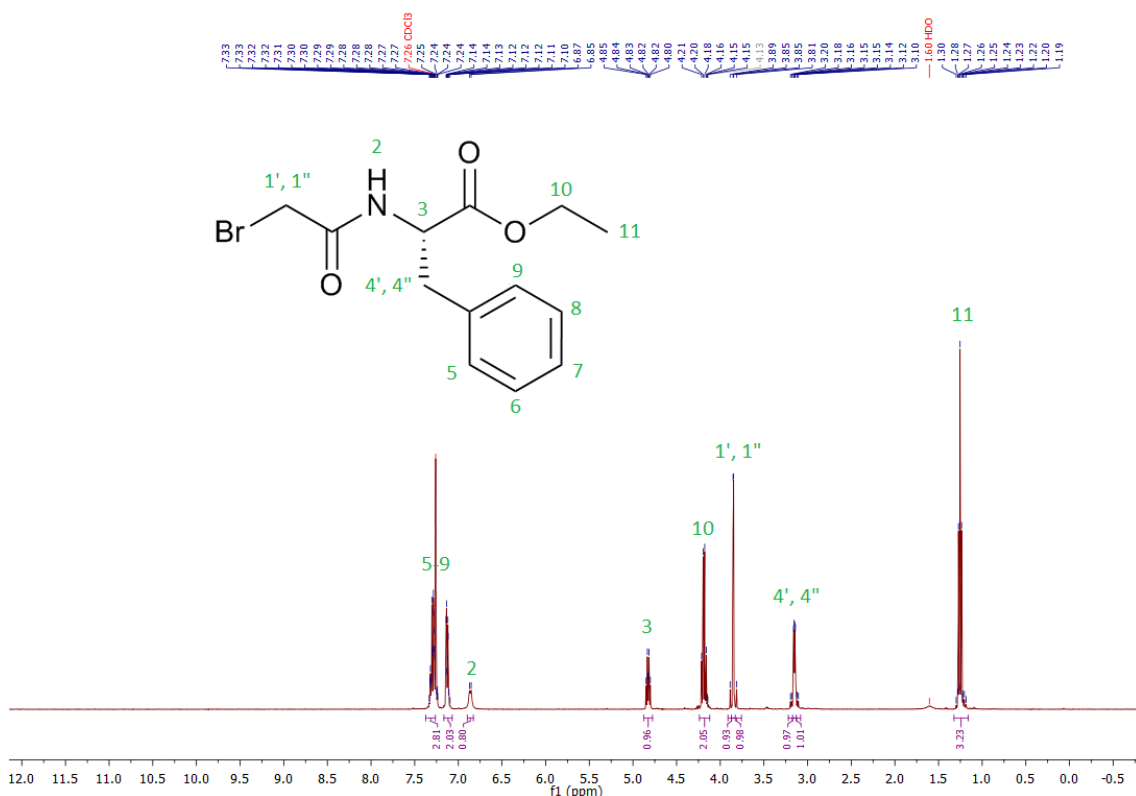
(**337**). The method outlined for the formation of (**337**) in the literature involves the reaction of an amino acid ester hydrochloride with an excess of  $\text{K}_2\text{CO}_3$  or TEA, and bromoacetyl bromide carried out at  $-78\text{ }^\circ\text{C}$ , conditions (**A**) (Table 2.1). This method results in the formation of coloured impurities if using TEA, possibly due to the Menshutkin reaction,<sup>38</sup> or TEA-Br having partial solubility in the organic layer that is not removed during an aqueous workup step. Changing the base for  $\text{Na}_2\text{CO}_3$  as in conditions (**B**) demonstrated that impurities were also present at the end of the reaction time due to the rate of neutralisation of the ester hydrochloride being too slow, thus encouraging the formation of side products. The synthesis route was modified so that the amino acid ester was neutralised to the free base form before being used in the reaction. An excess of  $\text{Na}_2\text{CO}_3$  was used as an auxiliary base to remove the HBr formed during the reaction. This pre-neutralisation step allowed the primary amine of the amino acid ester to rapidly and cleanly react with the bromoacetyl bromide subsequently added to the reaction and avoided the formation of unwanted side products. Room temperature reaction conditions were also employed with no formation of side products detected by TLC. Reaction conditions (**C**) resulted in a reaction mixture that could be purified by filtration to remove the  $\text{Na}_2\text{CO}_3$  followed by aqueous bicarbonate solution washings of the organic layer to remove any HBr and bromoacetic acid. Removal of the organic solvent *in vacuo* furnished the desired alkylating reagent in high yields as a white solid with no further purification required. Percentage yields from the various reaction conditions are summarised in Table 2.1. THF was also trialled as a replacement reaction solvent resulting in a good yield (74%) with a five hour reaction time and no chromatography required for purification, conditions (**D**). Similarly ethyl acetate was assessed as reaction solvent, conditions (**E**), however this time multiple impurities were detected by TLC after a five hour reaction time and no further work was carried out with this solvent.

**Table 2.1.** Summary of yields obtained for compound (**337**) acylation reaction optimisation.

Conditions	A	B	C	D	E
Yield ( <b>337</b> )	64% <sup>5</sup>	61%	89%	74%	N/A**
Starting Material	<b>336.HCl</b>	<b>336.HCl</b>	<b>336</b>	<b>336</b>	<b>336</b>
Base	TEA	$\text{Na}_2\text{CO}_3$	$\text{Na}_2\text{CO}_3$	$\text{Na}_2\text{CO}_3$	$\text{Na}_2\text{CO}_3$
Reaction time	5 h	5 h	3 h	5 h	5 h
Solvent	DCM	DCM	DCM	THF	Ethyl Acetate
Colum Chromatography Required?	Yes	No*	No	No	Yes

\*Bromoacetic acid detected by  $^1\text{H}$ -NMR, even after aqueous bicarbonate workup.

\*\* Multiple spots detected by TLC, no further work carried out.



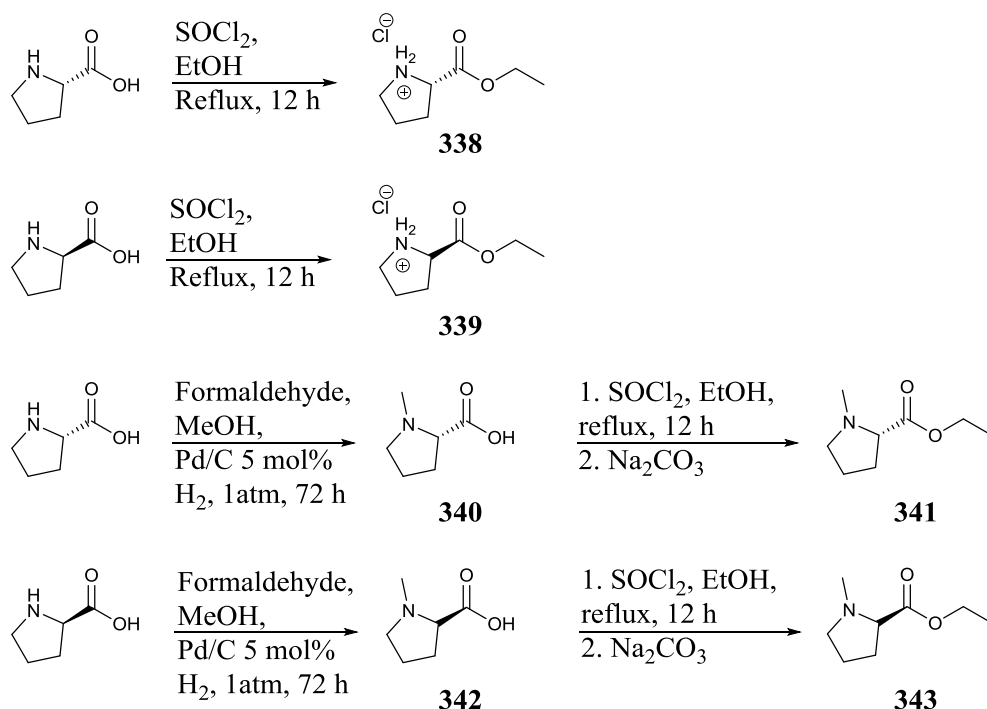
**Figure 2.4.**  $^1\text{H}$ -NMR of alkylating reagent (**337**) in  $\text{CDCl}_3$  after aqueous workup and drying.

From the  $^1\text{H}$ -NMR of alkylating reagent (**337**) (Figure 2.4) it can be seen that the L-phenylalanine sidechain appears as a 5 proton multiplet **5-9** in the aromatic region (7.33-7.10 ppm). The amide proton **2** appears as a doublet at 6.86 ppm coupling to the proton at the stereogenic centre at position **3** with  $J = 7.8$  Hz. At 4.83 ppm a doublet of triplets (dt) is visible with  $J = 7.8, 5.8$  Hz and can be attributed to the proton at stereogenic centre **3** coupling to the amide proton and the protons on the benzylic position of the L-phenylalanine sidechain **4**. One may expect to observe that the benzylic protons are inequivalent due to diastereotopic effects (i.e. the proton on the stereogenic centre **3** should be coupling to three inequivalent protons), giving rise to a doublet of doublet of doublets (ddd). However, when the two smaller coupling constants are the same in the ddd and overlap occurs then the ddd appears as a dt instead.<sup>39</sup> At 4.19 ppm the  $-\text{CO}_2\text{CH}_2-$  protons on the alkyl chain **10** are present, coupling to the neighbouring  $\text{CH}_3$  terminus **11** of the chain to give a quartet with  $J = 7.1$  Hz. Further upfield at 3.87 ppm and 3.83 ppm there are two doublets present which can be assigned as the protons **1'** and **1''**  $\alpha$  to the bromide atom. The presence of two doublets infers that these protons are not chemically equivalent and exhibit geminal coupling due to the protons diastereotopic nature. The protons **4'** and **4''** on the benzylic position of the L-phenylalanine sidechain occur as diastereotopic protons, coupling to the chiral proton **3** and to each other to give rise to two doublets of doublets at 3.17 ppm and 3.13 ppm with  $J = 6.0, 3.1$  Hz. Lastly the  $\text{CH}_3$  terminus of the alkyl chain **11** is

present at 1.25 ppm as a triplet, coupling to the neighbouring CH<sub>2</sub> protons on the alkyl chain with  $J = 7.1$  Hz.

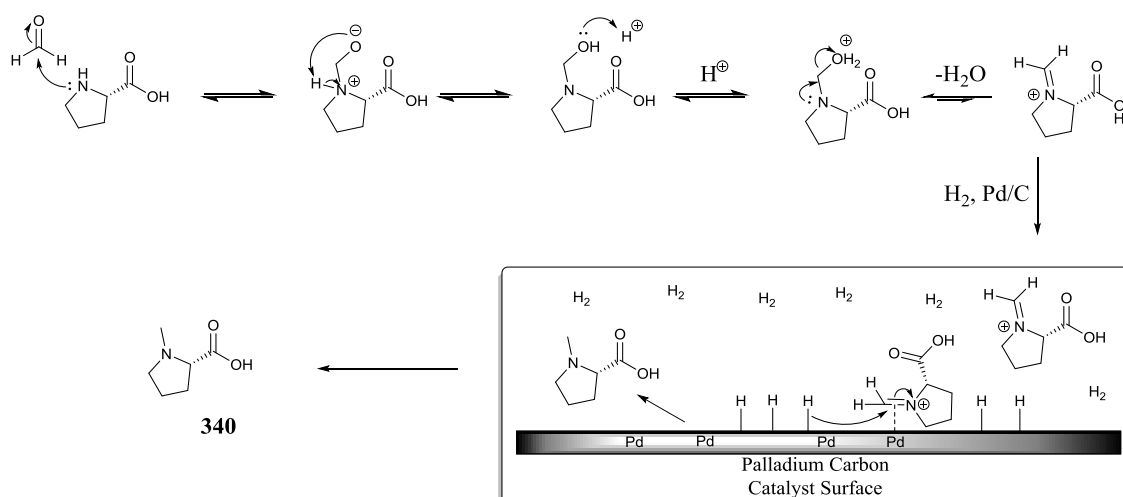
### 2.2.2.3 Synthesis of nitrogen heterocycles

Not all nitrogen heterocycles were commercially available and examples (**338-343**) were synthesised as outlined in Scheme 2.2. Synthesis of proline esters was accomplished as described for L-phenylalanine ester (**336**). Synthesis of *N*-methyl proline was by reductive amination of formaldehyde, using an excess of aqueous formaldehyde solution under a H<sub>2</sub> atmosphere in the presence of 1-5 mol% of Pd/C. The mechanism is outlined in Scheme 2.3. and the reaction was carried out according to the literature procedure of Lin *et al.*<sup>40</sup>

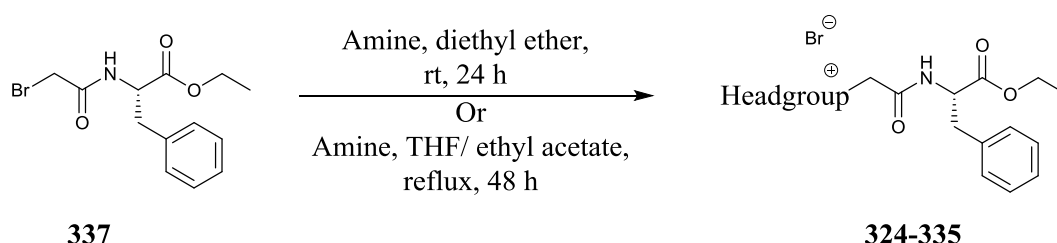


**Scheme 2.2.** General scheme for the synthesis of D- and L-Proline heterocycles (**338-343**).





**Scheme 2.3.** Reaction mechanism for the reductive alkylation of L-proline.



**Scheme 2.4.** Alkylation of tertiary amines with (337) to give ILs (324-335).

The reaction of (337) with amines of choice gave ILs (324-335), in up to excellent yield (e.g. ILs 325, 330 98%) although a wide range of yields (13-98%) was observed (Table 2.2). Reactivity of the amines used and the ease in which the target precipitated can be directly compared to the range in yields observed. Reduced yields for ILs (327, 331-335) is most likely due to the presence of electron withdrawing groups on the 3-position of a number of the heterocycles, specifically the ethyl esters present on the ethyl nicotinium IL (327) and on the prolinium derivatives (332-335), which reduce the overall nucleophilicity of the nitrogen heteroatom. Reduced yield for (329) is attributed to the slower rate of precipitation observed. No purification was required for the majority of the compounds except for final purification of (327) from unreacted ethyl nicotinate. Separation of the epimers (332-333) and (334-335) was carried out by silica gel chromatography. Separation of the epimers (332-333) and (334-335) was carried out by silica gel chromatography. For the reaction that produced epimer pair (332, 333) a ratio of 5:2 (IL 332: IL 333) was estimated by  $^1\text{H-NMR}$  before purification. Similarly for epimers (334, 335) a ratio of 5:2 was also observed (IL 335: IL 334). Determination of absolute stereochemistry for these derivatives is discussed in Section 2.2.2.4.

**Table 2.2.** Yields under different conditions for L-phenylalanine ILs (**324-335**).

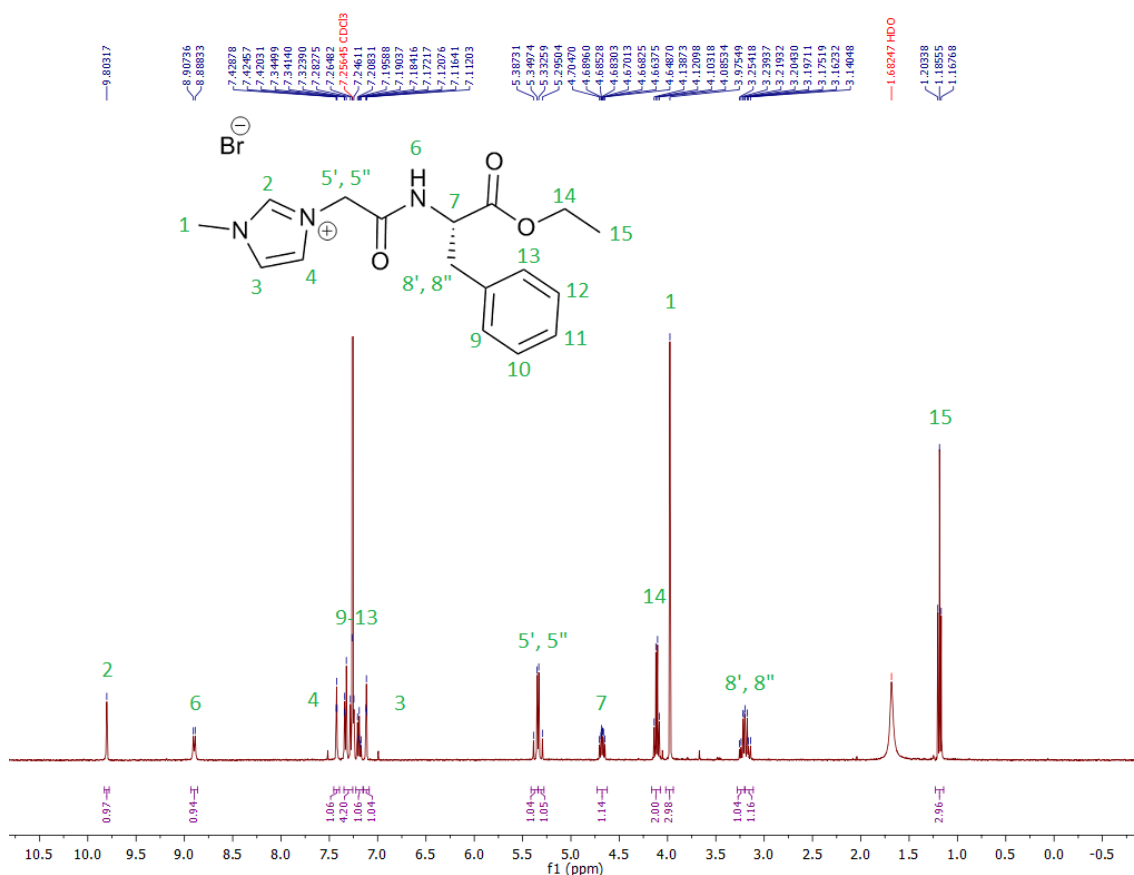
Compound	Reaction Conditions	Yield %
<b>324</b>	Diethyl Ether, rt, 24 h,	89
<b>325</b>	Diethyl Ether, rt, 24 h,	98
<b>326</b>	Diethyl Ether, rt, 24 h,	96
<b>327</b>	Diethyl Ether, rt, 24 h,	0*
<b>327</b>	THF, reflux, 48 h	56
<b>328</b>	Diethyl Ether, rt, 24 h,	88
<b>329</b>	Diethyl Ether, rt, 24 h,	34
<b>330</b>	Diethyl Ether, rt, 24 h,	99
<b>331</b>	Diethyl Ether, rt, 24 h,	91
<b>332</b>	Ethyl Acetate, reflux, 48 h	37
<b>332</b>	Diethyl Ether, rt, 24 h,	0*
<b>333</b>	Ethyl Acetate, reflux, 48 h	13
<b>333</b>	Diethyl Ether, rt, 24 h,	0*
<b>334</b>	Ethyl Acetate, reflux, 48 h	25
<b>335</b>	Ethyl Acetate, reflux, 48 h	34

\*No product detected by TLC 10% MeOH:DCM

From Table 2.3 a wide range of melting points for the ILs synthesised can also be observed (60-164 °C). Under the classical definition of an IL existing as a liquid below 100 °C all examples with the exception of (**328**, **329**, **331**) conform, though (**325**, **330**) have melting points very close to 100 °C.

**Table 2.3.** Melting points (uncorrected) obtained for L-phenylalanine ILs (**324-335**).

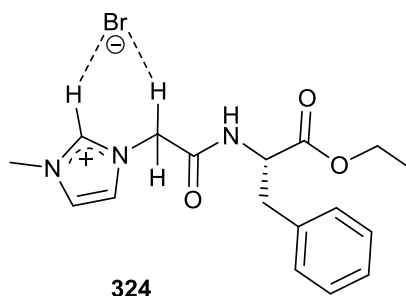
Compound	Melting Point °C
<b>324</b>	77-79
<b>325</b>	98-100
<b>326</b>	72-74
<b>327</b>	60-62
<b>328</b>	135-137
<b>329</b>	162-164
<b>330</b>	97-99
<b>331</b>	102-104
<b>332</b>	Liquid at RT
<b>333</b>	Liquid at RT
<b>334</b>	Liquid at RT
<b>335</b>	Liquid at RT



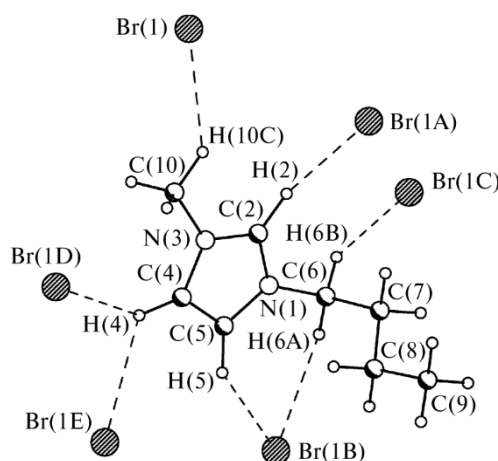
**Figure 2.5.**  $^1\text{H}$ -NMR of Imidazolium IL (**324**) in  $\text{CDCl}_3$  .

From the  $^1\text{H}$ -NMR of (**324**) (Figure 2.5) it can be seen that the single C-H proton on the imidazolium ring C<sub>2</sub> position **2** appears as a singlet far downfield at 9.80 ppm. Amide proton **6** is present as a doublet at 8.90 ppm with a coupling constant  $J = 1.7$  Hz, coupling to the proton on the stereogenic position **7**. The aromatic region of 7.42-7.11 ppm contains 7 protons, two methine protons from the imidazolium ring are present **3**, **4**, and the protons on the phenyl ring of the L-phenylalanine group **9-13**. CH<sub>2</sub> protons,  $\alpha$  to the carbonyl group of the amide linker **5'**, **5''** are present at 5.37 ppm and 5.31 ppm as two sets of doublets due to their diastereotopicity. It is proposed that the presence of the doublets could also be due to hydrogen bonding of the protons **5'**, **5''** to the bromide counterion introducing an inequivalency and hence geminal coupling of the protons with  $J = 15.0$  Hz. The mode of bonding is proposed in Figure 2.6. Protons **5'**, **5''** are present as two doublets at 3.87 ppm and 3.85 ppm in the alkylating reagent (**337**),  $\alpha$  to the bromide atom, and are shifted downfield in the  $^1\text{H}$ -NMR of (**324**) by 1.5 ppm due to the much higher electron withdrawing effect of the imidazolium group compared to the bromine. The proton at the stereogenic centre **7** is present as a doublet of doublet of doublets at 4.67 ppm due to the coupling of proton **7** to amide proton **6** and the inequivalent protons on the benzylic position of the phenylalanine sidechain **8'**, **8''**. At 4.11 ppm a quartet is observed due to the  $\alpha$ -protons of the ester group **14** coupling to the terminal CH<sub>3</sub> **15** with  $J = 7.2$  Hz. The singlet peak at 3.98 ppm is attributed to the *N*-methyl group on the imidazolium ring **1**. Diastereotopic

protons **8'**, **8''** of the phenylalanine side chain are present at 3.23 ppm and 3.17 ppm as two sets of doublet of doublets with  $J = 14.0, 6.0$  Hz, due to each protons vicinal coupling to proton **7** and geminal coupling. Lastly the terminal CH<sub>3</sub> group appears as a triplet at 1.18 ppm with  $J = 7.2$  Hz.

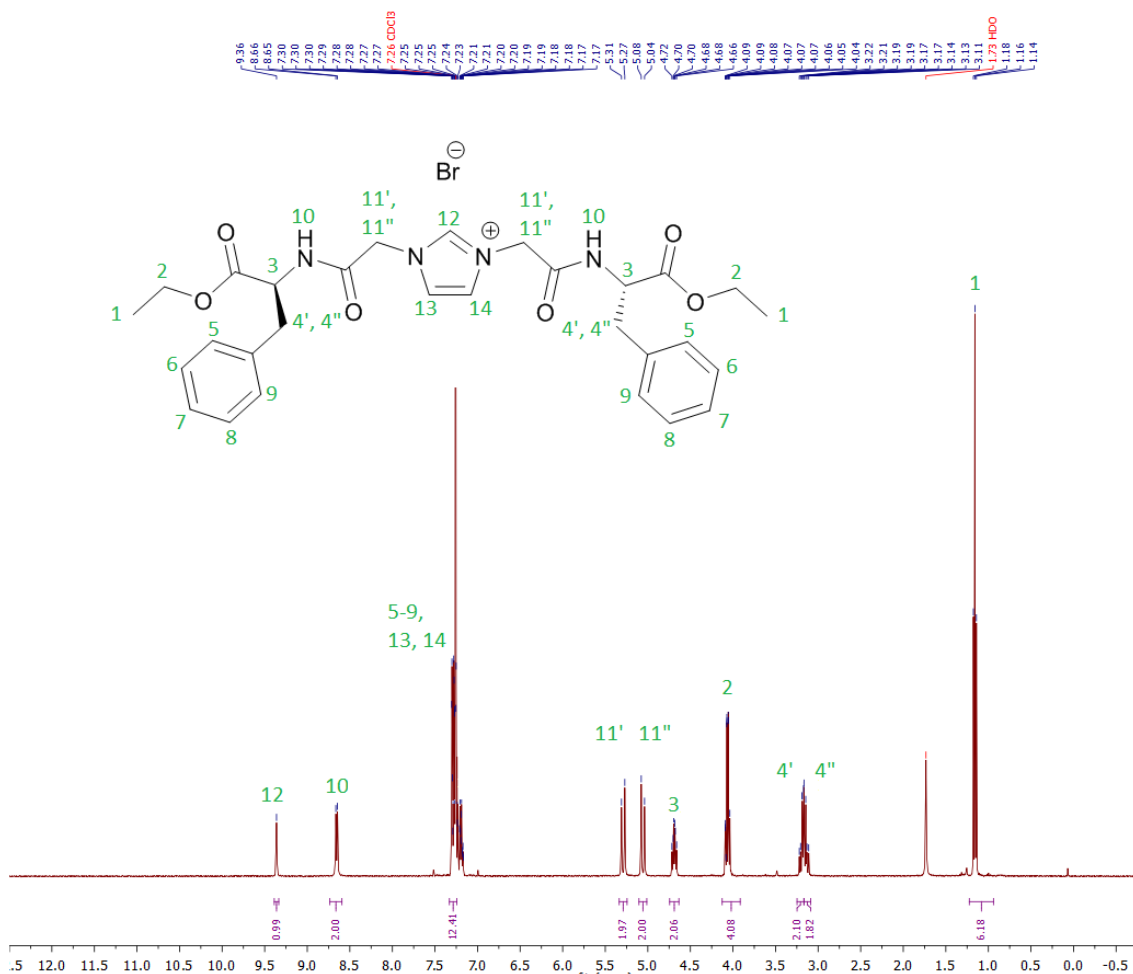


**Figure 2.6.** Proposed hydrogen bonding interaction between the imidazolium headgroup, amide linker and bromide counterion.



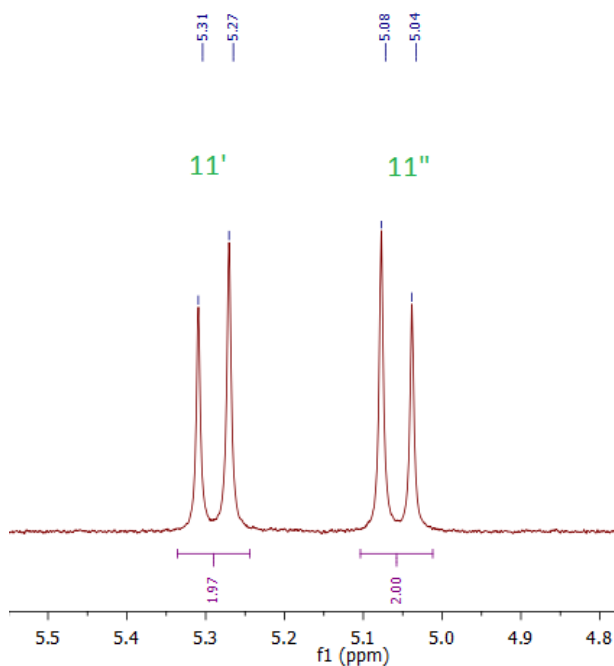
**Figure 2.7.** X-ray crystal structure and CH-Br contacts for [bmim][Br].

The proposed mode of binding to the proton attached to carbon C2 and also to the sidechain protons is supported by the x-ray crystal structures of a series of ILs published by Shaplov *et al.*, see [bmim][Br] (Figure 2.7).<sup>41</sup>



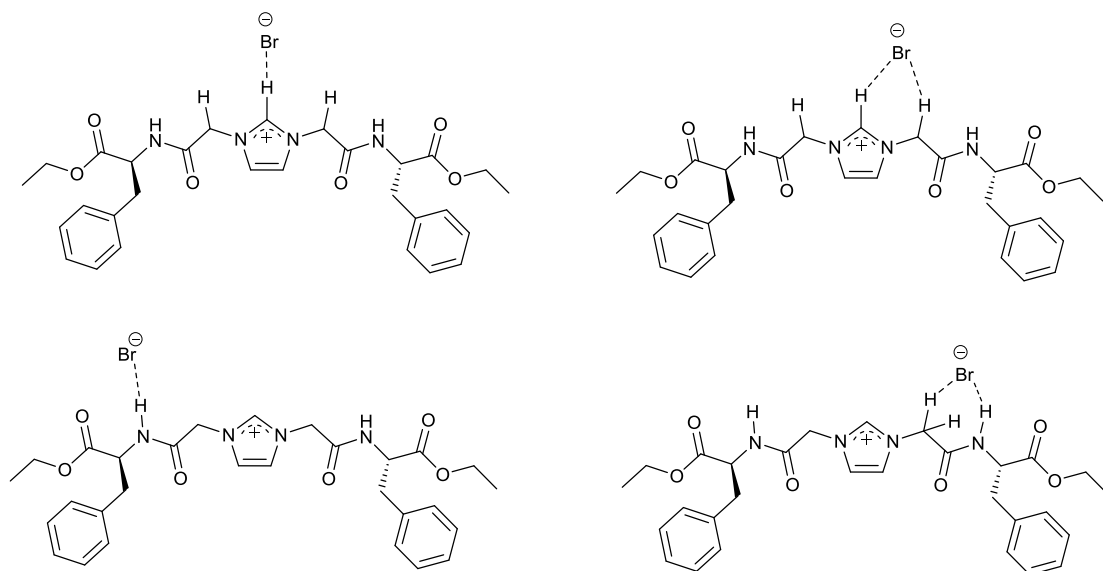
**Figure 2.8.**  $^1\text{H}$ -NMR of  $\text{C}_2$  Symmetric IL (**331**).

When a  $\text{C}_2$  symmetric derivative (**331**) was analysed, a very different  $^1\text{H}$ -NMR is observed (Figure 2.8).  $\text{CH}_2$  protons,  $\alpha$  to the carbonyl group of the amide linker **11'**, **11''** are now present as two distinct doublets,  $J = 15.6$  Hz, with much larger ppm separation than that present in (**324**). The roofing effect is also visible (Figure 2.9). It is proposed that the counterion is hydrogen bonding to the C2 proton on the imidazolium ring **12** and the two  $-\text{CH}_2$  protons on the amide linker (Figure 2.10). Benzylic protons **4'**, **4''** are visible as two sets of doublets of doublets at 3.14 ppm and 3.20 ppm due to their diastereotopicity, coupling geminally to give a doublet and vicinally with the stereogenic centre protons **3**, **17** to give another doublet, i.e. a doublet of doublets with  $J = 15.6$  Hz. Protons **3**, are visible as a triplet of doublets at 4.69 ppm with  $J = 8.2$  and 6.0 Hz, coupling to the amide protons **10** to give a doublet which in turn is further split by the coupling to the diastereotopic protons **4'**, **4''**.



**Figure 2.9.** Doublets and the roofing effect.

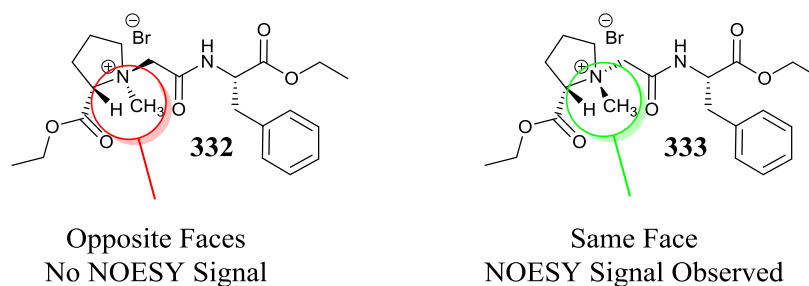
Proposed counterion binding modes are illustrated in Figure 2.10. The bromide anion could potentially hydrogen bond to the acidic C2 proton on the imidazole ring or to the *N*-H protons on the amide linker. Chemical shifts of the CH<sub>2</sub> protons observed,  $\alpha$  to the carbonyl groups, also suggests that hydrogen bonding to the anion could be taking place, as per Figure 2.6, 2.7. Furthermore a combination of each of the proposed binding modes could be taking place.



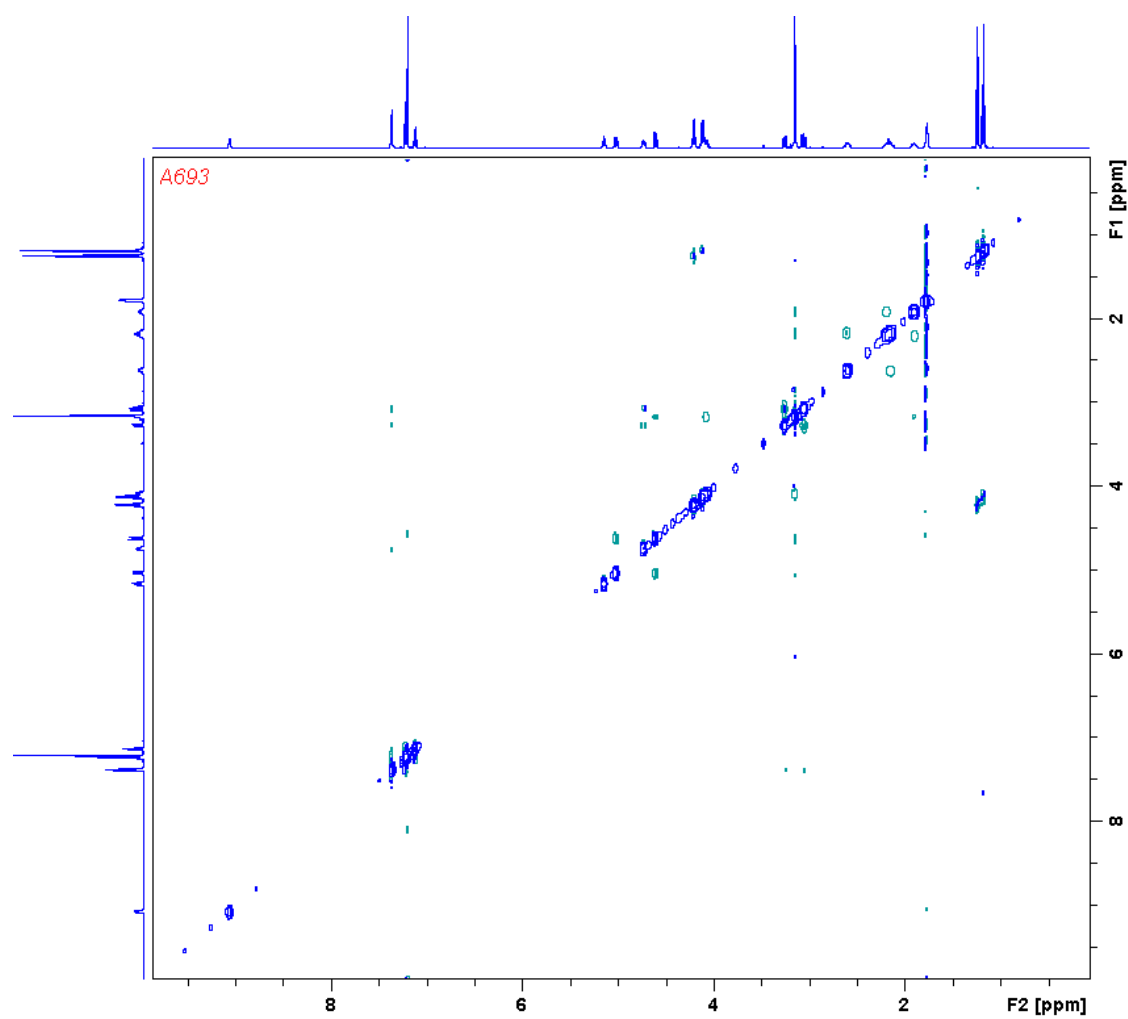
**Figure 2.10.** Proposed possible counter ion binding of C<sub>2</sub> symmetric IL (331).

#### 2.2.2.4 NOESY assignments of prolinium ILs

The absolute stereochemistry of prolinium derivatives (**332-335**) was determined by 2-dimensional NMR by utilising the nuclear overhauser effect i.e. a NOESY experiment. Under the experiments parameters, cross relaxation between individual nuclear spins is used to provide correlations between atoms that are spatially close, rather than through the sigma bond network. This type of experiment thus allows the determination of stereochemistry as groups that are close to each other on the same face, or cis, will exhibit a NOESY correlation and groups that are trans may not.<sup>42</sup> To determine the stereochemistry of the epimer pair (**332-333**) the alpha proton at the stereogenic centre of the *N*-methyl-L-prolinium headgroup was identified, as were the protons belonging to the *N*-methyl group on the same headgroup (Figure 2.11). Derivative (**332**) should therefore not provide a signal by NOESY and derivative (**333**) should.

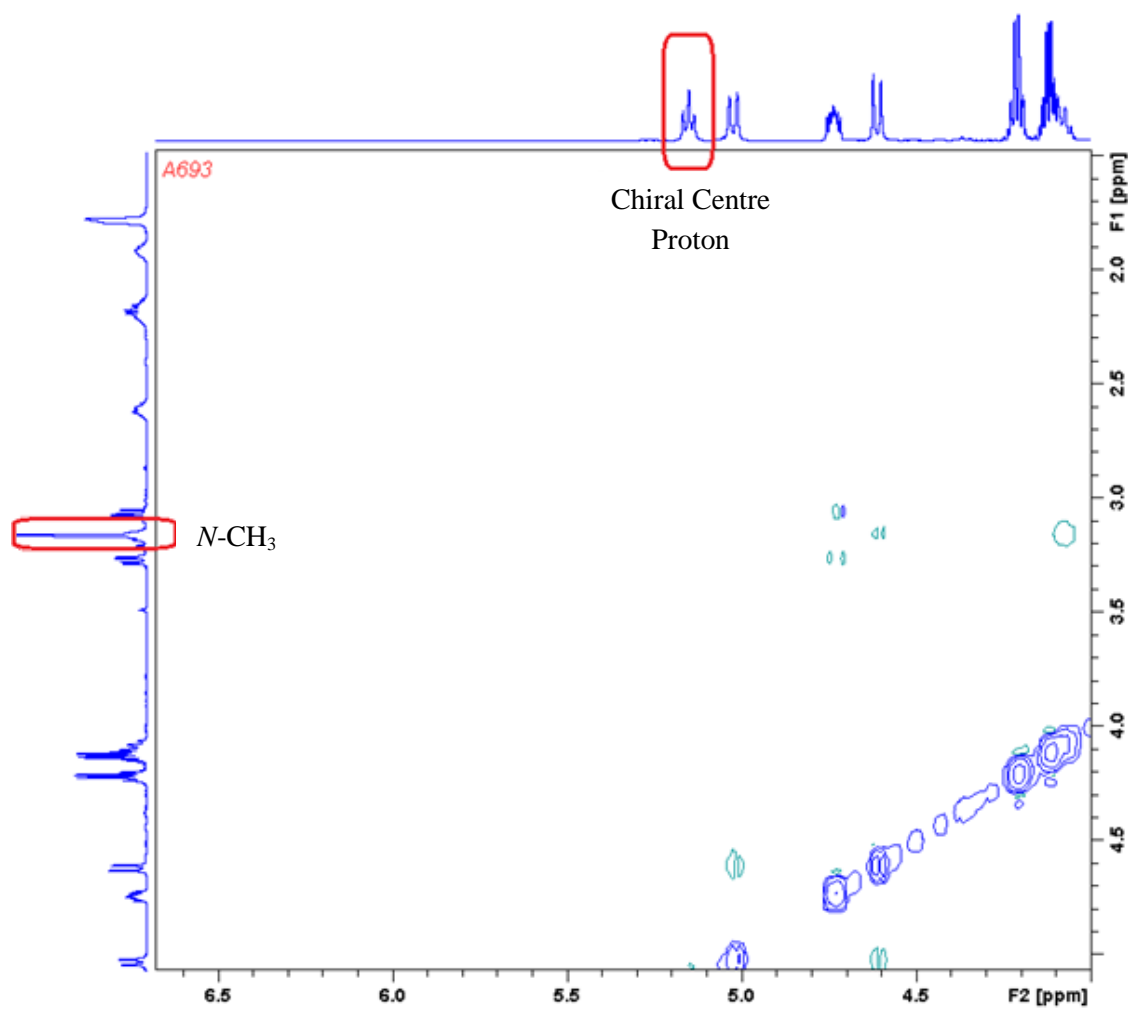


**Figure 2.11.** H to CH<sub>3</sub> NOESY rationale.

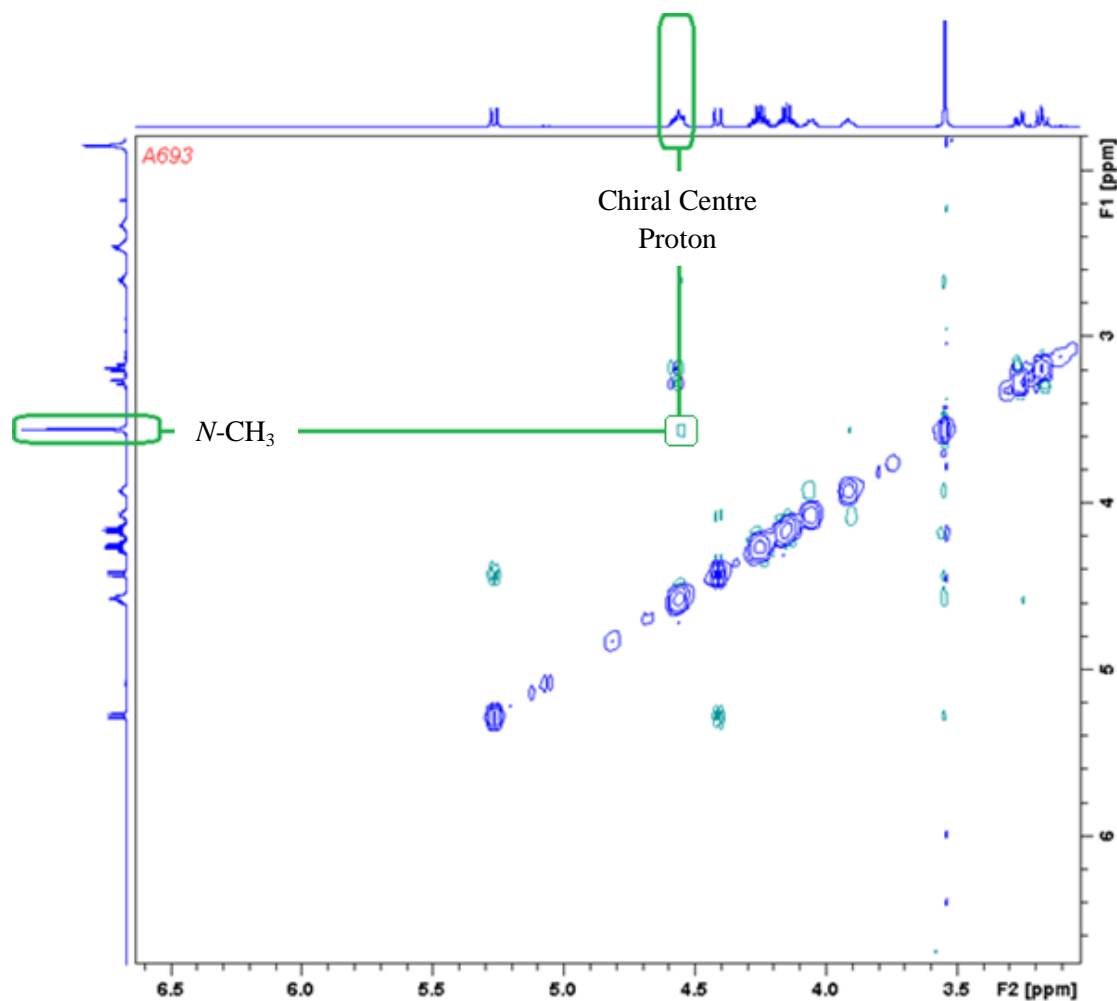


**Figure 2.12.** Example of a full NOESY spectra of (332).



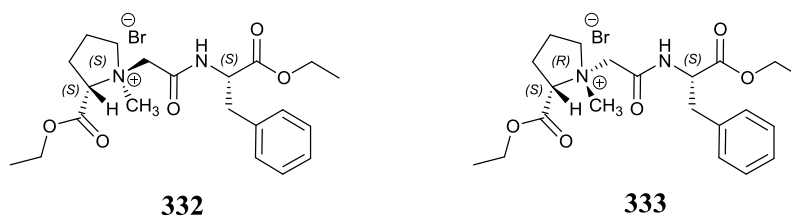


**Figure 2.13.** Close up of NOESY spectra of (332), note there is no NOESY signal correlating to the *N*-CH<sub>3</sub> and the H alpha to the carbonyl on the prolinium headgroup.



**Figure 2.14.** NOESY spectra of (**333**), note the NOESY signal produce at the intersection of the two green lines.

From the comparison of the two NOESY spectra produced (Figures 2.13-2.14) it can be concluded that (**332**) and (**333**) possessed the absolute stereochemistry as depicted in Figure 2.15.

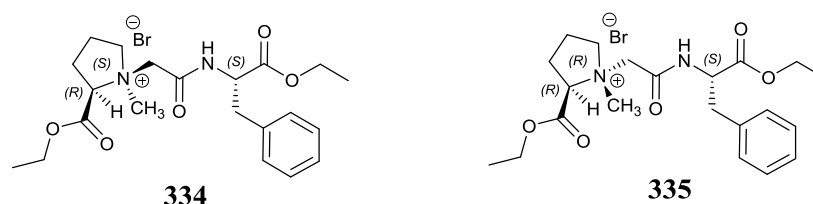


**Figure 2.15.** Absolute stereochemistry for (**332-333**) as determined by NOESY.

**332** = (1*S*,2*S*)-1-([[(2*S*)-1-ethoxy-1-oxo-3-phenylpropan-2-yl]carbamoyl]methyl)-2-(ethoxycarbonyl)-1-methylpyrrolidin-1-ium bromide

**333** = (1*R*,2*S*)-1-([[(2*S*)-1-ethoxy-1-oxo-3-phenylpropan-2-yl]carbamoyl]methyl)-2-(ethoxycarbonyl)-1-methylpyrrolidin-1-ium bromide

Similarly the absolute stereochemistry for (**334-335**) was determined as shown in Figure 2.16.



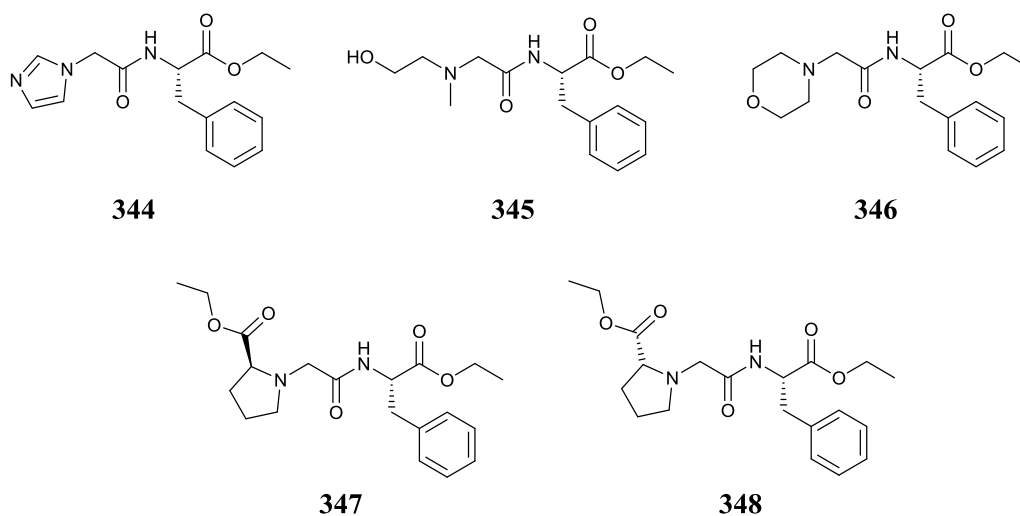
**Figure 2.16.** Absolute stereochemistry of ILs (**334-335**) as confirmed by NOESY experiments.

**334** = (1*S*,2*R*)-1-([[(2*S*)-1-ethoxy-1-oxo-3-phenylpropan-2-yl]carbamoyl]methyl)-2-(ethoxycarbonyl)-1-methylpyrrolidin-1-ium bromide.

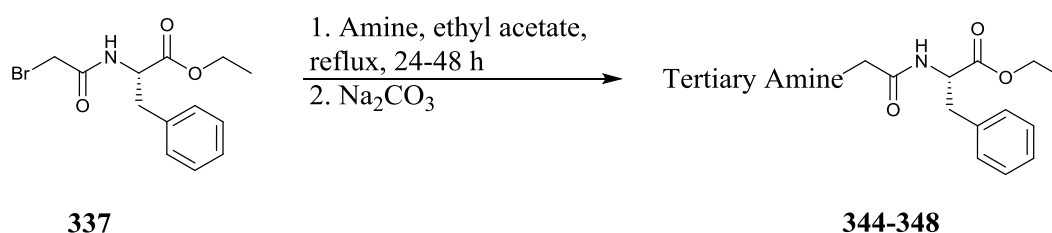
**335** = (1*R*,2*R*)-1-([[(2*S*)-1-ethoxy-1-oxo-3-phenylpropan-2-yl]carbamoyl]methyl)-2-(ethoxycarbonyl)-1-methylpyrrolidin-1-ium bromide.

#### 2.2.2.5 Synthesis of L-phenylalanine tertiary amino analogues

In parallel to the ILs synthesised in Section 2.2.2.2, a number of neutral tertiary amino derivatives (**344-348**) of the ILs were synthesised to investigate whether the charge on the quaternary amine affected the toxicity and biodegradability of the ILs (Figure 2.17). The neutral derivatives were synthesised according to modified routes (see Chapter 5, Section 5.3) than that in Scheme 2.1 and all were derived from alkylating reagent (**337**) to give compounds (**344-348**).



**Figure 2.17:** Tertiary amino derivatives synthesised.



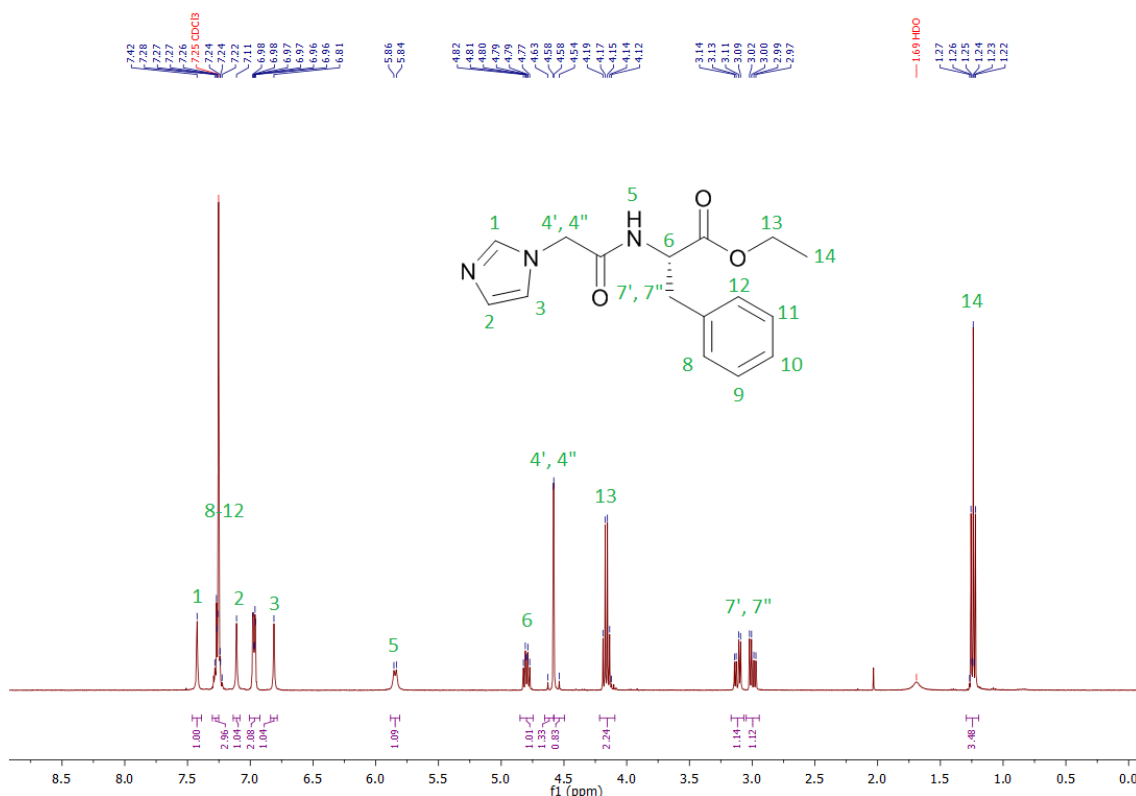
**Scheme 2.5.** Alkylation of secondary amines with (**337**) to give ILs (**344-348**).

The neutral derivatives (**344-348**) (Figure 2.17) represented a slightly more challenging synthesis as quaternisation of the tertiary amines formed during the reaction was possible, though unlikely for some of the more sterically hindered compounds (**347-348**) (Scheme 2.5). Also, as one equivalent of HBr is produced for every equivalent of product produced solid Na<sub>2</sub>CO<sub>3</sub> was stirred into the crude reaction products for ILs (**346-348**) for 1 hour to furnish the targets as their free base amines. Purification by column chromatography was employed for these compounds and in general the yields were lower than for their respective ILs (Table 2.4). One reason for this is that the driving force present in most IL formation reactions is precipitation of the product as soon as it is formed. Unfortunately the reactions did not proceed rapidly in diethyl ether and the products did not precipitate. Reaction conditions were altered to refluxing in ethyl acetate for 24-48 hours and no precipitation occurred under these conditions either, the products staying in solution. All of the neutral analogues synthesised were liquids at room temperature.

The yield for (**345**), 33%, is lower than that observed for the other tertiary amines (53-58%). This may be due to quaternisation of the tertiary amine with two equivalents of alkylating reagent (**337**). Another possible reason may be that a proportion of the target product was in HBr salt form and was not liberated to the free base form before purification, hence trapping a significant proportion on the silica gel utilised.

**Table 2.4.** Percentage yields obtained for for L-phenylalanine tertiary amino analogues.

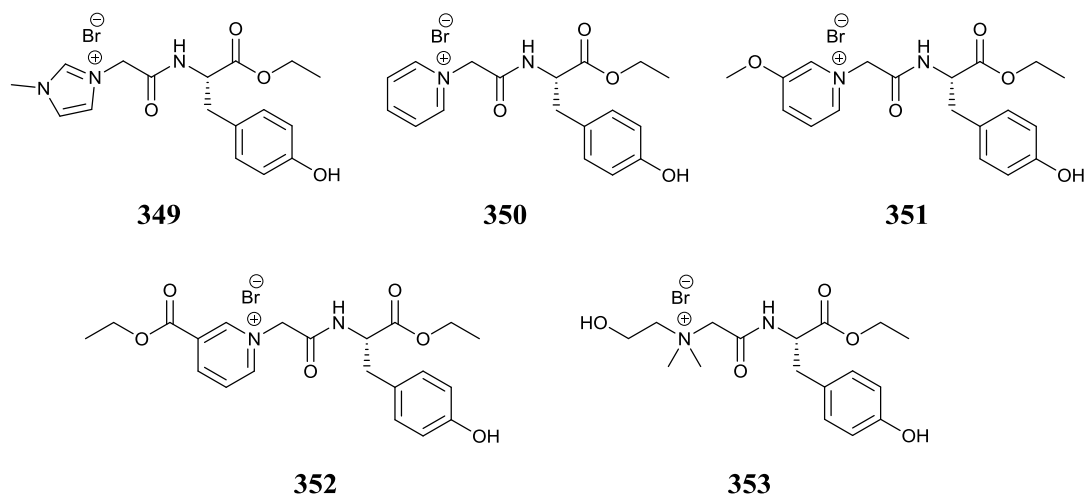
Compound	Yield %
<b>344</b>	55
<b>345</b>	34
<b>346</b>	57
<b>347</b>	53
<b>348</b>	58



**Figure 2.18.**  $^1\text{H}$ -NMR of neutral imidazole analogue (**344**) in  $\text{CDCl}_3$ .

From the  $^1\text{H}$ -NMR of (**344**) (Figure 2.18) it can be seen that the  $-\text{CH}_2$  protons  $\alpha$  to the carbonyl group of the amide linker **4'**, **4''** are not as shifted downfield as those present in the typical ILs present in Section 2.2.2.2 and are present as two doublets at 4.57 ppm and 4.56 ppm respectively with  $J = 17.2$  Hz. It can also be observed that the C2 proton of the imidazole ring **1** at 7.42 ppm is no longer shifted so far downfield in comparison to imidazolium IL (**324**) due to the reduced electron withdrawing environment present. Amide proton **5** is also shifted upfield considerably from 8.90 ppm in IL (**324**) to 5.94 ppm in this tertiary amino example.

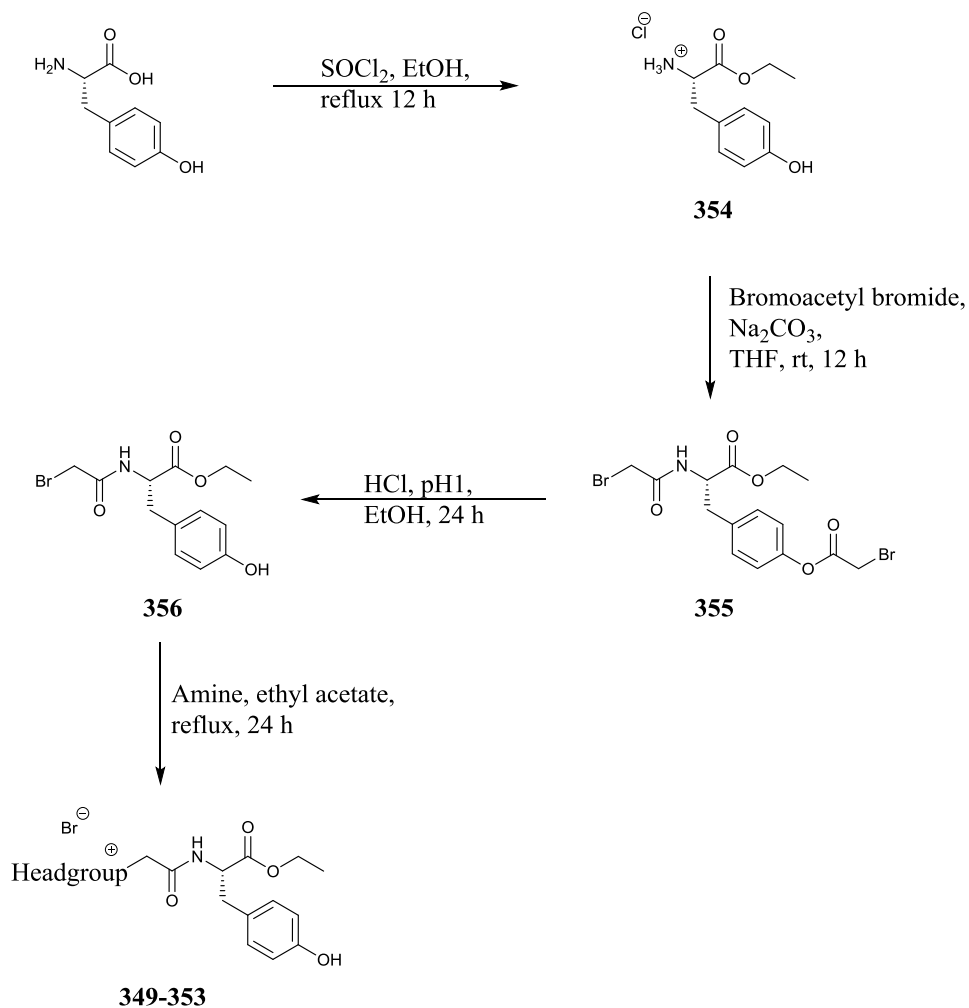
### 2.2.2.6 Synthesis of L-tyrosine analogues



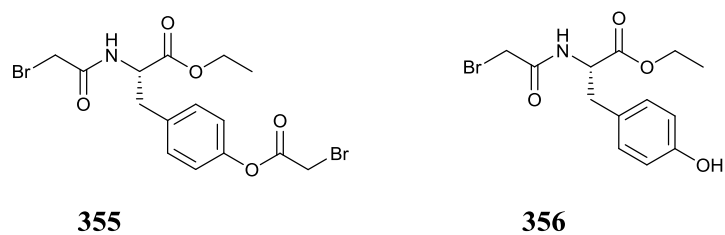
**Figure 2.19.** L-Tyrosine ILs (**349-353**) synthesised.

A subseries of ILs derived from L-tyrosine was also prepared (Figure 2.19) the aim of which was to investigate whether the additional –OH functionality in the tyrosine side chain would affect biodegradability and/or toxicity. As previously discussed, the enzyme PheOH can convert phenylalanine into tyrosine by an oxidative insertion mechanism<sup>15</sup> and there exists the possibility that the phenylalanine ILs studied in Section 2.2.2.2 could be converted *in vivo* to the tyrosine derivatives before undergoing biodegradation. The tyrosine derivatives were therefore synthesised to investigate the possibility of any enhanced biodegradation due to the presence of the phenolic –OH group.

The ILs were synthesised according to the route outlined in Scheme 2.6, a modification of Scheme 2.1 discussed previously in Section 2.2.2.2. **Step 1** of the synthesis was carried out as per Scheme 2.1 with an esterification reaction, this time with L-tyrosine and SOCl<sub>2</sub> to give L-tyrosine ethyl ester hydrochloride salt (**354**). Acylation of the ester (**354**) in **step 2** produced target  $\alpha$ -bromoamide (**356**) and over acylated phenolic ester (**355**) (Figure 2.20). Phenolic ester (**355**) was easily converted to (**356**) by acid hydrolysis in ethanol in **step 3** and a facile purification by precipitation furnished the desired compound in 54% yield.  $\alpha$ -Bromoamide (**356**) was then reacted with the nitrogen heterocycle of choice or dimethylamino ethanol (Scheme 2.6) in **step 4** to afford the series of L-tyrosine ILs (**349-353**).



**Scheme 2.6.** Synthetic route employed for the synthesis of L-tyrosine ILs.



**Figure 2.20.** L-Tyrosine alkylating reagents synthesised.

**Table 2.5.** Percentage yields and melting points for L-tyrosine ILs synthesised.

Compound	Yield %	Melting Point °C
<b>349</b>	83	38-40
<b>350</b>	99	30-32
<b>351</b>	99	117-119
<b>352</b>	71	53-55
<b>353</b>	79	141-143

The yields for the final tyrosine ILs (**349-353**) were in general moderate (e.g. 71%, **352**) to high (e.g. 99%, **350**, **351**). Derivative (**352**) was isolated in lower yields due to the harsher conditions and column chromatography required for final purification. Derivative (**349**) and (**353**) precipitated more slowly than expected and a longer reaction time or a solvent switch to ethyl acetate/THF and reflux conditions may aid in improving the yields (Table 2.5).

A broad range of melting points (30-32 to 141-143 °C) were observed for the tyrosine derivatives with the imidazolium IL (**349**) 38-40 °C, and pyridinium IL (**350**) 30-32 °C, the lowest. Introduction of an ester group to the pyridinium ring gave an increase in melting point (**350** vs **352**) to 53-55 °C and much higher melting points were observed for the 3-methoxy pyridinium derivative (**351**) 117-119 °C and the cholinium derivative (**353**) 141-143°C. The presence of the –OH group on the tyrosine ring greatly reduces the melting points of several of the ILs (**349**, **350** and **352**) when compared to their L-phenylalanine counterparts. A decrease of 40°C was observed for the imidazolium IL (**349** vs **324**), 68°C for pyridinium IL (**350** vs **325**), and a modest decrease in melting point of 7 °C for ethyl nicotinium (**352** vs **327**). Exceptions to this trend are the 3-methoxypyridinium IL (**326**) where an increase in melting point of 45 °C was observed and cholinium IL (**353**) with an increase of 40 °C when compared to their phenylalanine counterparts, **325** and **330** respectively.

#### 2.2.2.7 Green chemistry metrics

A number of green chemistry metrics were calculated for the amino acid esters (**336**, **338**, **339**, **341**, **343**, **354**), reductive alkylation products (**340**, **342**), alkylating reagents (**337**, **356**), L-phenylalanine ILs (**324-348**), neutral tertiary amino L-phenylalanine derivatives (**344-348**) and L-tyrosine ILs (**349-353**). The parameters calculated are as defined in Section 2.2.1. The metrics are presented in Table 2.6

It can be seen from the generated metrics that the synthesis of all the ILs had a 100% atom economy, a high E-factor, high GSK RME and a high stoichiometric factor. The Andraos RME is lower as it takes into account all solvent used in the IL washing steps. For the IL products that required purification by column chromatography (**327**, **332-335**, **352**), a much higher solvent intensity and mass intensity is also observed due to the amount of solvent required. Trituration and chromatography solvent should therefore be recycled in the future or if this process were to be scaled up in order to reduce the mass/solvent intensity, E-factor and material recovery parameters. Metrics generated for tertiary amino derivatives (**344-348**) are less desirable as lower yields and a higher consumption of solvent due to the purification by column chromatography was required.



Alkylating reagents (**337**, **356**) were both synthesised with moderate atom economy and a generally lower E-factor than the ILs. Moderate atom economy is observed due to the use of bromoacetyl bromide which is not fully incorporated into the product as one bromine atom is lost in the form of HBr. The presence of an auxiliary base also reduces the atom economy. Lower E-factor, which is desirable, is present due to the minimum amount of solvent employed when compared to the ILs, no column chromatography and no solvent washes are required.

Overall, the target ILs were all synthesised in sufficient quantities to undergo further investigations into their antimicrobial toxicity and biodegradability.

**Table 2.6.** Summary of green chemistry metrics for compounds synthesised in Section 2.2.2.

Compound	Atom Economy	Sheldon E-factor	GSK RME	Andraos RME	Mass Intensity	Solvent Intensity	Stoichiometric factor	Material Recovery Parameter	Yield %
<b>Amino Acid Esters</b>									
<b>336</b>	59%	20.8	0.425	0.046	21.8	11.8	0.735	0.108	99
<b>338</b>	81%	5.6	0.636	0.152	6.6	5.0	0.788	0.239	99
<b>339</b>	81%	5.8	0.635	0.147	6.8	5.2	0.788	0.231	99
<b>341</b>	90%	40.3	0.444	0.024	41.3	38.2	0.596	0.055	83
<b>343</b>	53%	29.5	0.231	0.033	30.5	24.5	1.000	0.142	43
<b>354</b>	71%	3.7	0.620	0.211	4.7	3.1	1.000	0.340	87
<b>Reductive Alkylation</b>									
<b>340</b>	89%	8.1	0.824	.123	8.1	6.9	0.958	0.148	98
<b>342</b>	89%	16.0	0.309	0.062	16.0	12.8	0.980	0.200	36
<b>Alkylating Reagents</b>									
<b>337</b>	63%	10.1	0.470	0.090	11.1	7.4	0.843	0.192	89
<b>356</b>	50%	55.1	0.281	0.018	56.1	17.9	0.873	0.063	54

Compound	Atom Economy	Sheldon E-factor	GSK RME	Andraos RME	Mass Intensity	Solvent Intensity	Stoichiometric factor	Material Recovery Parameter	Yield %
<b>L-Phenylalanine ILs</b>									
<b>324</b>	100 %	96.7	0.830	0.010	97.7	96.5	0.920	0.012	89
<b>325</b>	100 %	93.4	0.964	0.011	94.4	93.3	0.991	0.011	98
<b>326</b>	100 %	108.8	0.689	0.009	109.8	108.3	0.922	0.013	75
<b>327</b>	100 %	1081.5	0.523	0.001	1082.5	1080.6	0.934	0.002	56
<b>328</b>	100 %	120.7	0.812	0.008	121.7	120.5	0.918	0.010	88
<b>329</b>	100 %	126.5	0.335	0.008	127.5	124.5	0.991	0.023	34
<b>330</b>	100 %	88.1	0.901	0.011	89.1	88.0	0.917	0.012	99
<b>331</b>	80 %	33.0	0.718	0.029	34.0	32.6	0.986	0.041	91
<b>332</b>	100 %	1416.6	0.335	0.001	1417.6	1414.7	0.921	0.002	37
<b>333</b>	100 %	4088.3	0.122	0.001	4089.3	4081.1	0.921	0.002	13
<b>334</b>	100 %	1119.0	0.254	0.001	1120.0	1116.1	1.000	0.004	25
<b>335</b>	100 %	833.3	0.341	0.001	834.3	831.3	1.000	0.004	34

Compound	Atom Economy	Sheldon E-factor	GSK RME	Andraos RME	Mass Intensity	Solvent Intensity	Stoichiometric factor	Material Recovery Parameter	Yield %
<b>Neutral L-Phenylalanine derivatives</b>									
<b>344</b>	66%	1035.4	0.288	0.001	1036.4	1032.9	0.783	0.003	55
<b>345</b>	79%	2754.1	0.242	0.001	2755.1	2750.9	0.923	0.001	34
<b>346</b>	80%	476.6	0.433	0.002	477.6	474.6	0.958	0.005	56
<b>347</b>	53%	770.3	0.266	0.001	771.3	767.6	0.946	0.005	53
<b>348</b>	54%	463.4	0.305	0.002	464.4	461.1	0.966	0.007	58
<b>L-Tyrosine ILs</b>									
<b>349</b>	100%	294.0	0.819	0.003	295.0	293.8	0.979	0.004	83
<b>350</b>	100%	117.1	0.980	0.008	118.1	117.1	0.982	0.009	99
<b>351</b>	100%	120.7	0.971	0.008	121.7	120.7	0.982	0.008	99
<b>352</b>	100%	420.3	0.699	0.002	421.3	419.9	0.986	0.003	71
<b>353</b>	100%	150.7	0.773	0.007	151.7	150.4	0.985	0.009	79

## 2.3 Antimicrobial screening and biodegradation studies of 1<sup>st</sup> generation amino acid ILs and 3° amino analogues

### 2.3.1 Antimicrobial screening aim

The aim of the antimicrobial toxicity investigations was to determine the toxicity of the series of ILs and 3° amino compounds synthesised in this chapter. Information obtained from this investigation would then enable a rational design of “next generation” ILs based on any observed structure activity relationships (SAR) within the antimicrobial results. By keeping the amino acid backbone as either L-phenylalanine ethyl ester or L-tyrosine ethyl ester, any antimicrobial activity differences between compounds could tentatively be attributed to the headgroups effect on the overall molecule.

As previously discussed in Chapter 1, Section 1.2.5, toxicity is a parameter that must be investigated when determining the environmental compatibility and “greenness” of ILs. ILs have been described as possessing “green” properties, a description which has been repeated *ad nauseam*, often without any considerable investigation into the properties that will determine an ILs environmental impact. Exhibiting a negligible vapour pressure or non-flammability does not automatically classify an IL as being “green” since the toxicity and bioaccumulation that can occur from resistance to biodegradation is unknown. Antimicrobial toxicity and cytotoxicity properties of ILs have thus become a necessary parameter for investigation if ILs are to be considered benign. To date investigations have been carried out on the toxicity of ILs towards bacteria,<sup>43</sup> fungi,<sup>44</sup> invertebrates,<sup>45</sup> aquatic species,<sup>46</sup> plants,<sup>47</sup> and algae<sup>48</sup>.

Within the following section the antimicrobial activity of a number of ILs is presented. The ILs were screened against eight strains of bacteria, four gram positive and four gram negative, and 12 strains of fungi. Antimicrobial screening was carried out in collaboration with Dr. Marcel Špulák of the Department of Biological and Medical Sciences, Faculty of Pharmacy, Charles University, Hradec Králové, Czech Republic.

### 2.3.2 Antibacterial screening

To investigate the *in vitro* antibacterial activity of the aforementioned compounds, the following eight strains of bacteria from the collection available at Charles University, Czech Republic, were screened against:

Gram Positive:

- *S. aureus* (ATCC 65382) (SA)
- *Methicillin-res.S.a* (HK5996/08) (MRSA)
- *S. epidermidis* (HK6966/084 ) (SE)
- *Enterococcus sp.* (HK14365/085) (EF)

Gram Negative:

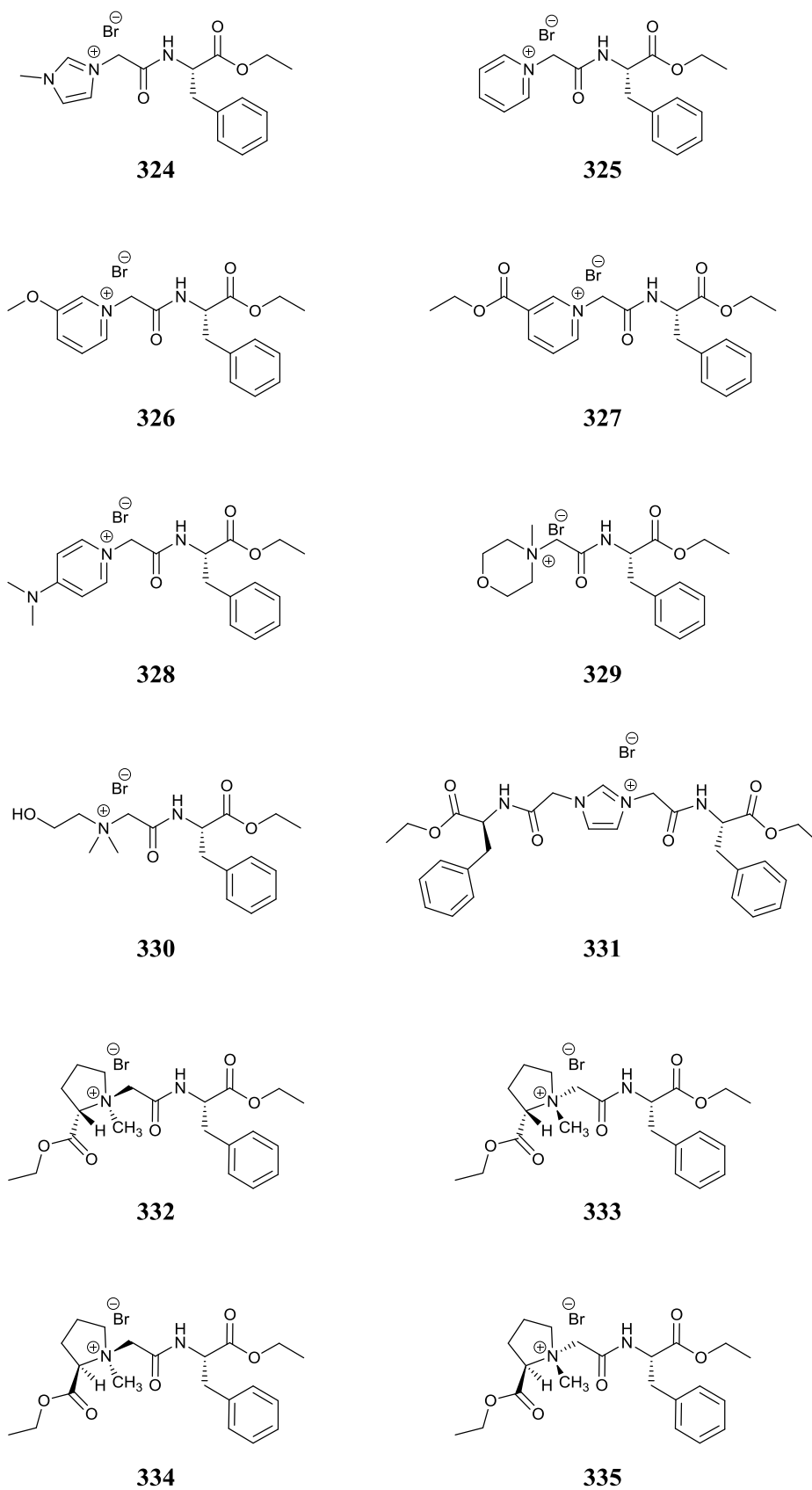
- *E. coli* (ATCC 87396) (EC)
- *K. pneumoniae* (HK11750/087) (KP)
- *K. pneumoniae* (HK14368/08) (KP-E)
- *P. aeruginosa* (ATCC 9027) (PA)

#### 2.3.2.1 Experimental Method

The experimental method is as described in Chapter 5, Section 5.8.1.

#### 2.3.2.2 Antibacterial results – L-phenylalanine ILs

From the results obtained in Table 2.7 for the L-phenylalanine ILs screened (Figure 2.21 depicting the same selection of ILs as Figure 2.3), it can be seen that in general a moderate to low antibacterial toxicity can be observed for the majority of the compounds screened. Where >500 (etc.)  $\mu\text{mol/L}$  is observed this is due to solubility of the compound being no greater than 500  $\mu\text{mol/L}$ , therefore any toxicity at higher concentrations cannot be observed. Where >2000  $\mu\text{mol/L}$  is observed then no discernible toxic effect has been demonstrated up to the screening concentration limit of 2000  $\mu\text{mol/L}$ .

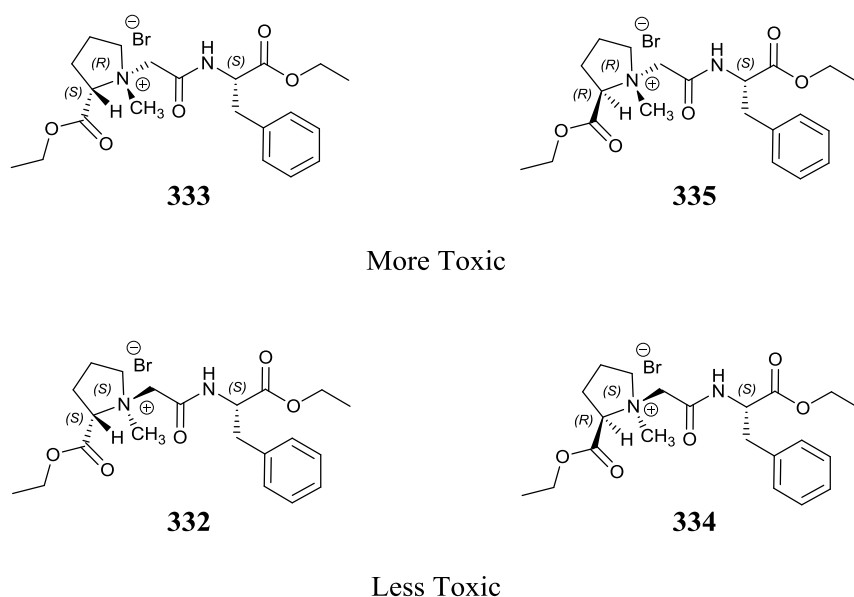


**Figure 2.21.** L-Phenylalanine ILs screened for antimicrobial activity.

**Table 2.7.** Antibacterial results obtained for L-phenylalanine ILs.

Microorganism	Time (h)	IL IC <sub>95</sub> μmol											
		324	325	326	327	328	329	330	331	332	333	334	335
Gram Positive													
SA	24h	2000,	2000,	>500,	1000,	>500,	2000,	2000,	500,	>2000,	1000,	>2000,	1000,
	48h	>2000	>2000	>500	1000	>500	2000	>2000	500	>2000	1000	>2000	1000
MRSA	24h	>2000,	>2000,	>500,	1000,	>500,	2000,	>2000,	1000,	>2000,	>1000,	>2000,	>2000,
	48h	>2000	>2000	>500	1000	>500	2000	>2000	1000	>2000	>1000	>2000	>2000
SE	24h	>2000,	>2000,	>500,	1000,	>500,	>2000,	>2000,	500,	2000,	1000,	>2000,	1000,
	48h	>2000	>2000	>500	1000	>500	>2000	>2000	500	2000	1000	>2000	1000
EF	24h	>2000,	>2000,	>500,	>1000,	>500,	>2000,	>2000,	1000,	>2000,	>1000,	>2000,	>2000,
	48h	>2000	>2000	>500	>1000	>500	>2000	>2000	1000	>2000	>1000	>2000	>2000
Gram Negative													
EC	24h	>2000,	>2000,	>500,	>1000,	>500,	>2000,	>2000,	2000,	>2000,	>1000,	>2000,	>2000,
	48h	>2000	>2000	>500	>1000	>500	>2000	>2000	2000	>2000	>1000	>2000	>2000
KP	24h	>2000,	>2000,	>500,	>1000,	>500,	>2000,	>2000,	>2000,	>2000,	>1000,	>2000,	>2000,
	48h	>2000	>2000	>500	>1000	>500	>2000	>2000	>2000	>2000	>1000	>2000	>2000
KP-E	24h	>2000,	>2000,	>500,	>1000,	>500,	>2000,	>2000,	>2000,	>2000,	>1000,	>2000,	>2000,
	48h	>2000	>2000	>500	>1000	>500	>2000	>2000	>2000	>2000	>1000	>2000	>2000
PA	24h	>2000,	>2000,	>500,	>1000,	>500,	>2000,	>2000,	2000,	>2000,	>1000,	>2000,	>2000,
	48h	>2000	>2000	>500	>1000	>500	>2000	>2000	2000	>2000	>1000	>2000	>2000



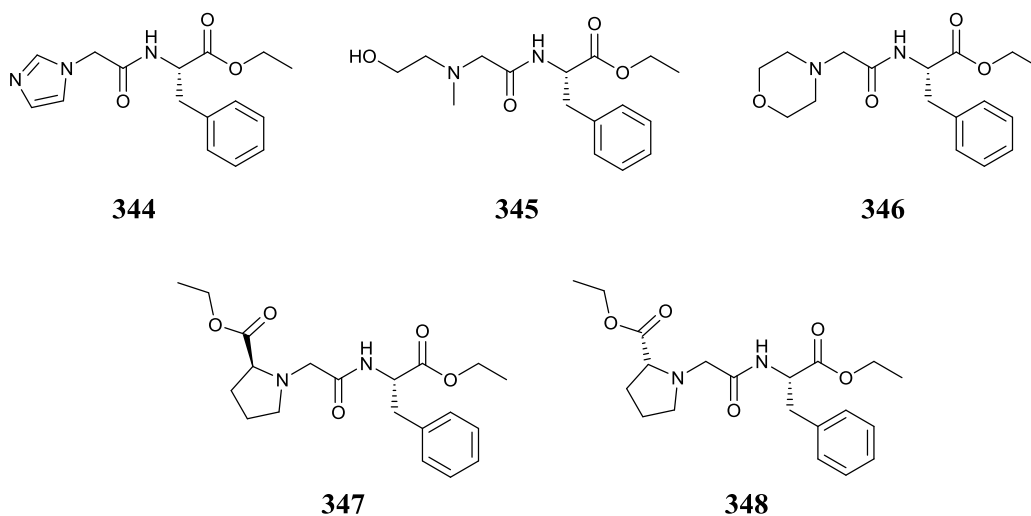


**Figure 2.22.** Diastereomeric pairs of *N*-methyl-prolinium ILs (**332-335**).

The lowest IC<sub>95</sub> observed was 500 µmol/L for (**331**) which is the C<sub>2</sub> symmetric bromide IL towards S.A and S.E. with a higher IC<sub>95</sub> observed for MRSA and E. sp. The next highest toxicity observed was 1000 µmol/L for derivatives (**327**, **333**, **335**) towards some gram positive bacteria. The prolinium derivatives, with *N*-methyl group orientated away from the observer, (**333**, **335**) displayed higher levels of toxicity than their respective epimers (**332**, **334**), see Figure 2.22.

There was no selectivity observed towards any of the bacterial strains, however the gram negative bacteria appeared more resilient towards the test compounds than the gram positive, as expected due to their double membrane cell wall composition.<sup>49</sup>

### 2.3.2.3 Antibacterial results – 3° amino compounds



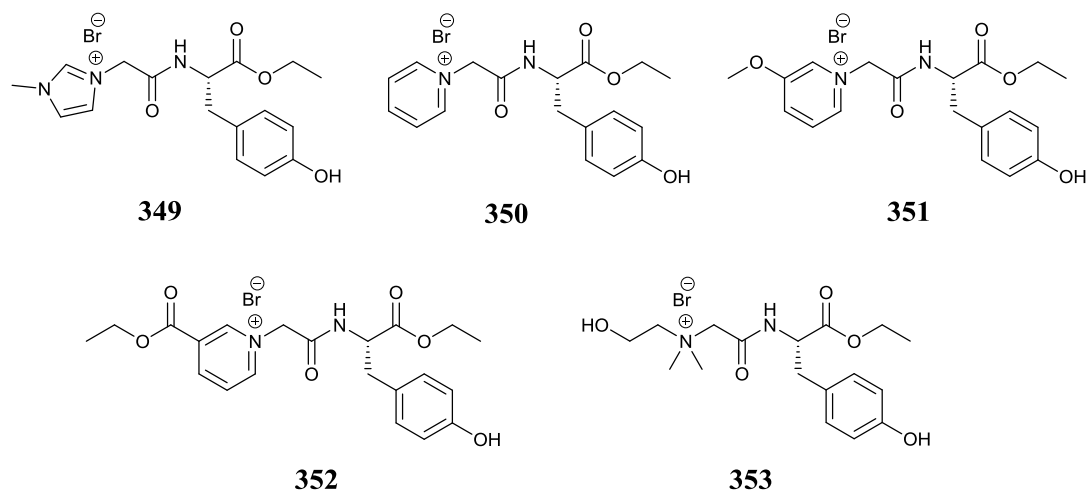
**Figure 2.23.** 3° Amino compounds screened for antimicrobial activity.

**Table 2.8.** Antibacterial results obtained for 3° amino compounds.

Microorganism	Time (h)	IL IC <sub>95</sub> μmol				
		344	345	346	347	348
Gram Positive						
SA	24h	1000,	1000,	2000,	125,	125,
	48h	1000	1000	2000	125	125
MRSA	24h	1000,	2000,	2000,	500,	1000,
	48h	1000	2000	2000	500	>2000
SE	24h	1000,	500,	>2000,	250,	>2000,
	48h	1000	500	>2000	250	>2000
EF	24h	>2000,	>2000,	>2000,	>1000,	>2000,
	48h	>2000	>2000	>2000	>1000	>2000
Gram Negative						
EC	24h	>2000,	>2000,	>2000,	>1000,	>2000,
	48h	>2000	>2000	>2000	>1000	>2000
KP	24h	>2000,	>2000,	>2000,	>1000,	>2000,
	48h	>2000	>2000	>2000	>1000	>2000
KP-E	24h	>2000,	>2000,	>2000,	>1000,	>2000,
	48h	>2000	>2000	>2000	>1000	>2000
PA	24h	>2000,	>2000,	>2000,	>1000,	>2000,
	48h	>2000	>2000	>2000	>1000	>2000

From the results obtained for the tertiary amino compounds (Figure 2.23 depicting the same tertiary amines as Figure 2.17), it can be observed that they possessed, in general, a higher toxicity than their L-phenylalanine IL counterparts. Imidazole derivative (**344**) was found to possess IC<sub>95</sub> of 1000 µmol/L towards SA, MRSA and SE, compared to 2000 µmol/L for the 1-methylimidazolium derivative (**324**) (Table 2.8). Tertiary amine (**344**) was also found to be less toxic than the C<sub>2</sub> symmetrical imidazolium IL (**331**). Methylethanolamine derivative (**345**) was observed to be more toxic when compared to cholinium counterpart (**330**) when screened against SA and an IC<sub>95</sub> four times greater towards SE was also observed. Tertiary amino morpholine derivative (**346**) exhibited the same low antimicrobial toxicity as IL counterpart (**329**). L-Proline tertiary amino compounds (**347**, **348**) displayed IC<sub>95</sub> values an order of magnitude greater than the N-methyl-L-prolinium derivatives (**332-335**) with IC<sub>95</sub> values of 125 µmol/L observed towards *S. aureus* and a moderate toxicity towards MRSA and *S. epidermidis* observed for derivative (**347**). The higher levels of toxicity associated with the tertiary amines is most likely due to the presence of reactive basic tertiary nitrogen groups.

### 2.3.2.4 Antibacterial results – L-tyrosine ILs



**Figure 2.24.** L-tyrosine ILs screened for antimicrobial activity.

**Table 2.9.** Antibacterial results obtained for L-tyrosine ILs.

Microorganism	Time (h)	IL IC <sub>95</sub> μmol				
		349	350	351	352	353
Gram Positive						
SA	24h	1000,	>2000,	>2000,	>2000,	2000,
	48h	1000	>2000	>2000	>2000	2000
MRSA	24h	2000,	2000,	>2000,	>2000,	>2000,
	48h	>2000	2000	>2000	>2000	>2000
SE	24h	500,	>2000,	>2000,	>2000,	1000,
	48h	1000	>2000	>2000	>2000	2000
EF	24h	>2000,	>2000,	>2000,	>2000,	>2000,
	48h	>2000	>2000	>2000	>2000	>2000
Gram Negative						
EC	24h	>2000,	>2000,	>2000,	>2000,	>2000,
	48h	>2000	>2000	>2000	>2000	>2000
KP	24h	>2000,	>2000,	>2000,	>2000,	>2000,
	48h	>2000	>2000	>2000	>2000	>2000
KP-E	24h	>2000,	>2000,	>2000,	>2000,	>2000,
	48h	>2000	>2000	>2000	>2000	>2000
PA	24h	>2000,	>2000,	>2000,	>2000,	>2000,
	48h	>2000	>2000	>2000	>2000	>2000

From the results illustrated in Table 2.9 it can be seen that the L-tyrosine ILs examined (Figure 2.24 depicting the same ILs as Figure 2.19), had in general a low to moderate toxicity. The L-

tyrosine imidazolium IL (**349**) displayed greater toxicity than that of L-phenylalanine analogue (**324**) towards *S. aureus*, 1000  $\mu\text{mol/L}$  vs 2000  $\mu\text{mol/L}$ . A greater toxicity towards *S. epidermidis* was also observed, 500  $\mu\text{mol/L}$  vs. 2000  $\mu\text{mol/L}$ . Of all the L-tyrosine derivatives screened, the 1-methylimidazolium compound (**349**) displayed the highest level of toxicity, 500-1000  $\mu\text{mol/L}$  for three of the four gram positive bacteria and had no discernible toxic effect towards the gram negative strains. No selectivity effects were observed for the L-tyrosine ILs.

#### 2.3.2.5 Antibacterial screening conclusions

In conclusion to the antibacterial screening a moderate to low toxicity was observed for the majority of the ILs screened, with the suggestion that stereochemistry plays a role in the toxicity results observed, especially with prolinium derivatives (**332-335**). The presence of a quaternary nitrogen centre appears to lower the toxicity significantly, with the tertiary amino derivatives exhibiting a much higher toxicity than their quaternary IL counterparts. An exception to this trend was observed for the morpholine derivatives (**329** and **346**) which had the same levels of toxicity towards the same strains of bacteria. The most toxic derivative IL screened was the  $\text{C}_2$  symmetrical IL (**331**) which exhibited an  $\text{IC}_{95}$  of 500  $\mu\text{mol/L}$  towards SA and SE, see Table 2.7. This result may be due to the added lipophilicity of the molecule and is somewhat in disagreement with the observations of Fatemi *et al.*<sup>50</sup> who suggested that increasing the symmetrical properties of an IL can reduce toxicity. However the toxicity measured in their case was measured towards Leukaemia rat cell lines and not bacteria and does not make for a direct comparison. The generally low toxicity observed for the ILs allows them to be considered potential green candidates.

#### 2.3.3 Antifungal screening

To investigate the *in vitro* anti-fungal activity of the ILs, the aforementioned compounds were screened against the following strains of fungi, available from the repository at Charles University, Czech Republic:

##### 9 Yeasts

- *Candida albicans* (ATCC 448597) (CA1)
- *Candida albicans* (ATCC 900288) (CA2)
- *Candida parapsilosis* (ATCC 220199 ) (CP)
- *Candida krusei* (ATCC 62581) (CK1)
- *Candida krusei* (E2811) (CK2)
- *Candida tropicalis* (156) (CT)
- *Candida glabrata* (20/I2) (CG)
- *Candida lusitaniae* (2446/I3 ) (CL)

- *Trichosporon asahii* (11884) (TA)

3 Filamentous fungi:

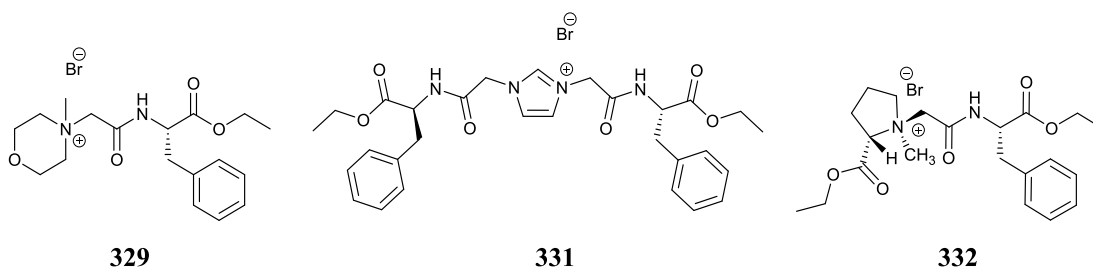
- *Aspergillus fumigatus* (2315) (AF)
- *Absidia corymbifera* (2726) (AC)
- *Trichophyton mentagrophytes* (445) (TM)

### 2.3.3.1 Experimental Method

The experimental method is as described in Chapter 5, Section 5.8.2.

### 2.3.3.2 Antifungal results – L-phenylalanine ILs

From the results obtained in Table 2.10, it can be seen that in general low antifungal toxicity can be observed for the majority of the compounds screened, with only three compounds (**329**, **331**, **332**) having  $IC_{80/50}$  values lower than 2000  $\mu\text{mol/L}$  (Figure 2.25). IL (**329**) showed an IC of 2000  $\mu\text{mol/L}$  towards 6 of the fungi, see Table 2.10. IL (**331**) similarly displayed and an IC of 2000  $\mu\text{mol/L}$  towards 5 of the fungi. IL (**332**) displayed an IC of 2000  $\mu\text{mol/L}$  towards only one of the fungi. No discernible toxic effect was observed for any of the other phenylalanine ILs examined. From this antifungal screening panel, it can be seen overall that the L-phenylalanine ILs had low toxic effect, at the concentrations screened at, towards any of the fungi.



**Figure 2.25.** ILs (**329**, **331**, **332**) were the only ILs to have any discernible toxic effect.

**Table 2.10.** L-Phenylalanine ILs screened for antifungal activity. \* IC<sub>50</sub> values were assessed for AF, AC and TM and IC<sub>80</sub> for all other strains.

Microorganism	Time (h)	IL IC <sub>80/50</sub> µmol*											
		324	325	326	327	328	329	330	331	332	333	334	335
<i>CA1</i>	24h	>2000,	>2000,	>2000,	> 1000,	> 500,	>2000,	>2000,	>2000,	>2000,	>2000,	>2000,	>2000,
	48h	>2000	>2000	>2000	>1000	>500	>2000	>2000	>2000	>2000	>2000	>2000	>2000
<i>CA2</i>	24h	>2000,	>2000,	>2000,	> 1000,	> 500,	>2000,	>2000,	>2000,	>2000,	>2000,	>2000,	>2000,
	48h	>2000	>2000	>2000	>1000	>500	>2000	>2000	>2000	>2000	>2000	>2000	>2000
<i>CP</i>	24h	>2000,	>2000,	>2000,	> 1000,	> 500,	>2000,	>2000,	>2000,	>2000,	>2000,	>2000,	>2000,
	48h	>2000	>2000	>2000	>1000	>500	>2000	>2000	>2000	>2000	>2000	>2000	>2000
<i>CK1</i>	24h	>2000,	>2000,	>2000,	> 1000,	> 500,	<b>2000,</b>	>2000,	<b>2000,</b>	>2000,	>2000,	>2000,	>2000,
	48h	>2000	>2000	>2000	>1000	>500	<b>2000</b>	>2000	>2000	>2000	>2000	>2000	>2000
<i>CK2</i>	24h	>2000,	>2000,	>2000,	> 1000,	> 500,	<b>2000,</b>	>2000,	>2000,	>2000,	>2000,	>2000,	>2000,
	48h	>2000	>2000	>2000	>1000	>500	<b>2000</b>	>2000	>2000	>2000	>2000	>2000	>2000
<i>CT</i>	24h	>2000,	>2000,	>2000,	> 1000,	> 500,	>2000,	>2000,	<b>2000,</b>	>2000,	>2000,	>2000,	>2000,
	48h	>2000	>2000	>2000	>1000	>500	>2000	>2000	<b>2000</b>	>2000	>2000	>2000	>2000
<i>CG</i>	24h	>2000,	>2000,	>2000,	> 1000,	> 500,	<b>2000,</b>	>2000,	>2000,	>2000,	>2000,	>2000,	>2000,
	48h	>2000	>2000	>2000	>1000	>500	<b>2000</b>	>2000	>2000	>2000	>2000	>2000	>2000
<i>CL</i>	24h	>2000,	>2000,	>2000,	> 1000,	> 500,	>2000,	>2000,	<b>2000,</b>	>2000,	>2000,	>2000,	>2000,
	48h	>2000	>2000	>2000	>1000	>500	>2000	>2000	<b>2000</b>	>2000	>2000	>2000	>2000
<i>TA</i>	24h	>2000,	>2000,	>2000,	> 1000,	> 500,	<b>2000,</b>	>2000,	>2000,	>2000,	>2000,	>2000,	>2000,
	48h	>2000	>2000	>2000	>1000	>500	<b>2000</b>	>2000	>2000	>2000	>2000	>2000	>2000
<i>AF</i>	24h	>2000,	>2000,	>2000,	> 1000,	> 500,	>2000,	>2000,	>2000,	>2000,	>2000,	>2000,	>2000,
	48h	>2000	>2000	>2000	>1000	>500	>2000	>2000	>2000	>2000	>2000	>2000	>2000
<i>AC</i>	24h	>2000,	>2000,	>2000,	> 1000,	> 500,	<b>2000,</b>	>2000,	>2000,	>2000,	>2000,	>2000,	>2000,
	48h	>2000	>2000	>2000	>1000	>500	>2000	>2000	>2000	>2000	>2000	>2000	>2000
<i>TM</i>	72h	>2000,	>2000,	>2000,	> 1000,	> 500,	<b>2000,</b>	>2000,	<b>2000,</b>	<b>2000,</b>	>2000,	>2000,	>2000,
	120h	>2000	>2000	>2000	>1000	>500	<b>2000</b>	>2000	<b>2000</b>	>2000	>2000	>2000	>2000

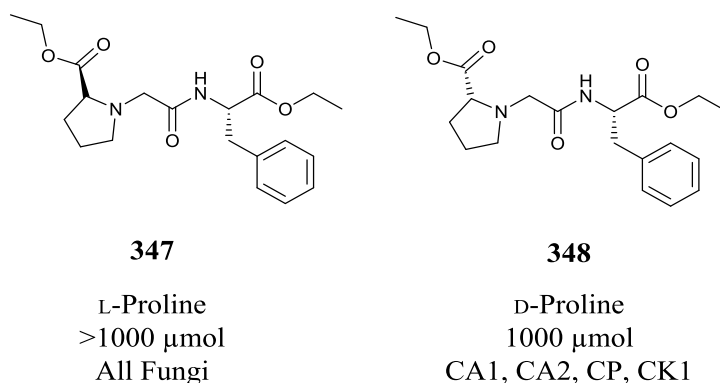
### 2.3.3.3 Antifungal results – 3° amino compounds

From the results obtained in Table 2.11, it can be seen that the 3° amino derivatives screened had in general low toxicity with only one derivative, D-proline tertiary amine (**348**), having an IC<sub>80</sub> of less than 2000 µmol/L. D-proline derivative (**348**) was also more toxic towards some fungi than its L-proline epimer (**347**), suggesting a relationship between stereochemistry and toxicity (Figure 2.26). When the tertiary amino D-proline derivative (**348**) is compared to IL counterparts (**334**, **335** - 2000 µmol/L for all fungi) it can be seen that the tertiary amino derivative has a greater toxic effect towards a number of fungi, specifically CA1, CA2, CP, CK1 and TM. For the remaining tertiary amino derivatives no discernible toxic effect was observed, up to the screening concentration limit of 2000 µmol/L, towards any of the fungi.

**Table 2.11.** Antifungal results obtained for L-phenylalanine tertiary amino derivatives.

Microorganism	Time (h)	IL IC <sub>80/50</sub> µmol*				
		344	345	346	347	348
<i>CA1</i>	24h	>2000,	>2000,	>2000,	> 1000,	<b>1000,</b>
	48h	>2000	>2000	>2000	>1000	>2000
<i>CA2</i>	24h	>2000,	>2000,	>2000,	> 1000,	<b>1000,</b>
	48h	>2000	>2000	>2000	>1000	<b>2000</b>
<i>CP</i>	24h	>2000,	>2000,	>2000,	> 1000,	<b>1000,</b>
	48h	>2000	>2000	>2000	>1000	<b>1000</b>
<i>CK1</i>	24h	>2000,	>2000,	>2000,	> 1000,	<b>1000,</b>
	48h	>2000	>2000	>2000	>1000	<b>1000</b>
<i>CK2</i>	24h	>2000,	>2000,	>2000,	> 1000,	<b>2000,</b>
	48h	>2000	>2000	>2000	>1000	<b>2000</b>
<i>CT</i>	24h	>2000,	>2000,	>2000,	> 1000,	>2000,
	48h	>2000	>2000	>2000	>1000	>2000
<i>CG</i>	24h	>2000,	>2000,	>2000,	> 1000,	>2000,
	48h	>2000	>2000	>2000	>1000	>2000
<i>CL</i>	24h	>2000,	>2000,	>2000,	> 1000,	>2000,
	48h	>2000	>2000	>2000	>1000	>2000
<i>TA</i>	24h	>2000,	>2000,	>2000,	> 1000,	>2000,
	48h	>2000	>2000	>2000	>1000	>2000
<i>AF</i>	24h	>2000,	>2000,	>2000,	> 1000,	>2000,
	48h	>2000	>2000	>2000	>1000	>2000
<i>AC</i>	24h	>2000,	>2000,	>2000,	> 1000,	>2000,
	48h	>2000	>2000	>2000	>1000	>2000
<i>TM</i>	72h	>2000,	>2000,	>2000,	> 1000,	<b>2000,</b>
	120h	>2000	>2000	>2000	>1000	<b>2000</b>

\* IC<sub>50</sub> values were assessed for AF, AC and TM and IC<sub>80</sub> for all other strains.



**Figure 2.26.** Comparison of stereochemistry and toxicity for tertiary amino derivatives (**347**, **348**).

#### 2.3.3.4 Antifungal results – L-tyrosine ILs

**Table 2.12.** Antifungal results obtained for L-tyrosine ILs.

Microorganism	Time (h)	IL IC <sub>80/50</sub> $\mu\text{mol}^*$				
		349	350	351	352	353
<i>CA1</i>	24h	>2000,	>2000,	>2000,	>2000,	>2000,
	48h	>2000	>2000	>2000	>2000	>2000
<i>CA2</i>	24h	>2000,	>2000,	>2000,	>2000,	>2000,
	48h	>2000	>2000	>2000	>2000	>2000
<i>CP</i>	24h	<b>2000,</b>	>2000,	>2000,	>2000,	>2000,
	48h	>2000	>2000	>2000	>2000	>2000
<i>CK1</i>	24h	>2000,	>2000,	>2000,	>2000,	>2000,
	48h	>2000	>2000	>2000	>2000	>2000
<i>CK2</i>	24h	>2000,	>2000,	>2000,	>2000,	>2000,
	48h	>2000	>2000	>2000	>2000	>2000
<i>CT</i>	24h	>2000,	>2000,	>2000,	>2000,	>2000,
	48h	>2000	>2000	>2000	>2000	>2000
<i>CG</i>	24h	>2000,	>2000,	>2000,	>2000,	>2000,
	48h	>2000	>2000	>2000	>2000	>2000
<i>CL</i>	24h	>2000,	>2000,	>2000,	>2000,	>2000,
	48h	>2000	>2000	>2000	>2000	>2000
<i>TA</i>	24h	>2000,	>2000,	>2000,	>2000,	>2000,
	48h	>2000	>2000	>2000	>2000	>2000
<i>AF</i>	24h	>2000,	>2000,	>2000,	>2000,	>2000,
	48h	>2000	>2000	>2000	>2000	>2000
<i>AC</i>	24h	>2000,	>2000,	>2000,	>2000,	>2000,
	48h	>2000	>2000	>2000	>2000	>2000
<i>TM</i>	72h	>2000,	>2000,	>2000,	>2000,	>2000,
	120h	>2000	>2000	>2000	>2000	>2000

\* IC<sub>50</sub> values were assessed for AF, AC and TM and IC<sub>80</sub> for all other strains.



As can be seen from Table 2.12, the L-tyrosine ILs screened had no discernible toxic effect towards the 12 strains of fungi, with the single exception of the imidazolium derivative (**349**) which had an IC<sub>80</sub> of 2000 µmol/L towards one strain of fungi, the *Candida parapsilosis*, after 24 hours. After 48 hours no inhibition was observed as the fungi had recovered.

#### 2.3.3.5 Antifungal screening conclusions

In conclusion to the antifungal screening a general low toxicity was observed for all the ILs screened. Of the tertiary amino derivatives (**344-348**) screened one derivative (**348**) exhibited moderate toxicity. In total only five compounds screened exhibited any toxic effect whatsoever towards the fungi. L-Phenylalanine ILs (**329, 331, 332**), tertiary amino (**348**) and L-tyrosine IL (**349**) showed activity of 2000 µmol/L or lower. As an overall trend, it appears that the derivatives examined are generally not toxic towards the panel of fungi, at the concentrations screened.

#### 2.3.4 Antimicrobial screening conclusions

In conclusion to the antimicrobial and antifungal screening it can be observed that the L-phenylalanine and L-tyrosine ILs had moderate to little toxic effect towards any of the bacteria and fungi screened against. Tertiary amino derivatives appeared to have a greater toxicity towards the same strains of bacteria and fungi. The presence of a quaternary nitrogen appears to have a reduction in the toxicity, though with such a small sample size it cannot be definitively said as to whether this is a general trend or an isolated incident. Stereochemistry of the prolinium derivatives also appeared to play an important part in the toxicity assessment with the orientation of the quaternary nitrogen's *N*-methyl group affecting the toxicity. Overall the generally low levels of toxicity support the proposal of a number of the ILs screened as green chemicals. In conjunction with the green synthesis metrics in Section 2.2.2.7 and the biodegradation studies carried out in Section 2.4, a full assessment of the ILs "greenness" can be made.

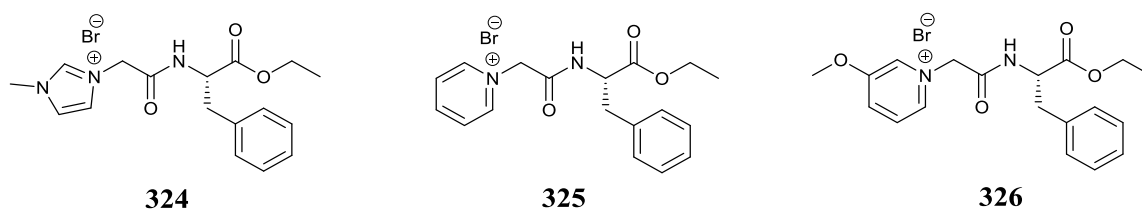
### 2.4 Biodegradation studies of amino acid ILs and 3° amino analogues

The aim of the work within this section was to investigate the biodegradability of the series of L-phenylalanine ILs, tertiary amino compounds and L-tyrosine ILs synthesised in this chapter. Necessity for investigating biodegradability of ILs has been thoroughly discussed in Chapter 1. Biodegradation screening was carried out using the Closed Bottle Test (CBT). The CBT is one of the methods of examining organic compounds for their aerobic biodegradability and is a simulation of the environment expected in surface ground water. Test conditions are designed to represent surface water conditions, such as low bacterial concentrations and low nutrient concentrations. See Chapter 1, Section 1.2.1.1 for description of CBT OECD 301D and Chapter

5, Section 5.9.1 for experimental method used. The first series of compounds to be screened was the L-phenylalanine series. As discussed previously, the backbone of L-phenylalanine ethyl ester was kept constant throughout this series so as to determine the effect of the headgroup on biodegradability. A second series of compounds, the tertiary amino derivatives, was prepared to investigate whether the absence of a positively charged quaternary nitrogen would affect the biodegradability. Lastly a series of L-tyrosine ILs was prepared to investigate whether the addition of the –OH group at the para position of the tyrosine side chain could affect the biodegradability. Results for each of the series are presented herein. Additionally, a subset of the L-phenylalanine ILs underwent further analysis. Samples from the beginning and the end of the CBTs were taken to determine primary elimination of the phenylalanine ethyl ester derivatives (ILs and tertiary amino derivatives) and to identify transformation products (TPs) via liquid chromatography/high resolution mass spectrometry (LC-orbitrap HRMS). A number of metabolite compounds were observed and their structures and breakdown pathways have been proposed. See Chapter 5, Section 5.9.2 for LC/MS method used.

#### 2.4.1 Biodegradation screening of L-phenylalanine ILs

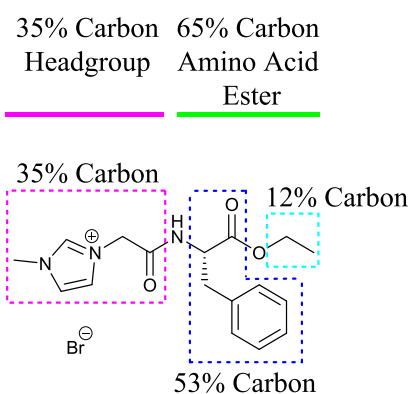
As can be seen from Table 2.13, of the ILs screened only one of the ILs, pyridinium IL (**325**), gave 63% biodegradation within the 28 day period (Figure 2.27). However IL (**325**) cannot be considered readily biodegradable as it did not reach the pass level of 60%, ten days after 10% biodegradation was observed (see Chapter 1, Section 1.2.1 for OECD 301D test specifications). The allotted test time was extended for IL (**325**) to 42 days, after which 76% biodegradation was observed suggesting IL (**325**) is inherently ultimately biodegradable. The next highest IL biodegradability was the 3-methoxy pyridinium IL (**326**, 52%) followed by 1-methylimidazolium (**324**, 47%) with a further reduction in biodegradability observed for the DMAP derivative (**328**, 33%) and ethyl nicotinium (**327**, 32%). It appears from the initial data that the pyridinium core is very sensitive to modification as the introduction of substituents on the 3 and 4 positions appears to greatly reduce biodegradability. C<sub>2</sub> symmetrical imidazolium IL (**331**) was also shown to be recalcitrant to biodegradation. Non-aromatic derivatives (morpholinium **329**, cholinium **330**) failed to degrade more than 17 and 24% respectively. For the prolinium derivatives (**332-335**) 21-24% biodegradation was observed. It can be further postulated that only the ester functionalities are undergoing biodegradation as the theoretical percentage biodegradation attributable to total ester degradation is 19%, a difference of 2-5% than that observed. Stereochemistry was not observed to play a role in the levels of biodegradation observed for the four prolinium derivatives.



**Figure 2.27.** L-phenylalanine ILs with the highest levels of biodegradability.

**Table 2.13.** Biodegradability and carbon distribution of examined L-phenylalanine IL compounds, colour coded according to the traffic light classification.<sup>51</sup>

IL	% Biodegradation	Amino Acid Ester Carbon %	Ester Carbon %
<b>L-Phenylalanine ILs</b>			
<b>324</b>	<b>47</b>	65	12
<b>325</b>	<b>63</b>	61	11
<b>326</b>	<b>52</b>	58	11
<b>327</b>	<b>32</b>	52	19
<b>328</b>	<b>33</b>	55	10
<b>329</b>	<b>17</b>	61	11
<b>330</b>	<b>24</b>	65	12
<b>331</b>	<b>40</b>	76	14
<b>332</b>	<b>24</b>	52	19
<b>333</b>	<b>22</b>	52	19
<b>334</b>	<b>23</b>	52	19
<b>335</b>	<b>21</b>	52	19



**Figure 2.28.** Carbon atom distribution of amino acid IL (**324**).

Figure 2.28 depicts the percentage distribution of carbon in imidazolium IL (**324**). By considering the carbon distribution over the various regions of the molecule and comparing the percentage biodegradation to the carbon distribution, a number of insights into the breakdown pathways of each IL can be considered. As can be seen for IL (**324**), total ester degradation of all IL in the CBT would provide 12% biodegradation, whilst total ester and amino acid

degradation would give 65% biodegradation. If biodegradation is observed to be higher than total ester degradation but lower than total ester and amino acid degradation then the compound may be undergoing different rates of biodegradation within the CBT. A certain proportion of the parent compound may undergo ester/amide hydrolysis and the rest of the parent compound remaining intact. Another possibility is that other portions of the molecule are undergoing biodegradation. All of the L-phenylalanine ILs except (**332-335**) undergo levels of biodegradation greater than total ester degradation, but less than total amino acid plus ester degradation.

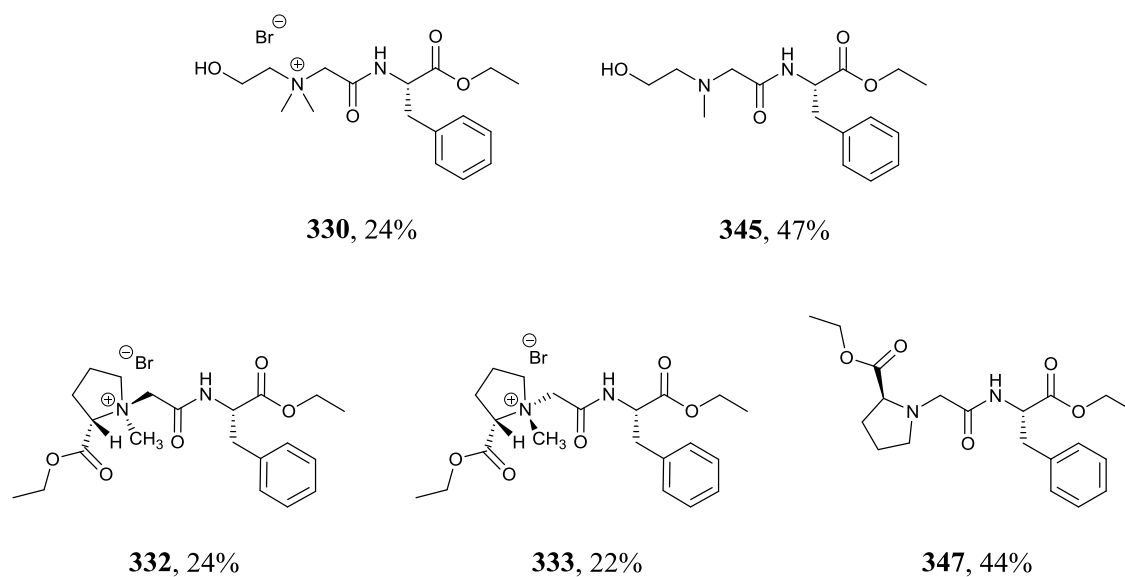
#### 2.4.2 Biodegradation screening of 3° amino analogues

A similar resistance to biodegradability was observed for the tertiary amino derivatives screened (Table 2.14). When the tertiary amino derivatives are compared to their IL counterparts it can be seen that imidazole derivative (**344**) underwent 40% biodegradation, 7% less than its IL counterpart (**324**, 47%). Tertiary amino derivative (**345**) underwent higher levels of biodegradation (+23%) than IL analogue (**330**) (Figure 2.29). Tertiary amino L-proline derivative (**347**) was also shown to undergo higher levels (+20-22%) of biodegradability than IL counterparts (**332**, **333**) (Figure 2.29). Similarly morpholine derivative (**346**, 28%) underwent 11% more biodegradation than the morpholinium derivative (**329**, 17%). Elevated levels of biodegradation suggest that the presence of a quaternary nitrogen atom can in some cases impede the biodegradation process thus tertiary amines can exhibit higher levels of biodegradation, an observation which is in agreement with the literature.<sup>3</sup> However, a larger sample size of tertiary amino compounds would need to be examined to draw any definite conclusions from any trends observed.

**Table 2.14.** Biodegradability and carbon distribution of examined tertiary amino compounds.

IL	% Biodegradation	Amino Acid Ester Carbon %	Ester Carbon %
<b>Tertiary Amine</b>			
<b>344</b>	<b>40</b>	69	13
<b>345</b>	<b>47</b>	69	13
<b>346</b>	<b>28</b>	65	12
<b>347</b>	<b>44</b>	55	20

Test extensions were applied for tertiary amines (**344**, **345**). After 42 days amine (**344**) had undergone 59% biodegradation and (**345**) had undergone 78%. It can be suggested that tertiary amines (**345**) could be inherently ultimately biodegradable.



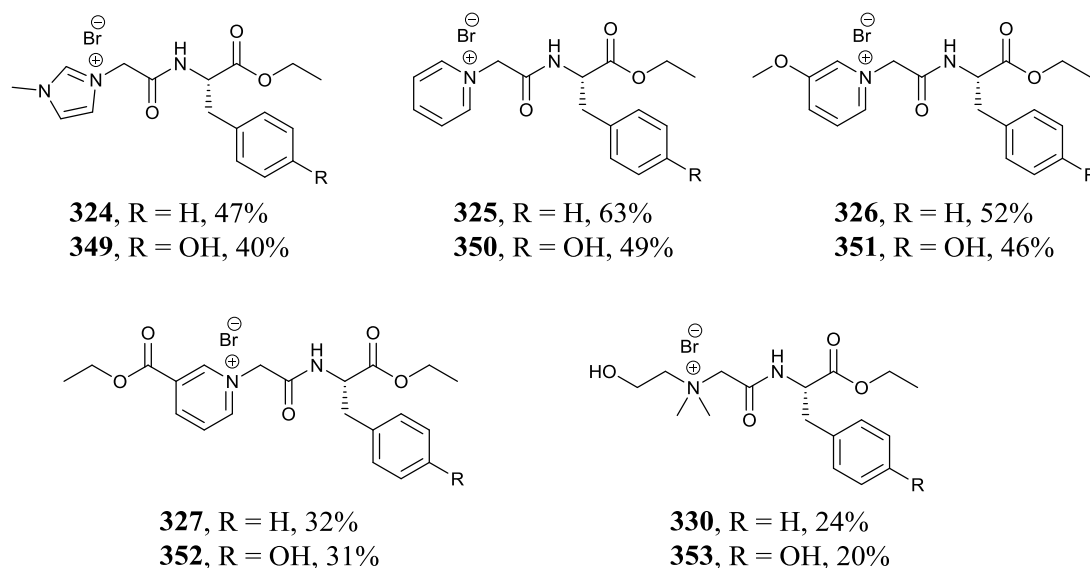
**Figure 2.29.** Comparison of IL biodegradation to tertiary amino biodegradation.

### 2.4.3 Biodegradation screening of L-tyrosine analogues

The presence of an additional –OH group on the L-tyrosine derived ILs appears to hinder biodegradation. When comparing L-phenylalanine derivative (**324**) to L-tyrosine derivative (**349**) the L-phenylalanine derivative displayed 7% more biodegradability than the L-tyrosine compound (Figure 2.30). A similar trend was observed for all L-tyrosine compounds with 5–13% less biodegradability. A 1% difference was observed between L-phenylalanine and L-tyrosine nicotinium (**327**) and (**352**).

**Table 2.15.** Biodegradability and carbon distribution of examined L-tyrosine compounds.

IL	% Biodegradation	Amino Acid Ester Carbon %	Ester Carbon %
<b>L-Tyrosine ILs</b>			
<b>349</b>	<b>40</b>	65	12
<b>350</b>	<b>49</b>	61	11
<b>351</b>	<b>46</b>	58	11
<b>352</b>	<b>31</b>	52	19
<b>353</b>	<b>20</b>	65	12



**Figure 2.30.** L-tyrosine IL biodegradation compared to L-phenylalanine for ILs.

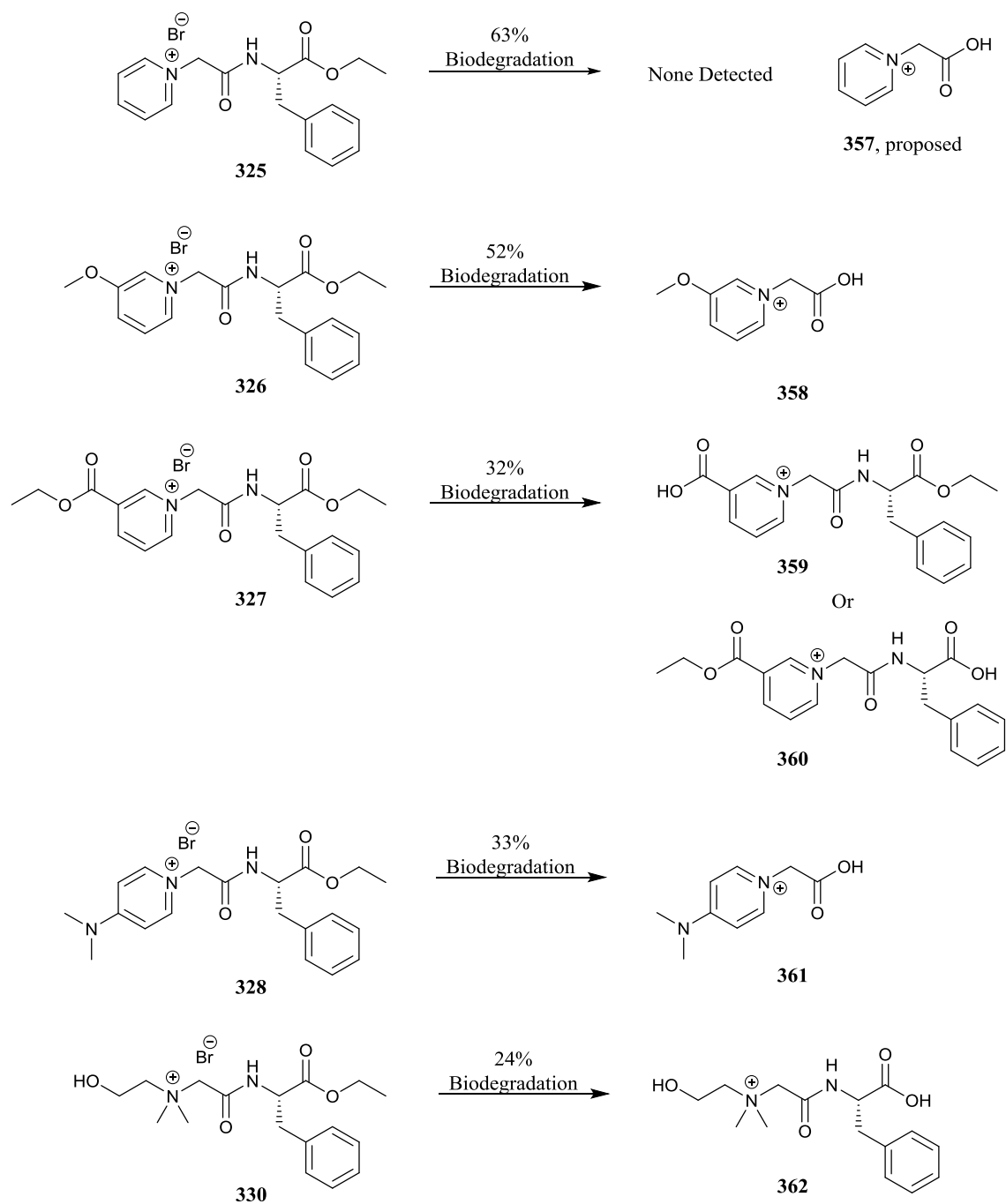
#### 2.4.4 Summary of IL and tertiary amino biodegradation

For all of the ILs and tertiary amines the percentage biodegradation observed is greater than that which can be attributed to ester degradation (though derivatives **332-335** are only 2-5% above this level). When the carbon content of the amino acid plus the ester is considered - and the assumption that the entire amino acid can undergo biodegradation is made - then the predicted levels of biodegradation suggest that a number of the ILs and tertiary amines (**324**, **325**, **329-331**, **344-346**, **349**, **350**, **353**) could undergo >60% biodegradation. All of the ILs except pyridinium IL (**325**) and the prolinium derivatives (**332-335**) are observed to have levels of biodegradation greater than full ester degradation but less than full amino acid degradation (**324**, **326-331**, **344-347**, **349-353**). Pyridinium IL (**325**) was observed to biodegrade 2% higher than the predicted levels attributable to total ester and amino acid degradation (61% predicted, 63% observed). However this rough approximation of carbon distribution and attributable degradation cannot be fully substantiated without a metabolite analysis of the closed bottle test. What exactly is breaking down? Is the rate of biodegradation such that some of the compound in the test undergoes high levels of mineralisation after a particular biochemical transformation? Is there some rate limiting step that once complete, allows the IL to biodegrade? Is ester hydrolysis occurring preferentially to amide bond hydrolysis or are both happening at the same time? Is there fully intact parent compound present in the closed bottle test vessel after the 28 day period? To answer these questions a detailed LCMS/MS analysis of a selection of ILs and 3° amino derived compounds was carried out.

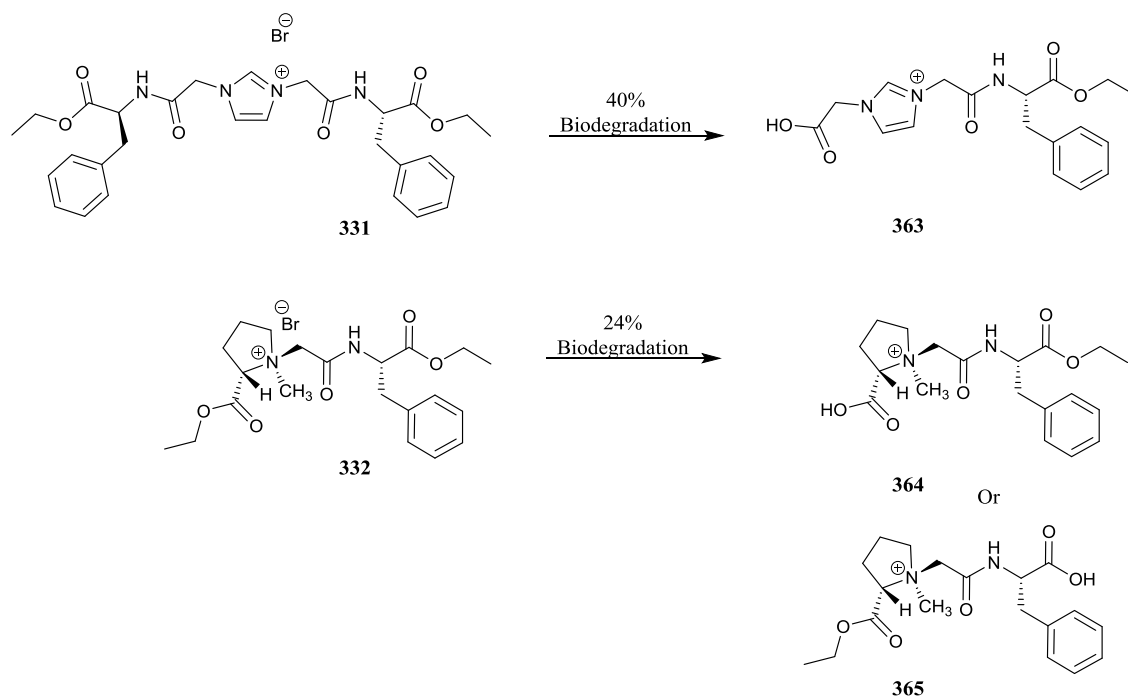
#### 2.4.5 LCMS/MS analysis of transformation products

In conjunction to the biodegradation screening conducted, an LCMS/MS analysis of the biodegradation transformation products was carried out after the 28 day test period by the research group of Prof. Klaus Kümmerer, Faculty for Sustainability, University of Lüneburg, Germany. Information gained from this test allowed for some initial elucidation into the breakdown pathways of the ILs examined. See Chapter 5, Section 5.9.2 for experimental conditions. The transformation products for the ILs and tertiary amines are presented in Schemes 2.7 and 2.10 respectively.

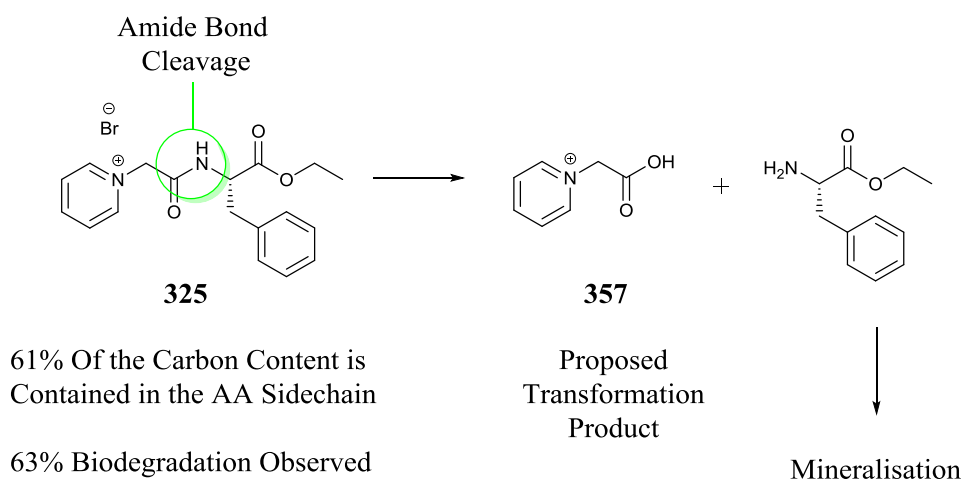
Based on the transformation products and percentage biodegradation for pyridinium IL (**325**), it can be inferred that the IL is breaking down by amide bond cleavage to a highly biodegradable L-phenylalanine residue and pyridinium acetic acid (**357**) (Scheme 2.8). It was observed that no transformation product was detected at the end of the test suggesting that pyridinium acetic acid is not accumulating. Pyridinium acetic acid can potentially undergo further levels of biodegradation as was observed by Besse-Hoggan *et al.* 2015.<sup>52</sup> It is currently unknown as to whether ester hydrolysis occurs before the amide bond is cleaved. To determine if pyridinium acetic acid was accumulating, a second CBT was conducted with a time extension beyond 28 days. After 42 days 76% biodegradation had occurred suggesting that the pyridinium ring is undergoing further degradation towards complete mineralisation.







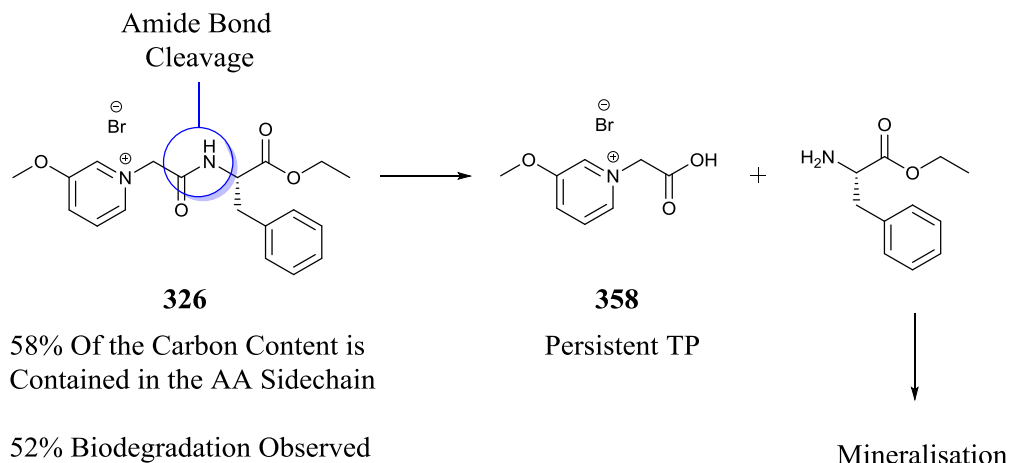
**Scheme 2.7.** Transformation products detected by LCMS for L-phenylalanine ILs.



**Scheme 2.8.** Potential biodegradation pathway for IL (**325**).

For ILs (**327**, **330**, **332**) (Scheme 2.7), ester hydrolysed products were discovered at the end of the 28 day test. No amide hydrolysed products were detected for these compounds. However for IL (**327**) 31% biodegradation was observed. Ester hydrolysis alone cannot account for the levels of biodegradation. Ester hydrolysis and mineralisation would theoretically produce 9% biodegradation. Therefore some other part of the molecule must be degrading rapidly and thus avoiding detection by LCMS/MS. A similar observation is made for IL (**330**, **332**). For prolinium derivatives (**332-335**) only one diastereomer (**332**) was analysed for metabolic breakdown products. However it can be inferred from the biodegradation percentages (21-23%

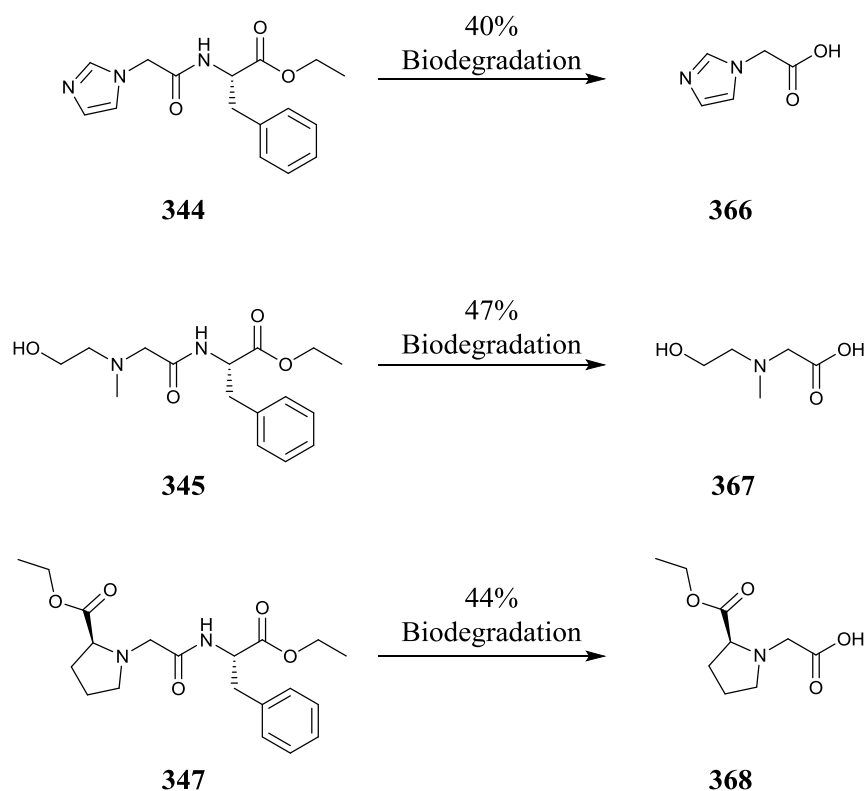
for all four derivatives) that ester hydrolysis is occurring, which is reinforced by the detection of TPs (**364**, **365**). At the end of the 28 day test, completely intact parent compound was also observed for each of the ILs screened.



**Scheme 2.9.** Potential biodegradation pathway of IL (**326**).

As can be seen from the potential biodegradation pathway of IL (**326**) (Scheme 2.9), there is not enough carbon in the sidechain to undergo a  $\geq 60\%$  mineralisation within the 28 day period. The aim of producing readily biodegradable ILs is not to just pass the test but rather produce readily biodegradable ILs that do not present a persistent transformation product. If simply passing the test was all that was required then a slightly longer ester chain length such as a butyl ester could be employed to predictably increase the levels of biodegradability whilst keeping toxicity at an acceptably low level.<sup>8, 53</sup>

Transformation products for the tertiary amino derivatives analysed are outlined in Scheme 2.10. Imidazole derivative (**344**) can be seen to breakdown by amide hydrolysis into imidazole acetic acid (**366**). Similarly the methylethanolamine derivative (**345**) can be seen to also undergo amide hydrolysis to (**367**) as does L-proline derivative (**347**) to (**368**). The lack of quaternisation on the nitrogen headgroup appears to allow for amide bond hydrolysis in all three examples. Of note is the presence of the ethyl ester in (**368**), after 28 days the ester remained intact on this TP. As with the ILs examined, completely intact parent compound was also observed for each of the tertiary amino derivatives screened.



**Scheme 2.10.** Transformation products detected for L-phenylalanine tertiary amino derivatives.

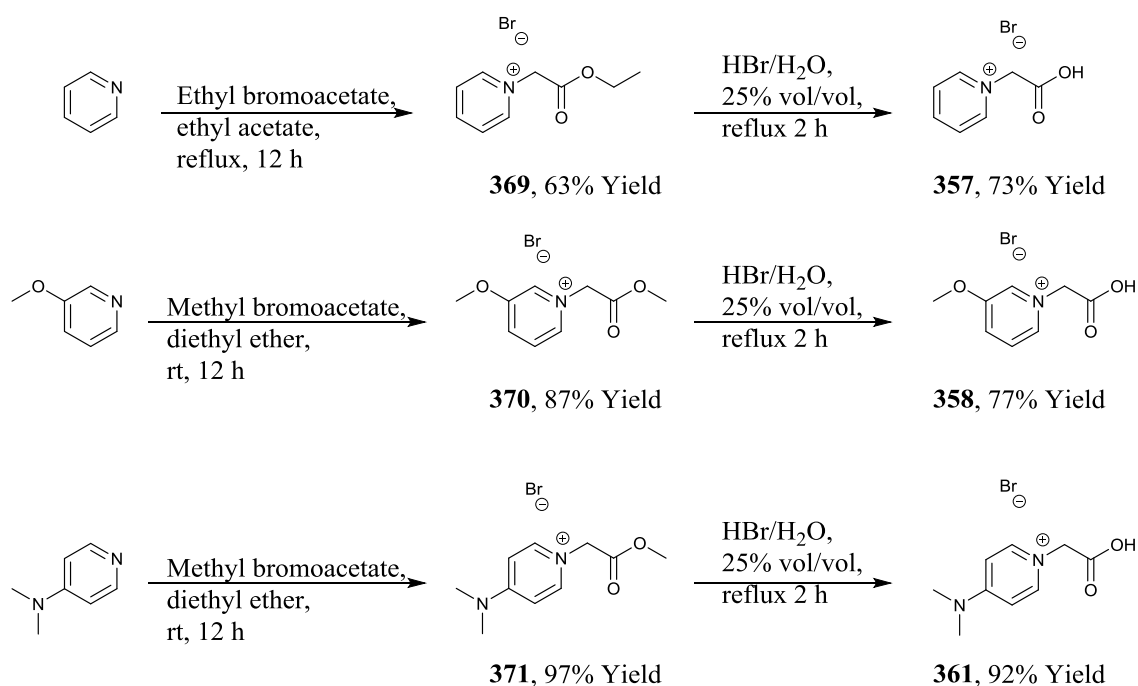
#### 2.4.6 Synthesis of transformation products

The final challenge in the unambiguous elucidation of the TP structures was the synthesis of the proposed products. Furthermore, authentic samples for further study, including TP antimicrobial toxicity and biodegradation were desired. Antimicrobial toxicity of the metabolic products would allow for a far more complete picture of the ILs overall toxicity. The question must be asked: what is the point in producing a biodegradable molecule if the transformation products are going to be more toxic than the parent compound? In addition it is also possible to assign structure, and tentatively stereochemistry, to the TPs if an authentic sample is available. The concept of submitting the transformation products of organic chemicals for further biodegradation screening has been carried out previously in the literature,<sup>54</sup> though to the authors knowledge, never with ILs. In 2015, Chaintreau *et al.* performed biodegradation screening (OECD 301D and OECD 301F) on a number of ketones. After the 28 day test period had elapsed, a number of persistent TPs were identified and the test duration was extended to 60 days. When the TPs were identified a number of them were synthesised and submitted for biodegradation screening themselves. Results from this screening showed that although the TPs were persistent in the original biodegradation screening (even though the test was extended beyond 28 days) when submitted for further screening (OECD 301D and OECD 301F) the persistent products underwent further biodegradation that was not observed in the original test.

The synthesis of the TPs detected in Section 2.4.5 is outlined herein. From the structures previously identified in Schemes 2.7 and 2.10, a number of synthetic routes to the target TPs were determined as follows:

#### 2.4.6.1 Ester acid hydrolysis – Route A

For TPs (**357**, **358**, **361**) the route involved synthesis of an ester of the target heterocycle followed by acid hydrolysis to give the carboxylic acid TP in a two step synthesis (Scheme 2.11). It was decided not to react the amine with bromoacetic acid to give the target in one step as the amines are nucleophilic bases and can compete with the acid base reaction to give lower yields.<sup>55</sup> The synthetic procedure is as outlined by Pukitis *et al.* who originally synthesised (**361**) from (**371**).<sup>56</sup> TP (**358**) has been previously reported by Oldfield *et al.*<sup>57</sup>

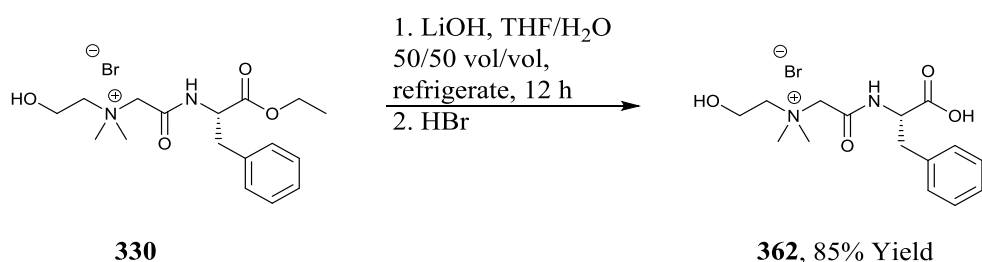


**Scheme 2.11.** Acid hydrolysis - Route A.

Target TPs were synthesised in good (e.g. **357**, 73%) to excellent yields (e.g. **361**, 92%) by route A as shown in Scheme 2.11.

#### 2.4.6.2 Ester base hydrolysis – Route B

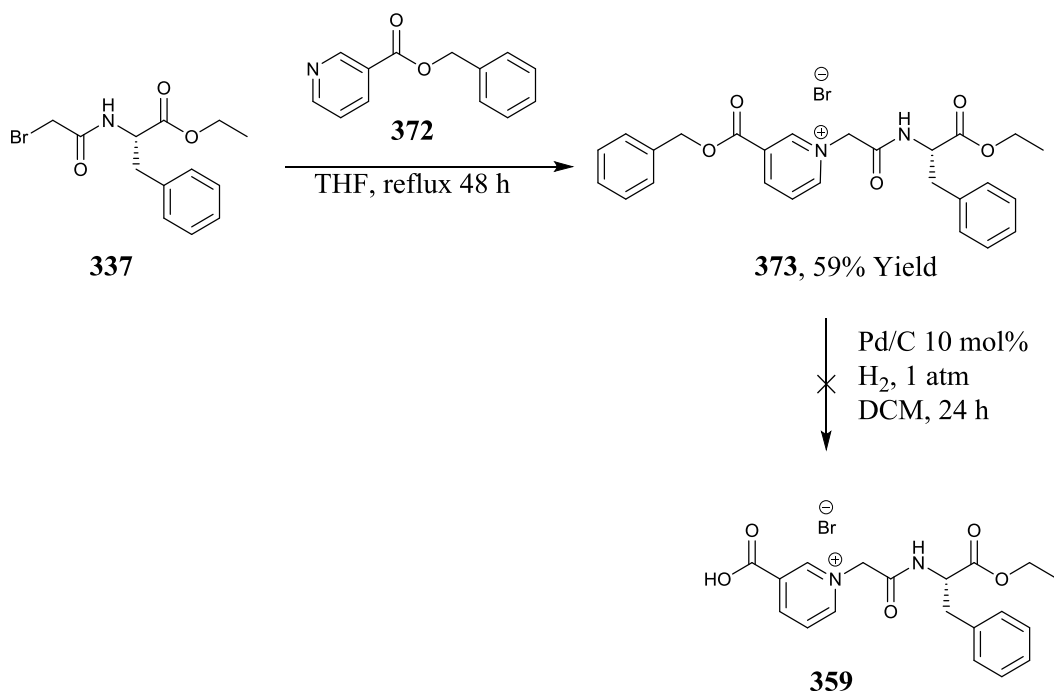
Base hydrolysis of cholinium IL (**330**) was chosen to furnish TP (**362**) in a one-step reaction providing the amide bond did not cleave under the conditions chosen. NaOH mediated hydrolysis cleaved the amide bond as did the use of HCl. To overcome this problem a LiOH mediated base hydrolysis procedure that is normally employed in ester deprotection in peptide synthesis was used (Route B, Scheme 2.12).<sup>58</sup> Target TP (**362**) was synthesised in 85% yield.



**Scheme 2.12.** Base hydrolysis, Route B.

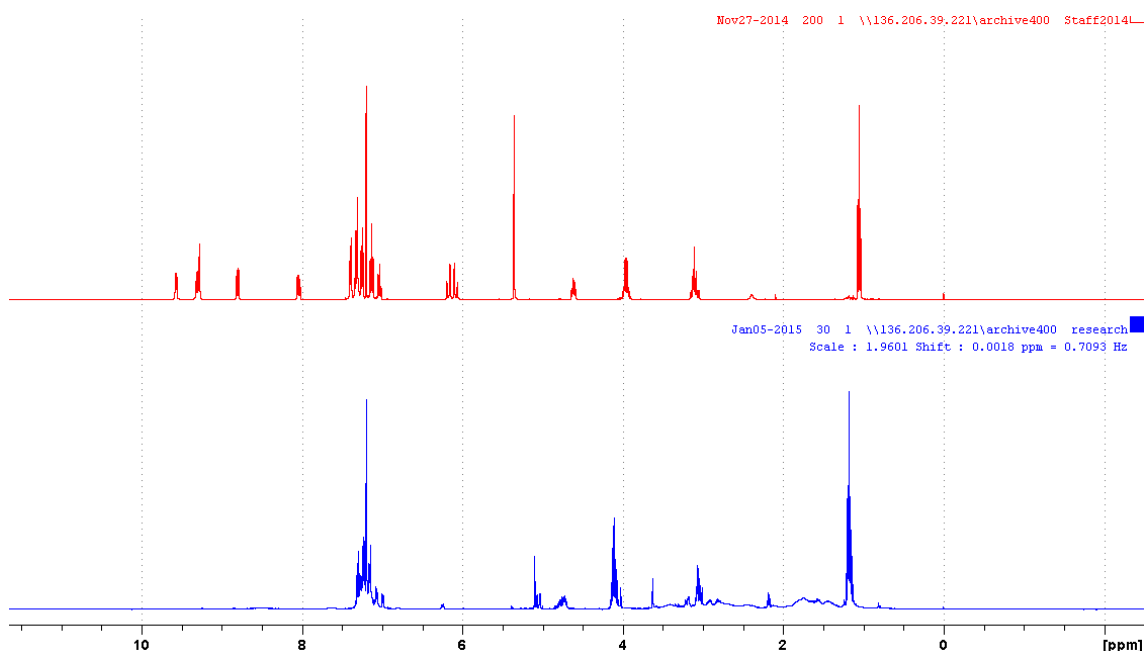
#### 2.4.6.3 Benzyl ester hydrogenolysis – Route C

For ILs (**327**, **331**, **332**) and tertiary amino derivative (**347**), a benzyl ester of the parent compound was synthesised followed by a deprotection hydrogenolysis reaction to the equivalent carboxylic acid TPs. For ILs (**327**, **332**) two possible TPs for each parent compound, one for each regioisomer, were proposed and thus two different benzyl ester parent molecules had to be synthesised in order to selectively deprotect the ester position of choice. For parent nicotinium IL (**327**) potential TPs were (**359**, **360**) thus the regioisomer benzyl esters (**373**, **376**) were synthesised as outlined in Scheme 2.13 and 2.14.



**Scheme 2.13.** Benzyl ester hydrogenolysis pathway for prolinium TP (**359**).

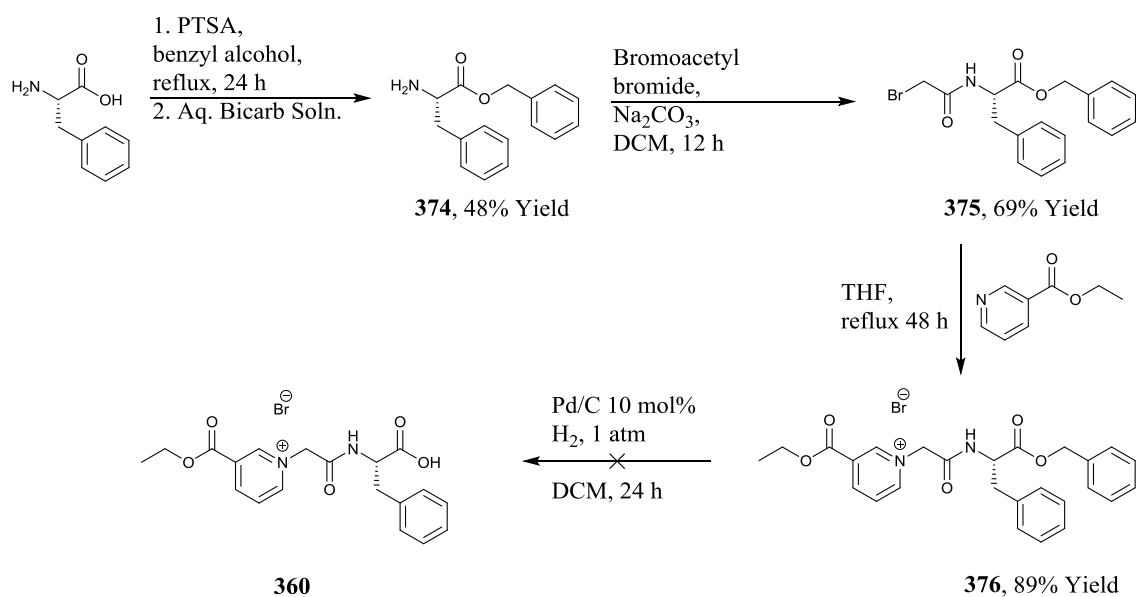
Benzyl nicotinate (**372**) was synthesised according to the procedure outlined by Khalafi-Nezhad *et al.*<sup>59</sup> Intermediate (**373**) was synthesised by the convergent synthesis of benzyl nicotinate (**372**) with alkylating reagent (**337**) in moderate yield (44%, Scheme 2.13). The initial synthesis plan proposed hydrogenolysis of the benzyl ester to give target TP (**359**).



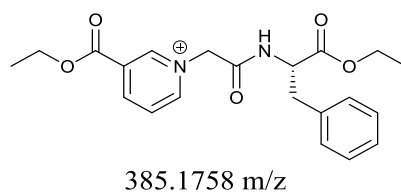
**Figure 2.31.**  $^1\text{H}$ -NMR spectra of benzyl ester (**373**) in red and crude material recovered after hydrogenolysis reaction in blue.

Benzyl deprotection by hydrogenolysis did not occur cleanly and gave multiple reduction products (as determined by TLC (10% MeOH:DCM and  $^1\text{H}$ -NMR spectra). Reactions solvents trialled included EtOH, MeOH and DCM, none of which facilitated a deprotection free of impurities and lead to what appeared to be reduction of the ethyl nicotinium ring (Figure 2.31). A redesigned synthesis route for IL (**359**) is further discussed in Section 2.4.6.4.

For TP (**360**) the proposed synthetic route (Scheme 2.14) was a linear synthesis beginning with the L-phenylalanine benzyl ester (**374**) prepared according to Baggett *et al.*<sup>60</sup> Reacting ester (**374**) with bromoacetyl bromide formed alkylating reagent (**375**) in good yields (69%). Though alkylating reagent (**375**) was previously reported by Toshifumi *et al.*<sup>61</sup> it was decided that the synthesis would be carried out as per the synthesis of (**337**) using  $\text{Na}_2\text{CO}_3$  instead of Toshifumi's *et al.* use of triethylamine.  $^1\text{H}$ -NMR and  $^{13}\text{C}$ -NMR of alkylating reagent (**375**) were in agreement with the literature.<sup>62</sup> Alkylating reagent (**375**) was subsequently reacted with ethyl nicotinate to give IL intermediate (**376**) in excellent yield (89%) after purification by column chromatography. Deprotection of IL (**376**) was attempted by hydrogenolysis to give target IL (**360**). However the hydrogenolysis reaction did not occur cleanly as per the previous benzyl IL (**373**) and gave a mixture of spots by TLC (10% MeOH:DCM). Analysis by  $^1\text{H}$ -NMR did not show the hydrogenolysis occurring cleanly. Analysis of the crude reaction mixture by LCMS identified a peak with  $m/z$  of 385.1735  $m/z$  corresponding to a diethyl ester cation (Figure 2.32) with the same  $m/z$  detected for IL (**327**). A redesigned synthesis route for IL (**360**) is further discussed in Section 2.4.6.4.

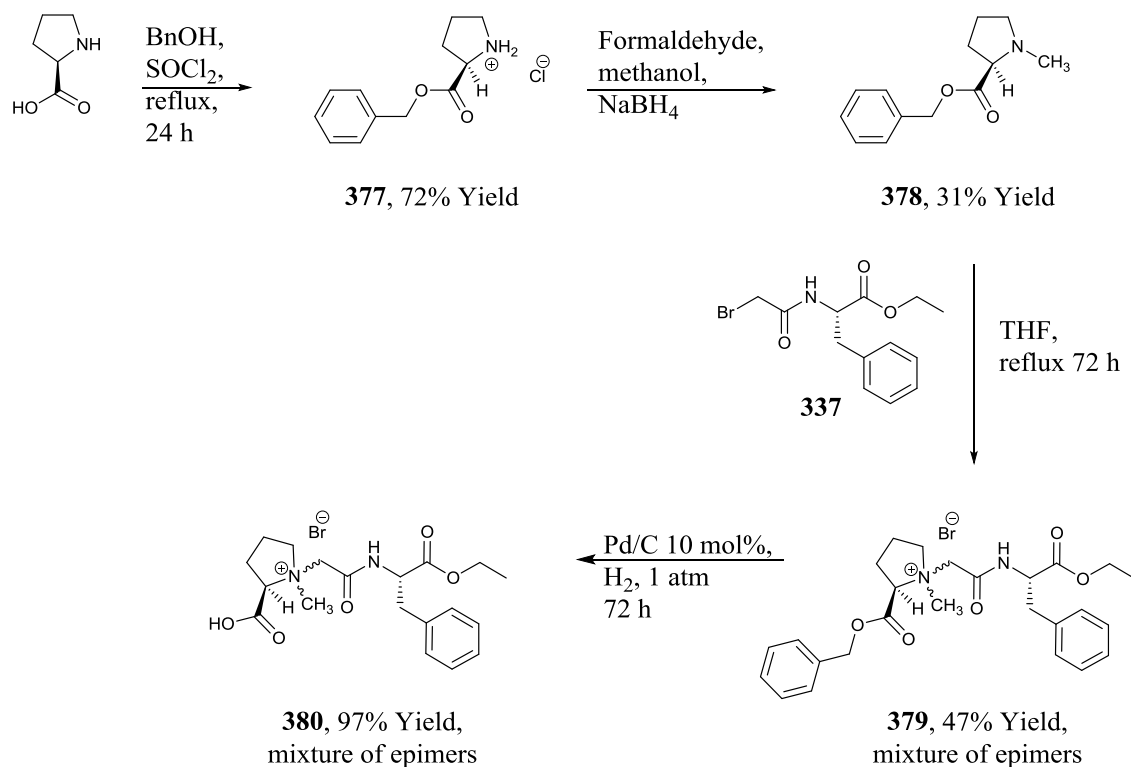


**Scheme 2.14.** Benzyl ester hydrogenolysis pathway for prolinium TPs (**360**).



**Figure 2.32.** Transesterified product produced from the hydrogenolysis reaction of (**376**).

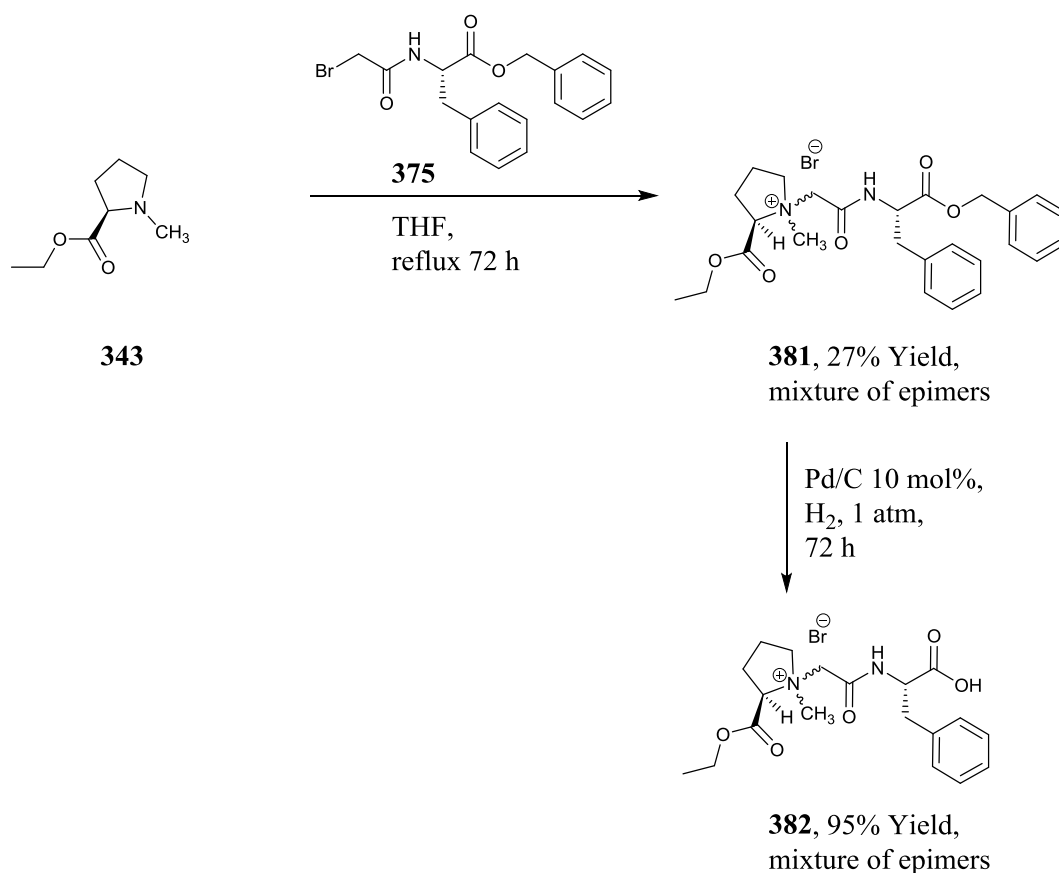
For L-prolinium IL (**332**) the potential TPs were determined to be ILs (**364**, **365**) thus benzyl esters were targeted for synthesis as per Scheme 2.15, 2.16. However due to stereochemical ambiguity reported during the biodegradation LC/MS analysis of L-prolinium IL (**332**) the D-prolinium benzyl esters and metabolite targets were synthesised as stereochemistry was not of concern to the LC/MS analysts. TP (**380**) was synthesised in place of (**364**) and (**382**) was synthesised in place of (**365**).



**Scheme 2.15.** Benzyl ester hydrogenolysis pathway for prolinium TP (**364/380**).

Synthesis of (**380**) began with the formation of D-proline benzyl ester hydrochloride (**377**) in good yield (72%) by Fischer-Speier esterification according to the method of Gagné *et al.*<sup>63</sup> (**377**) then underwent *N*-methylation by reductive alkylation using sodium borohydride and formaldehyde (and not with methyl iodide as carried out by Morphy *et al.*)<sup>64</sup> to give the *N*-methylated product (**378**) in moderate yield (31%). Reductive alkylation could not be carried out using Pd/C and H<sub>2</sub> as the benzyl ester would immediately undergo hydrogenolysis. Convergent synthesis of (**378**) and alkylation with (**337**) gave a mixture of IL epimers (**379**) which although purified from the reaction mixture could not be separated themselves by silica gel chromatography (*R<sub>f</sub>* < 0.01, 10% MeOH:DCM). The mixture of epimers then underwent hydrogenolysis to give TP (**380**) as a mixture of epimers (Scheme 2.15).

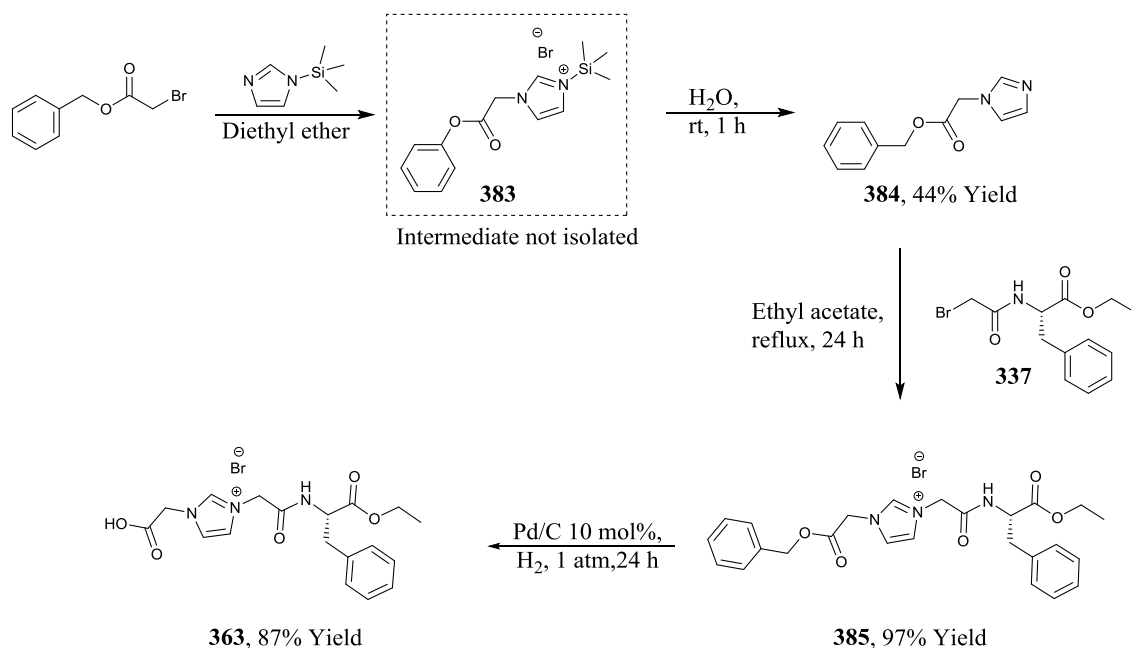




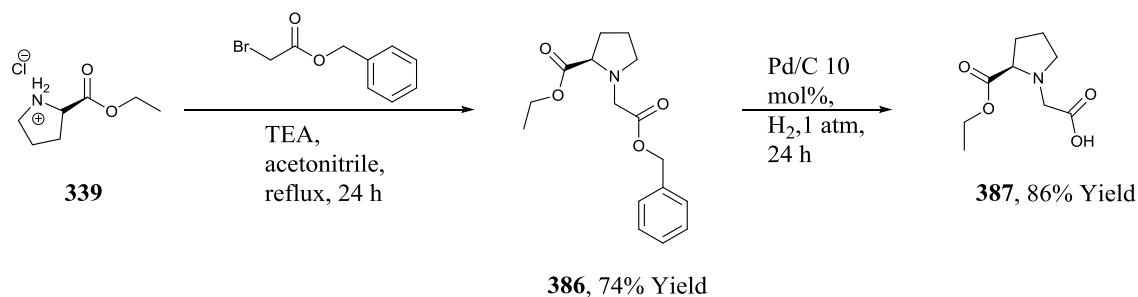
**Scheme 2.16.** Benzyl ester hydrogenolysis pathway for prolinium TP (**365/ 382**).

Similarly for L-prolinium TP (**365**) (Scheme 2.16), the D-prolinium derivative (**382**) was synthesised instead. A convergent synthesis from *N*-methyl-D-proline ethyl ester (**343**) with alkylating reagent (**375**) provided a mixture of IL epimers (**381**) in poor yield (27%). As per IL (**379**) the epimers could not be separated but were purified together by silica gel chromatography. Removal of the benzyl group by hydrogenolysis furnished TP (**382**) as a mixture of epimers.

For the synthesis of TPs (**380**, **382**) the benzyl ester hydrogenolysis strategy worked well for both compounds and could be applied to an L-prolinium synthesis in future if required. However due to the inseparable mixture of diastereomers present in both reactions, no definitive biodegradation or antimicrobial studies can be conducted with any certainty as to which diastereomer(s) may or may not be more biodegradable or may or may not have more or less toxic effect (if any).



TP (**363**) was also synthesised according to a benzyl ester hydrogenolysis route (Scheme 2.17). TMS-imidazole and benzylbromoacetate were reacted to form the IL intermediate (**383**) which rapidly precipitates as a white solid. Removal of solvent *in vacuo* and redissolving the intermediate in water (to remove the silyl protecting group) furnished intermediate (**384**) in moderate yield (44%) after purification by silica gel chromatography. Intermediate (**384**) was synthesised without the need to use a strong base to deprotonate imidazole before alkylation, as was the case with the synthesis outlined by Cerdan *et al.* using KOH to give the target (**384**)<sup>65</sup>. A convergent synthesis with (**337**) gave intermediate IL (**385**) in high yields (97%). Deprotection by hydrogenolysis afforded target TP (**363**) in high yield (87%). The synthesis was rapid, clean and efficient and required silica gel chromatography at only one stage, the purification of (**384**).

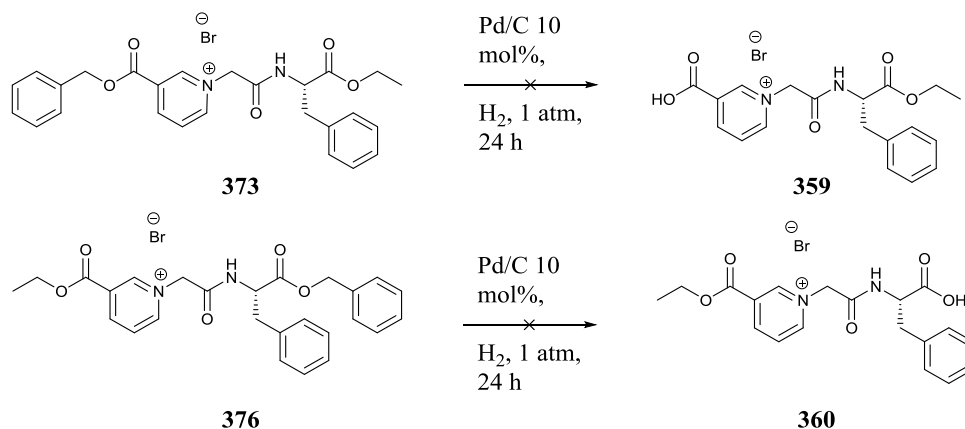


For the synthesis of L- target metabolite (**368**), once more due to the stereochemical ambiguity aforementioned, the target metabolite (**368**) was synthesised as the D-prolinium derivative

(**387**). Tertiary amino derivative (**387**) was similarly synthesised from monoalkylation of D-proline ethyl ester hydrochloride (**339**) to give the benzyl bromoacetate derivative (**386**) in good yield (74%). Debenzylation of (**386**) by hydrogenolysis gave target TP (**387**) in high yield (86%) (Scheme 2.18).

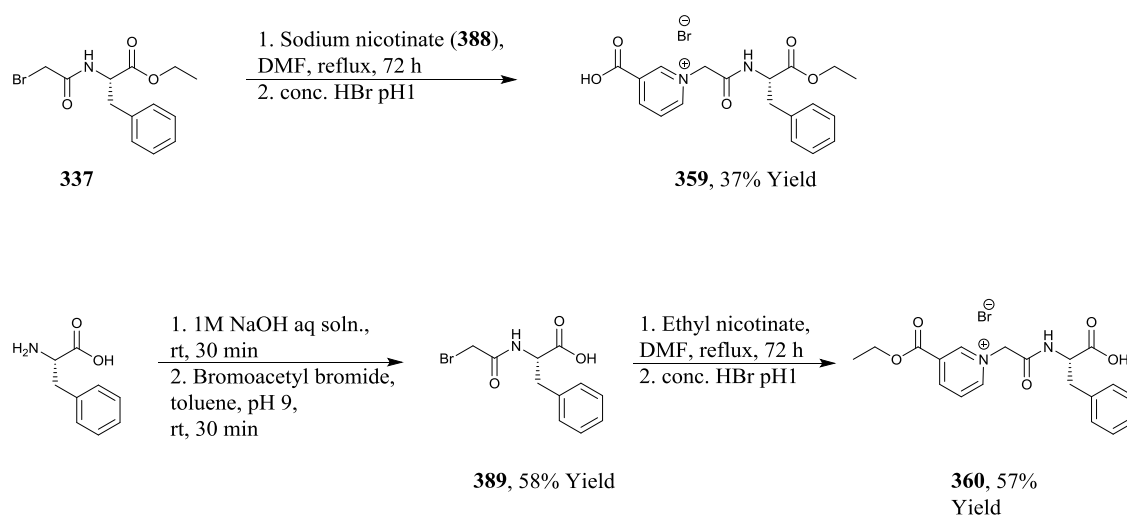
#### 2.4.6.4 Nicotinate TP synthesis redesign – route D

As the deprotection reaction by hydrogenolysis to remove the benzyl esters to give target compounds (**359**, **360**) (Scheme 2.19), did not proceed as expected, and clean deprotection could not be detected by  $^1\text{H-NMR}$ , a new route had to be considered.



**Scheme 2.19.** Failed benzyl deprotection reaction.

It was decided that instead of utilising benzyl esters as carboxylic acid protecting groups that utilising the target carboxylic acid from the very first stage of the reaction would be attempted. The redesigned synthesis is outlined in Scheme 2.20.



**Scheme 2.20.** Redesigned synthesis for TPs (**359**, **360**).

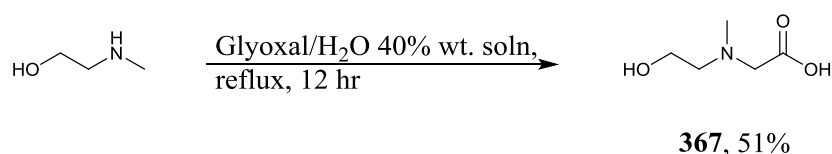
For the redesigned synthesis of **(359)** alkylating reagent **(337)** was reacted with sodium nicotinate **(388)** in refluxing DMF for 72 hours. After 72 hours the reaction mixture was acidified and purified by silica gel chromatography, to give the target product in moderate yields (37%) (Scheme 2.20). For the synthesis of TP **(360)** alkylating reagent **(389)** was synthesised according to the method outlined by Qin *et al.*<sup>66</sup> Alkylating reagent **(389)** was then reacted with ethyl nicotinate followed by purification by silica gel chromatography to give TP **(360)** in good yield (57%) (Scheme 2.20). The new synthetic route for **(359, 360)** gave the desired TPs, however a difficult separation by silica gel chromatography was required for the final purification. Carboxylic acid IL TPs are very polar and movement on normal phase silica gel made for a very slow purification.

#### 2.4.6.5 Imidazole acetic acid

TP **(366)** was commercially available and was purchased from TCI Europe.

#### 2.4.6.6 Formation of TP **(367)** – route E

TP **(367)** was formed through the 1 step reaction of glyoxal with 2-(methylamino)ethanol, according to the literature procedure outline by Farfán *et al.* Scheme 2.21,<sup>67</sup> in moderate yield (51%).



**Scheme 2.21.** Formation of TP **(367)**.

#### 2.4.6.7 Yield data for intermediate transformation product synthesis

As can be seen from Table 2.16, the ester yields observed ranged from good (e.g. **(372)**, 97%) to moderate (e.g. **374**, 48%). *N*-methylation of D-proline benzyl ester **(378)** proceeded with moderate yield (31%) whilst the *N*-alkylation of D-proline ethyl ester hydrochloride **(339)** with benzyl bromoacetate proceeded with 74% yield **(386)**. The intermediate benzyl acetate of imidazole, **(384)**, was produced in moderate yields (44%) potentially due to slow precipitation of the silyl IL intermediate **(383)** during the reaction. Synthesis of alkylating reagents **(375, 389)** proceeded in good yields (69%, 58% respectively). TP intermediate ILs were synthesised in poor (e.g. **381**, 27%) to excellent yields **(385, 97%)**. Poor yields associated with ILs **(373, 379, 381)** can be directly associated with the requirement for silica gel chromatography on these compounds to separate them from crude products containing multiple impurities by TLC.

**Table 2.16.** Percentage yields for intermediates synthesised.

Intermediate Compounds	Yield
<b>Esters</b>	
<b>372</b>	97%
<b>374</b>	48%
<b>377</b>	72%
<b><i>N</i>-alkylated products</b>	
<b>378</b>	31%
<b>384</b>	44%
<b>386</b>	74%
<b>Alkylating reagents</b>	
<b>375</b>	69%
<b>389</b>	58%
<b>IL TP intermediates</b>	
<b>369</b>	63%
<b>370</b>	87%
<b>371</b>	97%
<b>373</b>	44%
<b>376</b>	89%
<b>379</b>	47%
<b>381</b>	27%
<b>385</b>	97%

As can be seen from Table 2.17 a number of the TPs were synthesised in very poor (e.g. **382**, 4%) to excellent yields (**361**, 89%). Yields calculated are for the entire synthesis - whether linear or convergent - and include all synthetic transformations performed to reach the final TP. Synthesis routes that required >3 steps all suffered from a gradual drop in yield as can be expected from linear multi-step synthesis. Convergent synthesis methods employed for (**363**, **368**) gave higher overall yields (63-74%). Convergent synthesis for the D-prolinium TPs (**380**, **382**) suffered overall due to the poor yields observed for the *N*-alkylation of D-proline esters to give *N*-methylated products (**343**, 43%), (**378**, 31%) and the moderate to low yields observed for the formation of the benzyl ester ILs (**379**, 47%), (**381**, 27%). A two step linear synthesis such as that employed for (**358**, **361**) gives high final yields (67%, 89% respectively) due to the short nature of the synthesis. When compared to a three step linear synthesis such as that employed for (**359**), the additional third step in the synthesis reduces the overall yield significantly.

**Table 2.17.** Synthetic routes and final yields for TPs synthesised.

Transformation Product	Route	Total Steps	Final Step Yield	Overall Yield
<b>357</b>	A	2	73%	46%
<b>358</b>	A	2	77%	67%
<b>359</b>	D	3	37%	32%
<b>360</b>	D	2	57%	33%
<b>361</b>	A	2	92%	89%
<b>362</b>	B	4	75%	64%
<b>363</b>	C	5	87%	74%
<b>366</b>	TCI	N/A	N/A	N/A
<b>367</b>	E	1	51%	51%
<b>368</b>	C	3	86%	63%
<b>380</b>	C	6	97%	10%
<b>382</b>	C	6	95%	4%

The TPs and a number of their intermediates are also ILs, therefore their properties as ILs were also of interest. Melting points for the IL TPs are outlined in Table 2.18.

**Table 2.18.** Melting points for IL TPs and intermediates.

Final TPs	Melting Point °C
<b>357</b>	207-209
<b>358</b>	177-179
<b>359</b>	90-92
<b>360</b>	85-87
<b>361</b>	> 250
<b>362</b>	59-61
<b>380</b>	162-164
<b>382</b>	41-43
<b>IL TP Intermediates</b>	
<b>369</b>	133-135
<b>370</b>	36-38
<b>371</b>	227-229
<b>373</b>	50-52
<b>376</b>	63-65
<b>379</b>	159-161
<b>381</b>	42-44
<b>385</b>	57-59

As can be seen from Table 2.18 a number of the final TPs melt below 100 °C. TPs (**357**, **358**, **380**) were observed to have a significantly elevated melting point ~100 °C greater than the other TPs analysed. DMAP TP (**361**) had a melting point of > 250 °C. TP (**380**) was also observed to

melt at just 1-2 °C higher than its benzyl ester protected intermediate (**379**). All of the IL intermediates except (**369**, **371**, **379**) melted below 100 °C. None of the products synthesised were room temperature ILs.

The completion of the synthesis of detected TPs is a significant step in further understanding the environmental and toxicological interactions that may occur if ILs enter the terrestrial environment. Possessing a stock of synthesised and characterised TPs will allow for their further evaluation, whether by further investigations into their biodegradability or (eco)toxicity, to give a more complete picture of their lifecycle. The results of antimicrobial screening of the TPs are presented in Section 2.5.

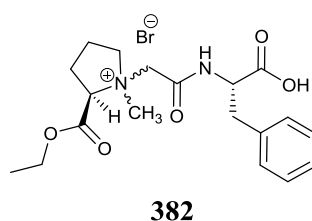
#### **2.4.7 Biodegradation screening conclusions**

From the results of the biodegradation screening it can be shown that one IL (**325**) was determined to be inherently ultimately biodegradable by the Closed Bottle Test (OECD 301D). L-phenylalanine ILs (**324**, **326-335**) appeared to be recalcitrant to biodegradation with a number of transformation products observed for ILs (**325-328**, **330-332**) screened. The remaining L-phenylalanine ILs were not examined for their transformation products. At the end of the 28 day test the presence of intact parent compound suggests that the ILs ester functionalities are more stable to aqueous conditions than expected (20 °C for 28 days). Tertiary amino derivatives examined (**345-347**) were shown to be more biodegradable than their IL counterparts, yet none of them passed the CBT. Tertiary amino compound (**345**) was determined to be inherently ultimately biodegradable after CBT test times were extended to 42 days. Results collected appear to be in agreement with Boethling's rules of thumb for designing compounds for degradation; tertiary amines are generally more biodegradable than quaternary amines.<sup>3</sup> The fact that one pyridinium IL (**325**) gave high levels of biodegradability in the CBT, and goes against the current trend of poorly biodegradable quaternary amines, shows that rational design of biodegradable ILs is challenging but not impossible. As can be seen from the observations made in Chapter 1 regarding biodegradability of pyridinium ILs, functionalization at the 3-position to give a methoxy pyridinium IL (**326**) reduces biodegradability. Similarly functionalization at the 4-position to give DMAP derivative (**328**) also appears to impede biodegradability. Additionally, the presence of an –OH moiety in the L-tyrosine derivatives screened hindered biodegradability from 5-13%.

### **2.5 Antimicrobial screening of transformation products**

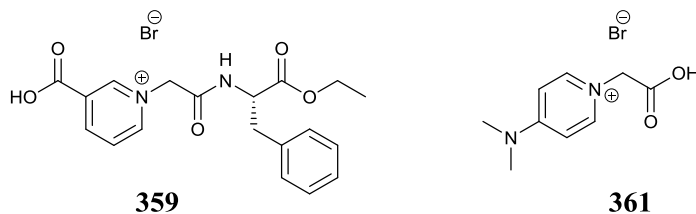
With the synthesis and characterisation of the TPs accomplished, the antimicrobial properties of the TPs were investigated as part of the same collaboration with Dr. Marcel Špulák, Faculty of

Pharmacy, Charles University, Czech Republic. The experimental methods, bacteria and fungi are the same as those outlined in Section 2.3. IL TPs (**358-363**, **380**, **382**) and tertiary amines (**366**, **368**) were examined for their antimicrobial toxicity. Overall the majority of the TPs possessed little to no discernible toxic effect towards the bacteria screened against up to the concentration limit of 2000  $\mu\text{mol/L}$ . The IL epimer mixture that comprised TP (**382**) displayed an  $\text{IC}_{95}$  of 500  $\mu\text{mol/L}$  towards the bacteria *S. aureus* and *S. epidermidis* (Table 2.19). The toxicity cannot be contributed to any one of the pair of isomers and thus is presented as the antimicrobial toxicity of a mixture.



**Figure 2.33.** IL (**382**).

Similarly, low levels of antifungal toxicity were observed. Just two ILs (**359**, **361**) showed any level of antifungal toxicity (Table 2.20). IL (**359**) had an  $\text{IC}_{95}$  of 2000  $\mu\text{mol/L}$  towards the two *Candida albicans* strains whilst IL (**361**) displayed an  $\text{IC}_{95}$  of 2000  $\mu\text{mol/L}$  towards the fungi *Candida parapsilosis* and *Trichophyton mentagrophytes*.



**Figure 2.34.** ILs (**359**, **361**).



**Table 2.19.** Antibacterial results obtained for TPS.

Microorganism	Time (h)	IL IC <sub>95</sub> μmol											
		357	358	359	360	361	362	363	366	367	368	380	382
Gram Positive													
SA	24h	>2000,	>2000,	>2000,	>2000,	>2000,	>2000,	>2000,	>2000,	>500,	>2000,	>1000,	500,
	48h	>2000	>2000	>2000	>2000	>2000	>2000	>2000	>2000	>500	>2000	>1000	500
MRSA	24h	>2000,	>2000,	>2000,	>2000,	>2000,	>2000,	>2000,	>2000,	>500,	>2000,	>1000,	>1000,
	48h	>2000	>2000	>2000	>2000	>2000	>2000	>2000	>2000	500	>2000	>1000	>1000
SE	24h	>2000,	>2000,	>2000,	>2000,	>2000,	>2000,	>2000,	>2000,	>500,	>2000,	>1000,	500,
	48h	>2000	>2000	>2000	>2000	>2000	>2000	>2000	>2000	>500	>2000	>1000	500
EF	24h	>2000,	>2000,	>2000,	>2000,	>2000,	>2000,	>2000,	>2000,	>500,	>2000,	>1000,	>1000,
	48h	>2000	>2000	>2000	>2000	>2000	>2000	>2000	>2000	>500	>2000	>1000	>1000
Gram Negative													
EC	24h	>2000,	>2000,	>2000,	>2000,	>2000,	>2000,	>2000,	>2000,	>500,	>2000,	>1000,	>1000,
	48h	>2000	>2000	>2000	>2000	>2000	>2000	>2000	>2000	>500	>2000	>1000	>1000
KP	24h	>2000,	>2000,	>2000,	>2000,	>2000,	>2000,	>2000,	>2000,	>500,	>2000,	>1000,	>1000,
	48h	>2000	>2000	>2000	>2000	>2000	>2000	>2000	>2000	>500	>2000	>1000	>1000
KP-E	24h	>2000,	>2000,	>2000,	>2000,	>2000,	>2000,	>2000,	>2000,	>500,	>2000,	>1000,	>1000,
	48h	>2000	>2000	>2000	>2000	>2000	>2000	>2000	>2000	>500	>2000	>1000	>1000
PA	24h	>2000,	>2000,	>2000,	>2000,	>2000,	>2000,	>2000,	>2000,	>500,	>2000,	>1000,	>1000,
	48h	>2000	>2000	>2000	>2000	>2000	>2000	>2000	>2000	>500	>2000	>1000	>1000

**Table 2.20.** L-Phenylalanine ILs screened for antifungal activity. \* IC<sub>50</sub> values were assessed for AF, AC and TM and IC<sub>80</sub> for all other strains.

Microorganism	Time (h)	IL IC <sub>80/50</sub> µmol*											
		357	358	359	360	361	362	363	366	367	368	380	382
<i>CAI</i>	24h	>2000,	>2000,	<b>2000,</b>	>2000,	>2000,	>2000,	>2000,	>2000,	>500,	>2000,	>1000,	>1000,
	48h	>2000	>2000	<b>2000</b>	>2000	>2000	>2000	>2000	>2000	>500	>2000	>1000	>1000
<i>CA2</i>	24h	>2000,	>2000,	<b>2000,</b>	>2000,	>2000,	>2000,	>2000,	>2000,	>500,	>2000,	>1000,	>1000,
	48h	>2000	>2000	<b>2000</b>	>2000	>2000	>2000	>2000	>2000	>500	>2000	>1000	>1000
<i>CP</i>	24h	>2000,	>2000,	>2000,	>2000,	<b>2000,</b>	>2000,	>2000,	>2000,	>500,	>2000,	>1000,	>1000,
	48h	>2000	>2000	>2000	>2000	<b>2000</b>	>2000	>2000	>2000	>500	>2000	>1000	>1000
<i>CKI</i>	24h	>2000,	>2000,	>2000,	>2000,	>2000,	>2000,	>2000,	>2000,	>500,	>2000,	>1000,	>1000,
	48h	>2000	>2000	>2000	>2000	>2000	>2000	>2000	>2000	>500	>2000	>1000	>1000
<i>CK2</i>	24h	>2000,	>2000,	>2000,	>2000,	>2000,	>2000,	>2000,	>2000,	>500,	>2000,	>1000,	>1000,
	48h	>2000	>2000	>2000	>2000	>2000	>2000	>2000	>2000	>500	>2000	>1000	>1000
<i>CT</i>	24h	>2000,	>2000,	>2000,	>2000,	>2000,	>2000,	>2000,	>2000,	>500,	>2000,	>1000,	>1000,
	48h	>2000	>2000	>2000	>2000	>2000	>2000	>2000	>2000	>500	>2000	>1000	>1000
<i>CG</i>	24h	>2000,	>2000,	>2000,	>2000,	>2000,	>2000,	>2000,	>2000,	>500,	>2000,	>1000,	>1000,
	48h	>2000	>2000	>2000	>2000	>2000	>2000	>2000	>2000	>500	>2000	>1000	>1000
<i>CL</i>	24h	>2000,	>2000,	>2000,	>2000,	>2000,	>2000,	>2000,	>2000,	>500,	>2000,	>1000,	>1000,
	48h	>2000	>2000	>2000	>2000	>2000	>2000	>2000	>2000	>500	>2000	>1000	>1000
<i>TA</i>	24h	>2000,	>2000,	>2000,	>2000,	>2000,	>2000,	>2000,	>2000,	>500,	>2000,	>1000,	>1000,
	48h	>2000	>2000	>2000	>2000	>2000	>2000	>2000	>2000	>500	>2000	>1000	>1000
<i>AF</i>	24h	>2000,	>2000,	>2000,	>2000,	>2000,	>2000,	>2000,	>2000,	>500,	>2000,	>1000,	>1000,
	48h	>2000	>2000	>2000	>2000	>2000	>2000	>2000	>2000	>500	>2000	>1000	>1000
<i>AC</i>	24h	>2000,	>2000,	>2000,	>2000,	>2000,	>2000,	>2000,	>2000,	>500,	>2000,	>1000,	>1000,
	48h	>2000	>2000	>2000	>2000	>2000	>2000	>2000	>2000	>500	>2000	>1000	>1000
<i>TM</i>	72h	>2000,	>2000,	>2000,	>2000,	<b>2000,</b>	>2000,	>2000,	>2000,	>500,	>2000,	>1000,	>1000,
	120h	>2000	>2000	>2000	>2000	<b>2000</b>	>2000	>2000	>2000	>500	>2000	>1000	>1000

It can be concluded from the antimicrobial screening that the TPs examined displayed negligible levels of toxicity at the concentrations screened at. The reduced levels of lipophilicity present in each compound may be an important factor in the low levels of toxicity observed.<sup>68, 69</sup> Low levels of toxicity such as those observed for the TPs suggests that IL biodegradation can produce relatively benign metabolic products and that the strategies employed within this chapter support the 4<sup>th</sup> principle of green chemistry: “designing safer chemicals”, and the 10<sup>th</sup> principle: “designing for degradation”.

## 2.6 Conclusions to 1st generation IL synthesis, biodegradation and antimicrobial toxicity screening

In conclusion a series of new L-phenylalanine ILs (**324-335**), tertiary amino analogues (**344-348**) and L-tyrosine ILs (**349-353**), have been synthesised and characterised by <sup>1</sup>H-NMR, <sup>13</sup>C-NMR, HRMS, IR, optical rotation and melting point. The target IL compounds were all produced in moderate to high yield yields with favourable green chemistry metrics established. ILs and tertiary amino analogues were produced in sufficient quantity and purity to facilitate an antimicrobial screening and biodegradation study. Of the ILs screened, both L-phenylalanine and L-tyrosine, possessed a low antimicrobial and low antifungal toxicity with only one IL (**331**) exhibiting an IC<sub>95</sub> of 500 µmol/L towards *S. aureus* and *S. epidermidis*. No other IL was observed with a lower IC<sub>95</sub>. All of the tertiary amino compounds examined (**344-348**) displayed higher levels of antimicrobial activity, especially towards *S. aureus* with IC<sub>95</sub> ranging from 125-1000 µmol/L with the tertiary amino proline derivatives (**347, 348**) displaying an IC<sub>95</sub> of 125 µmol/L towards *S. aureus*. The absence of a quaternary nitrogen atom in the tertiary amino compounds greatly increases the toxicity. From the results observed for the biodegradation screening, pyridinium IL (**325**) was observed to undergo 63% biodegradation within a 28 daytest period and 76% within a 42 day period and can be considered inherently ultimately biodegradable, but not readily biodegradable. Reduced levels of biodegradability (ranging from 17-51%) were observed for the rest of the ILs examined. None of the tertiary amino compounds (**344-347**) were considered readily biodegradable however a number of the tertiary amino derivatives (**345, 347**) underwent levels of biodegradation 20-22% higher than their IL counterparts (**330, 332/333**). Tertiary amino compounds (**344, 345**) also showed high levels of biodegradability (59% and 78% respectively) after test time extensions and (**345**) can be considered inherently ultimately biodegradable. This observation is in accordance with Boethling’s rules of thumb which suggests that generally tertiary amines undergo higher levels of biodegradation than quaternary amines.<sup>3</sup> A metabolite study on a number of ILs (**325-328**,

330-332) was carried out and persistent TPs were identified and subsequently synthesised; ILs (357-363, 380, 382) and tertiary amines (366, 367, 387). Overall, the TP's displayed little to no discernible antimicrobial toxicity and suggest that the IL metabolic products could be benign towards certain bacteria and fungi at the concentrations screened at. The TPs have since been submitted for investigation into their biodegradability to assess potential bioaccumulation. This work will be conducted by the research group of Prof. Klaus Kummerer, Faculty for Sustainability, University of Lüneburg, Germany.

It can be concluded that IL derivative (325) was the most "green" candidate of all the ILs examined. It can be rapidly synthesised in a short high yielding synthesis with favourable green chemistry metrics and did not require silica gel chromatography for purification at any stage. IL (325) also displayed very low levels of toxicity to bacteria screened against, displaying an MIC of 2000 µmol/L to *S. aureus* and >2000 µmol/L towards all other bacteria and fungi. IL (325) also can be categorised as inherently ultimately biodegradable and did not present any detectable transformation products. Overall the design and synthesis of low toxicity biodegradable ILs according to the 12 Principles of Green Chemistry and Boethling's Rules of Thumb has been a success in producing IL (325). For all of the ILs and tertiary amines, the antimicrobial toxicity and biodegradation data will prove invaluable in designing future generations of ILs. The data alone will be used in the future as data training sets for computational studies on the biodegradability and antimicrobial toxicity of ILs.

## 2.7 References

1. A. Jordan, A. Haisß, M. Spulak, Y. Karpichev, K. Kummerer and N. Gathergood, *Green Chem.*, 2016, DOI: 10.1039/C6GC00415F.
2. A. Haisß, A. Jordan, J. Westphal, E. Logunova, N. Gathergood and K. Kummerer, *Green Chem.*, 2016, DOI: 10.1039/C6GC00417B.
3. R. S. Boethling, E. Sommer and D. DiFiore, *Chem. Rev.*, 2007, 107, 2207-2227.
4. P. Anastas and N. Eghbali, *Chem. Soc. Rev.*, 2010, 39, 301-312.
5. D. Coleman, M. Spulak, M. T. Garcia and N. Gathergood, *Green Chem.*, 2012, 14, 1350-1356.
6. Y. Deng, S. Morrissey, N. Gathergood, A. M. Delort, P. Husson and M. F. C. Gomes, *Chemsuschem*, 2010, 3, 377-385.
7. S. Morrissey, B. Pegot, D. Coleman, M. T. Garcia, D. Ferguson, B. Quilty and N. Gathergood, *Green Chem.*, 2009, 11, 475-483.
8. N. Gathergood, P. J. Scammells and M. T. Garcia, *Green Chem.*, 2006, 8, 156-160.
9. M. T. Garcia, N. Gathergood and P. J. Scammells, *Green Chem.*, 2005, 7, 9-14.
10. N. Gathergood, M. T. Garcia and P. J. Scammells, *Green Chem.*, 2004, 6, 166-175.
11. N. Bodor, J. J. Kaminski and S. Selk, *J. Med. Chem.*, 1980, 23, 470-474.
12. R. A. Reck and H. J. Harwood, *Industrial and Engineering Chemistry*, 1953, 45, 1022-1026.

13. C. C. O. Alves, A. S. Franca and L. S. Oliveira, *LWT--Food Sci. Technol.*, 2013, 51, 1-8.
14. *Organic Chemicals in the Environment*, CRC Press, 2012.
15. P. F. Fitzpatrick, *Annu. Rev. Biochem.*, 1999, 68, 355-381.
16. A. Jordan and N. Gathergood, *Antibiotics*, 2013, 2, 419.
17. P. T. W. Anastas, J. C. , *Green Chemistry: Theory and Practice*, Oxford University Press: New York, 1998.
18. R. A. Sheldon, *C. R. Acad. Sci., Ser. IIC: Chim.*, 2000, 3, 541-551.
19. B. M. Trost, *Science*, 1991, 254, 1471-1477.
20. A. R. Ali, H. Ghosh and B. K. Patel, *Tetrahedron Lett.*, 2010, 51, 1019-1021.
21. C. Jungnickel, F. Stock, T. Brandsch and J. Ranke, *Environ. Sci. Pollut. Res.*, 2008, 15, 258-265.
22. J. M. DeSimone, *Science*, 2002, 297, 799-803.
23. B. A. Roberts and C. R. Strauss, *Acc. Chem. Res.*, 2005, 38, 653-661.
24. M. R. Infante, L. Perez, M. C. Moran, R. Pons, M. Mitjans, M. P. Vinardell, M. T. Garcia and A. Pinazo, *Eur. J. Lipid Sci. Technol.*, 2010, 112, 110-121.
25. P. J. Dunn, *Chem. Soc. Rev.*, 2012, 41, 1452-1461.
26. P. T. Anastas, M. M. Kirchhoff and T. C. Williamson, *Appl. Catal., A*, 2001, 221, 3-13.
27. C. Jungnickel, W. Mrozik, M. Markiewicz and J. Luczak, *Curr. Org. Chem.*, 2011, 15, 1928-1945.
28. J. Wang, *Acc. Chem. Res.*, 2002, 35, 811-816.
29. P. A. Duspara, M. S. Islam, A. J. Lough and R. A. Batey, *J. Org. Chem.*, 2012, 77, 10362-10368.
30. J. Andraos, *Org. Process Res. Dev.*, 2006, 10, 212-240.
31. J. Andraos, *Green chemistry metrics: measuring and monitoring sustainable processes*, Blackwell-Wiley, Oxford, 2008.
32. J. Andraos, *Org. Process Res. Dev.*, 2009, 13, 161-185.
33. J. Andraos, *Pure Appl. Chem.*, 2011, 83, 1361-1378.
34. D. J. C. Constable, C. Jimenez-Gonzalez and R. K. Henderson, *Org. Process Res. Dev.*, 2007, 11, 133-137.
35. A. D. Curzons, D. J. C. Constable, D. N. Mortimer and V. L. Cunningham, *Green Chemistry*, 2001, 3, 1-6.
36. C. Jiménez-González, D. Constable, A. Curzons and V. Cunningham, *Clean Techn Environ Policy*, 2002, 4, 44-53.
37. C. R. McElroy, A. Constantinou, L. C. Jones, L. Summerton and J. H. Clark, *Green Chem.*, 2015, 17, 3111-3121.
38. Z. Wang, *Menschutkin Reaction*, John Wiley & Sons, Inc., 2010.
39. J. Nowick, Multiplet Guide and Workbook, <http://www.chem.uci.edu/~jsnowick/groupweb/files/MultipletGuideV4.pdf>, Accessed 11/06/2015.
40. Y. H. Lin. Nan-horng, R. L. Elliott, M. S. Chorghade, S. J. Wittenberger, W. H. Bunnelle, B. A. Narayanan, P. Singam, T. K. J. Esch, D. O. Beer, C. C. Witzig, T. C. Herzig, A. R. Rao, *Method of Preparing Enantiomerically-pure 3-methyl-5-(1-alkyl-2(s)-pyrrolidinyl)isoxazoles*, Abbott Laboratories (One Abbott Park Road, Abbott Park, Illinois, 60064-3500, US) European Patent Number: EP0717741, 2001.
41. D. G. Golovanov, K. A. Lyssenko, Y. S. Vygodskii, E. I. Lozinskaya, A. S. Shaplov and M. Y. Antipin, *Russian Chemical Bulletin*, 2006, 55, 1989-1999.
42. J. Decatur, NOESY on the 400 and 500 Using Topspin, <http://www.columbia.edu/cu/chemistry/groups/nmr/noesy.pdf>, Accessed 08/07/2015.
43. K. M. Docherty and J. C. F. Kulpa, *Green Chem.*, 2005, 7, 185-189.
44. L. Myles, R. Gore, M. Spulak, N. Gathergood and S. J. Connon, *Green Chem.*, 2010, 12, 1157-1162.

45. Y.-R. Luo, W. San-Hu, X.-Y. Li, M.-X. Yun, J.-J. Wang and Z.-J. Sun, *Ecotoxicol. Environ. Saf.*, 2010, 73, 1046-1050.
46. S. P. M. Ventura, F. A. e Silva, A. M. M. Gonçalves, J. L. Pereira, F. Gonçalves and J. A. P. Coutinho, *Ecotoxicol. Environ. Saf.*, 2014, 102, 48-54.
47. S. Studzinska and B. Buszewski, *Anal. Bioanal. Chem.*, 2009, 393, 983-990.
48. K. J. Kulacki and G. A. Lamberti, *Green Chem.*, 2008, 10, 104-110.
49. M. Larry M. Bush, Overview of Bacteria, <http://www.merckmanuals.com/home/infections/bacterial-infections/overview-of-bacteria>, Accessed 27/8/15.
50. M. H. Fatemi and P. Izadiyan, *Chemosphere*, 2011, 84, 553-563.
51. R. G. Gore, L. Myles, M. Spulak, I. Beadham, T. M. Garcia, S. J. Connon and N. Gathergood, *Green Chem.*, 2013, 15, 2747-2760.
52. Y. Deng, I. Beadham, M. Ghavre, M. F. Costa Gomes, N. Gathergood, P. Husson, B. Legeret, B. Quilty, M. Sancelme and P. Besse-Hoggan, *Green Chem.*, 2015, 17, 1479-1491.
53. S. Stolte, S. Steudte, A. Igartua and P. Stepnowski, *Curr. Org. Chem.*, 2011, 15, 1946-1973.
54. M. Seyfried, C. G. van Ginkel, A. Boschung, F. Miffon, P. Fantini, E. Tissot, L. Baroux, P. Merle and A. Chaintreau, *Chemosphere*, 2015, 131, 63-70.
55. M. Ghavre, PhD, Dublin City University, 2012.
56. O. Y. Neilands, E. V. Shebenina and G. G. Pukitis, *Int. Arch. Allergy Appl. Immunol.*, 1999, 35, 1443-1450.
57. J. M. Sanders, Y. Song, J. M. W. Chan, Y. Zhang, S. Jennings, T. Kosztowski, S. Odeh, R. Flessner, C. Schwerdtfeger, E. Kotsikorou, G. A. Meints, A. O. Gómez, D. González-Pacanowska, A. M. Raker, H. Wang, E. R. van Beek, S. E. Papapoulos, C. T. Morita and E. Oldfield, *J. Med. Chem.*, 2005, 48, 2957-2963.
58. V. M. Krishnamurthy, V. Semetey, P. J. Bracher, N. Shen and G. M. Whitesides, *J. Am. Chem. Soc.*, 2007, 129, 1312-1320.
59. M. N. Soltani Rad, S. Behrouz, M. A. Faghihi and A. Khalafi-Nezhad, *Tetrahedron Lett.*, 2008, 49, 1115-1120.
60. C. J. Gray, M. Quibell, K. L. Jiang and N. Baggett, *Synthesis*, 1991, 1991, 141-146.
61. T. Miyazawa, *Bull. Chem. Soc. Jpn.*, 1980, 53, 3661-3669.
62. A. Basak, D. Mitra, M. Kar and K. Biradha, *Chem. Commun.*, 2008, DOI: 10.1039/B801644E, 3067-3069.
63. S. M. Voshell, S. J. Lee and M. R. Gagné, *J. Am. Chem. Soc.*, 2006, 128, 12422-12423.
64. A. R. Brown, D. C. Rees, Z. Rankovic and J. R. Morphy, *J. Am. Chem. Soc.*, 1997, 119, 3288-3295.
65. P. Zaderenko, M. S. Gil, P. Ballesteros and S. Cerdan, *J. Org. Chem.*, 1994, 59, 6268-6273.
66. H.-P. Li, S. Li, Z.-D. Wang and L. Qin, *J. Korean Chem. Soc.*, 2011, 55, 978-982.
67. N. Farfán, L. Cuéllar, J. M. Aceves and R. Contreras, *Synthesis*, 1987, 1987, 927-929.
68. L. Carson, P. K. W. Chau, M. J. Earle, M. A. Gilea, B. F. Gilmore, S. P. Gorman, M. T. McCann and K. R. Seddon, *Green Chem.*, 2009, 11, 492-497.
69. A. Buseti, D. E. Crawford, M. J. Earle, M. A. Gilea, B. F. Gilmore, S. P. Gorman, G. Laverty, A. F. Lowry, M. McLaughlin and K. R. Seddon, *Green Chem.*, 2010, 12, 420-425.

## **Chapter 3**

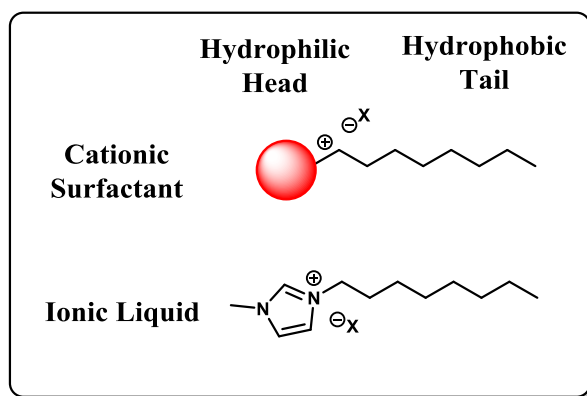
### *Synthesis of 2<sup>nd</sup> Generation Amino Acid ILs*

### 3.1 Aim

The aim of this chapter of work was to design and synthesise a series of 2<sup>nd</sup> generation amino acid ILs, derived from those presented in Chapter 2, with potential surface active properties (i.e. surfactants). Synthesis was carried out with respect to the 12 principles of green chemistry and Boethling's rules of thumb for designing molecules for their biodegradability and from the results presented in Chapter 2 regarding toxicity and biodegradability of ILs. The series of ILs presented within this chapter will be referred to as the "2<sup>nd</sup> generation" of amino acid ILs. Biodegradability and antimicrobial toxicity of this 2<sup>nd</sup> generation was a key point for investigation. An introduction to surfactants is given in this chapter, however the study of the surfactant properties of the 2<sup>nd</sup> generation ILs synthesised are presented separately in Chapter 4.

### 3.2 Introduction

The overlap between surfactant, or surface-active agents, and IL chemistry is one that has been observed from the very beginning of the current upsurge in IL research and development. Many of the structural features of ILs correspond with the functionalities present in surfactants.<sup>1</sup> (Most) ILs and surfactants are amphoteric classes of molecules i.e. they possess a polar, hydrophilic head(s) and a lipophilic, hydrophobic tail(s). A number of linear alkyl IL structures are analogous to those found in cationic surfactants and the research and design strategies of both fields, to promote biodegradation and control toxicity (based on application), are comparable. The structure of the 3-methyl-1-octyl imidazolium halide IL series, or [omim][X], is one of the many ILs that shares structural features with cationic surfactants (Figure 3.1).



**Figure 3.1.** Structural similarities between ILs and surfactants.

Since the implementation of the EU regulation on detergents in 2004 (Regulation (EC) No 648/2004), investigation into the ultimate biodegradability of surfactants has been a requirement. This legal requirement has driven a new wave of investigation into the preparation



of biodegradable surfactants that coincided with the advent of the first readily biodegradable ILs.<sup>2-4</sup> Strategies that have been employed to promote biodegradation are well documented, with the inclusion of hydrolysable ester bonds and cleavable amide links and are discussed in Chapter 1, Section 1.3.3 and Section 1.7.

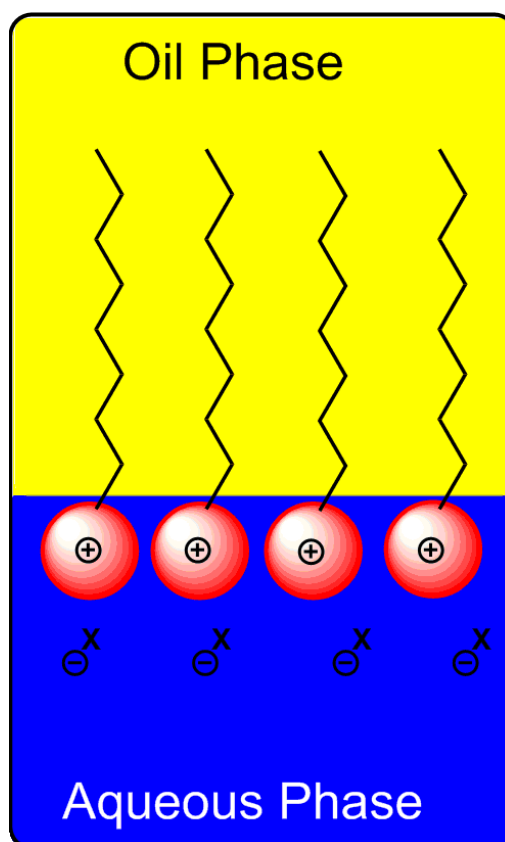
Under the EU regulation on detergents legislation, if a surfactant does not ultimately biodegrade then derogation may be applied for depending on the end use application and the calculated risk to the environment and health by the expected use of such a surfactant. Hence, antimicrobial toxicity data is vital.<sup>5</sup>

Surfactants are of interest due to their ability to adsorb onto surfaces or interfaces at relatively low concentrations. This property alters the interfacial energy of the surface or interface. Interface is the term used to define a boundary between two immiscible phases such as oil and water. Surface can also be used as a term when referring to an interface between one phase and a gas, e.g. air and water.<sup>6</sup>

Surfactants find a wide range of applications due to their phase boundary behaviour such as in detergents, emulsifiers, foaming agents, cleaning agents and phase transfer catalysis.<sup>6,7</sup> The ability to trap a significant proportion of the total mass of a system at a phase boundary, such as is present in an emulsion (a dispersion of minute droplets of oil in the aqueous phase), makes surfactants particularly useful, e.g. in cleaning an oil spill in an aquatic environment. When a surfactant's interfacial behaviour is so strong (when compared to the rest of the bulk phase of a system) then the entire system's behaviour can be dominated by what is occurring at the interface, an example of which is phase transfer catalysis.

The amphiphilic nature of surfactants means that if a surfactant is dissolved in an aqueous medium, the hydrophobic portion of the molecule can disrupt hydrogen bonding between water molecules. Thus the contact area between the hydrophobic portion of the surfactant and water is minimised. Repulsive behaviour can orientate the surfactant molecules as a mono-layer at the air-water surface boundary with the hydrophobic portion pointing almost entirely towards the air. Similar behaviour can be imagined for an oil-water interface where the hydrophobic portion is orientated towards the oil and the hydrophilic portion is orientated towards the water. As both the oil and the hydrophobic portion of the surfactant are non-polar species, the surfactant essentially allows "bridging" of the two phases as one portion of the surfactant exists in each phase. A reduction in the energy barrier is observed and the two phases are repelled to a lesser

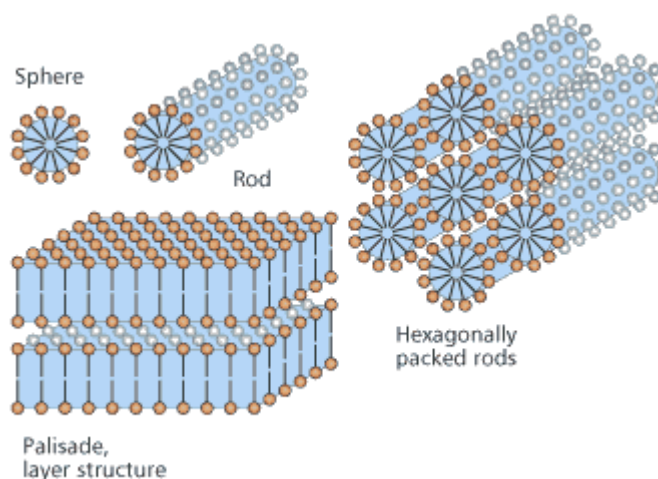
degree, hence a reduction in the surface tension is observable (Figure 3.2). The overall reduction of surface tension can eventually lead to an emulsified state.



**Figure 3.2.** Surfactant orientation at an oil-water interface.

Once an interface reaches saturation point there remains nowhere for additional molecules (i.e. higher concentrations) of surfactant to dissolve except for in one of the two phases. In an air-water system the excess concentration of surfactant begins to aggregate in the aqueous phase as colloidal sized particles (particles with diameters between 1 and 1000 nm) i.e micelles. Co-operative aggregation to hemi-micelles can also occur before surface saturation occurs. Bilayers and multilayer organisation is also possible as are rod shapes and hexagonal rods to name just a few (Figure 3.3). Solvents capable of hydrogen bonding from two or more centres are the only types reported capable of forming micelles due to the extended hydrogen bond network required to hold the aggregates together.<sup>6</sup> Micellisation is of importance for detergency (cleaning) applications as micelles allow for the dissolution and solubilisation of otherwise immiscible components (Figure 3.4). Micellisation is also of significance in drug delivery applications as drug molecules can be encapsulated within a micellar membrane allowing for greater control of delivery method and overall solubility. Drug molecules which are not water soluble can be enveloped within a micelle, which can in turn dissolve in an aqueous system.<sup>8</sup>

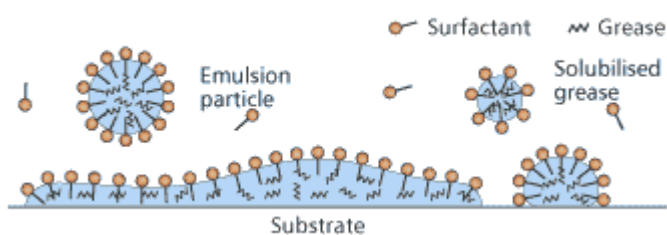
The concentration of surfactant required for the spontaneous formation of micelles is known as the critical micelle concentration (CMC). Many factors affect the micellisation process including temperature, the presence of electrolytes, and the presence of other organic molecules. Temperature increase can at first decrease the CMC, as the increase in temperature causes a reduction in hydration around the hydrophobic portion of a surfactant thus promoting micellisation. However if the temperature continues to increase then the water structure and hydrogen bonding that helps to maintain the micelle structure becomes disrupted and micellisation becomes unfavourable. The addition of electrolytes such as NaCl etc. can help to decrease the CMC as the addition of electrolytes aids in decreasing the ionic repulsion between charged headgroups in micelles, thus promoting micellisation. This effect is greater for cationic and anionic classes of surfactants followed by zwitter-ionic then non-ionic, see Section 3.2 for information on these classes of surfactants.



**Figure 3.3.** Micelles and some of the different forms that they can take.

Adapted from “Surfactants: the ubiquitous amphiphiles”

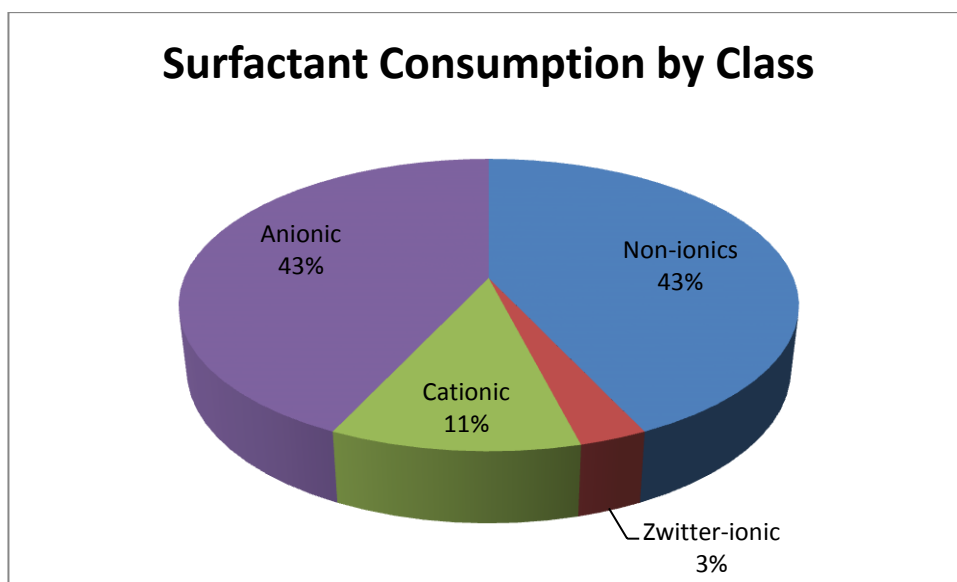
<http://www.rsc.org/chemistryworld/Issues/2003/July/amphiphiles.asp>.<sup>9</sup>



**Figure 3.4.** Detergent application of a surfactant.

### 3.3 Classes of surfactants

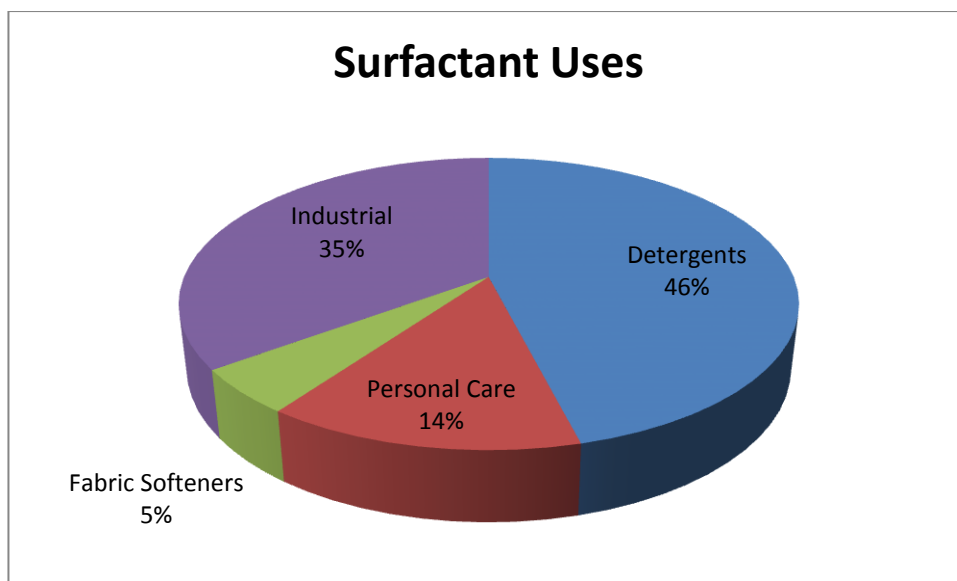
There exists four major classes of surfactants which can be categorised into two main groups: three ionic and one non-ionic. The three ionic classes are zwitter-ionic, anionic and cationic, each of which have considerably different properties, pros and cons.<sup>6</sup> Global consumption of surfactants by class is depicted in Figure 3.5. As can be seen, the anionic and non-ionic classes of surfactants combined dominate the global consumption of surfactants, followed by cationic and then zwitter-ionic surfactants. The breakdown of surfactant use and consumption by area can be seen in Figure 3.6.



**Figure 3.5.** Consumption of surfactants by class.<sup>10</sup>

Adapted from I. L. Matthew, in *Handbook of Detergents, Part F*, CRC Press, 2008, DOI: doi:10.1201/9781420014655.ch1

13 million metric tons of surfactants were produced in 2006 and it has been projected that upwards of 22 million tons will be produced annually by 2019 making surfactant production a lucrative market worth in the excess of €40 billion.<sup>11</sup>

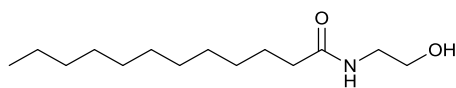


**Figure 3.6.** Uses of surfactants by sector/ application.<sup>10</sup>

Adapted from I. L. Matthew, in *Handbook of Detergents, Part F*, CRC Press, 2008, DOI: doi:10.1201/9781420014655.ch1

### 3.3.1 Non-Ionic

Non-ionic surfactants do not bear a charge at all on the surface active moiety and are not comprised of an anion-cation pair but instead a single uncharged chemical unit. The hydrophilic head of the unit is most often comprised of multiple heteroatoms such as a sugar unit or primary alcohols, whereas the hydrophobic tail can be comprised of a fatty acid/alcohol derivative (Figure 3.5). Due to the absence of a charge carrier the non-ionic surfactants have reduced electrostatic effect and do not strongly adsorb onto charged surfaces. Non-ionic surfactants are used as detergents and in the personal care and food products industry. Examples of non-ionic surfactants included polyethylene glycols (PEG), polysorbates, cocamide ethanolamines (**390**) (Figure 3.7) and nonylphenols.<sup>6, 12</sup>



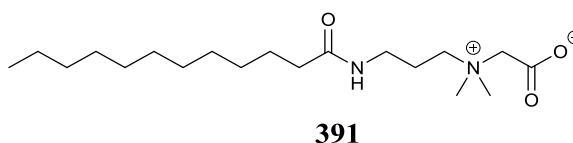
**390**

**Figure 3.7.** Cocamide monoethanolamine (**390**).

### 3.3.2 Zwitter-Ionic

Zwitter-Ionic surfactants bear both a positively and negatively charged portion on the same molecule and can be considered ampholytic. They also do not require a counterion to maintain charge balance. Some zwitter-ionic surfactant's ionisation states can be pH dependant, thus

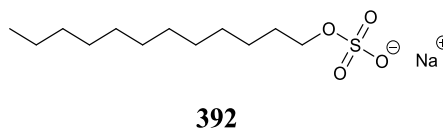
allowing for altering of physico-chemical properties by changing the acidity or basicity of the surfactant environment. This leads to the sub classification of amphoteric surfactants i.e. being able to act as both a base or an acid. At high pH zwitter-ionics can exhibit the surfactant properties of anionic surfactants and at low pH can exhibit cationic surfactant properties. As most surfaces in nature are negatively charged, zwitter-ionic surfactants can adsorb onto the surface without significantly altering the overall charge state of the surface. Zwitter-ionic surfactants find uses as dispersing aids, bactericides and corrosion inhibitors. Examples of zwitter-ionic surfactant classes include amidopropyl betaines (**391**) (Figure 3.8), amphotacetates and the sulphobetaines.<sup>6</sup>



**Figure 3.8.** Cocamidopropyl betaine (**391**).

### 3.3.3 Anionic

Anionic surfactants bear a negative charge on the surface active portion of the molecule and a positively charged counterion. Due to their negatively charged surface active portion the anionic surfactant family will be repelled by any negatively charged surfaces. Anionic surfactants can easily be prepared by neutralising fatty acids with a base to give the classic family of soaps. Other popular classes include sulphonic acid or phosphoric acid salts. Some anionic surfactants such as the fatty acid soaps can readily be insolubilised by electrolyte solutions (such as brine) and can be unstable under acidic conditions. Anionic surfactants play a large role in detergency and cleaning applications and are generally cheap to produce. Examples of anionic surfactants are the linear alkyl benzene sulphonates (LAS), alkyl sulphonates such as sodium dodecyl sulfate (**392**) (Figure 3.9), alkyl phosphates and metal carboxylates of fatty acids.<sup>6</sup>

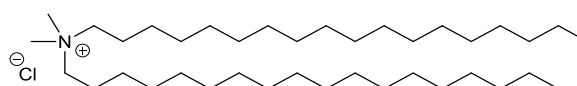


**Figure 3.9.** Sodium dodecyl sulphate (**392**).

### 3.3.4 Cationic

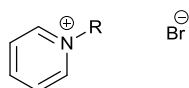
The cationic class of surfactants carry a positive charge on the surface active portion of the molecule and possess a negatively charged counterion. Cationic surfactants can readily adsorb onto negatively charged surfaces with the tail orientated away from the surface and thus create a water repellent barrier. In general cationic surfactants are more expensive than anionic and

display poorer detergent properties.<sup>6</sup> Cationic surfactants are also generally not compatible with anionic surfactants. Quaternary cationic charge carriers retain their water solubility regardless of pH. Cationic surfactants see a wide range of applications from herbicides and antimicrobials to fabric softeners and water repelling agents.<sup>6, 13</sup> As they readily adsorb onto surfaces they can impart their properties onto the surface. Examples of cationic surfactants include quaternary ammonium compounds (QAC's), such as distearyldimethylammonium chloride (**393**) (Figure 3.10), quaternary phosphonium, alkyl pyridinium surfactants and imidazolium based surfactants (Figures 3.11, 3.12).<sup>6</sup> A number of IL surfactants are also presented in Chapter 1, Section 1.7



**393**

**Figure 3.10.** Distearyldimethylammonium chloride



**394**, R = C<sub>10</sub>H<sub>21</sub>

**395**, R = C<sub>11</sub>H<sub>23</sub>

**396**, R = C<sub>12</sub>H<sub>25</sub>

**397**, R = C<sub>13</sub>H<sub>27</sub>

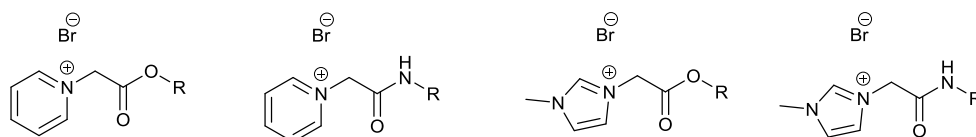
**398**, R = C<sub>14</sub>H<sub>29</sub>

**399**, R = C<sub>15</sub>H<sub>31</sub>

**400**, R = C<sub>16</sub>H<sub>33</sub>

**401**, R = C<sub>18</sub>H<sub>37</sub>

**Figure 3.11.** Alkyl pyridinium surfactants (n = 10-16, 18) reported by Rosen *et al.*<sup>14</sup> and Skerjanc *et al.*<sup>15</sup>



**402**, R = C<sub>6</sub>H<sub>13</sub>

**403**, R = C<sub>8</sub>H<sub>17</sub>

**404**, R = C<sub>10</sub>H<sub>21</sub>

**405**, R = C<sub>12</sub>H<sub>25</sub>

**406**, R = C<sub>14</sub>H<sub>29</sub>

**407**, R = C<sub>6</sub>H<sub>13</sub>

**408**, R = C<sub>8</sub>H<sub>17</sub>

**409**, R = C<sub>10</sub>H<sub>21</sub>

**410**, R = C<sub>12</sub>H<sub>25</sub>

**411**, R = C<sub>14</sub>H<sub>29</sub>

**412**, R = C<sub>6</sub>H<sub>13</sub>

**413**, R = C<sub>8</sub>H<sub>17</sub>

**414**, R = C<sub>10</sub>H<sub>21</sub>

**416**, R = C<sub>12</sub>H<sub>25</sub>

**416**, R = C<sub>14</sub>H<sub>29</sub>

**417**, R = C<sub>6</sub>H<sub>13</sub>

**418**, R = C<sub>8</sub>H<sub>17</sub>

**419**, R = C<sub>10</sub>H<sub>21</sub>

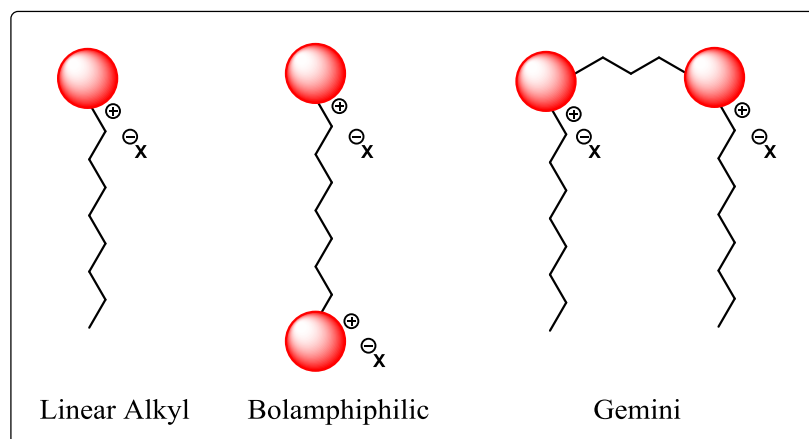
**420**, R = C<sub>12</sub>H<sub>25</sub>

**421**, R = C<sub>14</sub>H<sub>29</sub>

**Figure 3.12.** Alkyl ester and amide surfactants reported by Pérez *et al.*<sup>16, 17</sup> Imidazolium ILs (**412-414**) originally reported by Gathergood and Morrissey.<sup>3, 18</sup>

### 3.4 Subclasses of surfactants

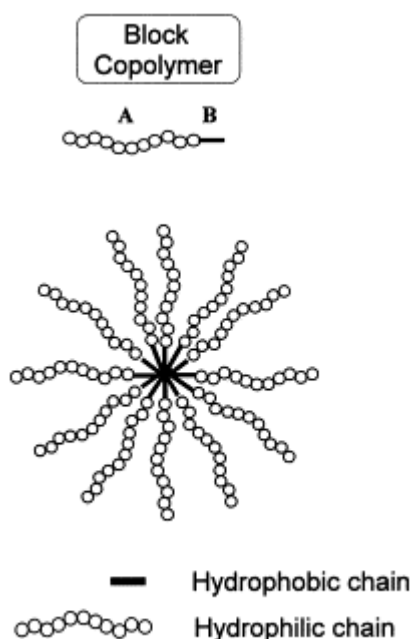
Within the classes of surfactant lie three main sub-classes. These sub-classes could be considered the overall structure or architecture of a surfactant molecule and are irrespective of whether the surfactant is charged or how it derives its charge. Structural composition of a surfactant and how its alkyl chain(s) are positioned give rise to the following classes of surfactants and are outline in Figure 3.13(cationic headgroups are depicted for illustrative purposes but they could also be anionic).



**Figure 3.13.** Subclasses of surfactants.

The surfactant properties and applications of polymers have also been widely reported but are not discussed in depth within the scope of this body of work. Polymeric surfactants derive their properties in much the same way as monomeric surfactants would; they are comprised of hydrophilic and hydrophobic regions that allow the polymer to interact at the interface of a two phase system. A polymeric surfactant structure is depicted in Figure 3.14. Block co-polymers of polyethylene and polypropylene glycols with molecular weights ranging from 1000-30,000  $\text{gmol}^{-1}$  have been reported as possessing surface active properties including wetting, gel forming, and drug delivery agents.<sup>19, 20</sup>





**Figure 3.14.** General structure of a polymeric surfactant.<sup>21</sup>

Adapted from Jones *et al. Eur. J. Pharm. Biopharm.*, 1999, 48, 101-111.<sup>21</sup>

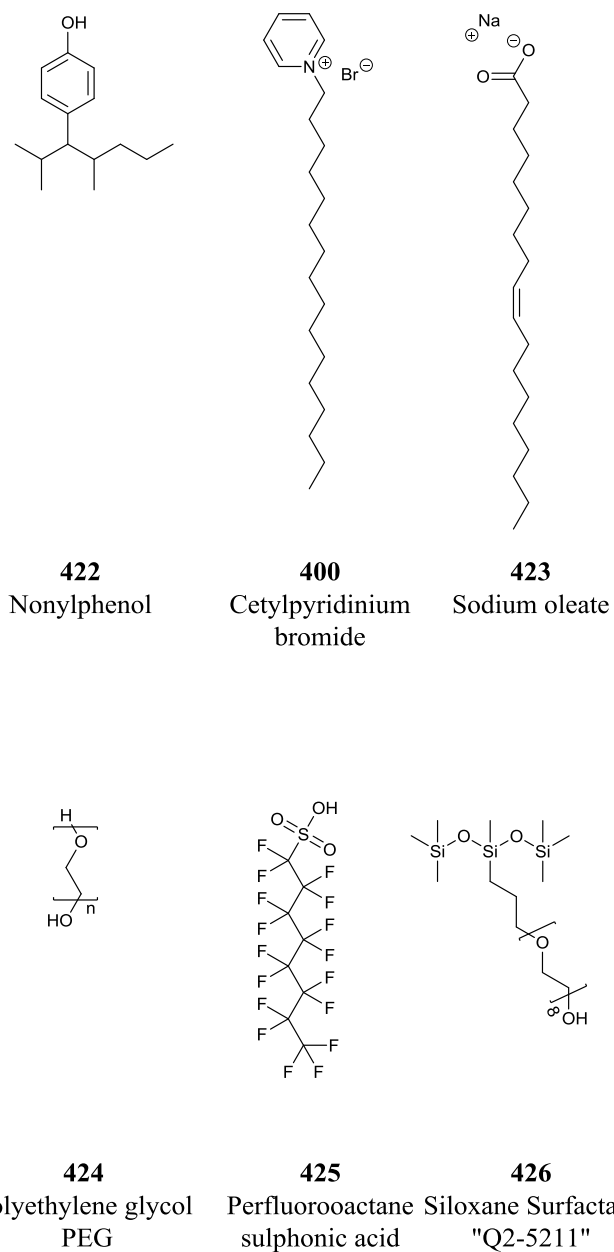
### 3.4.1 Linear alkyl

The most commonly employed surfactant structures are the linear alkyl derivatives. Linear alkyl derivatives contain a charged/polar head and a non-polar tail. As previously discussed in Section 3.3 the polar head, can be ionised or neutral. A linear alkyl surfactant's tail can be comprised of many different moieties (Figure 3.15).

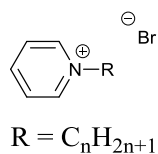
- Branched alkyl chains e.g. nonylphenol (**422**).<sup>22</sup>
- Linear alkyl chains e.g. cetylpyridinium bromide (**400**).<sup>22</sup>
- Unsaturated alkyl chains e.g. sodium oleate (**423**).<sup>23</sup>
- Polyoxygenated tails e.g. polyethylene glycol (**424**).<sup>6</sup>
- Perfluorinated tails e.g. perfluorooctanesulphonic acid (**425**).<sup>6</sup>
- Polysiloxanated tails e.g. "Q2-5211" (**426**).<sup>24</sup>

The size of the hydrophobic region (which can often be simplified to the length of the alkyl chain) is a key determining factor in the CMC and surface activity. The surface activity triples for each additional CH<sub>2</sub> unit according to Traube's rule which states that:" *in a homologous*

*series the interfacial activity increases with increasing size of the hydrophobic group and that the surfactant concentration at which a specific interfacial activity is achieved decreases with increasing size of the hydrophobic group*".<sup>13</sup> Simplified to a rule of thumb, the concentration required to produce equal lowering of surface tension decreases x3 for each additional CH<sub>2</sub> group in the surfactant's alkyl chain. Increased alkyl chain lengths can also be responsible for elevated melting points, closer packing at interfaces, reduced aqueous solubility and depending on length, differing levels of toxicity and biodegradability. A rule of thumb is that for every additional CH<sub>2</sub> unit added to the alkyl chain the CMC is reduced by half.<sup>27</sup> This trend is illustrated by the data in Table 3.1 for pyridinium surfactants of the formula depicted in Figure 3.16



**Figure 3.15.** Different classes of alkyl chains.

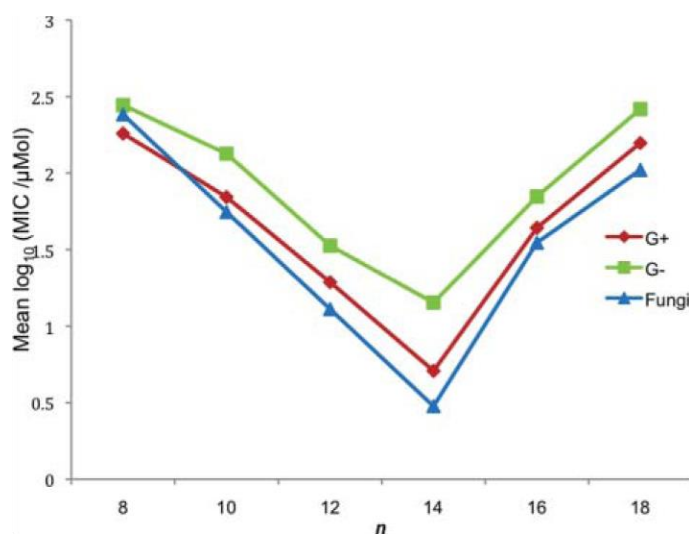


**Figure 3.16.** Linear alkyl pyridinium surfactants of general structure and formula ( $n = 10-16$ ).<sup>15</sup>

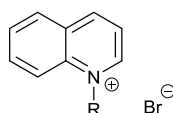
**Table 3.1.** CMC values for a homologous series of pyridinium bromide linear alkyl surfactants.<sup>15</sup>

Surfactant Chain Length	Number of Carbons in Sidechain	CMC (mM)
$C_{10}H_{21}$	10	44
$C_{11}H_{23}$	11	21
$C_{12}H_{25}$	12	11.4
$C_{13}H_{26}$	13	5.3
$C_{14}H_{29}$	14	2.7
$C_{15}H_{31}$	15	1.3
$C_{16}H_{33}$	16	0.64

Branching of alkyl chains reduces the melting point and packing. Cis double bonds also reduce the packing, however chains containing a trans double bond can pack almost as tightly as saturated alkyl chains. Branching of alkyl chains can also lead to a decrease in biodegradability.<sup>28-30</sup> Extending an alkyl chain up to a point will indeed decrease the CMC, however with extended chain lengths an increase in antimicrobial toxicity is observed. The trend of increasing toxicity will continue up to a point followed by a rapid decline in toxicity as aqueous solubility and thus bioavailability decreases.<sup>31, 32</sup> The trend is highlighted in Figure 3.17 published by Gilmore *et al.*<sup>32</sup>



**Figure 3.17.** MIC of alkylquinolinium ILs (Figure 3.18) screened by Gilmore *et al.*<sup>32</sup>



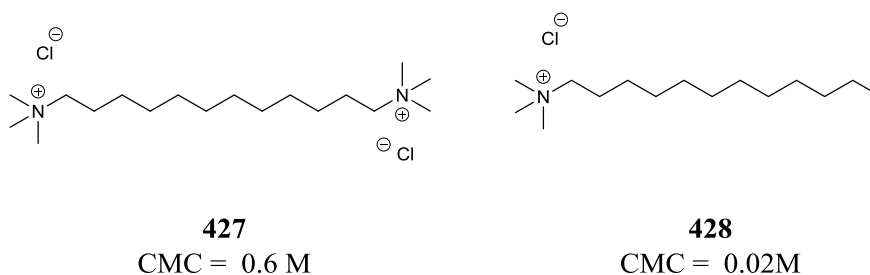
$$R = C_nH_{2n+1}$$

**Figure 3.18.** General structure of alkylquinolinium ILs screened by Gilmore *et al.*<sup>32</sup>

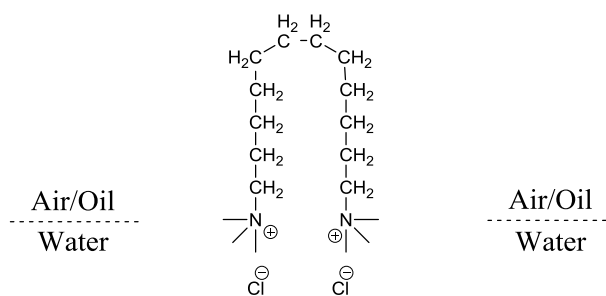
Polyoxypropylene units can increase the hydrophobic nature of a surfactant but the polyoxyethylene derivatives will actually decrease the hydrophobic nature. It has also been shown that addition of polyoxygenated units can reduce the overall antimicrobial toxicity of alkyl chains yet maintain levels of biodegradability.<sup>18</sup> The addition of fluorinated or siloxanated groups to the alkyl chain can lower the CMC below that which is attainable for hydrocarbon chains. Perfluorinated chains see widespread use in fire fighting applications and are known to be persistent pollutants exhibiting very poor biodegradability.<sup>26</sup>

### 3.4.2 Bolaform

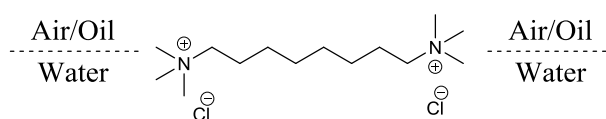
The bolaform, or bolaamphiphile, class of surfactants are a family of surfactants comprised of two charged groups located on opposite ends of the molecule (Figure 3.19). Charged regions of the molecules are tethered together with a chain of desired length and composition. Bolaform surfactants can behave at the air water interface in a number of ways. If the chain between the two heads is too short then no surface active properties are observed at all. As the chain length extends, the bolaform molecules can adopt a horizontal conformation lying flat on the surface. If the chain is extended even further then the bolaform surfactant can be pushed out of the water and into the air adopting a “wicket” conformation (Figure 3.20).<sup>6, 33</sup> Bolaform surfactants are often far poorer surfactants than linear alkyl surfactants with much less of an effective surface tension reducing range. The bolaform surfactants double charge confers much greater hydrophilicity than more traditional linear alkyl surfactants and CMC values for bolaform surfactants are often much higher than that of linear alkyl surfactants. Overall, bolaform compounds are less useful for surfactant applications (such as detergency) than linear alkyl surfactant molecules. A rule of thumb for the bolaform surfactants is that a bolaform surfactant will require almost 2x the number of carbon atoms as that of a comparable linear alkyl surfactant to achieve a similar CMC. Another way of stating this relationship is that when comparing a linear alkyl surfactant to a bolaform surfactant with the same number of carbon atoms in their alkyl chain/linker then the linear alkyl surfactant will have a CMC that is half of that observed for the bolaform (Figure 3.19).<sup>34</sup>



**Figure 3.19.** Comparison for bolaform surfactant  $C_{12}Me_6$  (**427**) and a  $C_{12}$  linear alkyl ammonium surfactant (**428**).<sup>34</sup>



Wicket Conformation

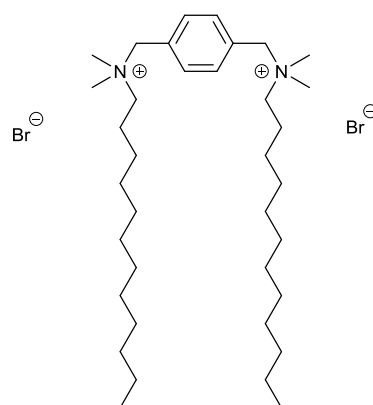


Flat / Horizontal Conformation

**Figure 3.20.** Potential bolaform conformations.<sup>33</sup>

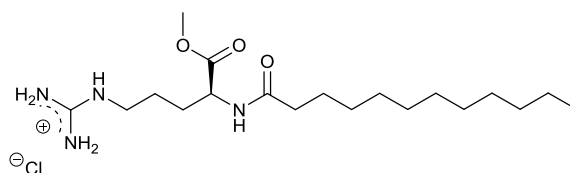
### 3.4.3 Gemini

The family of gemini surfactants are a class of surfactant where two linear alkyl derivatives are connected at, or very near to, the polar heads by a linker to form a dimeric type surfactant (Figure 3.21).<sup>6, 35, 36</sup> Linker types can include flexible alkyl or polyether chains or more rigid aromatic types.<sup>34</sup> Gemini surfactants appear to be far more effective at lowering the surface tension at interfaces than their corresponding monomeric linear alkyl surfactants. The reported CMC values are also lower, up to 2-3 orders of magnitude, than the monomeric linear alkyl derived surfactants of similar chain length (Figure 3.22).<sup>34, 37</sup> If a long flexible alkyl chain is used as a linker then the gemini surfactant can adopt a wicket conformation similar to that of the bolaform in Figure 3.20.<sup>36</sup> However if a rigid linker such as an aromatic moiety is used then the surfactant can lie horizontal on the surface. Apart from forming micelles, gemini surfactants can also form lipid like membranes.<sup>34</sup>

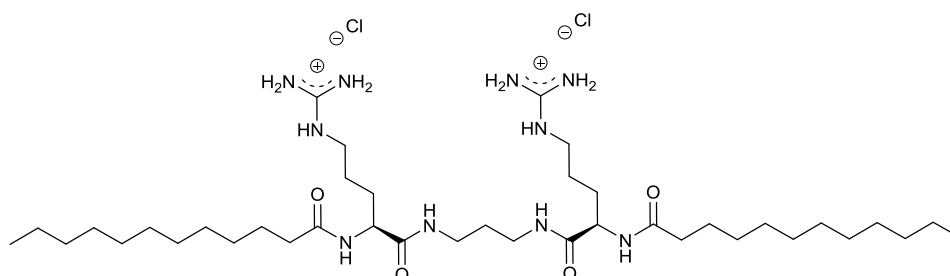


**429**

**Figure 3.21.** Gemini surfactant  $\text{C}_6\text{H}_4$ -1,4-bis- $[\text{CH}_2\text{N}^+(\text{CH}_3)_2\text{C}_{12}\text{H}_{25}]\cdot 2\text{Br}^-$



**430**, CMC = 6.0 mM



**431**, CMC = 0.005 mM

**Figure 3.22.** Comparison of CMC for linear alkyl surfactant (**430**) to gemini surfactant (**431**).<sup>37</sup>

### 3.5 Synthesis, antimicrobial toxicity and biodegradation studies of 2<sup>nd</sup> generation amino acid ILs

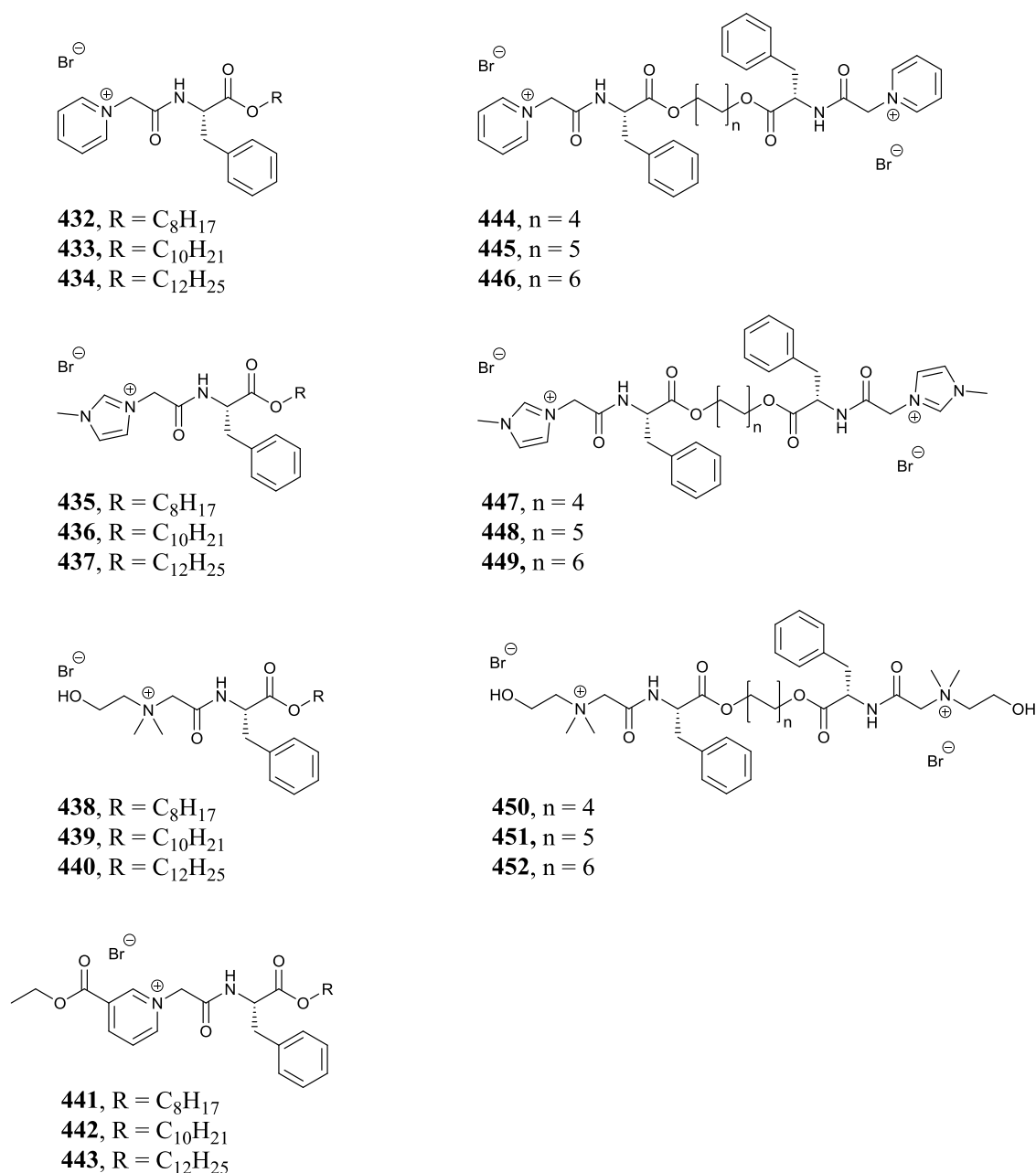
The aim of this section is to present the synthesis, antimicrobial toxicity and biodegradability of the 2<sup>nd</sup> generation of amino acid ILs. Research conducted in IL biodegradability and antimicrobial toxicity previously discussed in Chapters 1 and 2 has allowed for the rational design of a 2<sup>nd</sup> generation of amino acid derived ILs which can be synthesised from a number of renewable resources (e.g. L-phenylalanine,<sup>38</sup> and long chain alcohols such as octanol<sup>39</sup>). The design strategy chosen further embraces the framework outlined in the twelve principles of green chemistry and Boethling's rules of thumb and it is reported for the first time the chemical

synthesis, surfactant properties, antimicrobial activity and biodegradability of L-phenylalanine derived amino acid ionic liquid surfactants. Furthermore, investigations into how the aromatic sidechain of the L-phenylalanine moiety and the amino acid heteroatoms would affect the surfactant properties was of importance. Antimicrobial activity and biodegradability of this 2<sup>nd</sup> generation of amino acid ILs are discussed in detail in Section 3.6 and 3.7. Surfactant properties will be presented in Chapter 4.

Two classes of ILs were synthesised. The first class reported is a series of linear alkyl amino acid ILs comprised of ester chain lengths C<sub>8</sub>H<sub>17</sub>, C<sub>10</sub>H<sub>21</sub> and C<sub>12</sub>H<sub>25</sub>, whilst the second class are a bolaform class and are comprised of two amino acids linked together at the C-terminus by an ester chain linker. Linkers consisted of C<sub>8</sub>H<sub>16</sub>, C<sub>10</sub>H<sub>20</sub> and C<sub>12</sub>H<sub>24</sub>. Target ILs (**432-452**) are outlined in Figure 3.23. 2<sup>nd</sup> generation amino acid ILs were synthesised based on the synthesis, toxicity and biodegradability results of Chapter 2. Desired ester chain lengths of the ILs were determined from the beginning of the design process leading to a small series of targets. Choice of alkyl chains was due to the possibility that the amino acid's heteroatom content would lead to a lack of definition or distinction between the hydrophobic and hydrophilic regions of the surfactant candidate molecules, thus a long alkyl chain would increase the chances of promoting surfactant behaviour. If the C<sub>8</sub>-C<sub>12</sub> alkyl chain ILs proved to be poor surfactants then synthesis of shorter chains such as C<sub>4</sub> and C<sub>6</sub> would be fruitless.  $\alpha$ -Bromoamide alkylating reagents (**456-458**, **462-464**) developed within this chapter can be considered the key to the series of ILs, allowing for any number of nucleophilic substitutions to take place on the bromide atom leading to nearly limitless potential headgroups as final targets.

The most promising candidates from Chapter 2 for further investigation were the imidazolium (**324**), pyridinium (**325**), cholinium (**330**) ILs due to their favourable green chemistry metrics, antimicrobial toxicity and biodegradability. Though IL (**330**) was shown to only undergo ester cleavage in Chapter 2 Section 2.4.1 its rapid and green synthesis and non-aromatic linear headgroup made this derivative of interest for further study. Derivatives of ethyl nicotinium (**327**) were also planned based on the proviso that the green metrics for the first derivative synthesised were more promising than those calculated for (**327**) in Chapter 2 (poor E-factor, solvent intensity, mass intensity and reaction mass efficiency due to silica gel chromatography purification and moderate yields).



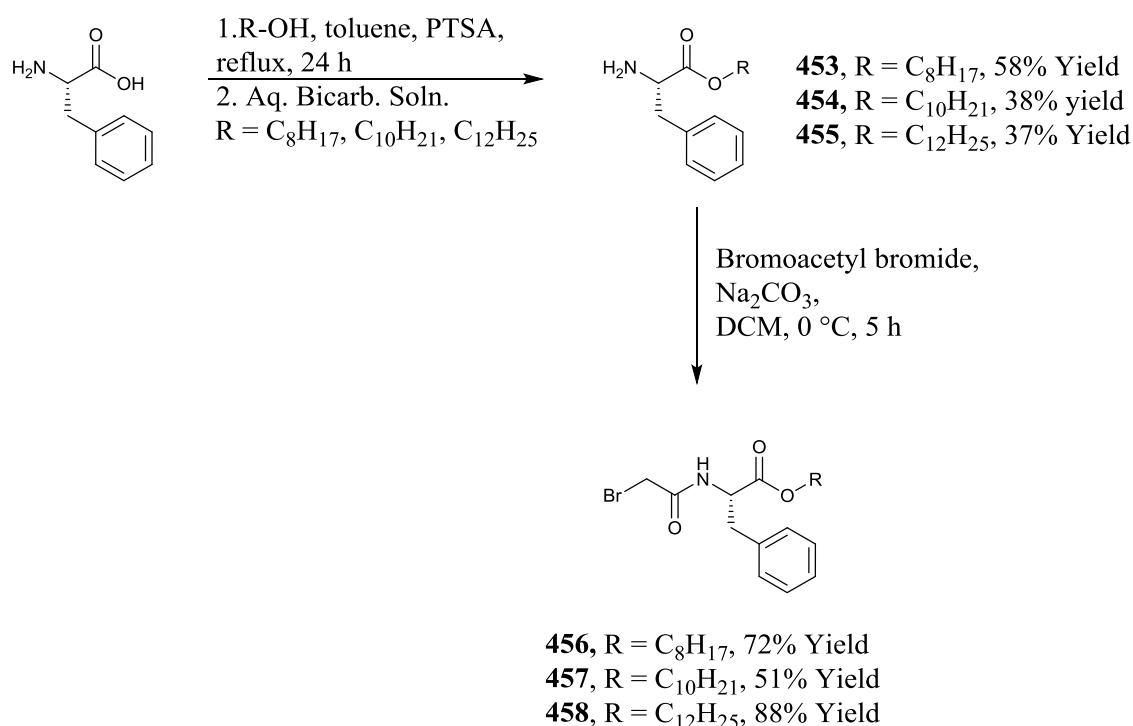


**Figure 3.23.** Surfactant targets (**432-452**).

### 3.5.1 Synthesis of 2<sup>nd</sup> generation L-phenylalanine linear alkyl ILs

Linear alkyl L-phenylalanine derived ILs were synthesised in three stages using a similar method to that outlined in Chapter 2, Section 2.2.2.2. **Step 1** involved acid catalysed esterification of L-phenylalanine with a long chain alcohol in toluene using *p*-toluene sulfonic acid (PTSA) as an acid catalyst to give esters (**453-455**). Use of SOCl<sub>2</sub> was unsuccessful as the resulting reaction mixture would not solubilise under the reaction conditions. Reaction workup required the neutralisation of the PTSA salt of the esters which resulted in the formation of an

emulsion that required several additions of brine and multiple extractions to retrieve the desired esters in an appreciable amount. This step is the lowest yielding step of the synthesis giving only moderate (e.g., **453**, 58%) to poor yields (e.g. **455**, 37%), (Table 3.2, Scheme 3.1). Inefficient removal of water, even though a Dean-Stark apparatus was employed, may also play a role in the poor yields. The quantities of crude PTSA ester salts recovered before neutralisation (Table 3.2) suggests that when the neutralisation step was carried out ~30% mass was lost in the resulting emulsions. Purification of the esters (**453-455**) produced was by precipitation from the reaction mixture with diethyl ether followed by vacuum filtration and washing with hexane. See Chapter 5 for experimental method.



**Scheme 3.1.** General synthetic route employed for step 1, synthesis of esters (**453-455**) and step 2, synthesis of alkylating reagents (**456-458**).

**Table 3.2:** Percentage yields for L-phenylalanine esterification reactions.

Product	Acid Employed	Crude Salt Product	Free Base Yield
Mass Recovery			
<b>453</b>	HCl (SOCl <sub>2</sub> )	0%	0%
<b>453</b>	PTSA	94%	58%
<b>454</b>	PTSA	65%	38%
<b>455</b>	PTSA	63%	37%

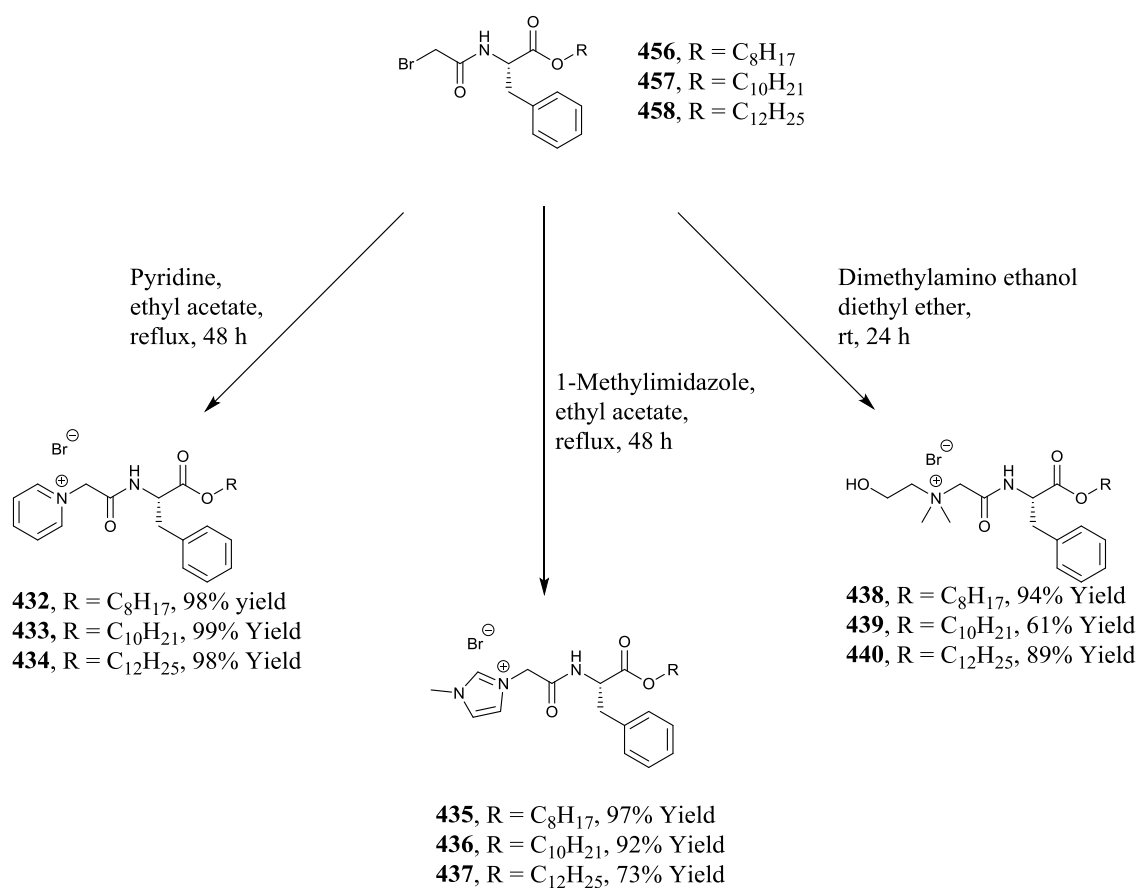
**Step 2** involved acylation of the esters with bromoacetyl bromide to form alkylating reagents (**456-458**) in moderate (e.g. **457**, 51%) to high yields (e.g. **458**, 88 %), (Table 3.3, Scheme 3.1). Purification of the  $\alpha$ -bromoamide alkylating reagents (**456-458**) was by aqueous workup and filtration through a short plug of silica to ensure complete removal of any lipophilic impurities.

**Table 3.3.** Percentage yields for alkylating reagents (**456-458**).

Compound	Yield %
<b>456</b>	72
<b>457</b>	51
<b>458</b>	88

**Step 3** involved alkylation of pyridine, dimethylamino ethanol or 1-methylimidazole to furnish the respective ILs (**432-440**) in high yields (Scheme 3.2). Solvent of choice for the IL forming reaction step is usually diethyl ether, however, precipitation of the IL products only occurred with the cholinium ILs (**438-440**). Instead, ethyl acetate and reflux conditions were employed for the pyridinium (**432-434**) and 1-methylimidazolium ILs (**435-437**). Final stage products (**432-440**) were purified by trituration. At no stage was silica gel chromatography a requirement for purification.

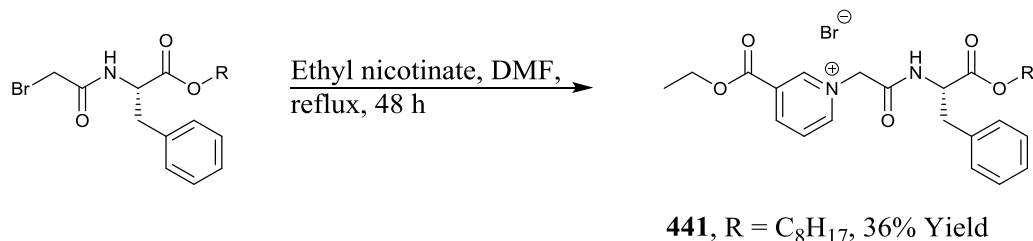
One additional C<sub>8</sub> IL (**441**), an ethyl nicotinate derivative, was synthesised. Neither diethyl ether, nor reflux conditions in ethyl acetate, produced the desired product (by TLC) after 48 hours. The reaction solvent was replaced with DMF and after 48 hours reflux a crude product was detected by TLC. Purification of the crude product by silica gel chromatography gave IL (**441**) in poor yield (36%) (Table 3.4, Scheme 3.3). At this stage of the synthesis it was decided to postpone further investigations into the ethyl nicotinium IL series due to the poor yield and unfavourable green metrics, see Table 3.5, therefore ILs (**442**, **443**) were not synthesised. With the exception of ethyl nicotinium (**441**), no silica gel chromatography was required for product purification thus leading to a simple, streamlined, synthetic approach and a considerable prevention of solvent waste.



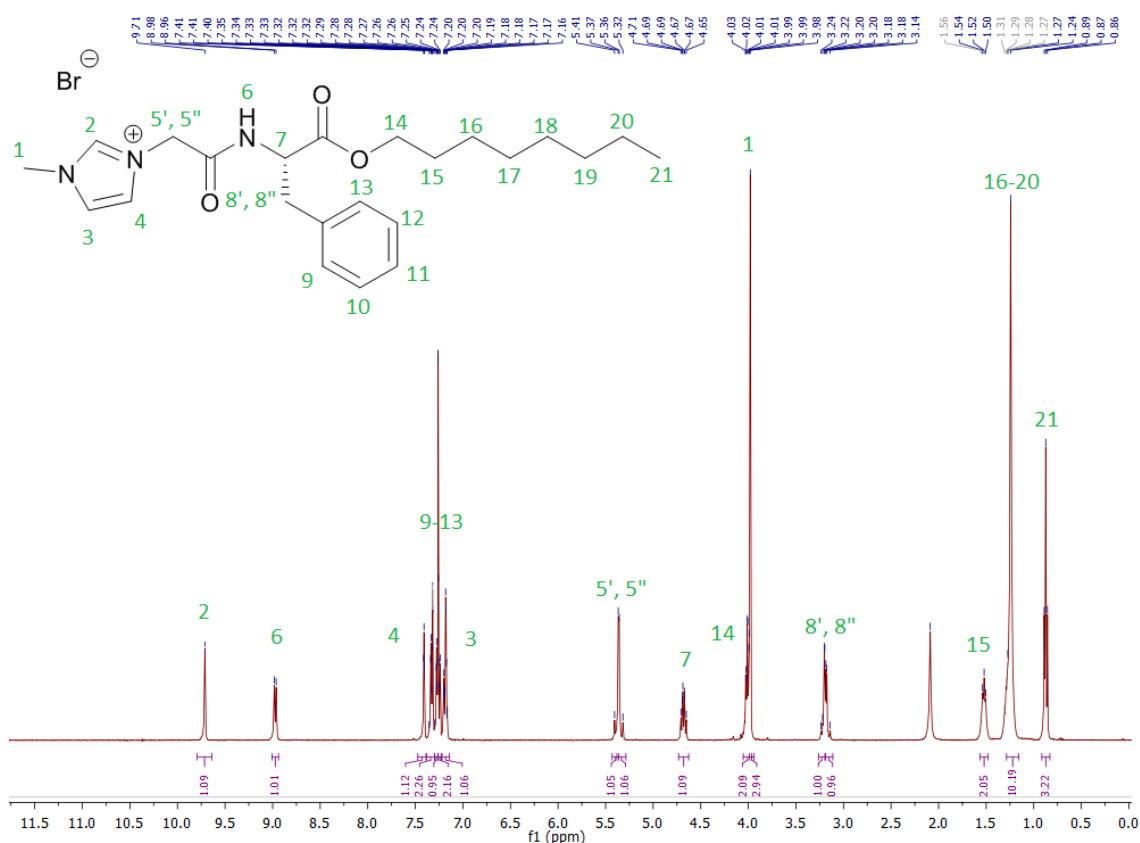
**Scheme 3.2.** General scheme for **step 3**, the synthesis of linear alkyl ILs from alkylating reagents.

**Table 3.4.** Percentage yields and melting points for ILs (**432-441**).

Compound	Yield %	Melting Point °C
<b>432</b>	98	93-95
<b>433</b>	99	101-103
<b>434</b>	98	107-109
<b>435</b>	97	64-66
<b>436</b>	92	80-82
<b>437</b>	73	94-96
<b>438</b>	94	80-82
<b>439</b>	61	57-59
<b>440</b>	89	63-65
<b>441</b>	36	43-45



**Scheme 3.3.** Synthesis of ethyl nicotinium IL (**441**).



**Figure 3.24.** <sup>1</sup>H-NMR of imidazolium IL (**435**) in CDCl<sub>3</sub>.

From the <sup>1</sup>H-NMR of (**435**) (Figure 3.24) it can be seen that the single C<sub>2</sub> proton **2** on the imidazolium ring appears as a singlet downfield at 9.71 ppm. Amide proton **6** is present as a doublet at 8.97 ppm with a coupling constant  $J = 7.7$  Hz, coupling to the proton on the stereogenic position **7**. The aromatic region of 7.41-7.16 ppm contains 7 protons, two methine protons from the imidazolium ring are present **3**, **4** and the protons on the phenyl ring of the L-phenylalanine sidechain **9-13**. CH<sub>2</sub> protons,  $\alpha$  to the carbonyl group of the amide linker, **5'**, **5''** are present at 5.39 ppm and 5.34 ppm as two sets of doublets due to their diastereotopicity, with  $J = 15.5$  Hz. It is proposed that the presence of the doublets could also be due to hydrogen

bonding of the protons **5'**, **5''** to the bromide counterion introducing an inequivalency and hence geminal coupling of the protons. This mode of binding has been previously discussed in Chapter 2, Section 2.2.2.2. Stereogenic proton **7** is present at 4.73-4.63 ppm as a multiplet. Protons **14**,  $\alpha$  to the ester oxygen, appear at 4.01 ppm as a multiplet due to their diastereotopicity. Methyl group protons **1** on the imidazolium ring appear at 3.98 ppm as a singlet. Amino acid sidechain protons at the benzylic position **8'**, **8''** are present as two sets of doublet of doublets at 3.21 and 3.18 ppm with  $J = 11.5, 4.0$  Hz. as they are diastereotopic, each coupling vicinally to the proton **7** at the stereogenic position and then geminally. Alkyl ester chain protons **15** are present as a multiplet at 1.60-1.46 ppm followed by the protons **16-20** as a multiplet between 1.34-1.14 ppm. Lastly the terminal CH<sub>3</sub> protons **20** on the alkyl chain are present as a triplet at 0.87 ppm with  $J = 6.8$  Hz.

### 3.5.1.1 Linear alkyl ILs green chemistry metrics

Green chemistry metrics are an important benchmark with which to analyse a synthetic route to a target. A number of green chemistry metrics have previously been calculated for the 1<sup>st</sup> generation of ILs outlined in Section 2.2.2.7. Following on from the information provided in Section 2.2.2.7, the following metrics were calculated for all of the linear alkyl compounds synthesised within, the results of which are outlined in Table 3.5.

The synthesis of the L-phenylalanine esters (**453-455**) resulted in low-moderate yields of the esters (37-58%) due to the difficulties presented with the workup phase of the reactions. Emulsion formation resulted in a difficult extraction, even when the emulsion was filtered over celite. Atom economy for the ester formation reactions is moderate due to the use of p-toluene sulphonic acid (PTSA) as an acid catalyst in stoichiometric quantities, none of which is incorporated into the final product. Atom economy is 57% for the octyl ester and increases as the ester chain length is increased to decyl (60%) and dodecyl (62%). Although caution must be excised when comparing these numbers as one can argue that the dodecyl synthesis is no greener than the octyl, just because the atom economy is slightly higher. E-factor, solvent and mass intensities were moderate (34-61) due to the quantities of solvent used to extract the product from the emulsions and the removal of expended PTSA salts as waste. GSK RME is moderate (0.21-0.30) and the Andraos RME is poor. Stoichiometric factor is high, >90% for all three esters (**453-455**) and the material recovery parameter is the highest of all three reaction steps.

Alkylating reagents (**456-458**) were synthesised in moderate to high yields (51-88%) with an improved atom economy of ~70% for all three compounds, compared to the ester forming

reactions. Atom economy still remains at a moderate level (68-71) due to the formation of stoichiometric quantities of HBr and subsequently bromoacetic acid from the workup stage of the reaction. E-factor, mass intensity and solvent intensity were in general higher than those calculated for the ester synthesis due to the stoichiometric quantities of auxiliary base employed in this stage of the reaction and the quantities of solvent and workup reagents used. GSK RME is moderate (~0.31-0.56) and the Andraos RME and material recovery parameters are both poor. Again the stoichiometric factor is high, at 0.89 for all three acylation reactions.

It can be seen from the generated metrics that the synthesis of ILs (**432-441**) proceeded with excellent yields, with >88% yields for all the ILs bar three examples (**437**, **439**, **441**). Atom economy for these nucleophilic substitution reactions is 100% as all reactants used in this step are incorporated into the final product. E-factor, mass intensity and solvent mass intensity are poorer when compared to the esterification and acylation reactions, however this can be attributed to the quantities of solvent required to wash the ILs in the final stage purification step. Environmental factors can be improved hugely if the solvent used in the washing step is recycled in the future. GSK RME is the highest of all three stages in the reactions ~90% for the majority of ILs (**432-436**, **438**) formed but there is no improvement in the Andraos RME due to the quantities of solvent employed. Stoichiometric factors were all excellent due to only a slight excess of alkylating reagent required in each of these reactions. Material recovery parameters are poor due to the quantities of solvents employed in the purification of the ILs. The least green parameters observed were for the ethyl nicotinum IL (**441**) due to the large volume of solvent required to purify the product by silica gel chromatography (300 mL of 7:93 MeOH:DCM).

**Table 3.5.** Green Chemistry metrics calculated for linear alkyl amino acid ILs and precursors.

Compound	Atom Economy	Sheldon E-factor	GSK RME	Andraos RME	Mass Intensity	Solvent Intensity	1/ Stoichiometric factor	Material Recovery Parameter	Yield %
<b>Amino Acid Esters</b>									
<b>453</b>	57 %	61.0	0.301	0.022	44.8	39.7	0.908	0.074	58
<b>454</b>	60 %	41.6	0.216	0.023	42.6	36.3	0.965	0.109	38
<b>455</b>	62 %	37.8	0.219	0.026	38.8	34.2	0.966	0.117	37
<b>Alkylating Reagents</b>									
<b>456</b>	68 %	56.0	0.438	0.018	57.0	53.0	0.891	0.040	72
<b>457</b>	70 %	81.1	0.315	0.012	82.1	76.4	0.894	0.039	51
<b>458</b>	71 %	41.7	0.560	0.023	42.7	39.6	0.899	0.042	88
<b>L-Phenylalanine ILs</b>									
<b>432</b>	100 %	58.2	0.962	0.017	59.2	58.1	0.976	0.018	99
<b>433</b>	100 %	76.3	0.976	0.013	77.3	76.3	0.978	0.013	99
<b>434</b>	100 %	73.8	0.965	0.013	74.8	73.7	0.987	0.014	98
<b>435</b>	100 %	99.3	0.973	0.010	100.3	99.3	0.991	0.010	97
<b>436</b>	100 %	86.9	0.909	0.011	87.9	86.8	0.987	0.013	92
<b>437</b>	100 %	101.6	0.719	0.010	102.6	101.2	0.991	0.014	72
<b>438</b>	100 %	70.7	0.923	0.014	71.7	70.6	0.971	0.015	94
<b>439</b>	100 %	117.0	0.599	0.008	118.0	116.3	0.983	0.014	61
<b>440</b>	100 %	56.6	0.886	0.017	57.6	56.5	0.998	0.020	89
<b>441</b>	100 %	1091.0	0.353	0.001	1092.0	1089.2	0.984	0.003	36



The overall picture that the metrics produce is that the esterification yields could be improved in the future, with potential longer reaction times and larger excesses of the alcohol to try and drive the equilibrium of the ester forming reaction. However, this approach should be mindful of the requirement to recover/recycle the excess of alcohol used. Alkylating reagent forming reactions (**step 2**) have varying yields and the overall yields may be improved by further extraction steps. Excessive use of extraction solvent can be balanced by implementing a solvent recycling process. Finally the IL forming reactions and the final step of the reactions suffer from large solvent use in the washing steps. This can be addressed as above, with recycling of the diethyl ether trituration solvent. If 90% of the diethyl ether is recycled then the IL E-Factor can be reduced to less than 15.

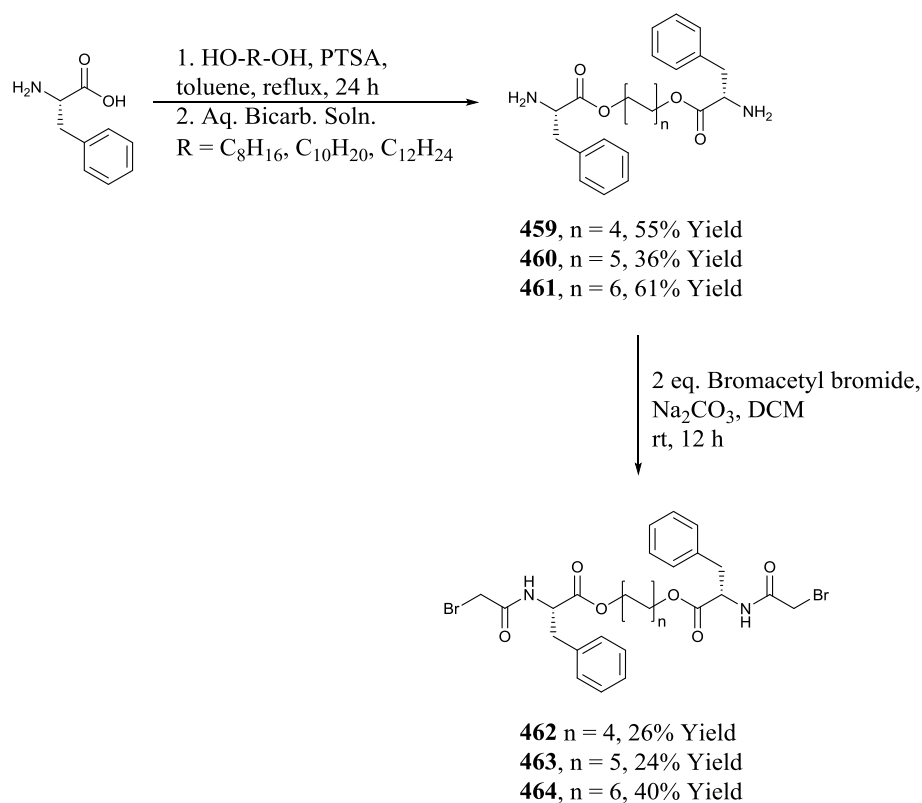
### 3.5.2 Synthesis of 2<sup>nd</sup> generation L-phenylalanine bolaform (dicationic) ILs

L-Phenylalanine derived dicationic ILs were synthesised in three steps using the method previously reported in Section 3.5.1. Desired ester chain lengths of the ILs were determined based on the linear alkyl ILs synthesised in Section 3.5.1. Linear alkyl ILs with C<sub>8</sub>H<sub>17</sub> ester chains were henceforth considered analogues of the dicationic ILs with a C<sub>8</sub>H<sub>16</sub> carbon spacer etc. **Step 1** of the reaction involved acid catalysed esterification of two equivalents of L-phenylalanine with one equivalent of diol in toluene using PTSA as an acid catalyst to give esters (**459-461**) (Scheme 3.4). SOCl<sub>2</sub> was not employed as the acid source as it was unsuccessfully applied in Section 3.5.1. Initially the reactions were carried out according to the literature procedure of Becker *et al.* which involved purification of the ester by recrystallization from hot water.<sup>40</sup> This procedure was found to be ineffective at the smaller scale reactions carried out in this section, thus the esters were purified by precipitation from the toluene reaction solvent using diethyl ether to give off-white crystalline solids which were then further purified by vacuum filtration and washed with hexane (Table 3.6). Hexane and ether used in this stage were recycled at 90-95% recovery using a rotary evaporator to redistill. Finally, to achieve the free amine products the bis-phenylalanine ester salts were added to sodium bicarbonate solution, stirred vigorously until neutralised then extracted using ethyl acetate. Comparable to the linear alkyl esters synthesised in Section 3.5.1, formation of an emulsion also occurred. Multiple additions of brine and several solvent extractions were performed to retrieve the desired esters in poor (e.g. **460**, 36%) to moderate (e.g. **461**, 61%) yields. From the percentage mass recovery difference between isolated PTSA salt before neutralisation and the free base mass recovery it can be said that ~15-20% of the product mass may have been lost during the aqueous neutralisation step (Table 3.6). Unfortunately due to incompatibility with the acylation conducted in **step 2**, the amino acid esters must be in the free base form and not in their PTSA salt form.

**Table 3.6.** Percentage yields for L-phenylalanine diol esterification reactions, step 1.

Product	Purification Method	PTSA Salt Product	
		Crude Mass Recovery	Free Base Yield
<b>459</b>	Recrystallization from Water	7%	0%
<b>460</b>	Recrystallization from Water	5%	0%
<b>461</b>	Recrystallization from Water	Not Carried Out	Not Carried Out
<b>459</b>	Precipitation from reaction	78%	55%
<b>460</b>	Precipitation from reaction	56%	36%
<b>461</b>	Precipitation from reaction	85%	61%

The second reaction stage was acylation of the bis-amino acids on both terminal nitrogen positions using bromoacetyl bromide to form alkylating reagents (**462-464**) in low (e.g. **462**, 26%) to moderate yields (**464**, 40%). All three acylated amino acids required purification by silica gel chromatography before further use (Scheme 3.4).



**Scheme 3.4.** General synthetic route employed for **step 1**, the synthesis of bis-amino acid esters (**459-461**) and **step 2**, the synthesis of alkylating reagents (**462-464**).

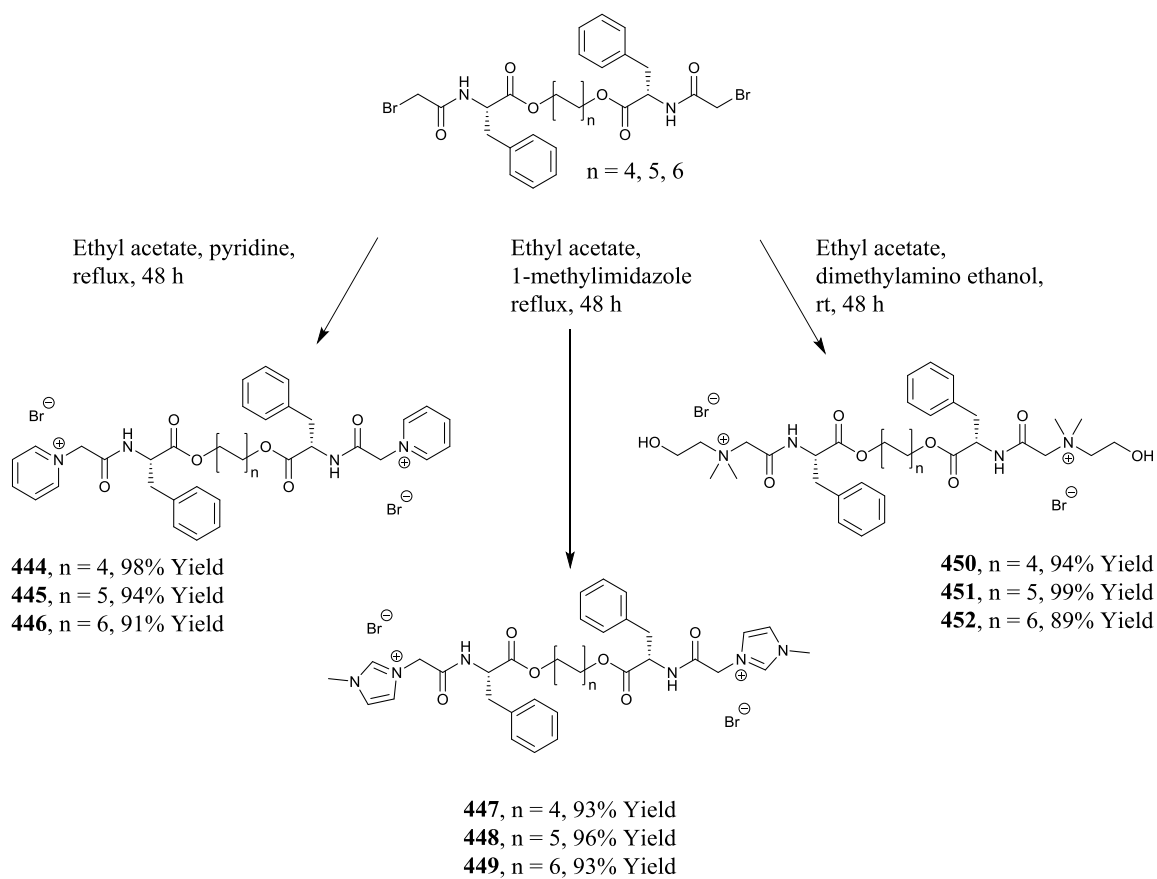
As can be seen from Table 3.7, the percentage yields for the alkylating reagents is much poorer when compared to the linear alkyl derivatives described in Section 3.5.1. One possible reason is that twice as much auxiliary base was required for this reaction to neutralise the HBr produced when the amino acid reacts with bromoacetyl bromide. Extra heterogeneous base required made stirring inconsistent and difficult. For the final alkylating reagent of the series (**464**), three equivalents of bromoacetyl bromide were used and this appears to have increased the yields by ~15%. Future optimisation of the di-acylation of the bis-amino acids will have to be carried out before any further investigations are carried out on this class of ILs. Replacement of the auxiliary base with a homogeneous amine base (other than TEA as it was shown in Section 2.2.2.2 to react poorly and cause coloured impurities), and/or the use of continuous effective stirring, such as that provided by an overhead stirrer, may elevate the yields of these products.

**Table 3.7.** Percentage yields for bis alkylating reagents (**435-437**).

Compound	Yield %
<b>462</b>	26
<b>463</b>	24
<b>464</b>	40

**Step 3** involved alkylation of pyridine, dimethylaminoethanol or 1-methylimidazole to furnish the respective dicationic ILs (**444-452**) in excellent yields (Scheme 3.5, Table 3.8). The synthesis of the final stage products was carried out under reflux conditions in ethyl acetate to facilitate the reaction. Once the dicationic product had formed it was observed to serendipitously precipitate. Conveniently, mono-cationic IL was not observed (TLC and <sup>1</sup>H-NMR of the crude reaction mixture) precipitating. Therefore isolation and purification of the end product was facile, a simple diethyl ether wash was sufficient for the purification of all ILs. As per Section 3.5.1, no silica gel chromatography was required for purification of the final products leading to a simple streamlined synthetic approach and a considerable prevention of solvent waste. Based on the recommendations provided by the metrics collected in Section 3.5.1.1 the trituration solvent used in the final wash step of the target ILs was also recycled (90-95% recovery) and re-distilled using a rotary evaporator for further use.

The synthesis outlined in Schemes 3.4 and 3.5 lead to a series of nine dicationic ILs (**444-452**). Once more it can be said that the  $\alpha$ -bromoamide alkylating reagents can lead to a nearly limitless numbers of potential headgroups as final targets.

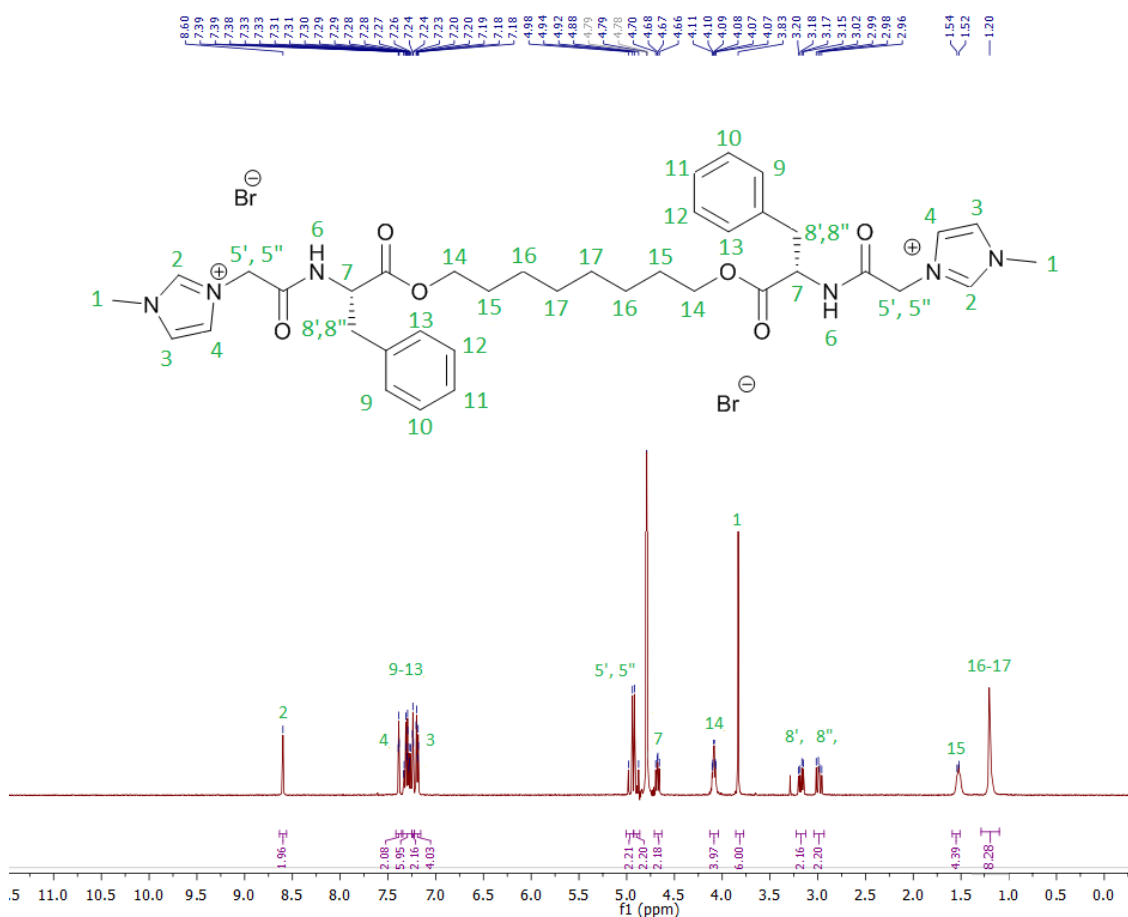


**Scheme 3.5.** General scheme for the synthesis of dicationic ILs (**444-452**).

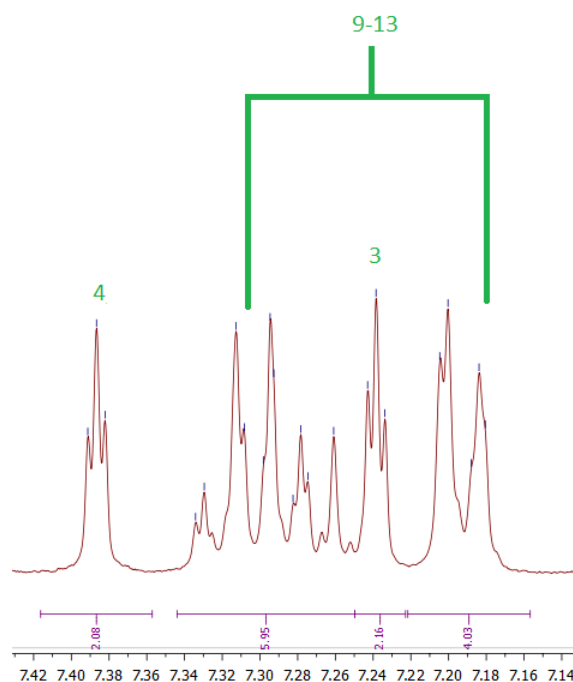
**Table 3.8.** Percentage yields and melting points for dicationic ILs synthesised.

Compound	Yield %	Melting Point °C
<b>444</b>	98	124-126
<b>445</b>	94	137-139
<b>446</b>	91	138-140
<b>447</b>	93	70-72
<b>448</b>	96	41-43
<b>449</b>	93	84-86
<b>450</b>	94	112-114
<b>451</b>	99	66-68
<b>452</b>	89	89-91

From the  $^1\text{H}$ -NMR of (**447**) (Figure 3.25) it can be seen that the C-H protons on both the imidazolium rings C<sub>2</sub> position **2** appear as a singlet downfield at 8.60 ppm. Amide N-H protons are not visible due to exchange with deuterium. The aromatic region of 7.39-7.18 ppm contains 14 protons, four methine protons from the imidazolium ring are present **3**, **4** and the protons on the phenyl rings of the L-phenylalanine sidechains **9-13** (Figure 3.26). CH<sub>2</sub> protons  $\alpha$  to the carbonyl group of the amide linker **5'**, **5''** are present at 4.96 ppm and 4.90 ppm as two sets of doublets with  $J = 16.7$  Hz. Single protons at each of the stereogenic positions **7** are present at 4.67 ppm as a multiplet. CH<sub>2</sub> protons alpha to the ester oxygen **22** are present as a multiplet at 4.08 ppm. Each methyl groups CH<sub>3</sub> protons **1** on the methylimidazolium ring are present as a singlet integrating as 6 at 3.83 ppm. Phenylalanine sidechain protons at the benzylic position **8'**, **8''** are present as two sets of doublets of doublets with  $J = 13.8, 6.3$  Hz. CH<sub>2</sub> protons beta to the ester oxygen **15** are present as a multiplet upfield at 1.53 ppm. Lastly the remaining protons on the alkyl spacer **16**, **17** are present as a multiplet at 1.20 ppm integrating as 8.



**Figure 3.25.**  $^1\text{H}$ -NMR of imidazolium IL (**447**) in  $\text{D}_2\text{O}$ .



**Figure 3.26.** Aromatic region.

#### 3.5.2.1 Dicationic ILs green chemistry metrics

As per the linear alkyl ILs synthesised in Section 3.5.1, the green chemistry metrics for the dicationic class of ILs synthesised were also calculated. From the results presented in Table 3.9 it can be seen that the metrics for the bis-phenylalanine esters (**459-461**) are similar to the linear alkyl esters synthesised in Section 3.5.1. However due to lessons learned from applying green chemistry metrics to previous ILs in this thesis such as the implementation of solvent recycling in the purification and recrystallization stage, there is a huge improvement of one order of magnitude (~35 reduced to ~3.5) in solvent intensity and an increase in material recovery. However when E-factors of the alkylating reagents (**462-464**) (ranging from 136-265) are compared to the linear alkyl alkylating reagents (**456-458**) (ranging from 41-81) a large increase in E-factor is observed. This is due to the requirement of silica gel chromatography in the purification of the bis-alkylating reagents. Chromatography solvent was not recycled and as such is reflected in Table 3.9. When comparing the metrics for the dicationic ILs (**444-452**) to the linear alkyl ILs (**432-441**) it can be seen once more that the atom economy is 100%. The E-Factors for the dicationic ILs are also considerably lower than that observed for the linear alkyl ILs due to full recycling of the trituration solvents used to purify the dicationic ILs. Synthesis of the dicationic ILs is also less mass intensive. GSK RME is also very high due to the high yielding synthesis and much lower net waste, thus leading to a high material recovery

parameter. Percentage yields for all the dicationic ILs were excellent and the Andraos RME is 2-3 times greater than that calculated for the linear alkyl derivatives.

The overall picture portrayed by the green chemistry metrics is that the synthesis of the dicationic ILs from start to finish employed much better green chemistry techniques and utilised the lessons learned while synthesising the previous class of linear alky ILs described in Section 3.5.1. Solvent recycling can be taken even further with recycling of the reaction solvents and chromatography solvents, thus lowering the volumes of solvent required. Yields for the bis-alkylating reagents require optimisation in the future to ensure that further investigations into these types of compounds can be carried out in an efficient manner. The possible optimisations have already been outlined in Section 3.5.2, *vide supra*.

**Table 3.9.** Green Chemistry metrics calculated for dicationic (bolaform) amino acid ILs (**417-425**) and precursors (**432-437**).

Compound	Atom Economy	Sheldon E-factor	GSK RME	Andraos RME	Mass Intensity	Solvent Intensity	1/ Stoichiometric factor	Material Recovery Parameter	Yield %
<b>Amino Acid Esters</b>									
<b>459</b>	51%	31.9	0.189	0.030	32.9	2.6	0.999	0.161	36
<b>460</b>	53%	31.2	0.279	0.031	32.2	2.7	0.959	0.111	55
<b>461</b>	61%	25.8	0.319	0.037	26.8	2.3	0.960	0.117	61
<b>Alkylating Reagents</b>									
<b>462</b>	65%	185.9	0.158	0.005	186.9	171.7	0.927	0.034	26
<b>463</b>	66%	265.9	0.147	0.004	266.9	247.4	0.938	0.026	24
<b>464</b>	52%	136.8	0.206	0.007	137.8	126.5	0.985	0.035	40
<b>L-Phenylalanine ILs</b>									
<b>444</b>	100%	31.1	0.982	0.031	32.1	31.1	1.000	0.032	98
<b>445</b>	100%	57.3	0.940	0.017	58.3	57.2	1.000	0.018	94
<b>446</b>	100%	42.0	0.910	0.023	43.0	41.9	1.000	0.026	91
<b>447</b>	100%	50.9	0.928	0.019	51.9	50.8	1.000	0.021	93
<b>448</b>	100%	81.1	0.958	0.012	82.1	81.0	1.000	0.013	96
<b>449</b>	100%	43.5	0.935	0.022	44.5	43.4	1.000	0.024	93
<b>450</b>	100%	31.2	0.944	0.031	32.2	31.1	1.000	0.033	94
<b>451</b>	100%	50.8	0.994	0.019	51.8	50.8	1.000	0.019	99
<b>452</b>	100%	42.4	0.891	0.023	43.4	42.3	1.000	0.026	89



### 3.6 Antimicrobial screening and biodegradation studies of 2<sup>nd</sup> generation amino acid ILs

The aim of this series of antimicrobial toxicity investigations was to determine the toxicity of the 2<sup>nd</sup> generation amino acid ILs described in this chapter. As discussed in Chapter 2, the toxicity of a number of ILs has previously been reported.<sup>41, 42</sup> More importantly, the structural similarities of the 2<sup>nd</sup> generation linear alkyl ILs synthesised in this chapter have a comparable structure to those of cationic surfactants, a number of which are broad spectrum antimicrobial agents themselves.<sup>43, 44</sup> Antimicrobial toxicity of dicationic/bolaform ILs has also been recently reported with the general trend observed that many are less toxic than monocationic ILs.<sup>45-47</sup> As previously discussed in Chapter 2, toxicity is a parameter that must be investigated when determining the environmental compatibility and “greenness” of ILs. Thus investigations within the field of IL research have been conducted to determine the toxicity of ILs towards bacteria<sup>48</sup>, fungi<sup>49</sup>, invertebrates<sup>50</sup>, aquatic species<sup>51</sup>, plants<sup>52</sup> and algae<sup>53</sup>.

Within the following section, the antimicrobial activity of a number of 2<sup>nd</sup> generation amino acid ILs are presented. ILs were screened against eight strains of bacteria, four gram positive and four gram negative, and twelve strains of fungi. Antimicrobial screening was carried out in collaboration with the Department of Biological and Medical Sciences, Faculty of Pharmacy, Charles University, Hradec Králové, Czech Republic. Antimicrobial testing carried out is according to the same procedure used in Chapter 2, Section 2.3. See Chapter 5, Section 5.8.

#### 3.6.1 Antibacterial screening of the 2<sup>nd</sup> generation linear alkyl amino acid ILs

To investigate the *in vitro* antibacterial effect of the linear alkyl ILs (**432-441**), the following eight strains of bacteria from the collection available at Charles University, Czech Republic, were screened against:

Gram Positive:

- *S. aureus* (ATCC 65382) (SA)
- *Methicillin-res.S.a* (HK5996/08) (MRSA)
- *S. epidermidis* (HK6966/084) (SE)
- *Enterococcus sp.* (HK14365/085) (EF)

Gram Negative:

- *E. coli* (ATCC 87396) (EC)
- *K. pneumoniae* (HK11750/087) (KP)
- *K. pneumoniae* (HK14368/08) (KP-E)
- *P. aeruginosa* (ATCC 9027) (PA)

The bacteria screened against were the same strains discussed in Chapter 2.

#### **3.6.1.1 Experimental Method**

The experimental method is as described in Chapter 5, Section 5.8.1.

### 3.6.1.2 Antibacterial Results – Linear Alkyl Surfactant ILs

**Table 3.10.** Antibacterial results obtained for L-phenylalanine ILs.

Microorganism		IL MIC <sub>95</sub> μmol									
Chain length	Time (h)	432 C <sub>8</sub>	435 C <sub>8</sub>	438 C <sub>8</sub>	441 C <sub>8</sub>	433 C <sub>10</sub>	436 C <sub>10</sub>	439 C <sub>10</sub>	434 C <sub>12</sub>	437 C <sub>12</sub>	440 C <sub>12</sub>
Gram Positive											
SA	24h	3.9,	7.81,	3.9,	15.62,	1.95,	1.95,	1.95,	1.95,	1.95,	1.95,
	48h	7.81	7.81	3.9	15.62	1.95	1.95	1.95	1.95	1.95	1.95
MRSA	24h	15.62,	31.25,	31.25,	31.25,	1.95,	3.9,	1.95,	3.9,	3.9,	1.95,
	48h	15.62	31.25	31.25	62.5	1.95	3.9	1.95	3.9	3.9	1.95
SE	24h	7.81,	15.62,	7.81,	7.81,	1.95,	3.9,	1.95,	1.95,	1.95,	1.95,
	48h	7.81	31.25	7.81	7.81	1.95	3.9	1.95	1.95	1.95	1.95
EF	24h	31.25,	31.25,	31.25,	62.5,	1.95,	3.9,	1.95,	3.9,	1.95,	1.95,
	48h	31.25	31.25	31.25	62.5	1.95	3.9	1.95	3.9	1.95	1.95
Gram Negative											
EC	24h	62.5,	62.5,	62.5,	125,	3.9,	31.25,	15.62,	62.5,	31.25,	7.81,
	48h	62.5	62.5	62.5	125	3.9	31.25	15.62	62.5	31.25	7.81
KP	24h	62.5,	62.5,	62.5,	62.5,	3.9,	31.25,	7.81,	62.5,	62.5,	7.81,
	48h	62.5	62.5	62.5	62.5	3.9	31.25	7.81	62.5	62.5	7.81
KP-E	24h	125,	125,	250,	125,	3.9,	31.25,	15.62,	62.5,	62.5,	15.62,
	48h	125	250	250	125	3.9	31.25	15.62	62.5	62.5	15.62
PA	24h	125,	125,	125,	250,	15.62,	31.25,	31.25,	62.5,	125,	62.5,
	48h	125	125	125	250	15.62	31.25	31.25	62.5	125	62.5

From the results obtained in Table 3.10 for the linear alkyl L-phenylalanine ILs screened (**432-441**) (Figure 3.23) it can be seen that in general a broad spectrum antibacterial toxicity can be observed for the majority of the compounds screened. A trend of increasing toxicity with increased alkyl chain length is also observed for the ILs screened against the gram positive bacteria. However, when the ILs were screened against the gram negative bacteria, it was observed that all of the C<sub>10</sub> examples were more toxic than the C<sub>8</sub> and C<sub>12</sub> examples. One potential explanation for this behaviour is due to the bioavailability and solubility of the C<sub>10</sub> examples. C<sub>8</sub> examples (**432, 435, 438, 441**) are less toxic due to their reduced lipophilicity and the C<sub>12</sub> examples (**434, 437, 440**) are less toxic due to their reduced solubility (even though they are more lipophilic the toxicity is reduced due to reduced bioavailability) *vide infra* Section 4.2. C<sub>10</sub> examples (**433, 436, 439**) appear to be in an optimum region where lipophilicity, solubility and thus bioavailability are at a maximum hence the highest levels of toxicity observed.<sup>31</sup> An alternative possibility is that the high toxicity is compound specific. Ethyl nicotinium C<sub>8</sub> derivative (**441**) was shown to be the least toxic example, see Table 3.10. It is believed that linear alkyl quaternary ammonium molecules, such as the ILs presented here, possess their antibacterial activity due to their effect on bacterial plasma membranes and as such belong to a class of antimicrobials defined as membrane-active agents.<sup>54</sup> The following sequence of events has been proposed in the literature to explain the antimicrobial activity of linear alkyl cationic species:<sup>55, 56</sup>

1. Adsorption of the antimicrobial agent to the cell wall followed by penetration into the cell wall
2. Reaction with the cytoplasmic membrane followed by membrane disorganisation
3. Leakage of intracellular material through the disrupted membrane
4. Degradation of proteins and nucleic acids within the cell
5. Cell wall lysis and cell death

### 3.6.2 Antifungal screening of the 2<sup>nd</sup> generation linear alkyl amino acid ILs

In tandem with the antibacterial screening, the linear alkyl ILs (**432-441**) were screened for their antifungal activity as per Chapter 2.

To investigate the *in vitro* anti fungal activity of the aforementioned compounds the following strains of fungi, available from the repository at Charles University, Czech Republic, were screened against:

#### 9 Yeasts

- *Candida albicans* (ATCC 448597) (CA1)
- *Candida albicans* (ATCC 900288) (CA2)
- *Candida parapsilosis* (ATCC 220199 ) (CP)
- *Candida krusei* (ATCC 62581) (CK1)
- *Candida krusei* (E2811) (CK2)
- *Candida tropicalis* (156) (CT)
- *Candida glabrata* (20/I2) (CG)
- *Candida lusitanae* (2446/I3 ) (CL)
- *Trichosporon asahii* (11884) (TA)

#### 3 Filamentous fungi:

- *Aspergillus fumigatus* (2315) (AF)
- *Absidia corymbifera* (2726) (AC)
- *Trichophyton mentagrophytes* (445) (TM)

The fungi screened against were the same strains discussed in Chapter 2.

#### 3.6.2.1 Experimental Method

The experimental method is as described in Chapter 5, Section 5.8.2.

#### 3.6.2.2 Antifungal Results – Linear Alkyl Surfactant ILs

From the results obtained for the antifungal screening of linear alkyl ILs (**432-441**) (Table 3.11), it can be seen that as alkyl chain length increases so does the antifungal activity. Antifungal activity for the C<sub>8</sub> examples (**432, 435, 438, 441**) is generally moderate 250-1000 µmol/L for imidazolium, cholinium and ethyl nicotinium derivatives (**435, 438, 441**).

**Table 3.11.** Antifungal results obtained for the linear alkyl ILs (**432-441**).

Microorganism	Time (h)	IL MIC $\mu\text{mol}^*$									
		<b>432</b> <b>C<sub>8</sub></b>	<b>435</b> <b>C<sub>8</sub></b>	<b>438</b> <b>C<sub>8</sub></b>	<b>441</b> <b>C<sub>8</sub></b>	<b>433</b> <b>C<sub>10</sub></b>	<b>436</b> <b>C<sub>10</sub></b>	<b>439</b> <b>C<sub>10</sub></b>	<b>434</b> <b>C<sub>12</sub></b>	<b>437</b> <b>C<sub>12</sub></b>	<b>440</b> <b>C<sub>12</sub></b>
<i>CA1</i>	24h	250,	500,	500,	500,	15.62,	31.25,	15.62,	3.9,	7.81,	1.95,
	48h	250	500	500	500	15.62	31.25	31.25	3.9	7.81	3.9
<i>CA2</i>	24h	250,	500,	500,	500,	15.62,	31.25,	15.62,	3.9,	7.81,	3.9,
	48h	250	1000	500	1000	31.25	62.5	31.25	3.9	7.81	3.9
<i>CP</i>	24h	125,	250,	500,	250,	15.62,	31.25,	31.25,	7.81,	7.81,	7.81,
	48h	250	500	500	500	31.25	31.25	31.25	7.81	7.81	7.81
<i>CK1</i>	24h	125,	250,	125,	125,	7.81,	31.25,	15.62,	7.81,	7.81,	3.9,
	48h	125	500	125	500	31.25	31.25	15.62	7.81	7.81	3.9
<i>CK2</i>	24h	125,	250,	62.5,	125,	7.81,	15.62,	15.62,	7.81,	7.81,	3.9,
	48h	125	500	125	250	31.25	31.25	15.62	7.81	7.81	3.9
<i>CT</i>	24h	250,	250,	250,	250,	7.81,	62.5,	31.25,	15.62,	7.81,	7.81,
	48h	250	250	250	250	31.25	62.5	31.25	15.62	15.62	7.81
<i>CG</i>	24h	500,	500,	1000,	500,	62.5,	62.5,	62.5,	7.81,	7.81,	3.9,
	48h	500	500	1000	500	62.5	62.5	62.5	7.81	15.62	3.9
<i>CL</i>	24h	250,	250,	250,	250,	62.5,	62.5,	125,	7.81,	31.25,	3.9,
	48h	500	250	500	500	62.5	62.5	125	7.81	31.25	3.9
<i>TA</i>	24h	1000,	1000,	500,	500,	125,	250,	250,	62.5,	125,	125,
	48h	1000	1000	500	1000	125	250	250	62.5	125	125
<i>AF</i>	24h	250,	500,	250,	125,	3.9	15.62,	31.25,	7.81,	7.81,	3.9,
	48h	250	1000	500	250	7.81	15.62	31.25	7.81	7.81	3.9
<i>AC</i>	24h	500,	500,	500	125,	31.25,	62.5,	31.25,	15.62,	15.62,	7.81,
	48h	500	500	500	250	31.25	62.5	31.25	15.62	15.62	7.81
<i>TM</i>	72h	1000,	1000,	500,	250,	62.5,	62.5,	31.25,	15.62,	7.81,	15.62,
	120h	1000	1000	500	250	62.5	62.5	31.25	15.62	7.81	15.62

\* IC<sub>50</sub> values were assessed for AF, AC and TM and IC<sub>80</sub> for all other strains.

C<sub>8</sub> pyridinium derivative (**432**) was more toxic with MIC values ranging from 125-1000 µmol/L. When the alkyl chain lengths were extended from C<sub>8</sub> to C<sub>10</sub> an order of magnitude increase in the toxicity is observed for all three C<sub>10</sub> compounds (**433**, **436**, **439**). MIC values for the C<sub>10</sub> ILs generally ranged from 15.62-250 µmol/L. Pyridinium C<sub>10</sub> compound (**433**) was more toxic than its imidazolium (**409**) and cholinium (**439**) counterparts with MIC values reaching as low as 3.9 µmol/L for the AF fungus. Finally, as the alkyl chain is further extended to C<sub>12</sub>, a broad spectrum antifungal activity is observed for all three C<sub>12</sub> compounds (**434**, **437**, **440**) with MIC values in the region of 3.9 – 125 µmol/L. Overall the TA strain of fungus appeared to be the most resistant to the linear alkyl ILs screened.

The mechanism of antifungal activity for linear alkyl quaternary ammonium compounds has been investigated in the literature. It has been shown that the cationic surfactant cetylpyridinium chloride can induce potassium ion leakage from yeasts such as *S. cerevisiae*. Linear alkyl cationic compounds mode of action on fungi is similar to that discussed for bacteria. QACs can insert into the plasma membrane of a fungus and cause disruption of the membrane and eventually lysis. QAC's have also been report as spore growth inhibitors.<sup>56</sup>

### 3.6.3 Antibacterial screening of the 2<sup>nd</sup> generation bolaform amino acid ILs

To investigate the *in vitro* antibacterial effect of the bolaform ILs (**444-452**) the following eight strains of bacteria from the collection available at Charles University, Czech Republic, were screened against:

Gram Positive:

- *S. aureus* (ATCC 65382) (SA)
- *Methicillin-res.S.a* (HK5996/08) (MRSA)
- *S. epidermidis* (HK6966/084 ) (SE)
- *Enterococcus sp.* (HK14365/085) (EF)

Gram Negative:

- *E. coli* (ATCC 87396) (EC)
- *K. pneumoniae* (HK11750/087) (KP)
- *K. pneumoniae* (HK14368/08) (KP-E)
- *P. aeruginosa* (ATCC 9027) (PA)

The bacteria screened against were the same strains discussed in Chapter 2.

### 3.6.3.1 Experimental Method

The experimental method is as described in Chapter 5, Section 5.8.1.

### 3.6.3.2 Antibacterial Results – Bolaform Surfactant ILs

As can be seen from the antibacterial result in Table 3.12 all of the bolaform ILs (**444-452**) possessed high levels of antimicrobial toxicity towards the gram positive bacteria (e.g. IL **444** 3.9  $\mu\text{mol IC}_{95}$  towards SE) and to a lesser extent towards the gram negative. It was also observed that an increase in toxicity occurred as the bolaform spacer was increased from C<sub>8</sub> to C<sub>10</sub> (e.g. IL **444** 31.25  $\mu\text{mol IC}_{95}$  towards EF decreasing to 15.62  $\mu\text{mol}$  for IL **445**) and again from C<sub>10</sub> to C<sub>12</sub> (e.g. IL **445** 15.62  $\mu\text{mol IC}_{95}$  towards EF decreasing to 3.9  $\mu\text{mol}$  for IL **446**). The results observed are consistent with the linear alkyl surfactants analysed in Section 3.6.1 in that high levels of antimicrobial toxicity are observed, most likely due to a high level of lipophilicity associated with these classes of molecules.



**Table 3.12.** Antibacterial results obtained for bolaform L-phenylalanine ILs.

Microorganism		IL MIC <sub>95</sub> μmol								
Chain length	Time (h)	444	447	450	445	448	451	446	449	452
		C <sub>8</sub>	C <sub>8</sub>	C <sub>8</sub>	C <sub>10</sub>	C <sub>10</sub>	C <sub>10</sub>	C <sub>12</sub>	C <sub>12</sub>	C <sub>12</sub>
Gram Positive										
SA	24h	7.81,	7.81,	15.62,	1.95,	1.95,	1.95,	1.95,	1.95,	7.81,
	48h	7.81	7.81	15.62	1.95	1.95	1.95	1.95	1.95	7.81
MRSA	24h	7.81,	15.62,	62.5,	1.95,	1.95,	1.95,	1.95,	1.95,	7.81,
	48h	7.81	15.62	62.5	1.95	1.95	1.95	1.95	1.95	7.81
SE	24h	3.9,	3.9,	3.9,	1.95,	1.95,	1.95,	1.95,	1.95,	1.95,
	48h	3.9	3.9	3.9	1.95	1.95	1.95	1.95	1.95	1.95
EF	24h	31.25,	125,	125,	15.62,	15.62,	7.81,	3.9,	3.9,	3.9,
	48h	31.25	125	125	15.62	15.62	7.81	3.9	3.9	3.9
Gram Negative										
EC	24h	15.62,	15.62,	31.25,	7.81,	7.81,	7.81,	1.95,	1.95,	3.9,
	48h	15.62	15.62	31.25	7.81	7.81	7.81	1.95	1.95	3.9
KP	24h	125,	500,	500,	62.5,	125,	62.5,	7.81,	7.81,	15.62,
	48h	125	500	500	62.5	125	62.5	7.81	7.81	15.62
KP-E	24h	250,	500,	500,	125,	125,	62.5,	7.81,	15.62,	15.62,
	48h	250	500	500	125	125	62.5	7.81	15.62	15.62
PA	24h	250,	500,	500,	125,	250,	125,	15.62,	31.25,	15.62,
	48h	250	500	500	125	250	125	15.62	31.25	15.62

### 3.6.4 Antifungal screening of the 2<sup>nd</sup> generation bolaform amino acid ILs

To investigate the *in vitro* anti fungal activity of the bolaform ILs (**444-452**) the following strains of fungi, available from the repository at Charles University, Czech Republic, were screened against:

#### 9 Yeasts

- *Candida albicans* (ATCC 448597) (CA1)
- *Candida albicans* (ATCC 900288) (CA2)
- *Candida parapsilosis* (ATCC 220199 ) (CP)
- *Candida krusei* (ATCC 62581) (CK1)
- *Candida krusei* (E2811) (CK2)
- *Candida tropicalis* (156) (CT)
- *Candida glabrata* (20/I2) (CG)
- *Candida lusitaniae* (2446/I3 ) (CL)
- *Trichosporon asahii* (11884) (TA)

#### 3 Filamentous fungi:

- *Aspergillus fumigatus* (2315) (AF)
- *Absidia corymbifera* (2726) (AC)
- *Trichophyton mentagrophytes* (445) (TM)

The fungi screened against were the same strains discussed in Chapter 2.

#### 3.6.4.1 Experimental Method

The experimental method is as described in Chapter 5, Section 5.8.2. Antifungal Results – Bolaform Surfactant ILs.

**Table 3.13.** Antifungal results obtained for bolaform L-phenylalanine ILs. (444-452).

Microorganism	Time (h)	IL MIC $\mu\text{mol}^*$								
		444 C <sub>8</sub>	447 C <sub>8</sub>	450 C <sub>8</sub>	445 C <sub>10</sub>	448 C <sub>10</sub>	451 C <sub>10</sub>	446 C <sub>12</sub>	449 C <sub>12</sub>	452 C <sub>12</sub>
<i>CAI</i>	24h	500,	1000,	>500,	62.5,	62.5,	62.5,	31.25,	15.62,	31.25,
	48h	500	1000	>500	62.5	62.5	62.5	31.25	15.62	31.25
<i>CA2</i>	24h	500,	1000,	>500,	62.5,	62.5,	125,	15.62,	31.25,	15.62,
	48h	500	1000	>500	62.5	62.5	125	15.62	31.25	15.62
<i>CP</i>	24h	250,	1000,	250,	7.81,	31.25,	31.25,	7.81,	3.9,	7.81,
	48h	250	1000	250	7.81	31.25	31.25	7.81	3.9	7.81
<i>CKI</i>	24h	1000,	1000,	500,	31.25,	62.5,	62.5,	7.81,	7.81,	15.62,
	48h	1000	1000	500	31.25	62.5	62.5	7.81	7.81	15.62
<i>CK2</i>	24h	500,	1000,	500,	31.25,	62.5,	62.5,	7.81,	15.62,	15.62,
	48h	500	1000	500	31.25	62.5	62.5	7.81	15.62	15.62
<i>CT</i>	24h	125,	250,	500,	15.62,	31.25,	15.62,	3.9,	15.62,	7.81,
	48h	125	250	500	15.62	31.25	15.62	3.9	15.62	7.81
<i>CG</i>	24h	500,	1000,	>500,	125,	125,	250,	31.25,	62.5,	31.25,
	48h	500	1000	>500	125	125	250	31.25	62.5	31.25
<i>CL</i>	24h	125,	500,	250,	31.25,	31.25,	15.62,	3.9,	15.62,	7.81,
	48h	125	500	250	31.25	31.25	15.62	3.9	15.62	7.81
<i>TA</i>	24h	125,	250,	500,	31.25,	62.5,	62.5,	31.25,	62.5,	31.25,
	48h	125	250	500	31.25	62.5	62.5	31.25	62.5	31.25
<i>AF</i>	24h	>1000,	>1000,	>500,	250,	500,	500,	62.5,	62.5,	125,
	48h	>1000	>1000	>500	250	500	500	62.5	62.5	125
<i>AC</i>	24h	>1000,	>1000,	>500,	250,	500,	125,	31.25,	31.25,	62.5,
	48h	>1000	>1000	>500	250	500	125	31.25	31.25	62.5
<i>TM</i>	72h	62.5,	62.5,	500,	500,	500,	62.5,	15.62,	31.25,	125,
	120h	62.5	62.5	500	500	500	62.5	15.62	31.25	125

\* IC<sub>50</sub> values were assessed for AF, AC and TM and IC<sub>80</sub> for all other strains.

### 3.6.4.2 Antifungal Results – Bolaform Surfactant ILs

In general, a trend of increasing antifungal toxicity with increasing alkyl chain length was observed for the bolaform ILs (Table 3.13). C<sub>8</sub> ILs (**444**, **447**, **450**) displayed a wide range of IC<sub>50</sub> and IC<sub>80</sub> values (62.5-1000). With an increase in alkyl chain linker to C<sub>10</sub> ILs (**445**, **448**, **451**) the levels of antifungal toxicity increased with the exceptions of the TM fungus which showed the opposite behaviour for ILs (**445**, **448**) where the IC<sub>50</sub> values increased from 62.5 to 500 µmol. This behaviour was not observed for IL (**451**). Finally, for the C<sub>12</sub> linked ILs (**446**, **449**, **452**) the highest levels of toxicity were observed, ranging from 3.9-125 µmol. The levels of toxicity observed for the bolaform ILs is of a comparable level to that of the linear alkyl ILs examined in section 3.6.2, the presence of a cationic charge on either end of the bolaform ILs having no apparent reduction in the levels of antifungal toxicity observed.

### 3.6.5 Antimicrobial Screening Conclusions

From the combined antibacterial and antifungal data collected for the linear alkyl ILs (**432-441**) it can be seen that in general a broad spectrum antibacterial activity was observed for the ILs screened. It was observed that as chain length increased so did toxicity towards the gram positive bacteria. A different trend was observed when compared against the gram negative bacteria with the highest levels of toxicity observed at the C<sub>10</sub> ester chain length, ILs (**433**, **436**, **439**). Ethyl nicotinium C<sub>8</sub> IL (**441**) was shown to be the least toxic derivative of the linear alkyl ILs but still within the same order of magnitude of toxicity as the other C<sub>8</sub> ILs.

From the antifungal screening conducted for the linear alkyl ILs, a general trend of increasing toxicity with increasing chain length can be observed. Ethyl nicotinium IL (**441**) is also observed to be just as toxic as its C<sub>8</sub> counterparts. As chain length is increased from C<sub>8</sub> to C<sub>10</sub> an order of magnitude increase in toxicity is observed for all three C<sub>10</sub> ILs (**433**, **436**, **439**). The C<sub>12</sub> ILs showed the highest level of antifungal toxicity with MIC values in the region of 3.9 – 125 µmol/L.

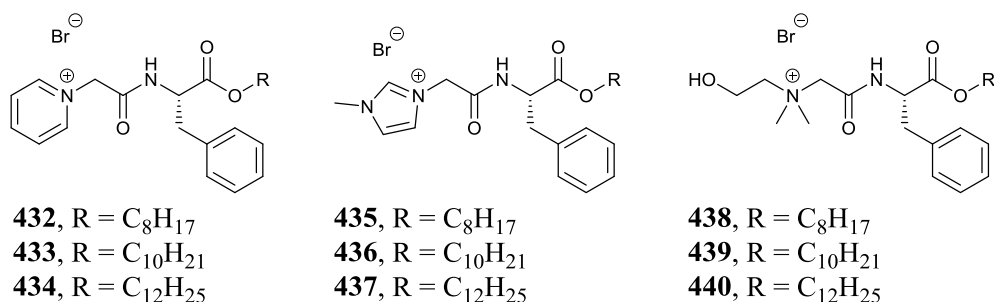
The bolaform ILs examined for their antimicrobial toxicity (**444-452**) displayed comparable levels of toxicity to their linear alkyl counterparts and showed increasing levels of toxicity with increasing alkyl chain length. Likewise, the antifungal results showed high levels of toxicity, comparable again to the linear alkyl ILs examined. The presence of two polar headgroups on the molecule did not appear to influence the levels of toxicity. The levels of toxicity for the bolaform ILs were also observed to be higher than those reported by Gindri *et al.*<sup>47</sup> most likely due to the increased lipophilicity of the bolaform ILs reported here.

### 3.7 Biodegradation Studies of 2<sup>nd</sup> Generation ILs

The aim of the work within this section was to investigate the biodegradability of the 2<sup>nd</sup> generation of L-phenylalanine ILs. The importance of investigating the biodegradability of the ILs synthesised has been previously discussed in Chapters 1-2. Furthermore the ILs undergoing examination are the 2<sup>nd</sup> generation derivatives of the ILs investigated in Chapter 2 and have been synthesised as potential surfactant performance chemicals. As discussed in Chapter 1, Section 1.7 and Chapter 3, Section 3.2, the need to produce readily biodegradable surfactants has been an on-going challenge for the past 50+ years and has recently been reinforced by the European Detergents Regulation 2005 which requires all surfactants to be ultimately biodegradable. Based on the biodegradation results obtained in Chapter 2 it was proposed that the ILs synthesised in this chapter could potentially breakdown into biodegradable fragments analogous to those detected in Chapter 2.

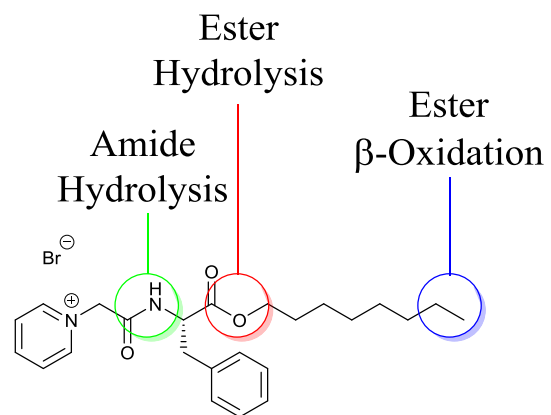
#### 3.7.1 Biodegradation Studies of Linear Alkyl ILs

The following linear alkyl ILs were examined for their biodegradability (Figure 3.27).



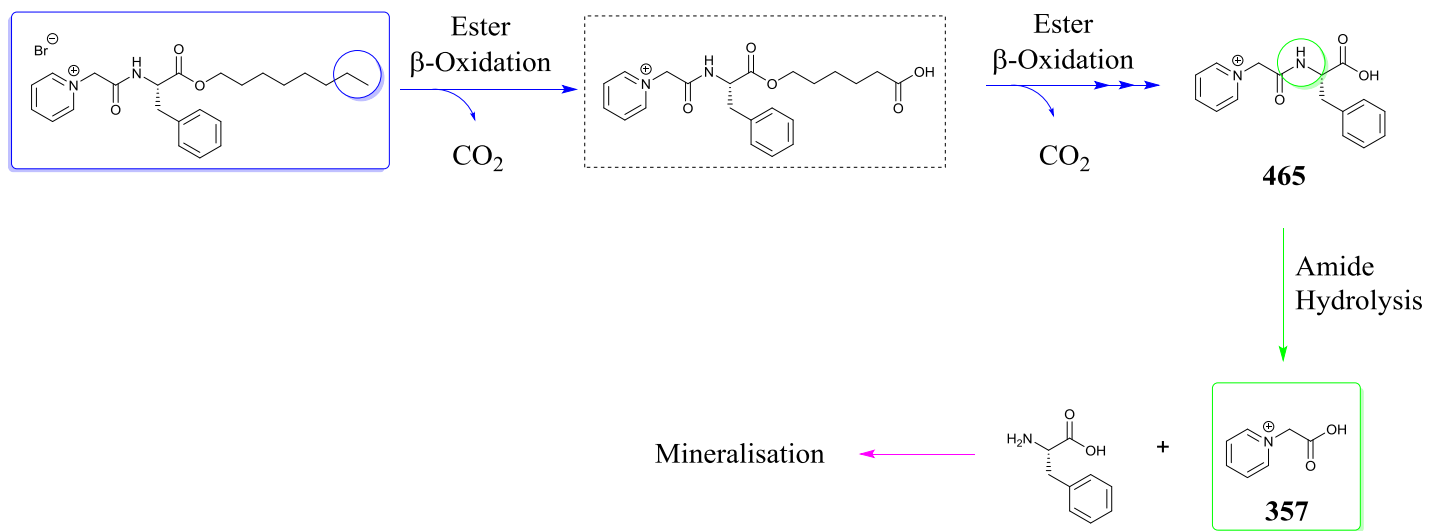
**Figure 3.27.** Linear Alkyl ILs (**432-440**) screened for their biodegradability.

From the structure activity biodegradation relationships examined in the metabolite examination, Chapter 2, Section 2.4.5, it was proposed that the linear alkyl ILs (**432-440**) (Figure 3.27), could potentially breakdown according to three likely pathways: amide hydrolysis, ester hydrolysis, and alkyl chain oxidation. An illustration of the potential breakdown sites are proposed for pyridinium IL (**432**) (Figure 3.28) and the pathways are outlined in Schemes 3.6, 3.7, 3.8.

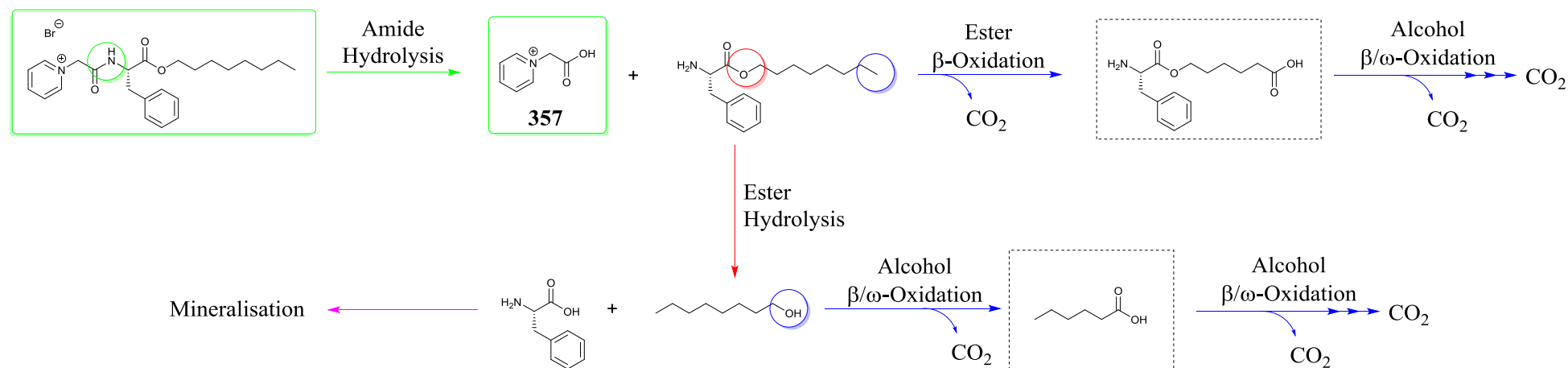


**Figure 3.28.** Potential breakdown sites on pyridinium IL (**432**).

**Scheme 3.6.** Proposed breakdown pathways of linear alkyl pyridinium IL (**432**) by ester oxidation.



**Scheme 3.7.** Proposed breakdown pathways of linear alkyl pyridinium IL (**432**) by ester oxidation.



**Scheme 3.8.** Proposed breakdown pathways of linear alkyl pyridinium IL (432) by amide hydrolysis.



### 3.7.1.1 Closed Bottle Test Method

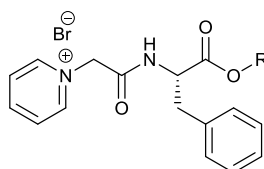
The CBT was carried out as per Chapter 5, Section 5.9.1

### 3.7.1.2 Linear alkyl IL biodegradation results

**Table 3.14.** Biodegradability and carbon distribution of examined L-phenylalanine ILs (**432-440**), colour coded according to the traffic light classification.<sup>57</sup>

IL	Biodegradation %	Amino Acid Ester Carbon %	Ester Carbon %
<b>L-Phenylalanine ILs</b>			
<b>432</b>	<b>53</b>	71	33
<b>433</b>	<b>36</b>	73	38
<b>434</b>	<b>4</b>	75	43
<b>435</b>	<b>48</b>	74	35
<b>436</b>	<b>44</b>	76	40
<b>437</b>	<b>15</b>	78	44
<b>438</b>	<b>36</b>	74	35
<b>439</b>	<b>27</b>	76	40
<b>440</b>	<b>20</b>	78	44

As can be seen from Table 3.14 of the ILs screened, none of the ILs examined passed the CBT. C<sub>8</sub> pyridinium (**432**) and imidazolium (**435**) derivatives underwent 53% and 48% biodegradation respectively. Cholinium C<sub>8</sub> derivative (**438**) underwent a lower level of biodegradation at 36%. When the C<sub>8</sub> biodegradation results are compared to the percentage carbon distribution of the molecules a number of insights can be made. Levels of biodegradation observed for the pyridinium IL (**432**), 53%, is above that which can be contributed to ester mineralisation alone (33%) and less than total amino acid degradation (71%). The identity of the biodegradation pathway is currently unknown and a metabolite analysis to determine the transformation products as per Chapter 2, Section 2.4.5, would provide invaluable information into the transformations taking place.



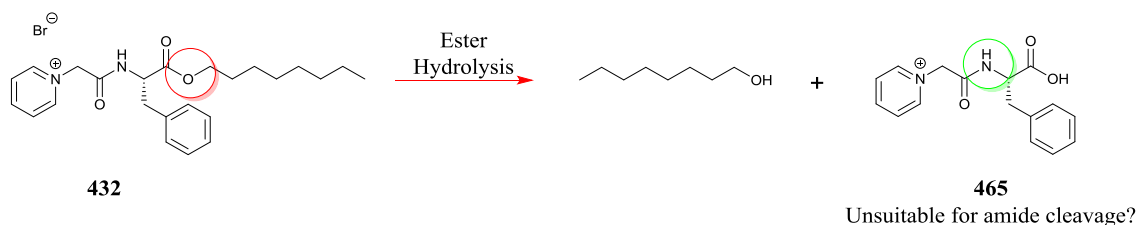
**325**, R = C<sub>2</sub>H<sub>5</sub>, 62%  
**432**, R = C<sub>8</sub>H<sub>17</sub>, 53%  
**433**, R = C<sub>10</sub>H<sub>21</sub>, 36%  
**434**, R = C<sub>12</sub>H<sub>25</sub>, 4%

**Figure 3.29.** Comparison of biodegradability for pyridinium ILs (**325**, **432-434**).

There are three possible reasons for the reduction in biodegradability observed for the octyl pyridinium IL (**432**) and decyl pyridinium IL (**433**) when compared to the short chain C<sub>2</sub>

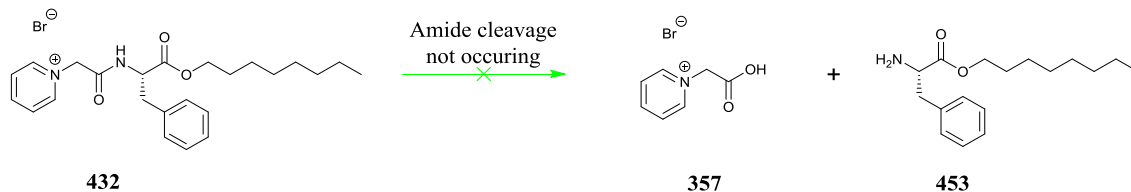
pyridinium IL (**325**) screened in Chapter 2 (Figure 3.29). The examples proposed below employ the C<sub>8</sub> pyridinium IL (**432**), however the same rationale can be applied to C<sub>10</sub> IL (**433**).

C<sub>8</sub> IL (**432**) could be undergoing slow rates of hydrolysis to the L-phenylalanine carboxylic acid transformation product (**465**) and this carboxylic acid may be an unsuitable substrate for amide cleavage (Scheme 3.9).



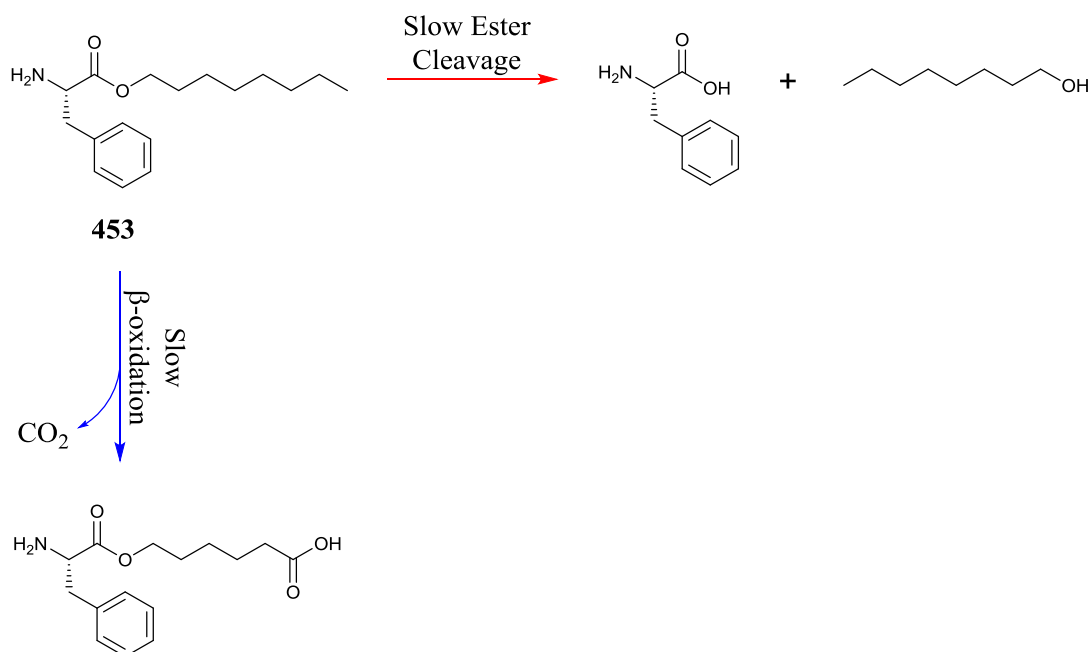
**Scheme 3.9.** Unsuitable amide cleavage after ester cleavage.

A second reason could be that octyl chain length parent IL (**432**) makes for an unsuitable substrate for amide cleavage in the first place (Scheme 3.9). This proposal is in agreement with the observation made in Chapter 2, Section 2.4.1 where pyridinium ethyl ester (**325**) (Figure 3.29), undergoes 62% biodegradation within the 28 day period, equating to almost the exact theoretical percentage degradation expected from amino acid and ester.



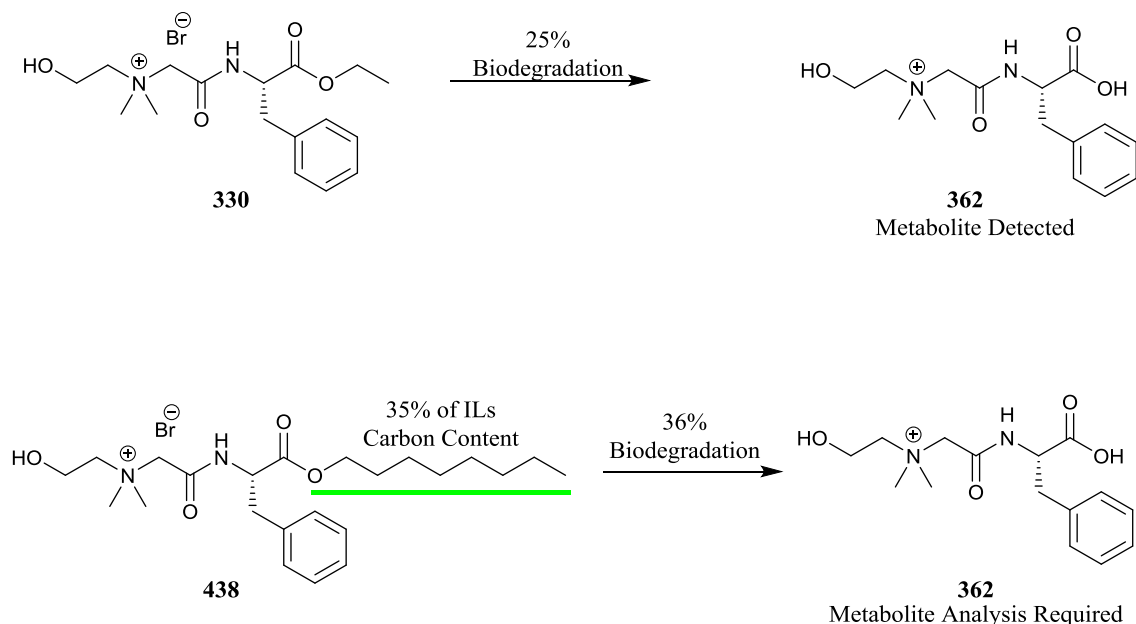
**Scheme 3.10.** Unsuitable amide cleavage before ester cleavage.

A final variation and extension upon Scheme 3.10 is that the octyl ester of L-phenylalanine may itself be an unsuitable substrate for ester cleavage and may be undergoing slow rates of ester hydrolysis or  $\beta$ -oxidation as shown in Scheme 3.11.



**Scheme 3.11.** Slow rates of biodegradation for amino acid octyl ester.

A middle ground between total ester degradation and total amino acid ester degradation suggests that the rate of biodegradation may be too slow to pass within the 28 day time limit and that rates of biodegradation for compounds cleaved at the ester or amide position could be different. If the tests were extended then ultimate biodegradability may be achieved for the  $\text{C}_8$  compounds.  $\text{C}_8$  cholinium IL (**438**) underwent 36% biodegradation which is almost exactly the carbon contribution from total ester degradation. Reduced biodegradability could be attributed to the cholinium IL undergoing a different biodegradation pathway to that observed for the pyridinium IL. In Chapter 2, a  $\text{C}_2$  ester cholinium IL (**330**) was seen to undergo ester cleavage only, with an amino acid carboxylate IL remaining, it may be that the  $\text{C}_8$  cholinium IL (**438**) is undergoing the same breakdown pathway as its  $\text{C}_2$  counterpart (Scheme 3.12) however only a metabolite study on these ILs can confirm the breakdown pathways.



**Scheme 3.12.** Cholinium C<sub>8</sub> biodegradation compared to Cholinium C<sub>2</sub> biodegradation.

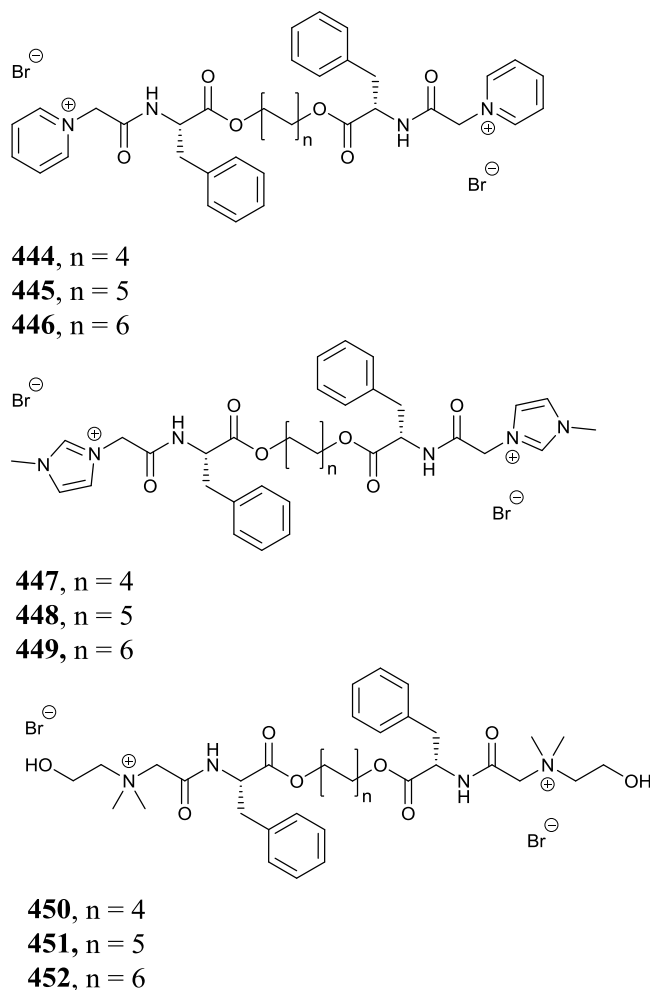
Upon extension of the alkyl chains to C<sub>10</sub>, a reduced biodegradability was observed for all three ILs (**433**, **436**, **439**). 36% Biodegradation was observed for pyridinium C<sub>10</sub> IL (**433**), 2% less than that which can be attributed to total ester mineralisation, 38%. 44% Biodegradation was observed for imidazolium C<sub>10</sub> IL (**436**), 4% above the theoretical degradation according to total ester degradation. Cholinium C<sub>10</sub> (**439**) displayed degradation levels 13% less than total ester degradation. See Table 3.14. From these values it cannot be inferred whether the amide bond of the C<sub>10</sub> ILs is undergoing hydrolysis. Reduced levels of biodegradability may be attributed to the broad spectrum antimicrobial activity of this series of ILs, previously determined in Section 3.6.

Further extension of the alkyl chains to C<sub>12</sub> to give ILs (**434**, **437**, **440**) saw a dramatic reduction in biodegradability. 4% biodegradation was observed for the pyridinium C<sub>12</sub> IL (**434**). All three C<sub>12</sub> ILs failed the toxicity control test carried out during the biodegradation screening and inhibited the WWTP organisms. Failure of the toxicity control helps to explain the sudden reduction in levels of biodegradability and is supported by the results obtained for the antimicrobial screening of the linear alkyl ILs, Section 3.6. According to Boethling's rules of thumb an extension in alkyl chain length should increase biodegradability.<sup>28</sup> However as the toxicity levels have increased with alkyl chain length, the potential increase in biodegradability is offset by the bacteria inability to degrade the IL. Indeed Boethling states that in many cases structural changes made to reduce the toxicity of small molecules can reduce biodegradability.<sup>28</sup> Though the C<sub>10</sub> and C<sub>12</sub> ILs undergo reduced levels of biodegradation, conclusions about their

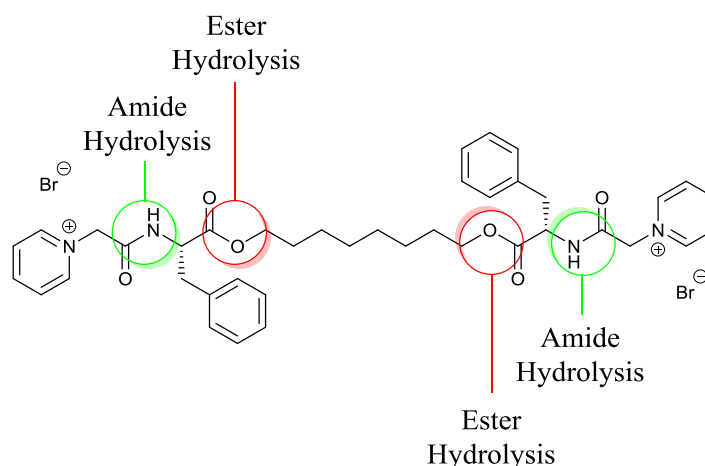
biodegradation pathways and ultimate biodegradability cannot be drawn without a full metabolite analysis and test time extensions.

### 3.7.2 Biodegradation Studies of Bolaform ILs

The following bolaform ILs were examined for their biodegradability (Figure 3.30). The biodegradability of bolaform and dicationic ILs has been reported in the literature and in general very poor results have been observed (< 5% biodegradation, see Chapter 1 Section 1.3.6).<sup>45,58,59</sup> Therefore the design features of the bolaform ILs such as the ester and amide linkages and the tentative QSABR observed in Chapter 2, Section 2.4.5 should allow for elevated levels of biodegradability. It is proposed that the bolaform ILs (**444-452**) (Figure 3.30) could potentially breakdown according to two likely pathways: amide hydrolysis and ester hydrolysis in a similar manner to that proposed for the linear alkyl ILs (Schemes 3.6, 3.7, 3.8). An illustration of the proposed breakdown sites for pyridinium IL (**444**) are depicted in Figure 3.31.



**Figure 3.30.** Linear Alkyl ILs (**444-452**) screened for their biodegradability



**Figure 3.31.** Potential biodegradation initiation points for IL (**444**).

### 3.7.2.1 Closed Bottle Test Method

The CBT was carried out as per Chapter 5, Section 5.2.1

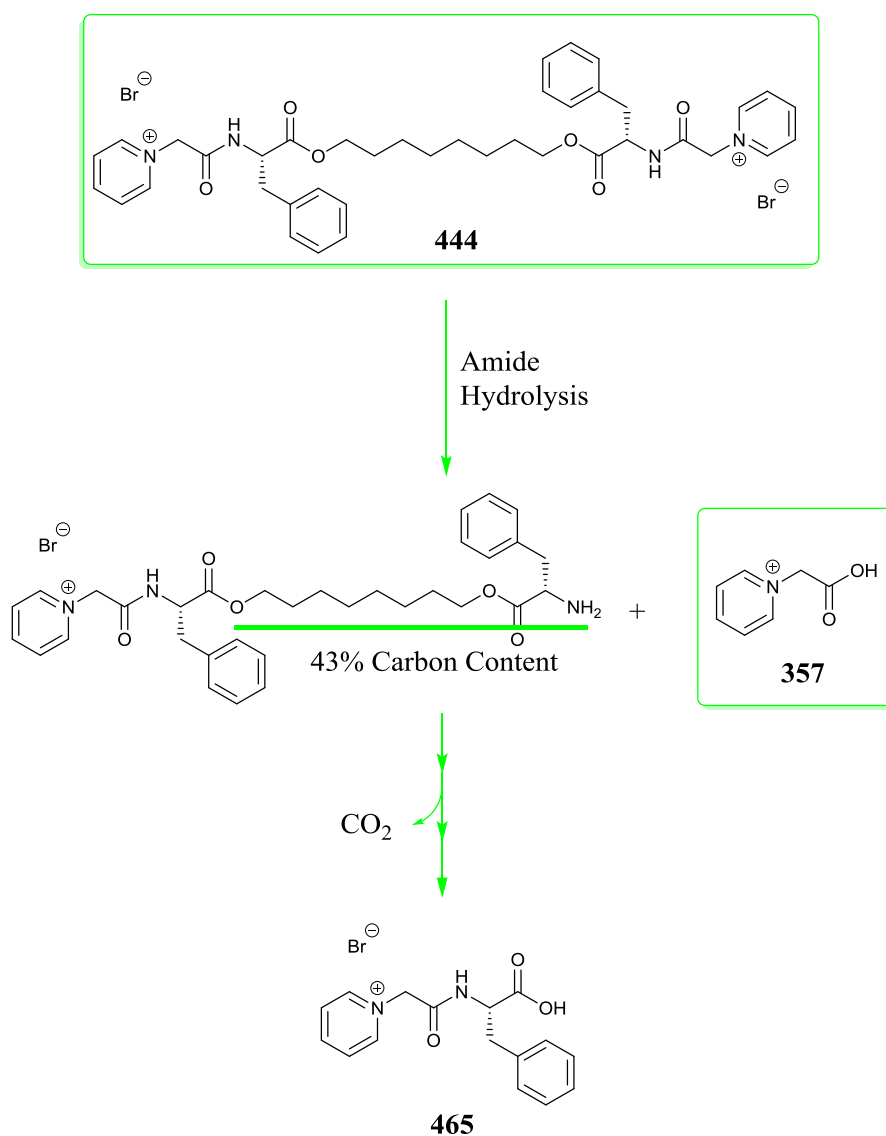
### 3.7.2.2 Linear alkyl IL biodegradation results

**Table 3.15.** Biodegradability and carbon distribution of examined L-phenylalanine ILs (444-452), colour coded according to the traffic light classification.<sup>57</sup>

IL	Biodegradation %	Amino Acid Ester Carbon %	Linker Carbon %
<b>L-Phenylalanine ILs</b>			
<b>444</b>	<b>47</b>	65	20
<b>445</b>	<b>40</b>	67	24
<b>446</b>	<b>18</b>	68	27
<b>447</b>	<b>53</b>	68	21
<b>448</b>	<b>44</b>	70	25
<b>449</b>	<b>40</b>	71	29
<b>450</b>	<b>28</b>	68	21
<b>451</b>	<b>24</b>	70	25
<b>452</b>	<b>19</b>	71	29

As can be seen from Table 3.15 of the ILs screened, none of the ILs examined passed the CBT. However the results presented are to the author's knowledge the highest levels of biodegradation observed for dicationic ILs reported in the literature by nearly +50%. The highest levels of biodegradation attained were for imidazolium C<sub>8</sub> linked IL (**447**), which displayed a tenfold increase over dicationic examples in the literature. It can be observed for each series of ILs that as spacer length is increased from C<sub>8</sub> to C<sub>10</sub> a decrease in biodegradability is observed, the same is also observed as the linker is increased from C<sub>10</sub> to C<sub>12</sub>. Cholinium C<sub>8</sub>

bolaform (**450**) displayed just 28% biodegradation and the cholinium class represents the lowest levels of bolaform biodegradability. Overall the highest levels of biodegradation within each headgroup class are observed for the C<sub>8</sub> linked ILs (**444**, **447**, **450**) (Table 3.15). It was also observed that all of the ILs with the exceptions of (**446**, **452**) had reached a plateau in their biodegradation after 28 days and were not expected to undergo further levels of biodegradation. The plateau phase obtained further poses the question of what exactly is breaking down within the test and why is it that the C<sub>8</sub> bolaforms observed higher levels than the C<sub>10</sub> and C<sub>12</sub> analogues. Levels of biodegradation obtained combined with the presence of the plateau phase suggest the ILs are breaking down into recalcitrant metabolites.



**Scheme 3.13.** Potential amide cleavage pathway for IL (**444**).

The example of IL (444), which displayed 47% biodegradation and had reached a plateau by the 28 day period could be accounted for by the pathway depicted in Scheme 3.13 where amide hydrolysis initially occurs followed by mineralisation of a portion of the linker chain and amino acids. Possible recalcitrant metabolites include (357) and (465) further reinforcing the need to examine (357) and (465) amongst other potential metabolites, for their biodegradability. The higher levels of biodegradability of the C<sub>8</sub> and C<sub>10</sub> pyridinium (444, 445) and C<sub>8</sub> and C<sub>10</sub> imidazolium (447, 448) analogues compared to the cholinium ILs (450-452), may be due to enzymatic considerations where the cholinium IL cannot fit into a specific region or binding site of a particular enzyme, whereas the imidazolium and pyridinium can.

The rapid reduction in biodegradability observed when the linker lengths are increased to C<sub>12</sub> may be due to a toxic effect or an incompatibility with esterase or amidase enzymes. However, this remains speculation as no toxicity controls were failed by any of the bolaform ILs. Antimicrobial toxicity results observed for the bolaform ILs screened in Chapter 3, Section 3.6 suggests that although the toxicity control did not fail in this CBT, a certain level of microbial inhibition is possible.

### **3.8 Conclusions to 2nd generation IL synthesis, biodegradation and antimicrobial toxicity screening**

In conclusion a series of new L-phenylalanine linear alkyl and bolaform ILs (432-441, 444-452), and alkylating reagents (456-458, 462-464) have been synthesised and characterised by <sup>1</sup>H-NMR, <sup>13</sup>C-NMR, HRMS, IR, optical rotation and melting point. Target IL compounds were produced in moderate to high yield yields with favourable green chemistry metrics established with the exception of ethyl nicotinium IL (441). Based on the poor synthesis and metrics for IL (441) it was decided to postpone synthesis of the ethyl nicotinium ILs (442, 443). Implementation of solvent recycling for the bolaform ILs (444-452) has shown to vastly improve the green chemistry metrics of the ILs synthesised. Linear alkyl and bolaform ILs were produced in sufficient quantity and purity to facilitate an antimicrobial screening and biodegradation study.

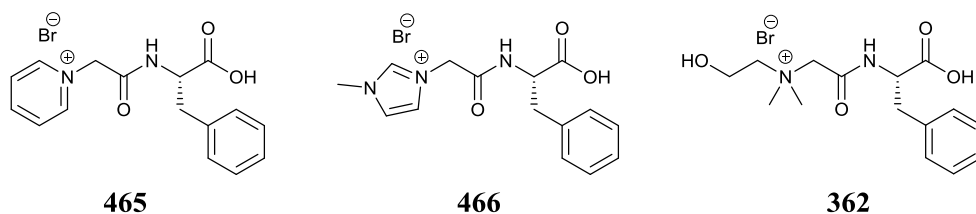
The linear alkyl ILs screened for their antimicrobial toxicity (432-441), possessed a broad spectrum antimicrobial activity towards the four gram positive bacteria screened against. A trend of increasing toxicity with increasing chain length was also observed. For the gram negative bacteria, the C<sub>10</sub> ILs (433, 436, 439) were shown to be more toxic towards the four bacteria than the C<sub>8</sub> or C<sub>12</sub> ILs. The reason for this higher level of toxicity for the C<sub>10</sub> examples



has been postulated as being a combination of solubility, lipophilicity and bioavailability. Linear alkyl ILs also showed a broad spectrum antifungal activity with increased activity observed as chain length was increased. The least toxic derivative screened was the ethyl nicotinium derivative (**441**), however it is important to note that the derivatives still possessed an activity in the region of 15.62-62.5  $\mu\text{mol/L}$   $\text{MIC}_{95}$  towards the gram positive bacteria and 125-250  $\mu\text{mol/L}$   $\text{MIC}_{95}$  towards the gram negative bacteria. Ethyl nicotinum IL (**441**) possessed moderate antifungal activity comparable to the other  $\text{C}_8$  analogues, 125-1000  $\mu\text{mol/L}$   $\text{IC}_{80}$ .

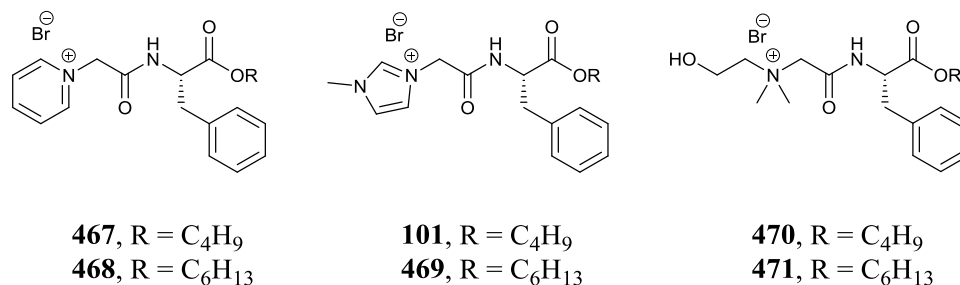
Bolaform ILs (**444-452**) also displayed high levels of antimicrobial and antifungal toxicity. Similar trends were observed for the bolaform ILs, with increasing toxicity linked to increasing alkyl spacer length.

From the results observed for the biodegradation screening, none of the linear alkyl ILs screened (**432-440**) could be classified as readily biodegradable. However a number of insights were drawn from the percentage biodegradation values observed. Biodegradation values calculated for the  $\text{C}_8$  derivatives (**432**, **435**, **438**) were above the percentage attributable to total ester degradation yet less than total ester + amino acid degradation (and only 7% below what is required to be considered readily biodegradable for  $\text{C}_8$  pyridinium IL (**432**)). The significance of such a result is that it can be proposed that the  $\text{C}_8$  ILs are undergoing a rate of biodegradation that is too slow for the 28 day test yet may continue on towards ultimate biodegradability. Biodegradation data for the bolaform ILs (**444-452**) was also obtained. Once again none of the ILs could be considered readily biodegradable however the results obtained are the highest levels of biodegradation reported for dicationic ILs in the literature. All of the bolaform ILs, with the exception of ILs (**446**, **452**), had reached a plateau in their biodegradability by the end of the 28 day test suggesting the presence of recalcitrant metabolite products such as those depicted in Figure 3.32. To determine whether potential metabolites such as an amino acid IL with an unprotected carboxylic acid group can undergo further biodegradation the following ILs (**362**, **465**, **466**) are proposed for further investigation into their biodegradability (Figure 3.32). Note IL (**362**) has been previously synthesised from Chapter 2, Section 2.4.5.



**Figure 3.32.** Proposed carboxylic acid ILs.

Furthermore, to investigate the suitability of ester chain lengths towards amidase, esterase and enzymes involved in  $\beta$ -oxidation, the following series of C<sub>4</sub>-C<sub>6</sub> alkyl chain length ILs (**101**, **467-471**) are proposed (Figure 3.33). Note IL (**101**) has already been reported in Chapter 1, Section 1.3.4.1 and underwent 61% biodegradation in the CO<sub>2</sub> headspace test ISO 14593.



**Figure 3.33.** Proposed intermediate length ILs (**101**, **467-471**).

It is suggested that the test times of 28 days are extended for all of the linear alkyl ILs (**432-440**) and the two bolaform ILs that hadn't reached a plateau (**446**, **452**), so as to determine the ultimate biodegradability. C<sub>10</sub> ILs examined (**433**, **436**, **439**) underwent reduced levels of biodegradability possibly attributable to increased levels of toxicity, however the toxicity control blank was not failed for the C<sub>10</sub> compounds. For C<sub>12</sub> ILs (**434**, **437**, **440**) the toxicity blank failed and this elevated level of toxicity, which is in agreement with the antimicrobial screening results, is the most likely cause for the dramatic reduction in levels of biodegradability observed for the C<sub>12</sub> ILs. In 10 years of screening IL and other organic compounds from the Gathergood group, these are the first to 'shut down' biodegradation processes due to high toxicity to the activated sludge used in the CBT.

In conclusion, the aims of this chapter have been met. A new series of surfactant candidate ILs has been synthesised in accordance to the 12 principles of green chemistry and have been designed for degradation. A number of green chemistry metrics have been calculated and the data gathered has allowed for an ongoing improvement in the synthetic techniques employed in the synthesis of this 2<sup>nd</sup> generation of amino acid ILs. Antimicrobial toxicity and biodegradability of the ILs has also been carried out with broad spectrum antimicrobial activity observed. Future investigation into the cytotoxicity of the 2<sup>nd</sup> generation ILs will provide an insight into how the ILs may interact with mammalian tissues. QAC's are amongst the most widely used antiseptics and the ILs synthesised within this chapter may be of value as ultimately biodegradable antiseptic surfactants, however QAC's are also known to possess a strong toxicity towards mammalian cells and further investigation is necessary.<sup>60</sup> It is proposed that the

biodegradation screening tests are extended beyond the 28 period so as to assess the ultimate biodegradability of the ILs undergoing examination.

### 3.9 References

1. N. V. Plechkova and K. R. Seddon, *Chem. Soc. Rev.*, 2008, 37, 123-150.
2. M. T. Garcia, N. Gathergood and P. J. Scammells, *Green Chem.*, 2005, 7, 9-14.
3. N. Gathergood, M. T. Garcia and P. J. Scammells, *Green Chem.*, 2004, 6, 166-175.
4. N. Gathergood, P. J. Scammells and M. T. Garcia, *Green Chem.*, 2006, 8, 156-160.
5. M. Ghavre, O. Byrne, L. Altes, P. K. Surolia, M. Spulak, B. Quilty, K. R. Thampi and N. Gathergood, *Green Chem.*, 2014, 16, 2252-2265.
6. M. J. Rosen and J. T. Kunjappu, *Surfactants and Interfacial Phenomena, 4th Edition*, Blackwell Science Publ, Oxford, 2012.
7. V. I. Pârvălescu and C. Hardacre, *Chem. Rev.*, 2007, 107, 2615-2665.
8. M. J. Lawrence, *Chem. Soc. Rev.*, 1994, 23, 417-424.
9. Surfactants: the ubiquitous amphiphiles, <http://www.rsc.org/chemistryworld/Issues/2003/July/amphiphiles.asp>, Accessed 03/08/2015, 2015.
10. I. L. Matthew, *Surfactant Production*, CRC Press, 2008.
11. Surfactants Market by Product Type, by Substrate Type, by Application - Trends & Forecast to 2020, <http://www.researchandmarkets.com/reports/3282601/surfactants-market-by-product-type-by-substrate>, Accessed 23/07/2015, 2015.
12. *Nonionics*, The Royal Society of Chemistry, 1995.
13. K. Kosswig, *Surfactants*, Wiley-VCH Verlag GmbH & Co. KGaA, 2000.
14. M. J. Rosen, M. Dahanayake and A. W. Cohen, *Colloids Surf.*, 1982, 5, 159-172.
15. J. Skerjanc, K. Kogej and J. Cerar, *Langmuir*, 1999, 15, 5023-5028.
16. M. T. Garcia, I. Ribosa, L. Perez, A. Manresa and F. Comelles, *Colloids Surf., B*, 2014, 123, 318-325.
17. M. T. Garcia, I. Ribosa, L. Perez, A. Manresa and F. Comelles, *Langmuir*, 2013, 29, 2536-2545.
18. S. Morrissey, B. Pegot, D. Coleman, M. T. Garcia, D. Ferguson, B. Quilty and N. Gathergood, *Green Chem.*, 2009, 11, 475-483.
19. M. J. Rosen, *Micelle Formation by Surfactants*, John Wiley & Sons, Inc., 2004.
20. A. V. Kabanov, V. P. Chekhonin, V. Y. Alakhov, E. V. Batrakova, A. S. Lebedev, N. S. Melik-Nubarov, S. A. Arzhakov, A. V. Levashov, G. V. Morozov, E. S. Severin and V. A. Kabanov, *FEBS Lett.*, 1989, 258, 343-345.
21. M.-C. Jones and J.-C. Leroux, *Eur. J. Pharm. Biopharm.*, 1999, 48, 101-111.
22. R. Varadaraj, J. Bock, P. Valint, S. Zushma and R. Thomas, *J. Phys. Chem.*, 1991, 95, 1671-1676.
23. J. M. Kuiper, R. T. Buwalda, R. Hulst and J. Engberts, *Langmuir*, 2001, 17, 5216-5224.
24. R. M. Hill, *Siloxane surfactants*, Springer Netherlands, 1997.
25. H. Jia, X. Bai, N. Li, L. Yu and L. Zheng, *CrystEngComm*, 2011, 13, 6179-6184.
26. EPA 505-F-14-001, [http://www2.epa.gov/sites/production/files/2014-04/documents/factsheet\\_contaminant\\_pfos\\_pfoa\\_march2014.pdf](http://www2.epa.gov/sites/production/files/2014-04/documents/factsheet_contaminant_pfos_pfoa_march2014.pdf), Accessed 24/07/2015, 2015.
27. D. Attwood, P. H. Elworthy and S. B. Kayne, *J. Phys. Chem.*, 1970, 74, 3529-3534.
28. R. S. Boethling, E. Sommer and D. DiFiore, *Chem. Rev.*, 2007, 107, 2207-2227.
29. R. S. Boethling, P. H. Howard, W. Meylan, W. Stiteler, J. Beauman and N. Tirado, *Environ. Sci. Technol.*, 1994, 28, 459-465.
30. P. H. Howard, R. S. Boethling, W. Stiteler, W. Meylan and J. Beauman, *Sci. Total Environ.*, 1991, 109, 635-641.

31. L. Carson, P. K. W. Chau, M. J. Earle, M. A. Gilea, B. F. Gilmore, S. P. Gorman, M. T. McCann and K. R. Seddon, *Green Chem.*, 2009, 11, 492-497.
32. A. Busetti, D. E. Crawford, M. J. Earle, M. A. Gilea, B. F. Gilmore, S. P. Gorman, G. Laverty, A. F. Lowry, M. McLaughlin and K. R. Seddon, *Green Chem.*, 2010, 12, 420-425.
33. F. M. Menger and S. Wrenn, *J. Phys. Chem.*, 1974, 78, 1387-1390.
34. R. Zana, *Bolaform and dimeric (gemini) surfactants*, Springer Netherlands, 1997.
35. J. L. Torres, E. Piera, M. R. Infante and P. Clapes, *Prep. Biochem. Biotechnol.*, 2001, 31, 259-274.
36. F. M. Menger and C. A. Littau, *J. Am. Chem. Soc.*, 1993, 115, 10083-10090.
37. A. Pinazo, X. Y. Wen, L. Perez, M. R. Infante and E. I. Franses, *Langmuir*, 1999, 15, 3134-3142.
38. C. C. O. Alves, A. S. Franca and L. S. Oliveira, *LWT--Food Sci. Technol.*, 2013, 51, 1-8.
39. J. Julis and W. Leitner, *Angew. Chem., Int. Ed.*, 2012, 51, 8615-8619.
40. J. Yu, F. Lin, P. Lin, Y. Gao and M. L. Becker, *Macromolecules*, 2014, 47, 121-129.
41. D. B. Zhao, Y. C. Liao and Z. D. Zhang, *Clean: Soil, Air, Water*, 2007, 35, 42-48.
42. P. T. P. Thi, C. W. Cho and Y. S. Yun, *Water Res.*, 2010, 44, 352-372.
43. J. Pernak, M. Smiglak, S. T. Griffin, W. L. Hough, T. B. Wilson, A. Pernak, J. Zabielska-Matejuk, A. Fojutowski, K. Kita and R. D. Rogers, *Green Chem.*, 2006, 8, 798-806.
44. M. T. Garcia, I. Ribosa, T. Guindulain, J. Sanchez-Leal and J. Vives-Rego, *Environ. Pollut.*, 2001, 111, 169-175.
45. S. Steudte, S. Bemowsky, M. Mahrova, U. Bottin-Weber, E. Tojo-Suarez, P. Stepnowski and S. Stolte, *RSC Adv.*, 2014, 4, 5198-5205.
46. F. A. E. Silva, F. Siopa, B. Figueiredo, A. M. M. Goncalves, J. L. Pereira, F. Goncalves, J. A. P. Coutinho, C. A. M. Afonso and S. P. M. Ventura, *Ecotoxicol. Environ. Saf.*, 2014, 108, 302-310.
47. I. M. Gindri, D. A. Siddiqui, P. Bhardwaj, L. C. Rodriguez, K. L. Palmer, C. P. Frizzo, M. A. P. Martins and D. C. Rodrigues, *RSC Adv.*, 2014, 4, 62594-62602.
48. K. M. Docherty and J. C. F. Kulpa, *Green Chem.*, 2005, 7, 185-189.
49. L. Myles, R. Gore, M. Spulak, N. Gathergood and S. J. Connon, *Green Chem.*, 2010, 12, 1157-1162.
50. Y.-R. Luo, W. San-Hu, X.-Y. Li, M.-X. Yun, J.-J. Wang and Z.-J. Sun, *Ecotoxicol. Environ. Saf.*, 2010, 73, 1046-1050.
51. S. P. M. Ventura, F. A. e Silva, A. M. M. Gonçalves, J. L. Pereira, F. Gonçalves and J. A. P. Coutinho, *Ecotoxicol. Environ. Saf.*, 2014, 102, 48-54.
52. S. Studzińska and B. Buszewski, *Anal. Bioanal. Chem.*, 2009, 393, 983-990.
53. K. J. Kulacki and G. A. Lamberti, *Green Chem.*, 2008, 10, 104-110.
54. W. B. Hugo and M. Frier, *Appl. Microbiol.*, 1969, 17, 118-127.
55. M. R. J. Salton, *J. Gen. Physiol.*, 1968, 52, 227-252.
56. G. McDonnell and A. D. Russell, *Clin. Microbiol. Rev.*, 1999, 12, 147-179.
57. L. Myles, R. G. Gore, N. Gathergood and S. J. Connon, *Green Chem.*, 2013, 15, 2740-2746.
58. L. Ford, J. R. Harjani, F. Atefi, M. T. Garcia, R. D. Singer and P. J. Scammells, *Green Chem.*, 2010, 12, 1783-1789.
59. A. Jordan and N. Gathergood, *Chem. Soc. Rev.*, 2015, DOI: 10.1039/C5CS00444F.
60. Â. S. Inácio, G. N. Costa, N. S. Domingues, M. S. Santos, A. J. M. Moreno, W. L. C. Vaz and O. V. Vieira, *Antimicrob. Agents Chemother.*, 2013, 57, 2631-2639.

## **Chapter 4**

### *Self-assembly and Surface Active Properties of 2<sup>nd</sup> Generation L-Phenylalanine Ionic Liquids*

## 4.1 Aim

The aim of this chapter was to investigate the surface activity and surfactant properties of the 2<sup>nd</sup> generation ILs described in Chapter 3. The premise for this investigation is described in the introduction to Chapter 3. A number of properties were investigated such as the critical micelle concentration (CMC), surface tension properties, liquid crystal behaviour at different temperatures, pH stability and susceptibility to hydrolysis.

## 4.2 Introduction

Determination of the CMC gives an indication as to how well a surfactant may perform in certain applications where the formation of micelles is beneficial e.g. cleaning, oil dispersion, foaming etc. Other information that can be obtained once the CMC is determined is the degree of ionisation ( $\alpha$ ) surrounding a micelle i.e. the degree of counterion dissociation. Degree of ionisation is a factor of how many counterions are associated around a micelle and how many are free in solution.<sup>1</sup> Dissociation of counterions means that the micelle can exist as a charged structure and the  $\alpha$  parameter can give insight into the stability of the micelles formed.<sup>2</sup> CMC was determined by two methods. The first was by conductivity and the second was by tensiometry. Both methods are discussed in full in Section 4.3, *vide infra*.

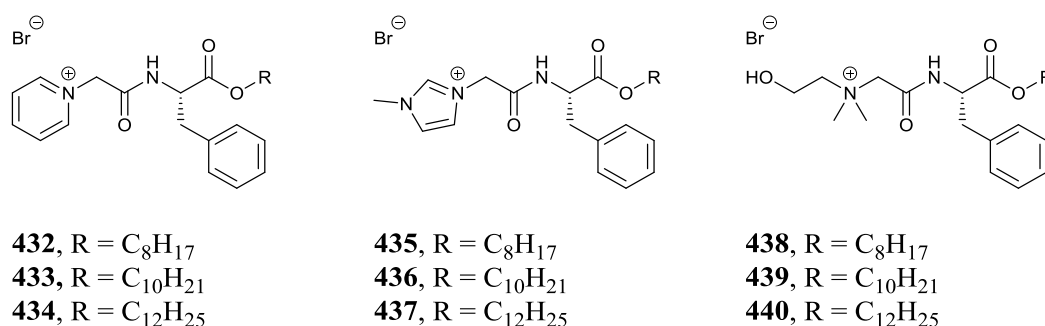
The second property investigated was the ILs ability to lower surface tension. Ability to lower surface tension at the interface of two phases is significant. Reduction in the repulsion forces between two otherwise immiscible phases can allow for dispersions of oil in water, emulsions, phase transfer catalysis etc.<sup>3-5</sup> A surfactant's effectiveness and efficiency at reducing surface tension can both be determined. Effectiveness is the maximum reduction in surface tension (effective range) achievable before surface saturation occurs and no more surfactant molecules can align at the surface and therefore the surface tension can be lowered no further.<sup>6</sup> At this point the excess concentration that can't access the saturated surface is forced to remain in the bulk solution and can begin to form aggregates such as micelles. Efficiency of a surfactant is the concentration of surfactant required to reduce surface tension by 20 mN/m.<sup>7</sup> Some surfactants may be efficient at lowering the surface tension by 20 mN/m but their effective range may be lacking. Such specific properties are application dependant i.e. whether efficiency, effectiveness or both are required and to what extent. A surfactant may have a high effective range but in achieving the lowest possible surface tension may require large concentrations. Thus the two components of efficiency and effectiveness must be considered. Furthermore the toxicity and biodegradability of the surfactants chosen for applications must be considered. Is it better to have a less efficient/effective surfactant if the overall toxicity is low and the biodegradability high?

To study the physicochemical properties of the surfactants a qualitative investigation into the liquid crystal forming behaviour was conducted using a polarised light microscope with heat controlled stage. A digital camera mounted on the stereo head of the microscope allowed for photography of the liquid crystal behaviour.

Lastly a preliminary investigation into the aqueous stability and hydrolysis in acidic and basic media was conducted for a number of surfactants.

### 4.3 Self-Aggregation and physicochemical properties of linear alkyl L-phenylalanine ILs.

The aggregation properties of the linear alkyl L-phenylalanine IL surfactants (**432-440**) (Figure 4.1) were determined by conductivity and tensiometry experiments. The results of these experiments are summarised in Table 4.1 and 4.5 respectively.

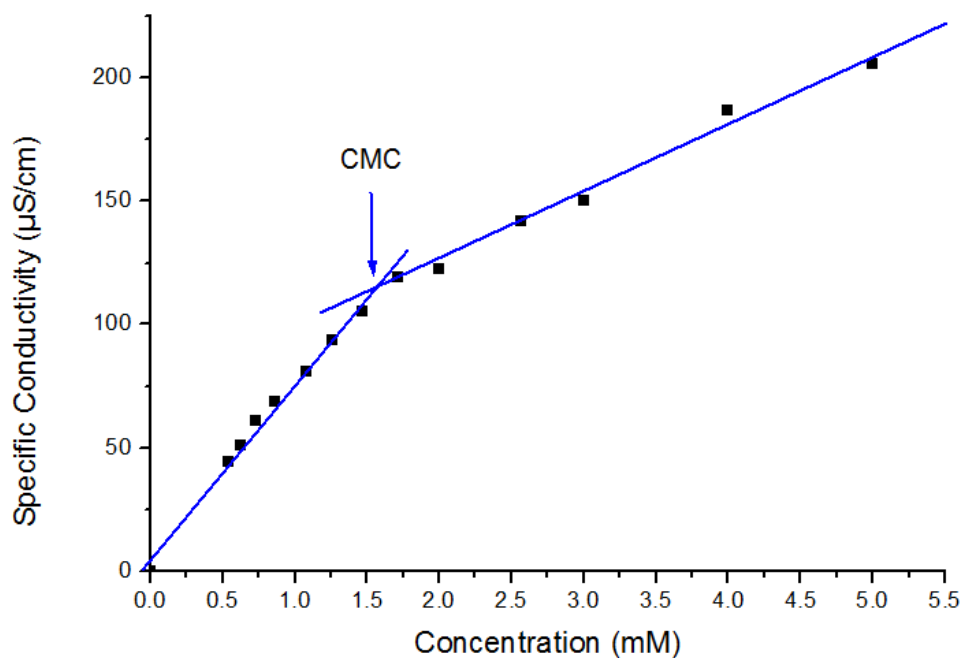


**Figure 4.1.** Linear alkyl ILs examined (**432-440**).

#### 4.3.1 Conductivity measurements

The change in specific conductivity with respect to concentration for aqueous solutions of the surfactants was measured. See Chapter 5, Section 5.10 for experimental details. The slope before the CMC has been reached is much steeper due to the concentration of free ions in solution. Once the CMC is achieved an abrupt change and reduction in the rate of increase in slope is observed due to the reduced ability of micelles to act as charge carriers as the free ions in solution are now involved in the aggregation process.<sup>8</sup> Surfactant counterions are bound to a certain degree to the micelle and this counterion binding parameter ( $\beta$ ) can be estimated by comparing the ratio of the two slopes to each other. Degree of ionisation ( $\alpha$ ) can also be determined by the following equation:  $\alpha = 1 - \beta$ . A typical conductivity plot is summarised in Figure 4.2. There are two distinct slopes observable for specific conductivity (Figure 4.2) and the CMC can be determined from the intersection of these two slopes. In total a conductivity vs.

concentration plot was constructed for each of the surfactant ILs undergoing investigation and are presented in Appendix II.



**Figure 4.2.** Plot of conductivity vs. concentration for imidazolium C<sub>10</sub> IL surfactant (**436**).

**Table 4.1.** Results obtained by conductimetry.

IL	Headgroup	Chain Length	CMC (mM)	$\alpha$	$\beta$	$\Delta G_{\text{mic}}^{\circ}$ (kJ/mol)
<b>432</b>	Pyridinium	8	4.00	0.697	0.303	-30.81
<b>433</b>	Pyridinium	10	1.30	0.47	0.53	-40.45
<b>434</b>	Pyridinium	12	0.20	0.407	0.593	-49.49
<b>435</b>	Imidazolium	8	3.70	0.497	0.503	-35.83
<b>436</b>	Imidazolium	10	1.70	0.377	0.623	-41.81
<b>437</b>	Imidazolium	12	0.22	0.455	0.545	-47.63
<b>438</b>	Cholinium	8	4.00	0.455	0.545	-36.52
<b>439</b>	Cholinium	10	1.50	0.427	0.573	-41.11
<b>440</b>	Cholinium	12	0.36	0.537	0.463	-43.32



As can be seen from Table 4.1, a progressive decrease in CMC was observed as ester chain length increased; a well-documented characteristic present in various surfactant classes with the progressive addition of each  $C_2H_4$  unit decreasing the CMC by a factor of  $\sim 4$  (the actual relationship is a progressive decrease of the CMC by half for every additional  $CH_2$  unit).<sup>3</sup> Very little difference was observed between the CMCs of the various headgroups. It can also be observed that as alkyl chain length increased so did the degree of counter-ion binding  $\beta$ .

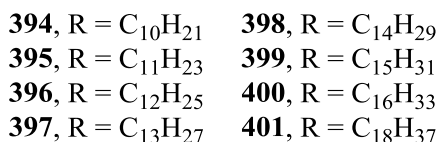
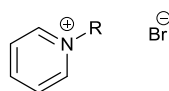
The spontaneity of the phenomenon of micellisation and aggregation of these surfactants in aqueous solution means that the Gibbs free energy ( $\Delta G^\circ_{mic}$ ) of micellisation can be determined as a negative value.  $\Delta G^\circ_{mic}$  was determined using the following equation:

$$\Delta G^\circ_{mic} = (2 - \beta)RT \ln x_{cmc}$$

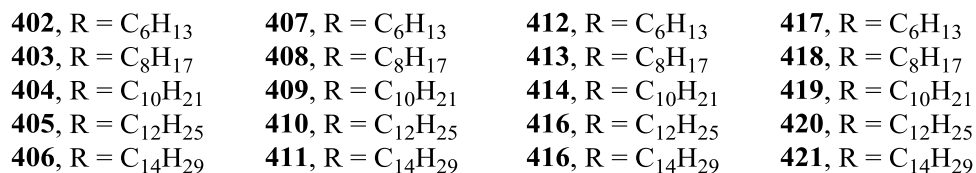
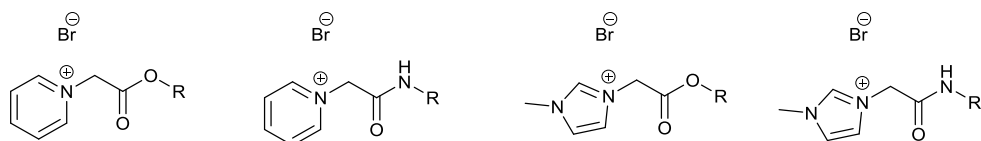
$\beta$  is the previously discussed counter-ion binding parameter (degree of association) and  $x_{cmc}$  is the critical micelle concentration expressed as a mole fraction of the solution measured. Results of the investigation into the  $\Delta G^\circ_{mic}$  show that as the alkyl chain length is increased, the energy required to form a micelle is decreased. This is due to the increase in hydrophobic repulsion interactions present with longer alkyl chains.

The CMC of the new IL surfactants (**432-435**) were compared to CMC values of linear alkyl surfactants reported in the literature, the observations of which are outlined in Table 4.2. Surfactants used for comparison include linear alkyl pyridinium surfactants depicted in Figure 4.3 (reported by Rosen *et al.*<sup>9</sup> and Skerjanc *et al.*<sup>10</sup>), and ester and amide functionalised imidazolium and pyridinium surfactants depicted in Figure 4.4 (investigated by Pérez *et al.*).<sup>8, 11</sup>

When compared to the ester functionalised pyridinium ILs examined by Pérez *et al.* the new amino acid surfactants reported here are comparable to ester surfactants with 3-4 more carbons. One reasonable explanation for this is that the phenylalanine sidechain residue is contributing to the overall lipophilicity of the surfactant therefore reducing the concentration required to form micelles. According to Rosen, a phenyl group as part of a hydrophobic group is equivalent to  $\sim 3.5$  carbon atoms.<sup>3</sup> This would help account for some of the decrease in CMC, the rest may be attributed to the remaining lipophilicity of the amino acid group; the amino acid heteroatoms themselves not contributing significant hydrophilicity to increase the CMC. The contribution of the phenyl sidechain is further exemplified when the predicted CMC values were determined and compared to the experimentally observed values.



**Figure 4.3.** Alkyl pyridinium surfactants (R = C<sub>n</sub>H<sub>2n+1</sub>, n = 10-16, 18) reported by Rosen *et al.*<sup>9</sup> and Skerjanc *et al.*<sup>10</sup>



**Figure 4.4.** Alkyl ester and amide surfactants reported by Pérez *et al.*<sup>8, 11</sup> Imidazolium IL (**412-414**) originally reported by Gathergood and Morrissey.<sup>12, 13</sup>

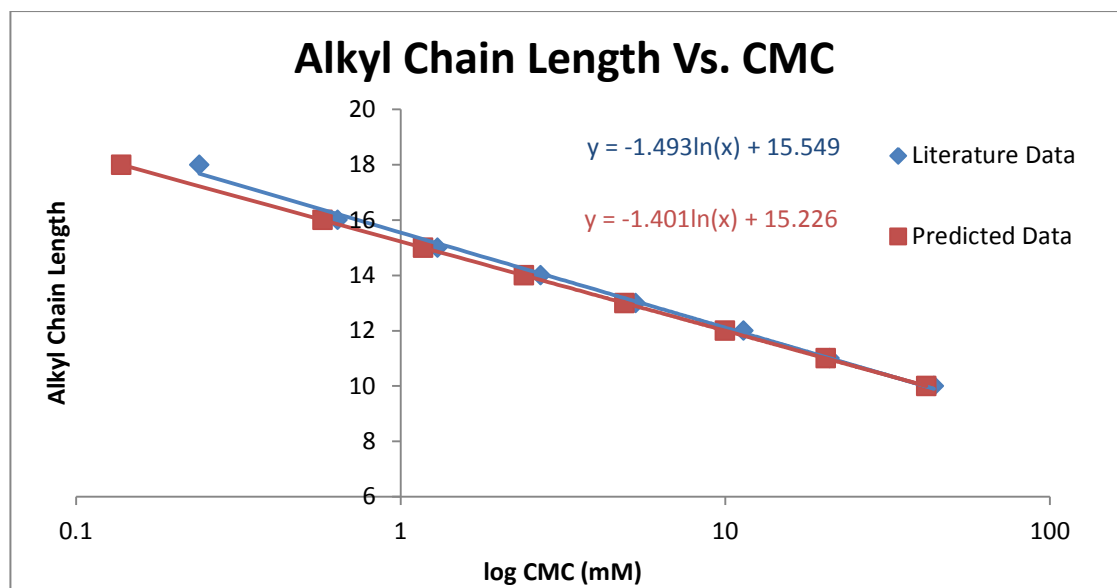
CMC can be tentatively predicted using the Stauff-Klevens rule<sup>14</sup>:

$$\log \text{CMC} = A - Bn$$

$A$  is a constant for the headgroup employed in the surfactant and  $B$  is an empirical constant constant for surfactant classes (originally approximated as  $\log_2(0.301)$  in Klevens original 1953 publication),  $n$  is the number of carbon atoms in the hydrophobic chain.<sup>14</sup> The value  $A$  for alkylpyridinium bromide surfactants (**394-401**) was determined to be 1.72 while  $B$  was determined to be 0.31 (at 30 °C).<sup>15, 16</sup> The accuracy of the predictions for ILs (**394-401**) compared to literature values are illustrated in Figure 4.5.

**Table 4.2.** Comparison of pyridinium surfactants reported by Rosen *et al.* (394-401), pyridinium ester (402-406) and amide (407-411) reported by Pérez *et al.*<sup>8, 11</sup> with new amino acid pyridinium IL surfactants (432-434). All surfactants were measured at 25 °C.

IL	Chain Length	Counterion	No. Carbons in Sidechain	CMC (mM)	Reference
<b>Linear Alkyl Pyridinium</b>					
394	C <sub>10</sub> H <sub>21</sub>	[Br]	10	44	10
395	C <sub>11</sub> H <sub>23</sub>	[Br]	11	21	10
396	C <sub>12</sub> H <sub>25</sub>	[Br]	12	11.4	9
397	C <sub>13</sub> H <sub>26</sub>	[Br]	13	5.3	10
398	C <sub>14</sub> H <sub>29</sub>	[Br]	14	2.7	10
399	C <sub>15</sub> H <sub>31</sub>	[Br]	15	1.3	10
400	C <sub>16</sub> H <sub>33</sub>	[Br]	16	0.64	10
401	C <sub>18</sub> H <sub>37</sub>	[Cl]	18	0.24	17
<b>Alkyl Ester Pyridinium</b>					
402	C <sub>6</sub> H <sub>13</sub>	[Br]	6	200	
403	C <sub>8</sub> H <sub>17</sub>	[Br]	8	73	8
404	C <sub>10</sub> H <sub>21</sub>	[Br]	10	17	8
405	C <sub>12</sub> H <sub>25</sub>	[Br]	12	4.1	8
406	C <sub>14</sub> H <sub>29</sub>	[Br]	14	0.91	8
<b>Alkyl Amide Pyridinium</b>					
407	C <sub>6</sub> H <sub>13</sub>	[Br]	6	262	11
408	C <sub>8</sub> H <sub>17</sub>	[Br]	8	73	11
409	C <sub>10</sub> H <sub>21</sub>	[Br]	10	18	11
410	C <sub>12</sub> H <sub>25</sub>	[Br]	12	4.6	11
411	C <sub>14</sub> H <sub>29</sub>	[Br]	14	1.2	11
<b>New Pyridinium Amino Acid ILs</b>					
432	C <sub>8</sub> H <sub>17</sub>	[Br]	8	4.00	n/a
433	C <sub>10</sub> H <sub>21</sub>	[Br]	10	1.30	n/a
434	C <sub>12</sub> H <sub>25</sub>	[Br]	12	0.20	n/a



**Figure 4.5.** Comparison of literature CMC values to predicted CMC values for linear alkyl pyridinium surfactants previously reported in the literature (**394-401**).

**Table 4.3.** Predicted CMC vs actual CMC for alkylpyridinium surfactants (**394-400**) and the new amino acid pyridinium ILs (**432-434**) reported in this chapter.

IL	Chain Length	No. Carbon atoms	Predicted CMC (mM)	Actual CMC (mM)
<b>Linear Alkyl Pyridinium</b>				
<b>394</b>	C <sub>10</sub> H <sub>21</sub>	10	41.69	44
<b>395</b>	C <sub>11</sub> H <sub>23</sub>	11	20.42	21
<b>396</b>	C <sub>12</sub> H <sub>25</sub>	12	10.00	11.4
<b>397</b>	C <sub>13</sub> H <sub>26</sub>	13	4.89	5.3
<b>398</b>	C <sub>14</sub> H <sub>29</sub>	14	2.39	2.7
<b>399</b>	C <sub>15</sub> H <sub>31</sub>	15	1.17	1.3
<b>400</b>	C <sub>16</sub> H <sub>33</sub>	16	0.58	0.64
<b>Amino Acid ILs</b>				
<b>432</b>	C <sub>8</sub> H <sub>17</sub>	8	173.78	4.0
<b>433</b>	C <sub>10</sub> H <sub>21</sub>	10	41.69	1.3
<b>434</b>	C <sub>12</sub> H <sub>25</sub>	12	10	0.2
<b>Amino Acid ILs - No. Carbon atoms including + 5 (Phenyl ring)</b>				
<b>432</b>	C <sub>8</sub> H <sub>17</sub>	13	4.89	4.0
<b>433</b>	C <sub>10</sub> H <sub>21</sub>	15	1.17	1.3
<b>434</b>	C <sub>12</sub> H <sub>25</sub>	17	0.28	0.2

When applying the Stauff-Klevens equation to the amino acid pyridinium ILs in Table 4.3 it can be seen that the equation can give estimates for the alkyl pyridinium surfactants examples taken from the literature. However, if the carbon count used in the new ILs (**432-434**) only takes into consideration the amino acids ester carbon quantity, then the prediction does not hold true. Only when the approximate additional lipophilicity from the amino acid sidechain phenyl group is included  $\sim +5$  does the prediction give meaningful results.

As can be seen from Table 4.4, the degree of binding for the surfactants increases as the alkyl chain length increases. This trend can also be compared to the CMC; the degree of binding increases as the hydrophobicity of the alkyl chain increases. When the amino acid ILs are compared to the alkyl pyridinium surfactants it can be seen that the degree of binding is lower. This may be due to the amino acid increasing the area per cationic headgroup in the micelle thus decreasing the number of counterions that can physically bind to the micelle before repulsion forces the remainder ( $\alpha$ ) into solution as free ions.

**Table 4.4.** Comparison of degree of binding,  $\beta$ , in linear alkyl pyridinium surfactants from the literature (**394-400**) and the new amino acid pyridinium ILs (**432-434**) reported in this chapter.

IL	Chain Length	Counterion	$\beta$	Reference
<b>Linear Alkyl Pyridinium</b>				
<b>394</b>	C <sub>10</sub> H <sub>21</sub>	[Br]	0.62	10
<b>395</b>	C <sub>11</sub> H <sub>23</sub>	[Br]	0.64	10
<b>396</b>	C <sub>12</sub> H <sub>25</sub>	[Br]	0.66	10
<b>397</b>	C <sub>13</sub> H <sub>26</sub>	[Br]	0.66	10
<b>398</b>	C <sub>14</sub> H <sub>29</sub>	[Br]	0.69	10
<b>399</b>	C <sub>15</sub> H <sub>31</sub>	[Br]	0.69	10
<b>400</b>	C <sub>16</sub> H <sub>33</sub>	[Br]	0.69	10
<b>Amino Acid ILs</b>				
<b>432</b>	C <sub>8</sub> H <sub>17</sub>	[Br]	0.303	n/a
<b>433</b>	C <sub>10</sub> H <sub>21</sub>	[Br]	0.530	n/a
<b>434</b>	C <sub>12</sub> H <sub>25</sub>	[Br]	0.593	n/a

### 4.3.2 Tensiometry measurements

The surface tension properties were determined according to the experimental method outlined in Chapter 5, Section 5.10. For each of the surfactant ILs examined, a plot of surface tension ( $\gamma$ ) vs. log concentration of the surfactant in aqueous solution was constructed. From the tensiometry plots a number of characteristics of the surfactants were determined. See Figure 4.6 for a typical plot determined for the surfactants analysed. CMC values were determined from the tensiometry plot from the intercept of the two distinct slopes present. The presence of two slopes can be attributed to the decrease in surface tension as surfactant concentration increases up to a minima where the surface becomes saturated by surfactant molecules. After this saturation has been reached the surfactant in solution begins forming micelles and the surface tension can be lowered no further.<sup>8</sup> For each of the linear alkyl ILs examined (432-440) a surface tension plot such as that presented in Figure 4.6 was constructed, see Appendix II for relevant graphs.

The surfactant efficiency ( $pC_{20}$ ) - the ability of a surfactant to reduce surface tension by 20 mN/m - was determined by the following equation:

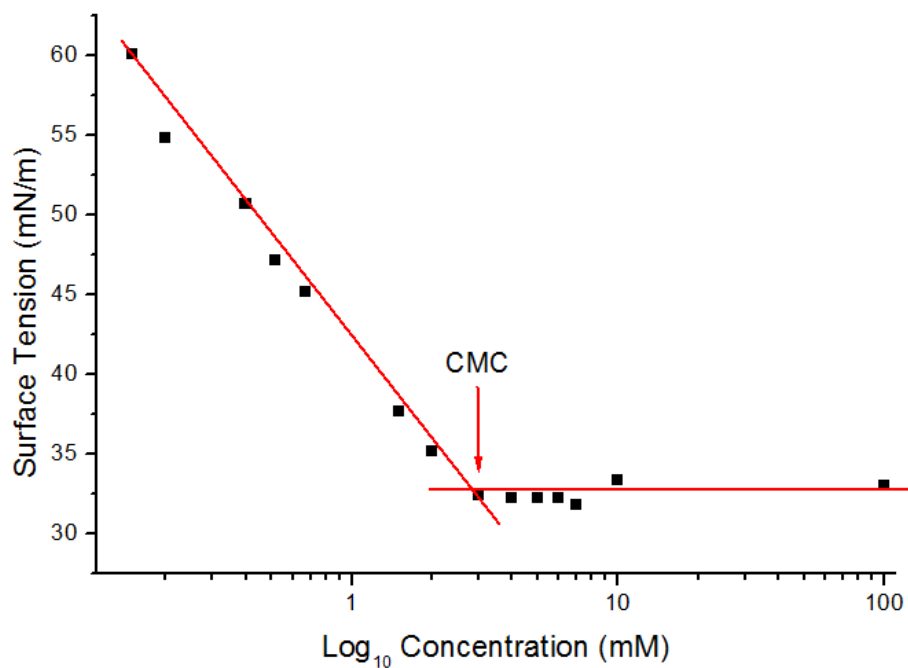
$$pC_{20} = -\log C_{20}$$

Where  $C_{20}$  is the concentration (in moles) required to reduce the surface tension by 20 mN/m<sup>11</sup>  
The larger the  $pC_{20}$  value, the more efficient the surfactant is.

The effectiveness of the surfactants ( $\pi_{CMC}$ ), was determined by the following equation:

$$\pi_{cmc} = \gamma_0 - \gamma_{cmc}$$

Where  $\gamma_0$  is the surface tension of pure water and  $\gamma_{cmc}$  is the surface tension observed at the CMC.<sup>11</sup>



**Figure 4.6.** Plot of Surface Tension vs. Log<sub>10</sub> Concentration for C<sub>8</sub> pyridinium IL surfactant (432).

The average area per molecule occupied by each surfactant molecule was also determined; using the Gibb's equation:

$$\Gamma = - \frac{1}{2.30_n \times RT} \times \left( \frac{d\gamma}{d\log_c} \right)_T$$

Where  $\Gamma$  is the surface excess concentration,  $\left( \frac{d\gamma}{d\log_c} \right)_T$  is the slope of the surface tension  $\gamma$  vs. log surfactant concentration dependence.  $R = 8.32 \text{ J/K mol}$  and  $T = 298.15 \text{ K}$ .  $n$  is the number of ionic species in solution and a value of two is used for the cation surfactants.

The surface excess concentration  $\Gamma$  is related to the area per surfactant molecule  $A$  using the following equation:

$$A = \frac{1}{N_A \times \Gamma}$$

Where  $N_A$  is Avogadro's constant.

**Table 4.5.** Surfactant properties for ILs (**432-440**) determined by tensiometry.

IL	Headgroup	Chain Length	CMC (mM)	$\gamma$ CMC (mN/m)	C <sub>20</sub> (mM)	pC <sub>20</sub>	Area per molecule $\text{\AA}^2 / \text{nm}^2$
<b>432</b>	Pyridinium	8	3.00	40.84	0.26	3.59	108.60 / 1.09
<b>433</b>	Pyridinium	10	0.70	36.65	0.03	4.49	105.26 / 1.05
<b>434</b>	Pyridinium	12	0.15	35.84	0.01	5.28	154.82 / 1.55
<b>435</b>	Imidazolium	8	2.50	38.24	0.19	3.71	108.13 / 1.08
<b>436</b>	Imidazolium	10	1.50	35.46	0.05	4.28	151.61 / 1.52
<b>437</b>	Imidazolium	12	0.25	36.77	0.01	4.99	154.58 / 1.55
<b>438</b>	Cholinium	8	2.00	37.03	0.11	3.96	126.52 / 1.27
<b>439</b>	Cholinium	10	1.70	35.04	0.04	4.36	126.52 / 1.27
<b>440</b>	Cholinium	12	0.20	35.85	0.02	4.82	112.58 / 1.13

From the results determined in Table 4.5, the CMC was determined for each of the IL surfactants and displayed a general decrease in CMC as alkyl chain length increased and was in agreement with the results obtained by conductivity, see Table 4.7 for method comparison. Overall effectiveness  $\gamma$ CMC was shown to be in the region of ~35-40 mN/m and varied very little across the surfactants when headgroup was changed. C<sub>8</sub> surface active ILs (**432**, **435**, **438**) appeared to have the largest  $\gamma$ CMC with a reduction in effectiveness observed as alkyl chain length is increased. The effective range for the surface active ILs examined was determined to be typical for long chain cationic surfactants and displayed a larger effective range than traditional linear alkyl pyridinium surfactants.  $\gamma$ CMC was comparable to the C<sub>6</sub>-C<sub>10</sub> ester functionalised pyridinium ILs synthesised and characterised by Pérez *et al.* Table 4.6.<sup>8</sup>



**Table 4.6.** Comparison of surface tension properties of new pyridinium surfactants to those reported in the literature.

IL	Surfactant	$\gamma$ CMC (mN/m)	pC <sub>20</sub>	Area Per Molecule nm <sup>2</sup>	Reference
<b>Linear Alkyl Pyridinium</b>					
<b>394</b>	C <sub>10</sub> H <sub>21</sub>	32	1.9	-	3, 9
<b>396</b>	C <sub>12</sub> H <sub>25</sub>	35	2.3	0.5	3, 9
<b>398</b>	C <sub>14</sub> H <sub>29</sub>	31	2.9	0.6	3, 9
<b>Alkyl Ester Pyridinium</b>					
<b>402</b>	C <sub>6</sub> H <sub>13</sub>	38	1.6	0.9	8
<b>403</b>	C <sub>8</sub> H <sub>17</sub>	39	2.1	0.7	8
<b>404</b>	C <sub>10</sub> H <sub>21</sub>	41	2.7	0.7	8
<b>405</b>	C <sub>12</sub> H <sub>25</sub>	43	3.5	0.6	8
<b>406</b>	C <sub>14</sub> H <sub>29</sub>	48	4.0	0.4	8
<b>Alkyl Amide Pyridinium</b>					
<b>407</b>	C <sub>6</sub> H <sub>13</sub>	-	-	-	
<b>408</b>	C <sub>8</sub> H <sub>17</sub>	42	1.8	-	11
<b>409</b>	C <sub>10</sub> H <sub>21</sub>	45	2.8	-	11
<b>410</b>	C <sub>12</sub> H <sub>25</sub>	37	3.6	-	11
<b>411</b>	C <sub>14</sub> H <sub>29</sub>	36	4.1	-	11
<b>New Pyridinium Amino Acid ILs</b>					
<b>432</b>	C <sub>8</sub> H <sub>17</sub>	41	3.6	1.1	n/a
<b>433</b>	C <sub>10</sub> H <sub>21</sub>	37	4.5	1.1	n/a
<b>434</b>	C <sub>12</sub> H <sub>25</sub>	36	5.3	1.6	n/a

The pC<sub>20</sub>, or efficiency parameter, was observed to increase as alkyl chain length increased as less surfactant was required to reduce the surface tension by 20 mN/m. This may be due to the increase in negative free energy of adsorption at the air/water interface for the additional methylene groups present as the chain length increases.<sup>8</sup> The amino acid surfactant ILs reported here had a greater efficiency than any of the reported linear alkyl or ester functionalised pyridinium examples (Table 4.6). Unfortunately no  $\gamma$ CMC or pC<sub>20</sub> data was available in the literature for C<sub>6</sub>H<sub>13</sub> or C<sub>16</sub>H<sub>33</sub> alkyl pyridinium bromide surfactants. Area per molecule for the

surfactants was determined and is presented in nm<sup>2</sup>. Area per molecule was determined to be >1 nm<sup>2</sup> for each surfactant analysed, a larger area than that observed for the linear alkyl/amide examples from the literature, Table 4.6. This larger area can be attributed to the bulky amino acid that links the headgroup to the alkyl chain.

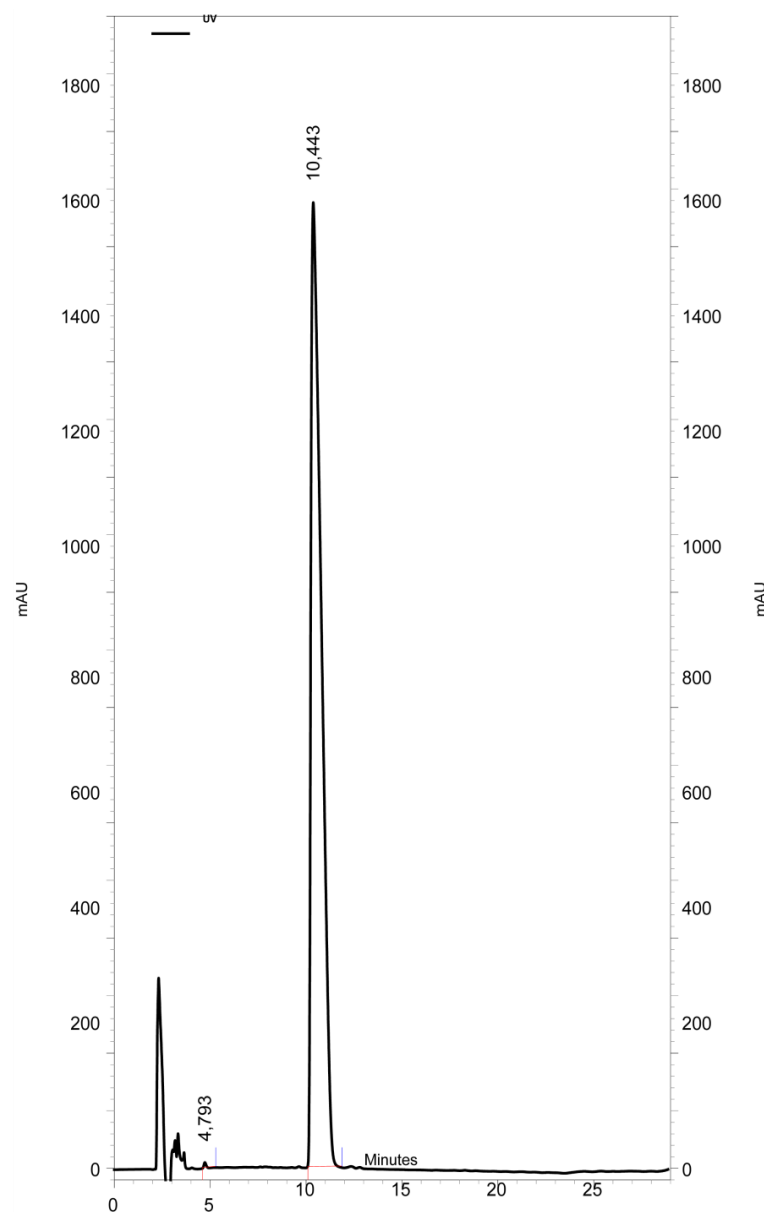
**Table 4.7.** Comparison of CMC by conductivity and by tensiometry.

IL	Headgroup	Chain Length	CMC	CMC
			Tensiometry (mM)	Conductivity (mM)
<b>432</b>	Pyridinium	8	3.00	4.00
<b>433</b>	Pyridinium	10	0.70	1.30
<b>434</b>	Pyridinium	12	0.15	0.20
<b>435</b>	Imidazolium	8	2.50	3.70
<b>436</b>	Imidazolium	10	1.50	1.70
<b>437</b>	Imidazolium	12	0.25	0.22
<b>438</b>	Cholinium	8	2.00	4.00
<b>439</b>	Cholinium	10	1.70	1.50
<b>440</b>	Cholinium	12	0.20	0.36

As can be seen from Table 4.7, the CMC was also determined by tensiometry and confirms the validity of the results observed by conductivity. There are many more methods that could be used to determine the CMC, some of the most popular include fluorescence spectroscopy<sup>11</sup>, <sup>1</sup>H and <sup>23</sup>Na NMR experiments<sup>18</sup> and dynamic light scattering (DLS).<sup>18</sup>

### 4.3.3 HPLC Models

The purity of all of the surfactants was determined by HPLC/UV to ensure >98% purity by the method outlined in Chapter 5, Section 5.10.5.



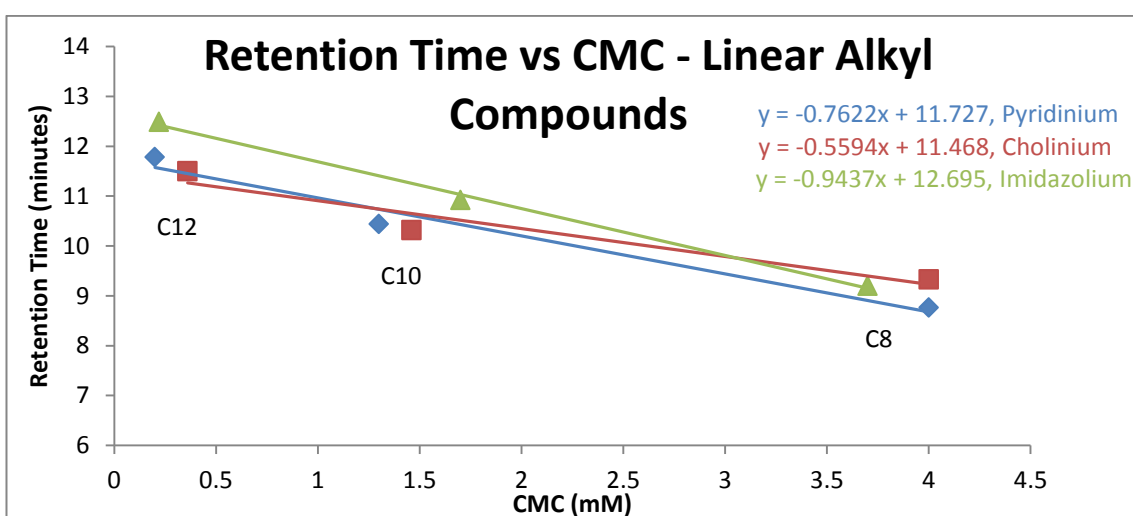
**Figure 4.7.** HPLC/UV trace for IL C<sub>10</sub> Pyridinium IL (**433**).

Retention Time Minutes	Area mAU	Area %	Height	Height %
4.79	358179	0,14	40979	0,61
10.44	251752507	99,86	6700948	99,39

**Table 4.8.** HPLC/UV retention time results.

Analysis of the surfactant by HPLC/UV showed that all of the linear alkyl ILs synthesised had a purity of greater than >98%.

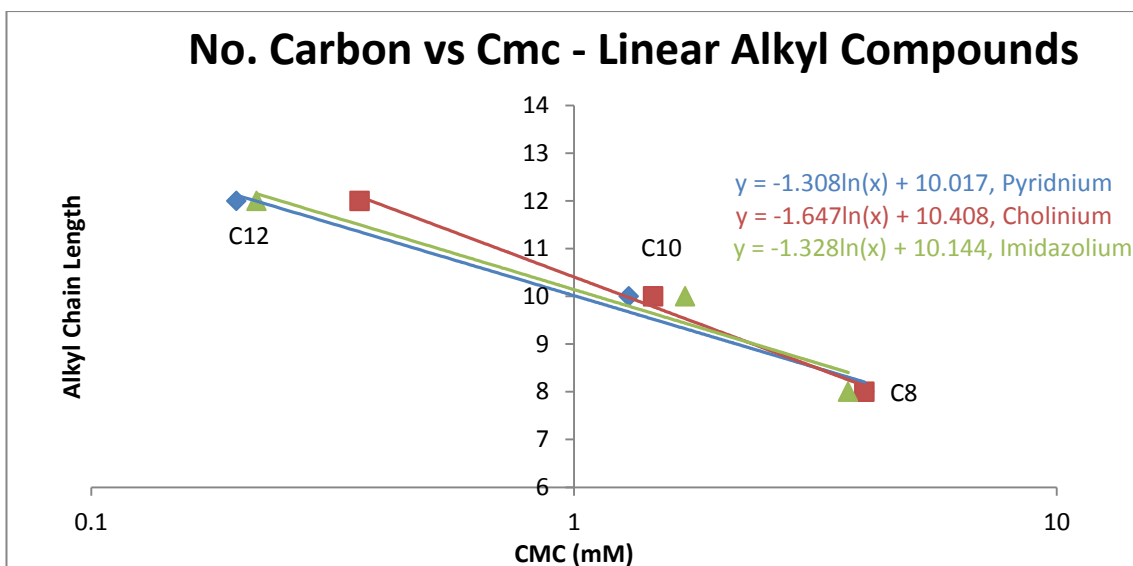
From the HPLC/UV analysis it was also possible to construct a model based on retention time and CMC. With an increase in lipophilicity there is also a subsequent increase in retention time as a  $C_{18}$  column was employed as the stationary phase. An increase in lipophilicity results in a decrease in CMC until solubility limits are reached. Therefore the retention time can be described as proportional to the CMC and a linear relationship was observed when retention time was plotted against CMC (Figure 4.8). Retention time, in the literature, has also be used to estimate the log octanol-water partition coefficients (logP) for surfactants in conjunction with the traditional shake-flask method (the shake-flask method itself is unsuitable due to the amphiphilic nature of surfactants).<sup>19</sup> Furthermore the interconnected relationships between logP and toxicity have also been reported.<sup>20</sup>



**Figure 4.8.** Retention time vs CMC for linear alkyl surfactants (432-440) examined by conductivity.

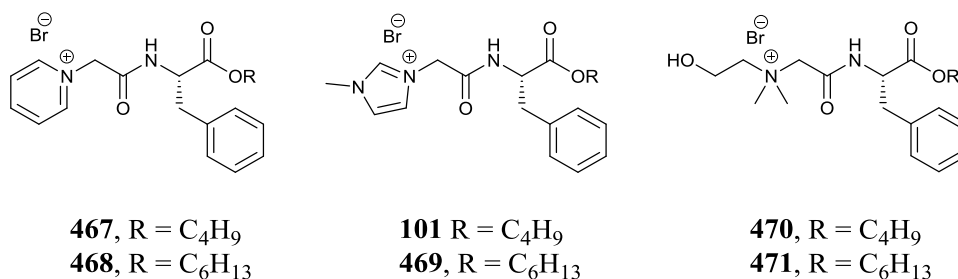
Figure 4.8 represents the HPLC retention time model developed for approximating the CMC of the surfactants examined. If further surfactants were developed with different alkyl chain lengths in this series then the HPLC retention time values could be used to extrapolate an approximate CMC value.

Figure 4.9 is a further development of the idea behind the HPLC model and represents another method in determining the approximate CMC of any further surfactants that could be developed from the linear alkyl series so far examined. The benefit of these models is that CMC can be “tailored” with a specific target CMC in mind. Both relationships presented will give an estimated figure in conjunction with the Stauff-Klevensequequation  $\log \text{CMC} = A - Bn$  described in Section 4.3.1.



**Figure 4.9.** No of Carbon atoms in the linear alkyl chain vs CMC (conductivity).

If a further series of C<sub>4</sub> and C<sub>6</sub> surfactants (Figure 4.10) were synthesised then the CMC values may be predicted using the Stauff-Klevens equation.



**Figure 4.10.** Potential C<sub>4</sub> and C<sub>6</sub> surfactants (**101**, **467-471**).

For pyridinium ILs, literature values of  $A = 1.72$  and  $B = 0.31$  were used.<sup>16</sup>

For imidazolium ILs, literature values of  $A = 1.78$  and  $B = 0.32$  were used.<sup>15</sup>

For cholinium ILs, literature values of  $A = 1.96$  and  $B = 0.30$  were used.<sup>15</sup>

Using the Stauff-Klevens rule, the predicted values for future C<sub>4</sub> and C<sub>6</sub> linear alkyl surfactants were calculated. When the predicted values were compared to the CMC values calculated from the equations of the line in Figure 4.9, a general disagreement between the values was observed, see Table 4.9. This discrepancy suggests that the literature values for  $A$  and  $B$  employed in the Stauff-Klevens equation used to predict the C<sub>4</sub> and C<sub>6</sub> surfactant's CMCs are not appropriate. While the  $A$  and  $B$  values previously used for longer chain pyridinium ILs in Section 4.3.1 may have given good correlations, any error associated with these values has been amplified by the larger CMC values predicted. New  $A$  and  $B$  values are therefore proposed for all three series of

amino acid ILs based on linear regressions plotted in Figure 4.9. It should be stated that the column in Table 4.9 entitled “Predicted CMC Carbon Count From Figure 4.9” is a derivation of the Stauff-Klevens rule and can be rewritten as follows to provide new *A* and *B* values according to Figure 4.9.

**Table 4.9.** Predicted CMC values for C<sub>4</sub> and C<sub>6</sub> surfactants.

<b>IL</b>	<b>Headgroup</b>	<b>Chain Length</b>	<b>Predicted CMC (mM) log(CMC) = <i>A</i> – <i>Bn</i></b>	<b>Predicted CMC From Figure 4.9</b>
<b>467</b>	Pyridinium	4	85.11	99.49
<b>468</b>	Pyridinium	6	20.41	21.56
<b>101</b>	Imidazolium	4	79.43	102.16
<b>469</b>	Imidazolium	6	18.19	22.65
<b>470</b>	Cholinium	4	181.97	48.94
<b>471</b>	Cholinium	6	45.71	14.53

Pyridinium:  $y = -1.308\ln(x) + 10.017 \rightarrow \text{Log(CMC)} = 3.326 - 0.332(y)$ . *A* = 3.326, *B* = 0.332

Imidazolium:  $y = -1.328\ln(x) + 10.144 \rightarrow \text{Log(CMC)} = 3.368 - 0.332(y)$ . *A* = 3.368, *B* = 0.332

Cholinium:  $y = -1.647\ln(x) + 10.408 \rightarrow \text{Log(CMC)} = 2.744 - 0.264(y)$ . *A* = 2.744, *B* = 0.264

Substituting the newly calculated *A* and *B* values, the following predicted CMC values are presented, Table 4.10.

With the newly calculated *A* and *B* values, there is a much better correlation between predicted values and observed CMC values, Table 4.10. Imidazolium C<sub>8</sub> and C<sub>10</sub> ILs (**435**, **436**) are the least accurately described of the series of ILs using this equation.

**Table 4.10.** Comparison of actual CMC and predicted CMC values using linear regression from Figure 4.9.

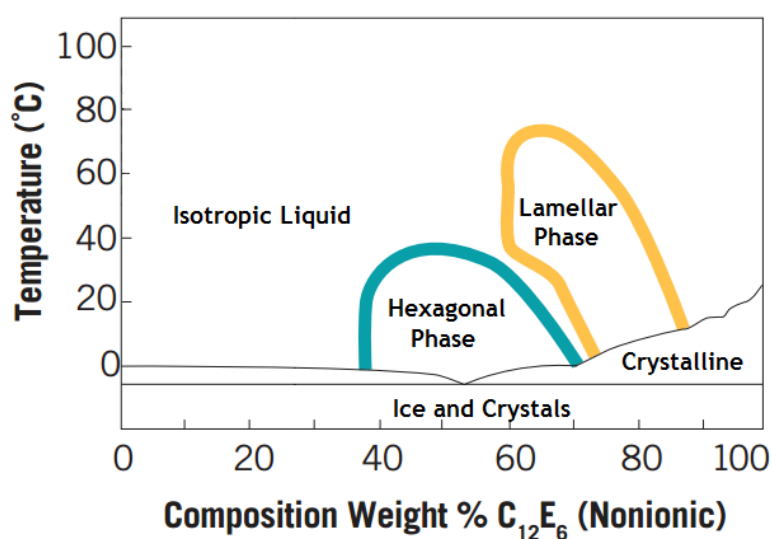
IL	Headgroup	Chain Length	Predicted CMC (mM)*	Actual CMC (mM)(conductimetry)
<b>434</b>	Pyridinium	12	0.22	0.20
<b>433</b>	Pyridinium	10	1.01	1.30
<b>432</b>	Pyridinium	8	4.67	4.00
<b>468</b>	Pyridinium	6	21.57	-
<b>467</b>	Pyridinium	4	99.54	-
<b>437</b>	Imidazolium	12	0.24	0.22
<b>436</b>	Imidazolium	10	1.12	1.70
<b>435</b>	Imidazolium	8	5.15	3.70
<b>469</b>	Imidazolium	6	18.19	-
<b>101</b>	Imidazolium	4	79.43	-
<b>440</b>	Cholinium	12	0.38	0.36
<b>439</b>	Cholinium	10	1.27	1.50
<b>438</b>	Cholinium	8	4.29	4.00
<b>471</b>	Cholinium	6	45.71	-
<b>470</b>	Cholinium	4	181.97	-

\* Calculated using  $\log(\text{CMC}) = A - Bn$ .

#### 4.3.4 Optical Microscopy

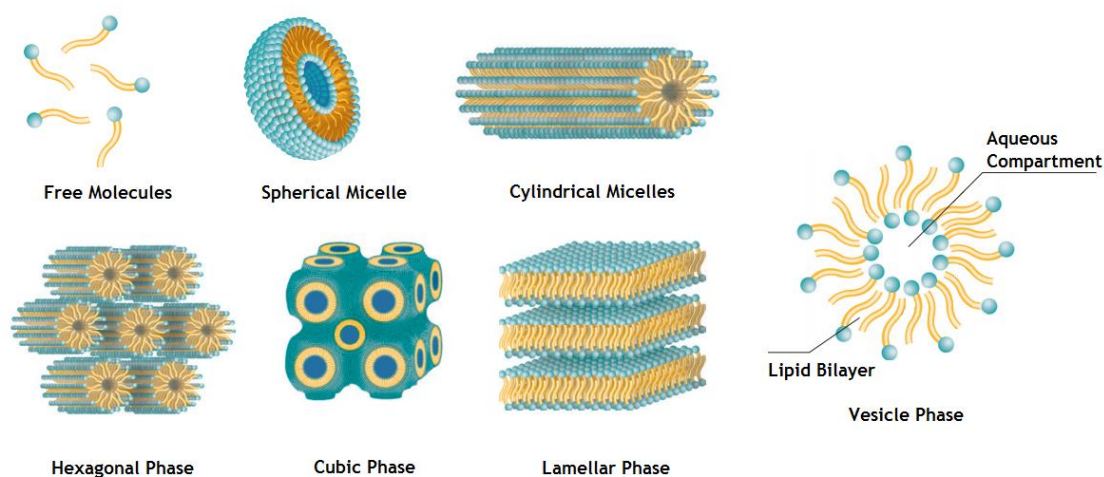
The IL surfactants (**432-434**, **437**, **440**) were analysed by polarised light optical microscopy to study their phase behaviour. It is possible to study the qualitative phase behaviour of binary water/surfactants mixtures as a function of temperature by optical microscopy according to the “flooding” (penetration) method of Lawrence described in Chapter 5, Section 5.10.4. In this

experiment, a drop of water was added onto anhydrous surfactant between a glass slide and a cover slip. Gradually different compositions of liquid crystals are produced and different separated mesophases develop.<sup>21</sup> These mesophases are lyotropic i.e. they are determined by interactions with other surfactant molecules in a bulk solvent phase. Mesophases are also anisotropic, i.e. they are structures in which one or more dimensions are highly extended. The use of a heated stage microscope also allowed for qualitative observations of how heat affected the formation and composition of mesophases as thermotropic properties can affect the phase formations. The various properties and mesophases obtainable are depicted in Figure 4.11 as a phase diagram. A number of different liquid crystal phases are depicted in Figure 4.12. The mesophasic liquid crystal behaviour is of particular interest for drug delivery applications as drug molecules can be “loaded” inside a particular mesophase and then delivered to a target.<sup>22</sup> Mesophases are also of interest for biological applications due to some of their similarities to biological membranes.<sup>22</sup>



**Figure 4.11.** Typical phase diagram for a non-ionic poly-ethoxylated surfactant. Adapted from P. Sciences, in *Particle Sciences - Technical Brief*, 2012, vol. 6.<sup>22</sup>



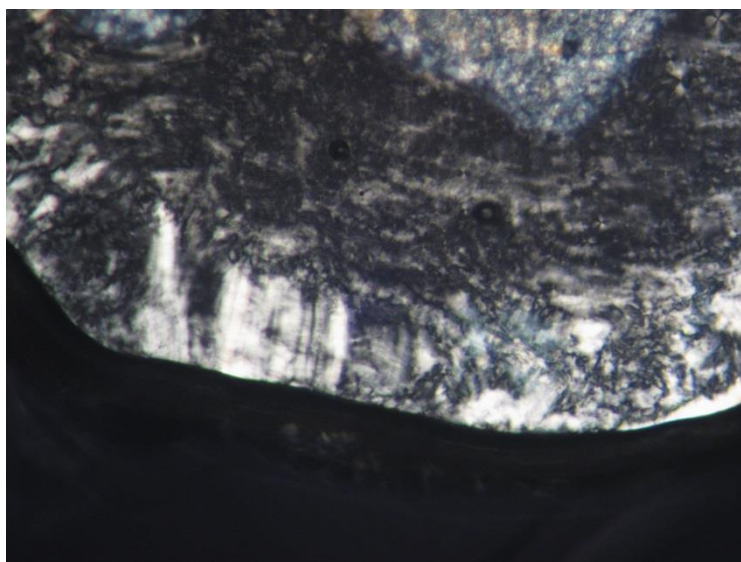


**Figure 4.12.** A selection of phases and mesophases that surfactants can form.

Adapted from P. Sciences, in *Particle Sciences - Technical Brief*, 2012, vol. 6,<sup>22</sup>  
and P. Sciences, in *Particle Sciences - Technical Brief*, 2010, vol. 1.<sup>23</sup>

Hexagonal and lamellar phase liquid crystals are anisotropic, i.e. are not uniform structures in all directions and therefore will scatter polarised light and appear as white areas when viewed.<sup>24</sup> Isotropic structures such as cubic phase crystals appear as black areas when exposed to polarized light but can be identified by exposing them to non-polarised light and comparing the before and after images.

In the following section a number of optical microscopy images captured using the aforementioned flooding/penetration method are presented. The experiments were also carried out over a range of temperatures ranging from 25 °C and 100 °C. A number of linear alkyl surfactants were analysed for their liquid crystal behaviour. The pyridinium C<sub>8</sub>, C<sub>10</sub> and C<sub>12</sub> (**432-434**) were analysed to determine whether chain length greatly affected the liquid crystal behaviour. Imidazolium C<sub>12</sub> (**437**) and cholinium C<sub>12</sub> (**440**) were also examined to determine whether headgroup affected the compositions observed.



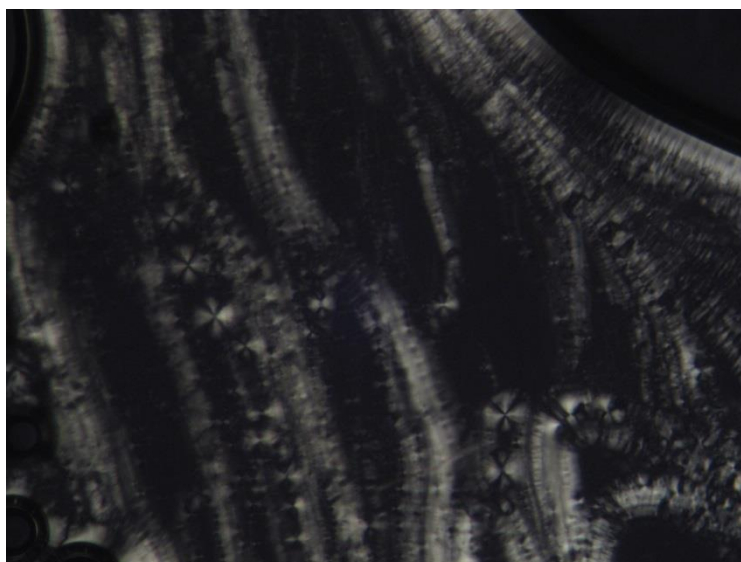
**Figure 4.13.** C<sub>8</sub> Pyr IL (432). 25 °C, x10 magnification

The image shown in Figure 4.13 is the solid hydrated surfactant and is referred to as a mosaic. The black area is the water added slowly diffusing into the surfactant.



**Figure 4.14.** C<sub>8</sub> Pyr IL (432) “Maltese Crosses” visibly forming. 35°C, x10 magnification

The formation of “Maltese crosses” is apparent (Figure 4.14). These crosses are representative of lamellar crystals.<sup>24</sup>



**Figure 4.15.** C<sub>8</sub> Pyr IL (432), Lamellar phase crystals. 35°C, x10 magnification

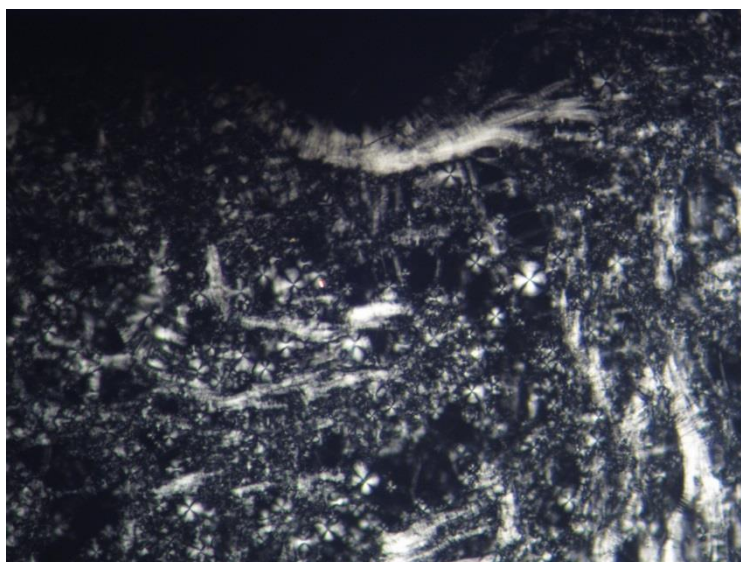
Oily streaks or tendrils are visible (Figure 4.15). These streaks represent lamellar phase liquid crystals.



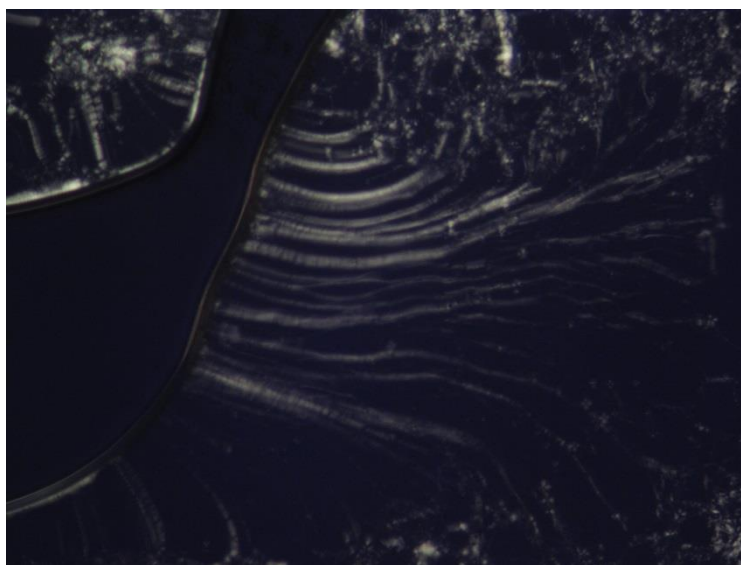
**Figure 4.16.** C<sub>8</sub> Pyr IL (432) Hexagonal phase liquid crystals. 55°C, x10 magnification

The formation of lyotropic hexagonal phase liquid crystals can be observed in the centre of the image (Figure 4.16). The hexagonal phase crystals appear as fans or sheet like structures. Heating from 25 °C to 35 °C to 55 °C shows a change as the phase thermotropically shifts from one mesomorph to another, as depicted by the sample phase diagram in Figure 4.4. After 65 °C solubilisation of (432) occurred rapidly.

The images captured for C<sub>10</sub> Pyridinium were very similar to those observed for C<sub>8</sub>.



**Figure 4.17.**  $C_{10}$  Pyr IL (**433**), an abundance of lamellar phase liquid crystals are visible. 30 °C, x10 magnification.

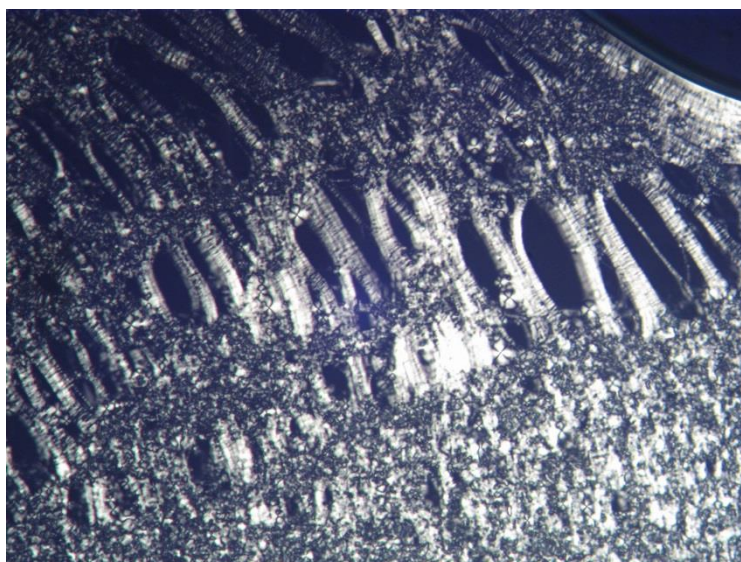


**Figure 4.18.**  $C_{10}$  Pyr IL (**433**), an abundance of lamellar phase liquid crystals are visible. 30 °C, x10 magnification.

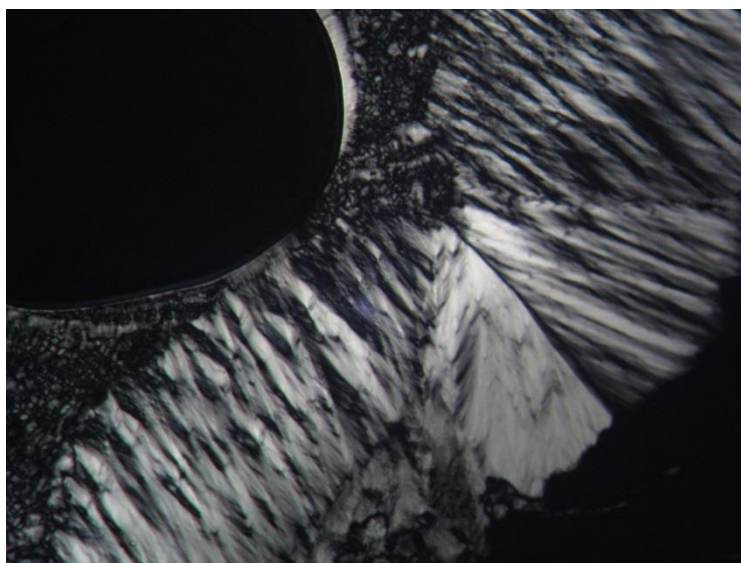
At 30 °C IL (**433**) was observed to be predominately in the lamellar phase as can be seen in Figures 4.17 and 4.18. No hexagonal phase liquid crystals were observed however for (**433**).

Upon extension of the alkyl chain length to  $C_{12}$ , the surfactant (**434**) was observed under the same experimental conditions, Figure 4.19.



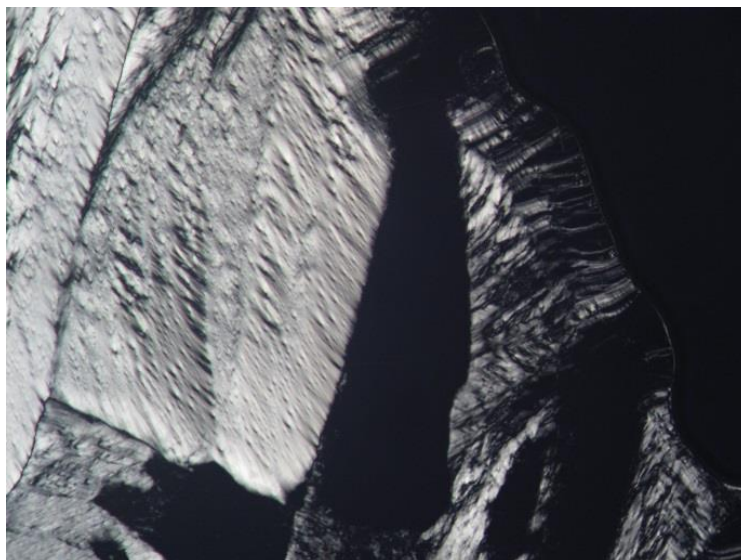


**Figure 4.19.** C<sub>12</sub> Pyr IL (434), lamellar phase crystals visible as streaks and Maltese crosses. 45 °C, x10 magnification.

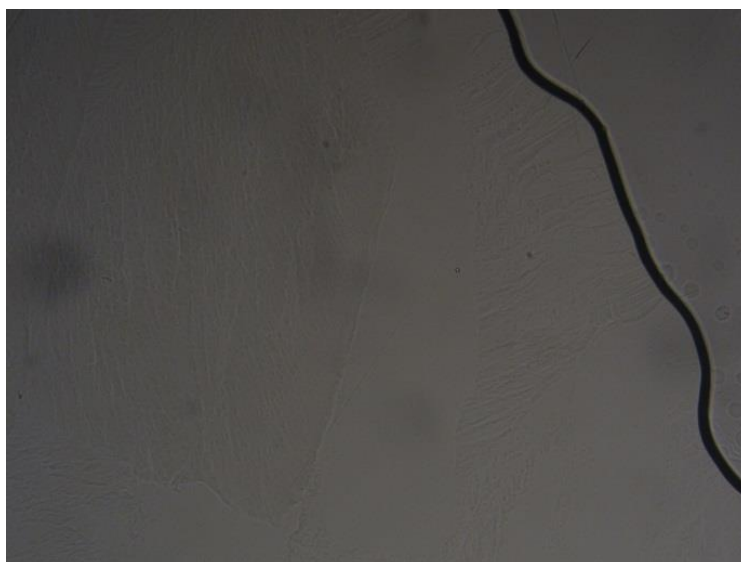


**Figure 4.20.** C<sub>12</sub> Pyr IL (434) Hexagonal phase liquid crystals. 70 °C, x10 magnification.

When the temperature was increased to 70 °C the formation of hexagonal phase liquid crystals occurred as can be seen from the image captured (Figure 4.20).



**Figure 4.21.** C<sub>12</sub>Pyr IL (434). Cubic liquid crystals observed under a polarised light source

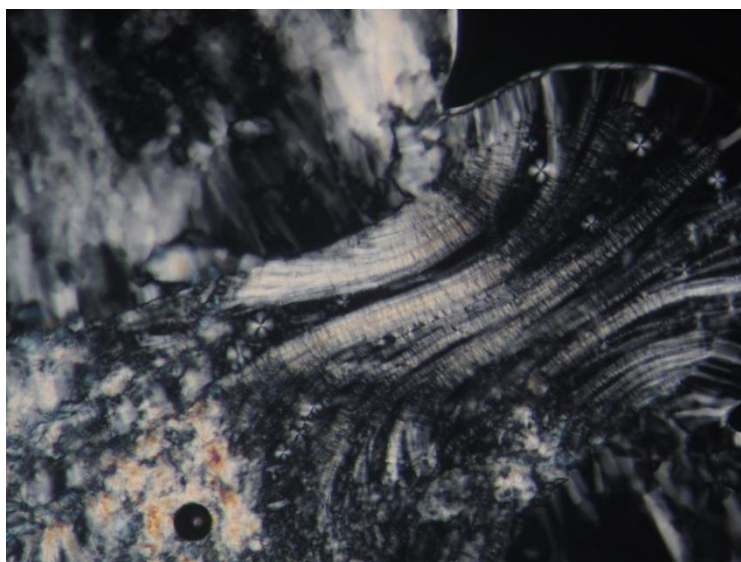


**Figure 4.22.** The same frame as Figure 4.21, cubic phase observed under non-polarised light

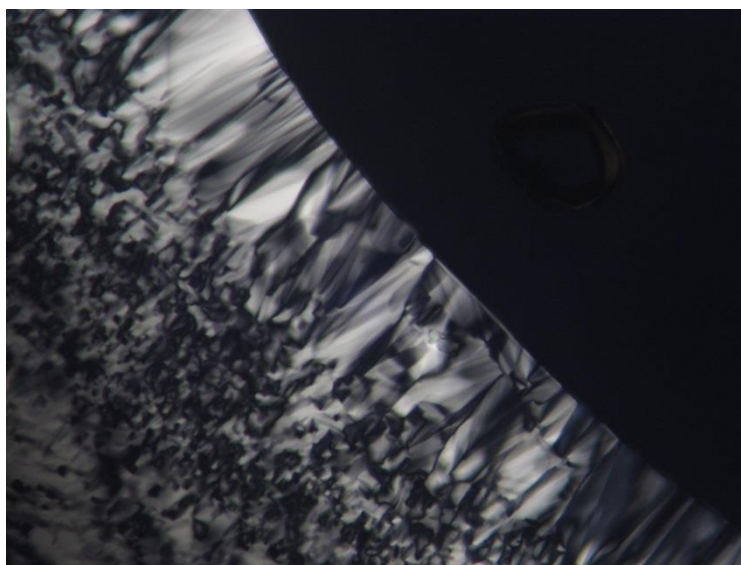
Both images are observed at 90 °C, x10 magnification.

The dark area in the centre of the image (Figure 4.21) represents cubic liquid crystals. Confirmation that they are indeed isotropic comes when the light shone through the microscope is switched to a non-polarised source (Figure 4.22). The dark area appears as white along with the rest of the hexagonal phase crystals present.

When the headgroup was altered from a pyridinium to an imidazolium or cholinium similar structures were observed to form readily. Alkyl chains were maintained at C<sub>12</sub>.

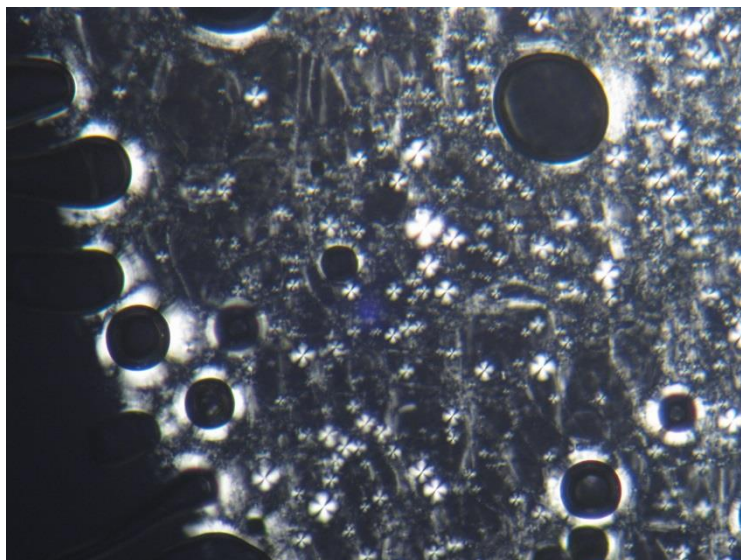


**Figure 4.23.** Lamellar phase liquid crystals observed for imidazolium C<sub>12</sub> IL (**437**). 40 °C, x10 magnification.

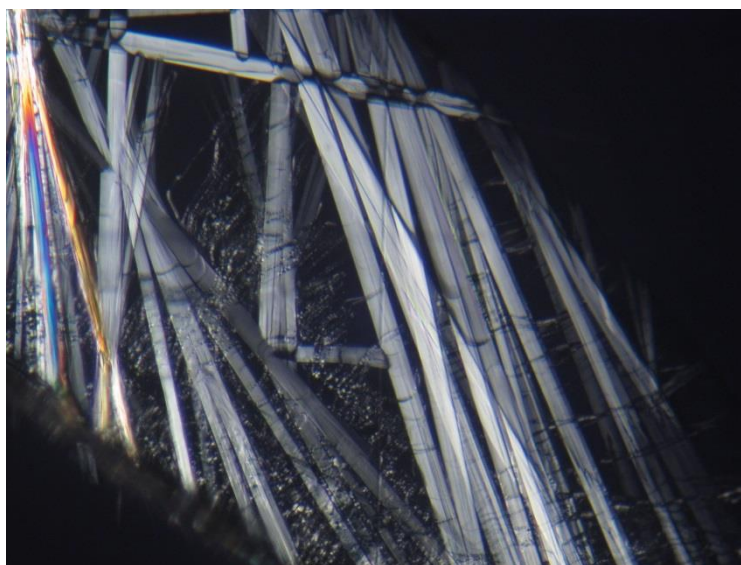


**Figure 4.24.** Hexagonal phase liquid crystals observed for IL (**437**). 60 °C, x10 magnification.





**Figure 4.25.** A forest of Maltese crosses observed for  $C_{12}$  imidazolium IL (**437**).70 °C, x10 magnification.

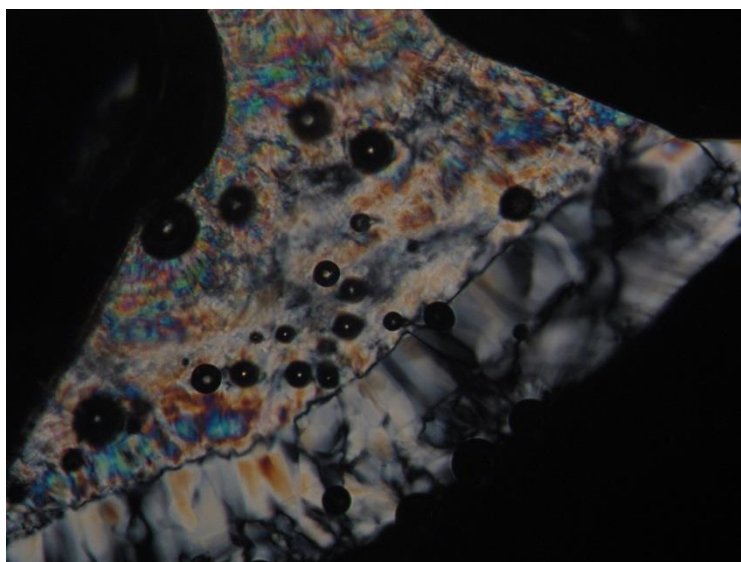


**Figure 4.26.** Needles growing upon cooling back to room temperature.

When imidazolium  $C_{12}$  IL (**437**) was cooled back to room temperature, thin needles of crystals were observed to rapidly form (Figure 4.26).

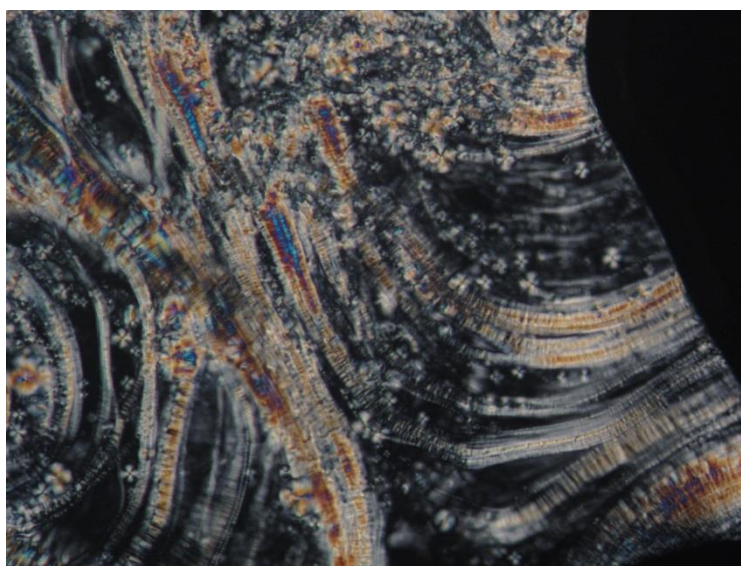
When the headgroup was switched to cholinium the following set of images were captured.



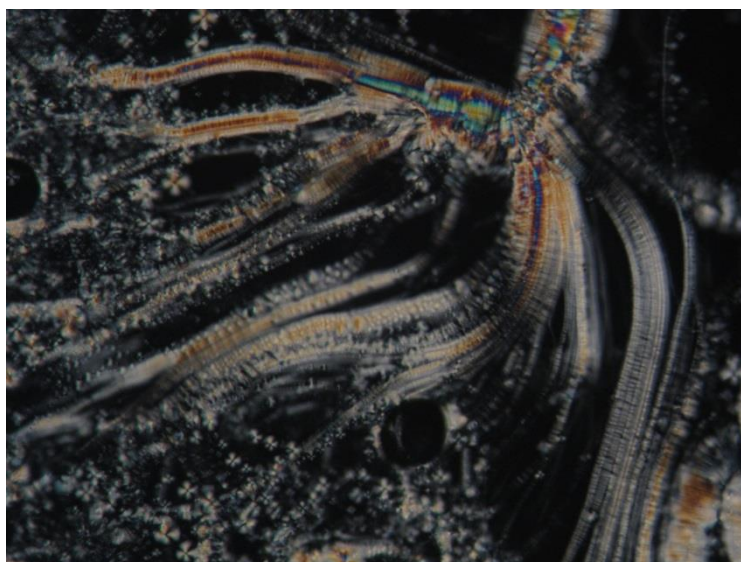


**Figure 4.27.** Cholinium C<sub>12</sub> (440), mosaic and hexagonal phase 20 °C, x10 magnification.

A rough textured and colourful mosaic can be observed (Figure 4.27). This mosaic is hydrated solid surfactant. On the lower half of the image grey hexagonal phase crystals can be seen expanding and encroaching on the bulk of the hydrated solid.



**Figure 4.28.** Lamellar phase liquid crystals observed for C<sub>12</sub> cholinium IL (440). 60 °C, x10 magnification.



**Figure 4.29.** Lamellar phase liquid crystals observed for C<sub>12</sub> cholinium IL (440). 60 °C, x10 magnification.

It was noted that the formation of lamellar phase liquid crystals did not occur at lower temperatures for C<sub>12</sub> cholinium IL (**440**) and only became apparent >50 °C. Overall it can be noted that to fully identify and determine the nature of the liquid crystals, and the surfactants tendency to form lyotropic or thermotropic liquid crystals, additional investigations would be required. Differential scanning calorimetry (DSC) would enable the identification of the phase transitions. Investigations solely into the thermotropic properties could also be conducted using dry surfactant and not adding water so as to observe the liquid crystal properties solely attributable to temperature change.<sup>25, 26</sup>

#### 4.3.5 Aqueous stability measurements

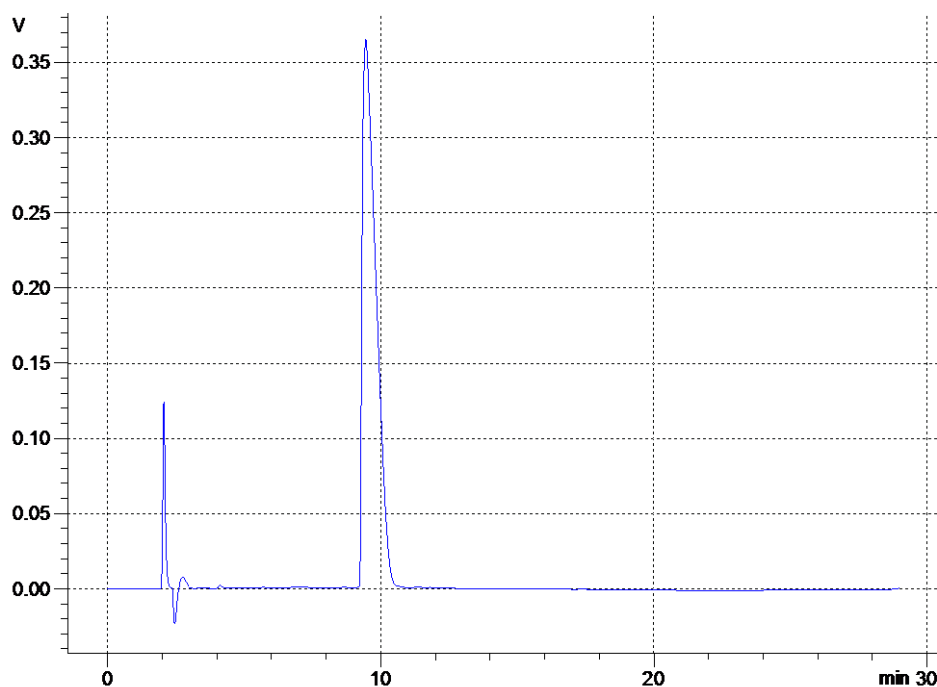
Qualitative aqueous hydrolysis of a number of surfactant IL samples (**433**, **436**, **439**) were measured over a one week period at 50 °C and repeated at pH 2 and pH 10, both at 25 °C. The aim of this study was to determine the onset of degradation and is a preliminary study into the overall stability of the ILs examined. HPLC/UV traces for each measurement are available in Appendix II.

##### 4.3.5.1 Hydrolysis study, pH 7, 50 °C

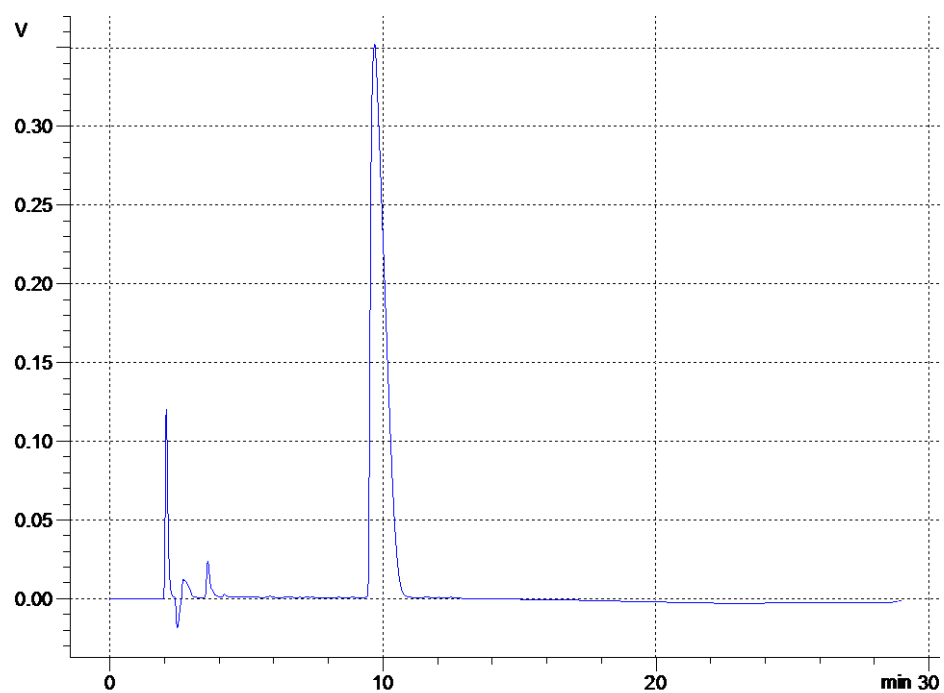
The results of the stability study show that hydrolysis was observed at 24 hours for each compound examined with the presence of a new product peak eluting at 3-4 minutes.

An example trace collected for the HPLC/UV analysis is displayed in Figure 4.30 and 4.31. The traces show pyridinium C<sub>10</sub> (**433**) at t = 0 h and t = 168 h and the appearance of degradation peaks due to hydrolysis. A UV visible hydrolysis product elutes much more rapidly than the parent product suggesting that the hydrolysis product is more polar than the parent compound. If

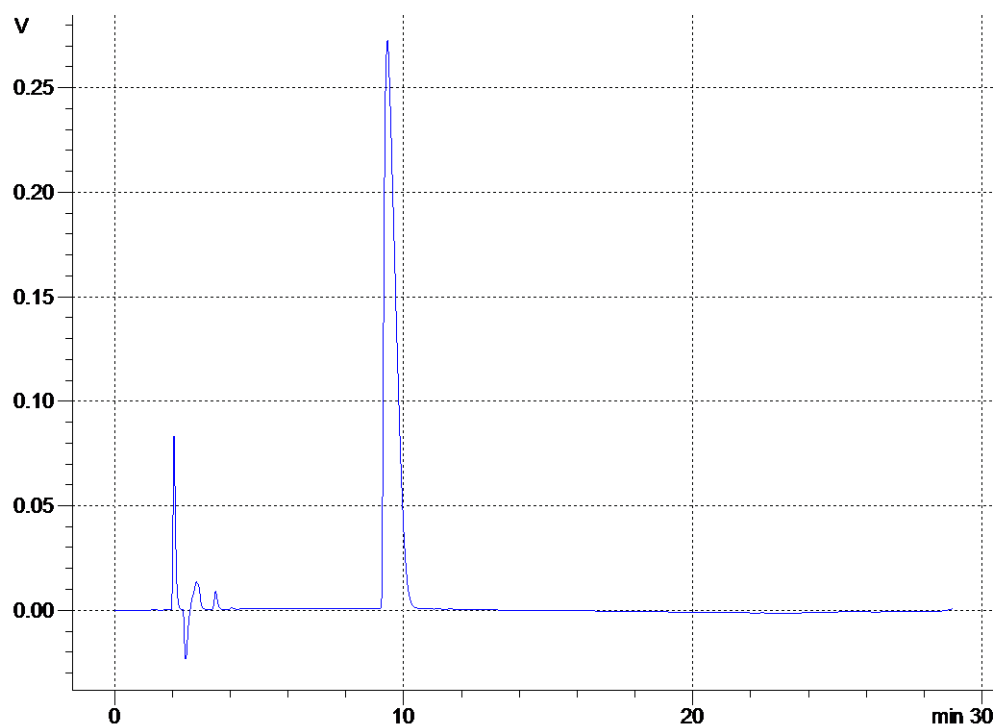
the ester functionality of the molecule is hydrolysed then the resultant amino acid carboxylic acid ionic liquid would indeed be far more polar than the parent compound. Amide hydrolysis would also produce a highly polar IL product. To confirm the hydrolysis pathway would require an MS study or isolation of the hydrolysed product and was not within the scope of this investigation. Similar HPLC/UV traces were prepared for C<sub>10</sub> imidazolium (**436**) (Figures 4.32-4.34) and C<sub>10</sub> cholinium (**439**) (Figures 4.35-4.36). Imidazole C<sub>10</sub> is observed undergoing hydrolysis at t = 24 h with a peak observed eluting at 3-4 minutes (Figure 4.33). The rapid onset for imidazolium degradation may be due to the inherent Brønsted acidity associated with imidazolium ILs.<sup>27-29</sup> For the cholinium IL (**439**), a shoulder to the main peak can be observed occurring at 168 hours after the hydrolysis experiment began (Figure 4.36).



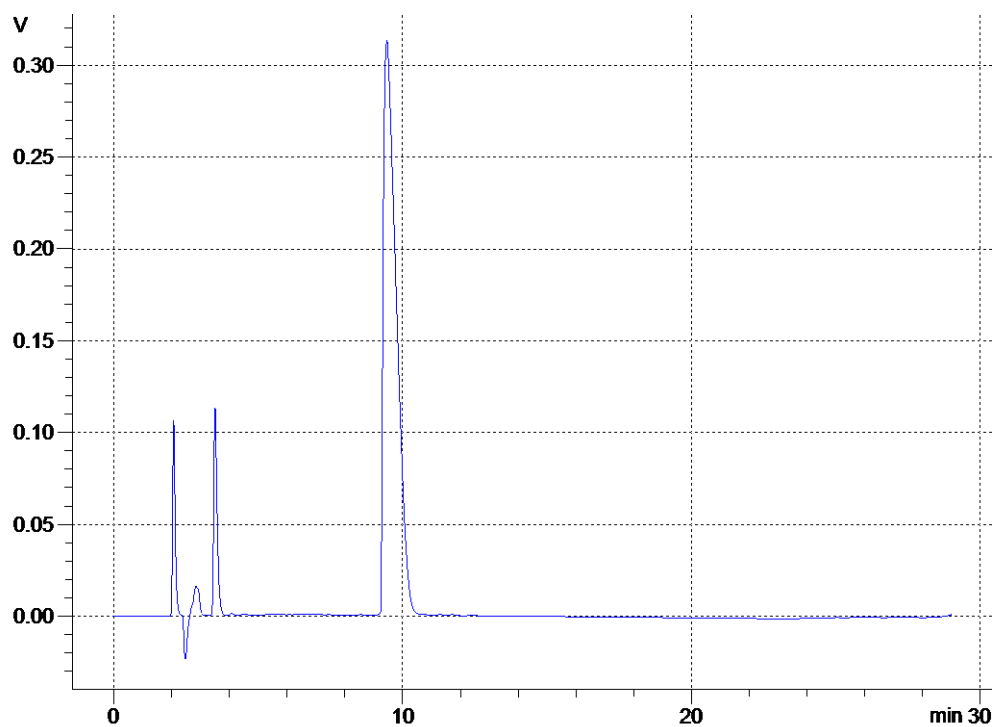
**Figure 4.30.** Pyridinium C<sub>10</sub> (**433**) concentration = 2.5 mM, pH = 7, 50°C, at t = 0 h.



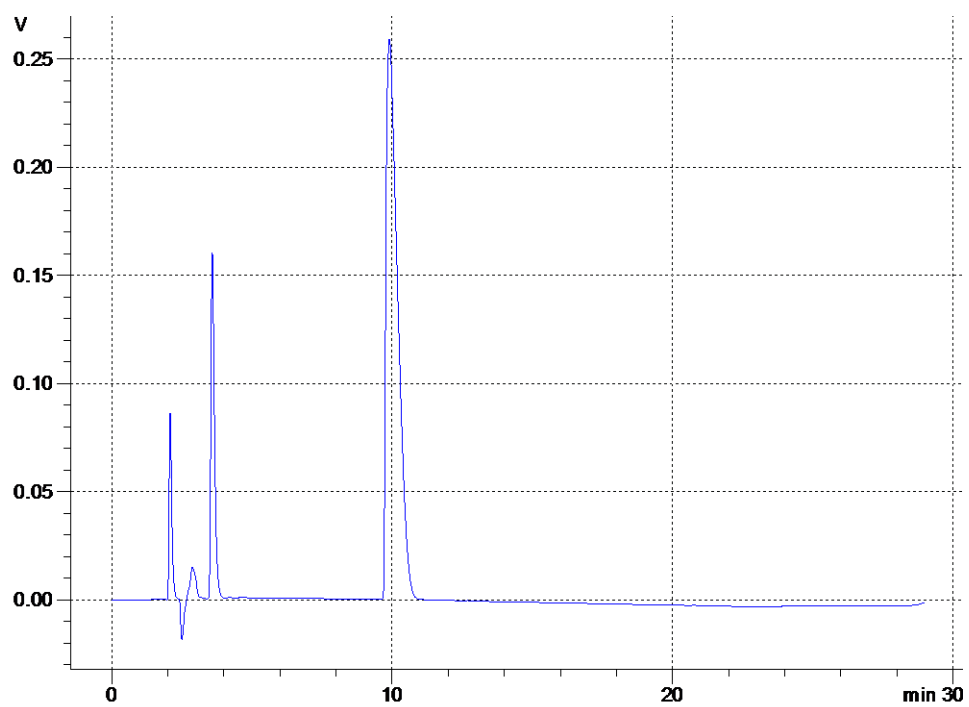
**Figure 4.31.** Pyridinium C<sub>10</sub> (**433**), pH = 7, 50°C, t = 168 h.



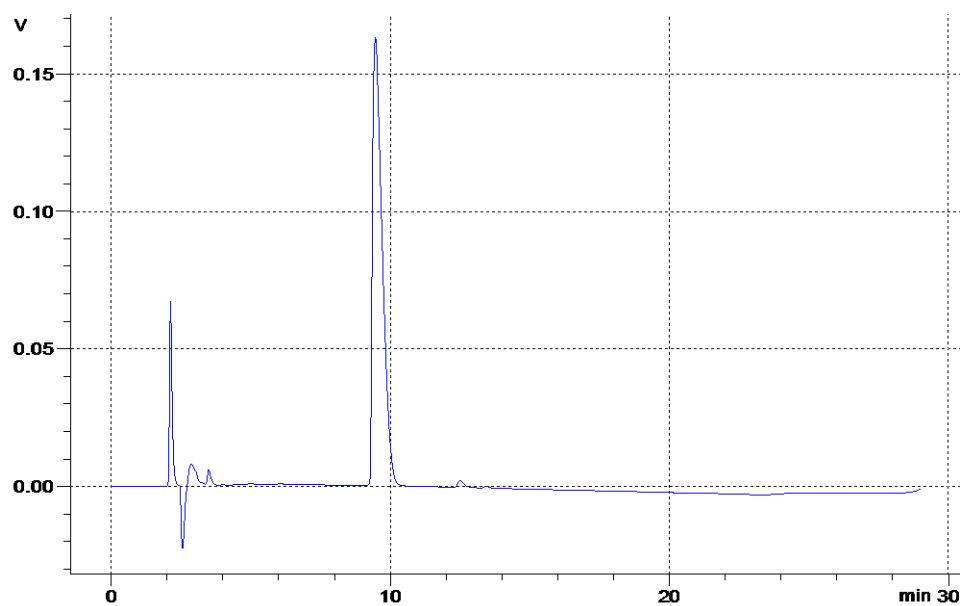
**Figure 4.32.** Imidazole C<sub>10</sub> (**436**), concentration = 2.5 mM, pH = 7, 50°C, t = 0 h. Parent peak eluting at 9.5 minutes



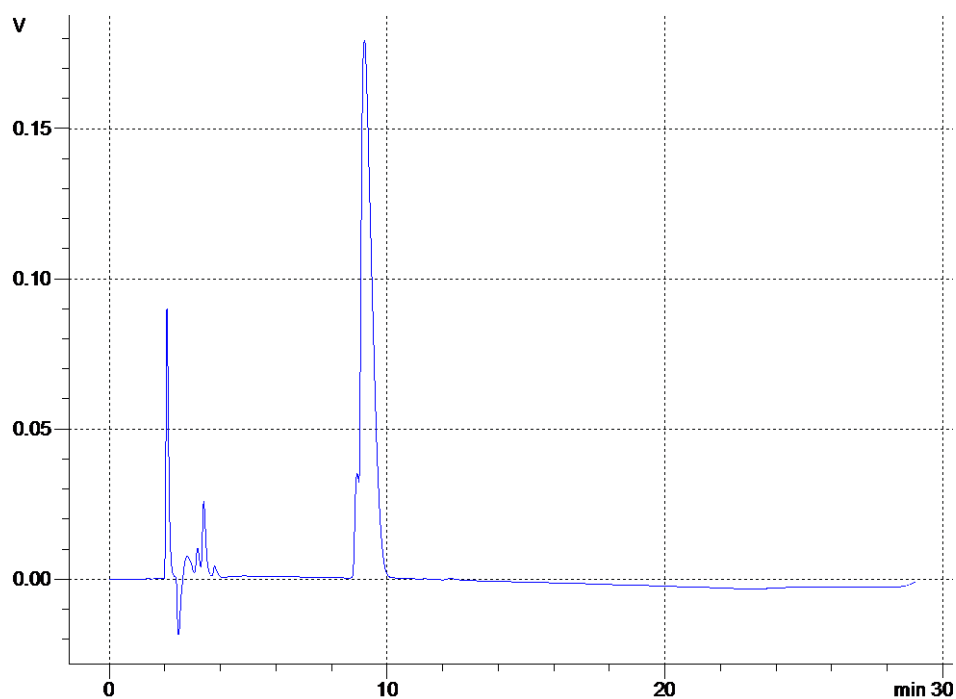
**Figure 4.33.** Imidazole C<sub>10</sub> (**436**), pH = 7, 50°C, t = 24 h. Parent peak eluting at 9.5 minutes.  
Hydrolysis product eluting at 3.5 minutes.



**Figure 4.34.** Imidazole C<sub>10</sub> (**436**), pH = 7, 50°C, t = 168 h.



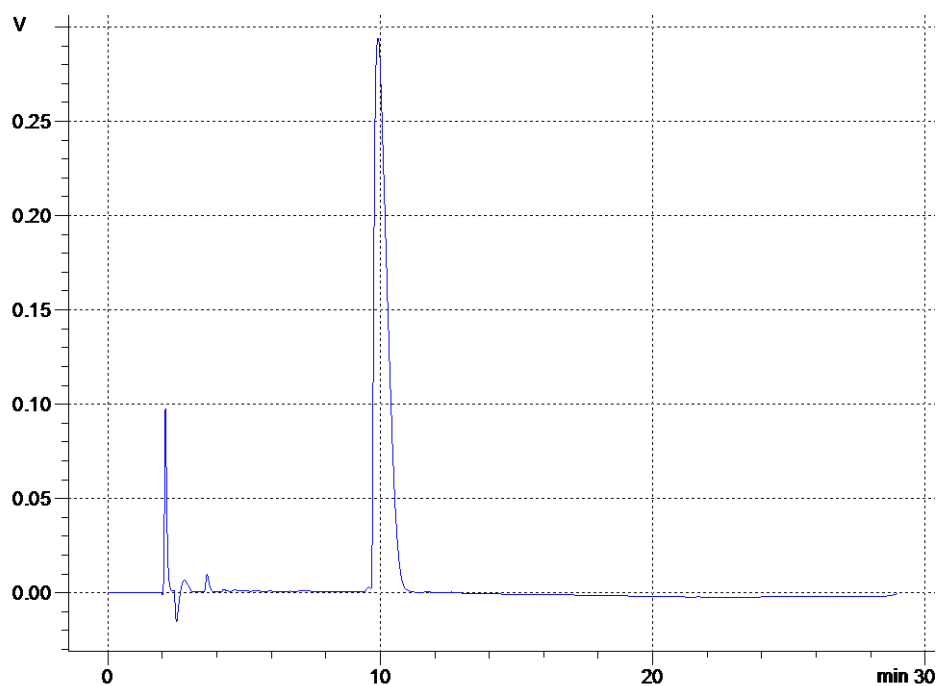
**Figure 4.35.** HPLC/UV trace of cholinium C<sub>10</sub> (**439**), concentration 2.5 mM, 50°C pH = 7, t = 0 h.



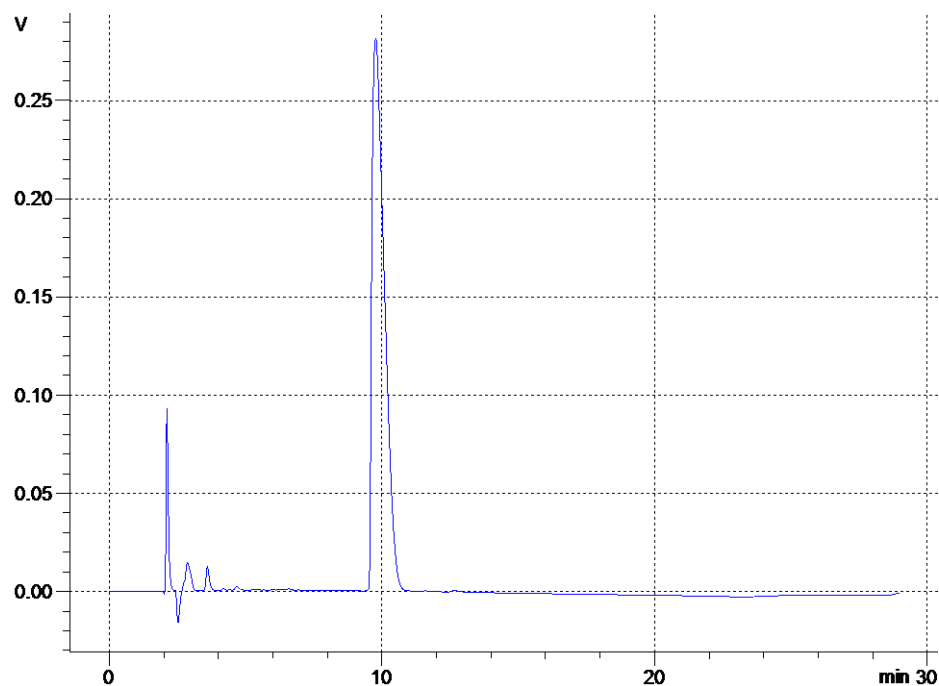
**Figure 4.36.** HPLC/UV trace of cholinium C<sub>10</sub> (**439**), 50°C pH = 7, t = 168 h displaying shoulder to main peak and rapidly eluting hydrolysis product at 3-5 minutes.

#### 4.3.5.2 Acid hydrolysis study, pH 2, 25 °C

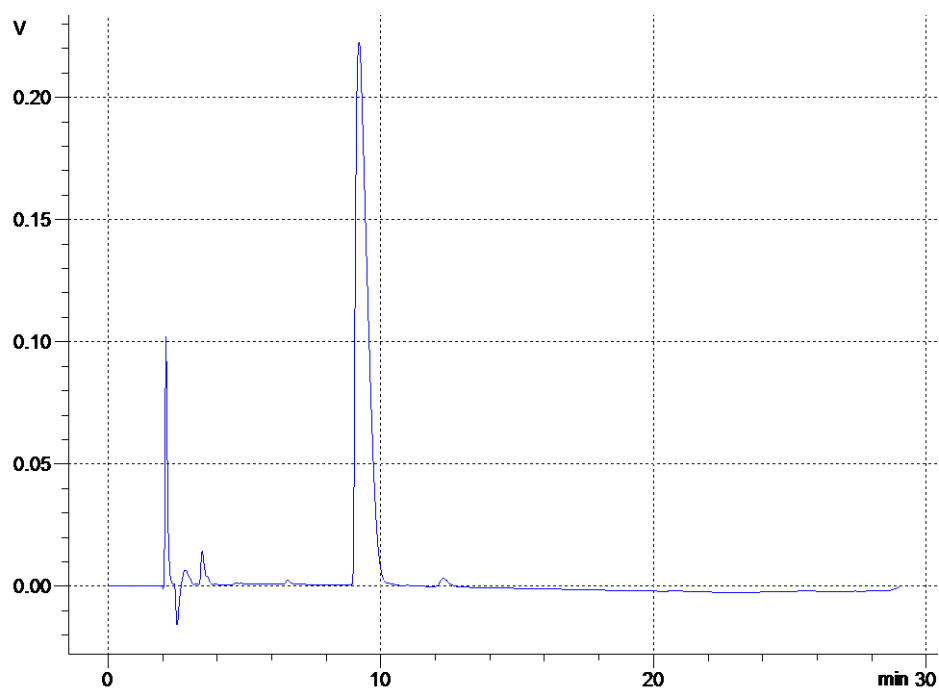
The stability study was repeated at 25 °C and the pH was altered to 2. The aim was to assess the acidic stability of the surfactant molecules in aqueous media. Overall from the HPLC traces provided (Figures 4.37-4.39), there appears to be acid hydrolysis occurring for all 3 ILs examined, however the peak eluting at 3-5 minutes is much smaller than that observed for the pH 7, 50 °C conditions previously described. Tentatively, it may appear that the ILs have a characteristic resistance to acid hydrolysis as the presence of sharp peaks eluting at 3-5 minutes were not detected until 168 hours and even then the peaks detected were far smaller than those present at pH7, 50 °C . A quantitative examination of the degradation is proposed for future work.



**Figure 4.37.** Pyridinium C<sub>10</sub> (433) at pH 2, concentration 2.5 mM, 25°C, t = 168 h.



**Figure 4.38.** Imidazolium C<sub>10</sub> (436) at pH2, initial concentration 2.5 mM, 25°C, t = 168 h.



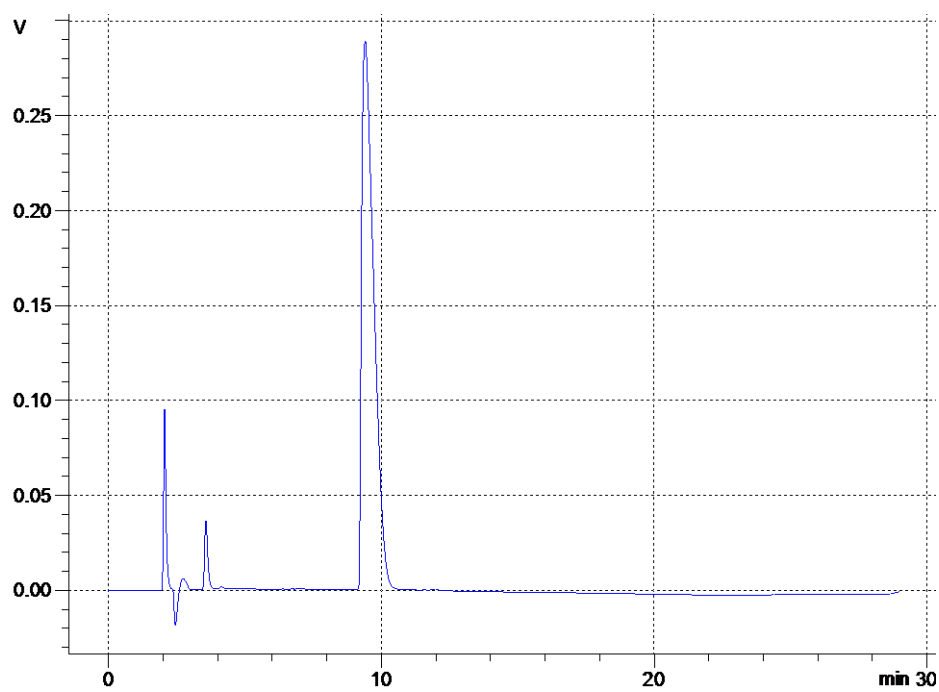
**Figure 4.39.** Cholinium C<sub>10</sub> (439) at pH2, initial concentration 2.5 mM, 25°C, t = 168 h.

#### 4.3.5.3 Base hydrolysis study, pH 10, 25 °C

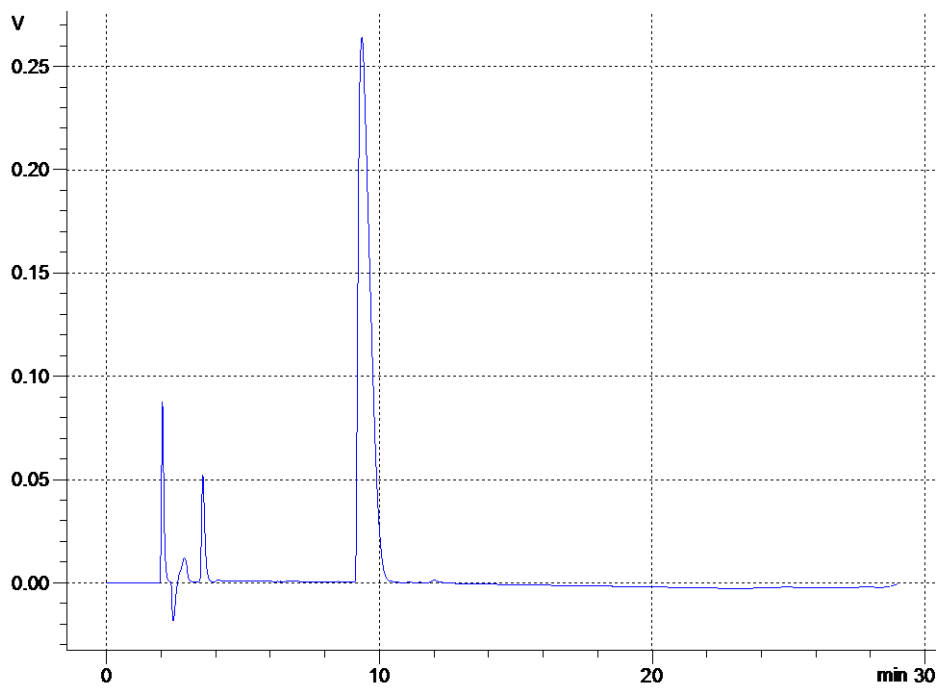
For the samples run at pH 10, higher levels of hydrolysis were observed after the 7 day period. The onset for alkaline hydrolysis was observed at t = 24 hours. Overall the ILs appear to be more susceptible to alkaline hydrolysis as can be seen from Figures 4.40-4.42. The



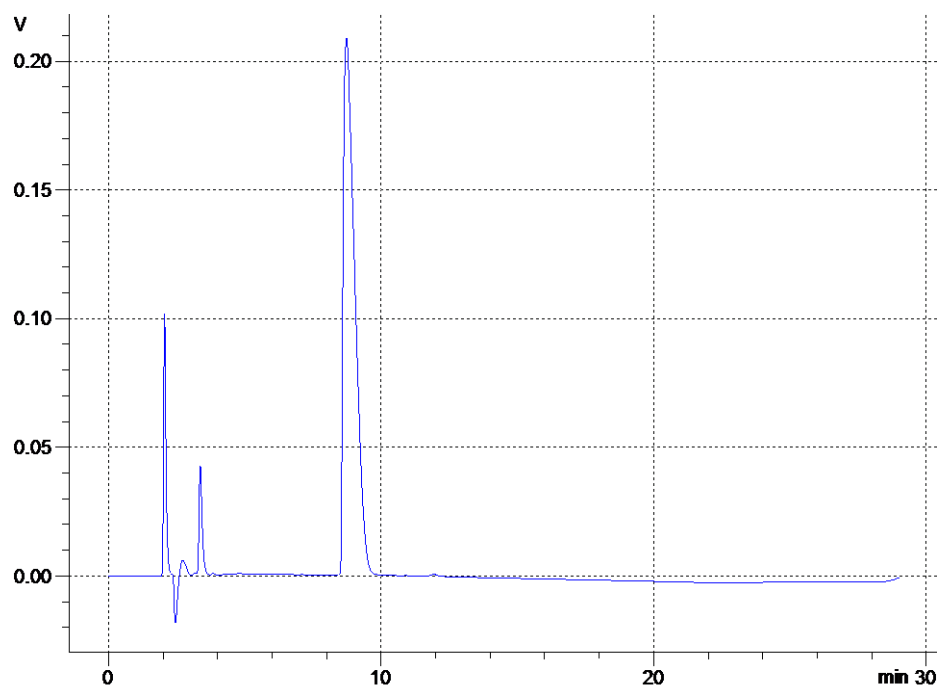
susceptibility of the amide and ester to hydrolysis also appears to occur more rapidly than that observed for acidic conditions.



**Figure 4.40.** Pyridinium C<sub>10</sub> (**433**) at pH 10, initial concentration 2.5 mM, 25°C, t = 24 h.



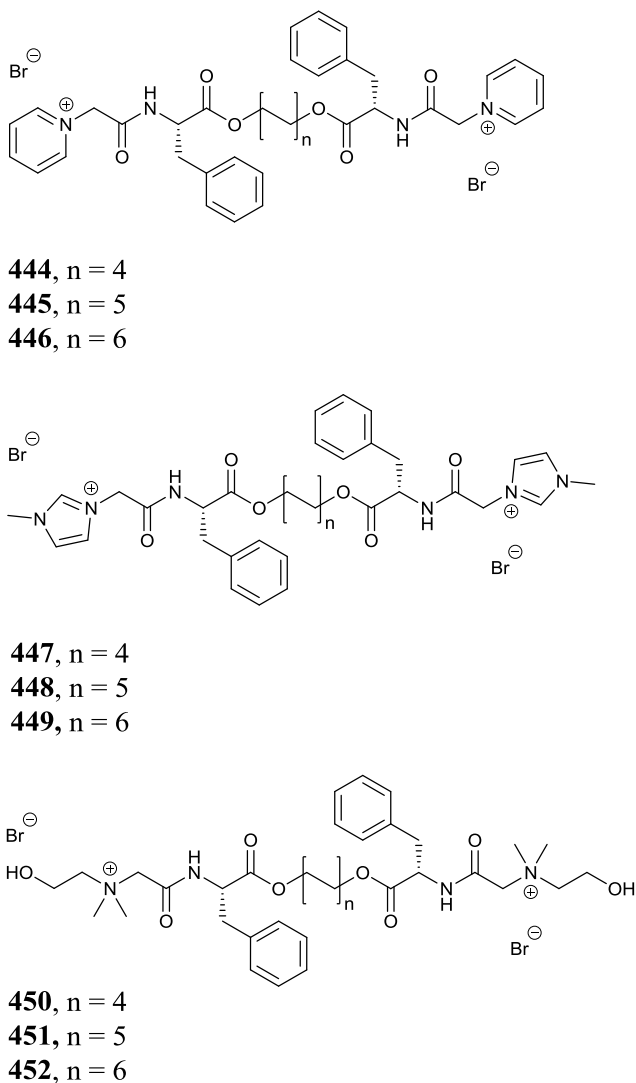
**Figure 4.41.** Imidazolium C<sub>10</sub> (**436**) at pH 10, initial concentration 2.5 mM, 25°C, t = 24 h.



**Figure 4.42.** Cholinium C<sub>10</sub> (**439**) at pH10, initial concentration 2.5 mM, 25°C, t = 24 h.

#### 4.4 Self-Aggregation and physico-chemical properties of bolaform L-phenylalanine ILs (444-452).

The aggregation properties of the bolaform L-phenylalanine IL surfactants (**444-452**) (Figure 4.43), were determined by conductivity and tensiometry experiments. Results of these experiments are summarised in Tables 4.11 and 4.12 respectively.



**Figure 4.43.** Bolaform ILs (**444- 452**) examined for their surfactant properties.

##### 4.4.1 Conductivity measurements

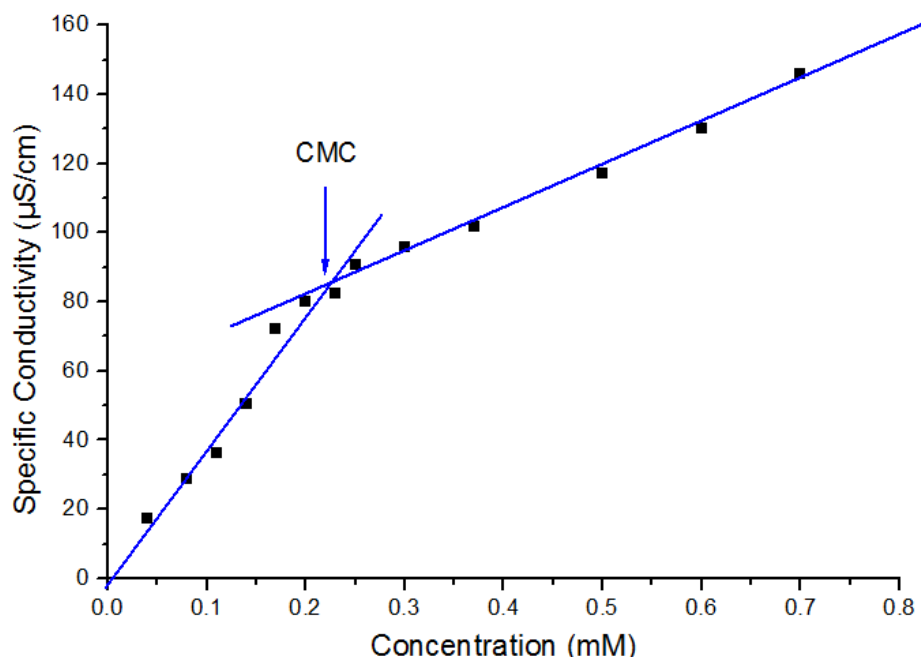
As per section 4.3.1 the change in specific conductivity of the bolaform ILs in aqueous media with respect to concentration was measured.

**Table 4.11.** Results obtained by conductimetry for bolaform ILs (**444-452**).

<b>IL</b>	<b>Headgroup</b>	<b>Spacer Length</b>	<b>CMC mM</b>	<b><math>\alpha</math></b>	<b><math>\beta</math></b>	<b><math>\Delta G_{\text{mic}}^{\circ}</math> (kJ/mol)</b>
<b>444</b>	Pyridinium	8	2.00	0.68	0.32	-33.34
<b>445</b>	Pyridinium	10	0.70	0.71	0.29	-15.62
<b>446</b>	Pyridinium	12	0.20	0.31	0.69	-24.01
<b>447</b>	Imidazolium	8	2.00	0.72	0.28	-32.35
<b>448</b>	Imidazolium	10	0.75	0.77	0.23	-13.62
<b>449</b>	Imidazolium	12	0.27	0.52	0.48	-20.00
<b>450</b>	Cholinium	8	2.50	0.71	0.29	-31.89
<b>451</b>	Cholinium	10	0.60	0.81	0.19	-14.67
<b>452</b>	Cholinium	12	0.27	0.74	0.26	-17.06

From the results shown in Table 4.11 it can be seen that the CMC values for the bolaform compounds decrease as the spacer length that joins each headgroup is increased in length. CMC values overall are approximately twice as low as their linear alkyl surfactant counterparts previously described in 4.3.1. This lower CMC was not expected and goes against the trends observed in the literature that suggest that a bolaform surfactant will have a CMC twice as large as that observed for a linear alkyl surfactant of the same carbon count (in the hydrophobic region).

Counterion binding  $\beta$  is in general much lower than the values observed for the linear alkyl surfactants and there is a proportional increase in the degree of ionisation  $\alpha$ .  $\Delta G_{\text{mic}}^{\circ}$  calculated was also generally lower ~20-30 kJ/mol than the linear alkyl surfactants and this represents a much less energetically favourable micellisation process occurring, most likely due to the repulsion forces present between the two cationic headgroups and other surfactant molecules in solution. The lowest  $\Delta G_{\text{mic}}^{\circ}$  observed were for the 8 carbon spacer bolaform surfactants.



**Figure 4.44.** CMC as determined by conductimetry for  $C_{12}$  linked pyridinium bolaform (**446**).

The  $C_8$  bolaform ILs (**444**, **447**, **450**) have a CMC ~half as large as their linear alkyl counterparts (**432**, **435**, **438**). For the  $C_{10}$  bolaform ILs (**445**, **448**, **450**) the trend continues. However when the  $C_{12}$  bolaform surfactants (**446**, **449**, **452**) are compared to their linear alkyl counterparts (**434**, **437**, **440**) a similar CMC is observed (0.20 mM-0.36 mM), Table 4.12. When compared to linear alkyl examples previously reported in the literature (and presented in Section 4.3.1) the bolaform surfactants here with a  $C_8$  spacer have the equivalent CMC values as a  $C_{14}$ - $C_{15}$  linear alkyl pyridinium surfactant.<sup>10</sup>  $C_{10}$  spacer bolaform ILs are equivalent to ~ $C_{16}$  linear alkyl surfactants<sup>10</sup> and the  $C_{12}$  are equivalent to ~ $C_{18}$ .<sup>17</sup> As per the new linear alkyl amino acid surfactants reported in Section 4.3.1 the carbon count and lipophilicity of the phenylalanine sidechain must be accounted for. If the relationship presented by Rosen (previously discussed in section 4.3.1.)<sup>3</sup> is applied then a  $C_8$  bolaform with two phenyl groups  $((8 + (2 \times 3.5)))$  would count as a ~15 carbon surfactant and indeed this is the relationship observed and can justify the CMC values that are lower than expected.

**Table 4.12.** Comparison of CMC for bolaform and linear alkyl ILs.

Headgroup	Linear Alkyl IL	Chain Length	CMC (mM)	Bolaform IL	Spacer Length	CMC (mM)
Pyridinium	<b>432</b>	8	4.00	<b>444</b>	8	2.00
Pyridinium	<b>433</b>	10	1.30	<b>445</b>	10	0.70
Pyridinium	<b>434</b>	12	0.20	<b>446</b>	12	0.20
Imidazolium	<b>435</b>	8	3.70	<b>447</b>	8	2.00
Imidazolium	<b>436</b>	10	1.70	<b>448</b>	10	0.75
Imidazolium	<b>437</b>	12	0.22	<b>449</b>	12	0.27
Cholinium	<b>438</b>	8	4.00	<b>450</b>	8	2.50
Cholinium	<b>439</b>	10	1.50	<b>451</b>	10	0.60
Cholinium	<b>440</b>	12	0.36	<b>452</b>	12	0.27

#### 4.4.2 Tensiometry measurements

As per section 4.3.2 the surface tension properties were examined by tensiometry for the bolaform ILs synthesised. It was unknown before the surface tension was examined as to whether the carbon spacers chosen would be long enough to give a reasonable reduction in surface tension and whether the bolaform ILs would adopt a flat conformation at the air water interface, a wicket conformation, or would they just dissolve in the aqueous phase. Investigation into the surface activity of the bolaform ILs (**444-452**) provided typical surface tension plots such as that depicted in Figure 4.44. All of the surface tension plots are available in Appendix II.

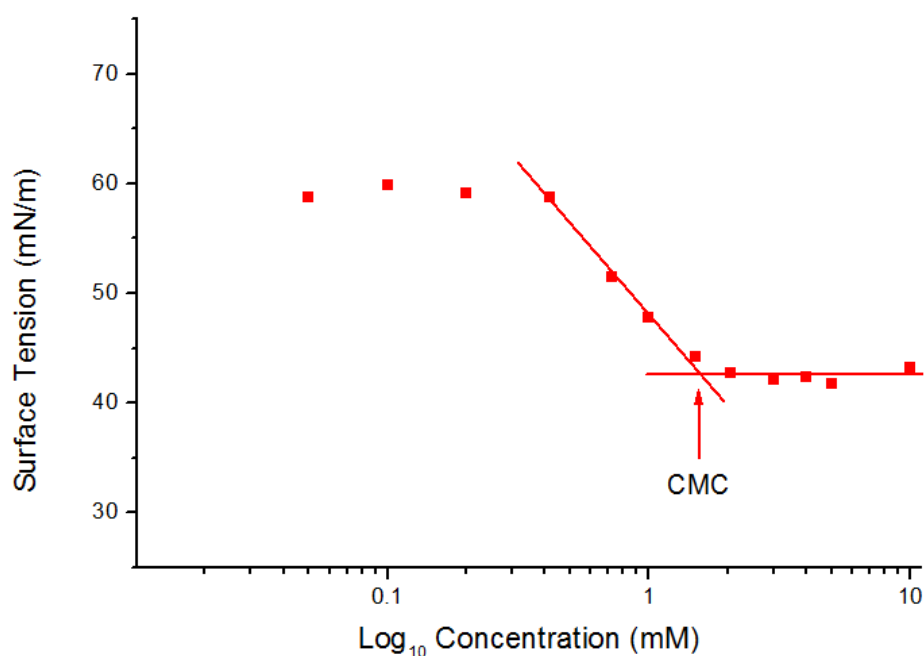
**Table 4.13.** Tensiometry results obtained for bolaform ILs.

IL	Headgroup	Spacer Length	CMC (mM)	$\gamma$ CMC (mN/m)	C <sub>20</sub> (mM)	PC <sub>20</sub>	Area per molecule $\text{\AA}^2 / \text{nm}^2$
<b>444</b>	Pyridinium	8	2.00	29.08	8.50E-04	3.07	81.50/ 0.81
<b>445</b>	Pyridinium	10	0.70	23.91	1.20E-04	3.92	297.26/ 2.97
<b>446</b>	Pyridinium	12	0.60	25.34	7.20E-05	4.14	286.80 / 2.87
<b>447</b>	Imidazolium	8	1.50	29.42	4.60E-04	3.34	81.10/ 0.81
<b>448</b>	Imidazolium	10	0.75	23.90	1.10E-04	3.96	216.90/ 2.17
<b>449</b>	Imidazolium	12	0.60	24.12	2.80E-04	3.55	150.40/ 1.50
<b>450</b>	Cholinium	8	-	-	-	-	-
<b>451</b>	Cholinium	10	2.75	33.98	4.97E-04	3.30	118.95/ 1.19
<b>452</b>	Cholinium	12	0.40	23.79	2.60E-04	3.59	166.83/ 1.67

From the results presented in Table 4.13, it can be seen that again a decrease in CMC is observed as the alkyl chain length increases, as expected. When it comes to the effectiveness, the  $\gamma$ CMC is far worse than the linear alkyl derivatives. Where the pyridinium C<sub>8</sub> linear alkyl derivative (**432**) was able to reduce the surface tension by ~41 mN/m, the bolaform C<sub>8</sub> pyridinium (**444**) was only able to reduce the surface tension by 29 mN/m. As the spacer length was increased from C<sub>8</sub> to C<sub>10</sub>-C<sub>12</sub> a large drop off in the effectiveness was also observed going generally from 30 to ~24-25 mN/m. Bolaform C<sub>8</sub> cholinium derivative (**450**) did not display appreciable surface active properties and the tensiometry plot is depicted in Figure 4.46. Efficiency or PC<sub>20</sub> for the bolaform surfactants was lower than the linear alkyl derivatives; C<sub>8</sub> bolaform ILs all had calculated PC<sub>20</sub> of ~3-3.30 whereas a linear alkyl C<sub>8</sub> had 3.59-3.96. As the

bolaform spacer was increased the efficiency was seen to increase to ~4. On comparison, the C<sub>12</sub> linear alkyl amino acid surfactants all reached an efficiency rating of ~5.

The area per molecule for the bolaform surfactants generally exceeds that observed for the linear alkyl examples. This is due to the orientation of the bolaform surfactant at the air water interface. For the C<sub>10</sub> bolaform compounds, large values suggest that the surfactant is lying flat across the surface, but when the spacer length is increased to 12, the chain is pushed into the air to a certain degree, lowering the surface area that the surfactant occupies. Much smaller values are observed for the C<sub>8</sub> linked bolaform surfactants. Values of 0.81 nm<sup>2</sup> are observed and suggest a completely different orientation of the C<sub>8</sub> surfactants (similar to that of the linear alkyl derivatives) than that observed for the C<sub>10</sub> and C<sub>12</sub> examples.

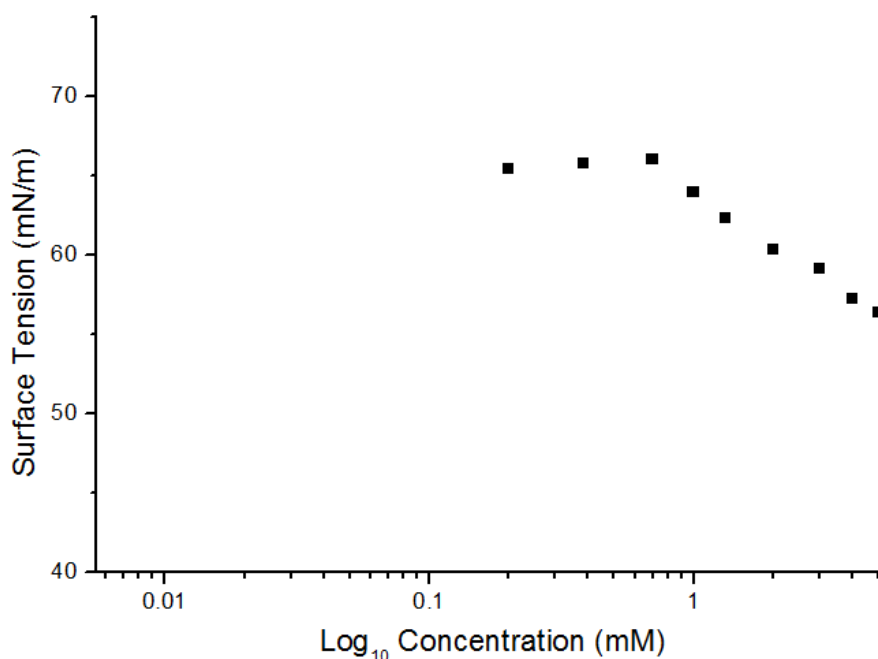


**Figure 4.45.** Tensiometry curve for C<sub>8</sub> pyridinium bolaform (**444**).

Figure 4.45 depicts a typical tensiometry curve for the bolaform surfactant (**444**). Of note is the much lower effectiveness in reducing the surface tension. At the far left of the plot, at concentrations in the 0.1 mM range, the tensiometry plot shows a plateau. This plateau represents the area where the concentration is too low to reduce the surface tension. The surface tension of pure water has a literature value of 71.99 mN/m at 25 °C<sup>30</sup>, however the plateau area of the tensiometry curve begins below 71.99 mN/m at ~60 mN/m. There are a number of possible reasons for this. The first is that the water used was not pure. This can be ruled out due



to the water being tested for surface tension properties before samples were made. The second is that minute amounts of lipophilic impurities present in the surfactant sample are known to reduce the initial surface tension of the water.<sup>31</sup> This reason is more likely, even though the surfactants were triturated multiple times during their synthesis and HPLC/UV analysis showed  $\geq 98\%$  purity, 1-2% trace impurities can be enough to lower the initial surface tension, even in micro-molar concentrations.<sup>31</sup>



**Figure 4.46.** Surface tension plot of C<sub>8</sub> cholinium bolaform (**450**).

As previously discussed in Chapter 3, Section 3.4.2, bolaform surfactants can adopt a number of different conformations at an air-water interface. From the plot of C<sub>8</sub> cholinium bolaform (**450**) it can be seen that very little reduction in surface tension was observed, even at higher concentrations (1-10 mM). It can be inferred from this result that the C<sub>8</sub> cholinium bolaform surfactant does not behave in the same way as their imidazolium and pyridinium counterparts. The reason for this may be attributed to the increased polarity of the cholinium headgroup due to the presence of a quaternary nitrogen and a primary alcohol. As the spacer length is increased for the cholinium bolaform series it can be observed that the C<sub>10</sub> (**451**) and C<sub>12</sub> (**452**) begin to show surface activity. The C<sub>10</sub> cholinium derivatives CMC is still higher than the C<sub>8</sub> pyridinium (**444**) and C<sub>8</sub> imidazolium (**447**) bolaform surfactants. If further investigations were to be conducted into this surfactant class the first modification attempted should be increasing the spacer lengths considerably to observe the effect on CMC.

**Table 4.14.** Comparison of CMC results by tensiometry and conductimetry.

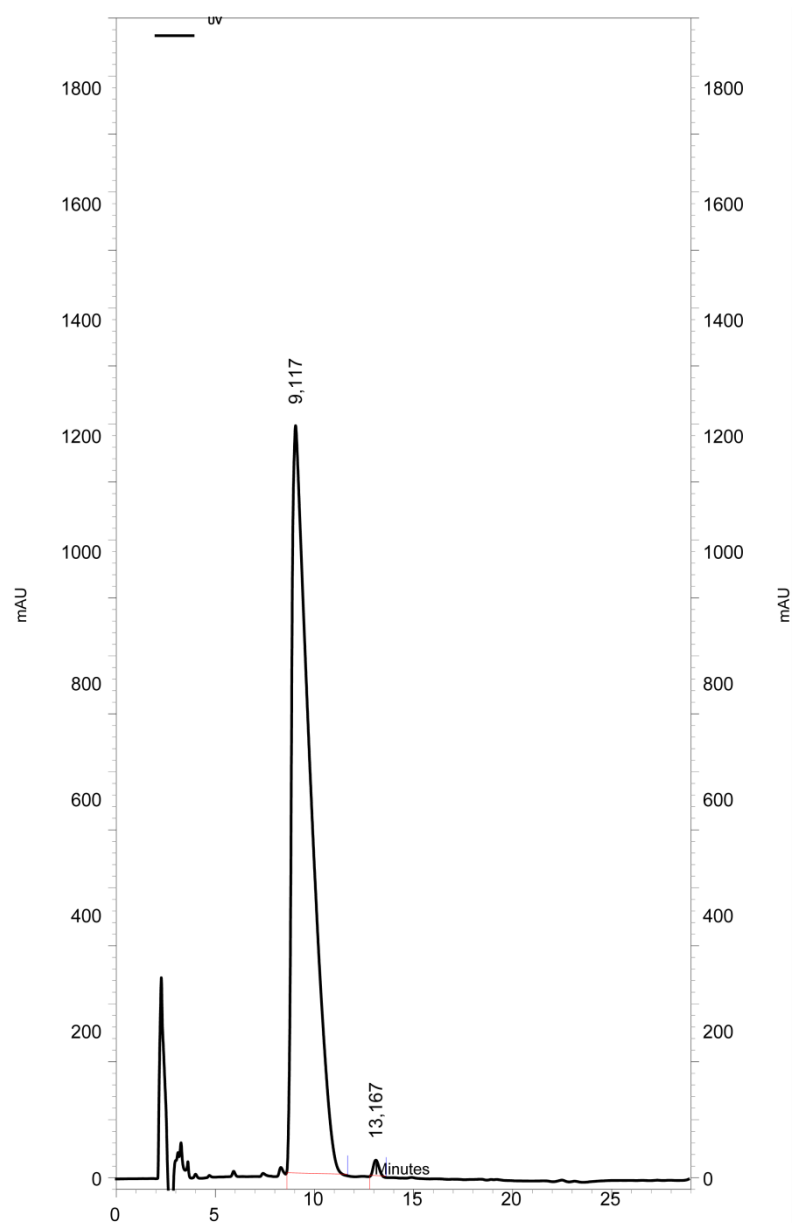
IL	Headgroup	CMC Conductivity (mM)	CMC Tensiometry (mM)
444	Pyridinium	2.00	2.00
445	Pyridinium	0.70	0.70
446	Pyridinium	0.20	0.60
447	Imidazolium	2.00	1.50
448	Imidazolium	0.75	0.75
449	Imidazolium	0.27	0.60
450	Cholinium	2.50	-
451	Cholinium	0.60	2.75
452	Cholinium	0.27	0.40

The comparison of CMC by conductimetry and tensiometry (Table 4.14) helps to confirm the accuracy of the CMC determination. Very little difference is observed between the experimental values for conductimetry and tensiometry.

#### 4.4.3 HPLC Models

The purity of all of the surfactants, as per section 4.3.3, was determined by HPLC/UV to ensure >98% purity of all surfactants.

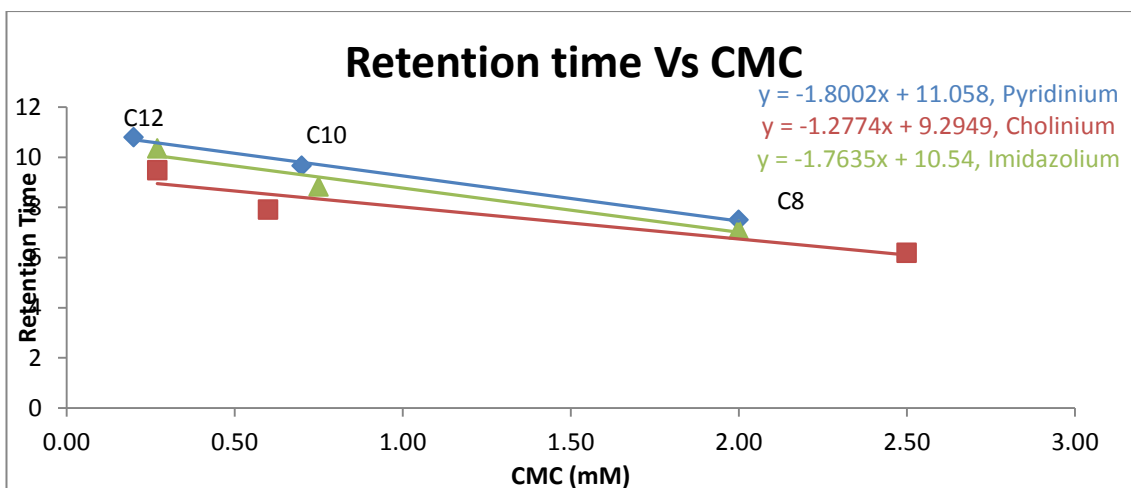
An example HPLC/UV trace (Figure 4.47 and Table 4.15), showed that bolaform IL (**444**) synthesised had a greater than >98% purity. HPLC/UV analysis was carried out for all bolaform ILs. As per section 4.3.3 it was also possible to construct a model based on retention time and CMC



**Figure 4.47.** HPLC/UV trace for IL C<sub>8</sub> pyridinium bolaform (**444**).

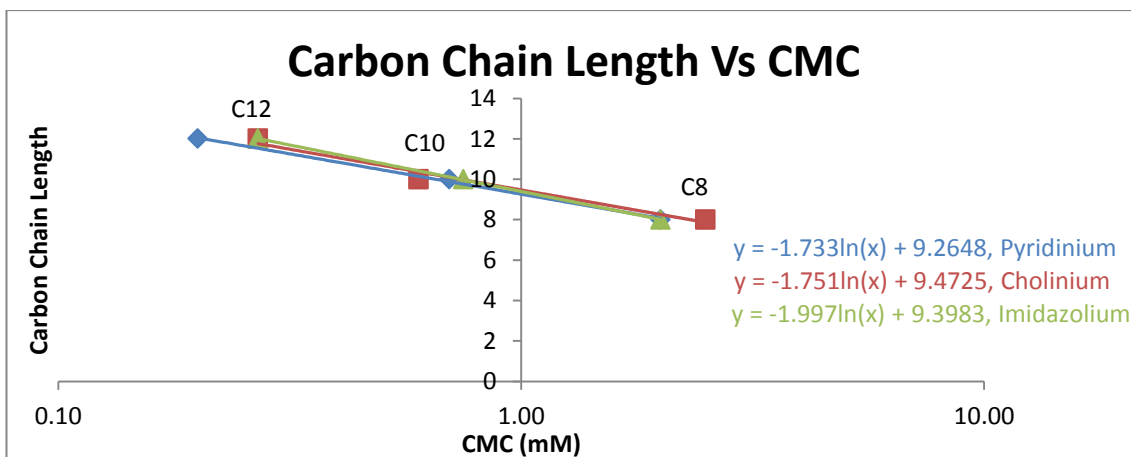
Retention Time Minutes	Area	Area %	Height	Height %
9.12	336365765	99,30	5164733	97,81
13.17	2368078	0,70	115793	2,19

**Table 4.15.** HPLC/UV retention time results.



**Figure 4.48.** Retention time vs CMC for bolaform surfactants (444-452) examined by conductivity.

There is a good correlation between retention time and CMC with just one of the cholinium points lying below the line by >1 minute of retention time (Figure 4.48). If bolaform surfactants with longer spacers were synthesised then HPLC/UV retention time could provide an estimate of their CMC.



**Figure 4.49.** No of Carbon atoms in the linear alkyl chain vs CMC (conductivity).

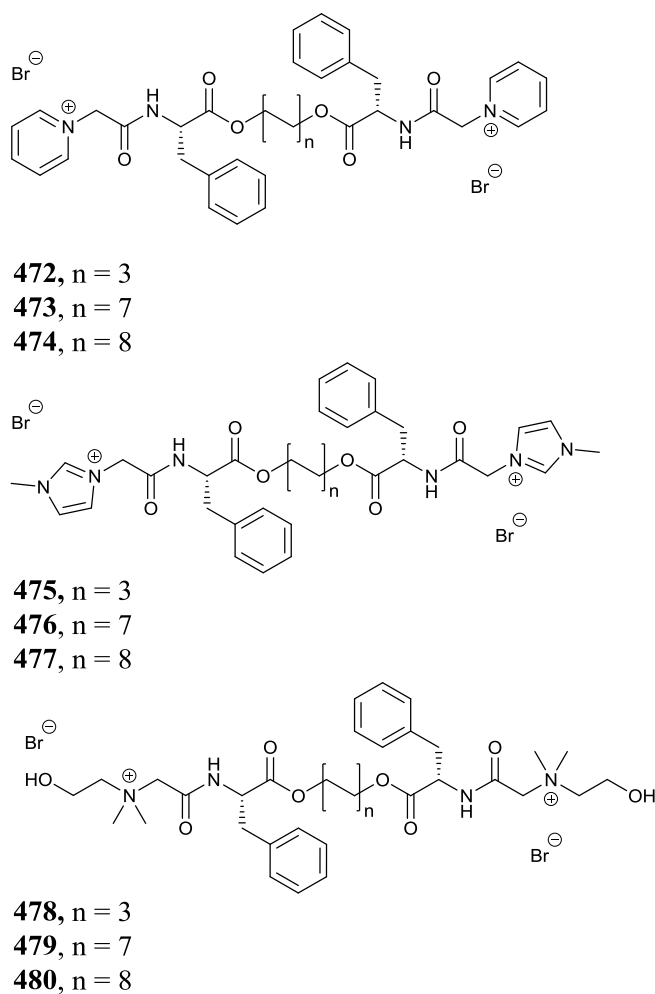
Figure 4.49 shows a good correlation between carbon spacer length and CMC as expected. From these models an estimate, in conjunction with the equation  $\log\text{CMC} = A - Bn$  previously described in section 4.3.1, can give a reasonable indication of CMC. As per section 4.3.3, new  $A$  and  $B$  values can be determined from the equations of the lines (Figure 4.49).

Pyridinium bolaform:  $y = -1.733\ln(x) + 9.2648 \rightarrow \log(x) = 2.322 - 0.251(y)$ .  $A = 2.322$ ,  $B = -0.251$

Imidazolium bolaform:  $y = -1.997\ln(x) + 9.3983 \rightarrow \log(x) = 2.044 - 0.217(y)$ .  $A = 2.044$ ,  $B = 0.217$

Cholinium bolaform:  $y = -1.751\ln(x) + 9.4725 \rightarrow \log(x) = 2.337 - 0.248(y)$ .  $A = 2.337$ ,  $B = 0.248$

From the calculated  $A$  and  $B$  values, a reasonable model of further bolaform surfactants of these classes may be constructed. However, caution must be exercised as the structural conformation that the bolaform surfactants assume is uncertain and can lead to varying values and properties. The predicted values are outlined in Table 4.16. As can be seen, a good agreement between predicted values and actual CMC is observed. Predicted CMC values for  $C_6$ ,  $C_{14}$  and  $C_{16}$  spaced bolaform surfactants (**472-480**) have also been included (Figure 4.50).



**Figure 4.50.** Bolaform ILs with  $C_6$ ,  $C_{14}$  and  $C_{16}$  spacers.

**Table 4.16.** Calculated CMC and actual CMC values for bolaform surfactant ILs.

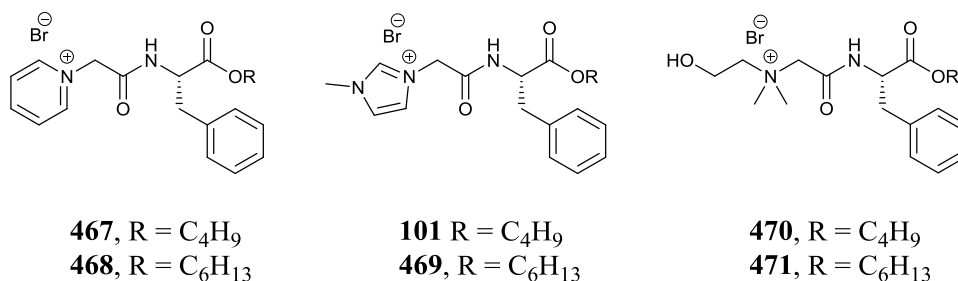
<b>IL</b>	<b>Headgroup</b>	<b>Spacer Length</b>	<b>Predicted CMC (mM)*</b>	<b>CMC (mM) (conductimetry)</b>
<b>472</b>	Pyridinium	6	6.55	-
<b>444</b>	Pyridinium	8	2.06	2.00
<b>445</b>	Pyridinium	10	0.65	0.70
<b>446</b>	Pyridinium	12	0.20	0.20
<b>473</b>	Pyridinium	14	0.06	-
<b>474</b>	Pyridinium	16	0.02	-
<b>475</b>	Imidazolium	6	5.52	-
<b>447</b>	Imidazolium	8	2.03	2.00
<b>448</b>	Imidazolium	10	0.75	0.75
<b>449</b>	Imidazolium	12	0.28	0.27
<b>476</b>	Imidazolium	14	0.10	-
<b>477</b>	Imidazolium	16	0.04	-
<b>478</b>	Cholinium	6	7.06	-
<b>450</b>	Cholinium	8	2.25	2.50
<b>451</b>	Cholinium	10	0.72	0.60
<b>452</b>	Cholinium	12	0.23	0.27
<b>479</b>	Cholinium	14	0.07	-
<b>480</b>	Cholinium	16	0.02	-

\*Calculated using  $\log(\text{CMC}) = A - Bn$

## 4.5 Conclusion

In conclusion two series of novel amino acid ionic liquid surfactants have been synthesised and a number of their surfactant properties have been characterised including CMC by conductivity and tensiometry, surface active properties by tensiometry including efficiency and effectiveness, aqueous stability in neutral, alkaline and basic media, and liquid crystal behaviour by optical microscopy. Addition of an amino acid linker containing a lipophilic side chain has demonstrated that the linker (L-phenylalanine) can contribute to the self-assembling properties, contributing lipophilicity to the micelle. In effect, the C<sub>8</sub> linear alkyl IL surfactants have an equivalent CMC to that of a surfactant 3-4 carbon atoms longer, as do C<sub>10</sub> and C<sub>12</sub>.

The effectiveness (in the ability to reduce surface tension) of the linear alkyl surfactants reported in this chapter is greater than that observed for linear alkyl surfactants found in the literature (even linear alkyl surfactants with  $\geq 4$  more carbon atoms). Effectiveness appears to be greatest for the C<sub>8</sub> linear alkyl amino acid surfactants and decreases for the C<sub>10-12</sub>. Efficiency of the linear alkyl surfactants reported are around twice that of similar linear alkyl surfactants. Area per molecule calculations for the linear alkyl surfactants showed a range of surface areas (1.05-1.55 nm<sup>2</sup>). A surface area of this size, when compared to analogous examples in the literature ( $\sim 0.5$  nm<sup>2</sup>) can be attributed to the bulk of the amino acid sidechain. Construction of HPLC retention time models will allow for rapid prediction of CMC of future generations of surfactants based upon the classes reported within this chapter. Adjusted *A* and *B* values for use in the Stauff-Klevens equation will allow for predicting CMC values of potential future surfactants with a reasonable degree of accuracy. It is proposed, in conjunction with the antimicrobial and biodegradation results in Chapter 3, that the following range of intermediate chain length ILs are synthesised to investigate just how short the chain length can be lowered before micellisation and surface activity ceases to occur (Figure 4.51).



**Figure 4.51.** Intermediate length C<sub>4</sub> and C<sub>6</sub> linear alkyl ILs.

Optical microscopy studies showed a wide range of liquid crystal behaviour for the surfactant ILs examined. A multitude of structures were observed over a wide range of temperatures (20-100 °C). Amongst the liquid crystals observed were hexagonal phase, lamellar phase and cubic phase. The study was qualitative in nature and could be further developed in the future by way of a quantitative study to produce phase diagrams for the surfactants of interest.

Aqueous, acid and alkaline hydrolysis experiments conducted on a number of surfactants gave an insight into the stability of the linear alkyl ILs examined. It can be observed from the preliminary study that the cholinium and imidazolium ILs (**436**, **439**) undergo hydrolysis at pH 7, 50 °C but the pyridinium IL (**433**) could potentially be more stable. Rapid onset of degradation was not observed for any of the three ILs at pH 2, 25 °C. Rapid base mediated hydrolysis is observed for the three ILs examined (**433**, **436**, **439**). A quantitative examination of the ILs stability will be of future importance for application considerations.

The bolaform ILs assessed showed CMC values that were generally lower than their linear alkyl counterparts. This observation was unexpected due to the general trend presented by Rosen *et al.* which suggests that bolaform surfactants must have 2x the number of carbon atoms to reach a similar CMC as that of linear alkyl surfactants.<sup>3</sup> One possible reason for this may be due to the reduced surface activity of the bolaform surfactants; there are more free molecules in solution forcing the formation of micelles at lower concentrations as the surface is not as saturated as that which is present in linear alkyl surfactants – even though the  $\Delta G_{mic}^{\circ}$  is lower. Another possible explanation is the presence of an additional amino acid in the bolaform ILs. A C<sub>8</sub> bolaform IL with two L-phenylalanine moieties present has ~+3.5 extra theoretical carbon atoms for each phenyl sidechain in the hydrophobic region, than that of a C<sub>8</sub> linear alky surfactant.

When the surface activity was examined for the bolaform surfactants a lower efficiency and lower effective range - than that which was observed for the linear alkyl surfactants - was observed. As per the linear alkyl surfactants, *A* and *B* values were calculated for the bolaform surfactants to provide insight into estimating the CMC of potential future bolaform surfactants of this type. The bolaform class of surfactants represents a niche class of surface active agents and may be of interest for biological and medicinal applications due to their similarities to biological membranes.<sup>32</sup>



## 4.6 References

1. M. J. Rosen, *Micelle Formation by Surfactants*, John Wiley & Sons, Inc., 2004.
2. B. L. Bales, *J. Phys. Chem. B*, 2001, 105, 6798-6804.
3. M. J. Rosen and J. T. Kunjappu, *Surfactants and Interfacial Phenomena, 4th Edition*, Blackwell Science Publ, Oxford, 2012.
4. K. Holmberg, B. Jönsson, B. Kronberg and B. Lindman, *Introduction to Surfactants*, John Wiley & Sons, Ltd, 2003.
5. K. Kosswig, *Surfactants*, Wiley-VCH Verlag GmbH & Co. KGaA, 2000.
6. M. J. Rosen, *J. Colloid Interface Sci.*, 1976, 56, 320-327.
7. M. J. Rosen, *J. Am. Oil Chem. Soc.*, 1974, 51, 461-465.
8. M. T. Garcia, I. Ribosa, L. Perez, A. Manresa and F. Comelles, *Langmuir*, 2013, 29, 2536-2545.
9. M. J. Rosen, M. Dahanayake and A. W. Cohen, *Colloids Surf.*, 1982, 5, 159-172.
10. J. Skerjanc, K. Kogej and J. Cerar, *Langmuir*, 1999, 15, 5023-5028.
11. M. T. Garcia, I. Ribosa, L. Perez, A. Manresa and F. Comelles, *Colloids Surf., B*, 2014, 123, 318-325.
12. S. Morrissey, B. Pegot, D. Coleman, M. T. Garcia, D. Ferguson, B. Quilty and N. Gathergood, *Green Chem.*, 2009, 11, 475-483.
13. N. Gathergood, M. T. Garcia and P. J. Scammells, *Green Chem.*, 2004, 6, 166-175.
14. H. B. Klevens, *J. Am. Oil Chem. Soc.*, 1953, 30, 74-80.
15. J. Wang and H. Wang, *Aggregation in Systems of Ionic Liquids*, Springer Berlin Heidelberg, 2014.
16. R. L. Venable and R. V. Nauman, *J. Phys. Chem.*, 1964, 68, 3498-&.
17. E. C. Evers and C. A. Kraus, *J. Am. Chem. Soc.*, 1948, 70, 3049-3054.
18. F. M. Menger and C. A. Littau, *J. Am. Chem. Soc.*, 1993, 115, 10083-10090.
19. J. Short, J. Roberts, D. W. Roberts, G. Hodges, S. Gutsell and R. S. Ward, *Ecotoxicol. Environ. Saf.*, 2010, 73, 1484-1489.
20. D. W. Roberts and J. Costello, *QSAR Comb. Sci.*, 2003, 22, 220-225.
21. A. S. C. Lawrence, *Discuss. Faraday Soc.*, 1958, 25, 51-58.
22. P. Sciences, in *Particle Sciences - Technical Brief*, 2012, vol. 6.
23. P. Sciences, in *Particle Sciences - Technical Brief*, 2010, vol. 1.
24. F. Tadros Tharwat, *An Introduction to Surfactants*, 2014.
25. Y. Wang and E. Marques, *J. Therm. Anal. Calorim.*, 2010, 100, 501-508.
26. S. Manet, Y. Karpichev, D. Dedovets and R. Oda, *Langmuir*, 2013, 29, 3518-3526.
27. L. Myles, R. G. Gore, N. Gathergood and S. J. Connon, *Green Chem.*, 2013, 15, 2740-2746.
28. R. G. Gore, L. Myles, M. Spulak, I. Beadham, T. M. Garcia, S. J. Connon and N. Gathergood, *Green Chem.*, 2013, 15, 2747-2760.
29. L. Myles, R. Gore, M. Spulak, N. Gathergood and S. J. Connon, *Green Chem.*, 2010, 12, 1157-1162.
30. N. B. Vargaftik, B. N. Volkov and L. D. Voljak, *J. Phys. Chem. Ref. Data*, 1983, 12, 817-820.
31. P. Quagliotto, N. Barbero, C. Barolo, E. Artuso, C. Compari, E. Fisicaro and G. Viscardi, *J. Colloid Interface Sci.*, 2009, 340, 269-275.
32. R. Zana, *Bolaform and dimeric (gemini) surfactants*, Springer Netherlands, 1997.

## **Chapter 5**

### *Experimental*

## 5.1 Experimental

### 5.1.1 Chemicals

All chemicals used in Chapters 2-3 were purchased from Sigma Aldrich or TCI Europe. Methanol and ethanol were distilled over magnesium turnings activated by iodine before use. DCM and ethyl acetate were pre-dried over magnesium sulphate and then distilled over  $\text{CaH}_2$  before use. THF and diethyl ether were dried over sodium wire and benzophenone and distilled before use. DMF used was purchased from Sigma Aldrich as an anhydrous sureseal preparation. Sigma Aldrich (Riedel de Haën) 220-440 mesh, 60 Å pore size, 35-75 µm particle size, silica gel was used for flash and thin layer chromatography.

### 5.1.2 NMR

The majority of NMR analysis was performed on a Bruker AC 400 MHz spectrometer operating at 400 MHz for  $^1\text{H}$ -NMR and 100 MHz for  $^{13}\text{C}$ -NMR. Samples were run in deuterated chloroform ( $\text{CDCl}_3$ ), deuterated water ( $\text{D}_2\text{O}$ ), deuterated methanol ( $\text{MeOD}$ ), or deuterated dimethyl sulfoxide ( $\text{DMSO}$ ) where appropriate. A 600 MHz Bruker spectrometer, operating at 600 MHz for  $^1\text{H}$ -NMR and 150 MHz for  $^{13}\text{C}$ -NMR was also used for analysis of some examples. All chemical shifts are reported in parts per million (ppm) are relative to the internal standard TMS and coupling constants ( $J$ ) are measured in Hertz (Hz). Multiplicity is stated as follows: s-singlet, d-doublet, t-triplet, q-quartet, dd-doublet of doublets, dt doublet of triplets, dq-doublet of quartets, tt-triplet of triplets, tq-triplet of quartets, ddd-doublet of doublet of doublets, m-multiplet, bs-broad singlet.

### 5.1.3 IR analysis

All IR analysis was carried out on a Perkin Elmer 100 FT-IR spectrometer with ATR. The strength of reported peaks are described as weak (w), medium (m), broad (b), strong (s) and very strong (vs).

### 5.1.4 Melting point

Melting points were determined using a Lennox automated melting point apparatus and the values are expressed in degrees Celsius ( $^{\circ}\text{C}$ ). The parameters for the melting point analysis were set at 5  $^{\circ}\text{C}$  per minute ramp and melting point was determined manually. Melting points are uncorrected.

### 5.1.5 Optical Rotation

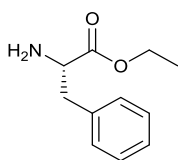
Optical rotations were measured using a Perkin Elmer 343 Polarimeter in chloroform, methanol or ethanol at 20  $^{\circ}\text{C}$  and values are expressed in degrees

### 5.1.6 ESI-MS

High resolution mass spectrometry (HRMS) with accurate mass measurement to four decimal places was obtained for new ILs, new tertiary amines and new alkylating reagents described in Chapters 2-3. The analysis was conducted in the ABCRF Mass Spectrometry Lab, Cavanagh Building, in University College Cork. Accurate mass measurement was obtained using a Waters Micromass LCT Premier run in ESI+ mode. An external reference standard of leucine enkephalin was used in order to confirm mass accuracy and a sulfadimethoxine concentration test was performed to ensure the accuracy of peaks in the ion count range of  $1 \times 10^3 - 1 \times 10^6$ .

## 5.2 Experimental preparation of Chapter 2 L-phenylalanine ILs

### 5.2.1 Preparation of L-phenylalanine ethyl ester (336) - general procedure "A"



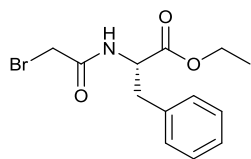
To a stirred suspension of ethanol (86 ml, 1.5 mol) and L-phenylalanine (25.00 g, 151.3 mmol) at 0 °C was added dropwise  $\text{SOCl}_2$  (26.3 ml, 303 mmol). The solution was allowed to warm to room temperature then heated under reflux conditions for 12 hours. Solubilisation of the reaction mixture was observed after 30 minutes reflux. After 12 hours the reaction mixture was allowed to cool to room temperature and a stream of nitrogen was bubbled through it for 30 minutes. After 30 minutes, ethanol was removed *in vacuo* to furnish the product as a hydrochloride salt in 99% yield. The salt product could then be retained for long term storage or neutralised as follows for immediate use. The salt product was dissolved in deionised water (50 ml) in a 1 litre separating funnel and a saturated aqueous bicarbonate solution was added slowly (50 ml). Neutralisation of the solution was accomplished and the free base amino acid ester was extracted using ethyl acetate (5 x 50 ml). The organic layer was washed with brine (3 x 50 ml) and dried over anhydrous magnesium sulphate followed by gravity filtration. Ethyl acetate was removed *in vacuo* to yield the title compound (**336**) as a pale yellow oil in 99% yield, (28.89 g, 149.5 mmol).

Molecular formula:  $\text{C}_{11}\text{H}_{15}\text{NO}_2$ ; Molecular weight:  $193.246 \text{ g mol}^{-1}$ .

$^1\text{H}$ -NMR (400 MHz,  $\text{CDCl}_3$ )  $\delta$  (ppm): 7.35 (m, 5H), 4.19 (q,  $J = 7.1 \text{ Hz}$ , 2H), 3.74 (dd,  $J = 7.9$ , 5.3 Hz, 1H), 3.10 (dd,  $J = 13.5$ , 5.3 Hz, 1H), 2.89 (dd,  $J = 13.5$ , 7.9 Hz, 1H), 1.27 (t,  $J = 7.1 \text{ Hz}$ , 3H).  $^{13}\text{C}$ -NMR (100 MHz,  $\text{CDCl}_3$ )  $\delta$  (ppm): 175.07, 137.31, 129.34, 128.55, 126.82, 60.95, 55.88, 41.16, 14.22

$^1\text{H}$ -NMR and  $^{13}\text{C}$ -NMR were in agreement with the literature.<sup>1</sup>

### 5.2.2 Preparation of L-phenylalanine ethyl ester $\alpha$ -bromoamide alkylating reagent (**337**) - general procedure “B”



To a stirred solution of L-phenylalanine ethyl ester (**336**) (6.23 g, 32.2 mmol) in DCM (50 ml) was added solid  $\text{Na}_2\text{CO}_3$  (5.13 g, 48.4 mmol) and dropwise, bromoacetyl bromide (3.4 ml, 39 mmol). The reaction mixture was allowed to cool to room temperature and stirred for 5 hours.

After 5 hours the  $\text{Na}_2\text{CO}_3$  was removed by gravity filtration. The DCM layer was washed with saturated sodium bicarbonate solution (3 x 50 ml), dried over anhydrous magnesium sulphate and gravity filtered. The DCM was removed *in vacuo* to afford the title compound as a white solid in 89% yield, (0.998 g, 28.6 mmol).

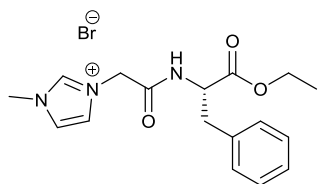
Molecular formula:  $\text{C}_{13}\text{H}_{16}\text{BrNO}_3$ ; Molecular weight: 314.179  $\text{g mol}^{-1}$ .

$^1\text{H}$ -NMR (400 MHz,  $\text{CDCl}_3$ )  $\delta$  (ppm): 7.32 – 7.27 (m, 3H), 7.14-7.12 (m, 2H), 6.86 (d,  $J$  = 6.8 Hz, 1H), 4.70 (dt,  $J$  = 7.8, 5.8 Hz, 1H), 4.25 (q,  $J$  = 7.1 Hz, 2H), 3.86 (d,  $J$  = 13.7 Hz, 1H), 3.83 (d,  $J$  = 13.6 Hz, 1H), 3.17 (dd,  $J$  = 14.0, 5.8 Hz, 1H), 3.13 (dd,  $J$  = 14.0, 5.8 Hz, 1H), 1.25 (t,  $J$  = 7.1 Hz, 3H)  $^{13}\text{C}$ -NMR (100 MHz,  $\text{CDCl}_3$ )  $\delta$  (ppm): 170.87, 165.15, 135.42, 129.37, 128.64, 127.30, 61.78, 53.76, 37.76, 28.71, 14.13

$^1\text{H}$ -NMR and  $^{13}\text{C}$ -NMR were in agreement with the literature.<sup>2</sup>

### 5.2.3 Preparation of IL (**324**) - general procedure “C”

3-({[(2S)-1-Ethoxy-1-oxo-3-phenylpropan-2-yl]carbamoyl}methyl)-1-methyl-1H-imidazol-3-ium bromide (**324**).



To a stirred solution of L-phenylalanine ethyl ester  $\alpha$ -bromoamide (**337**) (0.607 g, 1.93 mmol) in diethyl ether (10 ml) was added 1-methylimidazole (140  $\mu\text{l}$ , 1.76 mmol). The reaction was stirred at room temperature under an  $\text{N}_2$  atmosphere for 24 hours. After 24 hours a waxy precipitate had formed. The supernatant was decanted and the waxy crude product was washed with diethyl ether (3 x 25 ml) to afford the title compound (**324**) as a white solid in 89% yield, (0.622 g, 1.57 mmol).

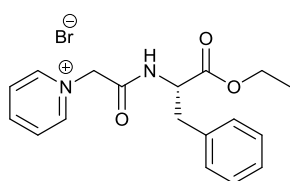
Molecular formula:  $\text{C}_{17}\text{H}_{22}\text{BrN}_3\text{O}_3$ ; Molecular weight: 396.285  $\text{g mol}^{-1}$ ; Mp: 77-79° C.

$[\alpha]_{\text{D}}^{20}$  = +7.49 (0.4 c,  $\text{CHCl}_3$ );  $^1\text{H}$ -NMR (400 MHz,  $\text{CDCl}_3$ )  $\delta$  (ppm): 9.80 (s, 1H), 8.89 (d,  $J$  = 7.6 Hz, 1H), 7.42 (t,  $J$  = 1.6, 1H), 7.34 (t,  $J$  = 1.6, 1H), 7.32 – 7.11 (m, 5H), 5.37 (d,  $J$  = 15.2,

1H), 5.31 (d,  $J = 14.8$ , 1H), 4.67 (ddd,  $J = 8.6, 7.8, 6.0$  Hz, 1H), 4.11 (q,  $J = 7.2$  Hz, 2H), 3.98 (s, 3H), 3.23 (dd,  $J = 14.0, 6.0$  Hz, 1H), 3.17 (dd,  $J = 14.0, 8.8$  Hz, 1H) 1.18 (t,  $J = 7.2$  Hz, 3H).  $^{13}\text{C-NMR}$  (100 MHz,  $\text{CDCl}_3$ )  $\delta$  (ppm): 171.16, 164.77, 137.75, 136.69, 129.53, 128.40, 126.78, 123.65, 122.48, 61.47, 54.83, 51.58, 37.41, 36.77, 14.05.  $\text{IR}$  (neat) ( $\text{cm}^{-1}$ ): 3202 (w), 3027 (w), 1732 (s), 1676 (vs), 1527 (m), 1373 (m), 1261 (m), 1218 (vs), 1178 (vs), 1107 (s), 767 (m), 749 (m).  $\text{ESI-MS}$  (+ve)  $m/z$ : Found  $[\text{M}-\text{Br}]^+$  316.1657,  $\text{C}_{17}\text{H}_{22}\text{N}_3\text{O}_3^+$  requires 316.1656.  $^1\text{H-NMR}$  and  $^{13}\text{C-NMR}$  were in agreement with the literature.<sup>2</sup>

#### 5.2.4 Preparation of IL (325)

(S)-1-(2-((1-Ethoxy-1-oxo-3-phenylpropan-2-yl)amino)-2-oxoethyl)pyridin-1-ium bromide (325).



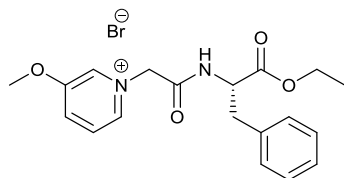
According to the general procedure “C”, using L-phenylalanine ethyl ester  $\alpha$ -bromoamide (337) (0.581 g, 1.85 mmol) and pyridine (135  $\mu\text{l}$ , 1.68 mmol), the title compound (325) was isolated as a white solid in 98% yield, (0.643 g, 1.64 mmol).

Molecular formula:  $\text{C}_{18}\text{H}_{21}\text{BrN}_2\text{O}_3$ ; Molecular weight: 393.281  $\text{g mol}^{-1}$ ; Mp: 98-100°C.

$[\alpha]_{\text{D}}^{20} = +2.26$  (0.4 c,  $\text{CHCl}_3$ );  $^1\text{H-NMR}$  (400 MHz,  $\text{CDCl}_3$ )  $\delta$  (ppm): 9.36 (d,  $J = 7.6$  Hz, 1H), 9.22 (d,  $J = 4.8$  Hz, 2H), 8.41 (t,  $J = 8.0$  Hz, 1H), 7.96 (t,  $J = 7.6$  Hz, 2H), 7.37-7.25 (m, 2H), 7.24-7.14 (m, 3H), 6.04 (d,  $J = 14.4$  Hz, 1H), 5.98 (d,  $J = 14.8$  Hz, 1H), 4.70-4.65 (m, 1H), 4.12-4.06 (m, 2H), 3.25 (dd,  $J = 14.0, 8.2$  Hz, 1H), 3.18 (dd,  $J = 14.0, 8.0$  Hz, 1H), 1.17 (t,  $J = 7.2$  Hz, 3H).  $^{13}\text{C-NMR}$  (100 MHz,  $\text{CDCl}_3$ ):  $\delta$  170.95, 163.97, 146.06, 145.31, 136.61, 129.61, 128.43, 127.63, 126.80, 62.12, 61.55, 54.95, 37.53, 14.07.  $\text{IR}$  (neat) ( $\text{cm}^{-1}$ ): 3184 (w), 3042 (w), 1736 (vs), 1686 (vs), 1632 (m), 1560 (s), 1484 (s), 1368 (s), 1264 (s), 1188 (vs).  $\text{ESI-MS}$  (+ve)  $m/z$ : Found  $[\text{M}-\text{Br}]^+$  313.1543,  $\text{C}_{18}\text{H}_{21}\text{N}_2\text{O}_3^+$  requires 313.1547.

#### 5.2.5 Preparation of IL (326)

(S)-1-(2-((1-Ethoxy-1-oxo-3-phenylpropan-2-yl)amino)-2-oxoethyl)-3-methoxypyridin-1-ium bromide (326).



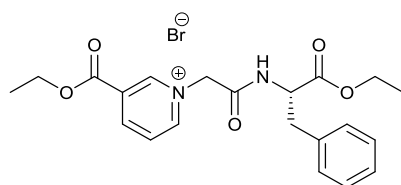
According to the general procedure “C”, using L-phenylalanine ethyl ester  $\alpha$ -bromoamide (337) (1.046 g, 3.329 mmol) and 3-methoxypyridine (320  $\mu\text{l}$ , 3.18 mmol), the title compound (326) was isolated as a white, hygroscopic solid in 96% yield, (1.295 g, 3.059 mmol).

Molecular formula: C<sub>19</sub>H<sub>23</sub>BrN<sub>2</sub>O<sub>4</sub>; Molecular weight: 423.307 g mol<sup>-1</sup>; Mp: 72-74°C.

$[\alpha]_D^{20} = -7.2$  (2.0 c, CHCl<sub>3</sub>); <sup>1</sup>H-NMR (400 MHz, CDCl<sub>3</sub>)  $\delta$  (ppm): 9.39 (d,  $J = 7.8$  Hz, 1H), 9.32 (d,  $J = 1.1$  Hz, 1H), 8.54 (d,  $J = 5.8$  Hz, 1H), 7.87-7.85 (ddd, 9.0, 2.4, 0.8 Hz, 1H), 7.77 (dd,  $J = 8.8, 5.8$  Hz, 1H), 7.35-7.33 (m, 2H), 7.23-7.12 (m, 3H), 5.94 (d,  $J = 14.1$  Hz, 1H) 5.88 (d,  $J = 14.1$  Hz, 1H), 4.66 (ddd,  $J = 8.9, 8.1, 5.9$  Hz, 1H), 4.10 (s, 3H), 4.09-4.03 (m, 2H), 3.24 (dd,  $J = 13.9, 5.8$  Hz, 1H), 3.17 (dd,  $J = 13.8, 8.0$  Hz, 1H), 1.16 (t,  $J = 7.2$ , 3H). <sup>13</sup>C-NMR (100 MHz, CDCl<sub>3</sub>)  $\delta$  (ppm): 170.83, 163.93, 158.38, 138.15, 136.66, 132.40, 131.99, 129.56, 128.36, 127.58, 126.75, 62.23, 61.51, 58.29, 54.91, 37.40, 14.07. IR (neat) (cm<sup>-1</sup>): 3187 (w), 3028 (w), 1736 (s), 1683 (vs), 1507 (vs), 1294 (vs), 1198 (b). ESI-MS (+ve) m/z: Found [M-Br]<sup>+</sup> 343.1649, C<sub>19</sub>H<sub>23</sub>N<sub>2</sub>O<sub>4</sub><sup>+</sup> requires 343.1652

### 5.2.6 Preparation of IL (327)

(S)-1-(2-((1-Ethoxy-1-oxo-3-phenylpropan-2-yl)amino)-2-oxoethyl)-3-(ethoxycarbonyl)pyridin-1-ium bromide (**327**).



To a stirred solution of L-phenylalanine ethyl ester  $\alpha$ -bromoamide (**337**) (0.507 g, 1.61 mmol) in THF (25 ml) was added ethyl nicotinate (200  $\mu$ l, 1.46 mmol). The reaction was stirred under reflux conditions for 24 hours.

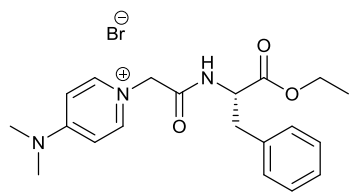
After 24 hours the THF was removed *in vacuo* to afford a brown crude product. The crude product was purified by silica gel chromatography (gradient elution of 5:95 MeOH:DCM to 10:90 MeOH:DCM) to afford the title compound (**327**) as an orange solid in 56% yield, (0.381 g, 0.819 mmol).

Molecular formula: C<sub>21</sub>H<sub>25</sub>BrN<sub>2</sub>O<sub>5</sub>; Molecular weight: 465.344 g mol<sup>-1</sup>; Mp: 60-62°C.

$[\alpha]_D^{20} = +1.4$  (2.0 c, CHCl<sub>3</sub>); <sup>1</sup>H-NMR (400 MHz, CDCl<sub>3</sub>)  $\delta$  (ppm): 9.71 (d,  $J = 6.0$  Hz, 1H), 9.37 (m, 2H), 8.93-8.90 (m, 1H), 8.10 (dd,  $J = 8.0, 6.4$  Hz, 1H), 7.37-7.35 (m, 2H), 7.25-7.22 (m, 2H), 7.17-7.13 (m, 1H), 6.26 (d,  $J = 15.2$  Hz, 1H), 6.19 (d,  $J = 15.2$  Hz, 1H), 4.72-4.67 (m, 1H), 4.48 (q,  $J = 7.2$  Hz, 2H), 4.11-4.05 (m, 2H), 3.25-3.14 (m, 2H), 1.44 (t,  $J = 7.2$  Hz, 3H), 1.15 (t,  $J = 7.1$  Hz, 3H). <sup>13</sup>C-NMR (100 MHz, CDCl<sub>3</sub>)  $\delta$  (ppm): 171.00, 163.80, 160.96, 149.75, 146.96, 145.36, 136.74, 130.41, 129.72, 128.49, 127.73, 126.87, 63.63, 62.88, 61.59, 55.14, 37.73, 14.28, 14.14. IR (neat) (cm<sup>-1</sup>): 3180 (w), 3027 (w), 1730 (vs), 1683 (vs), 1296 (vs), 1188 (b), 1110 (m), 1014 (s). ESI-MS (+ve) m/z: Found [M-Br]<sup>+</sup> 385.1755, C<sub>20</sub>H<sub>26</sub>N<sub>3</sub>O<sub>3</sub><sup>+</sup> requires 385.1758

### 5.2.7 Preparation of IL (328)

(S)-4-(Dimethylamino)-1-(2-((1-ethoxy-1-oxo-3-phenylpropan-2-yl)amino)-2-oxoethyl)pyridin-1-ium bromide (**328**).



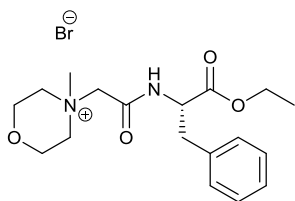
According to the general procedure “C”, using L-phenylalanine ethyl ester  $\alpha$ -bromoamide (**337**) (0.446 g, 1.42 mmol) and dimethylaminopyridine (0.158 g, 1.29 mmol), the title compound (**328**) was isolated as a white solid in 88% yield, (0.498 g, 1.14 mmol).

Molecular formula:  $C_{20}H_{26}BrN_3O_3$ ; Molecular weight: 436.350  $g\ mol^{-1}$ ; Mp: 135-137°C.

$[\alpha]_D^{20} = -13.2$  (2.0 c,  $CHCl_3$ ).  $^1H$ -NMR (400 MHz,  $CDCl_3$ )  $\delta$  (ppm): 9.26 (d,  $J = 7.2$  Hz, 1H), 8.36 (d,  $J = 7.8$  Hz, 2H), 7.35-7.33 (m, 2H), 7.21-7.19 (m, 2H), 7.15-7.11 (m, 1H), 6.73 (d,  $J = 7.8$ , 2H), 5.38 (d,  $J = 14.6$ , 1H), 5.31 (d,  $J = 14.6$  Hz, 1H), 4.58 (dd,  $J = 14.9$ , 7.4 Hz, 1H), 4.06 (q,  $J = 6.8$  Hz, 2H), 3.22 (s, 6H), 3.21-3.19 (m, 2H), 1.13 (t,  $J = 7.1$  Hz, 3H).  $^{13}C$ -NMR (100 MHz,  $CDCl_3$ )  $\delta$  (ppm): 170.70, 165.33, 156.37, 143.17, 136.86, 129.62, 128.35, 126.62, 107.43, 61.33, 58.62, 55.12, 40.43, 37.30, 14.09. IR (neat) ( $cm^{-1}$ ): 3165 (w), 3012 (w), 1743 (s), 1678 (vs), 1651 (vs), 1574 (m), 1404 (w), 1181 (b), 1024 (w), 818 (s). ESI-MS (+ve) m/z: Found  $[M-Br]^{+}$  356.1969,  $C_{20}H_{26}N_3O_3^{+}$  requires 356.1969.

### 5.2.8 Preparation of IL (329)

(S)-4-(2-((1-Ethoxy-1-oxo-3-phenylpropan-2-yl)amino)-2-oxoethyl)-4-methylmorpholin-4-ium bromide (**329**).



According to the general procedure “C”, using L-phenylalanine ethyl ester  $\alpha$ -bromoamide (**337**) (1.165 g, 3.708 mmol) and *N*-methylmorpholine (370  $\mu$ L, 3.37 mmol), the title compound (**329**) was isolated as a white solid in 34% yield, (0.482 g, 1.16 mmol).

Molecular formula:  $C_{18}H_{27}BrN_2O_4$ ; Molecular weight: 415.328  $g\ mol^{-1}$  Mp: 162-164°C.

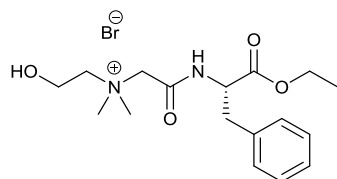
$[\alpha]_D^{20} = -22.71$  (0.5 c,  $CHCl_3$ ).  $^1H$ -NMR (400 MHz,  $CDCl_3$ )  $\delta$  (ppm): 9.40 (d,  $J = 8.0$  Hz, 1H), 7.43-7.41 (m, 2H), 7.29-7.26 (m, 2H), 7.20-7.17 (m, 1H), 5.06 (d,  $J = 13.8$  Hz, 1H), 4.79 (d,  $J = 14.1$  Hz, 1H), 4.76-4.72 (m, 1H), 4.15 (q,  $J = 7.2$  Hz, 2H), 4.08-4.03 (m, 2H), 3.91 (d,  $J = 10.2$  Hz, 2H), 3.85-3.75 (m, 1H), 3.57 – 3.49 (m, 1H), 3.47 (s, 3H), 3.36-3.33 (m, 1H), 3.33 (dd,  $J = 14.0$ , 4.6 Hz, 1H), 3.11 (dd,  $J = 14.1$ , 10.8 Hz, 1H), 1.24 (t,  $J = 7.2$  Hz, 3H).  $^{13}C$ -NMR (100 MHz,  $CDCl_3$ )  $\delta$  (ppm): 170.80, 162.78, 136.73, 129.62, 128.44, 126.82, 61.67, 61.30, 60.57,



60.50, 54.43, 51.40, 37.03, 14.12. IR (neat) (cm<sup>-1</sup>): 3186 (w), 3019 (w), 1735 (s), 1674 (vs), 1534 (s), 1456 (w), 1247 (b), 1120 (m), 1029 (m), 897 (m). ESI-MS (+ve) m/z: Found [M-Br]<sup>+</sup> 335.1963, C<sub>18</sub>H<sub>27</sub>N<sub>2</sub>O<sub>4</sub><sup>+</sup> requires 335.1965.

### 5.2.9 Preparation of IL (330)

(*S*)-2-((1-Ethoxy-1-oxo-3-phenylpropan-2-yl)amino)-*N*-(2-hydroxyethyl)-*N,N*-dimethyl-2-oxoethan-1-aminium bromide (**330**).



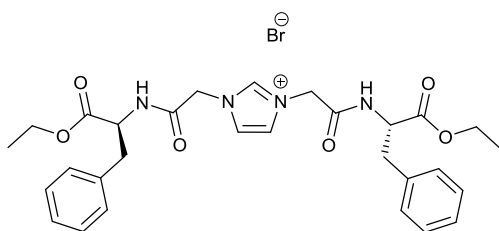
According to the general procedure “C”, using L-phenylalanine ethyl ester α-bromoamide (**337**) (0.594 g, 1.89 mmol) and dimethylaminoethanol (175 μl, 1.70 mmol), the title compound (**330**) was isolated as a white solid in 99% yield, (0.682 g, 1.69 mmol).

Molecular formula: C<sub>17</sub>H<sub>27</sub>BrN<sub>2</sub>O<sub>4</sub>; Molecular weight: 403.317 gmol<sup>-1</sup>; Mp: 97-99 °C.

[α]<sub>D</sub><sup>20</sup> = -45.24 (0.4 c, CHCl<sub>3</sub>). <sup>1</sup>H-NMR (400 MHz, CDCl<sub>3</sub>) δ (ppm): 9.01 (d, *J* = 7.6 Hz, 1H), 7.40-7.38 (m, 2H), 7.30-7.20 (m, 3H), 4.80 (d, *J* = 14 Hz, 1H), 4.74 (ddd, *J* = 10.3, 7.9, 4.8 Hz, 1H), 4.67 (t, *J* = 5.2 Hz, 1H), 4.43 (d, *J* = 14 Hz, 1H), 4.16 (q, *J* = 7.2 Hz, 2H), 4.12-4.08 (m, 2H), 3.65 (ddd, *J* = 13.5, 6.2, 2.5 Hz, 1H), 3.56 (ddd, *J* = 13.7, 6.8, 2.8 Hz, 1H), 3.36 (s, 3H), 3.29 (s, 3H), 3.29 (dd, *J* = 13.6 Hz, 5.1 Hz, 1H), 3.11 (dd, *J* = 14.0, 10.3 Hz, 1H), 1.24 (t, *J* = 7.2 Hz, 3H). <sup>13</sup>C-NMR (100 MHz, CDCl<sub>3</sub>) δ (ppm): 171.01, 163.08, 136.47, 129.52, 128.55, 127.01, 67.47, 63.29, 61.73, 55.86, 54.42, 53.40, 37.21, 14.11. IR (neat) (cm<sup>-1</sup>): 3345 (m), 3207 (m), 3056 (w), 1741 (s), 1686 (vs), 1547 (s), 1281 (s), 1210 (s), 1177 (s), 1079 (m). ESI-MS (+ve) m/z: Found [M-Br]<sup>+</sup> 323.1959, C<sub>17</sub>H<sub>27</sub>N<sub>2</sub>O<sub>4</sub><sup>+</sup> requires 323.1965.

### 5.2.10 Preparation of IL (331)

1,3-Bis(2-(((*S*)-1-ethoxy-1-oxo-3-phenylpropan-2-yl)amino)-2-oxoethyl)-1H-imidazol-3-ium bromide (**331**).



To a stirred solution of L-phenylalanine ethyl ester α-bromoamide (**337**) (3.260 g, 10.38 mmol) in diethyl ether (25 ml) was added TMS-imidazole (0.715 g, 5.10 mmol). The reaction was stirred at room temperature under an N<sub>2</sub> atmosphere for 24 hours.

After 24 hours a white precipitate of TMS-imidazolium ionic liquid had formed. The diethyl

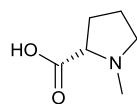
ether was removed *in vacuo* and the white precipitate was rapidly dissolved in ethyl acetate (25 ml). The reaction mixture was then heated under reflux for 24 hours. After 24 hours the reaction was cooled to room temperature and the solvent removed *in vacuo*. The resulting white solid was washed with diethyl ether (3 x 50 ml). Further drying under high vacuum afforded the title compound (**331**) as a white solid in 91% yield, (2.857 g, 4.641 mmol).

Molecular formula: C<sub>29</sub>H<sub>35</sub>BrN<sub>4</sub>O<sub>6</sub>; Molecular weight: 615.525 gmol<sup>-1</sup>; Mp: 102-104°C.

[ $\alpha$ ]<sub>D</sub><sup>20</sup> = +8.20 (1.0 c, CHCl<sub>3</sub>). <sup>1</sup>H-NMR (400 MHz, CDCl<sub>3</sub>)  $\delta$  (ppm): 9.36 (s, 1H), 8.65 (d, *J* = 7.72 Hz, 2H), 7.30-7.17 (m, 12H), 5.28 (d, *J* = 15.6 Hz, 2H), 5.05 (d, *J* = 15.6, 2H), 4.71-4.66 (m, 2H), 4.06 (q, *J* = 7.2 Hz, 4H), 3.20 (dd, *J* = 13.8, 6.0 Hz, 2H), 3.14 (dd, *J* = 13.9, 8.6 Hz, 2H), 1.16 (t, *J* = 7.2 Hz, 6H). <sup>13</sup>C-NMR (100 MHz, CDCl<sub>3</sub>)  $\delta$  (ppm): 171.31, 164.50, 137.63, 129.46, 128.46, 126.91, 122.79, 61.61, 54.72, 51.51, 37.43, 14.01. IR (neat) (cm<sup>-1</sup>): 3336 (w), 3092 (w), 3047 (w), 2988 (w), 2951 (w), 2899 (w), 1732 (vs), 1663 (vs), 1537 (m), 1198 (s), 747 (m), 701 (m). ESI-MS (+ve) m/z: Found [M-Br]<sup>+</sup> 535.2555, C<sub>29</sub>H<sub>35</sub>N<sub>4</sub>O<sub>6</sub><sup>+</sup> requires 535.2551.

## 5.2.11 Preparation of L-prolinium IIs (332-333) and their intermediates (340, 341)

### 5.2.11.1 Preparation of N-methyl-L-proline (340) – General Procedure “D”



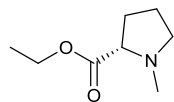
To a stirred solution of L-proline (2.086 g, 18.12 mmol) in methanol (20 ml) was added 40% v/v formaldehyde solution (aq.) 2.2 ml, 22 mmol). The solution was stirred for 30 minutes before 10% Pd/C was added (0.316 g, 2.80 mol%). The reaction was stirred vigorously under a H<sub>2</sub> atmosphere for 48 hours. After 48 hours determination of reaction completion was accomplished by <sup>1</sup>H-NMR in D<sub>2</sub>O. The hydrogen atmosphere was removed and the reaction flask was degassed with a stream of N<sub>2</sub>. The reaction mixture was then filtered over a pad of celite to remove the Pd/C. Solvent was removed *in vacuo* and the crude product was further dried under high vacuum for 48 hours to afford the title compound (**340**) as a white waxy solid in 98% yield (1.390 g, 10.77 mmol).

Molecular formula: C<sub>6</sub>H<sub>11</sub>NO<sub>2</sub>; Molecular weight: 129.159 gmol<sup>-1</sup>.

<sup>1</sup>H-NMR (400 MHz, D<sub>2</sub>O)  $\delta$  (ppm): 4.10 (dd, *J* = 9.4, 7.1 Hz, 1H), 3.72– 3.66 (m, 1H), 3.17– 3.10 (m, 1H), 2.90 (s, 3H), 2.55 – 2.45 (m, 1H), 2.17 – 2.00 (m, 2H), 1.99 – 1.89 (m, 1H). <sup>13</sup>C-NMR (100 MHz, D<sub>2</sub>O)  $\delta$  (ppm): 173.16, 70.05, 56.23, 40.55, 28.55, 22.60

$^1\text{H}$ -NMR and  $^{13}\text{C}$ -NMR was in agreement with the literature.<sup>3</sup>

#### 5.2.11.2 Preparation of *N*-methyl-L-proline ethyl ester (**341**)



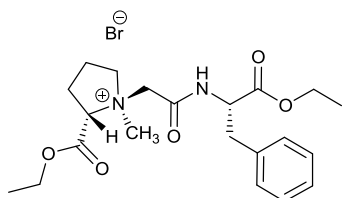
According to the general procedure “A” using *N*-methyl-L-proline (**340**) (1.512 g, 11.71 mmol), ethanol (30 ml) and  $\text{SOCl}_2$  (1.70 ml, 23.4 mmol) the target compound was isolated as a HCl salt. The salt product was stirred in DCM (25 ml) and  $\text{Na}_2\text{CO}_3$  (1.272 g, 12.00 mmol) for 1 hour to neutralise. After 1 hour the reaction mixture was gravity filtered and solvent was removed *in vacuo* to afford the title compound (**341**) as a red oil in 83% yield, (1.283 g, 8.17 mmol).

Molecular formula:  $\text{C}_8\text{H}_{15}\text{NO}_2$ ; Molecular weight:  $157.213 \text{ g mol}^{-1}$ .

$^1\text{H}$ -NMR (400 MHz,  $\text{D}_2\text{O}$ )  $\delta$  (ppm): 4.27 (q,  $J = 7.2 \text{ Hz}$ , 2H), 4.25-4.20 (m, 1H), 3.76-3.66 (m, 1H), 3.24-3.11 (m, 1H), 3.21 (s, 3H), 2.56-2.51 (m, 1H), 2.19-2.12 (m, 2H), 2.03-1.96 (m, 1H), 1.25 (t,  $J = 7.2 \text{ Hz}$ , 3H).  $^{13}\text{C}$ -NMR (100 MHz,  $\text{CDCl}_3$ )  $\delta$  (ppm): 173.78, 67.68, 60.68, 56.41, 40.93, 29.68, 23.10, 14.31.

#### 5.2.11.3 Preparation of **IL** (**332**)

(1*S*,2*S*)-1-({[(2*S*)-1-Ethoxy-1-oxo-3-phenylpropan-2-yl]carbamoyl}methyl)-2-(ethoxycarbonyl)-1-methylpyrrolidin-1-ium bromide (**332**).



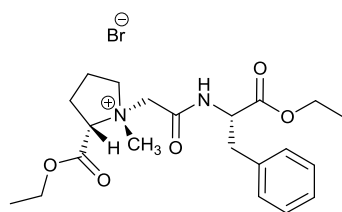
To a stirred solution of L-phenylalanine ethyl ester  $\alpha$ -bromoamide (**337**) (0.564 g, 1.79 mmol) in DMF (5 ml) was added *N*-methyl-L-proline-ethyl ester (**341**) (0.250 g, 1.61 mmol). The reaction was stirred under reflux conditions for 48 hours. After 48 hours the reaction mixture was allowed to cool to room temperature and the DMF was removed *in vacuo*. Analysis by TLC (1:10 MeOH:DCM) showed the presence of two spots separated by 0.05 R<sub>f</sub> and were presumed to be diastereomers of the target compound. The crude product was purified by silica gel chromatography (gradient elution of 5:95 MeOH:DCM to 10:90 MeOH:DCM) to afford the title compound (**332**) as a pale yellow oil in 37% yield (0.281 g, 0.596 mmol).

Molecular formula:  $\text{C}_{21}\text{H}_{31}\text{BrN}_2\text{O}_5$ ; Molecular weight:  $471.392 \text{ g mol}^{-1}$ .

$[\alpha]_D^{20} = -52.9$  (2.5 c, EtOH).  $^1\text{H-NMR}$  (600 MHz,  $\text{CDCl}_3$ )  $\delta$  (ppm): 9.05 (d,  $J = 8.2$  Hz, 1H), 7.38 – 7.37 (m, 2H), 7.23–7.20 (m, 2H), 7.13 – 7.11 (m, 1H), 5.14 (t,  $J = 9.5$  Hz, 1H), 5.04 (d,  $J = 13.2$  Hz, 1H), 4.73 (ddd,  $J = 10.6, 8.1, 4.7$  Hz, 1H), 4.61 (d,  $J = 13.2$  Hz, 1H), 4.21 (qd,  $J = 7.2, 2.1$  Hz, 2H), 4.14–4.09 (m, 3H), 3.26 (dd,  $J = 14.1, 4.8$  Hz, 1H), 3.17–3.14 (m, 1H), 3.15 (s, 3H), 3.06 (dd,  $J = 14.1, 10.7$  Hz, 1H), 2.61–2.59 (m, 1H), 2.21 – 2.10 (m, 2H), 1.98–1.90 (m, 1H), 1.24 (t,  $J = 7.2$  Hz, 3H), 1.18 (t,  $J = 7.2$  Hz, 3H).  $^{13}\text{C-NMR}$  (150 MHz,  $\text{CDCl}_3$ )  $\delta$  (ppm): 170.34, 165.63, 163.13, 136.73, 129.86, 128.46, 126.78, 73.00, 64.26, 63.37, 62.48, 61.73, 54.58, 45.71, 37.12, 24.16, 18.94, 14.15, 14.00. **IR** (neat) ( $\text{cm}^{-1}$ ): 3715 (w), 2981 (b), 1735 (vs), 1678 (vs), 1548 (m), 1454 (m), 1371 (m), 1202 (b), 1020 (m), 700 (s). **ESI-MS** (+ve)  $m/z$ : Found  $[\text{M}-\text{Br}]^+$  391.2230,  $\text{C}_{21}\text{H}_{31}\text{N}_2\text{O}_5^+$  requires 391.2227.

#### 5.2.11.4 Preparation of IL (333)

(1*R*,2*S*)-1-(2-(((*S*)-1-Ethoxy-1-oxo-3-phenylpropan-2-yl)amino)-2-oxoethyl)-2-(ethoxycarbonyl)-1-methylpyrrolidin-1-ium bromide (**333**).



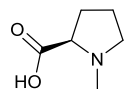
The title compound was isolated during purification of (**332**), as a pale yellow oil in 13% yield (0.099 g, 0.21 mmol).

**Molecular formula:**  $\text{C}_{21}\text{H}_{31}\text{BrN}_2\text{O}_5$ ; **Molecular weight:** 471.392  $\text{g mol}^{-1}$ .

$[\alpha]_D^{20} = -46.7$  (3.0c, EtOH).  $^1\text{H-NMR}$  (400 MHz,  $\text{CDCl}_3$ )  $\delta$  (ppm): 9.49 (d,  $J = 7.4$  Hz, 1H), 7.36 – 7.32 (m, 2H), 7.24 – 7.20 (m, 2H), 7.17 – 7.08 (m, 1H), 5.16 (d,  $J = 13.6$  Hz, 1H), 4.58 – 4.52 (m, 1H), 4.53 – 4.45 (m, 1H), 4.33 (d,  $J = 13.5$  Hz, 1H), 4.23 – 4.14 (m, 2H), 4.12 – 4.03 (m, 2H), 4.03 – 3.95 (m, 1H), 3.88 – 3.80 (m, 1H), 3.51 (s, 3H), 3.19 (dd,  $J = 13.9, 4.7$  Hz, 1H), 3.11 (dd,  $J = 14.0, 10.2$  Hz, 1H), 2.65 – 2.55 (m, 1H), 2.45 – 2.34 (m, 2H), 2.33 – 2.21 (m, 1H), 1.22 (t,  $J = 7.1$  Hz, 3H), 1.15 (t,  $J = 7.1$  Hz, 3H).  $^{13}\text{C-NMR}$  (100 MHz,  $\text{CDCl}_3$ )  $\delta$  (ppm): 170.80, 166.97, 163.70, 136.78, 129.48, 128.51, 126.88, 73.60, 64.96, 63.20, 61.62, 58.75, 55.40, 51.01, 37.28, 26.11, 19.42, 14.13, 13.91. **IR** (neat) ( $\text{cm}^{-1}$ ): 3183 (w), 2981 (b), 1737 (vs), 1682 (s), 1552 (m), 1455 (m), 1372 (w), 1211 (b), 1027 (m), 702 (m). **ESI-MS** (+ve)  $m/z$ : Found  $[\text{M}-\text{Br}]^+$  391.2227,  $\text{C}_{21}\text{H}_{31}\text{N}_2\text{O}_5^+$  requires 391.2227.

## 5.2.12 Preparation of D-prolinium ILs (334-335) and their intermediates (342, 343)

### 5.2.12.1 Preparation of *N*-methyl-D-proline (342)

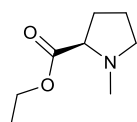


According to the general procedure “C” using D-proline (3.079 g, 26.74 mmol), the title compound (**342**) was isolated as a white crystalline solid in 36% yield, (1.235g, 9.562 mmol).

Molecular formula: C<sub>6</sub>H<sub>11</sub>NO<sub>2</sub>; Molecular weight: 129.159 g mol<sup>-1</sup>.

<sup>1</sup>H-NMR (400 MHz, D<sub>2</sub>O) δ (ppm): 3.84 (dd, *J* = 10.2, 6.9 Hz, 1H), 3.67– 3.61 (m, 1H), 3.10– 3.03 (m, 1H), 2.84 (s, 3H), 2.44 – 2.39 (m, 1H), 2.08– 1.88 (m, 3H). <sup>13</sup>C-NMR (100 MHz, D<sub>2</sub>O) δ (ppm): 173.16, 70.05, 56.23, 40.55, 28.55, 22.60.

### 5.2.12.2 Preparation of *N*-methyl-D-proline ethyl ester (343)



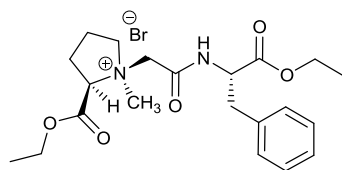
According to the general procedure “A” using *N*-methyl-D-proline (**342**) (1.235 g, 9.562 mmol), ethanol (20 ml), SOCl<sub>2</sub> (0.69 ml, 9.6 mmol) (the title compound (**343**) was isolated as a pale yellow oil in 43% yield, (0.649 g, 4.13 mmol).

Molecular formula: C<sub>8</sub>H<sub>15</sub>NO<sub>2</sub>; Molecular weight: 157.213 g mol<sup>-1</sup>.

<sup>1</sup>H-NMR (400 MHz, CDCl<sub>3</sub>) δ (ppm): 4.21 (q, *J* = 7.2 Hz, 2H), 3.18-3.14 (m, 1H), 2.99-2.96 (m, 1H), 2.42 (s, 3H), 2.34 (dd, *J* = 9.8, 8.8 Hz, 1H), 2.20-2.10 (m, 1H), 2.00-1.88 (m, 2H), 1.84-1.75 (m, 1H), 1.28 (t, *J* = 7.2 Hz, 3H). <sup>13</sup>C-NMR (100 MHz, CDCl<sub>3</sub>) δ (ppm): 173.57, 67.70, 60.87, 56.45, 40.93, 29.72, 23.16, 14.40.

### 5.2.12.3 Preparation of IL (334)

(1*S*,2*R*)-1-(2-(((*S*)-1-Ethoxy-1-oxo-3-phenylpropan-2-yl)amino)-2-oxoethyl)-2-(ethoxycarbonyl)-1-methylpyrrolidin-1-ium bromide (**334**).



To a stirred solution of L-phenylalanine ethyl ester α-bromoamide (**337**) (0.951 g, 3.02 mmol) in ethyl acetate (25 ml) was added *N*-methyl-D-proline-ethyl ester (**343**) (0.475 g, 3.02 mmol). The reaction was stirred under reflux conditions for 48 hours. After 48 hours the reaction was allowed to cool to room temperature and the solvent was removed *in vacuo* to afford a crude product. Analysis by TLC

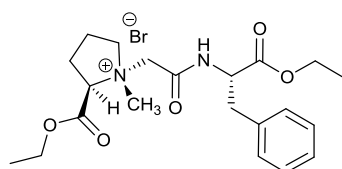
(1:10 MeOH:DCM) showed the presence of two spots separated by 0.05 R<sub>f</sub> and were presumed to be diastereomers. The crude product was purified by silica gel chromatography (gradient elution of 5:95 MeOH:DCM to 10:90 MeOH:DCM) to afford the title compound (**334**) as a pale yellow oil in 25% yield (0.358 g, 0.759 mmol).

Molecular formula: C<sub>21</sub>H<sub>31</sub>BrN<sub>2</sub>O<sub>5</sub>; Molecular weight: 471.392 g mol<sup>-1</sup>.

[α]<sub>D</sub><sup>20</sup> = +1.92 (0.1 c, EtOH). <sup>1</sup>H-NMR (400 MHz, CDCl<sub>3</sub>) δ (ppm): 9.26 (d, *J* = 8.6 Hz, 1H), 7.38 – 7.36 (m, 2H), 7.24 – 7.12 (m, 3H), 4.87 – 4.78 (m, 3H), 4.42 (d, *J* = 14.2 Hz, 1H), 4.20 (qd, *J* = 7.1, 1.7 Hz, 2H), 4.12 (q, *J* = 7.2 Hz, 2H), 3.87 – 3.81 (m, 1H), 3.46 – 3.39 (m, 1H), 3.34 (s, 3H), 3.26 (dd, *J* = 13.8, 4.6 Hz, 1H), 3.04 (dd, *J* = 13.9, 10.9 Hz, 1H), 2.61–2.53 (m, 1H), 2.48 – 2.39 (m, 1H), 2.33 – 2.18 (m, 1H), 2.28 – 2.22 (m, 1H), 1.26 (t, *J* = 7.2 Hz, 3H), 1.21 (t, *J* = 7.3 Hz, 3H). <sup>13</sup>C-NMR (100 MHz, CDCl<sub>3</sub>) δ (ppm): 170.62, 166.69, 163.14, 139.84, 129.72, 128.46, 126.91, 74.30, 64.48, 63.07, 61.66, 58.17, 54.12, 50.51, 37.39, 25.56, 19.40, 14.18, 13.94. IR (neat) (cm<sup>-1</sup>): 3183 (w), 2981 (b), 1737 (vs), 1682 (vs), 1552 (m), 1455 (m), 1372 (w), 1211 (b), 1027 (m), 702 (w). ESI-MS (+ve) m/z: Found [M–Br]<sup>+</sup> 391.2223, C<sub>21</sub>H<sub>31</sub>N<sub>2</sub>O<sub>5</sub><sup>+</sup> requires 391.2227.

#### 5.2.12.4 Preparation of IL (**335**)

(1*R*,2*R*)-1-(2-(((*S*)-1-Ethoxy-1-oxo-3-phenylpropan-2-yl)amino)-2-oxoethyl)-2-(ethoxycarbonyl)-1-methylpyrrolidin-1-ium bromide (**335**).



The title compound (**335**), was isolated during purification of (**334**), as a pale yellow oil in 34% yield (0.486 g, 1.03 mmol).

Molecular formula: C<sub>21</sub>H<sub>31</sub>BrN<sub>2</sub>O<sub>5</sub>; Molecular weight: 471.392 g mol<sup>-1</sup>.

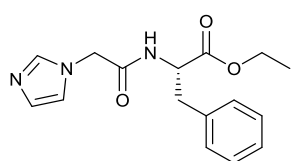
[α]<sub>D</sub><sup>20</sup> = +1.86 (1.0 c, EtOH). <sup>1</sup>H-NMR (400 MHz, CDCl<sub>3</sub>) δ (ppm): 9.28 (d, *J* = 7.3 Hz, 1H), 7.43 – 7.41 (m, 2H), 7.30 – 7.27 (m, 2H), 7.22–7.21 (m, 1H), 5.32 (d, *J* = 13.1 Hz, 1H), 5.11 (t, *J* = 9.5 Hz, 1H), 4.62 (ddd, *J* = 10.4, 7.4, 4.8 Hz, 1H), 4.48–4.43 (m, 1H), 4.42 (d, *J* = 13.0 Hz, 1H), 4.27 (qd, *J* = 7.2, 1.3 Hz, 2H), 4.16 (qd, *J* = 7.2, 2.7 Hz, 2H), 3.86–3.79 (m, 1H), 3.31 – 3.28 (m, 1H), 3.26 (s, 3H), 3.13 (dd, *J* = 14.0, 10.4 Hz, 1H), 2.72–2.63 (m, 1H), 2.39 – 2.31 (m, 1H), 2.28–2.21 (m, 1H), 2.13–2.02 (m, 1H), 1.30 (t, *J* = 7.1 Hz, 3H), 1.23 (t, *J* = 7.1 Hz, 3H). <sup>13</sup>C-NMR (100 MHz, CDCl<sub>3</sub>) δ (ppm): 170.57, 165.61, 163.38, 136.61, 129.62, 128.56, 126.92,

73.41, 64.84, 63.39, 62.64, 61.66, 55.23, 45.47, 36.82, 24.24, 18.97, 14.16, 14.01. IR (neat) (cm<sup>-1</sup>): 3175 (w), 2981 (b), 1737 (vs), 1678 (vs), 1548 (m), 1545 (m), 1371 (w), 1202 (b), 1020 (s), 700 (w). ESI-MS (+ve) m/z: Found [M-Br<sup>-</sup>]<sup>+</sup> 391.2215, C<sub>21</sub>H<sub>31</sub>N<sub>2</sub>O<sub>5</sub><sup>+</sup> requires 391.2227.

### 5.3 Experimental preparation of Chapter 2 L-phenylalanine tertiary amino compounds

#### 5.3.1 Preparation of tertiary amine (344)

Ethyl (2-(1*H*-imidazol-1-yl)acetyl)-L-phenylalaninate (**344**).



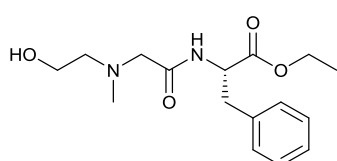
To a stirred solution of L-phenylalanine ethyl ester  $\alpha$ -bromoamide (**337**) (1.010 g, 3.215 mmol) in diethyl ether (20 ml) was added TMS-imidazole (0.321 g, 2.29 mmol). The reaction was stirred at room temperature under an N<sub>2</sub> atmosphere for 24 hours. After 24 hours a white precipitate of TMS-imidazolium ionic liquid had formed. Diethyl ether was removed *in vacuo* and the white precipitate was dissolved in 5 ml of water and stirred for 30 minutes to facilitate the removal of the TMS group. Water was removed *in vacuo* and the resulting crude product was purified by silica gel chromatography (eluent 10:90 MeOH:DCM) to afford the title compound (**344**) as a pale yellow oil in 55% yield, (0.383g, 1.27 mmol).

Molecular formula: C<sub>16</sub>H<sub>19</sub>N<sub>3</sub>O<sub>3</sub>; Molecular weight: 301.346gmol<sup>-1</sup>.

$[\alpha]_D^{20} = +19.6$  (2.0 c, CHCl<sub>3</sub>). <sup>1</sup>H-NMR (400 MHz, CDCl<sub>3</sub>)  $\delta$  (ppm): 7.42 (s, 1H), 7.29 – 7.26 (m, 3H), 7.11 (s, 1H), 6.98 – 6.95 (m, 2H), 6.81 (s, 1H), 5.84 (d, *J* = 7.9 Hz, 1H), 4.82-4.77 (m, 1H), 4.61 (d, *J* = 17.2 Hz, 1H), 4.56 (d, *J* = 17.7 Hz, 1H), 4.16 (q, *J* = 7.1 Hz, 2H), 3.12 (dd, *J* = 13.9, 5.7 Hz, 1H), 3.00 (dd, *J* = 14.0, 6.5 Hz, 1H), 1.24 (t, *J* = 7.1 Hz, 3H). <sup>13</sup>C-NMR (100 MHz, CDCl<sub>3</sub>)  $\delta$  (ppm): 170.81, 166.40, 137.50, 135.31, 130.94, 129.14, 128.86, 127.47, 119.58, 61.92, 53.11, 50.00, 37.56, 14.18. IR (neat) (cm<sup>-1</sup>): 3202 (w), 2982 (b), 1735 (s), 1673 (s), 1548 (m), 1509 (m), 1454 (w), 1372 (w), 1199 (b), 1107 (s), 1079 (s), 1030 (s), 744 (s), 701 (s). ESI-MS (+ve) m/z: Found [M+H]<sup>+</sup> 302.1493, C<sub>16</sub>H<sub>20</sub>N<sub>3</sub>O<sub>3</sub><sup>+</sup> requires 302.1499.

#### 5.3.2 Preparation of tertiary amine (345)

Ethyl *N*-(2-hydroxyethyl)-*N*-methylglycyl-L-phenylalaninate (**345**).



To a stirred solution of L-phenylalanine ethyl ester  $\alpha$ -bromoamide (**337**) (0.505 g, 1.60 mmol) in diethyl ether (25 ml)

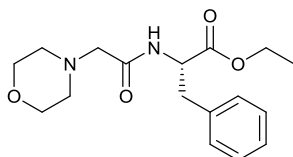
was added 2-(methylamino)ethanol (115  $\mu$ l, 1.43 mmol). The reaction was stirred at room temperature under an N<sub>2</sub> atmosphere for 24 hours. After 24 hours a waxy precipitate had formed. The supernatant was decanted and the waxy crude product was purified by silica gel chromatography (gradient elution of 1:99 MeOH:DCM to 5:95 MeOH:DCM) to afford the title compound (**345**) as a pale yellow oil in 34% yield, (0.148 g, 0.48 mmol).

Molecular formula: C<sub>16</sub>H<sub>24</sub>N<sub>2</sub>O<sub>4</sub>; Molecular weight: 308.378 gmol<sup>-1</sup>.

$[\alpha]_D^{20} = +29.1$  (0.9 c, CHCl<sub>3</sub>). <sup>1</sup>H-NMR (400 MHz, CDCl<sub>3</sub>)  $\delta$  (ppm): 7.74 (d,  $J = 8.8$  Hz, 1H) 7.29-7.22 (m, 3H), 7.14-7.12 (m, 2H), 4.86 (ddd,  $J = 8.7, 7.0, 6.1$  Hz, 1H), 4.15 (q,  $J = 7.2$  Hz, 2H), 3.63 – 3.49 (m, 2H), 3.15 (dd,  $J = 13.9, 5.9$  Hz, 1H), 3.07 (dd,  $J = 14.0, 6.8$  Hz, 1H), 3.05 (d,  $J = 16.7$  Hz, 1H), 2.99 (d,  $J = 16.9$  Hz, 1H), 2.56-2.46 (m, 2H), 2.35 (bs, 1H), 2.28 (s, 3H), 1.22 (t,  $J = 7.2$  Hz, 3H). <sup>13</sup>C-NMR (100 MHz, CDCl<sub>3</sub>)  $\delta$  (ppm): 172.46, 170.78, 136.06, 129.22, 128.57, 127.15, 61.73, 61.24, 60.07, 59.61, 52.54, 43.50, 37.90, 14.09. IR (neat) (cm<sup>-1</sup>): 3298 (b), 2939 (w), 1737 (s), 1656 (vs), 1517 (s), 1455 (m), 1373 (w), 1199 (b), 1129 (w), 1079 (w), 1040 (m), 746 (m), 702 (s). ESI-MS (+ve) m/z: Found [M+H]<sup>+</sup> 309.1809, C<sub>16</sub>H<sub>25</sub>N<sub>2</sub>O<sub>4</sub><sup>+</sup> requires 309.1809

### 5.3.3 Preparation of tertiary amine (**346**)

Ethyl (2-morpholinoacetyl)-L-phenylalaninate (**346**).



To a stirred solution of L-phenylalanine ethyl ester  $\alpha$ -bromoamide (**337**) (1.073 g, 3.415 mmol) in THF (50 ml) was added morpholine (280  $\mu$ l, 3.25 mmol). The reaction was stirred under reflux conditions for 24 hours. After 24 hours the reactions was allowed to cool to room temperature and solid Na<sub>2</sub>CO<sub>3</sub> (0.371 g, 3.50 mmol) was added to the reaction and stirred vigorously for 1 hour. After one hour the Na<sub>2</sub>CO<sub>3</sub> was removed by gravity filtration and the solvent was removed *in vacuo*. The crude product was purified by silica gel chromatography (eluent 50:50 ethyl acetate:hexane) to afford the title compound (**346**) as a brown oil in 56% yield, (0.587 g, 1.83 mmol).

Molecular formula: C<sub>17</sub>H<sub>24</sub>N<sub>2</sub>O<sub>4</sub>; Molecular weight: 320.389 gmol<sup>-1</sup>

$[\alpha]_D^{20} = +15.4$  (1.0 c, CHCl<sub>3</sub>). <sup>1</sup>H-NMR (400 MHz, CDCl<sub>3</sub>)  $\delta$  (ppm): 7.56 (bs, 1H), 7.30-7.21 (m, 3H), 7.14-7.13 (m, 2H), 4.85 (ddd,  $J = 8.4, 6.9, 5.7$  Hz, 1H), 4.17 (q,  $J = 7.2$  Hz, 2H), 3.58 (m, 3.61-3.54, 4H), 3.19 (dd,  $J = 14.0, 5.7$  Hz, 1H), 3.10 (dd,  $J = 14.0, 7.0$  Hz, 1H), 3.02-2.92 (m, 2H), 2.46 (s, 2H), 2.34 (s, 2H), 1.25 (t,  $J = 7.2$  Hz, 3H). <sup>13</sup>C-NMR (100 MHz, CDCl<sub>3</sub>)  $\delta$

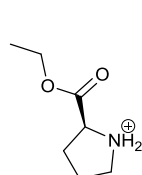


(ppm): 171.68, 136.09, 129.29, 128.74, 127.29, 66.90, 61.66, 53.61, 52.46, 37.77, 14.26. IR (neat) (cm<sup>-1</sup>): 3344 (w), 2962 (w), 2856 (w), 2822 (w), 1737 (s), 1676 (s), 1507 (s), 1454 (m), 1373 (w), 1190 (b), 1114 (vs), 1032 (m), 865 (m), 747 (vs), 700 (m). ESI-MS (+ve) m/z: Found [M+H]<sup>+</sup> 321.1809, C<sub>17</sub>H<sub>25</sub>N<sub>2</sub>O<sub>4</sub><sup>+</sup> requires 321.1809.

### 5.3.4 Preparation of tertiary amine (347)

#### 5.3.4.1 Preparation of L-proline ethyl ester hydrochloride (338)

L-proline ethyl ester hydrochloride (**338**).



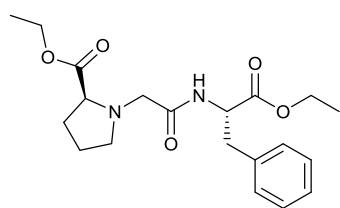
According to the general procedure “A”, using L-proline (5.011g, 43.52 mmol), the title compound (**338**) was isolated as a pale yellow oil in 99% yield, (7.751 g, 43.15 mmol).

Molecular formula: C<sub>7</sub>H<sub>14</sub>ClNO<sub>2</sub>; Molecular weight: 179.644 gmol<sup>-1</sup>.

<sup>1</sup>H-NMR (400 MHz, D<sub>2</sub>O) δ (ppm): 4.43 (dd, *J* = 8.7, 7.2 Hz, 1H), 4.26 (q, *J* = 7.2 Hz, 2H), 3.44-3.32 (m, 2H), 2.44-2.35 (m, 1H), 2.20 – 2.08 (m, 1H), 2.06-1.98 (m, 2H), 1.25 (t, *J* = 7.2 Hz, 3H). <sup>13</sup>C-NMR (100 MHz, D<sub>2</sub>O) δ (ppm): 168.59, 62.38, 58.15, 44.86, 26.91, 22.00, 14.10. <sup>1</sup>H-NMR and <sup>13</sup>C-NMR were in agreement with the literature.<sup>4</sup>

#### 5.3.4.2 Preparation of tertiary amine (347)

Ethyl (2-(((S)-1-Ethoxy-1-oxo-3-phenylpropan-2-yl)amino)-2-oxoethyl)-L-prolinate (**347**).



To a stirred solution of L-phenylalanine ethyl ester α-bromoamide (**337**) (0.581 g, 1.85 mmol) in THF (10 ml) was added L-proline ethyl ester hydrochloride (**338**) (0.302 g, 1.68 mmol) and solid Na<sub>2</sub>CO<sub>3</sub> (0.356g, 3.36 mmol). The reaction mixture was stirred at room temperature for 24 hours. After 24 hours the Na<sub>2</sub>CO<sub>3</sub> was removed by gravity filtration and the solvent was removed *in vacuo*. The crude product was purified by silica gel chromatography (eluent 50:50 ethyl acetate:hexane) to afford the title compound (**347**) as a yellow oil in 53% yield, (0.334 g, 0.887 mmol).

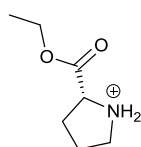
Molecular formula: C<sub>20</sub>H<sub>28</sub>N<sub>2</sub>O<sub>5</sub>; Molecular weight: 376.453 gmol<sup>-1</sup>.

$[\alpha]_D^{20} = -6.2$  (2.0 c,  $\text{CHCl}_3$ ).  $^1\text{H-NMR}$  (400 MHz,  $\text{CDCl}_3$ )  $\delta$  (ppm): 7.87 (d,  $J = 8.4$  Hz, 1H), 7.31 – 7.27 (m, 1H), 7.26 – 7.15 (m, 4H), 4.88-4.82 (m, 1H), 4.14 (q,  $J = 7.2$  Hz, 4H), 3.43-3.39 (m, 2H), 3.15-3.09 (m, 4H), 2.41 (dd,  $J = 8.0, 7.6$  Hz, 1H), 2.41 (dd,  $J = 16.6, 7.9$  Hz, 1H), 1.97-1.92 (m, 1H), 1.84-1.79 (m, 2H), 1.24 (t,  $J = 7.2$  Hz, 3H), 1.21 (t,  $J = 7.2$  Hz, 3H).  $^{13}\text{C-NMR}$  (100 MHz,  $\text{CDCl}_3$ )  $\delta$  (ppm): 173.79, 171.62, 170.76, 136.21, 129.35, 128.45, 126.96, 65.40, 61.28, 60.76, 57.67, 54.07, 52.68, 38.07, 29.59, 23.92, 14.29, 14.10. IR (neat) ( $\text{cm}^{-1}$ ): 3340 (w), 2980 (w), 1733 (s), 1679 (s), 1509 (m), 1454 (w), 1372 (w), 1187 (b), 1027 (m), 746 (w), 701 (m). ESI-MS (+ve) m/z: Found  $[\text{M}+\text{H}]^+$  377.2067,  $\text{C}_{20}\text{H}_{29}\text{N}_2\text{O}_5^+$  requires 377.2071.

### 5.3.5 Preparation of tertiary amine (348)

#### 5.3.5.1 Preparation of D-proline ethyl ester hydrochloride (339)

D-proline ethyl ester hydrochloride (**339**).



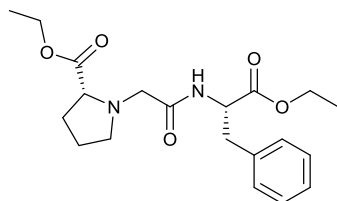
According to the general procedure “A” using D-proline (1.897 g, 16.48 mmol), the title compound (**339**) was isolated as a pale yellow oil in 99% yield, (2.194 g, 16.31 mmol).

Molecular formula:  $\text{C}_7\text{H}_{14}\text{ClNO}_2$ ; Molecular weight:  $179.644 \text{ g mol}^{-1}$ .

$^1\text{H-NMR}$  (400 MHz,  $\text{CDCl}_3$ )  $\delta$  (ppm): 10.26 (bs, 1H), 8.91 (bs, 1H), 4.48-4.42 (m, 1H), 4.23 (q,  $J = 7.1$  Hz, 2H), 3.59-3.45 (m, 2H), 2.43-2.34 (m, 1H), 2.16-1.98 (m, 3H), 1.27 (t,  $J = 7.2$  Hz, 3H).

#### 5.3.5.2 Preparation of tertiary amine (348)

Ethyl (2-(((S)-1-Ethoxy-1-oxo-3-phenylpropan-2-yl)amino)-2-oxoethyl)-D-prolinate (**348**).



To a stirred solution of L-phenylalanine ethyl ester  $\alpha$ -bromoamide (**337**) (0.803 g, 2.55 mmol) in THF (25 ml) was added D-proline ethyl ester hydrochloride of (**339**) (0.454 g, 2.53 mmol) and triethylamine (0.78 ml, 5.6 mmol) dropwise. The reaction mixture was stirred under reflux conditions for 48 hours.

After 48 hours the reaction mixture was cooled to room temperature and the triethylamine hydrobromide salts that had precipitated were removed by gravity filtration. Solvent was removed *in vacuo* and the crude product was purified by silica gel chromatography (eluent

50:50 ethyl acetate:hexane) to afford the title compound (**348**) as a yellow oil in 58% yield, (0.556 g, 1.48 mmol).

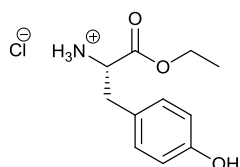
Molecular formula: C<sub>20</sub>H<sub>28</sub>N<sub>2</sub>O<sub>5</sub>; Molecular weight: 376.453 gmol<sup>-1</sup>.

$[\alpha]_D^{20} = +22.6$  (1.0 c, CHCl<sub>3</sub>). <sup>1</sup>H-NMR (400 MHz, CDCl<sub>3</sub>)  $\delta$  (ppm): 7.83 (d,  $J = 8.2$  Hz, 1H), 7.28-7.16 (m, 5H), 4.80 (td,  $J = 7.8, 5.7$  Hz, 1H), 4.17 (q,  $J = 7.2$  Hz, 2H), 4.14 (q,  $J = 7.1$  Hz, 2H), 3.39 (d,  $J = 16.7$  Hz, 1H), 3.37 (dd,  $J = 9.0, 5.1$  Hz, 1H), 3.21 (dd,  $J = 13.9, 5.7$  Hz, 1H), 3.11 (d,  $J = 16.8$  Hz, 1H), 3.06 (dd,  $J = 13.8, 7.6$  Hz, 1H), 2.79 (ddd,  $J = 8.9, 6.3, 5.0$  Hz, 1H), 2.42 (dd,  $J = 16.6, 7.8$  Hz, 1H), 2.15 – 2.08 (m, 1H), 1.97– 1.89 (m, 1H), 1.80 – 1.73 (m, 2H), 1.23 (t,  $J = 7.1$  Hz, 3H), 1.22 (t,  $J = 7.2$  Hz, 3H). <sup>13</sup>C-NMR (100 MHz, CDCl<sub>3</sub>)  $\delta$  (ppm): 174.08, 171.55, 171.06, 136.48, 129.36, 128.56, 127.06, 65.70, 61.40, 60.96, 57.94, 54.24, 52.98, 37.98, 29.78, 24.18, 14.31, 14.22. IR (neat) (cm<sup>-1</sup>): 3342 (w), 2980 (w), 1732 (s), 1675 (s), 1511 (m), 1454 (w), 1373 (w), 1182 (b), 1026 (m), 748 (s), 700 (m). ESI-MS (+ve) m/z: Found [M+H]<sup>+</sup> 377.2066, C<sub>20</sub>H<sub>29</sub>N<sub>2</sub>O<sub>5</sub><sup>+</sup> requires 377.2071.

## 5.4 Experimental preparation of Chapter 2 L-tyrosine ILs

### 5.4.1 Preparation of Chapter 2 L-tyrosine ethyl ester (**354**) and alkylating reagents (**355-356**)

#### 5.4.1.1 Preparation of L-Tyrosine ethyl ester hydrochloride (**354**).



According to the general procedure “A”, using L-tyrosine (9.882 g, 54.54 mmol), the title compound (**354**) was isolated as a white solid in 87% yield, (11.71 g, 47.67 mmol).

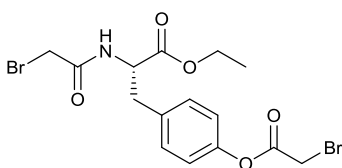
Molecular formula: C<sub>11</sub>H<sub>16</sub>ClNO<sub>3</sub>; Molecular weight: 245.703 gmol<sup>-1</sup>.

<sup>1</sup>H-NMR (400 MHz, DMSO)  $\delta$  (ppm): 9.46 (s, 1H), 8.52 (s, 3H), 7.02 (d,  $J = 8.5$  Hz, 2H), 6.72 (d,  $J = 8.5$  Hz, 2H), 4.16 – 4.09 (m, 3H), 3.07 (dd,  $J = 14.1, 5.8$  Hz, 1H), 2.96 (dd,  $J = 14.1, 7.3$  Hz, 1H), 1.13 (t,  $J = 7.1$  Hz, 3H).

<sup>1</sup>H-NMR was in agreement with the literature.<sup>5</sup>

#### 5.4.1.2 Preparation of alkylating reagent (355).

Ethyl (S)-2-(2-bromoacetamido)-3-(4-(2-bromoacetoxymethyl)phenyl)propanoate (**355**).

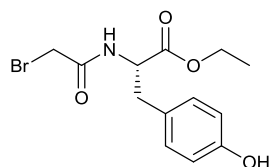


The title compound (**355**) was isolated from an over acylated preparation of (**356**), by silica gel chromatography (eluent 50:50 ethyl acetate:hexane) to afford compound (**355**) as a white solid in 5% yield (0.056 g, 0.12 mmol).

Molecular formula: C<sub>15</sub>H<sub>17</sub>Br<sub>2</sub>NO<sub>5</sub>; Molecular weight: 451.111 g mol<sup>-1</sup>; Mp: 101-103 °C.

$[\alpha]_D^{20} = +33.1$  (1.0 c, CHCl<sub>3</sub>). <sup>1</sup>H-NMR (400 MHz, CDCl<sub>3</sub>)  $\delta$  (ppm): 7.17 (d,  $J = 8.6$  Hz, 2H), 7.07 (d,  $J = 8.5$  Hz, 2H), 6.87 (d,  $J = 7.8$  Hz, 1H), 4.82 (dt,  $J = 7.8, 5.9$  Hz, 1H), 4.19 (q,  $J = 7.2$  Hz, 2H), 4.05 (s, 2H), 3.87 (d,  $J = 13.6$  Hz, 1H), 3.83 (d,  $J = 13.6$  Hz, 1H), 3.18 (dd,  $J = 13.8, 5.9$  Hz, 1H), 3.13 (dd,  $J = 13.9, 5.7$  Hz, 1H), 1.25 (t,  $J = 7.2$  Hz, 3H). <sup>13</sup>C-NMR (100 MHz, CDCl<sub>3</sub>)  $\delta$  (ppm): 170.79, 165.87, 165.27, 149.72, 133.83, 130.62, 133.83, 130.62, 121.39, 62.06, 53.79, 37.30, 28.80, 25.67, 14.24. IR (neat) (cm<sup>-1</sup>): 3426(m), 3303(m), 1721(s), 1672 (s), 1519 (m), 1227 (vs), 1199 (vs), 1101 (m), 822 (w). ESI-MS (+ve) m/z: Found [M+H]<sup>+</sup> 449.9550, C<sub>15</sub>H<sub>18</sub>Br<sub>2</sub>NO<sub>5</sub><sup>+</sup> requires 449.9546.

#### 5.4.1.3 Preparation of ethyl (2-bromoacetyl)-L-tyrosinate (356).



To a stirred solution of L-tyrosine ethyl ester hydrochloride (**354**), (3.648 g, 14.85 mmol), in DCM (50 ml) was added solid Na<sub>2</sub>CO<sub>3</sub> (3.462 g, 32.66 mmol). The reaction mixture was stirred vigorously for one hour to neutralise the L-tyrosine hydrochloride salt. The reaction mixture was then cooled to 0 °C and bromoacetyl bromide was added dropwise (2.6 ml, 30 mmol). The reaction mixture was allowed to warm to room temperature and stirred for 12 hours. After 12 hours the Na<sub>2</sub>CO<sub>3</sub> and other salts were removed by gravity filtration. The DCM layer was washed with saturated sodium bicarbonate solution (3 x 50 ml), dried over anhydrous magnesium sulphate and gravity filtered. TLC at this point (50:50 ethyl acetate: hexane) showed that over-acylation had occurred as expected on the *O*-position of the phenol side chain. The DCM was removed *in vacuo* and the solid crude product was dissolved in ethanol (10 ml) and acidified to pH 1 using conc. HCl. The solution was stirred for 24 hours until TLC showed the complete hydrolysis of the phenolic ester and the ethyl ester remaining intact. Precipitation of

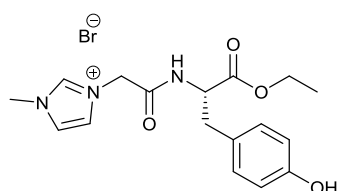
the product by dropwise addition of hexane afforded the title compound (**356**) as a white solid in 54% yield (4.337 g, 13.14 mmol).

Molecular formula: C<sub>13</sub>H<sub>16</sub>BrNO<sub>4</sub>; Molecular weight: 330.178 gmol<sup>-1</sup>; Mp: 111-113° C.

[ $\alpha$ ]<sub>D</sub><sup>20</sup> = +20.9 (1.0 c, CHCl<sub>3</sub>). <sup>1</sup>H-NMR (400 MHz, CDCl<sub>3</sub>)  $\delta$  (ppm): 6.99 (d, *J* = 8.5 Hz, 2H), 6.88 (d, *J* = 8.0 Hz, 1H), 6.74 (d, *J* = 8.5 Hz, 2H), 5.35 (s, 1H), 4.79 (dt, *J* = 8.0, 5.8 Hz, 1H), 4.20 (q, *J* = 7.1 Hz, 2H), 3.87 (d, *J* = 13.7 Hz, 1H), 3.83 (d, *J* = 13.7 Hz, 1H), 3.10 (dd, *J* = 14.1, 5.7 Hz, 1H), 3.04 (dd, *J* = 14.0, 5.9 Hz, 1H), 1.28 (t, *J* = 7.1 Hz, 3H). <sup>13</sup>C-NMR (100 MHz, CDCl<sub>3</sub>)  $\delta$  (ppm): 171.26, 165.51, 155.24, 130.76, 127.40, 115.78, 62.11, 54.11, 37.23, 28.95, 14.40. IR (neat) (cm<sup>-1</sup>): 3300(b), 1734(s), 1646 (s), 1547 (m), 1268 (m), 1194 (vs), 1101 (s), 1019 (m), 932 (w), 851 (w). ESI-MS (+ve) m/z: Found [M+H]<sup>+</sup> 330.0334, C<sub>13</sub>H<sub>17</sub>BrNO<sub>4</sub><sup>+</sup> requires 330.0335.

#### 5.4.2 Preparation of IL (**349**) – General Procedure “E”

(*S*)-3-(2-((1-Ethoxy-3-(4-hydroxyphenyl)-1-oxopropan-2-yl)amino)-2-oxoethyl)-1-methyl-1H-imidazol-3-ium bromide (**349**).



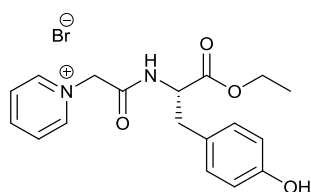
To a stirred solution of L-tyrosine ethyl ester  $\alpha$ -bromoamide (**356**) (0.504 g, 1.53 mmol) in ethyl acetate (50 ml) was added 1-methylimidazole (0.12 ml, 1.5 mmol). The reaction was stirred under reflux conditions for 24 hours. After 24 hours the reaction was allowed to cool to room temperature and the solvent was removed *in vacuo* to afford a crude product. The crude product was washed with diethyl ether (3 x 50 ml) to afford the title compound (**349**) as a white solid in 83% yield, (0.514 g, 1.25 mmol).

Molecular formula: C<sub>17</sub>H<sub>22</sub>BrN<sub>3</sub>O<sub>4</sub>; Molecular weight: 412.284 gmol<sup>-1</sup>; Mp: 38-40° C.

[ $\alpha$ ]<sub>D</sub><sup>20</sup> = +9.8 (0.6 c, EtOH). <sup>1</sup>H-NMR (400 MHz, DMSO)  $\delta$  (ppm): 9.30 (s, 1H), 9.08 (s, 1H), 8.98 (d, *J* = 7.5 Hz, 1H), 7.69 (t, *J* = 1.8 Hz, 1H), 7.63 (t, *J* = 1.8 Hz, 1H), 6.99 (d, *J* = 8.4 Hz, 2H), 6.68 (d, *J* = 8.4 Hz, 2H), 5.05 (d, *J* = 16.6 Hz, 1H), 5.00 (d, *J* = 16.8 Hz, 1H), 4.43 – 4.38 (m, 1H), 4.07 – 4.01 (m, 2H), 3.88 (s, 3H), 2.91 (dd, *J* = 13.8, 6.2 Hz, 1H), 2.83 (dd, *J* = 13.8, 8.2 Hz, 1H), 1.10 (t, *J* = 7.1 Hz, 3H). <sup>13</sup>C-NMR (100 MHz, DMSO)  $\delta$  (ppm): 171.07, 165.04, 156.16, 137.71, 130.10, 126.57, 123.67, 123.00, 115.12, 60.68, 54.42, 50.29, 36.17, 35.82, 13.97.

### 5.4.3 Preparation of IL (350)

(S)-1-(2-((1-Ethoxy-3-(4-hydroxyphenyl)-1-oxopropan-2-yl)amino)-2-oxoethyl)pyridin-1-ium bromide (**350**).



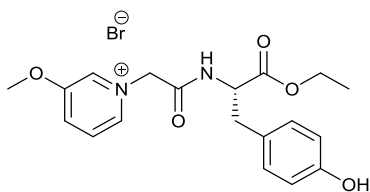
According to the general procedure “E”, using pyridine (250  $\mu$ l, 3.16 mmol), alkylating reagent (**356**) (1.065 g, 3.226 mmol) and ethyl acetate (50 mL), the title compound (**350**) was isolated as a white solid in 99% yield, (1.290 g, 3.152 mmol).

Molecular formula:  $C_{18}H_{21}BrN_2O_4$ ; Molecular weight: 409.280  $g\text{mol}^{-1}$ ; Mp: 30-32° C.

$[\alpha]_D^{20} = +15.4$  (1.0 c,  $CHCl_3$ ).  $^1H$ -NMR (400 MHz, DMSO)  $\delta$  (ppm): 9.30 (s, 1H), 9.19 (d,  $J = 7.5$  Hz, 1H), 8.92 (d,  $J = 5.3$  Hz, 2H), 8.66 (t,  $J = 7.8$  Hz, 1H), 8.17 (d,  $J = 7.1$  Hz, 1H), 7.01 (d,  $J = 8.5$  Hz, 2H), 6.68 (d,  $J = 8.4$  Hz, 2H), 5.52 (d,  $J = 16.0$  Hz, 2H), 5.48 (d,  $J = 16.1$  Hz, 1H), 4.45 – 4.40 (m, 1H), 4.07 – 3.99 (m, 2H), 2.91 (dd,  $J = 13.9, 6.5$  Hz, 1H), 2.86 (dd,  $J = 13.8, 7.8$  Hz, 1H), 1.09 (t,  $J = 7.1$  Hz, 3H).  $^{13}C$ -NMR (100 MHz, DMSO)  $\delta$  (ppm): 171.86, 165.44, 156.19, 146.22, 146.19, 130.15, 127.54, 126.43, 115.14, 61.32, 60.72, 54.53, 36.31, 13.95. IR (neat) ( $cm^{-1}$ ): 3197 (b), 3052 (b), 1732 (m), 1683 (s), 1514 (s), 1201 (bs), 1112 (m), 1021 (m), 853 (m). ESI-MS (+ve) m/z: Found  $[M-Br]^{+}$  329.1501,  $C_{18}H_{21}N_2O_4^{+}$  requires 329.1496.

### 5.4.4 Preparation of IL (351)

(S)-1-(2-((1-Ethoxy-3-(4-hydroxyphenyl)-1-oxopropan-2-yl)amino)-2-oxoethyl)-3-methoxypyridin-1-ium bromide (**351**).



According to the general procedure “E”, using 3-methoxy pyridine (280  $\mu$ l, 2.88 mmol), alkylating reagent (**356**) (0.973 g, 2.95 mmol) and ethyl acetate (50 mL), the title compound (**351**) was isolated as a white solid in 99% yield, (1.251 g, 2.848 mmol).

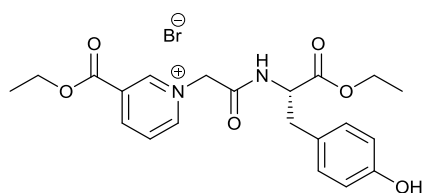
Molecular formula:  $C_{19}H_{23}BrN_2O_5$ ; Molecular weight: 439.306  $g\text{mol}^{-1}$ ; Mp: 117-119 °C.

$[\alpha]_D^{20} = +12.7$  (1.0 c,  $CHCl_3$ ).  $^1H$ -NMR (400 MHz, MeOD)  $\delta$  (ppm): 8.67 (dd,  $J = 2.7, 1.3$  Hz, 1H), 8.44 (d,  $J = 6.0$  Hz, 1H), 8.25 (ddd,  $J = 8.8, 2.6, 0.9$  Hz, 1H), 8.03 (dd,  $J = 8.9, 5.9$  Hz, 1H), 7.09 (d,  $J = 8.5$  Hz, 2H), 6.74 (d,  $J = 8.5$  Hz, 2H), 5.48 (d,  $J = 16.3$  Hz, 1H), 5.43 (d,  $J = 15.8$  Hz, 1H), 4.68 (dd,  $J = 8.7, 5.8$  Hz, 1H), 4.18 (q,  $J = 7.1$  Hz, 2H), 4.08 (s, 3H), 3.13 (dd,  $J = 14.0, 5.8$  Hz, 1H), 2.95 (dd,  $J = 14.0, 8.7$  Hz, 1H), 1.25 (t,  $J = 7.2$  Hz, 3H).  $^{13}C$ -NMR (100

MHz, DMSO)  $\delta$  (ppm): 172.66, 165.71, 159.97, 157.53, 139.52, 134.89, 132.38, 131.33, 129.21, 128.24, 116.26, 63.01, 62.57, 58.08, 56.03, 37.77, 14.36. IR (neat) (cm<sup>-1</sup>): 3196 (b), 3038 (b), 1731 (m), 1682 (m), 1509 (s), 1201 (bs), 1112 (m), 1012 (m), 826 (w). ESI-MS (+ve) m/z: Found [M-Br]<sup>+</sup> 359.1607, C<sub>19</sub>H<sub>23</sub>N<sub>2</sub>O<sub>5</sub><sup>+</sup> requires 359.1601.

#### 5.4.5 Preparation of IL (352)

(*S*)-1-(2-((1-Ethoxy-3-(4-hydroxyphenyl)-1-oxopropan-2-yl)amino)-2-oxoethyl)-3-(ethoxycarbonyl)pyridin-1-ium bromide (**352**).

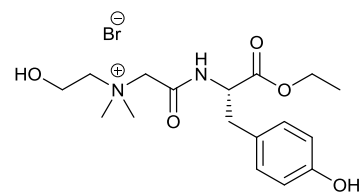


The target compound was synthesised according to the general procedure “E”, using ethyl nicotinate (0.40 ml, 2.98 mmol), alkylating reagent (**356**) (1.004 g, 3.041 mmol) and ethyl acetate (50 mL) to give a crude product as a brown solid. The crude product was purified by silica gel chromatography (eluent 5:95 MeOH:DCM) to afford the title compound (**352**) as an orange solid in 71% yield, (1.016 g, 2.111 mmol).

Molecular formula: C<sub>21</sub>H<sub>25</sub>BrN<sub>2</sub>O<sub>6</sub>; Molecular weight: 481.343 gmol<sup>-1</sup>; Mp: 53-55° C.

$[\alpha]_D^{20} = +9.0$  (1.0 c, CHCl<sub>3</sub>). <sup>1</sup>H-NMR (400 MHz, CDCl<sub>3</sub>)  $\delta$  (ppm): 9.34 (s, 1H), 9.21 (d, *J* = 6.1 Hz, 1H), 8.86 (d, *J* = 8.2 Hz, 1H), 8.82 (d, *J* = 8.3 Hz, 1H), 8.20 (dd, *J* = 8.1, 6.1 Hz, 1H), 7.05 (d, *J* = 8.2 Hz, 2H), 6.67 (d, *J* = 8.4 Hz, 2H), 6.14 (d, *J* = 15.5 Hz, 1H), 5.89 (d, *J* = 15.4 Hz, 1H), 4.72 (td, *J* = 8.6, 4.3 Hz, 1H), 4.47 – 4.35 (m, 2H), 4.13 (q, *J* = 6.9 Hz, 2H), 3.12 (dd, *J* = 14.1, 4.3 Hz, 1H), 2.97 (dd, *J* = 14.1, 9.1 Hz, 1H), 1.39 (t, *J* = 7.1 Hz, 3H), 1.25 (t, *J* = 7.1 Hz, 3H). <sup>13</sup>C-NMR (100 MHz, CDCl<sub>3</sub>)  $\delta$  (ppm): 171.11, 164.01, 161.25, 155.64, 149.02, 146.89, 145.75, 130.78, 130.16, 128.45, 127.27, 115.65, 63.55, 62.73, 61.85, 54.80, 36.58, 14.27, 14.23. IR (neat) (cm<sup>-1</sup>): 3191 (b), 3047 (b), 1729 (vs), 1685 (vs), 1514 (s), 1297 (s), 1191 (bs), 1111 (m), 1014 (m), 855 (m), 736 (m). ESI-MS (+ve) m/z: Found [M-Br]<sup>+</sup> 401.1713, C<sub>21</sub>H<sub>25</sub>N<sub>2</sub>O<sub>6</sub><sup>+</sup> requires 401.1707.

#### 5.4.6 Preparation of IL (353)



To a stirred solution of L-tyrosine ethyl ester  $\alpha$ -bromoamide (**356**) (1.027 g, 3.110 mmol) in diethyl ether (25 mL) was added dimethylaminoethanol (0.30 mL, 3.1 mmol). The reaction was stirred at room temperature under an N<sub>2</sub> atmosphere for 24 hours. After 24 hours a white precipitate had formed. The supernatant was

decanted and the white precipitate was washed with diethyl ether (3 x 50 mL) to afford the title product as a white solid in 79% yield, (1.004 g, 2.394 mmol)

Molecular formula: C<sub>17</sub>H<sub>27</sub>BrN<sub>2</sub>O<sub>5</sub>; Molecular weight: 419.316 gmol<sup>-1</sup>; Mp: 141-143° C.

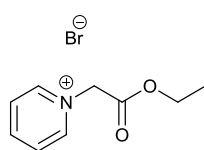
$[\alpha]_D^{20} = -3.0$  (1.0 c, CHCl<sub>3</sub>). <sup>1</sup>H-NMR (400 MHz, DMSO)  $\delta$  (ppm): 9.27 (s, 1H), 9.00 (d,  $J = 7.4$  Hz, 1H), 7.01 (d,  $J = 8.1$  Hz, 2H), 6.67 (d,  $J = 8.2$  Hz, 2H), 5.33 (s, 1H), 4.47 (d,  $J = 5.6$  Hz, 1H), 4.21 – 4.11 (m, 2H), 4.08 (q,  $J = 6.7$  Hz, 2H), 3.80 (s, 2H), 3.52 (s, 2H), 3.17 (s, 3H), 3.16 (s, 3H), 2.95 (dd,  $J = 14.3, 5.3$  Hz, 1H), 2.81 (dd,  $J = 13.7, 9.0$  Hz, 1H), 1.14 (t,  $J = 7.1$  Hz, 3H). <sup>13</sup>C-NMR (100 MHz, DMSO)  $\delta$  (ppm): 170.81, 163.39, 156.16, 130.17, 126.57, 115.11, 66.02, 62.50, 60.86, 54.97, 53.98, 52.07, 52.03, 35.78, 13.99. IR (neat) (cm<sup>-1</sup>): 3357 (b), 3188 (b), 3056 (m), 1737 (vs), 1665 (vs), 1556 (m), 1514 (m), 1369 (m), 1342 (m), 1287 (s), 1218 (vs), 1179 (vs), 1103 (m), 1071 (m), 1015 (m), 804 (m), 732 (m). ES-MS (+ve) m/z: Found [M-Br]<sup>+</sup> 339.1920, C<sub>19</sub>H<sub>23</sub>N<sub>2</sub>O<sub>5</sub><sup>+</sup> requires 339.1914

## 5.5 Experimental preparation of Chapter 2 IL and tertiary amino metabolites

### 5.5.1 Preparation of IL (357) – Acid hydrolysis route

#### 5.5.1.1 Preparation of IL (369)

1-(2-Ethoxy-2-oxoethyl)pyridin-1-ium bromide (**369**).



To a stirred solution of pyridine (320  $\mu$ l, 3.97 mmol) in ethyl acetate (25 ml) was added dropwise ethyl bromoacetate (0.50 ml, 4.4 mmol). The reaction was stirred under reflux conditions for 12 hours. After 12 hours a yellow precipitate had formed. The supernatant was decanted and the solid yellow crude product was isolated by vacuum filtration and washed with ethyl acetate (3 x 25 ml) to afford the title compound (**369**) as a yellow solid in 63% yield, (0.615 g, 2.50 mmol).

Molecular formula: C<sub>9</sub>H<sub>12</sub>BrNO<sub>2</sub>; Molecular weight: 246.104 gmol<sup>-1</sup>; Mp: 133-135° C.

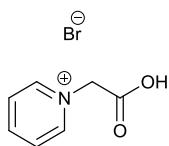
<sup>1</sup>H-NMR (400 MHz, CDCl<sub>3</sub>)  $\delta$  (ppm): 9.50 (dd,  $J = 6.7, 1.2$  Hz, 2H), 8.55 (tt,  $J = 7.9, 1.3$  Hz, 1H), 8.13 – 8.05 (m, 2H), 6.34 (s, 2H), 4.27 (q,  $J = 7.1$  Hz, 2H), 1.29 (t,  $J = 7.2$  Hz, 3H). <sup>13</sup>C-NMR (100 MHz, CDCl<sub>3</sub>)  $\delta$  (ppm): 165.86, 146.77, 146.08, 127.70, 63.45, 61.04, 14.12.



$^1\text{H}$ -NMR and  $^{13}\text{C}$ -NMR were in agreement with the literature.<sup>6</sup>

#### 5.5.1.2 Preparation of IL (357) - general procedure “F”

1-(carboxymethyl)pyridin-1-ium bromide (**357**).



Pyridinium IL (**369**) (0.345 g, 1.40 mmol) was stirred in a 25% (v/v) conc. HBr/H<sub>2</sub>O solution (10 ml) under reflux conditions for 2 hours. After two hours the solution was cooled to room temperature and dried *in vacuo*. The solid red crude product was washed with acetone (3 x 10 ml) to afford the title compound (**357**) as a white solid in 73% yield (0.224 g, 1.03 mmol).

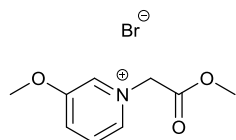
Molecular formula: C<sub>7</sub>H<sub>8</sub>BrNO<sub>2</sub>; Molecular weight: 218.050 g mol<sup>-1</sup>; Mp: 207-209° C.

$^1\text{H}$ -NMR (400 MHz, CDCl<sub>3</sub>)  $\delta$  (ppm): 8.80 – 8.73 (m, 2H), 8.57 (tt,  $J$  = 7.9, 1.3 Hz, 1H), 8.04 (s, 2H), 5.38 (s, 2H).  $^{13}\text{C}$ -NMR (100 MHz, D<sub>2</sub>O)  $\delta$  (ppm): 172.03, 148.80, 148.01, 130.45, 64.19.

#### 5.5.2 Preparation of IL (358) – Acid hydrolysis route

##### 5.5.2.1 Preparation of IL (370).

3-Methoxy-1-(2-methoxy-2-oxoethyl)pyridin-1-ium bromide (**370**).



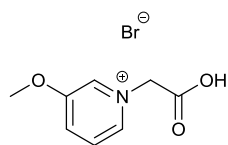
To a stirred solution of methoxy pyridine (460  $\mu\text{l}$ , 4.57 mmol) in diethyl ether (10 ml) was added dropwise methyl bromoacetate (430  $\mu\text{l}$ , 4.57 mmol). The reaction was stirred at room temperature under an N<sub>2</sub> atmosphere for 24 hours. After 24 hours a white precipitate had formed. The supernatant was decanted and the white solid crude product was washed with diethyl ether (3 x 25 ml) to afford the title compound (**370**) as a white hygroscopic solid in 87% yield, (1.042 g, 3.976 mmol).

Molecular formula: C<sub>9</sub>H<sub>12</sub>BrNO<sub>3</sub>; Molecular weight: 262.103 g mol<sup>-1</sup>; Mp: 36-38° C.

$^1\text{H}$ -NMR (400 MHz, CDCl<sub>3</sub>)  $\delta$  (ppm): 9.53 – 9.47 (m, 1H), 9.08 (d,  $J$  = 5.8 Hz, 1H), 8.03 – 7.87 (m, 2H), 6.39 (s, 2H), 4.12 (s, 3H), 3.80 (s, 3H).  $^{13}\text{C}$ -NMR (100 MHz, CDCl<sub>3</sub>)  $\delta$  (ppm): 160.49, 152.41, 133.47, 126.96, 126.87, 121.79, 54.90, 52.55, 47.85. IR (neat) (cm<sup>-1</sup>): 3033 (b), 2952 (b), 1748 (vs), 1625 (m), 1581 (vs), 1441 (s), 1296 (vs), 766 (s), 713 (s).

### 5.5.2.2 Preparation of IL (358)

1-(carboxymethyl)-3-methoxypyridin-1-ium bromide (**358**).



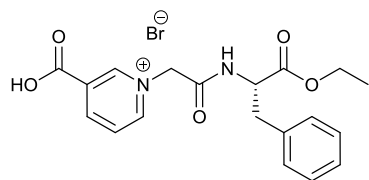
According to general procedure “F”, using IL (**370**) (0.709 g, 2.70 mmol), the title compound (**358**) was isolated as a white solid in 77% yield (0.516 g, 2.08 mmol).

Molecular formula: C<sub>8</sub>H<sub>10</sub>BrNO<sub>3</sub>; Molecular weight: 248.076 gmol<sup>-1</sup>; Mp: 177-179° C.

<sup>1</sup>H-NMR (400 MHz, D<sub>2</sub>O) δ (ppm): 8.44 (dd, *J* = 2.6, 1.3 Hz, 1H), 8.30 (dt, *J* = 5.9, 1.2 Hz, 1H), 8.06 (ddd, *J* = 8.9, 2.6, 1.0 Hz, 1H), 7.88 (dd, *J* = 8.9, 5.9 Hz, 1H), 5.29 (s, 2H), 3.90 (s, 3H). <sup>13</sup>C-NMR (100 MHz, D<sub>2</sub>O) δ (ppm): 169.26, 158.51, 137.98, 132.98, 131.44, 128.22, 61.67, 57.09. IR (neat) (cm<sup>-1</sup>): 2827 (b), 1737 (vs), 1583 (vs), 1508 (vs), 1291 (vs), 1192 (vs), 1057 (vs), 806 (vs), 776 (s), 693 (vs). ESI-MS (+ve) m/z: Found [M-Br]<sup>+</sup> 168.0661, C<sub>8</sub>H<sub>10</sub>NO<sub>3</sub><sup>+</sup> requires 168.0655.

### 5.5.3 Alternative preparation of IL (359)

(*S*)-3-Carboxy-1-(2-((1-ethoxy-1-oxo-3-phenylpropan-2-yl)amino)-2-oxoethyl)pyridin-1-ium bromide (**359**).



To a stirred solution of sodium nicotinate (0.480 g, 3.31 mmol) in DMF (25 ml) was added alkylating reagent (**337**) (3.210 g, 10.22 mmol). The reaction mixture was heated under reflux conditions for 72 hours and was observed to change from colourless to yellow. After 72 hours the reaction mixture was allowed to cool to room temperature. DMF was removed *in vacuo* and the crude orange product was purified by silica gel chromatography (eluent 5:95 MeOH:DCM) to afford the title compound (**359**) as an orange solid in 37% yield (0.532 g, 1.22 mmol).

Molecular formula: C<sub>19</sub>H<sub>21</sub>BrN<sub>2</sub>O<sub>5</sub>; Molecular weight: 437.290 gmol<sup>-1</sup>; Mp: 90-92° C.

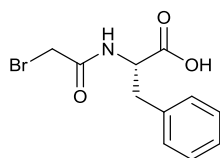
[α]<sub>D</sub><sup>20</sup> = -8.0 (0.1 c, EtOH). <sup>1</sup>H-NMR (400 MHz, D<sub>2</sub>O) δ (ppm): 8.92 (s, 1H), 8.86 (dt, *J* = 8.1, 1.4 Hz, 1H), 8.61 (dt, *J* = 6.2, 1.3 Hz, 1H), 8.04 (dd, *J* = 8.0, 6.2 Hz, 1H), 7.32 – 7.16 (m, 5H), 5.42 (d, *J* = 16.0 Hz, 1H), 5.34 (d, *J* = 16.0 Hz, 1H), 4.77 – 4.72 (m, 1H), 4.14 (q, *J* = 7.2 Hz, 2H), 3.24 (dd, *J* = 13.9, 5.5 Hz, 1H), 2.93 (dd, *J* = 13.8, 9.7 Hz, 1H), 1.16 (t, *J* = 7.2 Hz, 3H). <sup>13</sup>C-NMR (100 MHz, D<sub>2</sub>O) δ (ppm): 175.04, 169.21, 167.77, 149.14, 148.79, 138.76, 131.75, 131.23, 130.30, 129.76, 65.40, 64.15, 57.07, 37.00, 15.71. IR (neat) (cm<sup>-1</sup>): 2969 (b), 2779 (s),

2437 (m), 1733 (m), 1686 (s), 1641 (s), 1372 (s), 1211 (s), 1022 (vs), 705 (s), 668 (s). ESI-MS (+ve) *m/z*: Found [M-Br]<sup>+</sup> 357.1451, C<sub>19</sub>H<sub>21</sub>N<sub>2</sub>O<sub>5</sub><sup>+</sup> requires 357.1445.

#### 5.5.4 Alternative preparation of IL (360)

##### 5.5.4.1 Preparation of alkylating reagent (389)

(2-bromoacetyl)-L-phenylalanine (**389**).



To a stirred suspension of L-phenylalanine (0.865 g, 5.23 mmol) in deionised water (10 ml) at 0 °C was added a 1M NaOH solution (0.2 ml). The solution was stirred for 30 minutes until dissolution of the L-phenylalanine was achieved. After complete dissolution was observed, a solution of bromoacetyl bromide (0.50 ml, 5.7 mmol) in toluene (10 ml) was added to the stirred aqueous reaction mixture dropwise. Reaction pH was maintained at pH 9 by the concomitant addition of supplementary 1M NaOH if pH was determined to be decreasing by universal indicator paper checks every 5 minutes. After 30 minutes the reaction mixture was acidified to pH 1 and the target product was observed to precipitate as a white solid. Isolation of the target product was achieved by vacuum filtration of the reaction mixture followed by washing with ice cold deionised water (3 x 5 ml). Excess water was removed *in vacuo* to afford the title compound (**389**) as a white solid in 58% yield (0.861 g, 3.01 mmol).

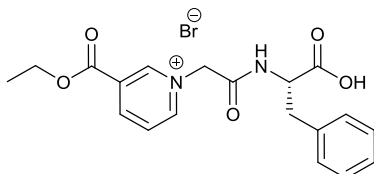
Molecular formula: C<sub>11</sub>H<sub>12</sub>BrNO<sub>3</sub>; Molecular weight: 286.125 gmol<sup>-1</sup>.

<sup>1</sup>H-NMR (400 MHz, CDCl<sub>3</sub>) δ (ppm): 7.38 – 7.26 (m, 3H), 7.21 – 7.13 (m, 2H), 6.83 (d, *J* = 7.7 Hz, 1H), 4.93 – 4.83 (m, 1H), 3.89 (d, *J* = 13.9 Hz, 1H), 3.84 (d, *J* = 13.9 Hz, 1H), 3.25 (dd, *J* = 14.0, 5.5 Hz, 1H), 3.17 (dd, *J* = 14.0, 6.1 Hz, 1H). <sup>13</sup>C-NMR (100 MHz, CDCl<sub>3</sub>) δ (ppm): 172.42, 165.88, 137.29, 129.10, 128.19, 126.50, 53.78, 36.47, 28.97.

No <sup>1</sup>H or <sup>13</sup>C-NMR spectra were reported in the literature procedure.<sup>10</sup>

##### 5.5.4.2 Final preparation of IL (360)

(*S*)-1-(2-((1-carboxy-2-phenylethyl)amino)-2-oxoethyl)-3-(ethoxycarbonyl)pyridin-1-ium bromide (**360**).



To a stirred solution of ethyl nicotinate (0.66 ml, 4.8 mmol) in DMF (25 ml) was added alkylating reagent (**389**) (0.703 g, 2.41 mmol). The reaction was heated under reflux conditions

for 72 hours and was observed to change from colourless to yellow. After 72 hours the reaction mixture was allowed to cool to room temperature. DMF was removed *in vacuo* and the crude orange product was purified by silica gel chromatography (eluent 5:95 MeOH:DCM) to afford the title compound (**360**) as an orange solid in 57% yield (0.604 g, 1.38 mmol).

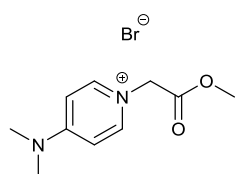
Molecular formula: C<sub>19</sub>H<sub>21</sub>BrN<sub>2</sub>O<sub>5</sub>; Molecular weight: 437.290 g mol<sup>-1</sup>; Mp: 85-87° C.

[α]<sub>D</sub><sup>20</sup> = +9.0 (0.1 c, EtOH). <sup>1</sup>H-NMR (400 MHz, D<sub>2</sub>O) δ (ppm): 9.18 (s, 1H), 9.02 (d, *J* = 8.2 Hz, 1H), 8.74 (d, *J* = 6.1 Hz, 1H), 8.17 – 8.09 (m, 1H), 7.32 – 7.19 (m, 5H), 5.45 (d, *J* = 16.1 Hz, 1H), 5.35 (d, *J* = 16.0 Hz, 1H), 4.70 (dd, *J* = 9.9, 5.1 Hz, 1H), 4.43 (q, *J* = 7.1 Hz, 2H), 3.26 (dd, *J* = 13.9, 4.9 Hz, 1H), 2.92 (dd, *J* = 13.7, 10.0 Hz, 1H), 1.34 (t, *J* = 7.1 Hz, 3H). <sup>13</sup>C-NMR (100 MHz, D<sub>2</sub>O) δ (ppm): 177.13, 167.39, 164.99, 150.98, 149.32, 149.14, 139.14, 133.31, 131.75, 131.20, 130.66, 129.66, 66.45, 64.26, 57.20, 39.50, 15.71. IR (neat) (cm<sup>-1</sup>): 3201 (b), 3029 (m), 2928 (m), 1729 (vs), 1682 (vs), 1540 (s), 1298 (vs), 1207 (vs), 1188 (vs), 741 (s), 643 (s). ESI-MS (+ve) m/z: Found [M-Br]<sup>+</sup> 357.1451, C<sub>19</sub>H<sub>21</sub>N<sub>2</sub>O<sub>5</sub><sup>+</sup> requires 357.1445.

### 5.5.5 Preparation of IL (361) – Acid hydrolysis route

#### 5.5.5.1 Preparation of IL (371)

4-(dimethylamino)-1-(2-methoxy-2-oxoethyl)pyridin-1-ium bromide (**371**).



To a stirred solution of dimethylaminopyridine (0.500 g, 4.09 mmol) in diethyl ether (10 ml) was added dropwise methyl bromoacetate (0.50 ml, 5.3 mmol). The reaction was stirred at room temperature under an N<sub>2</sub> atmosphere for 24 hours. After 24 hours a white precipitate had formed.

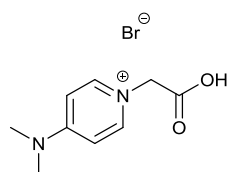
The supernatant was decanted and the white solid crude product was washed with diethyl ether (3 x 25 ml) to afford the title compound (**371**) as a white solid in 97% yield, (1.089 g, 3.957 mmol).

Molecular formula: C<sub>10</sub>H<sub>15</sub>BrN<sub>2</sub>O<sub>2</sub>; Molecular weight: 275.146 g mol<sup>-1</sup>; Mp: 227-229 ° C

<sup>1</sup>H-NMR (400 MHz, CDCl<sub>3</sub>) δ (ppm): 8.20 – 8.10 (m, 2H), 7.08 – 6.97 (m, 2H), 5.13 (s, 2H), 3.68 (s, 3H), 3.16 (s, 6H). <sup>13</sup>C-NMR (100 MHz, CDCl<sub>3</sub>) δ (ppm): 168.17, 156.07, 143.08, 107.43, 56.53, 52.82, 39.92. IR (neat) (cm<sup>-1</sup>): 3064 (m), 2940 (m), 1751 (vs), 1650 (vs), 1569 (vs), 1435 (s), 1207 (vs), 1178 (vs), 828 (s), 743 (s), 693 (s).

### 5.5.5.2 Preparation of IL (361)

1-(carboxymethyl)-4-(dimethylamino)pyridin-1-ium bromide (**361**).



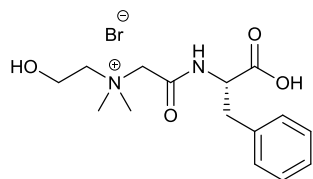
According to general procedure “F”, using IL (**371**) (0.596 g, 2.17 mmol), the title compound (**361**) was isolated as a white solid in 92% yield (0.519 g, 1.99 mmol).

Molecular formula: C<sub>9</sub>H<sub>13</sub>BrN<sub>2</sub>O<sub>2</sub>; Molecular weight: 261.119 g mol<sup>-1</sup>; Mp: >250°C.

<sup>1</sup>H-NMR (400 MHz, D<sub>2</sub>O) δ (ppm): 7.86 – 7.77 (m, 2H), 6.82 – 6.74 (m, 2H), 4.86 (s, 2H), 3.09 (s, 6H). <sup>13</sup>C-NMR (100 MHz, D<sub>2</sub>O) δ (ppm): 171.09, 156.43, 142.20, 107.33, 57.27, 39.47. IR (neat) (cm<sup>-1</sup>): 2807 (b), 1735 (s), 1650 (s), 1573 (s), 1178 (s), 824 (vs), 643 (vs). ESI-MS (+ve) m/z: Found [M-Br]<sup>+</sup> 181.0977, C<sub>9</sub>H<sub>13</sub>N<sub>2</sub>O<sub>2</sub><sup>+</sup> requires 181.0972.

### 5.5.6 Preparation of IL (362) – Base hydrolysis route

(S)-2-((1-carboxy-2-phenylethyl)amino)-N-(2-hydroxyethyl)-N,N-dimethyl-2-oxoethan-1-aminium bromide (**362**).



To a stirred solution of IL (**330**) (0.244 g, 0.65 mmol) in a 50% (v/v) THF/H<sub>2</sub>O solution (10 ml) was added LiOH (0.250 g, 5.96 mmol). The solution was allowed to stand in the fridge for 12 hours. After 12 hours the basic solution was acidified to pH 6 by dropwise addition of HBr. Evaporation of the solvent *in vacuo* yielded a waxy crude white product. The crude product was washed with acetonitrile (3 x 10 ml) to extract the title compound leaving the inorganic salt behind. Solvent was removed *in vacuo* to afford the title compound (**362**) as a white solid in 85% yield (0.211 g, 0.55 mmol).

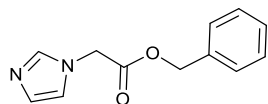
Molecular formula: C<sub>15</sub>H<sub>23</sub>BrN<sub>2</sub>O<sub>4</sub>; Molecular weight: 375.258 g mol<sup>-1</sup>; Mp: 59-61° C.

[α]<sub>D</sub><sup>20</sup> = +5.0 (0.1 c, EtOH). <sup>1</sup>H-NMR (400 MHz, DMSO) δ (ppm): 8.37 (d, *J* = 8.5 Hz, 1H), 7.30 – 7.14 (m, 5H), 7.14 – 7.02 (m, 1H), 5.36 (s, 1H), 4.21 (td, *J* = 9.7, 3.9 Hz, 2H), 4.13 (d, *J* = 14.2 Hz, 1H), 4.06 (d, *J* = 14.2 Hz, 1H), 3.48 – 3.38 (m, 2H), 3.22 – 3.10 (m, 2H), 3.09 (s, 3H), 3.06 (s, 3H), 2.70 (dd, *J* = 13.7, 10.0 Hz, 1H). <sup>13</sup>C-NMR (100 MHz, D<sub>2</sub>O) δ (ppm): 174.74, 162.46, 139.32, 129.53, 128.32, 126.31, 66.12, 63.72, 56.47, 55.17, 52.30, 52.16, 38.01. IR (neat) (cm<sup>-1</sup>): 3406 (s), 3236 (m), 1636 (s), 1614 (vs), 1395 (m), 1085 (m), 699 (m). ESI-MS (+ve) m/z: Found [M-Br]<sup>+</sup> 295.1660, C<sub>15</sub>H<sub>23</sub>N<sub>2</sub>O<sub>4</sub><sup>+</sup> requires 295.1652.

### 5.5.7 Preparation of IL (363) – Hydrogenolysis route

#### 5.5.7.1 Preparation of intermediate (384)

Benzyl 2-(1*H*-imidazol-1-yl)acetate (**384**).



To a stirred solution of TMS-imidazole (1.400 g, 9.981 mmol) in diethyl ether (25 ml) was added dropwise benzyl bromoacetate (0.88 ml, 10 mmol). The reaction was stirred at room temperature under an N<sub>2</sub> atmosphere for 2 hours at which point a white precipitate of TMS-imidazolium ionic liquid had formed. The diethyl ether was removed *in vacuo* and the white precipitate was dissolved in water (10 ml) and stirred for 1 hour. After 1 hour the water was removed *in vacuo* resulting in a crude white solid product. Purification of the crude product was accomplished by silica gel chromatography (eluent 5:95 MeOH:DCM) to afford the title compound (**384**) as a white solid in 44% yield (0.946 g, 4.37 mmol).

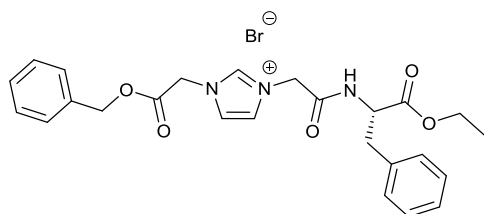
Molecular formula: C<sub>12</sub>H<sub>12</sub>N<sub>2</sub>O<sub>2</sub>; Molecular weight: 216.240 gmol<sup>-1</sup>

<sup>1</sup>H-NMR (400 MHz, CDCl<sub>3</sub>) δ (ppm): 7.61 (s, 1H), 7.40-7.35 (m, 5H), 7.34 (s, 1H), 6.97 (s, 1H), 5.21 (s, 2H), 4.76 (s, 2H). <sup>13</sup>C-NMR (100 MHz, CDCl<sub>3</sub>) δ (ppm): 167.33, 137.98, 134.70, 129.85, 128.84, 128.79, 128.58, 120.01, 67.78, 48.05.

<sup>1</sup>H-NMR and <sup>13</sup>C-NMR were in agreement with the literature.<sup>11</sup>

#### 5.5.7.2 Preparation of IL (385)

(*S*)-1-(2-(Benzyloxy)-2-oxoethyl)-3-(2-((1-ethoxy-1-oxo-3-phenylpropan-2-yl)amino)-2-oxoethyl)-1*H*-imidazol-3-ium bromide (**385**).



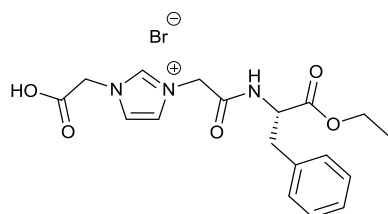
To a stirred solution of ethyl alkylating reagent (**337**) (0.667 g, 2.13 mmol) in diethyl ether (25 ml) and ethyl acetate (5 ml) was added imidazole intermediate (**384**) (0.383 g, 1.77 mmol). An off-white precipitate was observed forming after 30 minutes. The reaction was stirred at room temperature for 72 hours. After 72 hours the solvent was decanted and the resulting white crude product was washed with diethyl ether (3 x 25 ml) to afford the title compound (**385**) as an off white solid in 97% yield (0.913 g, 1.72 mmol).

Molecular formula: C<sub>25</sub>H<sub>28</sub>BrN<sub>3</sub>O<sub>5</sub>; Molecular weight: 527.415 g mol<sup>-1</sup>; Mp: 57-59° C.

[ $\alpha$ ]<sub>D</sub><sup>20</sup> = +9.5 (1.95 c, CHCl<sub>3</sub>). <sup>1</sup>H-NMR (400 MHz, CDCl<sub>3</sub>)  $\delta$  (ppm): 9.58 (s, 1H), 8.95 (d, *J* = 7.7 Hz, 1H), 7.46 – 7.28 (m, 9H), 7.25 – 7.07 (m, 3H), 5.36 – 5.28 (m, 3H), 5.27 – 5.18 (m, 1H), 5.17 (s, 2H), 4.69 – 4.59 (m, 1H), 4.08 – 3.96 (m, 2H), 3.17 (d, *J* = 2.0 Hz, 1H), 3.14 (dd, *J* = 12.0, 3.9 Hz, 1H), 1.12 (t, *J* = 7.1 Hz, 3H). <sup>13</sup>C-NMR (100 MHz, CDCl<sub>3</sub>)  $\delta$  (ppm): 171.47, 165.96, 164.78, 138.39, 136.76, 134.45, 129.66, 129.06, 128.93, 128.89, 128.62, 127.01, 123.41, 123.04, 68.73, 61.71, 54.98, 51.75, 50.56, 37.52, 14.18. IR (neat) (cm<sup>-1</sup>): 3033 (b), 1736 (vs), 1684 (vs), 1551 (s), 1178 (vs), 1024 (s), 743 (s), 697 (vs). ESI-MS (+ve) m/z: Found [M-Br]<sup>+</sup> 450.2027, C<sub>25</sub>H<sub>28</sub>N<sub>3</sub>O<sub>5</sub><sup>+</sup> requires 450.2023.

### 5.5.7.3 Preparation of IL (363)

(*S*)-1-(Carboxymethyl)-3-(2-((1-ethoxy-1-oxo-3-phenylpropan-2-yl)amino)-2-oxoethyl)-1H-imidazol-3-ium bromide (**363**).



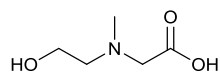
To a stirred solution of IL (**385**) (0.450 g, 0.853 mmol) in DCM (25 ml) was added 10% Pd/C (0.045 g). The reaction mixture was stirred vigorously under 1 atmosphere of H<sub>2</sub> for 12 hours. After 12 hours the reaction mixture was degassed with a stream of N<sub>2</sub> and filtered over a pad of celite. The celite filter pad was washed with DCM (3 x 25 ml). The combined filtrate was collected and organic solvent was removed *in vacuo*. The resulting crude product was washed with chloroform (3 x 25 ml) to afford the title compound (**363**) as an off white solid in 87% yield (0.325 g, 0.738 mmol).

Molecular formula: C<sub>18</sub>H<sub>22</sub>BrN<sub>3</sub>O<sub>5</sub>; Molecular weight: 440.294 g mol<sup>-1</sup>; Mp: 162-164° C.

[ $\alpha$ ]<sub>D</sub><sup>20</sup> = +4.0 (0.1 c, EtOH). <sup>1</sup>H-NMR (400 MHz, D<sub>2</sub>O)  $\delta$  (ppm): 8.71 (t, *J* = 1.6 Hz, 1H), 7.45 (t, *J* = 1.9 Hz, 1H), 7.36 – 7.16 (m, 6H), 5.05 – 4.88 (m, 4H), 4.74 – 4.68 (m, 1H), 4.14 (qd, *J* = 7.2, 1.3 Hz, 2H), 3.23 (dd, *J* = 13.9, 5.7 Hz, 1H), 2.96 (dd, *J* = 13.9, 9.4 Hz, 1H), 1.16 (t, *J* = 7.2 Hz, 3H). <sup>13</sup>C-NMR (100 MHz, D<sub>2</sub>O)  $\delta$  (ppm): 172.61, 170.12, 166.42, 137.85, 136.20, 129.11, 128.65, 127.14, 123.48, 123.07, 62.76, 54.41, 50.54, 50.48, 36.62, 13.09. IR (neat) (cm<sup>-1</sup>): 3311 (b), 3108 (m), 2981 (m), 1726 (vs), 1664 (vs), 1555 (s), 1537 (s), 1215 (s), 1195 (s), 1178 (s), 691 (s). ESI-MS (+ve) m/z: Found [M-Br]<sup>+</sup> 360.1561, C<sub>18</sub>H<sub>22</sub>N<sub>3</sub>O<sub>5</sub><sup>+</sup> requires 360.1554.

### 5.5.8 Preparation of tertiary amine (367)

*N*-(2-hydroxyethyl)-*N*-methylglycine (**367**).



To a stirred solution of 40 wt.% glyoxal/H<sub>2</sub>O (3.75 ml, 33.0 mmol) was added 2-(methylamino)ethanol (2.40 ml, 30.0 mmol). The reaction mixture was stirred under reflux conditions for 12 hours. After 12 hours the reaction mixture was cooled to room temperature and the water was removed *in vacuo*. The resulting brown crude product was recrystallised from ethanol/acetone to afford the title compound (**367**) as a white crystalline solid in 51% yield (2.048 g, 15.38 mmol).

Molecular formula: C<sub>5</sub>H<sub>11</sub>NO<sub>3</sub>; Molecular weight: 133.147 g mol<sup>-1</sup>.

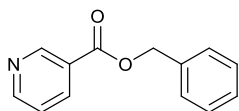
<sup>1</sup>H-NMR (400 MHz, D<sub>2</sub>O) δ (ppm): 3.86 (t, *J* = 5.4 Hz, 2H), 3.73 (bs, 2H), 3.30 (bs, 2H), 2.90 (s, 3H). <sup>13</sup>C-NMR (100 MHz, D<sub>2</sub>O) δ (ppm): 170.20, 58.40, 57.59, 55.37, 41.34. ESI-MS (+ve) *m/z*: Found [M+H]<sup>+</sup> 134.0815 C<sub>5</sub>H<sub>12</sub>NO<sup>+</sup> requires 134.0812.

<sup>1</sup>H-NMR and <sup>13</sup>C-NMR were in agreement with the literature.<sup>12</sup>

### 5.5.9 Preparation of IL (373) – Failed hydrogenolysis route

#### 5.5.9.1 Preparation of ester (372)

Benzyl nicotinate (**372**).



To a round bottom flask was added benzyl alcohol (0.76 ml, 7.8 mmol), tosylimidazole (2.083 g, 9.372 mmol), triethylamine (1.75 ml, 12.5 mmol), sodium nicotinate (2.265 g, 15.61 mmol), tetrabutylammonium iodide (0.430 g, 1.16 mmol) and DMF (20 ml). The reaction was stirred under reflux conditions for 6 hours and was observed darkening to a brown colour. After 6 hours the reaction mixture was cooled to room temperature and diluted with water (20 ml). The crude product was extracted using DCM (3 x 20 ml). Purification was achieved by silica gel chromatography (gradient elution of ethyl acetate:hexane 30:70 to 50:50 ethyl acetate:hexane). The title compound (**372**) was isolated as a pale yellow oil in 97% yield (1.610 g, 7.550 mmol).

Molecular formula: C<sub>13</sub>H<sub>11</sub>NO<sub>2</sub>; Molecular weight: 213.236 g mol<sup>-1</sup>.

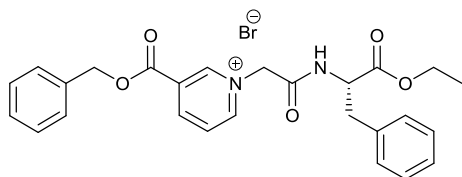


<sup>1</sup>H-NMR (400 MHz, CDCl<sub>3</sub>) δ (ppm): 9.27 (s, 1H), 8.78 (d, *J* = 4.8 Hz, 1H), 8.32 (dt, *J* = 8.0, 1.9 Hz, 1H), 7.46 – 7.34 (m, 6H), 5.40 (s, 2H). <sup>13</sup>C-NMR (100 MHz, CDCl<sub>3</sub>) δ (ppm): 165.14, 153.52, 151.00, 137.23, 135.49, 128.73, 128.56, 128.38, 126.06, 123.37, 67.17.

<sup>1</sup>H-NMR and <sup>13</sup>C-NMR were in agreement with the literature. <sup>7</sup>

### 5.5.9.2 Preparation of IL (373)

(*S*)-3-((Benzyloxy)carbonyl)-1-(2-((1-ethoxy-1-oxo-3-phenylpropan-2-yl)amino)-2-oxoethyl)pyridin-1-ium bromide (**373**).



According to a modified general procedure “E,” using benzyl nicotinate (0.998 g, 4.68 mmol), ethyl alkylating reagent (**337**), (2.061 g, 6.559 mmol) and THF (25 ml) under reflux conditions, the title compound was isolated as a crude solid orange product. Purification of the crude product was achieved by silica gel chromatography (gradient elution of 1:99 MeOH:DCM to 5:95 MeOH:DCM) to afford the title compound (**373**) as a hygroscopic orange solid in 59% yield (1.449 g, 2.747 mmol).

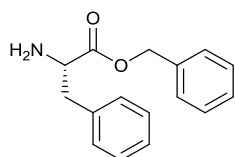
Molecular formula: C<sub>26</sub>H<sub>27</sub>BrN<sub>2</sub>O<sub>5</sub>; Molecular weight: 527.415 g mol<sup>-1</sup>; Mp: 50-52° C.

[α]<sub>D</sub><sup>20</sup> = +1.5 (1.3 c, CHCl<sub>3</sub>). <sup>1</sup>H-NMR (400 MHz, CDCl<sub>3</sub>) δ (ppm): 9.72 (dt, *J* = 6.1, 1.4 Hz, 1H), 9.40 – 9.33 (m, 2H), 8.92 (dt, *J* = 8.2, 1.5 Hz, 1H), 8.10 (dd, *J* = 8.1, 6.1 Hz, 1H), 7.53 – 7.32 (m, 7H), 7.28 – 7.19 (m, 2H), 7.18 – 7.09 (m, 1H), 6.19 (d, *J* = 15.1 Hz, 1H), 6.14 (d, *J* = 15.1 Hz, 1H), 5.47 (s, 2H), 4.70 (ddd, *J* = 9.1, 7.9, 5.9 Hz, 1H), 4.12 – 4.03 (m, 2H), 3.25 (dd, *J* = 13.8, 5.9 Hz, 1H), 3.18 (dd, *J* = 13.8, 9.0 Hz, 1H), 1.17 (t, *J* = 7.1 Hz, 3H). <sup>13</sup>C-NMR (100 MHz, CDCl<sub>3</sub>) δ (ppm): 171.01, 163.73, 160.87, 149.89, 146.97, 145.43, 136.67, 134.12, 130.11, 129.69, 129.26, 129.15, 128.99, 128.47, 127.74, 126.86, 69.15, 62.83, 61.62, 55.09, 37.70, 14.14. IR (neat) (cm<sup>-1</sup>): 3194 (b), 3032 (b), 1731 (vs), 1684 (vs), 1547 (m), 1377 (m), 1292 (vs), 1185 (vs), 1112 (s), 735 (s), 698 (vs). ESI-MS (+ve) m/z: Found [M-Br]<sup>+</sup> 447.1927, C<sub>26</sub>H<sub>27</sub>N<sub>2</sub>O<sub>5</sub><sup>+</sup> requires 447.1914.

### 5.5.10 Preparation of IL (376) – Failed hydrogenolysis route

#### 5.5.10.1 Preparation of ester (374)

L-Phenylalanine benzyl ester (**374**).



To a stirred suspension of L-phenylalanine (5.046 g, 30.55 mmol) in toluene (25 ml) was added benzyl alcohol (6.5 ml, 62 mmol) and PTSA

(11.62 g, 61.09 mmol). The reaction was stirred under reflux conditions using a Dean-Stark apparatus for 24 hours. After 24 hours the reaction mixture was cooled to room temperature and the PTSA salt of the crude product was precipitated by portionwise addition of diethyl ether (3 x 50 ml). The solid precipitate was isolated by vacuum filtration and washed with toluene (3 x 50 ml). The PTSA salt of the title compound (**374**) (8.721 g) was dissolved in a saturated sodium bicarbonate solution (50 ml) in a 250 ml beaker and stirred for 10 minutes until neutralisation had occurred. The solution was transferred to a separating funnel and the free base title compound (**374**) was extracted using DCM (3 x 50 ml). Removal of solvent *in vacuo* afforded the title compound (**374**) as a brown oil in 48% yield (3.722 g, 14.58 mmol).

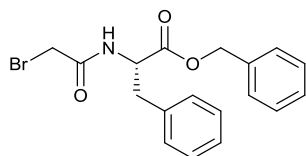
Molecular formula: C<sub>16</sub>H<sub>17</sub>NO<sub>2</sub>; Molecular weight: 255.317 gmol<sup>-1</sup>.

<sup>1</sup>H-NMR (400 MHz, CDCl<sub>3</sub>) δ (ppm): 7.43 – 7.21 (m, 10H), 7.21 – 7.10 (m, 2H), 5.15 (d, *J* = 12.2 Hz, 1H), 5.12 (d, *J* = 12.4 Hz, 1H), 3.80 (dd, *J* = 7.6, 5.5 Hz, 1H), 3.10 (dd, *J* = 13.6, 5.5 Hz, 1H), 2.91 (dd, *J* = 13.5, 7.6 Hz, 1H).

<sup>1</sup>H-NMR was in agreement with the literature.<sup>8</sup>

#### 5.5.10.2 Preparation of alkylating reagent (**375**)

Benzyl (2-bromoacetyl)-L-phenylalaninate (**375**).



To a stirred solution of L-phenylalanine benzyl ester (**374**) (0.781 g, 3.06 mmol) in DCM (25 ml) was added solid Na<sub>2</sub>CO<sub>3</sub> (0.486 g, 4.59 mmol). To this reaction mixture was added bromoacetyl bromide dropwise (290 µl, 3.34 mmol). The reaction was stirred for 12 hours. After 12 hours the Na<sub>2</sub>CO<sub>3</sub> was removed by gravity filtration. The DCM layer was washed with saturated sodium bicarbonate solution (3 x 25 ml), dried over anhydrous magnesium sulphate and gravity filtered. The DCM was removed *in vacuo* to afford the title compound (**375**) as a white solid in 69% yield, (0.788 g, 2.10 mmol).

Molecular formula: C<sub>18</sub>H<sub>18</sub>BrNO<sub>3</sub>; Molecular weight: 376.250 gmol<sup>-1</sup>.

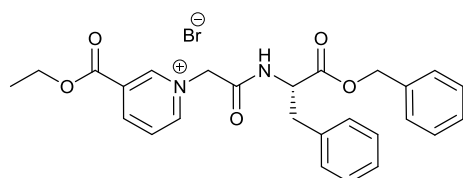
<sup>1</sup>H-NMR (400 MHz, CDCl<sub>3</sub>) δ (ppm): 7.43 – 7.34 (m, 3H), 7.34 – 7.28 (m, 2H), 7.25 – 7.19 (m, 3H), 7.05 – 6.97 (m, 2H), 6.85 (d, *J* = 8.0 Hz, 1H), 5.19 (d, *J* = 12.1 Hz, 1H), 5.13 (d, *J* = 12.1 Hz, 1H), 4.94 – 4.84 (m, 1H), 3.86 (d, *J* = 13.7 Hz, 1H), 3.82 (d, *J* = 13.6 Hz, 1H), 3.16 (dd, *J* =

12.0, 5.8 Hz, 1H), 3.12 (dd,  $J = 12.4, 5.7$  Hz, 1H).  $^{13}\text{C-NMR}$  (100 MHz,  $\text{CDCl}_3$ )  $\delta$  (ppm): 170.76, 165.17, 135.20, 134.95, 129.42, 128.76, 127.38, 67.57, 53.77, 37.72, 28.77.

$^1\text{H-NMR}$  and  $^{13}\text{C-NMR}$  were in agreement with the literature.<sup>9</sup>

### 5.5.10.3 Preparation of IL (376)

(*S*)-1-(2-((1-(benzyloxy)-1-oxo-3-phenylpropan-2-yl)amino)-2-oxoethyl)-3-(ethoxycarbonyl)pyridin-1-ium bromide (**376**).



To a stirred solution of ethyl nicotinate (250  $\mu\text{l}$ , 1.81 mmol) in ethyl acetate (25 ml) was added benzyl alkylating reagent (**375**) (0.751 g, 2.00 mmol). The reaction mixture was stirred under reflux conditions for 48 hours and was observed to change to an orange colour. After 48 hours the reaction mixture was cooled to room temperature and the solvent was removed *in vacuo*. The resulting solid orange crude product was purified by silica gel chromatography (eluent 5:95 MeOH:DCM) to afford the title product (**376**) as an orange solid in 89% yield (0.850 g, 1.61 mmol).

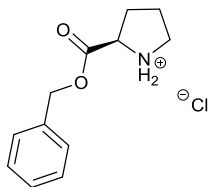
Molecular formula:  $\text{C}_{26}\text{H}_{27}\text{BrN}_2\text{O}_5$ ; Molecular weight: 527.415  $\text{g mol}^{-1}$ ; Mp: 63-65° C.

$[\alpha]_{\text{D}}^{20} = +5.5$  (1.75 c,  $\text{CHCl}_3$ ).  $^1\text{H-NMR}$  (400 MHz,  $\text{CDCl}_3$ )  $\delta$  (ppm): 9.64 (dt,  $J = 6.1, 1.4$  Hz, 1H), 9.48 (d,  $J = 7.9$  Hz, 1H), 9.35 (s, 1H), 8.85 (dt,  $J = 8.2, 1.5$  Hz, 1H), 8.06 – 7.97 (m, 1H), 7.36 – 7.27 (m, 5H), 7.24 – 7.18 (m, 4H), 7.17 – 7.11 (m, 1H), 6.26 (d,  $J = 15.1$  Hz, 1H), 6.10 (d,  $J = 15.1$  Hz, 1H), 5.08 (d,  $J = 12.3$  Hz, 1H), 4.99 (d,  $J = 12.3$  Hz, 1H), 4.82 – 4.71 (m, 1H), 4.48 (q,  $J = 7.1$  Hz, 2H), 3.30 – 3.15 (m, 2H), 1.44 (t,  $J = 7.1$  Hz, 3H).  $^{13}\text{C-NMR}$  (100 MHz,  $\text{CDCl}_3$ )  $\delta$  (ppm): 170.93, 163.82, 160.90, 149.55, 146.90, 145.37, 136.49, 135.29, 130.43, 129.71, 128.67, 239.59, 128.45, 138.36, 127.72, 126.95, 67.31, 63.71, 62.78, 55.16, 37.57, 14.29. IR (neat) ( $\text{cm}^{-1}$ ): 3031 (b), 1729 (vs), 1684 (vs), 1543 (m), 1497 (m), 1455 (m), 1369 (m), 1296 (vs), 1190 (vs), 1110 (m), 1012 (m), 736 (s), 698 (vs). ESI-MS (+ve) m/z: Found  $[\text{M-Br}]^+$  447.1928,  $\text{C}_{26}\text{H}_{27}\text{N}_2\text{O}_5^+$  requires 447.1914.

### 5.5.11 Preparation of IL (380) – Hydrogenolysis route

#### 5.5.11.1 Preparation of ester (377)

D-Proline benzyl ester hydrochloride (**377**).



To a stirred suspension of D-proline (5.75 g, 49.9 mmol) and benzyl alcohol (24 ml, 2.5 mol) was added  $\text{SOCl}_2$  (7.25 ml, 99.9 mmol). The reaction mixture was stirred at room temperature for 12 hours. The title compound (**377**) was precipitated by portionwise addition of diethyl ether (3 x 50 ml).

The title compound (**377**) was dried under high vacuum for 48 hours to give a brown solid in 72% yield (8.707g, 36.02 mmol).

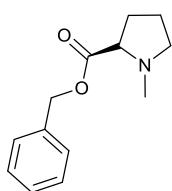
Molecular formula:  $\text{C}_{12}\text{H}_{16}\text{ClNO}_2$ ; Molecular weight:  $241.715 \text{ g mol}^{-1}$ .

$^1\text{H-NMR}$  (400 MHz,  $\text{D}_2\text{O}$ )  $\delta$  (ppm): 7.45 – 7.30 (m, 5H), 5.28 (d,  $J = 12.0 \text{ Hz}$ , 1H), 5.23 (d,  $J = 12.0 \text{ Hz}$ , 1H), 4.46 (dd,  $J = 8.8, 7.1 \text{ Hz}$ , 1H), 3.45 – 3.26 (m, 2H), 2.45 – 2.30 (m, 1H), 2.17 – 2.04 (m, 1H), 2.04 – 1.95 (m, 2H).  $^{13}\text{C-NMR}$  (100 MHz,  $\text{D}_2\text{O}$ )  $\delta$  (ppm): 169.62, 134.51, 128.93, 128.81, 128.50, 68.62, 59.41, 46.14, 28.01, 23.11.

$^1\text{H-NMR}$  and  $^{13}\text{C-NMR}$  were in agreement with the literature.<sup>13</sup>

#### 5.5.11.2 Preparation of N-methyl-D-proline benzyl ester (378)

N-Methyl-D-proline benzyl ester (**378**).



To a stirred solution of D-proline benzyl ester hydrochloride (**377**) (4.862 g, 23.69 mmol) in methanol (25 ml) was added  $\text{NaHCO}_3$  (1.990 g, 23.69 mmol). The solution as stirred for 5 minutes followed by the addition of formaldehyde solution 40% v/v (4.1 ml, 47 mmol). The reaction mixture was stirred for 2 hours followed by the portionwise addition of  $\text{NaBH}_4$  (1.135 g, 29.96 mmol).

After a further 30 minutes the aqueous reaction mixture was added to a separating funnel and the product was extracted with DCM (3 x 20 ml). DCM was removed *in vacuo* to afford a crude product as a colourless oil. The crude product was purified by silica gel chromatography (eluent 50:50 ethyl acetate:hexane) to afford the title compound (**378**) as a colourless oil in 31% yield (1.614 g, 7.360 mmol).

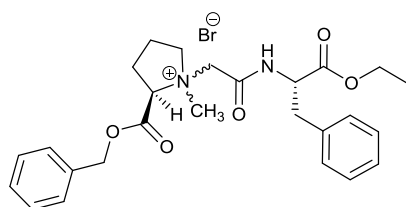
Molecular formula:  $\text{C}_{13}\text{H}_{17}\text{NO}_2$ ; Molecular weight:  $219.284 \text{ g mol}^{-1}$ .

$^1\text{H}$ -NMR (400 MHz,  $\text{CDCl}_3$ )  $\delta$  (ppm): 7.32 – 7.15 (m, 5H), 5.11 (d,  $J$  = 12.3 Hz, 1H), 5.07 (d,  $J$  = 12.4 Hz, 1H), 3.09 – 2.99 (m, 1H), 2.91 (dd,  $J$  = 8.8, 6.9 Hz, 1H), 2.31 (s, 3H), 2.27 – 2.16 (m, 1H), 2.13 – 1.99 (m, 1H), 1.94 – 1.78 (m, 2H), 1.75 – 1.62 (m, 1H).  $^{13}\text{C}$ -NMR (100 MHz,  $\text{CDCl}_3$ )  $\delta$  (ppm): 173.76, 136.08, 128.67, 128.35, 127.72, 67.50, 66.40, 56.41, 40.99, 29.71, 23.23.

$^1\text{H}$ -NMR and  $^{13}\text{C}$ -NMR were in agreement with the literature.<sup>14</sup>

### 5.5.11.3 Preparation of IL (379)

(2R)-2-((Benzyloxy)carbonyl)-1-(2-(((S)-1-ethoxy-1-oxo-3-phenylpropan-2-yl)amino)-2-oxoethyl)-1-methylpyrrolidin-1-ium bromide (**379**).



To a stirred solution of *N*-methyl-D-proline benzyl ester (**378**) (1.029 g, 4.693 mmol) in THF (25 ml) was added ethyl alkylating reagent (**337**) (1.769 g, 5.631 mmol). The reaction was heated under reflux conditions for 72 hours. After 72 hours the reaction was allowed to cool to room

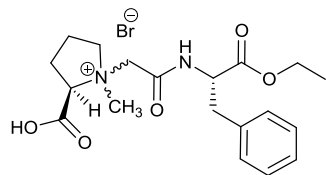
temperature and the solvent was removed *in vacuo*. The resulting crude product was purified by silica gel chromatography (gradient elution of 1:99 MeOH:DCM to 5:95 MeOH:DCM) to afford the title compound (**379**) as a white solid, mixture of epimers (1:3.3 ratio), in 47% yield (1.180 g, 2.212 mmol).

Molecular formula:  $\text{C}_{26}\text{H}_{33}\text{BrN}_2\text{O}_5$ ; Molecular weight: 533.463  $\text{g mol}^{-1}$ ; Mp: 159-161° C.

$[\alpha]_{\text{D}}^{20}$  = -8.0 (0.1 c, EtOH).  $^1\text{H}$ -NMR (400 MHz,  $\text{CDCl}_3$ )  $\delta$  (ppm): 9.27 – 8.98 (m, 1H), 7.39 – 6.96 (m, 10H), 5.28 – 4.99 (m, 2H), 4.99 – 4.67 (m, 2H), 4.58 – 4.33 (m, 1H), 4.07 (q,  $J$  = 7.1 Hz, 2H), 4.00 – 3.72 (m, 2H), 3.75 (s, 1H), 3.50 – 3.33 (m, 1H), 3.28 (s, 2H), 3.24 – 3.08 (m, 2H), 3.08 – 2.94 (m, 1H), 2.54 – 2.25 (m, 1H), 2.29 – 1.86 (m, 2H), 1.18 – 1.12 (m, 3H).  $^{13}\text{C}$ -NMR (100 MHz,  $\text{CDCl}_3$ )  $\delta$  (ppm): 171.46, 170.62, 170.50, 136.75, 135.89, 133.81, 129.83, 129.39, 129.19, 128.88, 126.85, 73.23, 68.70, 65.20, 62.58, 61.50, 54.89, 45.83, 37.01, 24.31, 19.15, 14.14. IR (neat) ( $\text{cm}^{-1}$ ): 3029 (m), 2981 (m), 1736 (vs), 1680 (vs), 1550 (s), 1453 (s), 1443 (s), 1213 (vs), 1024 (s), 739 (s), 699 (vs). ESI-MS (+ve) m/z: Found  $[\text{M}-\text{Br}]^+$  453.2396,  $\text{C}_{26}\text{H}_{33}\text{N}_2\text{O}_5^+$  requires 453.2384.

#### 5.5.11.4 Preparation of IL (380) – General procedure “G”

(2*R*)-2-Carboxy-1-(2-(((*S*)-1-ethoxy-1-oxo-3-phenylpropan-2-yl)amino)-2-oxoethyl)-1-methylpyrrolidin-1-ium bromide (**380**).



To a stirred solution of IL (**379**) (0.136 g, 0.255 mmol) in DCM was added 10% Pd/C (0.025 g). The reaction mixture was stirred at room temperature under 1 atmosphere of H<sub>2</sub> for 72 hours. After 72 hours the reaction mixture was degassed with a stream of nitrogen and filtered over a pad of celite. Solvent was removed from the filtrate to afford the title compound (**380**) as a mixture of epimers (1:3.3 ratio) as a pale yellow solid in 97% yield (0.108 g, 0.244 mmol).

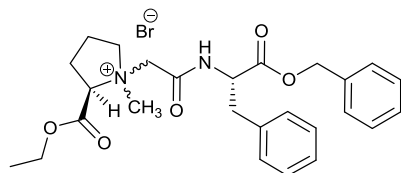
Molecular formula: C<sub>19</sub>H<sub>27</sub>BrN<sub>2</sub>O<sub>5</sub>; Molecular weight: 443.338 g mol<sup>-1</sup>; Mp: 39-41° C.

[ $\alpha$ ]<sub>D</sub><sup>20</sup> = -32.0 (0.1 c, EtOH). <sup>1</sup>H-NMR (400 MHz, D<sub>2</sub>O)  $\delta$  (ppm): 7.27 – 7.07 (m, 5H), 4.60 – 4.52 (m, 1H), 4.48 – 4.32 (m, 1H), 4.32 – 4.22 (m, 1H), 4.07 (q, *J* = 7.1 Hz, 2H), 4.01 – 3.82 (m, 1H), 3.71 – 3.60 (m, 1H), 3.51 – 3.32 (m, 1H), 3.25 – 3.14 (m, 1H), 2.95 (s, 0.7H), 2.82 (dd, *J* = 14.0, 10.2 Hz, 1H), 2.72 (s, 2.3H), 2.40 – 2.25 (m, 1H), 2.23 – 2.05 (m, 1H), 2.04 – 1.87 (m, 2H), 1.09 (t, *J* = 7.1 Hz, 3H). <sup>13</sup>C-NMR (100 MHz, D<sub>2</sub>O)  $\delta$  (ppm): 172.35, 168.74, 163.95, 136.28, 129.14, 128.72, 127.19, 74.56, 66.21, 63.09, 62.81, 53.98, 44.35, 36.55, 23.27, 18.40, 13.15. IR (neat) (cm<sup>-1</sup>): 3197 (b), 3035 (w), 2985 (w), 1734 (s), 1680 (vs), 1546 (m), 1209 (b), 1022 (s), 730 (m), 699 (vs). ESI-MS (+ve) m/z: Found [M-Br]<sup>+</sup> 363.1922, C<sub>26</sub>H<sub>33</sub>N<sub>2</sub>O<sub>5</sub><sup>+</sup> requires 363.1914.

#### 5.5.12 Preparation of IL (382) – Hydrogenolysis route

##### 5.5.12.1 Preparation of IL (381)

(2*R*)-1-(2-(((*S*)-1-(Benzyloxy)-1-oxo-3-phenylpropan-2-yl)amino)-2-oxoethyl)-2-(ethoxycarbonyl)-1-methylpyrrolidin-1-ium bromide (**381**).



To a stirred solution of *N*-methyl-D-proline ethyl ester hydrochloride (**343**) (0.196 g, 1.09 mmol) in THF (25 ml) was added triethylamine (0.15 ml, 4.3 mmol) and benzyl alkylating reagent (**375**) (0.490 g, 1.31 mmol). The reaction was heated under reflux conditions for 48 hours. After 48 hours the reaction was allowed to cool to room temperature and the solvent was removed *in vacuo*. The resulting crude product was

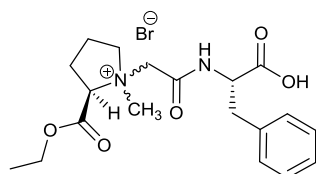
purified by silica gel chromatography (gradient elution of 1:99 MeOH:DCM to 5:95 MeOH:DCM) to afford the title compound (**381**) as a white solid, mixture of epimers (1:4 ratio), in 27% yield (0.158 g, 0.296 mmol).

Molecular formula: C<sub>26</sub>H<sub>33</sub>BrN<sub>2</sub>O<sub>5</sub>; Molecular weight: 533.463 g mol<sup>-1</sup>; Mp: 42-44° C.

[α]<sub>D</sub><sup>20</sup> = -12.0 (0.1 c, EtOH). <sup>1</sup>H-NMR (400 MHz, CDCl<sub>3</sub>) δ (ppm): 9.33 (d, *J* = 7.4 Hz, 1H), 7.44 – 7.27 (m, 7H), 7.24 – 7.00 (m, 3H), 5.20 (dd, *J* = 12.8, 7.2 Hz, 2H), 5.03 (dd, *J* = 21.0, 11.0 Hz, 2H), 4.72 – 4.62 (m, 1H), 4.36 (d, *J* = 13.3 Hz, 1H), 4.29 – 4.18 (m, 3H), 3.55 (ddd, *J* = 11.7, 8.6, 2.7 Hz, 1H), 3.39 – 3.25 (m, 1H), 3.16 (d, *J* = 3.9 Hz, 3H), 3.14 – 3.04 (m, 1H), 2.68 – 2.51 (m, 1H), 2.20 – 1.81 (m, 3H), 1.28 (t, *J* = 7.1 Hz, 3H). <sup>13</sup>C-NMR (100 MHz, CDCl<sub>3</sub>) δ (ppm): 170.47, 165.56, 163.43, 136.48, 135.27, 129.67, 129.58, 128.64, 128.55, 128.48, 128.38, 126.96, 73.56, 67.36, 64.75, 63.40, 62.64, 55.39, 45.33, 36.76, 24.19, 18.85, 14.02. IR (neat) (cm<sup>-1</sup>): 3031 (m), 2981 (m), 1737 (vs), 1679 (vs), 1549 (s), 1455 (s), 1208 (vs), 1028 (s), 739 (s), 698 (vs). ESI-MS (+ve) m/z: Found [M-Br]<sup>+</sup> 453.2396, C<sub>26</sub>H<sub>33</sub>N<sub>2</sub>O<sub>5</sub><sup>+</sup> requires 453.2384.

#### 5.5.12.2 Preparation of IL (**382**)

(2*R*)-1-(2-(((*S*)-1-carboxy-2-phenylethyl)amino)-2-oxoethyl)-2-(ethoxycarbonyl)-1-methylpyrrolidin-1-ium (**382**).



According to general procedure “G”, using IL (**381**) (0.101 g, 0.189 mmol), the title compound was isolated as a pale yellow solid, mixture of epimers (1:4 ratio), in 95% yield (0.081 g, 0.18 mmol).

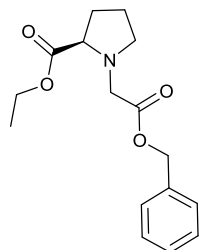
Molecular formula: C<sub>19</sub>H<sub>27</sub>BrN<sub>2</sub>O<sub>5</sub>; Molecular weight: 443.338 g mol<sup>-1</sup>; Mp: 41-43° C.

[α]<sub>D</sub><sup>20</sup> = -13.0 (0.1 c, EtOH). <sup>1</sup>H-NMR (400 MHz, D<sub>2</sub>O) δ (ppm): 7.28 – 7.10 (m, 5H), 4.75 – 4.71 (m, 1H), 4.47 – 4.36 (m, 1H), 4.29 (d, *J* = 14.8 Hz, 1H), 4.16 (q, *J* = 7.1 Hz, 2H), 4.03 (d, *J* = 14.8 Hz, 1H), 3.74 – 3.63 (m, 1H), 3.50 – 3.35 (m, 1H), 3.30 – 3.20 (m, 1H), 2.98 (s, 0.6H), 2.88 – 2.77 (m, 1H), 2.73 (s, 2.4H), 2.49 – 2.30 (m, 1H), 2.29 – 2.13 (m, 1H), 2.11 – 1.89 (m, 2H), 1.15 (t, *J* = 7.2 Hz, 3H). <sup>13</sup>C-NMR (100 MHz, D<sub>2</sub>O) δ (ppm): 174.37, 166.30, 163.57, 136.59, 129.15, 128.70, 127.14, 73.42, 66.78, 63.74, 63.21, 53.94, 44.92, 36.68, 23.20, 18.58, 13.01. IR (neat) (cm<sup>-1</sup>): 3192 (b), 2920 (m), 2918 (m), 1734 (s), 1679 (vs), 1548 (m), 1205 (b), 1025 (s), 731 (s), 701(vs).

### 5.5.13 Preparation of tertiary amine (387)

#### 5.5.13.1 Preparation of ester (386)

Ethyl (2-(benzyloxy)-2-oxoethyl)-D-prolinate (**386**).



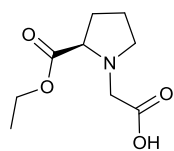
To a stirred solution of D-proline ethyl ester hydrochloride (**339**) (0.250 g, 1.39 mmol) in acetonitrile (15 ml) at room temperature was added dropwise triethylamine (0.43 ml, 3.1 mmol). The reaction mixture was stirred for 30 minutes followed by the dropwise addition of benzyl bromoacetate (0.24 ml, 1.5 mmol). The reaction mixture was stirred for 6 hours. After 6 hours volatile organics were removed *in vacuo* and the resulting crude product was purified by silica gel chromatography (eluent 10:90 ethyl acetate:hexane) to afford the title compound (**386**) as a pale yellow oil in 74% yield (0.299 g, 1.03 mmol).

Molecular formula: C<sub>16</sub>H<sub>21</sub>NO<sub>4</sub>; Molecular weight: 291.347 g mol<sup>-1</sup>.

$[\alpha]_D^{20} = +88.6$  (1.8 c, CHCl<sub>3</sub>). <sup>1</sup>H-NMR (400 MHz, CDCl<sub>3</sub>)  $\delta$  (ppm): 7.40 – 7.30 (m, 5H), 5.15 (s, 2H), 4.24 – 4.07 (m, 2H), 3.68 (d,  $J = 17.4$  Hz, 1H), 3.65 – 3.62 (m, 1H), 3.59 (d,  $J = 17.3$  Hz, 1H), 3.22 – 3.12 (m, 1H), 2.87 – 2.76 (m, 1H), 2.26 – 2.11 (m, 1H), 2.05 – 1.78 (m, 3H), 1.25 (t,  $J = 7.1$  Hz, 3H). <sup>13</sup>C-NMR (100 MHz, CDCl<sub>3</sub>)  $\delta$  (ppm): 173.90, 170.74, 135.78, 128.68, 128.44, 66.38, 63.73, 60.77, 53.40, 52.96, 29.80, 23.87, 14.34. IR (neat) (cm<sup>-1</sup>): 2980 (b), 1733 (vs), 1175 (vs), 1155(vs), 1094 (s), 736 (s), 697 (vs). ESI-MS (+ve) m/z: Found [M+H]<sup>+</sup> 292.1538, C<sub>16</sub>H<sub>22</sub>NO<sub>4</sub><sup>+</sup> requires 292.1543.

#### 5.5.13.2 Preparation of tertiary amine (387)

(*R*)-2-(2-(Ethoxycarbonyl)pyrrolidin-1-yl)acetic acid (**387**).



To a stirred solution of (**386**) (0.127 g, 0.44 mmol) in 50:50 ethanol:ethyl acetate was added 10% Pd/C (0.011 g). The reaction mixture was stirred vigorously under 1 atmosphere of H<sub>2</sub> for 12 hours. After 12 hours the reaction mixture was degassed with a stream of N<sub>2</sub> and filtered over a pad of celite. The celite filter pad was washed with 50:50 ethanol:ethyl acetate (3 x 25 ml). The combined filtrate was collected and organic solvent was removed *in vacuo* to afford the title compound (**387**) as a pale yellow oil in 86% yield (0.076 g, 0.38 mmol).



Molecular formula: C<sub>9</sub>H<sub>15</sub>NO<sub>4</sub>; Molecular weight: 201.222 g mol<sup>-1</sup>.

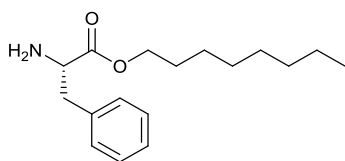
$[\alpha]_D^{20} = -46.15$  (0.1 c, EtOH). <sup>1</sup>H-NMR (400 MHz, D<sub>2</sub>O)  $\delta$  (ppm): 4.42 (dd,  $J = 9.3, 6.1$  Hz, 1H), 4.30 (q,  $J = 7.1$  Hz, 2H), 4.01 (d,  $J = 16.2$  Hz, 1H), 3.91 – 3.76 (m, 2H), 3.27 (ddd,  $J = 11.6, 8.4, 7.1$  Hz, 1H), 2.59 – 2.43 (m, 1H), 2.27 – 2.08 (m, 2H), 2.12 – 1.97 (m, 1H), 1.28 (t,  $J = 7.1$  Hz, 3H). <sup>13</sup>C-NMR (100 MHz, D<sub>2</sub>O)  $\delta$  (ppm): 170.28, 169.74, 67.32, 63.68, 57.47, 56.07, 28.15, 22.63, 13.01. IR (neat) (cm<sup>-1</sup>): 2981 (b), 1733 (vs), 1619 (vs), 1372 (s), 1186 (b), 1022 (s). ESI-MS (+ve) m/z: Found  $[M+H]^+$  202.1077 C<sub>9</sub>H<sub>16</sub>NO<sub>4</sub><sup>+</sup> requires 202.1074

## 5.6 Experimental preparation of Chapter 3 linear alkyl amino acid surfactant ILs

### 5.6.1 Preparation of Chapter 3 linear alkyl amino acid esters (453-455)

#### 5.6.1.1 Preparation of ester (453) – general procedure “H”

Octyl L-phenylalaninate (**453**).



To a stirred suspension of L-phenylalanine (8.094 g, 48.99 mmol), in toluene (50 ml) was added PTSA (10.251 g, 59.53 mmol), and 1-octanol (9.5 ml, 60 mmol). The suspension was heated under reflux conditions for 12 hours using a Dean-Stark apparatus. After 2 hours, a homogenous solution was obtained. After 12 hours the solution was allowed to cool to room temperature. Addition of diethyl ether (50 ml) caused precipitation of the product as a crude PTSA salt. The crude PTSA salt product was isolated by vacuum filtration and washed with hexane (3 x 50 ml). The crude product PTSA salt was then neutralised by stirring in an aqueous sodium bicarbonate solution (150 ml) and then transferred to a separating funnel. The title compound (**453**) was extracted with ethyl acetate (3 x 50 ml), breaking the emulsion formed with brine (3 x 50 ml). The organic phase was dried over magnesium sulphate, filtered and volatiles removed *in vacuo* to afford the title compound (**453**) as a pale yellow oil in 58% yield (7.900 g, 28.48 mmol).

Molecular formula: C<sub>17</sub>H<sub>27</sub>NO<sub>2</sub>; Molecular weight: 277.408 g mol<sup>-1</sup>.

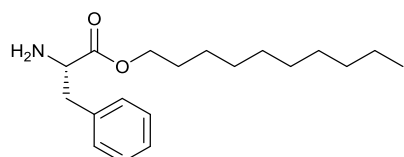
<sup>1</sup>H-NMR (400 MHz, CDCl<sub>3</sub>)  $\delta$  (ppm): 7.32 – 7.19 (m, 5H), 4.09 (t,  $J = 6.8$  Hz, 2H), 3.76 (dd,  $J = 7.6, 5.6$  Hz, 1H), 3.10 (dd,  $J = 13.6, 5.2$  Hz, 1H), 2.90 (dd,  $J = 13.6, 7.6$  Hz, 1H), 1.60-1.57 (m, 2H), 1.30 -1.24 (m, 10 H), 0.88 (t,  $J = 6.4$  Hz, 3H). <sup>13</sup>C-NMR (100 MHz, CDCl<sub>3</sub>)  $\delta$  (ppm):

174.81, 137.12, 129.42, 128.68, 126.98, 65.39, 55.84, 40.93, 31.89, 29.27, 28.63, 25.97, 22.75, 14.22.

$^1\text{H}$ -NMR and  $^{13}\text{C}$ -NMR were in agreement with the literature.<sup>15</sup>

### 5.6.1.2 Preparation of ester (454)

Decyl L-phenylalaninate (**454**).



g, 26.26 mmol).

According the general procedure “H”, using L-phenylalanine (12.361 g, 74.828 mmol), PTSA (15.657 g, 82.31) and decanol (15 ml, 78 mmol), the title compound (**454**) was isolated as a pale yellow oil in 38% yield (8.602

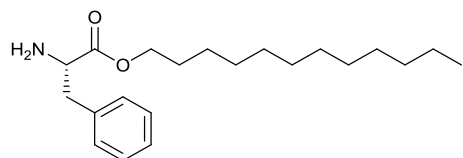
Molecular formula:  $\text{C}_{19}\text{H}_{31}\text{NO}_2$ ; Molecular weight:  $305.462 \text{ g mol}^{-1}$ .

$^1\text{H}$ -NMR (400 MHz,  $\text{CDCl}_3$ )  $\delta$  (ppm): 7.32 – 7.19 (m, 5H), 4.09 (t,  $J = 6.8 \text{ Hz}$ , 2H), 3.75 (dd,  $J = 7.6, 5.6 \text{ Hz}$ , 1H), 3.11 (dd,  $J = 13.6, 5.2 \text{ Hz}$ , 1H), 2.90 (dd,  $J = 13.6, 7.6 \text{ Hz}$ , 1H), 1.61-1.56 (m, 2H), 1.32 -1.22 (m, 14 H), 0.88 (t,  $J = 6.4 \text{ Hz}$ , 3H).

$^1\text{H}$ -NMR was in agreement with the literature.<sup>16</sup>

### 5.6.1.3 Preparation of ester (455)

Dodecyl L-phenylalaninate (**455**)



According the general procedure “H”, using L-phenylalanine (12.255 g, 74.188 mmol), PTSA (15.524 g, 81.612 mmol) and dodecanol (13.823 g, 74.182 mmol) the title compound was isolated as a pale yellow oil in 37% yield (9.130 g, 27.38 mmol).

Molecular formula:  $\text{C}_{21}\text{H}_{35}\text{NO}_2$ ; Molecular weight:  $333.516 \text{ g mol}^{-1}$ .

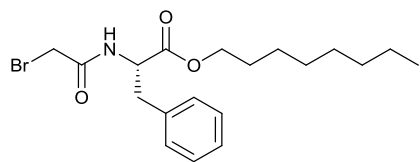
$^1\text{H}$ -NMR (400 MHz,  $\text{CDCl}_3$ )  $\delta$  (ppm): 7.30 – 7.19 (m, 5H), 4.09 (t,  $J = 6.8 \text{ Hz}$ , 2H), 3.74 (dd,  $J = 7.6, 5.6 \text{ Hz}$ , 1H), 3.10 (dd,  $J = 13.6, 5.2 \text{ Hz}$ , 1H), 2.89 (dd,  $J = 13.6, 7.6 \text{ Hz}$ , 1H), 1.61-1.58 (m, 2H), 1.31-1.19 (m, 18 H), 0.88 (t,  $J = 6.4 \text{ Hz}$ , 3H).

$^1\text{H}$ -NMR was in agreement with the literature.<sup>16</sup>

## 5.6.2 Preparation of Chapter 3 linear alkyl alkylating reagents (456-458)

### 5.6.2.1 Preparation of alkylating reagent (456)

Octyl (2-bromoacetyl)-L-phenylalaninate (**456**).



According to general procedure “B”, using L-phenylalanine octyl ester (**453**) (7.900 g, 28.48 mmol),  $\text{Na}_2\text{CO}_3$  (3.924 g, 37.02 mmol), bromoacetyl bromide (2.95 ml, 33.9 mmol) and DCM (100 ml) the crude

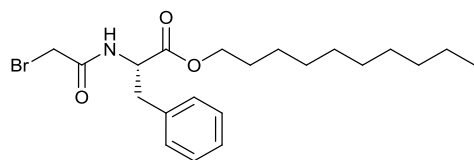
product was isolated as an off white solid. Purification was achieved by passing the crude product through a short plug of silica gel using 150 ml of 10% ethyl acetate: hexane. Solvent was removed *in vacuo* and the product was further dried under high vacuum for 24 hours to afford the title compound (**456**) as a white solid in 72% yield (8.184 g, 20.55 mmol).

Molecular formula:  $\text{C}_{19}\text{H}_{28}\text{BrNO}_3$ ; Molecular weight: 398.341  $\text{g mol}^{-1}$ ; Mp: 39-40 °C.

$[\alpha]_D^{20} = +16.8$  (1.0 c,  $\text{CHCl}_3$ ),  $+0.9$  (1.0 c, EtOH).  $^1\text{H-NMR}$  (400 MHz,  $\text{CDCl}_3$ )  $\delta$  (ppm): 7.35 – 7.21 (m, 3H), 7.16 – 7.09 (m, 2H), 6.86 (d,  $J = 7.9$  Hz, 1H), 4.89 – 4.79 (m, 1H), 4.17 – 4.03 (m, 2H), 3.87 (d,  $J = 13.7$  Hz, 1H), 3.83 (d,  $J = 13.8$  Hz, 1H), 3.17 (dd,  $J = 12.5, 2.6$  Hz, 1H), 3.13 (dd,  $J = 12.2, 2.5$  Hz, 1H), 1.64 – 1.56 (m, 2H), 1.35 – 1.22 (m, 10H), 0.89 (t,  $J = 6.8$  Hz, 3H).  $^{13}\text{C-NMR}$  (100 MHz,  $\text{CDCl}_3$ )  $\delta$  (ppm): 171.00, 165.16, 135.49, 129.43, 128.74, 127.40, 66.02, 53.87, 37.92, 31.87, 29.25, 28.81, 28.52, 25.92, 22.75, 14.22. IR (neat) ( $\text{cm}^{-1}$ ): 3298 (b), 2920 (m), 2854 (m), 1737 (s), 1719 (vs), 1649 (vs), 1542 (vs), 1280 (s), 1236 (s), 1208 (s), 1182 (m), 1139 (m), 699 (s). ESI-MS (+ve) m/z: Found  $[\text{M}+\text{H}]^+$  398.1338,  $\text{C}_{19}\text{H}_{29}\text{BrNO}_3^+$  requires 398.1325.

### 5.6.2.2 Preparation of alkylating reagent (457)

Decyl (2-bromoacetyl)-L-phenylalaninate (**457**).



According to the general procedure “B”, using L-phenylalanine decyl ester (**454**) (8.020 g, 26.26 mmol),  $\text{Na}_2\text{CO}_3$  (3.618 g, 34.14 mmol), bromoacetyl bromide (2.75 ml, 31.5 mmol) and DCM (100 ml),

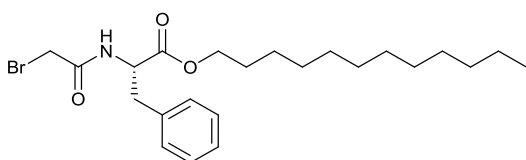
the title compound was isolated as a white solid in 51% yield (5.675 g, 13.31 mmol).

Molecular formula:  $\text{C}_{21}\text{H}_{32}\text{BrNO}_3$ ; Molecular weight: 426.395  $\text{g mol}^{-1}$ ; Mp: 43-44 °C.

$[\alpha]_D^{20} = +15.4$  (1.0 c,  $\text{CHCl}_3$ ),  $+2.4$  (1.0 c, EtOH).  $^1\text{H-NMR}$  (400 MHz,  $\text{CDCl}_3$ )  $\delta$  (ppm): 7.35 – 7.21 (m, 3H), 7.16 – 7.09 (m, 2H), 6.86 (d,  $J = 7.9$  Hz, 1H), 4.89 – 4.79 (m, 1H), 4.17 – 4.03 (m, 2H), 3.87 (d,  $J = 13.7$  Hz, 1H), 3.83 (d,  $J = 13.8$  Hz, 1H), 3.17 (dd,  $J = 12.5, 2.6$  Hz, 1H), 3.13 (dd,  $J = 12.2, 2.5$  Hz, 1H), 1.64 – 1.56 (m, 2H), 1.35 – 1.22 (m, 14H), 0.89 (t,  $J = 6.8$  Hz, 3H).  $^{13}\text{C-NMR}$  (100 MHz,  $\text{CDCl}_3$ )  $\delta$  (ppm): 170.96, 165.11, 135.46, 129.40, 128.70, 127.36, 65.99, 53.83, 37.89, 31.96, 29.60, 29.56, 29.38, 29.26, 28.78, 28.49, 25.89, 22.76, 14.21.  $\text{IR}$  (neat) ( $\text{cm}^{-1}$ ): 3298 (b), 2920 (m), 2854 (m), 1719 (vs), 1649 (vs), 1542 (vs), 1280 (s), 1208 (s), 1182 (m), 1139 (m), 971 (m), 699 (s).  $\text{ESI-MS}$  (+ve)  $m/z$ : Found  $[\text{M}+\text{Na}]^+$  448.1462,  $\text{NaC}_{21}\text{H}_{32}\text{BrNO}_3^+$  requires 448.1458.

### 5.6.2.3 Preparation of alkylating reagent (458)

Dodecyl (2-bromoacetyl)-L-phenylalaninate (458).



According to the general procedure “B”, using L-phenylalanine dodecyl ester (455) (9.130 g, 27.38 mmol),  $\text{Na}_2\text{CO}_3$  (3.772 g, 35.59 mmol), bromoacetyl bromide (2.9 ml, 33 mmol) and

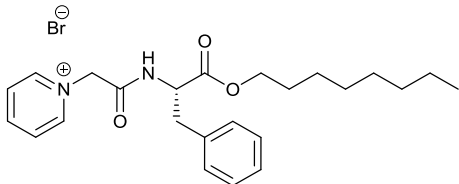
DCM (100 ml), the title compound was isolated as a white solid in 88% yield (10.940 g, 24.073 mmol).

Molecular formula:  $\text{C}_{23}\text{H}_{36}\text{BrNO}_3$ ; Molecular weight: 454.449  $\text{gmol}^{-1}$ ; Mp: 55-56 °C.

$[\alpha]_D^{20} = +14.7$  (1.0 c,  $\text{CHCl}_3$ ),  $+1.0$  (1.0 c, EtOH).  $^1\text{H-NMR}$  (400 MHz,  $\text{CDCl}_3$ )  $\delta$  (ppm): 7.35 – 7.21 (m, 3H), 7.16 – 7.09 (m, 2H), 6.87 (d,  $J = 7.9$  Hz, 1H), 4.89 – 4.79 (m, 1H), 4.16 – 4.05 (m, 2H), 3.85 (d,  $J = 13.6$  Hz, 1H), 3.84 (d,  $J = 13.6$  Hz, 1H), 3.17 (dd,  $J = 12.1, 6.0$  Hz, 1H), 3.12 (dd,  $J = 12.3, 5.7$  Hz, 1H), 1.66 – 1.51 (m, 2H), 1.35-1.22 (m, 18H), 0.88 (d,  $J = 6.9$  Hz, 3H).  $^{13}\text{C-NMR}$  (100 MHz,  $\text{CDCl}_3$ )  $\delta$  (ppm): 171.01, 165.15, 135.40, 129.45, 128.76, 127.42, 66.05, 53.89, 37.95, 32.04, 29.78, 29.76, 29.70, 29.62, 29.48, 29.31, 28.84, 28.55, 25.94, 22.83, 14.27.  $\text{IR}$  (neat) ( $\text{cm}^{-1}$ ): 3311 (b), 2918 (s), 2850 (m), 1734 (vs), 1647 (vs), 1533 (vs), 1496 (m), 1199 (vs), 986 (m), 699 (s).  $\text{ESI-MS}$  (+ve)  $m/z$ : Found  $[\text{M}+\text{Na}]^+$  476.1783,  $\text{NaC}_{23}\text{H}_{36}\text{BrNO}_3^+$  requires 476.1771.

### 5.6.3 Preparation of IL (432)

(S)-1-(2-((1-(Octyloxy)-1-oxo-3-phenylpropan-2-yl)amino)-2-oxoethyl)pyridin-1-ium bromide (**432**).



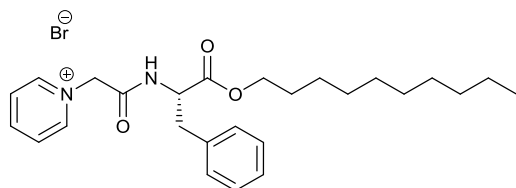
According to general procedure “E”, using octyl(2-bromoacetyl)-L-phenylalaninate (**456**) (1.926 g, 4.835 mmol), pyridine (380  $\mu$ l, 4.72 mmol) and ethyl acetate (25 ml) the title compound (**432**) was isolated as a white solid in 98% yield (2.210 g, 4.629 mmol).

Molecular formula:  $C_{24}H_{33}BrN_2O_3$ ; Molecular weight: 477.443  $gmol^{-1}$ ; Mp: 93-95  $^{\circ}C$ .

$[\alpha]_D^{20} = +1.5$  (1.0 c, EtOH).  $^1H$ -NMR (400 MHz,  $CDCl_3$ )  $\delta$  (ppm): 9.27 (d,  $J = 7.8$  Hz, 1H), 9.19 – 9.12 (m, 2H), 8.40 (tt,  $J = 7.8, 1.4$  Hz, 1H), 7.96 (dd,  $J = 7.9, 6.5$  Hz, 2H), 7.38 – 7.30 (m, 2H), 7.30 – 7.12 (m, 3H), 5.99 (s, 2H), 4.69 (ddd,  $J = 8.9, 7.7, 6.0$  Hz, 1H), 4.07 – 3.96 (m, 2H), 3.23 (dd,  $J = 13.9, 6.1$  Hz, 1H), 3.16 (dd,  $J = 13.9, 8.9$  Hz, 1H), 1.66 – 1.41 (m, 2H), 1.36 – 1.12 (m, 10H), 0.87 (t,  $J = 6.8$  Hz, 3H).  $^{13}C$ -NMR (100 MHz,  $CDCl_3$ )  $\delta$  (ppm): 171.08, 163.97, 146.17, 145.29, 136.39, 129.69, 128.53, 127.69, 126.89, 65.85, 65.26, 55.05, 37.67, 31.89, 29.28, 29.25, 28.49, 25.87, 22.75, 14.22. IR (neat) ( $cm^{-1}$ ): 3335 (b), 2915 (m), 2815 (m), 1737 (vs), 1661 (vs), 1629 (s), 1534 (s), 1478 (s), 1349 (m), 1198 (s), 974 (s), 724 (s), 702 (s), 678 (s). ESI-MS (+ve) m/z: Found  $[M-Br]^{+}$  397.2488,  $C_{24}H_{33}N_2O_3^{+}$  requires 397.2486.

### 5.6.4 Preparation of IL (433)

(S)-1-(2-((1-(Decyloxy)-1-oxo-3-phenylpropan-2-yl)amino)-2-oxoethyl)pyridin-1-ium bromide (**433**).



According to the general procedure “E”, decyl (2-bromoacetyl)-L-phenylalaninate (**457**) (1.461 g, 3.43 mmol), pyridine (270  $\mu$ l, 3.36 mmol) and ethyl acetate (25 ml), the title compound was isolated as a white solid in 99% yield (1.683 g, 3.329 mmol).

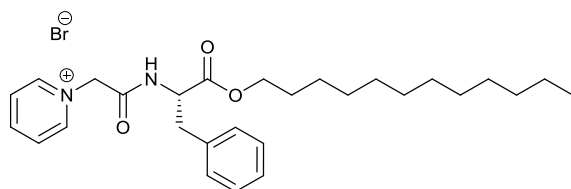
Molecular formula:  $C_{26}H_{37}BrN_2O_3$ ; Molecular weight: 505.497  $gmol^{-1}$ ; Mp: 101-103  $^{\circ}C$ .

$[\alpha]_D^{20} = +2.0$  (1.0 c, EtOH).  $^1H$ -NMR (400 MHz,  $CDCl_3$ )  $\delta$  (ppm): 9.30 (d,  $J = 7.8$  Hz, 1H), 9.21 – 9.14 (m, 2H), 8.40 (tt,  $J = 7.8, 1.4$  Hz, 1H), 8.01 – 7.92 (m, 2H), 7.39 – 7.31 (m, 2H), 7.28 –

7.13 (m, 3H), 6.06 (d,  $J = 14.8$  Hz, 1H), 6.01 (d,  $J = 14.7$  Hz, 1H), 4.69 (ddd,  $J = 8.8, 7.7, 6.1$  Hz, 1H), 4.10 – 3.87 (m, 2H), 3.23 (dd,  $J = 13.8, 6.1$  Hz, 1H), 3.17 (dd,  $J = 13.9, 8.8$  Hz, 1H), 1.56 – 1.47 (m, 2H), 1.35 – 1.12 (m, 14H), 0.87 (t,  $J = 7.0$  Hz, 3H).  $^{13}\text{C-NMR}$  (100 MHz,  $\text{CDCl}_3$ )  $\delta$  (ppm): 171.16, 164.06, 146.28, 145.38, 136.82, 129.84, 128.66, 127.80, 127.02, 66.00, 62.34, 55.20, 37.77, 32.13, 29.79, 29.74, 29.56, 29.47, 28.64, 26.01, 22.93, 14.38.  $\text{IR}$  (neat) ( $\text{cm}^{-1}$ ): 3335 (b), 2915 (m), 2815 (m), 1737 (s), 1661 (s), 1629 (m), 1534 (m), 1478 (m), 1349 (m), 1198 (m), 974 (m), 724 (m), 702 (m), 678 (m).  $\text{ESI-MS}$  (+ve)  $m/z$ : Found  $[\text{M}-\text{Br}^-]^+$  425.2803,  $\text{C}_{26}\text{H}_{37}\text{N}_2\text{O}_3^+$  requires 425.2799.

### 5.6.5 Preparation of IL (434)

(*S*)-1-(2-((1-(Dodecyloxy)-1-oxo-3-phenylpropan-2-yl)amino)-2-oxoethyl)pyridin-1-ium bromide (**434**).



According to the general procedure “C”, using dodecyl (2-bromoacetyl)- L-phenylalaninate (**458**) (1.541 g, 3.391 mmol), pyridine (270  $\mu\text{l}$ , 3.32 mmol) and ethyl

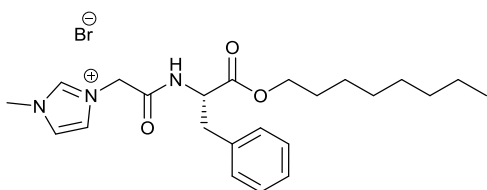
acetate (25 ml), the title compound (**434**) was isolated as a pale pink solid in 98% yield (1.742 g, 3.265 mmol).

Molecular formula:  $\text{C}_{28}\text{H}_{41}\text{BrN}_2\text{O}_3$ ; Molecular weight:  $533.551 \text{ g mol}^{-1}$ ; Mp: 107-109  $^\circ\text{C}$ .

$[\alpha]_{\text{D}}^{20} = +2.6$  (1.0 c, EtOH).  $^1\text{H-NMR}$  (400 MHz,  $\text{CDCl}_3$ )  $\delta$  (ppm): 9.28 (d,  $J = 7.8$  Hz, 1H), 9.19 – 9.11 (m, 2H), 8.40 (tt,  $J = 7.8, 1.4$  Hz, 1H), 7.96 (dd,  $J = 7.9, 6.5$  Hz, 2H), 7.37 – 7.30 (m, 2H), 7.28 – 7.10 (m, 3H), 6.06 (d,  $J = 14.9$  Hz, 1H), 6.03 (d,  $J = 14.9$  Hz, 1H), 4.74 – 4.64 (m, 1H), 4.07 – 3.91 (m, 2H), 3.22 (dd,  $J = 13.6, 6.4$  Hz, 1H), 3.16 (dd,  $J = 13.6, 8.8$  Hz, 1H), 1.63 – 1.43 (m, 2H), 1.33 – 1.08 (m, 18H), 0.86 (t,  $J = 7.0$  Hz, 3H).  $^{13}\text{C-NMR}$  (100 MHz,  $\text{CDCl}_3$ )  $\delta$  (ppm): 171.25, 164.13, 146.31, 145.42, 136.82, 129.82, 128.66, 127.80, 127.02, 65.99, 62.36, 55.17, 37.80, 32.15, 29.90, 29.88, 29.84, 29.74, 29.60, 29.48, 28.63, 26.01, 22.93, 14.38.  $\text{IR}$  (neat) ( $\text{cm}^{-1}$ ): 3335 (b), 2915 (vs), 2815 (vs), 1737 (vs), 1661 (vs), 1629 (s), 1534 (s), 1478 (s), 1349 (s), 1198 (m), 974 (m), 724 (s), 702 (m), 678 (m).  $\text{ESI-MS}$  (+ve)  $m/z$ : Found  $[\text{M}-\text{Br}^-]^+$  453.3113,  $\text{C}_{28}\text{H}_{41}\text{N}_2\text{O}_3^+$  requires 453.3112.

### 5.6.6 Preparation of IL (435)

(S)-1-Methyl-3-(2-((1-(octyloxy)-1-oxo-3-phenylpropan-2-yl)amino)-2-oxoethyl)-1H-imidazol-3-ium bromide (**435**).



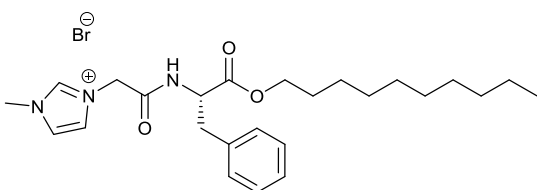
According to the general procedure “E”, using octyl (2-bromoacetyl)-L-phenylalaninate (**456**) (1.060 g, 2.661 mmol), 1-methylimidazole (210  $\mu$ l, 2.63 mmol) and ethyl acetate (25 ml), the title compound (**435**) was isolated as a white solid in 97% yield (1.244 g, 2.589 mmol).

Molecular formula:  $C_{23}H_{34}BrN_3O_3$ ; Molecular weight: 480.447  $g\ mol^{-1}$ ; Mp: 64-66  $^{\circ}C$ .

$[\alpha]_D^{20} = +5.4$  (1.0 c, EtOH).  $^1H$ -NMR (400 MHz,  $CDCl_3$ )  $\delta$  (ppm): 9.71 (s, 1H), 8.97 (d,  $J = 7.7$  Hz, 1H), 7.41 (t,  $J = 1.7$  Hz, 1H), 7.38 – 7.29 (m, 2H), 7.29 – 7.26 (m, 1H), 7.26 – 7.23 (m, 1H), 7.21 – 7.14 (m, 2H), 5.39 (d,  $J = 15.5$  Hz, 1H), 5.34 (d,  $J = 15.5$  Hz, 1H), 4.73 – 4.63 (m, 1H), 4.01 (m, 2H), 3.98 (s, 3H), 3.26 – 3.19 (m, 1H), 3.17 (dd,  $J = 11.5, 4.0$  Hz, 1H), 1.60 – 1.46 (m, 2H), 1.34-1.14 (m, 10H), 0.87 (t,  $J = 6.8$  Hz, 3H).  $^{13}C$ -NMR (100 MHz,  $CDCl_3$ )  $\delta$  (ppm): 171.36, 164.81, 137.86, 136.73, 129.60, 128.51, 126.88, 123.76, 122.46, 65.79, 54.89, 51.67, 37.54, 36.87, 31.87, 29.28, 29.24, 28.48, 25.87, 22.74, 14.21. IR (neat) ( $cm^{-1}$ ): 3431 (b), 3340 (b), 2915 (m), 1736 (vs), 1666 (vs), 1533 (s), 1352 (s), 1201 (vs), 1167 (vs), 974 (s), 752 (s), 702 (s). ESI-MS (+ve) m/z: Found  $[M-Br]^{+}$  400.2603,  $C_{23}H_{34}N_3O_3^{+}$  requires 400.2595.

### 5.6.7 Preparation of IL (436)

(S)-3-(2-((1-(Decyloxy)-1-oxo-3-phenylpropan-2-yl)amino)-2-oxoethyl)-1-methyl-1H-imidazol-3-ium bromide (**436**).



According to the general procedure “E”, using decyl (2-bromoacetyl)-L-phenylalaninate (**457**) (1.317 g, 3.089 mmol), 1-methylimidazole (240  $\mu$ l, 3.03 mmol) and ethyl acetate (25 ml) the title compound (**436**) was isolated as a white solid in 92% yield (1.424 g, 2.800 mmol).

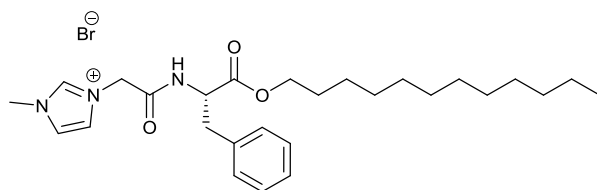
Molecular formula:  $C_{25}H_{38}BrN_3O_3$ ; Molecular weight: 508.501  $g\ mol^{-1}$ ; Mp: 80-82  $^{\circ}C$ .

$[\alpha]_D^{20} = +5.2$  (1.0 c, EtOH).  $^1H$ -NMR (400 MHz,  $CDCl_3$ )  $\delta$  (ppm): 9.80 (s, 1H), 8.94 (d,  $J = 7.7$  Hz, 1H), 7.42 (t,  $J = 1.5$  Hz, 1H), 7.37 – 7.30 (m, 2H), 7.29 – 7.24 (m, 2H), 7.24 – 7.16 (m, 1H), 7.13 (t,  $J = 1.6$  Hz, 1H), 5.38 (d,  $J = 15.4$  Hz, 1H), 5.32 (d,  $J = 15.4$  Hz, 1H), 4.73 – 4.63 (m, 1H), 4.03 (m, 2H), 3.98 (s, 3H), 3.22 (dd,  $J = 12.9, 5.3$  Hz, 1H), 3.17 (dd,  $J = 12.9, 7.6$  Hz, 1H),

1.61 – 1.47 (m, 2H), 1.34 – 1.15 (m, 14H), 0.87 (t,  $J = 6.8$  Hz, 3H).  $^{13}\text{C-NMR}$  (100 MHz,  $\text{CDCl}_3$ )  $\delta$  (ppm): 171.49, 164.94, 137.92, 136.80, 129.67, 128.60, 126.97, 123.83, 122.58, 65.89, 54.96, 51.71, 37.62, 36.93, 32.06, 29.72, 29.67, 29.49, 29.41, 28.56, 25.96, 22.85, 14.30.  $\text{IR}$  (neat) ( $\text{cm}^{-1}$ ): 3431 (b), 3340 (b), 2915 (m), 1736 (vs), 1666 (vs), 1533 (s), 1352 (s), 1201 (vs), 1168 (vs), 974 (s), 752 (vs), 702 (s).  $\text{ESI-MS}$  (+ve)  $m/z$ : Found  $[\text{M}-\text{Br}]^+$  428.2913,  $\text{C}_{25}\text{H}_{38}\text{N}_3\text{O}_3^+$  requires 428.2908

### 5.6.8 Preparation of IL (437)

(*S*)-3-(2-((1-(Dodecyloxy)-1-oxo-3-phenylpropan-2-yl)amino)-2-oxoethyl)-1-methyl-1H-imidazol-3-ium bromide (**437**).



According to the general procedure “E”, using dodecyl (2-bromoacetyl)-L-phenylalaninate (**458**) (1.438 g, 3.164 mmol), 1-methylimidazole (250  $\mu\text{l}$ , 3.13 mmol) and ethyl acetate (25 ml), the title

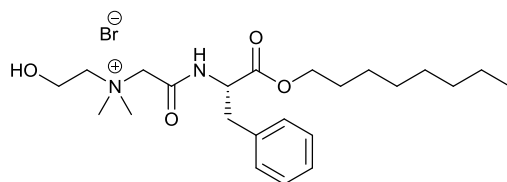
compound (**437**) was isolated as a white solid in 73% yield (1.221 g, 2.276 mmol).

**Molecular formula:**  $\text{C}_{27}\text{H}_{42}\text{BrN}_3\text{O}_3$ ; **Molecular weight:** 536.555  $\text{g mol}^{-1}$ ; **Mp:** 94-96  $^{\circ}\text{C}$ .

$[\alpha]_{\text{D}}^{20} = +5.3$  (1.0 c, EtOH).  $^1\text{H-NMR}$  (400 MHz,  $\text{CDCl}_3$ )  $\delta$  (ppm): 9.75 (s, 1H), 8.94 (d,  $J = 7.7$  Hz, 1H), 7.42 (t,  $J = 1.5$  Hz, 1H), 7.37 – 7.29 (m, 2H), 7.34 – 7.22 (m, 2H), 7.23 – 7.16 (m, 1H), 7.15 (t,  $J = 1.5$  Hz, 1H), 5.38 (d,  $J = 15.5$  Hz, 1H), 5.33 (d,  $J = 15.5$  Hz, 1H), 4.74 – 4.63 (m, 1H), 4.02 (m, 2H), 3.98 (s, 3H), 3.22 (dd,  $J = 12.5, 4.9$  Hz, 1H), 3.17 (dd,  $J = 12.5, 7.0$  Hz, 1H), 1.62 – 1.46 (m, 2H), 1.34 – 1.22 (m, 18H), 0.87 (t,  $J = 7.2$  Hz, 3H).  $^{13}\text{C-NMR}$  (100 MHz,  $\text{CDCl}_3$ )  $\delta$  (ppm): 171.28, 164.72, 137.92, 136.70, 129.63, 128.52, 126.88, 123.83, 122.29, 65.84, 54.89, 51.74, 37.51, 36.87, 32.02, 29.77, 29.75, 29.71, 29.61, 29.46, 29.35, 28.51, 25.89, 22.80, 14.24.  $\text{IR}$  (neat) ( $\text{cm}^{-1}$ ): 3432 (b), 3340 (b), 2916 (m), 1735 (vs), 1666 (vs), 1535 (s), 1352 (s), 1202 (s), 1162 (m), 970 (m), 753 (m), 703 (m).  $\text{ESI-MS}$  (+ve)  $m/z$ : Found  $[\text{M}-\text{Br}]^+$  456.3227,  $\text{C}_{27}\text{H}_{42}\text{N}_3\text{O}_3^+$  requires 456.3221.

### 5.6.9 Preparation of IL (438)

(*S*)-*N*-(2-Hydroxyethyl)-*N,N*-dimethyl-2-((1-(octyloxy)-1-oxo-3-phenylpropan-2-yl)amino)-2-oxoethan-1-aminium bromide (**438**).



The title compound was synthesised according to general procedure “C”, using octyl (2-bromoacetyl)-L-phenylalaninate (**456**) (1.559 g,



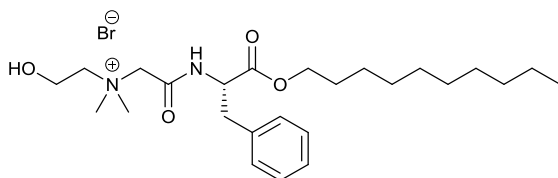
3.914 mmol), dimethylethanolamine (380  $\mu$ l, 3.84 mmol) and diethyl ether (25 ml). Product was observed precipitating as a white solid after 30 min. The solution was stirred at room temperature (48 hours) until no more dimethylethanolamine could be detected by TLC 10% MeOH: DCM visualised using ninhydrin stain. The crude product was washed with diethyl ether (3 x 50 ml) to afford the title compound (**438**) as a white solid in 94% yield (1.750 g, 3.590 mmol).

Molecular formula:  $C_{23}H_{39}BrN_2O_4$ ; Molecular weight: 487.479  $g\ mol^{-1}$ ; Mp: 80-82  $^{\circ}C$ .

$[\alpha]_D^{20} = -18.2$  (1.0 c, EtOH).  $^1H$ -NMR (400 MHz,  $CDCl_3$ )  $\delta$  (ppm): 8.95 (d,  $J = 7.9$  Hz, 1H), 7.40 – 7.32 (m, 2H), 7.31 – 7.15 (m, 3H), 4.80 – 4.72 (m, 1H), 4.70 (d,  $J = 14.0$  Hz, 1H), 4.45 (d,  $J = 14.0$  Hz, 1H), 4.15 – 4.00 (m, 4H), 3.75 – 3.59 (m, 2H), 3.36 (s, 3H), 3.30 (s, 3H), 3.26 (dd,  $J = 14.0, 5.1$  Hz, 1H), 3.09 (dd,  $J = 13.9, 10.0$  Hz, 1H), 1.65 – 1.52 (m, 2H), 1.34 – 1.18 (m, 10H), 0.88 (t,  $J = 7.5$  Hz, 3H).  $^{13}C$ -NMR (100 MHz,  $CDCl_3$ )  $\delta$  (ppm): 171.11, 163.06, 136.53, 129.59, 128.62, 127.06, 67.72, 65.99, 63.24, 55.96, 54.54, 53.70, 37.28, 31.86, 29.26, 29.23, 28.51, 25.88, 22.72, 14.19. IR (neat) ( $cm^{-1}$ ): 3323 (b), 3222 (b), 2921 (b), 1738 (vs), 1689 (vs), 1547 (s), 1347 (s), 1279 (s), 1215 (m), 1180 (s), 1083 (s), 979 (s), 763 (s), 681 (s). ESI-MS (+ve)  $m/z$ : Found  $[M-Br]^{+}$  407.2905,  $C_{23}H_{39}N_2O_4^{+}$  requires 407.2904.

#### 5.6.10 Preparation of IL (**439**)

(*S*)-2-((1-(Decyloxy)-1-oxo-3-phenylpropan-2-yl)amino)-*N*-(2-hydroxyethyl)-*N,N*-dimethyl-2-oxoethan-1-aminium bromide (**439**).



According to the general procedure “C”, using decyl (2-bromoacetyl)-L-phenylalaninate (**457**) (1.471 g, 3.450 mmol), dimethylethanolamine (340  $\mu$ l, 3.38 mmol) and diethyl ether (25 ml), the title compound

(**439**) was isolated as a white solid in 61% yield (1.062 g, 2.060 mmol).

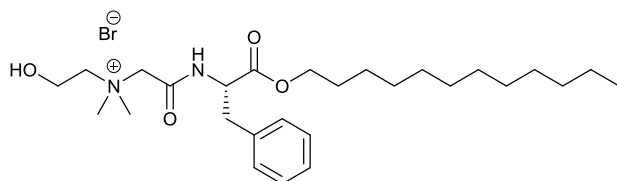
Molecular formula:  $C_{25}H_{43}BrN_2O_4$ ; Molecular weight: 505.497  $g\ mol^{-1}$ ; Mp: 57-59  $^{\circ}C$ .

$[\alpha]_D^{20} = -5.6$  (1.0 c, EtOH).  $^1H$ -NMR (400 MHz,  $CDCl_3$ )  $\delta$  (ppm): 8.93 (d,  $J = 7.9$  Hz, 1H), 7.39 – 7.15 (m, 5H), 4.75 (ddd,  $J = 10.0, 7.9, 5.1$  Hz, 1H), 4.67 (d,  $J = 14.1$  Hz, 1H), 4.45 (d,  $J = 14.1$  Hz, 1H), 4.15 – 4.00 (m, 4H), 3.75 – 3.61 (m, 2H), 3.36 (s, 3H), 3.30 (s, 3H), 3.25 (dd,  $J = 14.0, 5.1$  Hz, 1H), 3.08 (dd,  $J = 14.0, 10.0$  Hz, 1H), 1.61 – 1.53 (m, 2H), 1.33 – 1.13 (m, 14H), 0.87 (t,  $J = 7.0$  Hz, 3H).  $^{13}C$ -NMR (100 MHz,  $CDCl_3$ )  $\delta$  (ppm): 171.16, 163.11, 136.53, 129.59,

128.63, 127.08, 67.67, 66.01, 63.30, 55.97, 54.52, 53.62, 37.32, 31.98, 29.64, 29.59, 29.41, 29.33, 28.53, 25.90, 22.78, 14.23. IR (neat) (cm<sup>-1</sup>): 3323 (b), 3231 (b), 2920 (vs), 1738 (vs), 1689 (vs), 1547 (s), 1200 (vs), 1083 (s), 681 (s). ESI-MS (+ve) m/z: Found [M-Br]<sup>+</sup> 435.3226, C<sub>25</sub>H<sub>43</sub>N<sub>2</sub>O<sub>4</sub><sup>+</sup> requires 435.3217.

### 5.6.11 Preparation of IL (440)

(S)-2-((1-(Dodecyloxy)-1-oxo-3-phenylpropan-2-yl)amino)-N-(2-hydroxyethyl)-N,N-dimethyl-2-oxoethan-1-aminium bromide (**440**).



According to a modified general procedure “C”, using dodecyl (2-bromoacetyl)-L-phenylalaninate (**458**) (1.946 g, 4.282 mmol),

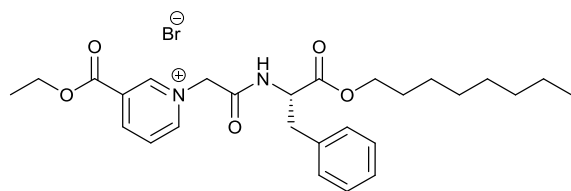
dimethylethanolamine (430 µl, 4.27 mmol) and diethyl ether (25 ml) were stirred at room temperature for 25 hours. The product did not readily precipitate and the crude product was isolated after solvent was removed *in vacuo*. General procedure “C” was modified to employ hexane as the trituration solvent (3 x 50 ml) as opposed to diethyl ether due to increased solubility of the title compound (**440**) in diethyl ether. The trituated product was dried under high vacuum to give the title product as a white solid in 89% yield (2.062 g 3.793 mmol).

Molecular formula: C<sub>27</sub>H<sub>47</sub>BrN<sub>2</sub>O<sub>4</sub>; Molecular weight: 543.587 gmol<sup>-1</sup>; Mp: 63-65 °C.

[α]<sub>D</sub><sup>20</sup> = -5.8 (1.0 c, EtOH). <sup>1</sup>H-NMR (400 MHz, CDCl<sub>3</sub>) δ (ppm): 8.91 (d, *J* = 8.0 Hz, 1H), 7.38 – 7.12 (m, 5H), 4.74 (ddd, *J* = 9.9, 7.9, 5.2 Hz, 1H), 4.65 (d, *J* = 14.1 Hz, 1H), 4.45 (d, *J* = 14.1 Hz, 1H), 4.14 – 4.00 (m, 4H), 3.74 – 3.64 (m, 2H), 3.35 (s, 3H), 3.30 (s, 3H), 3.24 (dd, *J* = 13.9, 5.1 Hz, 1H), 3.08 (dd, *J* = 14.1, 10.0 Hz, 1H), 1.57 (q, *J* = 6.9 Hz, 2H), 1.36-1.17(m, 18H), 0.87 (t, *J* = 6.6 Hz, 3H). <sup>13</sup>C-NMR (100 MHz, CDCl<sub>3</sub>) δ (ppm): 171.23, 163.18, 136.58, 129.63, 128.68, 127.13, 67.67, 66.06, 63.38, 56.01, 54.55, 53.60, 37.38, 32.06, 29.81, 29.79, 29.74, 29.66, 29.50, 29.40, 28.58, 25.96, 22.83, 14.28. IR (neat) (cm<sup>-1</sup>): 3320 (b), 3230 (b), 2920 (vs), 1738 (vs), 1689 (vs), 1546 (vs), 1180 (vs), 1084 (s), 694 (s). ESI-MS (+ve) m/z: Found [M-Br]<sup>+</sup> 463.3539, C<sub>27</sub>H<sub>47</sub>N<sub>2</sub>O<sub>4</sub><sup>+</sup> requires 463.3530.

### 5.6.12 Preparation of IL (441)

(S)-3-(Ethoxycarbonyl)-1-(2-((1-(octyloxy)-1-oxo-3-phenylpropan-2-yl)amino)-2-oxoethyl)pyridin-1-ium bromide (**441**).



The title compound was synthesised according to a modified general procedure “E”, using using octyl (2-bromoacetyl)-L-phenylalaninate (**456**) (0.741 g, 1.86 mmol), ethyl nicotinate (240  $\mu$ l, 1.82 mmol) and

DMF (5 ml). The reaction was heated at 100  $^{\circ}$ C for 48 hours. After 48 hours the reaction mixture was allowed to cool to room temperature and the DMF was removed *in vacuo* to afford a brown crude product. Purification of the crude product was accomplished by silica gel chromatography (eluent 7:93 MeOH:DCM) to afford the title compound (**441**) as an orange solid in 36% yield (0.359 g, 0.653 mmol).

Molecular formula:  $C_{27}H_{37}BrN_2O_5$ ; Molecular weight: 549.506  $gmol^{-1}$ ; Mp: 43-45  $^{\circ}$ C.

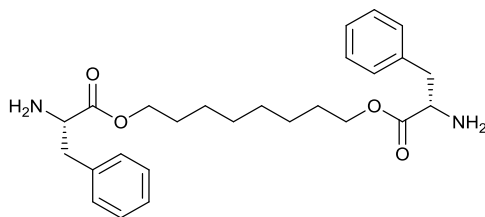
$[\alpha]_D^{20} = -0.7$  (1.0 c, EtOH).  $^1H$ -NMR (400 MHz,  $CDCl_3$ )  $\delta$  (ppm): 9.65 (d,  $J = 6.0$  Hz, 1H), 9.40 – 9.31 (m, 2H), 8.91 (d,  $J = 8.1$  Hz, 1H), 8.10 (dd,  $J = 7.9, 6.2$  Hz, 1H), 7.38 – 7.31 (m, 2H), 7.29 – 7.20 (m, 2H), 7.20 – 7.10 (m, 1H), 6.21 (d,  $J = 15.3$  Hz, 1H), 6.15 (d,  $J = 15.3$  Hz, 1H), 4.78 – 4.64 (m, 1H), 4.50 (q,  $J = 7.1$  Hz, 2H), 4.10 – 3.94 (m, 2H), 3.28 – 3.11 (m, 2H), 1.59 – 1.47 (m, 1H), 1.45 (t,  $J = 7.1$  Hz, 3H), 1.34 – 1.16 (s, 10H), 0.87 (t,  $J = 6.9$  Hz, 3H).  $^{13}C$ -NMR (100 MHz,  $CDCl_3$ )  $\delta$  (ppm): 171.18, 163.75, 160.93, 149.69, 147.00, 145.42, 136.67, 130.48, 129.69, 128.55, 127.76, 126.92, 65.88, 63.69, 62.85, 55.14, 37.78, 31.90, 29.30, 29.27, 28.50, 25.88, 22.76, 14.31, 14.23. IR (neat) ( $cm^{-1}$ ): 3192 (b), 3031 (m), 2926 (s), 2856 (m), 1733 (vs), 1687 (vs), 1547 (m), 1467 (m), 1370 (m), 1299 (vs), 1203 (vs), 1113 (m), 1016 (m), 742 (m), 701 (m). ESI-MS (+ve) m/z: Found  $[M-Br]^{+}$  469.2704,  $C_{27}H_{37}N_2O_5^{+}$  requires 469.2697.

## 5.7 Experimental preparation of Chapter 3 bolaform amino acid surfactant ILs

### 5.7.1 Preparation of Chapter 3 bolaform amino acid esters (459-561)

#### 5.7.1.1 Preparation of ester (459)

Octane-1,8-diyl (2*S*,2'*S*)-bis(2-amino-3-phenylpropanoate) (**459**).



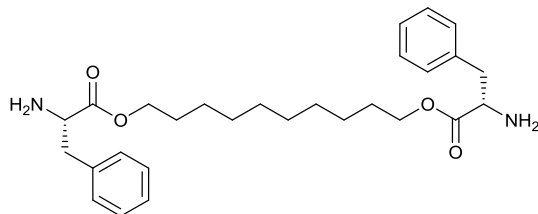
According to the general procedure “H”, using L-phenylalanine (15.029 g, 90.981 mmol), 1,8-octane diol (7.236 g, 49.49 mmol), PTSA (19.037 g, 100.05 mmol) and toluene (100 ml), the title compound (**459**) was isolated as a pale yellow oil in 36% yield (7.810 g, 17.73 mmol)

Molecular formula: C<sub>26</sub>H<sub>36</sub>N<sub>2</sub>O<sub>4</sub>; Molecular weight: 440.584 g mol<sup>-1</sup>.

<sup>1</sup>H-NMR (400 MHz, CDCl<sub>3</sub>) δ (ppm): 7.33 – 7.17 (m, 10H), 4.08 (t, *J* = 6.7 Hz, 4H), 3.71 (dd, *J* = 7.7, 5.5 Hz, 2H), 3.07 (dd, *J* = 13.5, 5.4 Hz, 2H), 2.86 (dd, *J* = 13.5, 7.8 Hz, 2H), 1.70-1.45 (m, 4H), 1.35 – 1.26 (m, 8H). <sup>13</sup>C-NMR (100 MHz, CDCl<sub>3</sub>) δ (ppm): 175.14, 137.27, 129.30, 128.55, 126.82, 65.04, 55.88, 41.21, 29.09, 28.52, 25.81.

#### 5.7.1.2 Preparation of ester (460)

Decane-1,10-diyl (2*S*,2'*S*)-bis(2-amino-3-phenylpropanoate) (**460**).



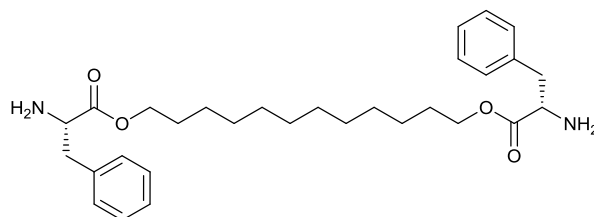
According to the general procedure “H” using L-phenylalanine (9.629 g, 58.29 mmol), 1,10-decane diol (5.079 g, 29.14 mmol), PTSA (12.197 g, 64.120 mmol) and toluene (75 ml), the title compound (**460**) was isolated as an orange oil in 55% yield (7.512 g, 16.029 mmol).

Molecular formula: C<sub>28</sub>H<sub>40</sub>N<sub>2</sub>O<sub>4</sub>; Molecular weight: 468.638 gmol<sup>-1</sup>.

<sup>1</sup>H-NMR (400 MHz, CDCl<sub>3</sub>) δ (ppm): 7.43 – 7.10 (m, 10H), 4.19 – 4.03 (m, 2H), 3.66 (t, *J* = 6.6 Hz, 2H), 3.12 (dd, *J* = 13.3, 5.5 Hz, 2H), 2.91 (dd, *J* = 13.7, 7.7 Hz, 2H), 2.86 (dd, *J* = 13.5, 7.8 Hz, 2H), 1.64-1.53 (m, 4H), 1.33 – 1.28 (m, 12H). <sup>13</sup>C-NMR (100 MHz, CDCl<sub>3</sub>) δ (ppm): 175.12, 137.33, 129.44, 128.70, 126.98, 65.31, 55.94, 41.20, 29.29, 28.67, 25.85.

### 5.7.1.3 Preparation of ester (461)

Dodecane-1,12-diyl (2*S*,2'*S*)-bis(2-amino-3-phenylpropanoate) (**461**).



According to the general procedure “H”, using L-phenylalanine (9.890 g, 59.87 mmol), 1,12-dodecane diol (6.057 g, 29.93 mmol), PTSA (12.527 g, 65.856 mmol) and toluene (75 ml), the title compound (**461**) was isolated as an orange oil in 61% yield (9.093 g, 18.31 mmol).

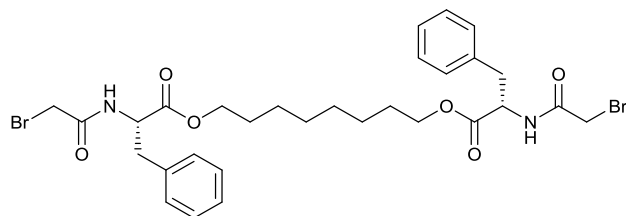
Molecular formula: C<sub>30</sub>H<sub>44</sub>N<sub>2</sub>O<sub>4</sub>; Molecular weight: 496.692 gmol<sup>-1</sup>.

<sup>1</sup>H-NMR (400 MHz, CDCl<sub>3</sub>) δ (ppm): 7.40 – 7.01 (m, 10H), 4.09 (t, *J* = 6.7 Hz, 2H), 3.80 – 3.69 (m, 2H), 3.63 (td, *J* = 6.6, 1.3 Hz, 2H), 3.09 (dd, *J* = 13.5, 5.3 Hz, 2H), 2.88 (dd, *J* = 13.5, 7.8 Hz, 2H), 1.64 – 1.50 (m, 4H), 1.38 – 1.24 (m, 16H). <sup>13</sup>C-NMR (100 MHz, CDCl<sub>3</sub>) δ (ppm): 175.23, 137.40, 129.44, 128.69, 126.96, 65.31, 56.00, 41.29, 29.33, 28.68, 25.87.

### 5.7.2 Preparation of Chapter 3 bolaform alkylating reagents (462-465)

#### 5.7.2.1 Preparation of alkylating reagent (462)

Octane-1,8-diyl (2*S*,2'*S*)-bis(2-(2-bromoacetamido)-3-phenylpropanoate) (**462**).



According to the general procedure “B”, using bis-ester (**459**) (6.923 g, 15.71 mmol), bromoacetyl bromide (3.05 ml, 35.0 mmol), Na<sub>2</sub>CO<sub>3</sub> (3.995 g, 37.70 mmol) and DCM (50 ml) a

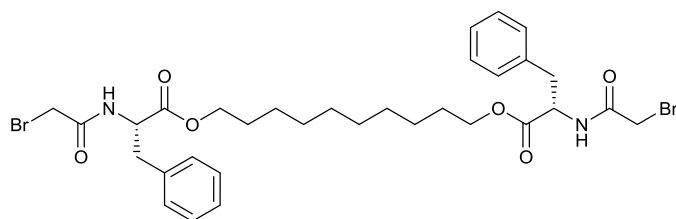
crude product was isolated as a white solid. The crude product was purified by silica gel chromatography (eluent 30:70 ethyl acetate:hexane), to afford the title compound (**462**) as white solid in 26% yield (2.822 g, 4.135 mmol).

Molecular formula: C<sub>30</sub>H<sub>38</sub>Br<sub>2</sub>N<sub>2</sub>O<sub>6</sub>; Molecular weight: 682.450 gmol<sup>-1</sup>; Mp: 97-99 °C.

$[\alpha]_D^{20} = +30.2$  (1.0 c, CHCl<sub>3</sub>). <sup>1</sup>H-NMR (400 MHz, CDCl<sub>3</sub>)  $\delta$  (ppm): 7.34 – 7.19 (m, 6H), 7.16 – 7.08 (m, 4H), 6.88 (d,  $J = 7.9$  Hz, 2H), 4.88 – 4.78 (m, 2H), 4.19 – 4.03 (m, 4H), 3.86 (d,  $J = 13.6$  Hz, 2H), 3.81 (d,  $J = 13.5$  Hz, 2H), 3.17 (dd,  $J = 12.8, 4.8$  Hz, 2H), 3.12 (dd,  $J = 12.8, 4.9$  Hz, 2H), 1.64 – 1.54 (m, 4H), 1.29 (s, 8H). <sup>13</sup>C-NMR (100 MHz, CDCl<sub>3</sub>)  $\delta$  (ppm): 171.02, 165.19, 135.50, 129.44, 128.77, 127.42, 65.90, 53.88, 39.79, 29.14, 28.83, 28.51, 25.84. IR (neat) (cm<sup>-1</sup>): 2935 (m), 2847 (w), 1727 (vs), 1650 (vs), 1536 (s), 1202 (vs), 1183 (s), 1138 (m), 1275 (m), 1232 (s), 1205 (vs), 1174 (s), 698 (vs). ESI-MS (+ve) m/z: Found [M+H]<sup>+</sup> 681.1174, C<sub>30</sub>H<sub>39</sub>Br<sub>2</sub>N<sub>2</sub>O<sub>6</sub><sup>+</sup> requires 681.1169.

#### 5.7.2.2 Preparation of alkylating reagent (**463**)

Decane-1,10-diyl (2*S*,2'*S*)-bis(2-(2-bromoacetamido)-3-phenylpropanoate) (**463**).



According to the general procedure “B”, using bis-ester (**460**) (5.403 g, 11.54 mmol), bromoacetyl bromide (2.25 ml, 25.8 mmol), Na<sub>2</sub>CO<sub>3</sub> (2.813 g, 26.54 mmol) and DCM (50 ml) the crude product was isolated as a white solid. The crude product was purified by silica gel chromatography (eluent 30:70 ethyl acetate:hexane), to afford the title compound (**463**) as white solid in 24% yield (1.959 g, 2.757 mmol).

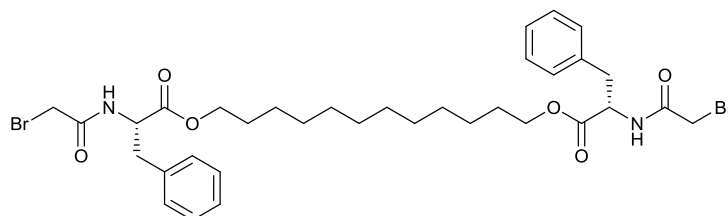
Molecular formula: C<sub>32</sub>H<sub>42</sub>Br<sub>2</sub>N<sub>2</sub>O<sub>6</sub>; Molecular weight: 710.504 gmol<sup>-1</sup>; Mp: 88-90 °C.

$[\alpha]_D^{20} = +30.5$  (1.0 c, CHCl<sub>3</sub>). <sup>1</sup>H-NMR (400 MHz, CDCl<sub>3</sub>)  $\delta$  (ppm): 7.35 – 7.21 (m, 6H), 7.16 – 7.08 (m, 4H), 6.87 (d,  $J = 7.9$  Hz, 2H), 4.88 – 4.79 (m, 2H), 4.18 – 4.03 (m, 4H), 3.86 (d,  $J = 14.0$  Hz, 2H), 3.83 (d,  $J = 13.9$  Hz, 2H), 3.17 (dd,  $J = 12.9, 5.8$  Hz, 2H), 3.12 (dd,  $J = 12.6, 4.6$  Hz, 2H), 1.66 – 1.54 (m, 4H), 1.33 – 1.19 (m, 12H). <sup>13</sup>C-NMR (100 MHz, CDCl<sub>3</sub>)  $\delta$  (ppm): 170.99, 165.14, 135.48, 129.42, 128.74, 127.40, 65.96, 53.86, 37.92, 29.48, 29.24, 28.81, 28.51, 25.89. IR (neat) (cm<sup>-1</sup>): 2920 (m), 2849 (w), 1727 (vs), 1654 (vs), 1537 (s), 1355 (s), 1222 (s),

1192 (vs), 1183 (vs), 693 (vs). ESI-MS (+ve) m/z: Found  $[M+H]^+$  709.1495,  $C_{32}H_{43}Br_2N_2O_6^+$  requires 709.1482.

### 5.7.2.3 Preparation of alkylating reagent (464)

Dodecane-1,12-diyl (2*S*,2'*S*)-bis(2-(2-bromoacetamido)-3-phenylpropanoate) (**464**).



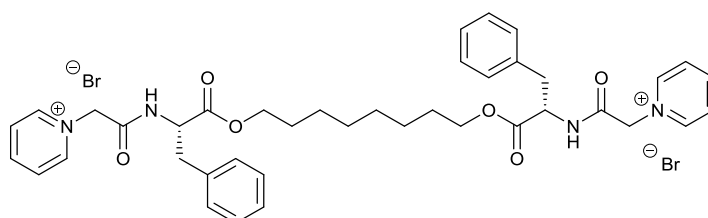
According to the general procedure “B”, using bis-dodecyl ester (**461**) (6.396 g, 12.88 mmol), bromoacetyl bromide (3.4 ml, 39.0 mmol),  $Na_2CO_3$  (4.369 g, 41.22 mmol) and DCM (50 ml) the crude product was isolated as a white solid. The crude product was purified by silica gel chromatography (eluent 30:70 ethyl acetate: hexane) to afford the title compound (**464**) as white solid in 40% yield (3.832 g, 5.188 mmol).

Molecular formula:  $C_{34}H_{46}Br_2N_2O_6$ ; Molecular weight: 738.558  $gmol^{-1}$ ; Mp: 64-66 °C.

$[\alpha]_D^{20} = +20.1$  (1.0 c,  $CHCl_3$ ).  $^1H$ -NMR (400 MHz,  $CDCl_3$ )  $\delta$  (ppm): 7.33 – 7.22 (m, 6H), 7.15 – 7.10 (m, 4H), 6.86 (d,  $J = 7.8$  Hz, 2H), 4.87 – 4.80 (m, 2H), 4.15 – 4.05 (m, 4H), 3.86 (d,  $J = 13.6$  Hz, 2H), 3.83 (d,  $J = 13.7$  Hz, 2H), 3.16 (dd,  $J = 13.5, 5.8$  Hz, 2H), 3.12 (dd,  $J = 13.6, 6.2$  Hz, 2H), 1.63 – 1.58 (m, 4H), 1.31 – 1.24 (m, 16H).  $^{13}C$ -NMR (100 MHz,  $CDCl_3$ )  $\delta$  (ppm): 170.99, 165.15, 135.48, 129.42, 128.73, 127.39, 65.99, 53.85, 37.91, 29.62, 29.56, 29.27, 28.80, 28.51, 25.90. IR (neat) ( $cm^{-1}$ ): 2924 (b), 2853 (w), 1732 (vs), 1650 (vs), 1529 (s), 1362 (s), 1228 (s), 1201 (vs), 974 (vs), 699 (vs). ESI-MS (+ve) m/z: Found  $[M+H]^+$  737.1802,  $C_{34}H_{47}Br_2N_2O_6^+$  requires 737.1795.

### 5.7.3 Preparation of IL (444)

1,1'-((4*S*,17*S*)-4,17-Dibenzyl-2,5,16,19-tetraoxo-6,15-dioxo-3,18-diazaicosane-1,20-diyl)bis(pyridin-1-ium) bromide (**444**).



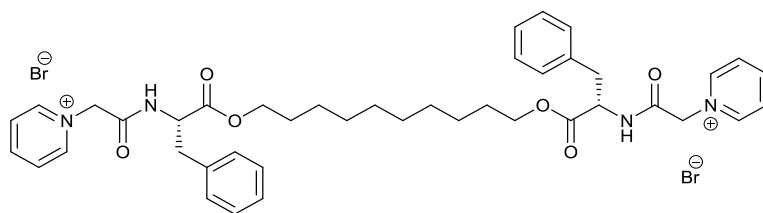
According to the general procedure “E”, using bis-alkylating reagent (**462**) (0.880 g, 1.29 mmol), pyridine (210  $\mu$ l, 2.58 mmol) and ethyl acetate (25 ml), the title compound (**444**) was isolated as a white solid in 98% yield (1.065 g, 1.267 mmol).

Molecular formula:  $C_{40}H_{48}Br_2N_4O_6$ ; Molecular weight: 840.654  $gmol^{-1}$ ; Mp: 124-126  $^{\circ}C$ .

$[\alpha]_D^{20} = + 3.2$  (1.0 c, MeOH).  $^1H$ -NMR (400 MHz,  $D_2O$ )  $\delta$  (ppm): 8.62 – 8.51 (m, 6H), 8.06 – 7.97 (m, 4H), 7.27 – 7.08 (m, 10H), 5.43 (d,  $J = 16.1$  Hz, 2H), 5.37 (d,  $J = 16.1$  Hz, 2H), 4.63 (dd,  $J = 8.3, 7.0$  Hz, 2H), 4.02 – 3.86 (m, 4H), 3.07 (dd,  $J = 13.8, 6.9$  Hz, 2H), 2.99 (dd,  $J = 13.8, 8.3$  Hz, 2H), 1.45 – 1.26 (m, 4H), 1.10 – 0.93 (m, 8H).  $^{13}C$ -NMR (100 MHz,  $D_2O$ )  $\delta$  (ppm): 172.54, 165.29, 146.72, 145.42, 136.01, 129.11, 128.66, 127.98, 127.18, 66.21, 61.48, 54.64, 36.96, 28.29, 27.66, 25.08. IR (neat) ( $cm^{-1}$ ): 3219 (b), 3039 (b), 2926 (m), 2744 (w), 1738 (s), 1679 (vs), 1634 (s), 1555 (m), 1488 (s), 1200 (s), 693 (m). ESI-MS (+ve) m/z: Found  $[M-2Br]^+$  340.1790,  $C_{40}H_{48}N_4O_6^{2+}$  requires  $(680.3563)/2 = 340.1782$

#### 5.7.4 Preparation of IL (**445**)

1,1'-((4*S*,19*S*)-4,19-Dibenzyl-2,5,18,21-tetraoxo-6,17-dioxa-3,20-diazadocosane-1,22-diyl)bis(pyridin-1-ium) (**445**).



According to the general procedure “E”, using bis-alkylating reagent (**463**) (0.502 g, 0.707 mmol), pyridine (110  $\mu$ l, 1.41 mmol) and ethyl acetate (25 ml), the title compound (**445**) was isolated as a white solid in 94% yield (0.579 g, 0.667 mmol).

Molecular formula:  $C_{42}H_{52}Br_2N_4O_6$ ; Molecular weight: 868.708  $gmol^{-1}$ ; Mp: 137.139  $^{\circ}C$ .

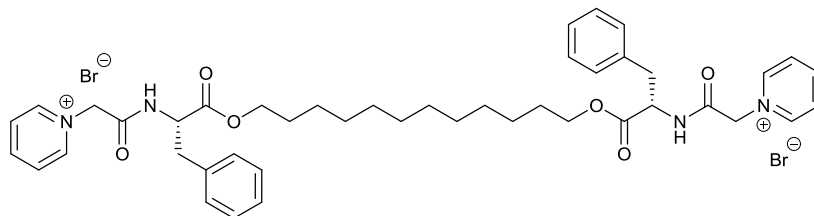
$[\alpha]_D^{20} = + 3.4$  (1.0 c, MeOH).  $^1H$ -NMR (400 MHz,  $D_2O$ )  $\delta$  (ppm): 8.65 – 8.52 (m, 6H), 8.11 – 8.00 (m, 4H), 7.34 – 7.15 (m, 10H), 5.42 (d,  $J = 15.9$  Hz, 2H), 5.35 (d,  $J = 16.2$  Hz, 2H), 4.73 – 4.65 (m, 2H), 4.15 – 3.93 (m, 4H), 3.16 (dd,  $J = 13.9, 6.4$  Hz, 2H), 3.01 (dd,  $J = 13.8, 8.8$  Hz, 2H), 1.55 – 1.38 (m, 4H), 1.27 – 1.06 (m, 12H).  $^{13}C$ -NMR (100 MHz,  $D_2O$ )  $\delta$  (ppm): 172.35, 165.20, 146.71, 145.44, 136.05, 129.12, 128.57, 127.98, 127.07, 65.86, 61.53, 54.58, 37.10, 29.01, 28.84, 27.87, 25.44. IR (neat) ( $cm^{-1}$ ): 3166 (b), 3034 (b), 2911 (m), 2853 (w), 1738 (s),



1668 (vs), 1634 (m), 1527 (s), 1487 (s), 1200 (s), 689 (vs). ESI-MS (+ve) m/z: Found  $[M-2Br]^+$  345.1936,  $C_{42}H_{52}N_4O_6^{2+}$  requires  $(708.3876)/2 = 354.1938$ .

#### 5.7.5 Preparation of IL (446)

1,1'-((4*S*,21*S*)-4,21-Dibenzyl-2,5,20,23-tetraoxo-6,19-dioxa-3,22-diazatetracosane-1,24-diyl)bis(pyridin-1-ium) bromide (**446**).



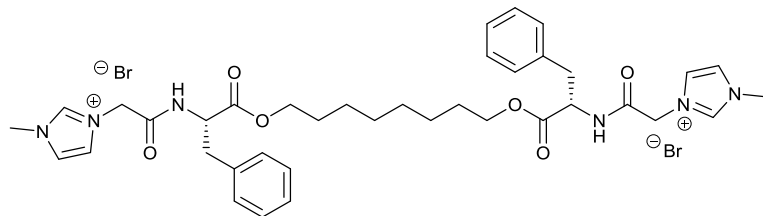
According to the general procedure “E”, using bis-alkylating reagent (**464**) (0.716 g, 0.969 mmol), pyridine (150  $\mu$ l, 1.92 mmol) and ethyl acetate (25 ml), the title compound (**446**) was isolated as a white solid in 91% yield (0.790 g, 0.881 mmol).

Molecular formula:  $C_{44}H_{56}Br_2N_4O_6$ ; Molecular weight:  $896.762 \text{ gmol}^{-1}$ ; Mp: 138-140  $^{\circ}\text{C}$ .

$[\alpha]_D^{20} = +5.1$  (1.0 c, MeOH).  $^1\text{H-NMR}$  (400 MHz,  $\text{CDCl}_3$ )  $\delta$  (ppm): 8.61 – 8.56 (m, 4H), 8.53 (tt,  $J = 7.9, 1.4 \text{ Hz}$ , 2H), 8.03 – 7.94 (m, 4H), 7.20 – 7.02 (m, 10H), 5.63 – 5.30 (m, 4H), 4.64 – 4.49 (m, 2H), 3.89 (dt,  $J = 12.0, 6.3 \text{ Hz}$ , 2H), 3.79 (dt,  $J = 11.2, 6.1 \text{ Hz}$ , 2H), 2.99 (d,  $J = 7.7 \text{ Hz}$ , 4H), 1.34 – 1.18 (m, 4H), 1.16 – 0.87 (m, 16H).  $^{13}\text{C-NMR}$  (100 MHz,  $\text{CDCl}_3$ )  $\delta$  (ppm): 172.23, 165.15, 146.69, 145.45, 136.09, 129.14, 128.52, 127.97, 127.00, 65.69, 61.56, 54.53, 38.76, 37.17, 29.46, 29.35, 29.12, 27.98, 25.61. IR (neat) ( $\text{cm}^{-1}$ ): 3180 (b), 3030 (b), 2920 (s), 2849 (m), 1734 (vs), 1672 (vs), 1628 (m), 1531 (s), 1487 (vs), 1200 (vs), 693 (vs). ESI-MS (+ve) m/z: Found  $[M-2Br]^+$  368.2104,  $C_{44}H_{56}N_4O_6^{2+}$  requires  $(736.4189)/2 = 368.2095$ .

#### 5.7.6 Preparation of IL (447)

3,3'-((4*S*,17*S*)-4,17-Dibenzyl-2,5,16,19-tetraoxo-6,15-dioxa-3,18-diazaicosane-1,20-diyl)bis(1-methyl-1H-imidazol-3-ium) bromide (**447**).



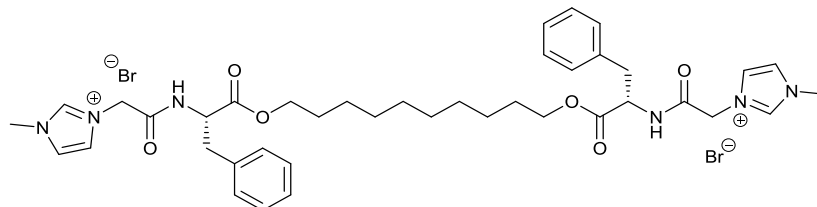
According to the general procedure “E”, using bis-alkylating reagent (**462**) (0.567 g, 0.831 mmol), 1-methylimidazole (130  $\mu$ l, 1.66 mmol) and ethyl acetate (25 ml), the title compound (**447**) was isolated as a white solid in 93% yield (0.652 g, 0.770 mmol).

Molecular formula: C<sub>38</sub>H<sub>50</sub>Br<sub>2</sub>N<sub>6</sub>O<sub>6</sub>; Molecular weight: 846.662 g mol<sup>-1</sup>; Mp: 70-72 °C.

[ $\alpha$ ]<sub>D</sub><sup>20</sup> = +6.3 (1.0 c, MeOH). <sup>1</sup>H-NMR (400 MHz, D<sub>2</sub>O)  $\delta$  (ppm): 8.60 (s, 2H), 7.39 (t,  $J$  = 1.8 Hz, 2H), 7.34 – 7.25 (m, 6H), 7.24 (t,  $J$  = 1.8 Hz, 2H), 7.22 – 7.16 (m, 4H), 4.96 (d,  $J$  = 16.7 Hz, 2H), 4.90 (d,  $J$  = 16.7 Hz, 2H), 4.68 (dd,  $J$  = 8.9, 6.3 Hz, 2H), 4.13 – 4.04 (m, 4H), 3.83 (s, 6H), 3.18 (dd,  $J$  = 13.8, 6.3 Hz, 2H), 2.99 (dd,  $J$  = 13.9, 8.9 Hz, 2H), 1.57 – 1.49 (m, 4H), 1.28 – 1.11 (m, 8H). <sup>13</sup>C-NMR (100 MHz, D<sub>2</sub>O)  $\delta$  (ppm): 172.86, 166.59, 136.06, 129.09, 128.70, 127.23, 123.45, 123.13, 66.55, 54.33, 50.35, 36.74, 35.79, 28.01, 27.51, 24.89. IR (neat) (cm<sup>-1</sup>): 3309 (b), 3033 (b), 2920 (m), 1728 (vs), 1660 (vs), 1549 (s), 1205 (vs), 1173 (vs), 698 (s). ESI-MS (+ve) m/z: Found [M-2Br]<sup>+</sup> 343.1895, C<sub>38</sub>H<sub>50</sub>N<sub>6</sub>O<sub>6</sub><sup>2+</sup> requires (686.3781)/2 = 343.1891.

### 5.7.7 Preparation of IL (448)

3,3'-((4*S*,19*S*)-4,19-Dibenzyl-2,5,18,21-tetraoxo-6,17-dioxa-3,20-diazadocosane-1,22-diyl)bis(1-methyl-1H-imidazol-3-ium) bromide (**448**).



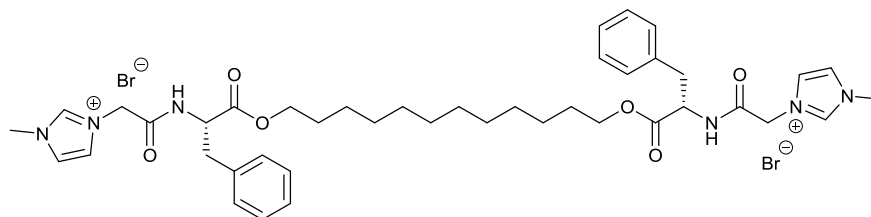
According to the general procedure “E”, using bis-alkylating reagent (**463**) (0.348 g, 0.489 mmol), 1-methylimidazole (77  $\mu$ l, 0.96 mmol) and ethyl acetate (25 ml), the title compound (**448**) was isolated as a beige solid in 96% yield (0.409 g, 0.468 mmol).

Molecular formula: C<sub>40</sub>H<sub>54</sub>Br<sub>2</sub>N<sub>6</sub>O<sub>6</sub>; Molecular weight: 874.716 g mol<sup>-1</sup>; Mp: 41-43 °C.

[ $\alpha$ ]<sub>D</sub><sup>20</sup> = + 6.0 (1.0 c, MeOH). <sup>1</sup>H-NMR (400 MHz, D<sub>2</sub>O)  $\delta$  (ppm): 7.38 (d,  $J$  = 2.0 Hz, 2H), 7.26 – 7.13 (m, 10H), 7.09 (d,  $J$  = 6.9 Hz, 2H), 4.97 (d,  $J$  = 16.7 Hz, 2H), 4.91 (d,  $J$  = 11.0 Hz, 2H), 4.65 – 4.56 (m, 2H), 4.02 – 3.85 (m, 4H), 3.80 (s, 6H), 3.04 (dd,  $J$  = 13.8, 6.8 Hz, 2H), 2.96 (dd,  $J$  = 13.7, 8.4 Hz, 2H), 1.43 – 1.29 (m, 4H), 1.12 – 0.98 (m, 12H). <sup>13</sup>C-NMR (100 MHz, D<sub>2</sub>O)  $\delta$  (ppm): 172.65, 166.46, 136.04, 129.07, 128.62, 127.14, 123.45, 123.15, 66.19, 54.42, 50.40, 36.93, 35.83, 28.82, 28.61, 27.76, 25.32. IR (neat) (cm<sup>-1</sup>): 3310 (b), 3063 (b), 2922 (m), 2850 (m), 1729 (vs), 1662 (vs), 1551 (s), 1204 (vs), 1173 (vs), 700 (s). ESI-MS (+ve) m/z: Found [M-2Br]<sup>+</sup> 357.2063, C<sub>40</sub>H<sub>54</sub>N<sub>6</sub>O<sub>6</sub><sup>2+</sup> requires (714.4094)/2 = 357.2047.

### 5.7.8 Preparation of IL (449)

3,3'-((4*S*,21*S*)-4,21-Dibenzyl-2,5,20,23-tetraoxo-6,19-dioxa-3,22-diazatetracosane-1,24-diyl)bis(1-methyl-1*H*-imidazol-3-ium) bromide (**449**).



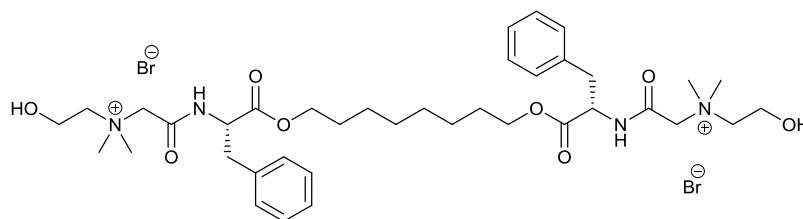
According to the general procedure “E”, using bis-alkylating reagent (**464**) (0.669 g, 0.906 mmol), 1-methylimidazole (140  $\mu$ l, 1.79 mmol) and ethyl acetate (25 ml), the target compound (**449**) was isolated as a beige solid in 93% yield (0.763 g, 0.845 mmol).

Molecular formula:  $C_{42}H_{58}Br_2N_6O_6$ ; Molecular weight: 902.770  $gmol^{-1}$ ; Mp: 84-86  $^{\circ}C$ .

$[\alpha]_D^{20} = +3.3$  (1.0 c, MeOH).  $^1H$ -NMR (400 MHz,  $D_2O$ )  $\delta$  (ppm): 7.38 (d,  $J = 2.0$  Hz, 2H), 7.23 (d,  $J = 2.0$  Hz, 2H), 7.19 – 7.01 (m, 10H), 5.03 – 4.90 (m, 4H), 4.62 – 4.53 (m, 2H), 3.96 – 3.78 (m, 4H), 3.79 (s, 6H), 2.96 (d,  $J = 7.5$  Hz, 4H), 1.31 – 1.25 (m, 4H), 1.12 – 1.07 (m, 16H).  $^{13}C$ -NMR (100 MHz,  $D_2O$ )  $\delta$  (ppm): 172.38, 166.30, 136.08, 129.10, 128.52, 127.00, 123.45, 123.18, 65.79, 54.33, 50.49, 37.11, 35.90, 29.49, 29.39, 29.14, 28.01, 25.65. IR (neat) ( $cm^{-1}$ ): 3395 (b), 3069 (b), 2921 (s), 2851 (m), 1732 (vs), 1661 (vs), 1544 (s), 1206 (vs), 1172 (vs), 701 (s). ESI-MS (+ve)  $m/z$ : Found  $[M-2Br]^{2+}$  371.2228,  $C_{42}H_{58}N_6O_6^{+}$  requires  $(742.4407)/2 = 371.2204$ .

### 5.7.9 Preparation of IL (450)

(4*S*,17*S*)-4,17-Dibenzyl-*N*1,*N*20-bis(2-hydroxyethyl)-*N*1,*N*1,*N*20,*N*20-tetramethyl-2,5,16,19-tetraoxo-6,15-dioxa-3,18-diazaicosane-1,20-diaminium bromide (**450**).



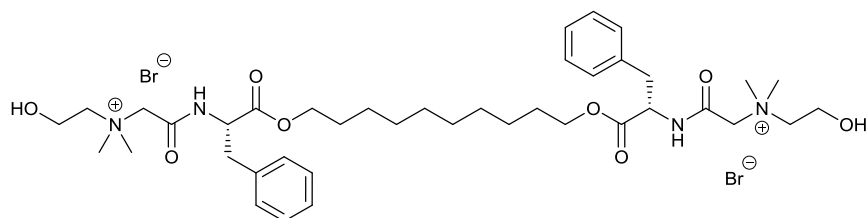
According to the general procedure “E”, using bis-alkylating reagent (**462**) (0.895 g, 1.31 mmol), dimethylaminoethanol (270  $\mu$ l, 2.62 mmol) and ethyl acetate (25 ml), the title compound (**450**) was isolated as a white solid in 94% yield (1.064 g, 1.236 mmol).

Molecular formula:  $C_{38}H_{60}Br_2N_4O_8$ ; Molecular weight: 860.726  $gmol^{-1}$ ; Mp: 112-114  $^{\circ}C$ .

$[\alpha]_D^{20} = -1.6$  (1.0 c, MeOH).  $^1\text{H-NMR}$  (400 MHz,  $\text{D}_2\text{O}$ )  $\delta$  (ppm): 7.37 – 7.18 (m, 10H), 4.73 (dd,  $J = 9.3, 6.1$  Hz, 2H), 4.18 – 4.06 (m, 6H), 4.00 (d,  $J = 15.2$  Hz, 2H), 3.93 – 3.85 (m, 4H), 3.55 – 3.48 (m, 4H), 3.21 (dd,  $J = 14.0, 6.0$  Hz, 2H), 3.13 (s, 6H), 3.12 (s, 6H), 2.96 (dd,  $J = 13.9, 9.3$  Hz, 2H), 1.60 – 1.50 (m, 4H), 1.23 (s, 8H).  $^{13}\text{C-NMR}$  (100 MHz,  $\text{D}_2\text{O}$ )  $\delta$  (ppm): 172.68, 163.88, 136.09, 129.09, 128.77, 127.30, 66.67, 66.01, 63.11, 55.39, 54.13, 52.89, 52.84, 36.55, 27.97, 27.52, 24.85.  $\text{IR}$  (neat) ( $\text{cm}^{-1}$ ): 3294 (b), 2920 (m), 2858 (m), 1729 (vs), 1672 (vs), 1540 (s), 1452 (m), 1196 (s), 738 (s), 689 (s).  $\text{ESI-MS}$  (+ve)  $m/z$ : Found  $[\text{M-2Br}]^+$  350.2203,  $\text{C}_{38}\text{H}_{60}\text{N}_4\text{O}_8^{2+}$  requires  $(700.4400)/2 = 350.2200$ .

#### 5.7.10 Preparation of IL (451)

(4*S*,19*S*)-4,19-Dibenzyl-*N*1,*N*22-bis(2-hydroxyethyl)-*N*1,*N*1,*N*22,*N*22-tetramethyl-2,5,18,21-tetraoxo-6,17-dioxa-3,20-diazadocosane-1,22-diaminium bromide (**451**).



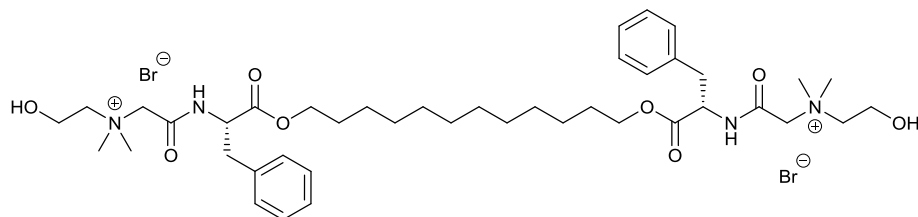
According to the general procedure “E”, using bis-alkylating reagent (**463**) (0.529 g, 0.745 mmol), dimethylaminoethanol (150  $\mu\text{l}$ , 1.47 mmol) and ethyl acetate (25 ml), the title compound (**451**) was isolated as a white solid in 99% yield (0.657 g, 0.739 mmol).

Molecular formula:  $\text{C}_{40}\text{H}_{64}\text{Br}_2\text{N}_4\text{O}_8$ ; Molecular weight:  $888.780 \text{ g mol}^{-1}$ ; Mp:  $66\text{--}68^\circ \text{C}$ .

$[\alpha]_D^{20} = -6.7$  (1.0 c, MeOH).  $^1\text{H-NMR}$  (400 MHz,  $\text{D}_2\text{O}$ )  $\delta$  (ppm): 7.34 – 7.21 (m, 6H), 7.20 – 7.14 (m, 4H), 4.73 – 4.68 (m, 2H), 4.17 – 3.96 (m, 8H), 3.96 – 3.83 (m, 4H), 3.57 – 3.50 (m, 4H), 3.15 (s, 12H), 3.14 – 3.05 (m, 2H), 2.98 (dd,  $J = 13.9, 9.0$  Hz, 2H), 1.56 – 1.40 (m, 4H), 1.28 – 1.10 (m, 12H).  $^{13}\text{C-NMR}$  (100 MHz,  $\text{D}_2\text{O}$ )  $\delta$  (ppm): 172.27, 163.76, 135.99, 129.07, 128.66, 127.19, 66.12, 63.11, 55.38, 53.99, 52.81, 52.79, 36.79, 28.99, 28.78, 27.88, 25.45.  $\text{IR}$  (neat) ( $\text{cm}^{-1}$ ): 3289 (b), 2920 (m), 2852 (m), 1731 (vs), 1671 (vs), 1553 (m), 1466 (m), 1200 (s), 1176 (s), 742 (m), 698 (m).  $\text{ESI-MS}$  (+ve)  $m/z$ : Found  $[\text{M-2Br}]^{2+}$  364.2358,  $\text{C}_{40}\text{H}_{64}\text{N}_4\text{O}_8^+$  requires  $(728.4713)/2 = 364.2357$ .

### 5.7.11 Preparation of IL (452)

(4*S*,21*S*)-4,21-Dibenzyl-*N*1,*N*24-bis(2-hydroxyethyl)-*N*1,*N*1,*N*24,*N*24-tetramethyl-2,5,20,23-tetraoxo-6,19-dioxa-3,22-diazatetracosane-1,24-diaminium bromide (**452**).



According to the general procedure “E”, using bis-alkylating reagent (**464**) (0.707 g, 0.957 mmol), dimethylaminoethanol (190  $\mu$ l, 1.91 mmol) and ethyl acetate (25 ml), the title compound was isolated as a white solid in 89% yield (0.783 g, 0.854 mmol).

Molecular formula:  $C_{42}H_{68}Br_2N_4O_8$ ; Molecular weight: 916.834  $gmol^{-1}$ ; Mp: 89-91  $^{\circ}C$ .

$[\alpha]_D^{20} = -2.6$  (1.0 c,  $CHCl_3$ ).  $^1H$ -NMR (400 MHz,  $D_2O$ )  $\delta$  (ppm): 7.31 – 7.19 (m, 6H), 7.18 – 7.10 (m, 4H), 4.71 – 4.65 (m, 2H), 4.12 (d,  $J = 15.8$  Hz, 2H), 4.09 – 3.93 (m, 6H), 3.93 – 3.84 (m, 4H), 3.61 – 3.47 (m, 4H), 3.14 (s, 12H), 3.09 (dd,  $J = 14.0, 6.5$  Hz, 2H), 2.97 (dd,  $J = 13.9, 8.9$  Hz, 2H), 1.54 – 1.36 (m, 4H), 1.19 (s, 16H).  $^{13}C$ -NMR (100 MHz,  $D_2O$ )  $\delta$  (ppm): 172.12, 163.73, 135.99, 129.08, 128.62, 127.14, 66.11, 65.92, 63.12, 55.38, 53.92, 52.77, 36.87, 29.49, 29.13, 28.03, 25.68. IR (neat) ( $cm^{-1}$ ): 3285 (b), 2922 (s), 2852 (m), 1732 (vs), 1670 (vs), 1550 (s), 1468 (m), 1199 (vs), 1177 (vs), 742 (s), 698 (s). ESI-MS (+ve) m/z: Found  $[M-2Br]^+$  378.2514,  $C_{42}H_{68}N_4O_8^{2+}$  requires  $(756.5026)/2 = 378.2513$ .

## 5.8 Antimicrobial Screening

The antimicrobial screening was carried out in collaboration with Dr. Marcel Špulák, Faculty of Pharmacy, Charles University, Czech Republic.

### 5.8.1 Antibacterial Screening

In vitro antibacterial testing was carried out on the following strains of bacteria available from the collection maintained at the Department of Biological and Medical Sciences, Faculty of Pharmacy, Charles University, Hradec Králové, Czech Republic:

Gram Positive:

- *S. aureus* (ATCC 65382)
- *Methicillin-res.S.a* (HK5996/08)
- *S. epidermidis* (HK6966/084 )

- *Enterococcus* sp. (HK14365/085)

Gram Negative:

- *E. coli* (ATCC 87396)
- *K. pneumoniae* (HK11750/087)
- *K. pneumoniae* (HK14368/08)
- *P. aeruginosa* (ATCC 9027)

The ATCC strains served as the quality control strains. All the bacterial isolates were maintained on Mueller-Hinton dextrose agar (MH, HiMedia, adersky-Envitek, Czech Republic), prior to being tested. Mueller-Hinton agar buffered to pH 7.4 ( $\pm$  0.2) was employed as the test medium. To the wells of the microdilution tray were added 200  $\mu$ L of the agar medium, 10  $\mu$ l of inoculum suspension and 2-fold serial dilutions of the test compound (2000 to 0.488  $\mu$ mol l<sup>-1</sup>). DMSO served as diluent for all the test compounds with a final concentration of no greater than 2%. The inoculum was prepared in Mueller-Hinton medium to give a final concentration of 0.5 McFarland scale ( $1.5 \times 10^8$  cfu ml<sup>-1</sup>). The test trays were incubated at 37 °C and MICs were read visually after 24 h and 48 h. The MICs were defined as 95% inhibition of the growth of control (MIC<sub>95</sub>) and were determined twice and in duplicate. The deviations from the usually obtained values were no higher than the nearest concentration value up and down the dilution scale.

### 5.8.2 Antifungal Screening

In vitro antifungal testing was carried out on the following strains of fungi available from the collection maintained at the Department of Biological and Medical Sciences, Faculty of Pharmacy, Charles University, Hradec Králové, Czech Republic:

Yeasts:

- *Candida albicans* (ATCC 448597)
- *Candida albicans* (ATCC 900288)
- *Candida parapsilosis* (ATCC 220199 )
- *Candida krusei* (ATCC 62581)
- *Candida krusei* (E2811)
- *Candida tropicalis* (156)
- *Candida glabrata* (20/I2)
- *Candida lusitanae* (2446/I3 )
- *Trichosporon asahii* (11884)

Filamentous fungi:

- *Aspergillus fumigatus* (2315)
- *Absidia corymbifera* (2726)
- *Trichophyton mentagrophytes* (445)

Three ATCC strains (*Candida albicans* ATCC 90028, *Candida parapsilosis* ATCC 22019, *Candida krusei* ATCC 6258) served as the quality control strains. All the fungal isolates were maintained on Sabouraud dextrose agar prior to being tested. Minimum Inhibitory Concentrations were determined by modified CLSI standard of microdilution format of the NCCLS M27-A3 and M38-A2 document guidelines.<sup>17, 18</sup> The deviations from the usually obtained values were no higher than the nearest concentration value up and down the dilution scale. DMSO (100 %) served as a diluent for all compounds; the final concentration of DMSO did not exceed 2 %. RPMI 1640 (Sevapharma, Prague) medium supplemented with L-glutamine and buffered with 0.165 M morpholinepropanesulfonic acid (Serva) to pH 7.0 by 10 N NaOH was used as the test medium. The wells of the microdilution tray contained 100 µl of the RPMI 1640 medium with 2-fold serial dilutions of the compounds (2000 or 1000 to 0.48 µmol l<sup>-1</sup>) and 100 µl of inoculum suspension. Fungal inoculum in RPMI 1640 was prepared to give a final concentration of  $5 \times 10^3 \pm 0.2$  cfu ml<sup>-1</sup>. The trays were incubated at 35°C and MICs were read visually for filamentous fungi and photometrically for yeasts as an absorbance at 540 nm after 24 h and 48 h. The MIC/IC50 values for the dermatophytic strain (*T. mentagrophytes*) were determined after 72 h and 120 h and for *A. fumigatus*, *A. corymbifera* after 24 and 48 h. For all other strains MIC/IC80 values were evaluated. The MICs were defined as 50% or 80% inhibition of the growth of control. MICs were determined twice and in duplicate. The deviations from the usually obtained values were no higher than the nearest concentration value up and down the dilution scale.

## 5.9 Biodegradation Screening

### 5.9.1 Closed Bottle Test Method

The testing was carried out at 20°C in the dark for 28 days in the Institute of Sustainable and Environmental Chemistry at Leuphana University according to OECD method 301D.<sup>19-21</sup> A compound can be classified as readily biodegradable if it undergoes more than 60% biodegradation within the 28 day test. The compound must also reach 60% biodegradation within a ten day period as soon as 10% biodegradation is observed.<sup>21</sup>

The testing carried out involves four separate test vessels making up one series. Each series was carried out in duplicate.

- Test blank vessel – mineral medium + inoculum

- Quality control vessel - mineral medium + sodium acetate + inoculum
- Test series vessel – mineral medium + inoculum + test compound
- Toxicity control – mineral medium + sodium acetate + inoculum + test compound

The test blank records the overall theoretical oxygen demand (ThOD) of the bacteria and their growth with no sources of organic carbon.

The quality control series employs readily biodegradable sodium acetate to demonstrate that the bacteria are performing as expected, degrading the prescribed amount of sodium acetate within 14 days.

The test series vessel contains the organic compound under examination as the only source of organic carbon. The oxygen demand of this vessel can therefore be directly compared to the amount of organic carbon undergoing degradation from the test compound.

The toxicity control contains a quantity of sodium acetate and the test compound calculated to provide ThOD of 5 mg l<sup>-1</sup>. If the difference in ThOD compared to the predicted ThOD is more than 25% observed then a potential inhibitory effect due to antimicrobial effects of the test compound may be occurring and a compound is labelled as toxic.

The levels of aerobic biodegradation were measured using a sensor unit within the bottle containing an oxygen electrode (Oxi 196 with EO 196-1.5WTW Weilheim, Germany). The times of measurement were Day: 0, 0 (3 hours), 1, 7, 14, 21 and 28.

## **5.9.2 LCMS Metabolite Study**

### **5.9.2.1 Materials**

LC-MS grade acetonitrile was purchased from VWR (VWR International, GmbH, Darmstadt, Germany). The aqueous buffer solutions were prepared using ultrapure water 18.2 MΩ·cm (Ultra Clear UV TM, Barsbüttel, Germany) and formic acid for analysis (Merck KGaA, Darmstadt, Germany).

### **5.9.2.2 Instrumentation**

The analysis was performed on a Dionex Ultimate 3000 UHPLC, equipped with a solvent rack (SRD-3600), a binary pump (HPG-3400-RS), an auto-sampler (WPS-3000-TRS), and column oven (TCC-3000) coupled with a LTQ Orbitrap XL (Thermo Scientific, Dreieich, Germany) equipped with a HES source.

### **5.9.2.3 LC-MS method**

The separations were carried out on a Hypersil Gold CN (100/3mm, 3µm, Thermo Scientific) equipped with an HILIC guard column (Macherey-Nagel, Düren, Germany) kept at 30°C with a flow rate of 400 µl min<sup>-1</sup> using a gradient of acetonitrile and 0.05% formic acid in water (V:V).



The gradient started with 97% acetonitrile, held for 1 minute, decreased to 60% over 11 minutes, held for 3 minutes, then increased back to the initial condition of 97% within 3 minutes and terminated by 7 minutes re-equilibration time. The mass spectra were acquired in positive centroid mode with a resolving power of 30000. The parameters for the heated electrospray source for sheath and auxiliary gas flow rates were 15 and 5 arbitrary units, respectively. The spray voltage and the vaporizer temperature were set to 4 kV and 200 °C, the capillary voltage and the capillary temperature were set to -9 V and 275 °C and the tube lens voltage was kept at 100 V.

## **5.10 Self assembly and physico-chemical surfactant property investigations**

### **5.10.1 Aqueous sample preparation**

Water from a Milli-Q system was used in all sample preparation. Stock solutions were prepared by weight, shaken first by hand for ca. 1 minute and then sonicated for 15 minutes at 25°C in a sonicator bath (Ultrasons-H, Selecta S.A.) to ensure complete dissolution of each sample. Samples of lower concentration were prepared by dilution from stock solutions. The samples were kept at 25°C for at least 2 h for equilibration.

### **5.10.2 Conductivity measurements**

Conductivity was measured at 25°C using an Orion Conductivity Cell 011010A with platinized platinum electrode in conjunction with a Thermo Orion 550 A instrument with a cell constant of 0.998 cm<sup>-1</sup>. Temperature for all measurements was maintained at 25°C using a thermostatically controlled water bath. Cell constant was calibrated with NaCl solutions of known conductivities and was used for calculating the conductivity of the surfactant solution. The conductivity of water was subtracted from the measured conductivity of each sample. Measurements were made at increasing concentrations to minimise errors from possible contamination of the electrode.

### **5.10.3 Surface tension measurements**

Surface tension was measured at 25°C by the Wilhelmy plate technique using a Krüss K-12 tensiometer. Glass containers and plate were cleaned with chromic acid solution and rinsed thoroughly with distilled water. The plate was flame dried before each measurement. Surface tension was considered to be at equilibrium when the standard deviation of five consecutive measurements did not exceed 0.10 mN m<sup>-1</sup>.

### **5.10.4 Optical Microscopy**

The polarised optical microscopy method used to examine the surfactants was the flooding/penetration method according to Lawrence.<sup>22</sup> In this technique, water is allowed to diffuse onto anhydrous surfactants placed between a glass slide and a cover slip. After a short

time, gradients in composition are produced and different separated mesomorphic or mesophases develop around the crystalline surfactant allowing the determination of the liquid crystal structures formed. The microscope used was a Zeiss binocular microscope with heated stage and the images were examined at x10 and x40 optical magnification. Images were captured using a digital camera attached to the microscope head and pointing through an aperture above the turret objective lenses.

#### 5.10.5 HPLC-UV analysis

Purity of surfactants synthesised was analysed by HPLC, with a VWR L-2130 model using an L-2400 UV-vis detector at 215 nm and a LiChrospher 100 RP-18 (5  $\mu$ m) LiChroCART 250x4 mm C18 column at room temperature. A gradient elution profile was employed from the initial solvent composition of A/B 50/50 (by volume), changing during 30 minutes to a final composition of 100% B where A is 0.1% v/v TFA in H<sub>2</sub>O and B is 0.085% of TFA in H<sub>2</sub>O/CH<sub>3</sub>CN 1:4. The flow rate through the column was 1.0 ml min<sup>-1</sup>.

#### 5.10.6 Aqueous stability measurements

Aqueous stability of the L-phenylalanine surfactant ILs was determined by maintaining an aqueous solution (~10 mg in 5 ml) of the surfactant to be analysed at 50 °C for 1 week. The sample vials prepared were glass test tubes with a threaded lid. Parafilm was wrapped around the lid to prevent evaporation. The samples were maintained at the desired temperature in a thermostatically controlled water bath.

Degradation was measured by taking a 0.5 ml aliquot at 1 day intervals and analysing parent peak area decline by HPLC-UV using the parameters previously outlined in Section 5.10.5. The method outlined above was also repeated at pH 2 and pH 10, both at 25 °C over a 1 week period.

### 5.11 References

1. J. Hartwig, J. B. Metternich, N. Nikbin, A. Kirschning and S. V. Ley, *Org. Biomol. Chem.*, 2014, 12, 3611-3615.
2. D. Coleman, M. Spulak, M. T. Garcia and N. Gathergood, *Green Chem.*, 2012, 14, 1350-1356.
3. K. D. Daughtry, Y. Xiao, D. Stoner-Ma, E. Cho, A. M. Orville, P. Liu and K. N. Allen, *J. Am. Chem. Soc.*, 2012, 134, 2823-2834.
4. R. Almansa, D. Guijarro and M. Yus, *Tetrahedron: Asymmetry*, 2007, 18, 2828-2840.
5. M. Ousmer, N. A. Braun, C. Bavoux, M. Perrin and M. A. Ciufolini, *J. Am. Chem. Soc.*, 2001, 123, 7534-7538.
6. X. Sala, A. M. Rodríguez, M. Rodríguez, I. Romero, T. Parella, A. von Zelewsky, A. Llobet and J. Benet-Buchholz, *J. Org. Chem.*, 2006, 71, 9283-9290.
7. R. A. Green, D. Pletcher, S. G. Leach and R. C. D. Brown, *Org. Lett.*, 2015, 17, 3290-3293.
8. A. Sakakura, Y. Koshikari and K. Ishihara, *Tetrahedron Lett.*, 2008, 49, 5017-5020.

9. A. Basak, D. Mitra, M. Kar and K. Biradha, *Chem. Commun.*, 2008, DOI: 10.1039/B801644E, 3067-3069.
10. H.-P. Li, S. Li, Z.-D. Wang and L. Qin, *J. Korean Chem. Soc.*, 2011, 55, 978-982.
11. P. Zaderenko, M. S. Gil, P. Ballesteros and S. Cerdan, *J. Org. Chem.*, 1994, 59, 6268-6273.
12. N. Farfán, L. Cuéllar, J. M. Aceves and R. Contreras, *Synthesis*, 1987, 1987, 927-929.
13. S. M. Voshell, S. J. Lee and M. R. Gagné, *J. Am. Chem. Soc.*, 2006, 128, 12422-12423.
14. M. Stodulski, A. Mamińska and J. Mlynarski, *Tetrahedron: Asymmetry*, 2011, 22, 464-467.
15. M. de Loos, J. H. van Esch, R. M. Kellogg and B. L. Feringa, *Tetrahedron*, 2007, 63, 7285-7301.
16. K. Baczko, C. Larpent and P. Lesot, *Tetrahedron: Asymmetry*, 2004, 15, 971-982.
17. *Reference Method for Broth Dilution Antifungal Susceptibility Testing of Yeasts. Approved standard. Document M27-A3. Clinical Laboratory Standard Institute, Wayne, PA, 2008.*
18. *Reference Method for Broth Dilution Antifungal Susceptibility Testing of Filamentous Fungi. Approved standard. Document M38-A2. Clinical Laboratory Standard Institute, Wayne, PA, 2008.*
19. OECD, *Test No. 301: Ready Biodegradability*, OECD Publishing, 1992.
20. OECD, *OECD Guideline for Testing of Chemicals*, 1992.
21. OECD, *Revised Introduction to the OECD Guidelines for Testing of Chemicals, Section 3*, OECD Publishing, 2006.
22. A. S. C. Lawrence, *Discuss. Faraday Soc.*, 1958, 25, 51-58.

## **Chapter 6**

### *Conclusions and Future Work*

## 6.1 Conclusions and future work

A series of amino acid derived ILs (**324-335**, **349-353**) and tertiary amines (**344-348**) have been synthesised according to the 12 principles of green chemistry and Boethling's rules of thumb for designing biodegradable molecules and their antimicrobial toxicity and biodegradability have been assessed (Chapter 2). Green chemistry metrics were calculated for the synthesis of these compounds and favourable characteristics as well as areas that can be improved upon have been identified. Antimicrobial toxicity assessments have shown that in general the amino acid derived compounds had a low to moderate toxicity with the tertiary amines exhibiting a greater toxic effect than the quaternary. Biodegradation studies have shown that one pyridinium IL (**325**) and one tertiary amine (**345**) could be classified as inherently ultimately biodegradable. In conjunction to the biodegradation studies a preliminary examination of the metabolic products at the end of the 28 day test was conducted and has given insight into the breakdown pathways of the ILs and tertiary amines. No organic metabolic products were detected (apart from remaining parent compound) for pyridinium IL (**325**) suggesting complete mineralisation within the 28 day test. Metabolic products themselves have been synthesised and their antimicrobial toxicity results showed little to no toxic effect for the metabolites screened. Metabolite biodegradability is currently undergoing assessment to give a greater picture of the potential environmental fate and impact of the ILs and tertiary amines and their transformation products. From the assessments carried out in Chapter 2, pyridinium IL (**325**) was deemed to be the most green candidate synthesised and was proposed as a building block from which to design further generations of ILs.

Following on from the work carried out in Chapter 2, Chapter 3 reports a series of L-phenylalanine ILs subsequently designed from the most green candidates, including pyridinium IL (**325**), with the aim to produce surfactant ILs. These ILs were derivatives of those synthesised in Chapter 2 and represent a rational design in producing surface active molecules from shorter chain analogues. A series of linear alkyl ILs of chain length C<sub>8</sub>-C<sub>12</sub> (**432-434**) were synthesised. Analogous imidazolium (**435-437**), cholinium (**438-440**) and ethyl nicotinium (**441**) ILs were also synthesised due to their Chapter 2 counterparts' favourable characteristics in synthesis, antimicrobial toxicity, biodegradation or a combination of all three. In total 10 new linear alkyl ILs and three new alkylating reagents (**456-458**) were synthesised. Furthermore 9 new bolaform pyridinium (**444-446**), imidazolium (**447-449**) and cholinium (**450-452**) ILs and 3 new alkylating reagents (**462-464**) were also designed and synthesised using C<sub>8</sub>-C<sub>12</sub> linkers with the aim of producing low toxicity surface active molecules. Similar to the assessments carried out in Chapter 2, the green chemistry metrics were again determined for the 19<sup>th</sup> generation

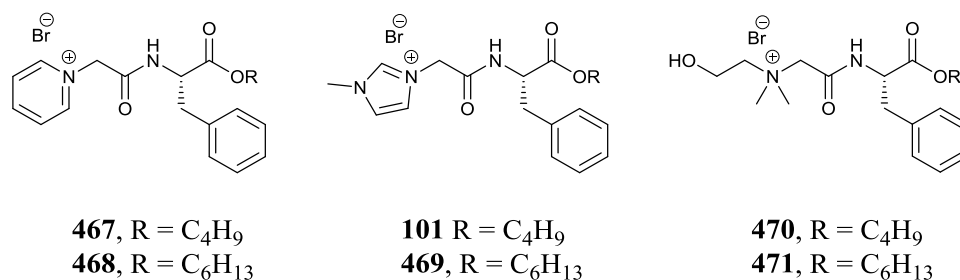
amino acid ILs, 6 alkylating reagents and 6 esters synthesised in Chapter 3. Overall the metrics produced for the linear alkyl ILs in Chapter 3 were more favourable due to the synthetic methodologies employed and the replacement of column chromatography with alternative purification methods using reduced quantities of organic solvent. From the unfavourable green chemistry metrics calculated for the ethyl nicotinium C<sub>8</sub> IL (**441**) it was decided to postpone the further investigation of C<sub>10</sub> (**442**) and C<sub>12</sub> (**443**) ethyl nicotinium ILs. It was decided that to improve the overall metrics for the bolaform ILs that solvent recycling would be employed for the derivatives. Diethyl ether and hexane trituration solvents were recycled at 95% recovery using a rotary evaporator to rapidly distil large quantities of solvent which was subsequently reused in further purification of other ILs. Moderate to poor yields were observed for the bolaform esters and alkylating reagents and this presents a key area for future optimisation if further investigations into this class of ILs is to be conducted.

Antimicrobial toxicity results for the linear alkyl ILs showed in general a broad spectrum antibacterial toxicity towards gram positive bacteria. Similarly a broad spectrum activity was observed towards gram negative bacteria with C<sub>10</sub> ILs displaying the most toxic effects. Moderate (e.g. **432**, 250-1000  $\mu\text{mol}^{-1}$  IC<sub>50</sub>) to high levels (e.g. **434**, 3.9-62.5  $\mu\text{mol}^{-1}$  IC<sub>50</sub>) of antifungal toxicity was also observed for all of the linear alkyl ILs. The lowest levels of antibacterial toxicity (though still considerable 15.62-250  $\mu\text{mol}^{-1}$  MIC<sub>95</sub>) were observed for the ethyl nicotinium C<sub>8</sub> IL (**441**) which suggests that future investigations into this IL as a surface active agent with lower antimicrobial toxicity could be promising. Bolaform ILs (**444-452**) displayed similar levels of antimicrobial activity to their linear alkyl counterparts with broad spectrum activity towards both fungi and bacteria observed and an increase in toxicity as alkyl chain spacer length was increased. Biodegradation studies of the linear alkyl ILs did not produce any readily biodegradable ILs even though their carbon content was significantly greater with respect to the ethyl ester ILs examined in Chapter 2. The C<sub>8</sub> (**432**, **435**, **438**) and C<sub>10</sub> (**433**, **436**, **439**) ILs examined may prove to be ultimately biodegradable if their test time is extended due to slower rates of biodegradability. The C<sub>12</sub> linear alkyl ILs (**434**, **437**, **440**) examined failed the toxicity control test of the biodegradation screening and are the first to do so in the preceding decade of research conducted within the Gathergood group. Bolaform ILs examined for their biodegradability (**444-452**) showed that the C<sub>10</sub> examples (**447-449**) were the most biodegradable of the bolaform ILs with moderate levels (e.g. **447**, 53%) observed. A rapid drop off when spacer length was increased to C<sub>12</sub> was observed for the bolaform ILs (**449-452**). This rapid drop-off could be due to enzymatic steric considerations or due to the broad spectrum antimicrobial effect of the bolaform ILs (though no toxicity controls were failed).

The surface active properties of the linear alkyl (**432-440**) and bolaform (**444-452**) ILs were assessed during two separate two month placements in the laboratory of Dr. Lourdes Pérez, CSIC, IQAC, Barcelona. Surfactant properties examined include critical micelle concentration by conductimetry and tensiometry, surface active properties by tensiometry, liquid crystal behaviour by optical microscopy and a preliminary investigation into aqueous stability in neutral, acidic and basic media. It was shown that the linear alkyl ILs synthesised all displayed excellent surface active properties such as large effective range and high levels of efficiency. Micelles were also observed forming at lower than expected concentrations. The amino acid sidechain was proposed to be contributing lipophilicity towards the alkyl chain thus reducing the concentrations of surfactant required for activity. Bolaform ILs synthesised also displayed surface activity at lower concentrations than expected due to a proposed amino acid contribution, however a lower effective range was observed for the bolaform ILs. Cholinium C<sub>8</sub> bolaform (**450**) was an exception to this observation, not displaying considerable surface tension reduction at all and was deemed to have poor surface tension reducing properties. Aqueous stability in a number of media was also investigated and the preliminary investigations showed a general resistance of the ILs to acid hydrolysis and a susceptibility toward base hydrolysis and hydrolysis in media at pH 7 with temperature elevated to 50 °C. Optical microscopy experiments were able to produce visual examples of the liquid crystal behaviour of a number of linear alkyl ILs (**432, 433, 434, 436, 439**). The images observed over a wide range of temperatures (20-100 °C) were able to give insight into the interactions of the ILs in aqueous media including hexagonal, lamellar and cubic phase liquid crystals. Crystals were also observed growing in real time, most likely due to the greatly increased coordination and crystallinity due to a combination of the L-phenylalanine sidechain and long alkyl chain, not generally observed for shorter chain ILs. HPLC models were constructed for the linear alkyl and bolaform ILs to aid in predicting the possible CMC values for future generations of L-phenylalanine derived ILs. Values for the Stauff-Klevens equation for the three series of ILs (pyridinium, imidazolium and cholinium) were also calculated to assist with such predictions.

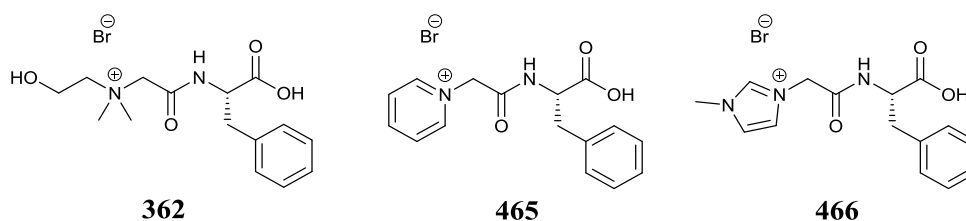
## 6.2 Future Work

The future work of this project lies immediately with the ongoing metabolite biodegradation studies. Additional investigations into the cytotoxicity of the surfactant ILs is also of the utmost importance if real world applications of these surfactants are to be considered. Further investigation into shorter chain linear alkyl ILs of C<sub>4</sub>-C<sub>6</sub> (**101, 467-471**) ester lengths should also be considered to investigate whether surface activity with reduced antimicrobial toxicity and potentially greater biodegradability of intermediate length alkyl chains can be achieved. The following ILs (Figure 6.1) have been proposed in Chapters 3 and 4 for future synthesis:



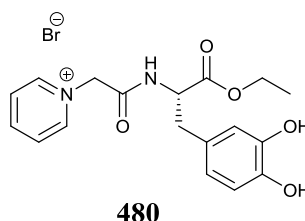
**Figure 6.1:** Future intermediate ester chain ILs.

Biodegradation studies of amino acid carboxylic acid ILs (**362**, **465-466**) (Figure 6.2) should also be investigated to determine whether an amino acid IL with an unprotected carboxylic acid can undergo biodegradation through the amino acid or by amide bond cleavage followed by mineralisation.



**Figure 6.2.** Amino acid carboxylic acid ILs.

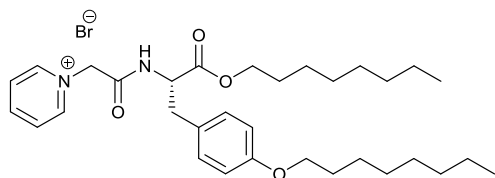
Biodegradation studies on L-DOPA derived ILs (Figure 6.3). would also be of interest as L-phenylalanine and L-tyrosine can both be converted into L-DOPA in biological systems.<sup>1</sup>



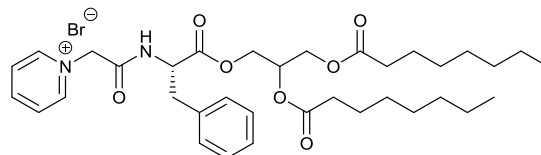
**Figure 6.3.** L-DOPA derived IL

Bolaform ILs with longer spacer units should also be considered as a C<sub>8</sub> chain length did not seem to be adequate for surface activity for the cholinium derivative (**450**). A series of surface active ILs could also potentially be synthesised from L-phenylalanine glycerol esters or L-tyrosine esters. This selection includes linear alkyl derivatives, dialkyl derivatives and gemini derivatives, using the already defined synthetic methodologies described within Chapters 2-3 of this body of work. A number of potential structures are outlined below, Figure 6.3.

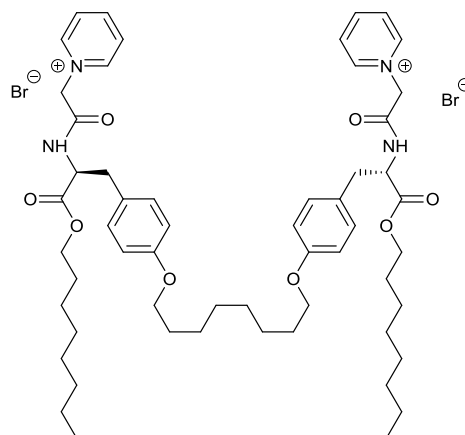




Dialkyl tyrosine surfactant



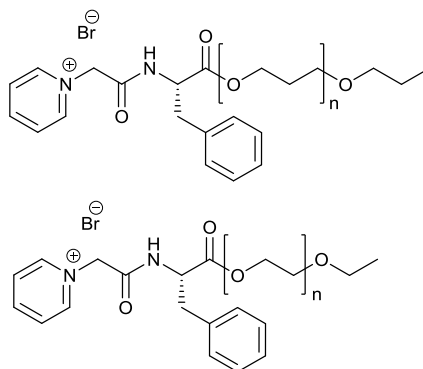
Dialkyl L-phenylalanine glycerol ester surfactant



Gemini tyrosine surfactant

**Figure 6.4.** Potential future generation L-phenylalanine and L-tyrosine derived surfactants.

To combat the high levels of toxicity associated with cationic surfactants a number of poly propylene or poly ethylene glycol esters of the ILs could be synthesised. As previously discussed in Chapters 3-4 polypropylene can effectively reduce the CMC and polyethylene can increase the CMC. It has also been shown in the literature that polyethylene containing IL esters can help in reducing toxicity.<sup>2</sup> Two such structures are proposed below in Figure 6.4.

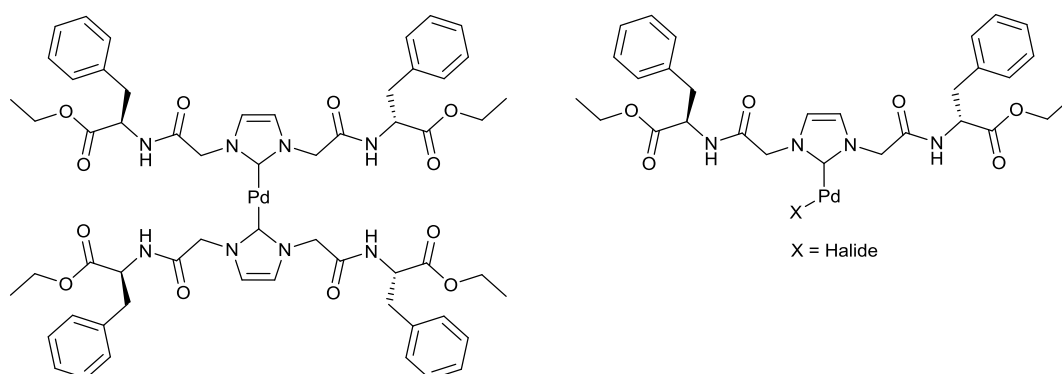


**Figure 6.5.** PEG and PPG L-phenylalanine derived surfactant ILs.

Potential applications of the surface active ILs include their use as broad spectrum antimicrobial and biodegradable cleaning agents. Determination of ultimate biodegradability and cytotoxicity will be required before further consideration of these applications. The imidazolium and

pyridinium surface active ILs may also present themselves as dual functioning Brønsted-acidic phase transfer catalysts due to their dual nature as surface active agents and the known acidity and liberation of acidic species associated with imidazolium ILs reported by Gathergood and Connon.<sup>3-7</sup>

Lastly the C<sub>2</sub> symmetrical IL reported in Chapter 2 could also be considered as an *N*-heterocyclic carbene ligand as depicted in Figure 6.5. The presence of sterically hindering/directing L-phenylalanine sidechain groups or indeed functionalised/unfunctionalised tyrosine sidechain may contribute towards the discovery of future generations of enantioselective catalyst ligands, though the acidity of the amide protons may complicate this avenue of investigation.



**Figure 6.6.** NHC ligand derived from IL (331).

## 6.2 References

1. K. J. Broadley, *Pharmacol. Ther.*, 2010, 125, 363-375.
2. S. Morrissey, B. Pegot, D. Coleman, M. T. Garcia, D. Ferguson, B. Quilty and N. Gathergood, *Green Chem.*, 2009, 11, 475-483.
3. L. Myles, R. G. Gore, N. Gathergood and S. J. Connon, *Green Chem.*, 2013, 15, 2740-2746.
4. L. Myles, N. Gathergood and S. J. Connon, *Chem. Commun.*, 2013, 49, 5316-5318.
5. R. G. Gore, L. Myles, M. Spulak, I. Beadham, T. M. Garcia, S. J. Connon and N. Gathergood, *Green Chem.*, 2013, 15, 2747-2760.
6. L. Myles, R. Gore, M. Spulak, N. Gathergood and S. J. Connon, *Green Chem.*, 2010, 12, 1157-1162.
7. B. Procuranti, L. Myles, N. Gathergood and S. J. Connon, *Synthesis*, 2009, 2009, 4082-4086.

# **Appendix I**

## *IL biodegradation under aerobic biodegradation conditions*

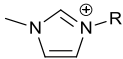
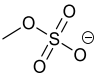

*The information within this appendix is the ESI for the ILs discussed in Chapter 1*

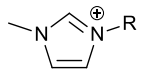
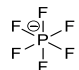
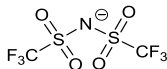
## Table of Contents

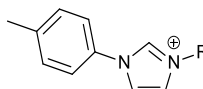
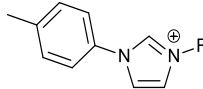
### Appendix - IL biodegradation under aerobic biodegradation conditions

Imidazolium ( <b>4, 8, 9, 68-102</b> )	A-4
Bis-Imidazolium ( <b>217-224</b> )	A-17
Thiazolium ( <b>103-104</b> )	A-20
Pyridinium ( <b>16, 105-124</b> )	A-21
Bis-Pyridinium ( <b>214-216</b> )	A-27
Morpholinium ( <b>125-136</b> )	A-29
1,4-Diazabicyclo[2.2.2]octanium (DABCO) ( <b>137-141</b> )	A-34
Piperidinium ( <b>142-148</b> )	A-36
Pyrrolidinium ( <b>149-156</b> )	A-39
Bis-Pyrrolidinium ( <b>225-227</b> )	A-43
Tetraalkyl Ammonium ( <b>56-58, 60, 67, 158,159,168-180</b> )	A-45
Protic ILs – Ethanolaminium ( <b>54, 55, 160-167</b> )	A-52
Cholinium ( <b>61-66, 157, 310-322</b> )	A-59
Phosphonium ( <b>181-213</b> )	A-70

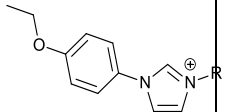
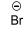
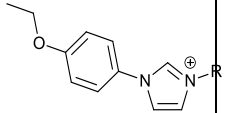
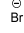
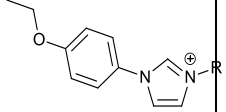
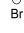
Surfactants ( <b>LAM</b> , <b>C3(CA)2</b> , <b>1010R (4)</b> , <b>1212R</b> , <b>1414R</b> , <b>HTAB</b> )	A-79
Tris-Imidazolium Surfactants ( <b>286-297</b> )	A-83
Tetrakis-Imidazolium Surfactants ( <b>298-309</b> )	A-87
References	A-90

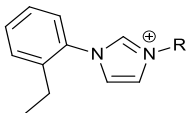
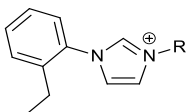
IL	Head Group	Side Chain R	Anion	Biodegradation %	Classification	Test Method	Inoculum	IL Conc.	Test Duration	Measured Parameter	Ref
<b>Imidazolium</b>											
<b>68</b>		C <sub>2</sub> H <sub>5</sub>		10	Not readily biodegradable	Respirometric BOD (OxiDirect® by Lovibond)	Waste-water organisms	100 mg/L	10 d	BOD	<sup>1</sup>
<b>8</b>	“	C <sub>2</sub> H <sub>5</sub>		0	Not primarily biodegradable	Primary Biodegradation by HPLC from modified OECD 301	Activated Sludge	200 µM	28 d		<sup>2</sup>

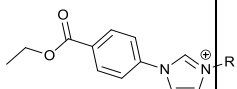
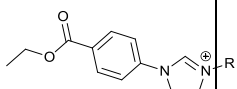
<b>8</b>		$\text{C}_2\text{H}_5$	$\ominus \text{Cl}$	n.d.	Not readily biodegradable	Manometric Respirometry (OECD 301F)	Activated Sludge	120-150 mg/L	28 d	BOD	<sup>2</sup>
<b>9</b>	“	$\text{C}_4\text{H}_9$	$\ominus \text{Cl}$	03	Not readily biodegradable	Respirometric BOD (OxiDirect® by Lovibond)	Waste-water organisms	100 mg/L	10 d	BOD	<sup>1</sup>
<b>4</b>	“	$\text{C}_4\text{H}_9$		0	Not readily biodegradable	$\text{BOD}_5$	Activated sludge	10 g/L	30 d	BOD	<sup>3</sup>
<b>29</b>	“	$\text{C}_4\text{H}_9$		0	Not readily biodegradable	$\text{BOD}_5$	Activated sludge	10 g/L	30 d	BOD	<sup>3</sup>

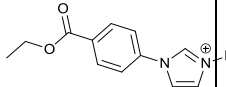
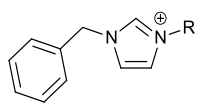
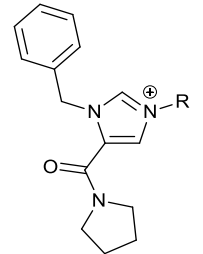
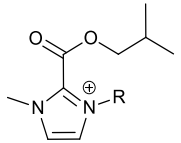
<b>12</b>	“	C <sub>6</sub> H <sub>13</sub>	$\ominus$ Cl	02	Not readily biodegradable	Respirometric BOD (OxiDirect® by Lovibond)	Waste-water organisms	100 mg/L	10 d	BOD	
<b>69</b>		C <sub>3</sub> H <sub>7</sub>	$\ominus$ Br	0	Not primarily biodegradable	Primary Biodegradation by HPLC from modified OECD 301	Activated Sludge	200 µM	28 d		<sup>2</sup>
<b>69</b>	“	“	“	n.d.	Not readily biodegradable	Manometric Respirometry (OECD 301F)	Activated Sludge	120-150 mg/L	28 d	BOD	<sup>2</sup>
<b>70</b>		C <sub>4</sub> H <sub>9</sub>	$\ominus$ Br	0	Not primarily biodegradable	Primary Biodegradation by HPLC from modified OECD 301	Activated Sludge	200 µM	28 d		<sup>2</sup>

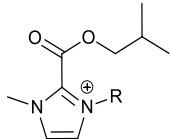
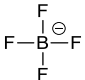
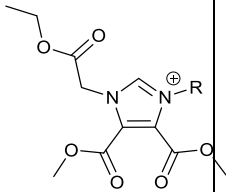
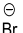
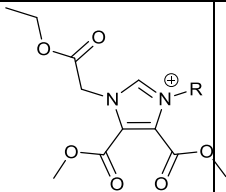
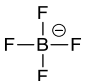
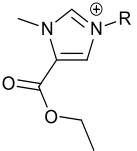
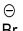


70	“	“	“	0	Not readily biodegradable	Manometric Respirometry (OECD 301F)	Activated Sludge	120-150 mg/L	28 d	BOD	2
71		C <sub>4</sub> H <sub>9</sub>		0	Not primarily biodegradable	Primary Biodegradation by HPLC from modified OECD 301	Activated Sludge	200 μM	28 d		2
71		C <sub>4</sub> H <sub>9</sub>		n.d.	Not readily biodegradable	Manometric Respirometry (OECD 301F)	Activated Sludge	120-150 mg/L	28 d	BOD	2
72		C <sub>5</sub> H <sub>11</sub>		0	Not primarily biodegradable	Primary Biodegradation by HPLC from modified OECD 301	Activated Sludge	200 μM	28 d		2

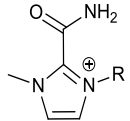
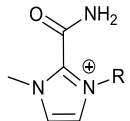
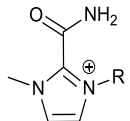

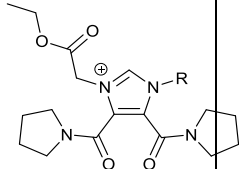
72	“	“	“	n.d.	Not readily biodegradable	Manometric Respirometry (OECD 301F)	Activated Sludge	120-150 mg/L	28 d	BOD	<sup>2</sup>
73		C <sub>4</sub> H <sub>9</sub>	<sup>⊖</sup> Br	0	Not primarily biodegradable	Primary Biodegradation by HPLC from modified OECD 301	Activated Sludge	200 μM	28 d		<sup>2</sup>
73	“	“	“	n.d.	Not readily biodegradable	Manometric Respirometry (OECD 301F)	Activated Sludge	120-150 mg/L	28 d	BOD	<sup>2</sup>
74		C <sub>4</sub> H <sub>9</sub>	<sup>⊖</sup> I	0	Not primarily biodegradable	Primary Biodegradation by HPLC from modified OECD 301	Activated Sludge	200 μM	28 d		<sup>2</sup>

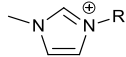
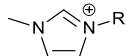

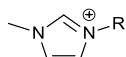
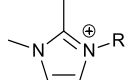
74	“	“	“	n.d.	Not readily biodegradable	Manometric Respirometry (OECD 301F)	Activated Sludge	120-150 mg/L	28 d	BOD	2
75		C <sub>6</sub> H <sub>13</sub>	Br <sup>⊖</sup>	100	<u>primarily biodegradable</u>	Primary Biodegradation by HPLC from modified OECD 301	Activated Sludge	200 μM	28 d		2
75	“	“	“	8	Not readily biodegradable	Manometric Respirometry (OECD 301F)	Activated Sludge	120-150 mg/L	28 d	BOD	2
76		C <sub>4</sub> H <sub>9</sub>	Br <sup>⊖</sup>	100	<u>primarily biodegradable</u>	Primary Biodegradation by HPLC from modified OECD 301	Activated Sludge	200 μM	28 d		2

76		$\text{C}_4\text{H}_9$	$\ominus$ Br	7	Not readily biodegradable	Manometric Respirometry (OECD 301F)	Activated Sludge	120-150 mg/L	28 d	BOD	2
78		$\text{CH}_2\text{CONC}_4\text{H}_8$	$\ominus$ Br	0	Not readily biodegradable	$\text{CO}_2$ Headspace test (ISO 14593)	Activated sludge	20 mg/L	28 d	$\text{THCO}_2$	4
79		$\text{CH}_2\text{COOCH}_3$	$\ominus$ Br	2	Not readily biodegradable	$\text{CO}_2$ Headspace test (ISO 14593)	Activated sludge	20 mg/L	28 d	$\text{THCO}_2$	4
80		$\text{CH}_3$	$\ominus$ I	30	Not readily biodegradable	$\text{CO}_2$ Headspace test (ISO 14593)	Activated sludge	20 mg/L	28 d	$\text{THCO}_2$	4

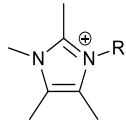
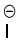
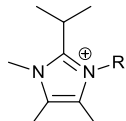

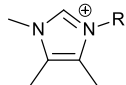

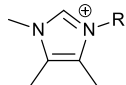

81		CH <sub>3</sub>		35	Not readily biodegradable	CO <sub>2</sub> Headspace test (ISO 14593)	Activated sludge	20 mg/L	28 d	THCO <sub>2</sub>	4
82		CH <sub>2</sub> C <sub>6</sub> H <sub>5</sub>		24	Not readily biodegradable	CO <sub>2</sub> Headspace test (ISO 14593)	Activated sludge	20 mg/L	28 d	THCO <sub>2</sub>	4
83		CH <sub>3</sub>		31	Not readily biodegradable	CO <sub>2</sub> Headspace test (ISO 14593)	Activated sludge	20 mg/L	28 d	THCO <sub>2</sub>	4
84		CH <sub>2</sub> COOCH <sub>3</sub>		10	Not readily biodegradable	CO <sub>2</sub> Headspace test (ISO 14593)	Activated sludge	20 mg/L	28 d	THCO <sub>2</sub>	4

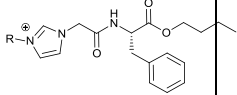
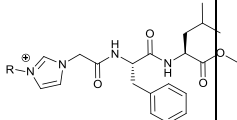
85		$\text{CH}_2\text{COOCH}_3$		5	Not readily biodegradable	CO <sub>2</sub> Headspace test (ISO 14593)	Activated sludge	20 mg/L	28 d	THCO <sub>2</sub>	4
86		$\text{CH}_2\text{C}_6\text{H}_5$		6	Not readily biodegradable	CO <sub>2</sub> Headspace test (ISO 14593)	Activated sludge	20 mg/L	28 d	THCO <sub>2</sub>	4
87		$\text{CH}_3$		12	Not readily biodegradable	CO <sub>2</sub> Headspace test (ISO 14593)	Activated sludge	20 mg/L	28 d	THCO <sub>2</sub>	4
88		$\text{CH}_3$		3	Not readily biodegradable	CO <sub>2</sub> Headspace test (ISO 14593)	Activated sludge	20 mg/L	28 d	THCO <sub>2</sub>	4

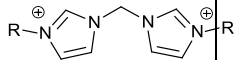
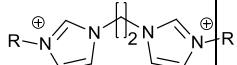
<b>89</b>		$\text{CH}_2\text{COOCH}_3$	$\ominus \text{Br}$	17	Not readily biodegradable	$\text{CO}_2$ Headspace test (ISO 14593)	Activated sludge	20 mg/L	28 d	$\text{THCO}_2$	<sup>4</sup>
<b>90</b>		$\text{CH}_2\text{CONC}_4\text{H}_8$	$\ominus \text{Br}$	12	Not readily biodegradable	$\text{CO}_2$ Headspace test (ISO 14593)	Activated sludge	20 mg/L	28 d	$\text{THCO}_2$	<sup>4</sup>
<b>91</b>		$\text{CH}_2\text{CONC}_4\text{H}_8$		14	Not readily biodegradable	$\text{CO}_2$ Headspace test (ISO 14593)	Activated sludge	20 mg/L	28 d	$\text{THCO}_2$	<sup>4</sup>
<b>92</b>		$\text{CH}_2\text{C}_6\text{H}_5$	$\ominus \text{Br}$	2	Not readily biodegradable	$\text{CO}_2$ Headspace test (ISO 14593)	Activated sludge	20 mg/L	28 d	$\text{THCO}_2$	<sup>4</sup>

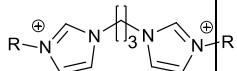
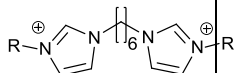
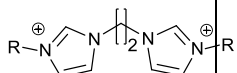
<b>93</b>		$\text{CH}_2\text{COOCH}_3$	$\ominus \text{Br}$	10	Not readily biodegradable	$\text{CO}_2$ Headspace test (ISO 14593)	Activated sludge	20 mg/L	28 d	$\text{THCO}_2$	<sup>4</sup>
<b>94</b>		$\text{CH}_2\text{COOCH}_3$		14	Not readily biodegradable	$\text{CO}_2$ Headspace test (ISO 14593)	Activated sludge	20 mg/L	28 d	$\text{THCO}_2$	<sup>4</sup>
<b>95</b>		$\text{CH}_2\text{CONC}_4\text{H}_8$	$\ominus \text{Br}$	3	Not readily biodegradable	$\text{CO}_2$ Headspace test (ISO 14593)	Activated sludge	20 mg/L	28 d	$\text{THCO}_2$	<sup>4</sup>
<b>96</b>		$\text{CH}_2\text{CONC}_4\text{H}_8$	$\ominus \text{Br}$	3	Not readily biodegradable	$\text{CO}_2$ Headspace test (ISO 14593)	Activated sludge	20 mg/L	28 d	$\text{THCO}_2$	<sup>4</sup>

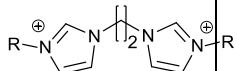
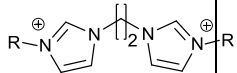
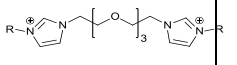
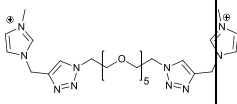
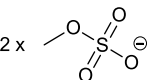


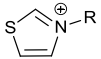
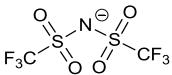
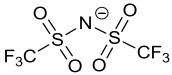
<b>97</b>		C <sub>2</sub> H <sub>5</sub>		2.11	Not readily biodegradable	Closed Bottle Test (TG 301 D)	Waste-water organisms	5 mg/L	28 d	BOD	<sup>5</sup>
<b>98</b>		C <sub>2</sub> H <sub>5</sub>		6.64	Not readily biodegradable	Closed Bottle Test (TG 301 D)	Waste-water organisms	5 mg/L	28 d	BOD	<sup>5</sup>
<b>99</b>		C <sub>2</sub> H <sub>5</sub>		6.23	Not readily biodegradable	Closed Bottle Test (TG 301 D)	Waste-water organisms	5 mg/L	28 d	BOD	<sup>5</sup>
<b>100</b>		C <sub>6</sub> H <sub>13</sub>		9.07	Not readily biodegradable	Closed Bottle Test (TG 301 D)	Waste-water organisms	5 mg/L	28 d	BOD	<sup>5</sup>

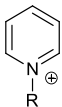
<b>101</b>		CH <sub>3</sub>	$\ominus$ Br	61	<u>Readily</u> <u>biodegradable</u>	CO <sub>2</sub> Headspace test (ISO 14593)	Activated sludge	20 mg C L <sup>-1</sup>	28 d	ThCO <sub>2</sub>	<sup>6</sup>
<b>102</b>		CH <sub>3</sub>	$\ominus$ Br	64	<u>Readily</u> <u>biodegradable</u>	CO <sub>2</sub> Headspace test (ISO 14593)	Activated sludge	20 mg C L <sup>-1</sup>	28 d	ThCO <sub>2</sub>	<sup>6</sup>

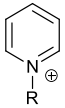
IL	Head Group	Side Chain R	Anion	Biodegradation %	Classification	Test Method	Inoculum	IL Conc.	Test Duration	Measured Parameter	Ref
<b>Bis-Imidazolium</b>											
<b>217</b>		CH <sub>3</sub>	$2 \times \text{I}^{\ominus}$	<5	Not readily biodegradable	Primary Biodegradation by IC from modified OECD 301 D	Activated Sludge	60-100 mg/L	28 d		<sup>7</sup>
<b>218</b>		CH <sub>3</sub>	$2 \times \text{Br}^{\ominus}$	<5	Not readily biodegradable	Primary Biodegradation by IC from modified OECD 301 D	Activated Sludge	60-100 mg/L	28 d		<sup>7</sup>

<b>219</b>		CH <sub>3</sub>	2 x Br <sup>⊖</sup>	<5	Not readily biodegradable	Primary Biodegradation by IC from modified OECD 301 D	Activated Sludge	60-100 mg/L	28 d		7
<b>220</b>		CH <sub>3</sub>	2 x Br <sup>⊖</sup>	<5	Not readily biodegradable	Primary Biodegradation by IC from modified OECD 301 D	Activated Sludge	60-100 mg/L	28 d		7
<b>220</b>	“	CH <sub>3</sub>	2 x Br <sup>⊖</sup>	0 ± 0.5	Not readily biodegradable	Manometric Respirometry (OECD 301F)	Activated Sludge	120-150 mg/L	28 d	BOD	7
<b>221</b>		C <sub>4</sub> H <sub>9</sub>	2 x Br <sup>⊖</sup>	<5	Not readily biodegradable	Primary Biodegradation by IC from modified OECD 301 D	Activated Sludge	60-100 mg/L	28 d		7

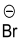
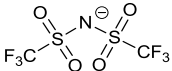
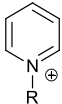


222		C <sub>6</sub> H <sub>13</sub>	2 x Br <sup>⊖</sup>	<5	Not readily biodegradable	Primary Biodegradation by IC from modified OECD 301 D	Activated Sludge	60-100 mg/L	28 d		7
222		C <sub>6</sub> H <sub>13</sub>	2 x Br <sup>⊖</sup>	2 ± 2.5	Not readily biodegradable	Manometric Respirometry (OECD 301F)	Activated Sludge	120-150 mg/L	28 d	BOD	7
223		CH <sub>3</sub>	2 x Cl <sup>⊖</sup>	<5	Not readily biodegradable	Primary Biodegradation by IC from modified OECD 301 D	Activated Sludge	60-100 mg/L	28 d		7
224		CH <sub>3</sub>	2 x 	<5	Not readily biodegradable	Primary Biodegradation by IC from modified OECD 301 D	Activated Sludge	60-100 mg/L	28 d		7

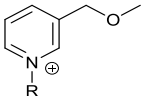
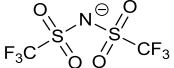
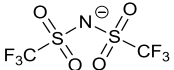
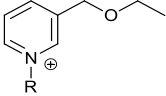
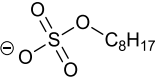
IL	Head Group	Side Chain R	Anion	Biodegradation %	Classification	Test Method	Inoculum	IL Conc.	Test Duration	Measured Parameter	Ref
<b>Thiazolium</b>											
<b>103</b>		C <sub>2</sub> H <sub>5</sub>		03	Not readily biodegradable	CO <sub>2</sub> Headspace test (ISO 14593)	Activated sludge	20 mg/L	28 d	THCO <sub>2</sub>	<sup>8</sup>
<b>104</b>	“	C <sub>2</sub> H <sub>4</sub> OH		07	Not readily biodegradable	CO <sub>2</sub> Headspace test (ISO 14593)	Activated sludge	20 mg/L	28 d	THCO <sub>2</sub>	<sup>8</sup>

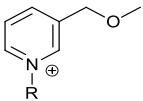
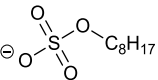
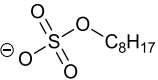
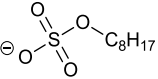
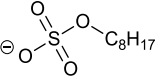
IL	Head Group	Side Chain R	Anion	Biodegradation %	Classification	Test Method	Inoculum	IL Conc.	Test Duration	Measured Parameter	Ref
<b>Pyridinium</b>											
<b>16</b>		C <sub>2</sub> H <sub>5</sub>	$\ominus$ Cl	0	Not readily biodegradable	Primary Biodegradation	Activated sludge	50 $\mu$ mol /L	28 d		9, 10
<b>105</b>	“	CH <sub>2</sub> CN	$\ominus$ Cl	Not reported	Hydrolysis of cyano group detected	Primary Biodegradation	Activated sludge	50 $\mu$ mol /L	28 d		9

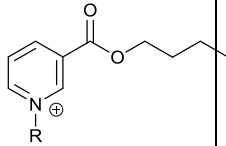
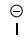
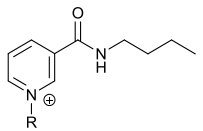
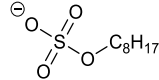
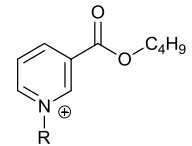
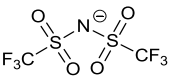
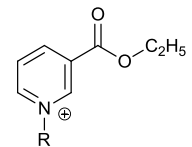
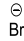
105	“	CH <sub>2</sub> CN	$\ominus$ Cl	-2 ± 0	<u>Inherently</u>	Manometric Respirometry (OECD 301F)	Activated sludge		28 d	BOD	<sup>9</sup>
106		C <sub>4</sub> H <sub>9</sub>	$\ominus$ Br	2	Not readily biodegradable	Manometric Respirometry (OECD 301F)	Activated sludge		28 d	BOD	<sup>9</sup> , <sup>11</sup>
107	“	C <sub>3</sub> H <sub>7</sub>	$\ominus$ Br	1 ± 0	Not readily biodegradable	Manometric Respirometry (OECD 301F)	Activated sludge		28 d	BOD	<sup>9</sup>
108	“	CH <sub>2</sub> C <sub>6</sub> H <sub>5</sub>	$\ominus$ Br	2	Not readily biodegradable	CO <sub>2</sub> Headspace test (ISO 14593)		20 mg/L	28 d	THCO <sub>2</sub>	<sup>4</sup>

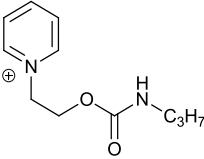
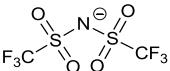
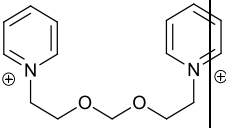
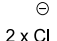


109	“	C <sub>2</sub> H <sub>4</sub> OH		65	<u>Readily biodegradable</u>	CO <sub>2</sub> Headspace test (ISO 14593, OECD 310)	Activated sludge	20 mg/L	28 d	THCO <sub>2</sub>	8
110	“	C <sub>2</sub> H <sub>4</sub> OH		62	<u>Readily biodegradable</u>	CO <sub>2</sub> Headspace test (ISO 14593, OECD 310)	Activated sludge	20 mg/L	28 d	THCO <sub>2</sub>	8
111		C <sub>2</sub> H <sub>4</sub> OH		100	<u>Inherently, ultimately biodegradable</u>	Primary Biodegradation	Activated sludge	50 μmol /L	28 d		9
111	“	C <sub>2</sub> H <sub>4</sub> OH		65 ± 10	<u>Inherently</u>	Manometric Respirometry (OECD 301F)	Activated sludge		28 d	BOD	9

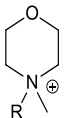
112	“	C <sub>2</sub> H <sub>4</sub> OH	$\ominus$ Cl	51 ± 0	<u>Inherently</u>	Manometric Respirometry (OECD 301F)	Activated sludge		28 d	BOD	<sup>9</sup>
113		C <sub>2</sub> H <sub>4</sub> OH		6	Not readily biodegradable	CO <sub>2</sub> Headspace test (ISO 14593)	Activated sludge	20 mg/L	28 d	THCO <sub>2</sub>	<sup>8</sup>
114	“	C <sub>4</sub> H <sub>9</sub>		01	Not readily biodegradable	CO <sub>2</sub> Headspace test (ISO 14593)	Activated sludge	20 mg/L	28 d	THCO <sub>2</sub>	<sup>8</sup>
115		C <sub>4</sub> H <sub>9</sub>		36	Not readily biodegradable	CO <sub>2</sub> Headspace test (ISO 14593)	Activated sludge	20 mg/L	28 d	THCO <sub>2</sub>	<sup>8</sup>

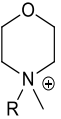
<b>116</b>		$\text{C}_4\text{H}_9$		32	Not readily biodegradable	CO <sub>2</sub> Headspace test (ISO 14593)	Activated sludge	20 mg/L	28 d	THCO <sub>2</sub>	8
<b>117</b>	“	$\text{C}_8\text{H}_{17}$		31	Not readily biodegradable	CO <sub>2</sub> Headspace test (ISO 14593)	Activated sludge	20 mg/L	28 d	THCO <sub>2</sub>	8
<b>118</b>	“	$\text{CH}_2\text{C}(\text{O})\text{OC}_2\text{H}_5$		47	Not readily biodegradable	CO <sub>2</sub> Headspace test (ISO 14593)	Activated sludge	20 mg/L	28 d	THCO <sub>2</sub>	8
<b>119</b>	“	$\text{CH}_2\text{C}(\text{O})\text{OC}_5\text{H}_{11}$		51	Not readily biodegradable	CO <sub>2</sub> Headspace test (ISO 14593)	Activated sludge	20 mg/L	28 d	THCO <sub>2</sub>	8

120		CH <sub>3</sub>		74	<u>Readily biodegradable</u>	CO <sub>2</sub> Headspace test (ISO 14593)	Waste-water organisms	40 mg/L	28 d	THCO <sub>2</sub>	11
121		C <sub>4</sub> H <sub>9</sub>		30	Not readily biodegradable	CO <sub>2</sub> Headspace test (ISO 14593)	Waste-water organisms	40 mg/L	28 d	THCO <sub>2</sub>	11
122		C <sub>2</sub> H <sub>4</sub> OH		71	<u>Readily biodegradable</u>	CO <sub>2</sub> Headspace test (ISO 14593)	Activated sludge	20 mg/L	28 d	THCO <sub>2</sub>	8
123		CH <sub>2</sub> C <sub>6</sub> H <sub>5</sub>		25	Not readily biodegradable	CO <sub>2</sub> Headspace test (ISO 14593)	Activated sludge	20 mg/L	28 d	THCO <sub>2</sub>	4

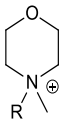
124		N/A		03	Not readily biodegradable	CO <sub>2</sub> Headspace test (ISO 14593)	Activated sludge	20 mg/L	28 d	THCO <sub>2</sub>	8
IL	Head Group	Side Chain R	Anion	Biodegradation %	Classification	Test Method	Inoculum	IL Conc.	Test Duration	Measured Parameter	Ref
Bis-Pyridinium											
214		N/A		05	Not readily biodegradable	CO <sub>2</sub> Headspace test (ISO 14593)	Activated sludge	20 mg/L	28 d	THCO <sub>2</sub>	8

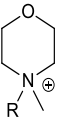
215	“	N/A	$2 \times \begin{array}{c} \text{O} \quad \text{O} \\ \diagdown \quad \diagup \\ \text{F}_3\text{C}-\text{S}-\text{N}^{\ominus}-\text{S}-\text{CF}_3 \\ \diagup \quad \diagdown \\ \text{O} \quad \text{O} \end{array}$	04	Not readily biodegradable	CO <sub>2</sub> Headspace test (ISO 14593)	Activated sludge	20 mg/L	28 d	THCO <sub>2</sub>	8
216	“	N/A	$2 \times \begin{array}{c} \text{F} \\   \\ \text{F}-\text{P}^{\ominus}-\text{F} \\   \\ \text{F} \end{array}$	03	Not readily biodegradable	CO <sub>2</sub> Headspace test (ISO 14593)	Activated sludge	20 mg/L	28 d	THCO <sub>2</sub>	8

IL	Head Group	Side Chain R	Anion	Biodegradation %	Classification	Test Method	Inoculum	IL Conc.	Test Duration	Measured Parameter	Ref
<b>Morpholinium</b>											
<b>125</b>		C <sub>2</sub> H <sub>5</sub>	$\ominus$ Br	30	Not readily biodegradable	CO <sub>2</sub> Headspace test (ISO 14593)	Activated sludge	20 mg/L	28 d	THCO <sub>2</sub>	<sup>12</sup>
<b>126</b>	“	C <sub>4</sub> H <sub>9</sub>	$\ominus$ Br	10	Not readily biodegradable	CO <sub>2</sub> Headspace test (ISO 14593)	Activated sludge	20 mg/L	28 d	THCO <sub>2</sub>	<sup>12</sup>

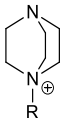
126	“	C <sub>4</sub> H <sub>9</sub>	$\ominus$ Br	-3±4	Not readily biodegradable	Primary Biodegradation	Activated sludge	50 $\mu$ mol /L	28 d		9
127		C <sub>6</sub> H <sub>13</sub>	$\ominus$ Br	04	Not readily biodegradable	CO <sub>2</sub> Headspace test (ISO 14593)	Activated sludge	20 mg/L	28 d	THCO <sub>2</sub>	12
128	“	C <sub>8</sub> H <sub>17</sub>	$\ominus$ Br	06	Not readily biodegradable	CO <sub>2</sub> Headspace test (ISO 14593)	Activated sludge	20 mg/L	28 d	THCO <sub>2</sub>	12
129	“	C <sub>10</sub> H <sub>21</sub>	$\ominus$ Br	07	Not readily biodegradable	CO <sub>2</sub> Headspace test (ISO 14593)	Activated sludge	20 mg/L	28 d	THCO <sub>2</sub>	12

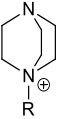


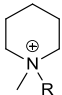
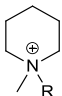
<b>130</b>	“	C <sub>2</sub> H <sub>4</sub> OH	$\ominus$ I	17 ± 1		Primary Biodegradation	Activated sludge	50 μmol /L	28 d		<sup>9</sup>
<b>130</b>	“	C <sub>2</sub> H <sub>4</sub> OH	$\ominus$ I	-1 ± 1 4 ± 1	Not readily biodegradable	Manometric Respirometry (OECD 301F)	Activated sludge		28 d 60 d	BOD	<sup>9</sup>
<b>131</b>		C <sub>3</sub> H <sub>6</sub> OH	$\ominus$ Cl	12 ± 8		Primary Biodegradation	Activated sludge	50 μmol /L	28 d		<sup>9</sup>
<b>131</b>	“	C <sub>3</sub> H <sub>6</sub> OH	$\ominus$ Cl	31 ± 16 59 ± 10	<u>Inherently</u>	Manometric Respirometry (OECD 301F)	Activated sludge		28 d 41 d	BOD	<sup>9</sup>

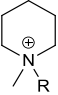
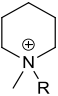
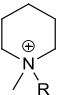
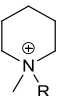
132	“	CH <sub>2</sub> CN	$\ominus$ Cl	54 ± 13	Hydrolysis of cyano group detected	Primary Biodegradation	Activated sludge	50 μmol /L	28 d		9
132	“	CH <sub>2</sub> CN	$\ominus$ Cl	0	Not readily biodegradable	Manometric Respirometry (OECD 301F)	Activated sludge		28 d	BOD	9
133	“	CH <sub>2</sub> C <sub>6</sub> H <sub>5</sub>	$\ominus$ Cl	0	Not readily biodegradable	Primary Biodegradation Modified OECD 301 D	Activated sludge	45 mg/L	28 d		13
133		CH <sub>2</sub> C <sub>6</sub> H <sub>5</sub>	$\ominus$ Cl	0	Not readily biodegradable	Manometric Respirometry (OECD 301F)	Activated sludge	20 mg/L 100 mg/L	28 d	BOD	

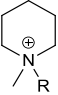
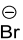
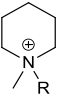
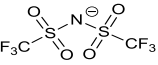
<b>134</b>	“	$\text{C}_2\text{H}_4\text{OCH}_3$	$\ominus$ Cl	$-1 \pm 4$	Not readily biodegradable	Primary Biodegradation	Activated sludge	50 $\mu\text{mol}$ /L	28 d		9
<b>135</b>	“	$\text{CH}_2\text{OC}_2\text{H}_5$	$\ominus$ Cl	$-3 \pm 4$	Not readily biodegradable	Primary Biodegradation	Activated sludge	50 $\mu\text{mol}$ /L	28 d		9
<b>136</b>	“	$\text{C}_2\text{H}_4\text{OC}_2\text{H}_5$	$\ominus$ Cl	$0 \pm 8$	Not readily biodegradable	Primary Biodegradation	Activated sludge	50 $\mu\text{mol}$ /L	28 d		9

IL	Head Group	Side Chain R	Anion	Biodegradation %	Classification	Test Method	Inoculum	IL Conc.	Test Duration	Measured Parameter	Ref
<b>1,4-Diazabicyclo[2.2.2]octanium (DABCO)</b>											
<b>137</b>		C <sub>2</sub> H <sub>5</sub>	$\ominus$ Br	40	Not readily biodegradable	CO <sub>2</sub> Headspace test (ISO 14593)	Activated sludge	20 mg/L	28 d	THCO <sub>2</sub>	<sup>12</sup>
<b>138</b>	“	C <sub>4</sub> H <sub>9</sub>	$\ominus$ Br	36	Not readily biodegradable	CO <sub>2</sub> Headspace test (ISO 14593)	Activated sludge	20 mg/L	28 d	THCO <sub>2</sub>	<sup>12</sup>

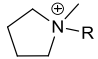
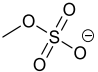
<b>139</b>	“	C <sub>6</sub> H <sub>13</sub>	$\ominus$ Br	23	Not readily biodegradable	CO <sub>2</sub> Headspace test (ISO 14593)	Activated sludge	20 mg/L	28 d	THCO <sub>2</sub>	<sup>12</sup>
<b>140</b>		C <sub>8</sub> H <sub>17</sub>	$\ominus$ Br	34	Not readily biodegradable	CO <sub>2</sub> Headspace test (ISO 14593)	Activated sludge	20 mg/L	28 d	THCO <sub>2</sub>	<sup>12</sup>
<b>141</b>	“	C <sub>10</sub> H <sub>21</sub>	$\ominus$ Br	34	Not readily biodegradable	CO <sub>2</sub> Headspace test (ISO 14593)	Activated sludge	20 mg/L	28 d	THCO <sub>2</sub>	<sup>12</sup>

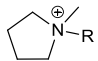
IL	Head Group	Side Chain R	Anion	Biodegradation %	Classification	Test Method	Inoculum	IL Conc.	Test Duration	Measured Parameter	Ref
Piperidinium											
142		C <sub>2</sub> H <sub>4</sub> OH	$\ominus$ Cl	29 ± 3 85 ± 1	<u>Inherently biodegradable</u>	Manometric Respirometry (OECD 301F)	Activated sludge		28 d 60 d	BOD	<sup>9</sup>
143		C <sub>3</sub> H <sub>6</sub> OH	$\ominus$ Cl	79 ± 2	<u>Inherently, ultimately biodegradable</u>	Manometric Respirometry (OECD 301F)	Activated sludge		28 d	BOD	<sup>9</sup>

<b>144</b>		$\text{CH}_2\text{CN}$	$\ominus \text{Cl}$	Not reported	Hydrolysis of cyano group detected	Primary Biodegradation	Activated sludge	50 $\mu\text{mol/L}$	28 d		<sup>9</sup>
<b>144</b>		$\text{CH}_2\text{CN}$	$\ominus \text{Cl}$	$5 \pm 2$	Not readily biodegradable	Manometric Respirometry (OECD 301F)	Activated sludge		28 d	BOD	<sup>9</sup>
<b>145</b>		$\text{CH}_2\text{OC}_2\text{H}_5$	$\ominus \text{Cl}$	$-2 \pm 2$	Not readily biodegradable	Primary Biodegradation	Activated sludge	50 $\mu\text{mol/L}$	28 d	BOD	<sup>9</sup>
<b>146</b>		$\text{C}_2\text{H}_4\text{OCH}_3$	$\ominus \text{Cl}$	$1 \pm 4$	Not readily biodegradable	Primary Biodegradation	Activated sludge	50 $\mu\text{mol/L}$	28 d	BOD	<sup>9</sup>

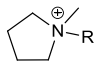
147		C <sub>4</sub> H <sub>9</sub>		-4 ± 3	Not readily biodegradable	Manometric Respirometry (OECD 301F)	Activated sludge		28 d	BOD	9, 11
148		C <sub>3</sub> H <sub>7</sub>		3 ± 2	Not readily biodegradable	Manometric Respirometry (OECD 301F)	Activated sludge		28 d	BOD	9

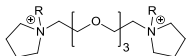


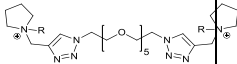
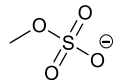
IL	Head Group	Side Chain R	Anion	Biodegradation %	Classification	Test Method	Inoculum	IL Conc.	Test Duration	Measured Parameter	Ref
<b>Pyrrolidinium</b>											
<b>149</b>		C <sub>4</sub> H <sub>9</sub>		6/9	Not readily biodegradable	CO2 evolution test (OECD 301B)	Waste-water organisms	40 mg/L	28 d	CO <sub>2</sub> Evolution	14
<b>149</b>	“	“	“	2/4	Not readily biodegradable	Manometric Respirometry (OECD 301F)	Waste-water organisms	75 mg/L	28 d	BOD	14

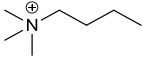
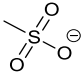
149	“	“	“	0	Not readily biodegradable	Primary Biodegradation by ion chromatography (samples taken from OECD 301B test)			28 d		14
150		C <sub>4</sub> H <sub>9</sub>	$\ominus$ Br	14 ± 13 70 ± 18	<u>Inherently, ultimately biodegradable</u>	Manometric Respirometry (OECD 301F)	Activated sludge		28 d 42 d	BOD	<sup>9</sup>
151	“	C <sub>3</sub> H <sub>6</sub> OH	$\ominus$ Cl	100	<u>Primarily biodegradable</u>	Primary Biodegradation	Activated sludge	50 μmol /L	28 d		<sup>9</sup>
151	“	C <sub>3</sub> H <sub>6</sub> OH	$\ominus$ Cl	67 ± 3	<u>Readily biodegradable</u>	Manometric Respirometry (OECD 301F)	Activated sludge		28 d	BOD	<sup>9</sup>

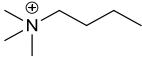
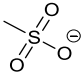
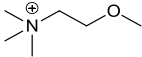
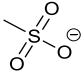
<b>152</b>	“	C <sub>2</sub> H <sub>5</sub>		-2 ± 3 -3 ± 8	Not readily biodegradable	Primary Biodegradation	Activated sludge	50 µmol /L	28 d 40 d		9
<b>153</b>	“	C <sub>2</sub> H <sub>4</sub> OH		8 ± 5 25 ± 21	Not readily biodegradable, potentially inherently	Primary Biodegradation	Activated sludge	50 µmol /L	28 d 43 d		9
<b>153</b>		C <sub>2</sub> H <sub>4</sub> OH		6 ± 9 42 ± 39	Not readily biodegradable, potentially inherently	Manometric Respirometry (OECD 301F)	Activated sludge		28 d 60 d	BOD	9
<b>154</b>	“	CH <sub>2</sub> CN		Not reported	Hydrolysis of cyano group detected	Primary Biodegradation	Activated sludge	50 µmol /L	28 d		9

<b>154</b>	“	CH <sub>2</sub> CN	$\ominus$ Cl	2 ± 2	Not readily biodegradable	Manometric Respirometry (OECD 301F)	Activated sludge		28 d	BOD	<sup>9</sup>
<b>155</b>	“	CH <sub>2</sub> CO- OCH <sub>2</sub> CH <sub>3</sub>	$\ominus$ Br	100	<u>Inherently,</u> <u>Ultimately</u> <u>Biodegradable</u>	Primary Biodegradation	Activated sludge	50 μmol /L	28 d		<sup>9</sup>
<b>155</b>	“	CH <sub>2</sub> CO- OCH <sub>2</sub> CH <sub>3</sub>	$\ominus$ Br	34 ± 11 74 ± 0.1	<u>Inherently,</u> <u>Ultimately</u> <u>Biodegradable</u>	Manometric Respirometry (OECD 301F)	Activated sludge		28 d 38 d	BOD	<sup>9</sup>
<b>156</b>		C <sub>8</sub> H <sub>17</sub>	$\ominus$ Cl	100	<u>Primarily</u> <u>biodegradable</u>	Primary Biodegradation	Activated sludge	50 μmol /L	28 d		<sup>9</sup>

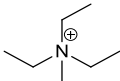
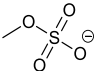
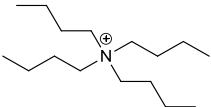
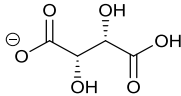
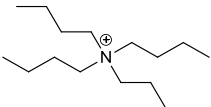
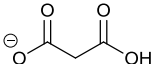
156	“	C <sub>8</sub> H <sub>17</sub>	$\ominus$ Cl	69 ± 1	<u>Readily</u> <u>biodegradable</u>	Manometric Respirometry (OECD 301F)	Activated sludge		28 d	BOD	<sup>9</sup>
IL	Head Group	Side Chain R	Anion	Biodegrad- ation %	Classification	Test Method	Inoculum	IL Conc.	Test Duration	Measured Parameter	Ref
<b>Bis-Pyrrolidinium</b>											
225		CH <sub>3</sub>	$\ominus$ 2 x Cl	<5	Not readily biodegradable	Primary Biodegradation by IC from modified OECD 301 D	Activated Sludge	60- 100 mg/L	28 d		<sup>7</sup>

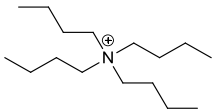
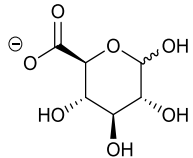
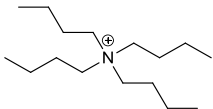
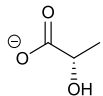
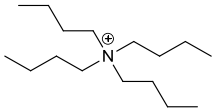
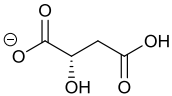
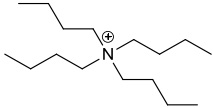
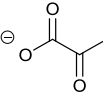
226		CH <sub>3</sub>	2 x 	<5	Not readily biodegradable	Primary Biodegradation by IC from modified OECD 301 D	Activated Sludge	60-100 mg/L	28 d		7
226	“	“	“	2 ± 2.5	Not readily biodegradable	Manometric Respirometry (OECD 301F)	Activated Sludge	120-150 mg/L	28 d	BOD	7

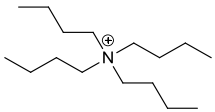
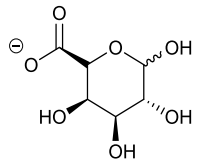
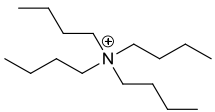
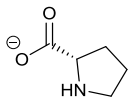
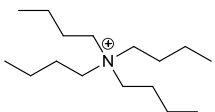
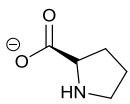
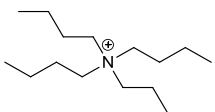
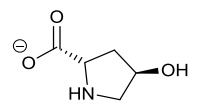
IL	Head Group (Cation)	Anion	Biodegradation %	Classification	Test Method	Inoculum	IL Conc.	Test Duration	Measured Parameter	Ref
<b>Tetraalkyl Ammonium</b>										
<b>158</b>			59/62	<u>Readily biodegradable</u>	CO2 evolution test (OECD 301B)	Waste-water organisms	40 mg/L	28 d	CO <sub>2</sub> Evolution	<sup>14</sup>
<b>158</b>	“	“	87/88	<u>Readily biodegradable</u>	Manometric Respirometry (OECD 301F)	Waste-water organisms	75 mg/L	28 d	BOD	<sup>14</sup>

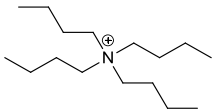
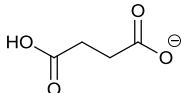
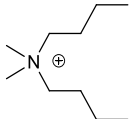
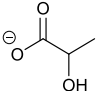
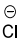
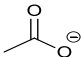
158			100±3	<u>Primarily biodegradable</u>	Primary Biodegradation by ion chromatography (samples taken from OECD 301B test)			9 d		14
159			17/18	Not readily biodegradable	CO2 evolution test (OECD 301B)	Waste-water organisms	40 mg/L	28 d	CO <sub>2</sub> Evolution	14
159	“	“	27/29	Not readily biodegradable	Manometric Respirometry (OECD 301F)	Waste-water organisms	75 mg/L	28 d	BOD	14
159	“	“	4±1		Primary Biodegradation by ion chromatography			28 d		14

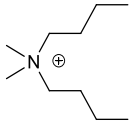
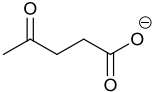
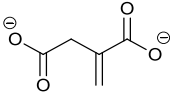
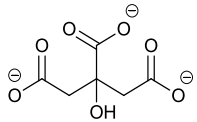
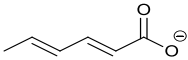


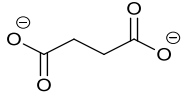
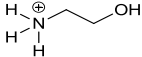
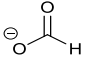
					(samples taken from OECD 301B test)					
173			4/5	Not readily biodegradable	Manometric Respirometry (OECD 301F)	Waste-water organisms	75 mg/L	28 d	BOD	14
56			15.5	Not readily biodegradable	Closed Bottle Test (TG 301 D)	Waste-water organisms		28 d	BOD	15
57			9.9	Not readily biodegradable	Closed Bottle Test (TG 301 D)	Waste-water organisms		28 d	BOD	15

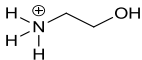
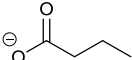
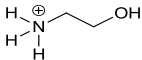
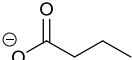
<b>58</b>			18.6	Not readily biodegradable	Closed Bottle Test (TG 301 D)	Waste-water organisms		28 d	BOD	15
<b>58</b>			15.5	Not readily biodegradable	Closed Bottle Test (TG 301 D)	Waste-water organisms		28 d	BOD	15
<b>168</b>			14.2	Not readily biodegradable	Closed Bottle Test (TG 301 D)	Waste-water organisms		28 d	BOD	15
<b>169</b>			12.2	Not readily biodegradable	Closed Bottle Test (TG 301 D)	Waste-water organisms		28 d	BOD	15

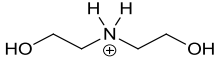
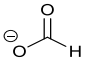
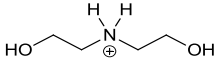
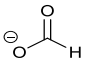
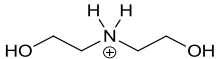
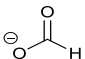
<b>170</b>			22.8	Not readily biodegradable	Closed Bottle Test (TG 301 D)	Waste-water organisms		28 d	BOD	15
<b>67</b>			15-20	Not readily biodegradable	CO <sub>2</sub> Headspace test (OECD 310)	Activated sludge	20 mg/L	28 d	THCO <sub>2</sub>	16
<b>171</b>			15-20	Not readily biodegradable	CO <sub>2</sub> Headspace test (OECD 310)	Activated sludge	20 mg/L	28 d	THCO <sub>2</sub>	16
<b>172</b>			20-25	Not readily biodegradable	CO <sub>2</sub> Headspace test (OECD 310)	Activated sludge	20 mg/L	28 d	THCO <sub>2</sub>	16

323			Nd	Not determined	Closed Bottle Test (TG 301 D)	Waste-water organisms		28 d	BOD	15
60			72	<u>Readily biodegradable</u>	Manometric Respirometry (OECD 301F)	Waste-water organisms		28 d	BOD	17
174	“		5	Not readily biodegradable	Manometric Respirometry (OECD 301F)	Waste-water organisms		28 d	BOD	17
175	“		77	<u>Readily biodegradable</u>	Manometric Respirometry (OECD 301F)	Waste-water organisms		28 d	BOD	17

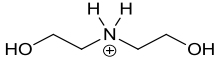
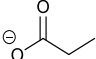
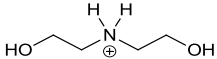
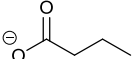
176			66	<u>Readily biodegradable</u>	Manometric Respirometry (OECD 301F)	Waste-water organisms		28 d	BOD	17
177	“		45	Not readily biodegradable	Manometric Respirometry (OECD 301F)	Waste-water organisms		28 d	BOD	17
178	“		69	<u>Readily biodegradable</u>	Manometric Respirometry (OECD 301F)	Waste-water organisms		28 d	BOD	17
179	“		54	Not readily biodegradable	Manometric Respirometry (OECD 301F)	Waste-water organisms		28 d	BOD	17

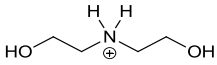
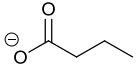
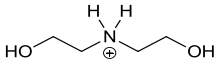
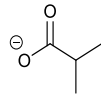
180	“		69	<u>Readily biodegradable</u>	Manometric Respirometry (OECD 301F)	Waste- water organisms		28 d	BOD	17
IL	Cation	Anion	Biodegradation %	Classification	Test Method	Inoculum	IL Conc.	Test Duration	Measured Parameter	Ref
<b>Protic ILs – Ethanolaminium</b>										
54			86	<u>Readily biodegradable</u>	Manometric Respirometry (OECD 301 F)	Activated Sludge	100 mg/L	28 d	BOD	18

54	“	“	100	<u>Primarily biodegradable</u>	Primary Biodegradation by ion chromatography (samples taken from OECD 301 F test)			5 d		18
55			95	<u>Readily biodegradable</u>	Manometric Respirometry (OECD 301F)	Activated Sludge	100 mg/L	28 d	BOD	18
55			100	<u>Primarily biodegradable</u>	Primary Biodegradation by ion chromatography (samples taken from OECD 301 F test)			5 d		18

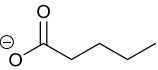
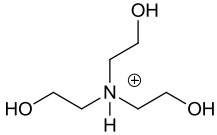
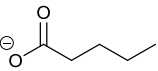
<b>160</b>			13	Not readily biodegradable	Manometric Respirometry (OECD 301F)	Activated Sludge	100 mg/L	28 d	BOD	18
<b>160</b>	“	“	100	<u>Primarily biodegradable</u>	Primary Biodegradation by ion chromatography (samples taken from OECD 301 F test)			5 d		18
<b>161</b>			69	<u>Readily biodegradable</u>	Manometric Respirometry (OECD 301F)	Activated Sludge	100 mg/L	28 d	BOD	18
<b>161</b>			65/ 100	<u>Primarily biodegradable</u>	Primary Biodegradation by ion chromatography			5d/ 28 d		18

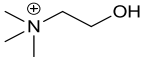
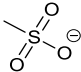


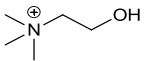
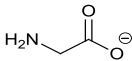
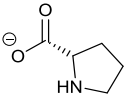
					(samples taken from OECD 301 F test)					
<b>162</b>			68	<u>Readily biodegradable</u>	Manometric Respirometry (OECD 301F)	Activated Sludge	100 mg/L	28 d	BOD	18
<b>162</b>	“	“	100	<u>Primarily biodegradable</u>	Primary Biodegradation by ion chromatography (samples taken from OECD 301 F test)			5 d		18
<b>163</b>			78	<u>Readily biodegradable</u>	Manometric Respirometry (OECD 301F)	Activated Sludge	100 mg/L	28 d	BOD	18

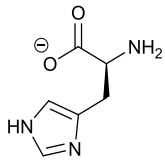
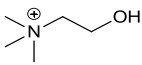
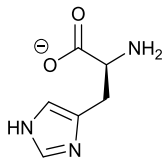
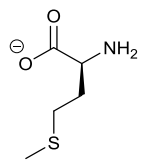
163			21/ 100	<u>Primarily biodegradable</u>	Primary Biodegradation by ion chromatography (samples taken from OECD 301 F test)			5 d/ 28 d		18
164			79	<u>Readily biodegradable</u>	Manometric Respirometry (OECD 301F)	Activated Sludge	100 mg/L	28 d	BOD	18
164	“	“	70/ 100	<u>Primarily biodegradable</u>	Primary Biodegradation by ion chromatography (samples taken from OECD 301 F test)			5 d/ 28d		18

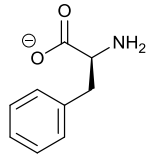
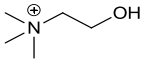
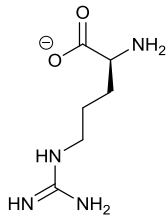
165			69	<u>Readily biodegradable</u>	Manometric Respirometry (OECD 301F)	Activated Sludge	100 mg/L	28 d	BOD	18
165			16/ 62	<u>Primarily biodegradable</u>	Primary Biodegradation by ion chromatography (samples taken from OECD 301 F test)			5 d/ 28 d		18
166			59	Not readily biodegradable	Manometric Respirometry (OECD 301F)	Activated Sludge	100 mg/L	28 d	BOD	18
166	“	“	34/ 100	<u>Primarily biodegradable</u>	Primary Biodegradation by ion chromatography			5 d/ 28 d		18

					(samples taken from OECD 301 F test)					
167	“		57	Not readily biodegradable	Manometric Respirometry (OECD 301F)	Activated Sludge	100 mg/L	28 d	BOD	18
167			33/ 100	<u>Primarily biodegradable</u>	Primary Biodegradation by ion chromatography (samples taken from OECD 301 F test)			5 d/ 28 d		18

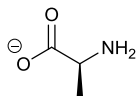
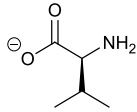
IL	Cation	Anion	Biodegradation %	Classification	Test Method	Inoculum	IL Conc.	Test Duration	Measured Parameter	Ref
<b>Cholinium</b>										
<b>157</b>			84/88	<u>Readily biodegradable</u>	CO2 evolution test (OECD 301B)	Waste-water organisms	40 mg/L	28 d	CO <sub>2</sub> Evolution	<sup>14</sup>
<b>157</b>	“	“	88/90	<u>Readily biodegradable</u>	Manometric Respirometry (OECD 301F)	Waste-water organisms	75 mg/L	28 d	BOD	<sup>14</sup>

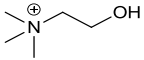
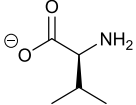
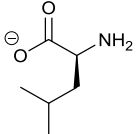
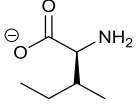
157	“	“	100±2	<u>Primarily biodegradable</u>	Primary Biodegradation by ion chromatography (samples taken from OECD 301B test)			5 d		14
61			76.4 ± 1.1	<u>Readily biodegradable</u>	CO <sub>2</sub> Headspace test (ISO 14593, OECD 310)	Activated sludge	20 mg/L	28 d	THCO <sub>2</sub>	19
61	“	“	82.6 ± 1.1	<u>Readily biodegradable</u>	Closed Bottle Test (TG 301 D)	Waste-water organisms	3 mg/L	28 d	BOD	19
62	“		70.5 ± 3.0	<u>Readily biodegradable</u>	CO <sub>2</sub> Headspace test (OECD 310)	Activated sludge	20 mg/L	28 d	THCO <sub>2</sub>	19

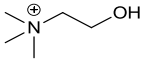
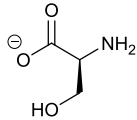
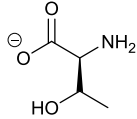
62	“	“	$71.3 \pm 0.1$	<u>Readily biodegradable</u>	Closed Bottle Test (TG 301 D)	Waste-water organisms	3 mg/L	28 d	BOD	<sup>19</sup>
63	“		$63.3 \pm 1.2$	<u>Readily biodegradable</u>	CO <sub>2</sub> Headspace test (OECD 310)	Activated sludge	20 mg/L	28 d	THCO <sub>2</sub>	<sup>19</sup>
63			$65.3 \pm 1.3$	<u>Readily biodegradable</u>	Closed Bottle Test (TG 301 D)	Waste-water organisms	3 mg/L	28 d	BOD	<sup>19</sup>
64	“		$63.6 \pm 1.2$	<u>Readily biodegradable</u>	CO <sub>2</sub> Headspace test (OECD 310)	Activated sludge	20 mg/L	28 d	THCO <sub>2</sub>	<sup>19</sup>

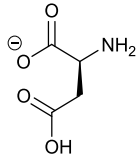
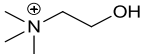
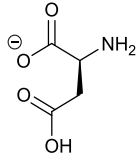
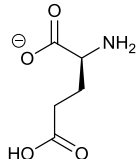
64	“	“	66.1 ± 0.9	<u>Readily biodegradable</u>	Closed Bottle Test (TG 301 D)	Waste-water organisms	3 mg/L	28 d	BOD	19
65	“		72.5 ± 0.3	<u>Readily biodegradable</u>	CO <sub>2</sub> Headspace test (OECD 310)	Activated sludge	20 mg/L	28 d	THCO <sub>2</sub>	19
65	“	“	70.8 ± 0.1	<u>Readily biodegradable</u>	Closed Bottle Test (TG 301 D)	Waste-water organisms	3 mg/L	28 d	BOD	19
66			65.5 ± 1.2	<u>Readily biodegradable</u>	CO <sub>2</sub> Headspace test (OECD 310)	Activated sludge	20 mg/L	28 d	THCO <sub>2</sub>	19

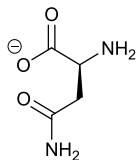
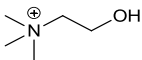
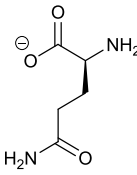


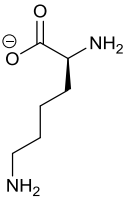
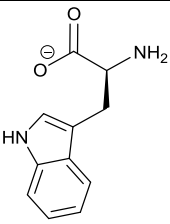
66	“	“	$67.6 \pm 0.2$	<u>Readily biodegradable</u>	Closed Bottle Test (TG 301 D)	Waste-water organisms	3 mg/L	28 d	BOD	<sup>19</sup>
310	“		$76.2 \pm 0.8$	<u>Readily biodegradable</u>	CO <sub>2</sub> Headspace test (OECD 310)	Activated sludge	20 mg/L	28 d	THCO <sub>2</sub>	<sup>19</sup>
310	“	“	$80.0 \pm 0.4$	<u>Readily biodegradable</u>	Closed Bottle Test (TG 301 D)	Waste-water organisms	3 mg/L	28 d	BOD	<sup>19</sup>
311	“		$67.5 \pm 0.6$	<u>Readily biodegradable</u>	CO <sub>2</sub> Headspace test (OECD 310)	Activated sludge	20 mg/L	28 d	THCO <sub>2</sub>	<sup>19</sup>

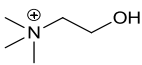
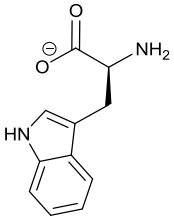
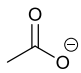
311			$69.4 \pm 0.6$	<u>Readily biodegradable</u>	Closed Bottle Test (TG 301 D)	Waste-water organisms	3 mg/L	28 d	BOD	<sup>19</sup>
312	“		$71.4 \pm 1.0$	<u>Readily biodegradable</u>	CO <sub>2</sub> Headspace test (OECD 310)	Activated sludge	20 mg/L	28 d	THCO <sub>2</sub>	<sup>19</sup>
312	“	“	$72.4 \pm 0.1$	<u>Readily biodegradable</u>	Closed Bottle Test (TG 301 D)	Waste-water organisms	3 mg/L	28 d	BOD	<sup>19</sup>
313	“		$70.5 \pm 0.3$	<u>Readily biodegradable</u>	CO <sub>2</sub> Headspace test (OECD 310)	Activated sludge	20 mg/L	28 d	THCO <sub>2</sub>	<sup>19</sup>

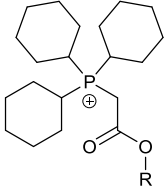
313	“	“	$71.6 \pm 0.8$	<u>Readily biodegradable</u>	Closed Bottle Test (TG 301 D)	Waste-water organisms	3 mg/L	28 d	BOD	<sup>19</sup>
314			$74.7 \pm 0.3$	<u>Readily biodegradable</u>	CO <sub>2</sub> Headspace test (OECD 310)	Activated sludge	20 mg/L	28 d	THCO <sub>2</sub>	<sup>19</sup>
314	“	“	$80.6 \pm 1.5$	<u>Readily biodegradable</u>	Closed Bottle Test (TG 301 D)	Waste-water organisms	3 mg/L	28 d	BOD	<sup>19</sup>
315	“		$71.5 \pm 0.8$	<u>Readily biodegradable</u>	CO <sub>2</sub> Headspace test (OECD 310)	Activated sludge	20 mg/L	28 d	THCO <sub>2</sub>	<sup>19</sup>

315	“	“	$74.3 \pm 1.5$	<u>Readily biodegradable</u>	Closed Bottle Test (TG 301 D)	Waste-water organisms	3 mg/L	28 d	BOD	<sup>19</sup>
316	“		$82.4 \pm 0.7$	<u>Readily biodegradable</u>	CO <sub>2</sub> Headspace test (OECD 310)	Activated sludge	20 mg/L	28 d	THCO <sub>2</sub>	<sup>19</sup>
316			$87.1 \pm 0.6$	<u>Readily biodegradable</u>	Closed Bottle Test (TG 301 D)	Waste-water organisms	3 mg/L	28 d	BOD	<sup>19</sup>
317	“		$80.8 \pm 0.5$	<u>Readily biodegradable</u>	CO <sub>2</sub> Headspace test (OECD 310)	Activated sludge	20 mg/L	28 d	THCO <sub>2</sub>	<sup>19</sup>

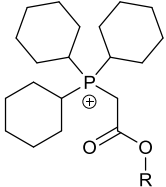
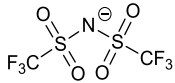
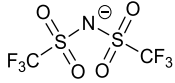
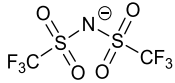
317	“	“	$86.3 \pm 0.2$	<u>Readily biodegradable</u>	Closed Bottle Test (TG 301 D)	Waste-water organisms	3 mg/L	28 d	BOD	<sup>19</sup>
318	“		$85.2 \pm 0.1$	<u>Readily biodegradable</u>	CO <sub>2</sub> Headspace test (OECD 310)	Activated sludge	20 mg/L	28 d	THCO <sub>2</sub>	<sup>19</sup>
318	“	“	$87.1 \pm 1.2$	<u>Readily biodegradable</u>	Closed Bottle Test (TG 301 D)	Waste-water organisms	3 mg/L	28 d	BOD	<sup>19</sup>
319			$81.4 \pm 0.1$	<u>Readily biodegradable</u>	CO <sub>2</sub> Headspace test (OECD 310)	Activated sludge	20 mg/L	28 d	THCO <sub>2</sub>	<sup>19</sup>

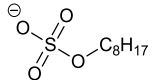
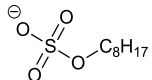
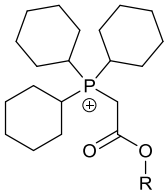
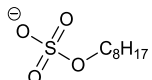
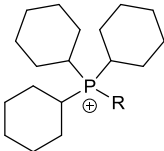

<b>319</b>	“	“	$86.6 \pm 1.4$	<u>Readily biodegradable</u>	Closed Bottle Test (TG 301 D)	Waste-water organisms	3 mg/L	28 d	BOD	<sup>19</sup>
<b>320</b>	“		$64.7 \pm 0.5$	<u>Readily biodegradable</u>	CO <sub>2</sub> Headspace test (OECD 310)	Activated sludge	20 mg/L	28 d	THCO <sub>2</sub>	<sup>19</sup>
<b>320</b>	“	“	$67.7 \pm 1.0$	<u>Readily biodegradable</u>	Closed Bottle Test (TG 301 D)	Waste-water organisms	3 mg/L	28 d	BOD	<sup>19</sup>
<b>321</b>	“		$62.1 \pm 0.3$	<u>Readily biodegradable</u>	CO <sub>2</sub> Headspace test (OECD 310)	Activated sludge	20 mg/L	28 d	THCO <sub>2</sub>	<sup>19</sup>

321			$65.9 \pm 0.2$	<u>Readily biodegradable</u>	Closed Bottle Test (TG 301 D)	Waste-water organisms	3 mg/L	28 d	BOD	<sup>19</sup>
322	“		$65.3 \pm 0.1$	<u>Readily biodegradable</u>	CO <sub>2</sub> Headspace test (OECD 310)	Activated sludge	20 mg/L	28 d	THCO <sub>2</sub>	<sup>19</sup>
322	“	“	$68.1 \pm 1.9$	<u>Readily biodegradable</u>	Closed Bottle Test (TG 301 D)	Waste-water organisms	3 mg/L	28 d	BOD	<sup>19</sup>

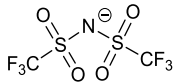
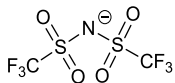
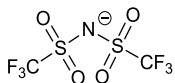
IL	Head Group	Side Chain R	Anion	Biodegrad- ation %	Classification	Test Method	Inoculum	IL Conc.	Test Duration	Measured Parameter	Ref
<b>Phosphonium</b>											
<b>181</b>		C <sub>3</sub> H <sub>7</sub>	$\ominus$ Br	4	Not readily biodegradable	CO <sub>2</sub> Headspace test (ISO 14593)	Activated sludge	20 mg/L	28 d	THCO <sub>2</sub>	<sup>20</sup>
<b>182</b>	“	C <sub>5</sub> H <sub>11</sub>	$\ominus$ Br	3	Not readily biodegradable	CO <sub>2</sub> Headspace test (ISO 14593)	Activated sludge	20 mg/L	28 d	THCO <sub>2</sub>	<sup>20</sup>

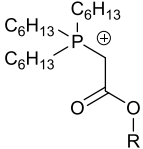
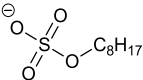
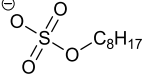
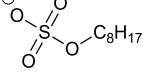
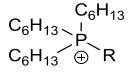



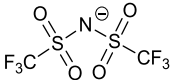
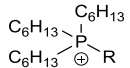
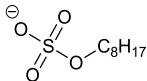
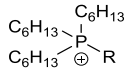
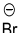
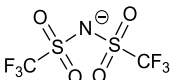
<b>183</b>	“	$C_7H_{15}$	$\ominus$ Br	2	Not readily biodegradable	CO <sub>2</sub> Headspace test (ISO 14593)	Activated sludge	20 mg/L	28 d	THCO <sub>2</sub>	20
<b>184</b>		$C_3H_7$		7	Not readily biodegradable	CO <sub>2</sub> Headspace test (ISO 14593)	Activated sludge	20 mg/L	28 d	THCO <sub>2</sub>	20
<b>185</b>	“	$C_5H_{11}$		2	Not readily biodegradable	CO <sub>2</sub> Headspace test (ISO 14593)	Activated sludge	20 mg/L	28 d	THCO <sub>2</sub>	20
<b>186</b>	“	$C_7H_{15}$		3	Not readily biodegradable	CO <sub>2</sub> Headspace test (ISO 14593)	Activated sludge	20 mg/L	28 d	THCO <sub>2</sub>	20

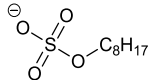
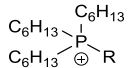
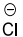
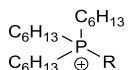
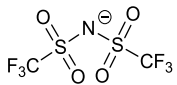
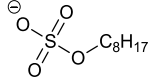
<b>187</b>	“	$C_3H_7$		18	Not readily biodegradable	CO <sub>2</sub> Headspace test (ISO 14593)	Activated sludge	20 mg/L	28 d	THCO <sub>2</sub>	20
<b>188</b>	“	$C_5H_{11}$		22	Not readily biodegradable	CO <sub>2</sub> Headspace test (ISO 14593)	Activated sludge	20 mg/L	28 d	THCO <sub>2</sub>	20
<b>189</b>		$C_7H_{15}$		21	Not readily biodegradable	CO <sub>2</sub> Headspace test (ISO 14593)	Activated sludge	20 mg/L	28 d	THCO <sub>2</sub>	20
<b>190</b>		$(CH_2)_4O-$ $C(O)CH_3$		9	Not readily biodegradable	CO <sub>2</sub> Headspace test (ISO 14593)	Activated sludge	20 mg/L	28 d	THCO <sub>2</sub>	20

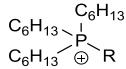
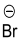
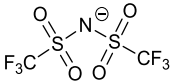
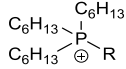
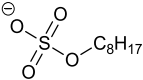
<b>191</b>	“	N/A		9	Not readily biodegradable	CO <sub>2</sub> Headspace test (ISO 14593)	Activated sludge	20 mg/L	28 d	THCO <sub>2</sub>	20
<b>192</b>	“	N/A		22	Not readily biodegradable	CO <sub>2</sub> Headspace test (ISO 14593)	Activated sludge	20 mg/L	28 d	THCO <sub>2</sub>	20
<b>193</b>		C <sub>3</sub> H <sub>7</sub>		12	Not readily biodegradable	CO <sub>2</sub> Headspace test (ISO 14593)	Activated sludge	15 mg/L	28 d	THCO <sub>2</sub>	20
<b>194</b>		C <sub>5</sub> H <sub>11</sub>		4	Not readily biodegradable	CO <sub>2</sub> Headspace test (ISO 14593)	Activated sludge	15 mg/L	28 d	THCO <sub>2</sub>	20

<b>195</b>	“	$C_7H_{15}$	$\ominus$ Br	10	Not readily biodegradable	CO <sub>2</sub> Headspace test (ISO 14593)	Activated sludge	15 mg/L	28 d	THCO <sub>2</sub>	20
<b>196</b>	“	$C_3H_7$		0	Not readily biodegradable	CO <sub>2</sub> Headspace test (ISO 14593)	Activated sludge	15 mg/L	28 d	THCO <sub>2</sub>	20
<b>197</b>	“	$C_5H_{11}$		2	Not readily biodegradable	CO <sub>2</sub> Headspace test (ISO 14593)	Activated sludge	15 mg/L	28 d	THCO <sub>2</sub>	20
<b>198</b>	“	$C_7H_{15}$		0	Not readily biodegradable	CO <sub>2</sub> Headspace test (ISO 14593)	Activated sludge	15 mg/L	28 d	THCO <sub>2</sub>	20

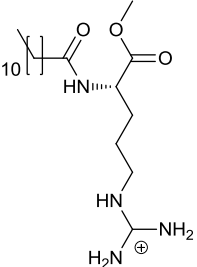
<b>199</b>		$\text{C}_3\text{H}_7$		15	Not readily biodegradable	CO <sub>2</sub> Headspace test (ISO 14593)	Activated sludge	15 mg/L	28 d	THCO <sub>2</sub>	20
<b>200</b>	“	$\text{C}_5\text{H}_{11}$		20	Not readily biodegradable	CO <sub>2</sub> Headspace test (ISO 14593)	Activated sludge	15 mg/L	28 d	THCO <sub>2</sub>	20
<b>201</b>	“	$\text{C}_7\text{H}_{15}$		30	Not readily biodegradable	CO <sub>2</sub> Headspace test (ISO 14593)	Activated sludge	15 mg/L	28 d	THCO <sub>2</sub>	20
<b>202</b>		$(\text{CH}_2)_4\text{O}-\text{C}(\text{O})\text{CH}_3$		0	Not readily biodegradable	CO <sub>2</sub> Headspace test (ISO 14593)	Activated sludge	15 mg/L	28 d	THCO <sub>2</sub>	20

203	“	“		0	Not readily biodegradable	CO <sub>2</sub> Headspace test (ISO 14593)	Activated sludge	15 mg/L	28 d	THCO <sub>2</sub>	20
204		(CH <sub>2</sub> ) <sub>4</sub> O-C(O)CH <sub>3</sub>		5	Not readily biodegradable	CO <sub>2</sub> Headspace test (ISO 14593)	Activated sludge	15 mg/L	28 d	THCO <sub>2</sub>	20
205		CH <sub>2</sub> CHCH <sub>2</sub>		8	Not readily biodegradable	CO <sub>2</sub> Headspace test (ISO 14593)	Activated sludge	15 mg/L	28 d	THCO <sub>2</sub>	20
206	“	“		0	Not readily biodegradable	CO <sub>2</sub> Headspace test (ISO 14593)	Activated sludge	15 mg/L	28 d	THCO <sub>2</sub>	20

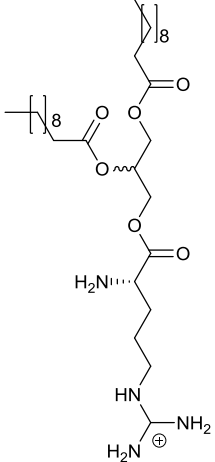
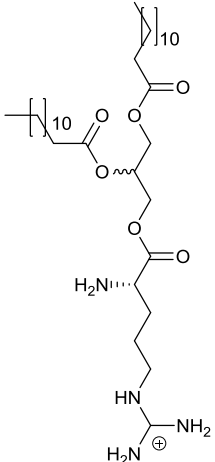
207	“	“		18	Not readily biodegradable	CO <sub>2</sub> Headspace test (ISO 14593)	Activated sludge	15 mg/L	28 d	THCO <sub>2</sub>	20
208		CH <sub>2</sub> OCH <sub>3</sub>		2	Not readily biodegradable	CO <sub>2</sub> Headspace test (ISO 14593)	Activated sludge	15 mg/L	28 d	THCO <sub>2</sub>	20
209		CH <sub>2</sub> OCH <sub>3</sub>		0	Not readily biodegradable	CO <sub>2</sub> Headspace test (ISO 14593)	Activated sludge	15 mg/L	28 d	THCO <sub>2</sub>	20
210	“	“		11	Not readily biodegradable	CO <sub>2</sub> Headspace test (ISO 14593)	Activated sludge	15 mg/L	28 d	THCO <sub>2</sub>	20

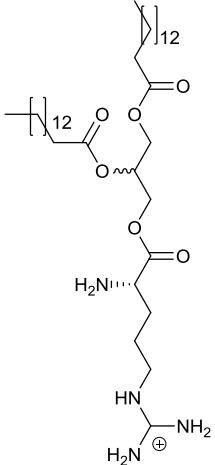
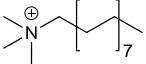
211		CH <sub>2</sub> CH <sub>2</sub> OH		0	Not readily biodegradable	CO <sub>2</sub> Headspace test (ISO 14593)	Activated sludge	15 mg/L	28 d	THCO <sub>2</sub>	20
212	“	“		0	Not readily biodegradable	CO <sub>2</sub> Headspace test (ISO 14593)	Activated sludge	15 mg/L	28 d	THCO <sub>2</sub>	20
213		CH <sub>2</sub> CH <sub>2</sub> OH		9	Not readily biodegradable	CO <sub>2</sub> Headspace test (ISO 14593)	Activated sludge	15 mg/L	28 d	THCO <sub>2</sub>	20

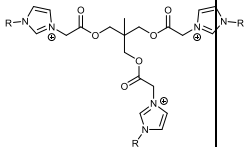


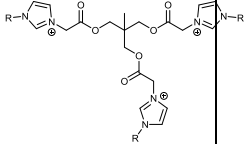
Surfactant	Head Group	Anion	Biodegradation %	Classification	Test Method	Inoculum	IL Conc.	Test Duration	Measured Parameter	Ref
Surfactants										
LAM		$\text{Cl}^-$	90	<u>Readily biodegradable</u>	Closed Bottle Test (TG 301 D)	Waste-water organisms		28 d	BOD	<sup>21</sup>

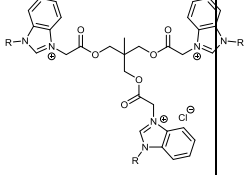
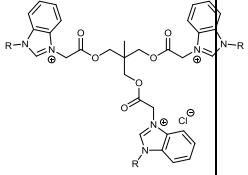
<b>C3(CA)2</b>		$\ominus$ 2 x Cl	87	<u>Ultimately Biodegradable</u>	Closed Bottle Test (TG 301 D)	Waste-water organisms		28 d	BOD	21
<b>1010R(4)</b>		$\ominus$ Cl	79	<u>Ultimately biodegradable</u>	Closed Bottle Test (TG 301 D)	Waste-water organisms			BOD	21

1010R(4)		$\ominus$ Cl	20	Not readily biodegradable	Closed Bottle Test (TG 301 D)	Waste-water organisms		28 d	BOD	22
1212R		$\ominus$ Cl	82	<u>Readily biodegradable</u>	Closed Bottle Test (TG 301 D)	Waste-water organisms		28 d	BOD	22

<b>1414R</b>		$\text{Cl}^{\ominus}$	61	<u>Readily biodegradable</u>	Closed Bottle Test (TG 301 D)	Waste-water organisms		28 d	BOD	22
<b>HTAB</b>		$\text{Br}^{\ominus}$	0.36	Not readily biodegradable	Closed Bottle Test (TG 301 D)	Waste-water organisms		28 d	BOD	22

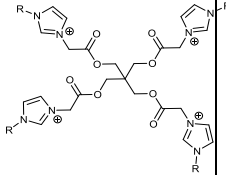
IL	Head Group	Side Chain R	Anion	Biodegradation %	Classification	Test Method	Inoculum	IL Conc.	Test Duration	Measured Parameter	Ref
<b>Tris-Imidazolium Surfactants</b>											
<b>286</b>		C <sub>4</sub> H <sub>9</sub>	$\ominus$ 3 x Cl	27	Not readily biodegradable	Closed Bottle Test (TG 301 D)	Waste-water organisms	100 mg/L	16 d	BOD	<sup>23</sup>
<b>287</b>	“	C <sub>6</sub> H <sub>13</sub>	$\ominus$ 3 x Cl	36	Not readily biodegradable	Closed Bottle Test (TG 301 D)	Waste-water organisms	100 mg/L	16 d	BOD	<sup>23</sup>

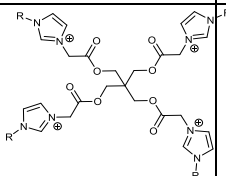
<b>288</b>	“	$C_8H_{17}$	$\ominus$ 3 x Cl	47	Not readily biodegradable	Closed Bottle Test (TG 301 D)	Waste- water organisms	100 mg/L	16 d	BOD	<sup>23</sup>
<b>289</b>		$C_{10}H_{21}$	$\ominus$ 3 x Cl	45	Not readily biodegradable	Closed Bottle Test (TG 301 D)	Waste- water organisms	100 mg/L	16 d	BOD	<sup>23</sup>
<b>290</b>	“	$C_{12}H_{25}$	$\ominus$ 3 x Cl	51	Not readily biodegradable	Closed Bottle Test (TG 301 D)	Waste- water organisms	100 mg/L	16 d	BOD	<sup>23</sup>
<b>291</b>	“	$CH_2C_6H_5$	$\ominus$ 3 x Cl	20	Not readily biodegradable	Closed Bottle Test (TG 301 D)	Waste- water organisms	100 mg/L	16 d	BOD	<sup>23</sup>

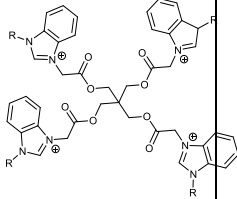
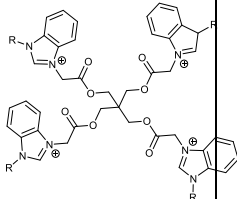
<b>292</b>		$C_4H_9$	$\ominus$ 3 x Cl	22	Not readily biodegradable	Closed Bottle Test (TG 301 D)	Waste-water organisms	100 mg/L	16 d	BOD	<sup>23</sup>
<b>293</b>	“	$C_6H_{13}$	$\ominus$ 3 x Cl	27	Not readily biodegradable	Closed Bottle Test (TG 301 D)	Waste-water organisms	100 mg/L	16 d	BOD	<sup>23</sup>
<b>294</b>		$C_8H_{17}$	$\ominus$ 3 x Cl	35.5	Not readily biodegradable	Closed Bottle Test (TG 301 D)	Waste-water organisms	100 mg/L	16 d	BOD	<sup>23</sup>
<b>295</b>	“	$C_{10}H_{21}$	$\ominus$ 3 x Cl	40	Not readily biodegradable	Closed Bottle Test (TG 301 D)	Waste-water organisms	100 mg/L	16 d	BOD	<sup>23</sup>

<b>296</b>	“	$\text{C}_{12}\text{H}_{25}$	$\text{Cl}^-$ 3 x Cl	45	Not readily biodegradable	Closed Bottle Test (TG 301 D)	Waste- water organisms	100 mg/L	16 d	BOD	23
<b>297</b>	“	$\text{CH}_2\text{C}_6\text{H}_5$	$\text{Cl}^-$ 3 x Cl	16	Not readily biodegradable	Closed Bottle Test (TG 301 D)	Waste- water organisms	100 mg/L	16 d	BOD	23



IL	Head Group	Side Chain R	Anion	Biodegrad- ation %	Classification	Test Method	Inoculum	IL Conc.	Test Duration	Measured Parameter	Ref
<b>Tetrakis-Imidazolium Surfactants</b>											
<b>298</b>		<b>C<sub>4</sub>H<sub>9</sub></b>	$\ominus$ 4 x Cl	35	Not readily biodegradable	Closed Bottle Test (TG 301 D)	Waste- water organisms	100 mg/L	16 d	BOD	<sup>24</sup>
<b>299</b>	“	<b>C<sub>6</sub>H<sub>13</sub></b>	$\ominus$ 4 x Cl	39	Not readily biodegradable	Closed Bottle Test (TG 301 D)	Waste- water organisms	100 mg/L	16 d	BOD	<sup>24</sup>

300	“	C <sub>8</sub> H <sub>17</sub>	$\ominus$ 4 x Cl	49	Not readily biodegradable	Closed Bottle Test (TG 301 D)	Waste- water organisms	100 mg/L	16 d	BOD	<sup>24</sup>
301		C <sub>10</sub> H <sub>21</sub>	$\ominus$ 4 x Cl	51.5	Not readily biodegradable	Closed Bottle Test (TG 301 D)	Waste- water organisms	100 mg/L	16 d	BOD	<sup>24</sup>
302	“	C <sub>12</sub> H <sub>25</sub>	$\ominus$ 4 x Cl	56	Not readily biodegradable	Closed Bottle Test (TG 301 D)	Waste- water organisms	100 mg/L	16 d	BOD	<sup>24</sup>
303	“	CH <sub>2</sub> C <sub>6</sub> H <sub>5</sub>	$\ominus$ 4 x Cl	22	Not readily biodegradable	Closed Bottle Test (TG 301 D)	Waste- water organisms	100 mg/L	16 d	BOD	<sup>24</sup>

304		C <sub>4</sub> H <sub>9</sub>	$\ominus$ 4 x Cl	28	Not readily biodegradable	Closed Bottle Test (TG 301 D)	Waste-water organisms	100 mg/L	16 d	BOD	24
305	“	C <sub>6</sub> H <sub>13</sub>	$\ominus$ 4 x Cl	33.5	Not readily biodegradable	Closed Bottle Test (TG 301 D)	Waste-water organisms	100 mg/L	16 d	BOD	24
306		C <sub>8</sub> H <sub>17</sub>	$\ominus$ 4 x Cl	42	Not readily biodegradable	Closed Bottle Test (TG 301 D)	Waste-water organisms	100 mg/L	16 d	BOD	24
307	“	C <sub>10</sub> H <sub>21</sub>	$\ominus$ 4 x Cl	44	Not readily biodegradable	Closed Bottle Test (TG 301 D)	Waste-water organisms	100 mg/L	16 d	BOD	24

308	“	C <sub>12</sub> H <sub>25</sub>	$\ominus$ 4 x Cl	47	Not readily biodegradable	Closed Bottle Test (TG 301 D)	Waste- water organisms	100 mg/L	16 d	BOD	<sup>24</sup>
309	“	CH <sub>2</sub> C <sub>6</sub> H <sub>5</sub>	$\ominus$ 4 x Cl	21.5	Not readily biodegradable	Closed Bottle Test (TG 301 D)	Waste- water organisms	100 mg/L	16 d	BOD	<sup>24</sup>

## References for Appendix

1. A. Romero, A. Santos, J. Tojo and A. Rodríguez, *J. Hazard. Mater.*, 2008, 151, 268-273.
2. S. Stolte, T. Schulz, C.-W. Cho, J. Arning and T. Strassner, *ACS Sustainable Chem. Eng.*, 2013, 1, 410-418.
3. G. Quijano, A. Couvert, A. Amrane, G. Darracq, C. Couriol, P. Le Cloirec, L. Paquin and D. Carrié, *Chem. Eng. J.*, 2011, 174, 27-32.
4. R. G. Gore, L. Myles, M. Spulak, I. Beadham, T. M. Garcia, S. J. Connon and N. Gathergood, *Green Chem.*, 2013, 15, 2747-2760.
5. E. Liwarska-Bizukojc, C. Maton, C. V. Stevens and D. Gendaszewska, *J. Chem. Technol. Biotechnol.*, 2014, 89, 763-768.
6. D. Coleman, M. Spulak, M. T. Garcia and N. Gathergood, *Green Chem.*, 2012, 14, 1350-1356.
7. S. Steudte, S. Bemowsky, M. Mahrova, U. Bottin-Weber, E. Tojo-Suarez, P. Stepnowski and S. Stolte, *RSC Adv.*, 2014, 4, 5198-5205.
8. L. Ford, J. R. Harjani, F. Atefi, M. T. Garcia, R. D. Singer and P. J. Scammells, *Green Chem.*, 2010, 12, 1783-1789.

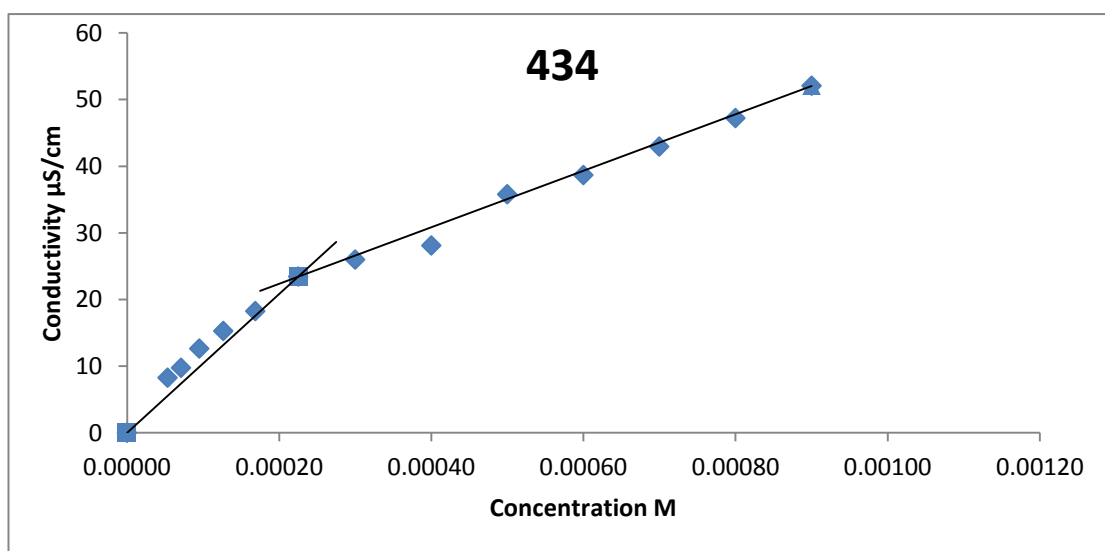
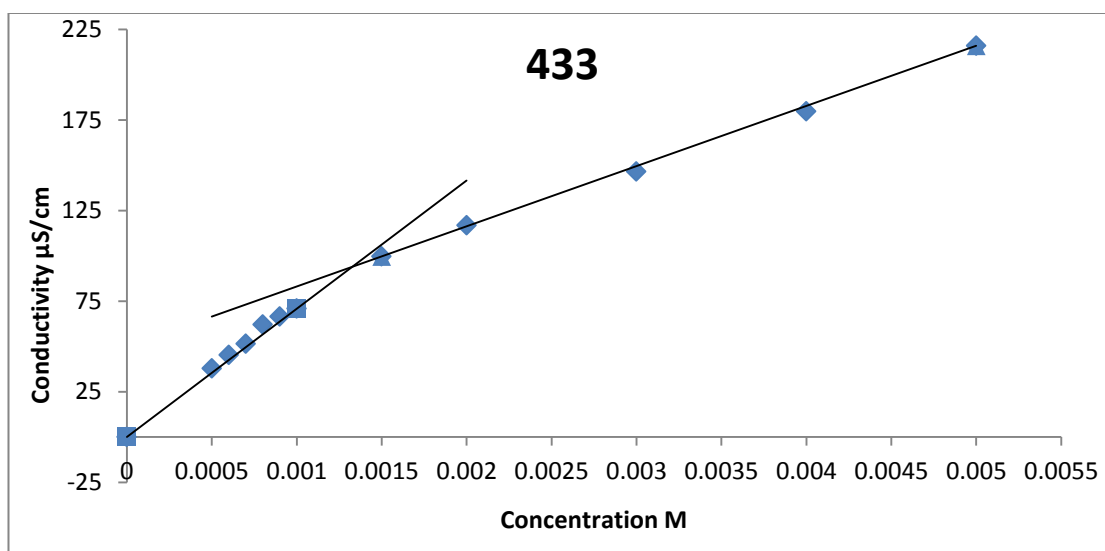
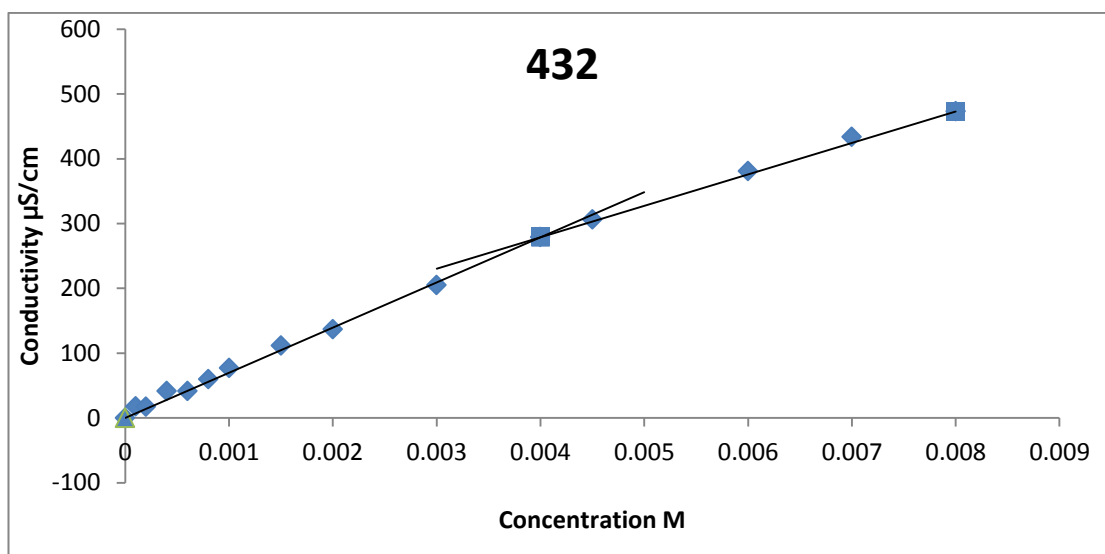
9. J. Neumann, S. Steudte, C.-W. Cho, J. Thoming and S. Stolte, *Green Chem.*, 2014, 16, 2174-2184.
10. S. Stolte, S. Abdulkarim, J. Arning, A. K. Blomeyer-Nienstedt, U. Bottin-Weber, M. Matzke, J. Ranke, B. Jastorff and J. Thoming, *Green Chem.*, 2008, 10, 214-224.
11. J. R. Harjani, R. D. Singer, M. T. Garcias and P. J. Scammells, *Green Chem.*, 2009, 11, 83-90.
12. C. Pretti, M. Renzi, S. E. Focardi, A. Giovani, G. Monni, B. Melai, S. Rajamani and C. Chiappe, *Ecotoxicol. Environ. Saf.*, 2011, 74, 748-753.
13. J. Pernak, N. Borucka, F. Walkiewicz, B. Markiewicz, P. Fochtman, S. Stolte, S. Steudte and P. Stepnowski, *Green Chem.*, 2011, 13, 2901-2910.
14. S. Stolte, S. Steudte, O. Areitioaurtena, F. Pagano, J. Thöming, P. Stepnowski and A. Igartua, *Chemosphere*, 2012, 89, 1135-1141.
15. N. Ferlin, M. Courty, S. Gatard, M. Spulak, B. Quilty, I. Beadham, M. Ghavre, A. Haiß, K. Kümmerer, N. Gathergood and S. Bouquillon, *Tetrahedron*, 2013, 69, 6150-6161.
16. N. Ferlin, M. Courty, A. N. Van Nhien, S. Gatard, M. Pour, B. Quilty, M. Ghavre, A. Haiß, K. Kummerer, N. Gathergood and S. Bouquillon, *RSC Adv.*, 2013, 3, 26241-26251.
17. F. Boissou, A. Muhlbauer, K. De Oliveira Vigier, L. Leclercq, W. Kunz, S. Marinkovic, B. Estrine, V. Nardello-Rataj and F. Jerome, *Green Chem.*, 2014, 16, 2463-2471.
18. B. Peric, J. Sierra, E. Martí, R. Cruañas, M. A. Garau, J. Arning, U. Bottin-Weber and S. Stolte, *J. Hazard. Mater.*, 2013, 261, 99-105.
19. X. D. Hou, Q. P. Liu, T. J. Smith, N. Li and M. H. Zong, *PLoS One*, 2013, 8.
20. F. Atefi, M. T. Garcia, R. D. Singer and P. J. Scammells, *Green Chemistry*, 2009, 11, 1595-1604.
21. M. R. Infante, L. Perez, M. C. Moran, R. Pons, M. Mitjans, M. P. Vinardell, M. T. Garcia and A. Pinazo, *Eur. J. Lipid Sci. Technol.*, 2010, 112, 110-121.
22. A. Pinazo, N. Lozano, L. Perez, M. C. Moran, M. R. Infante and R. Pons, *C. R. Chim.*, 2011, 14, 726-735.
23. N. N. Al-Mohammed, R. S. Duali Hussen, Y. Alias and Z. Abdullah, *RSC Adv.*, 2015, 5, 2869-2881.

24. N. N. Al-Mohammed, R. S. Duali Hussen, T. H. Ali, Y. Alias and Z. Abdullah, *RSC Adv.*, 2015, 5, 21865-21876.

## ***Appendix II***

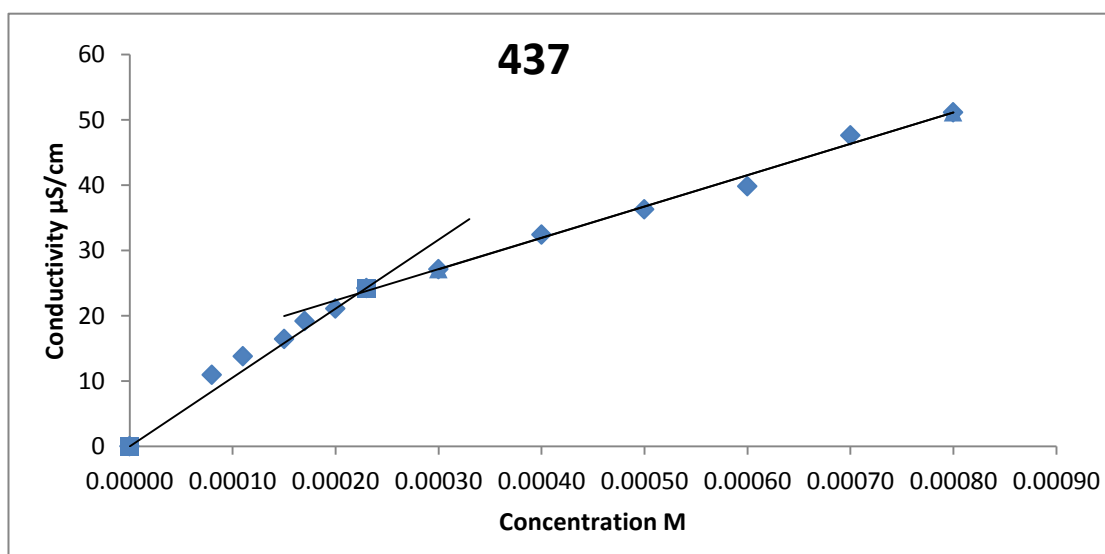
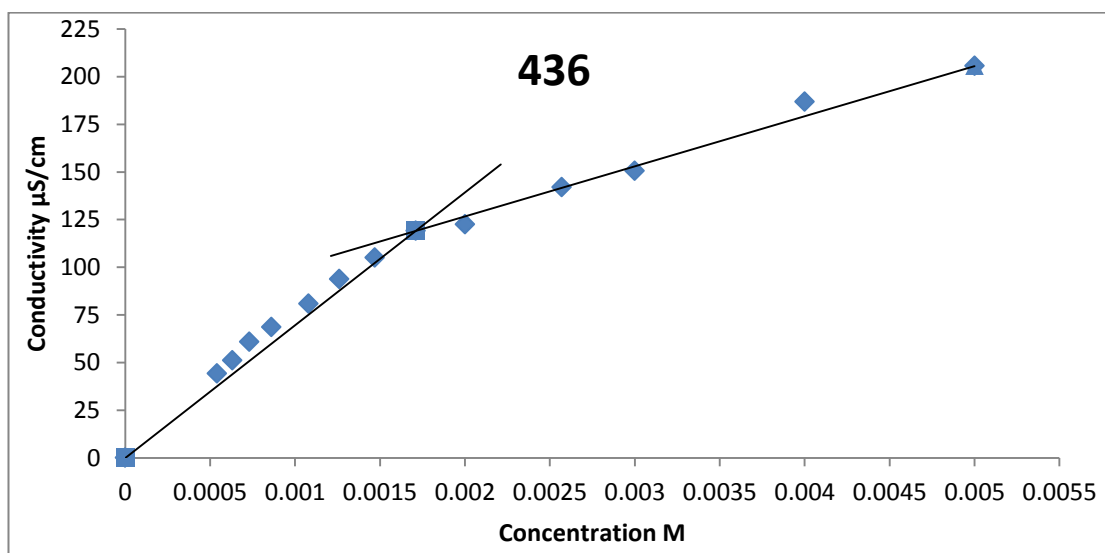
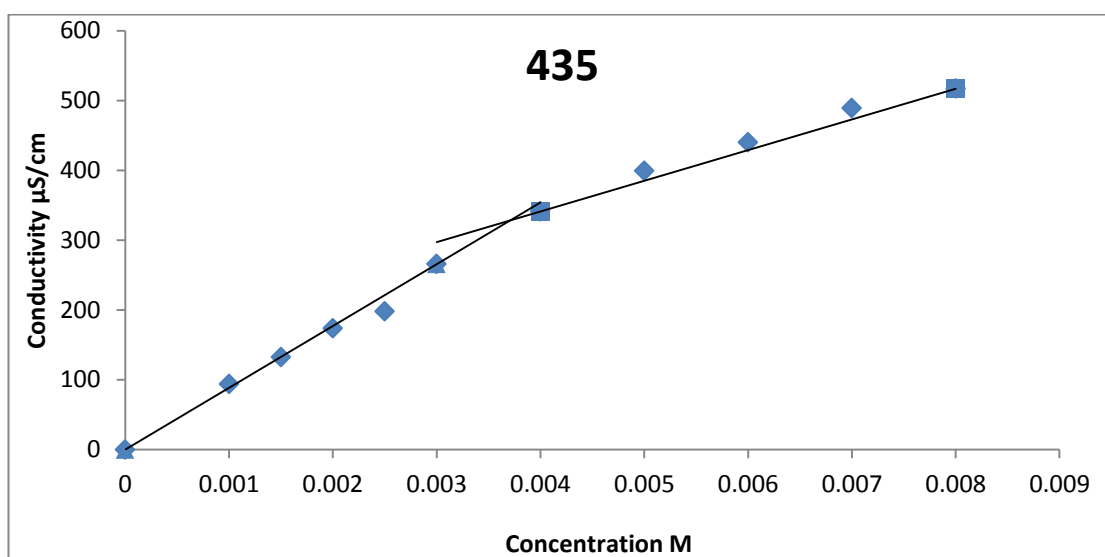
*Critical micelle concentration, tensiometry and  
HPLC curves for ILs examined in Chapter 4*

### Conductivity curves for linear alkyl pyridinium surfactants (432-434)

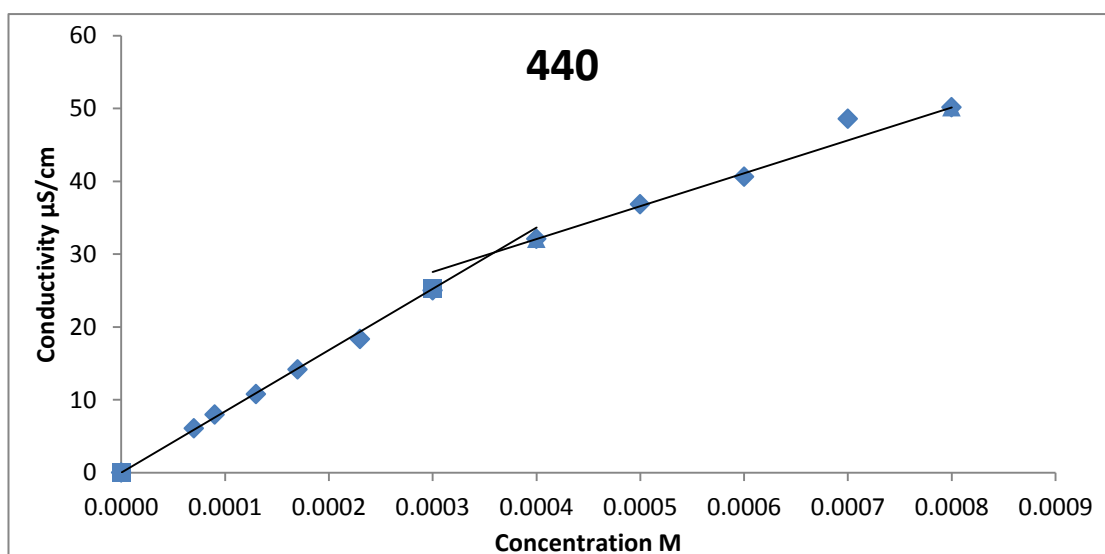
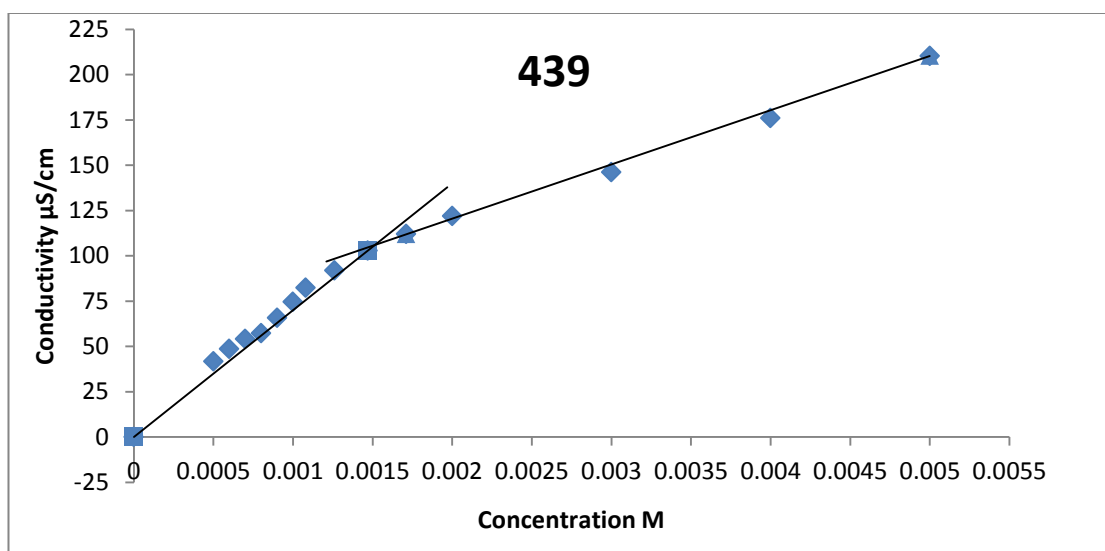
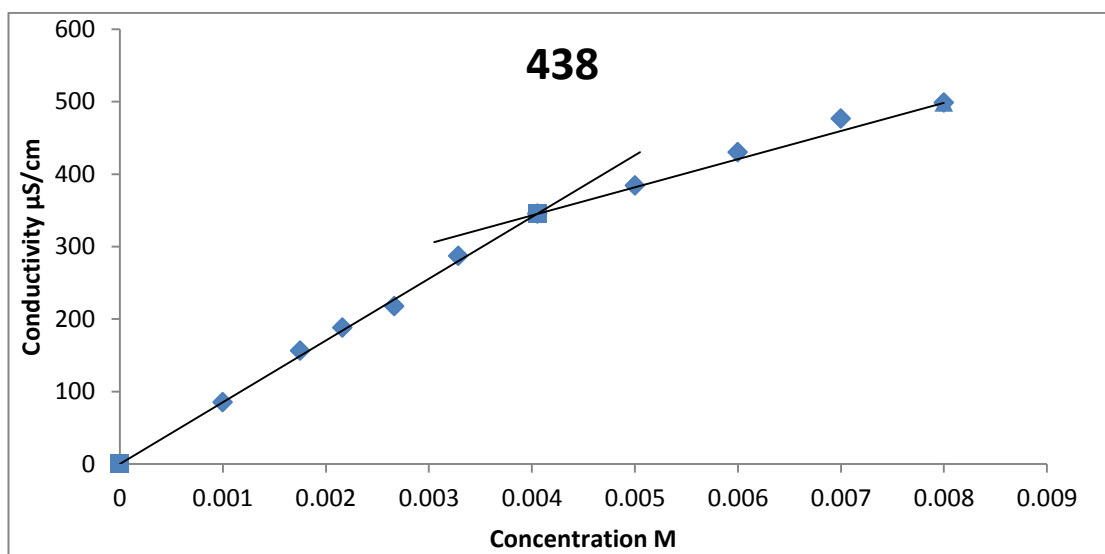




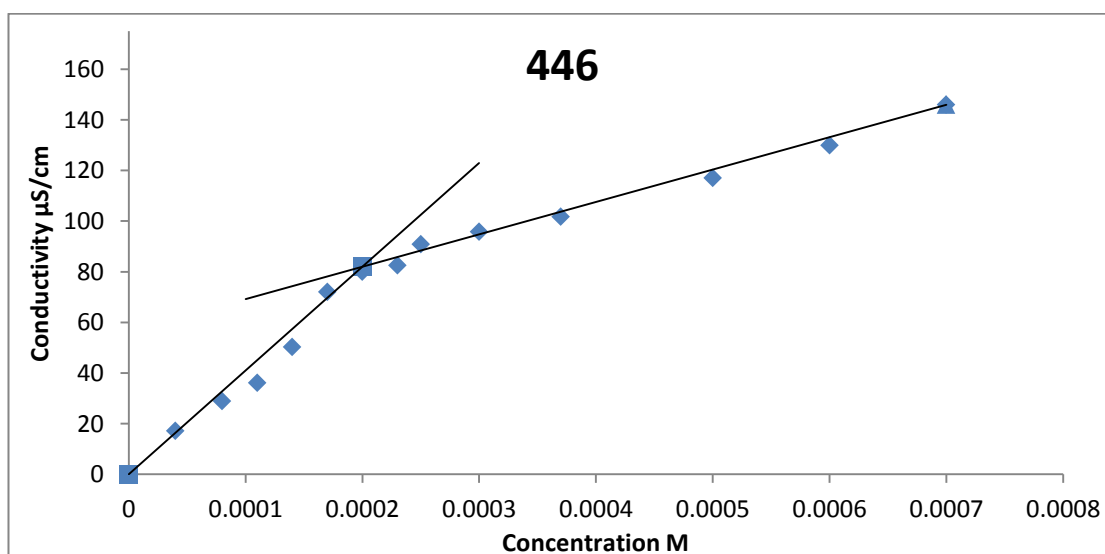
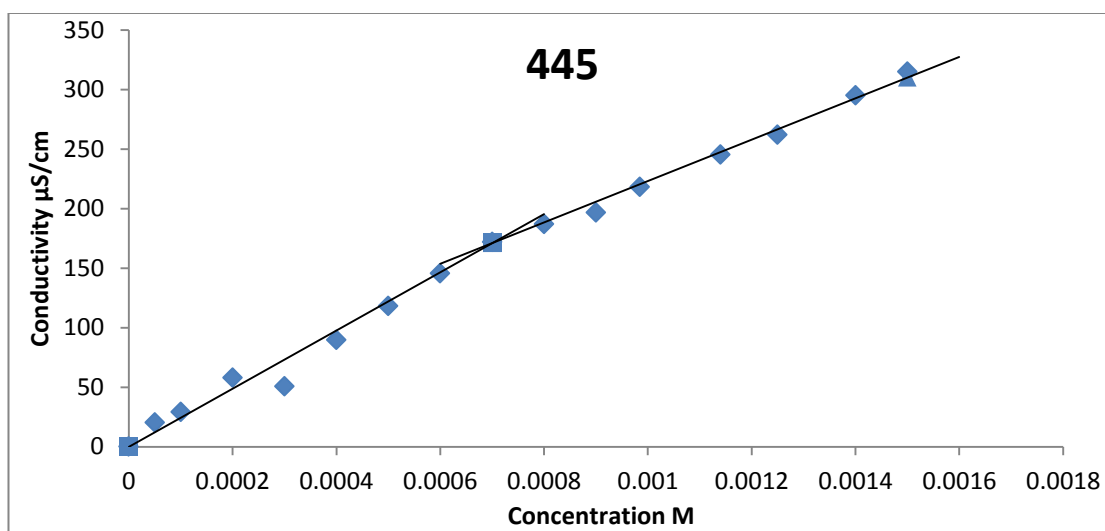
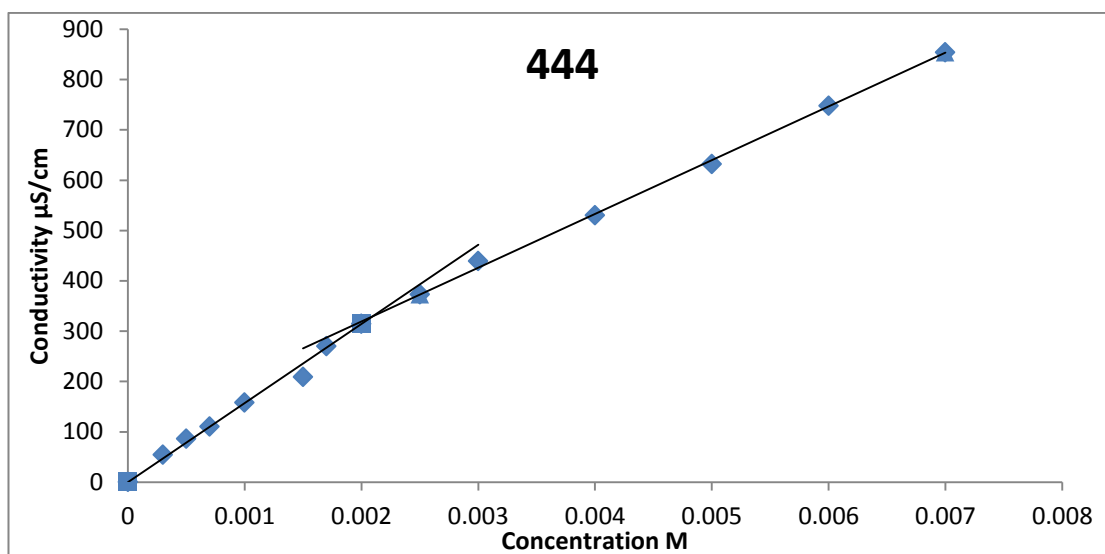
## Conductivity curves for linear alkyl imidazolium surfactants (435-437)



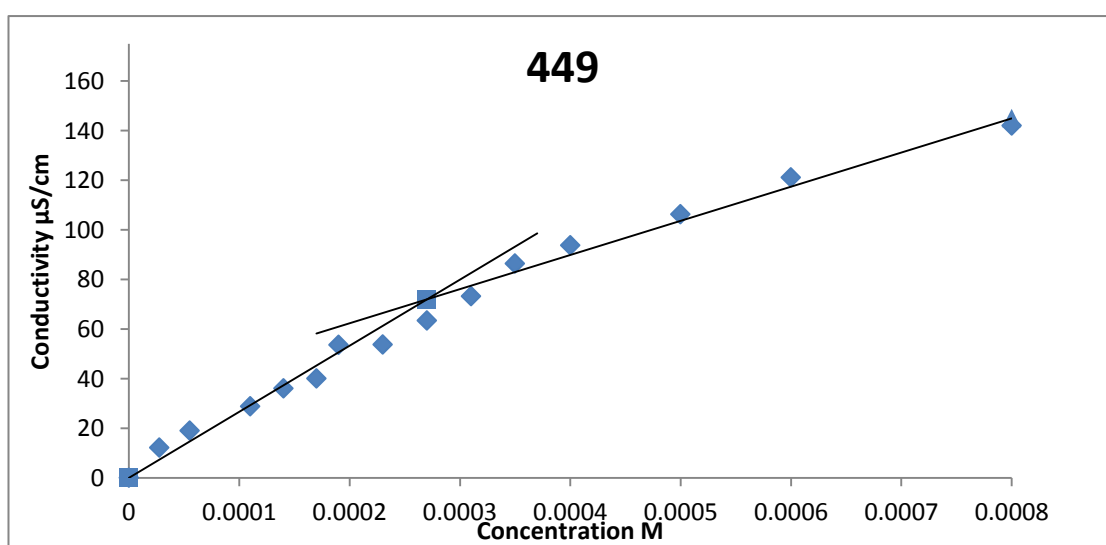
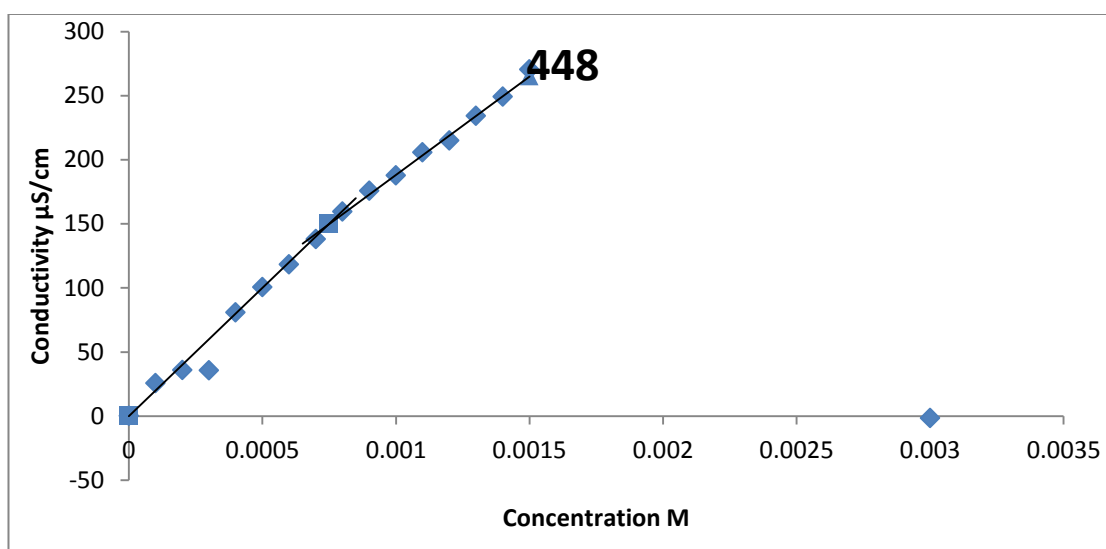
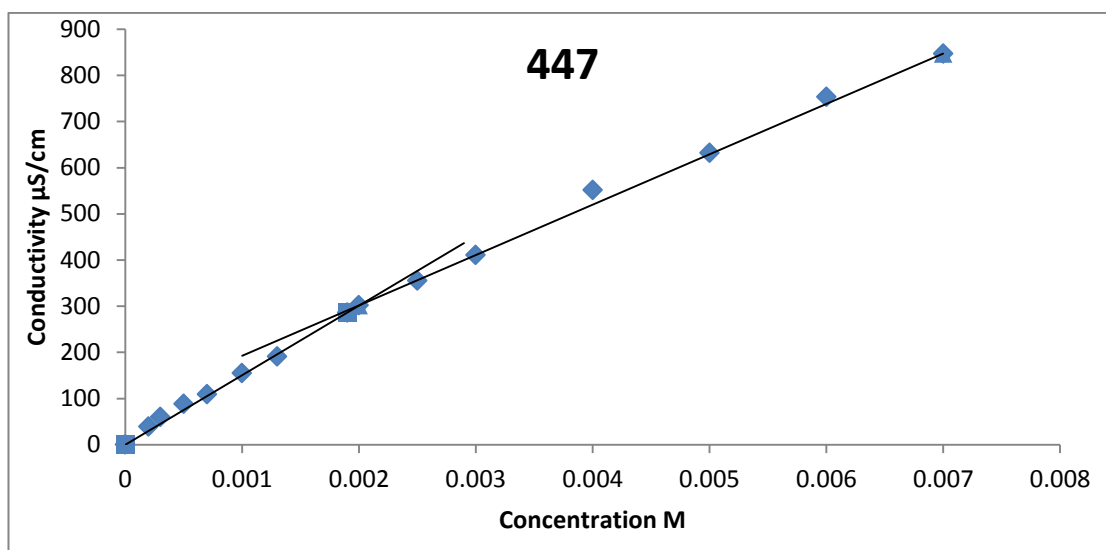
### Conductivity curves for linear alkyl cholinium surfactants (438-440)



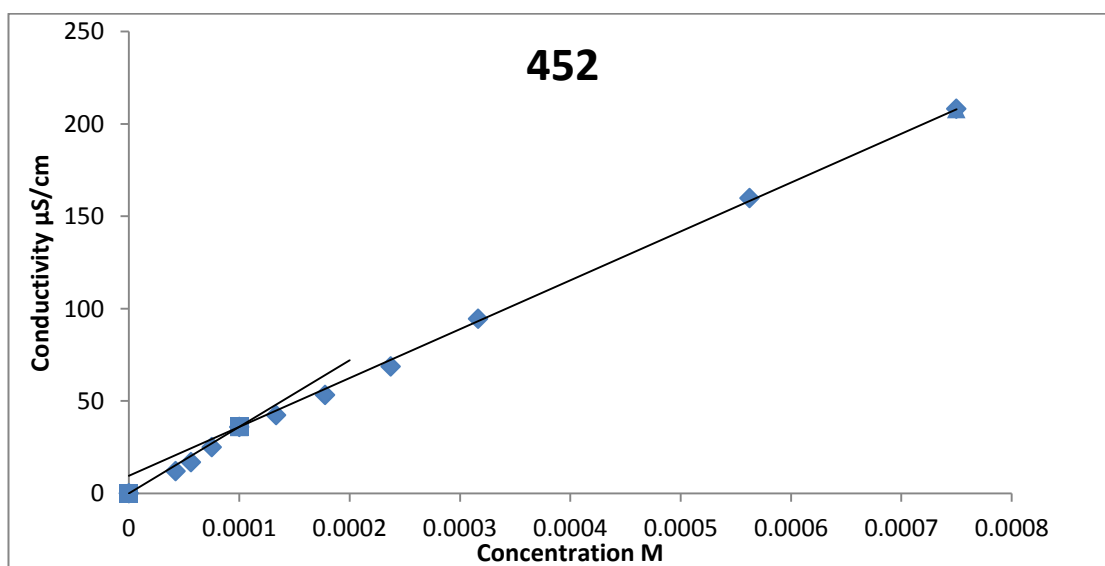
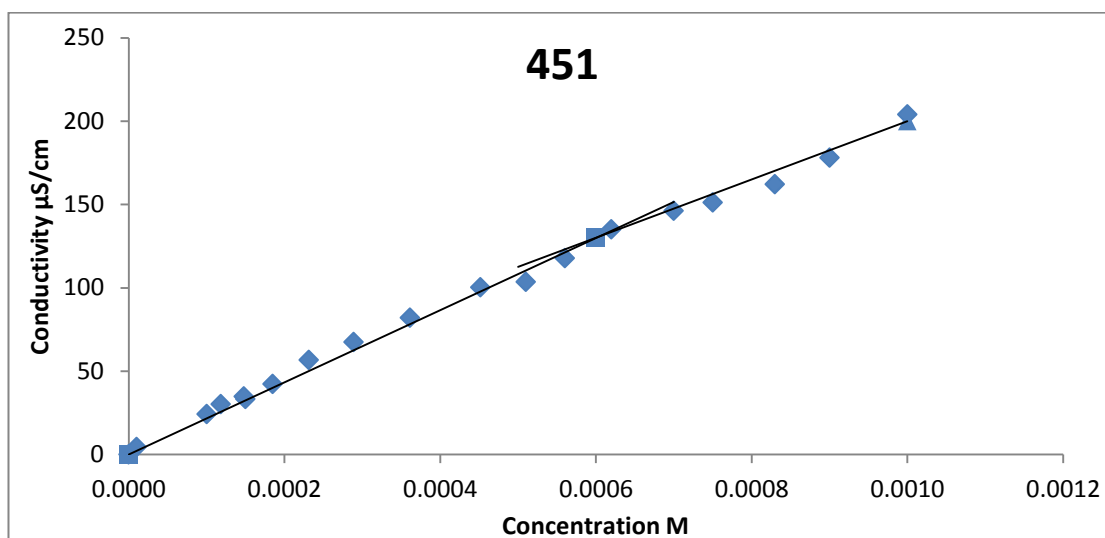
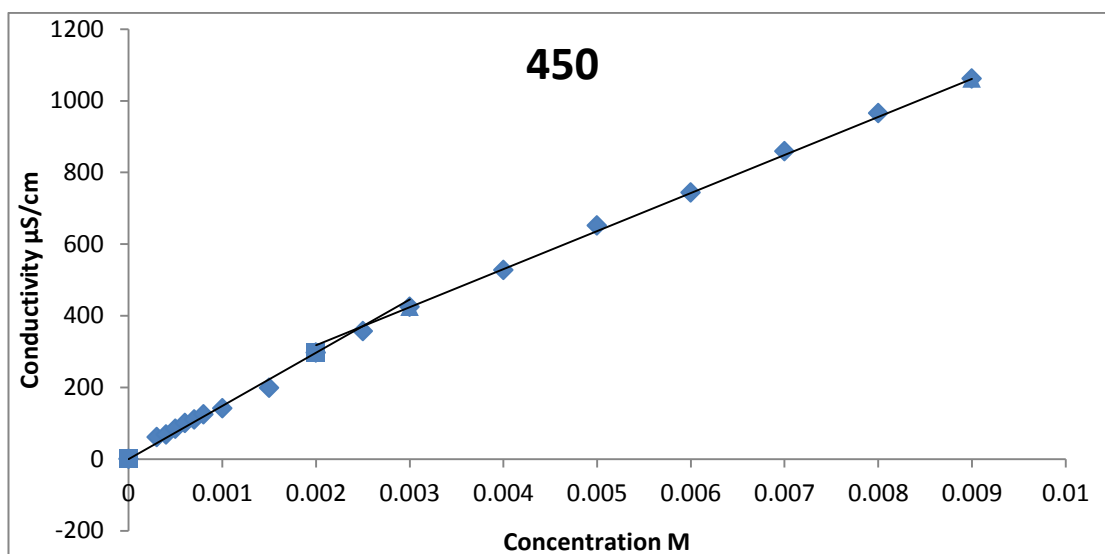
### Conductivity curves for bolaform pyridinium surfactants (444-446)



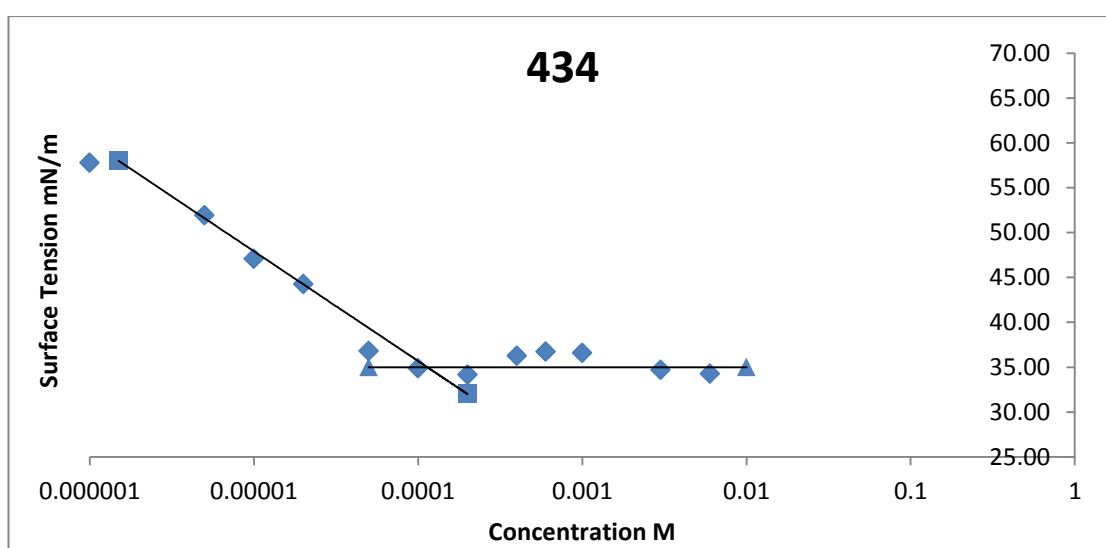
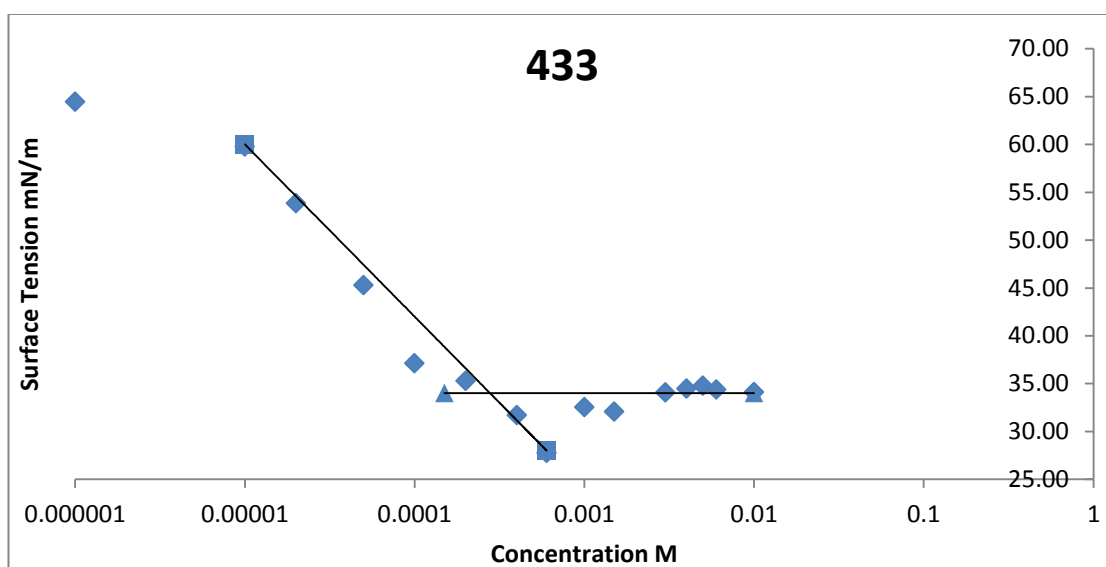
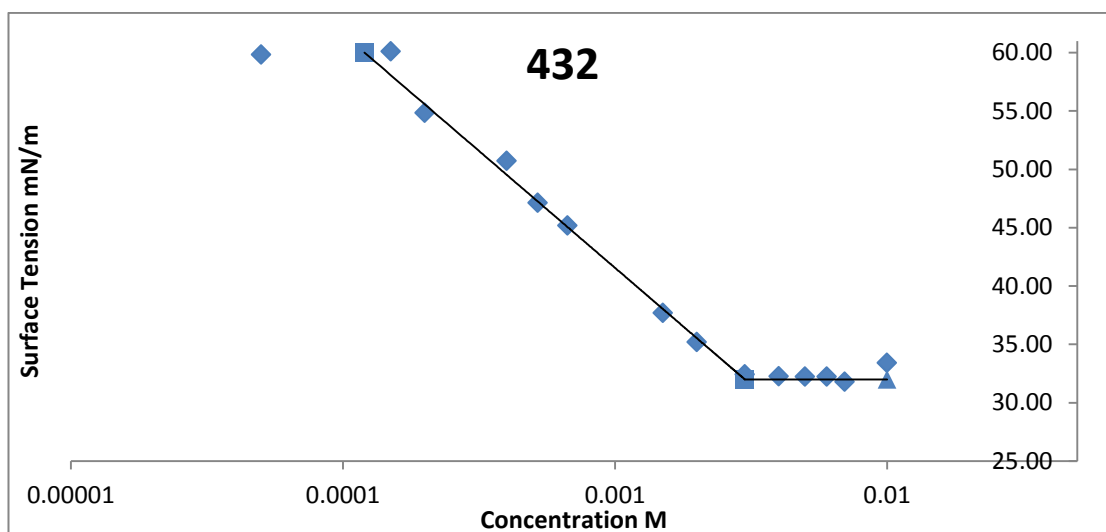
### Conductivity curves for bolaform imidazolium surfactants (447-449)



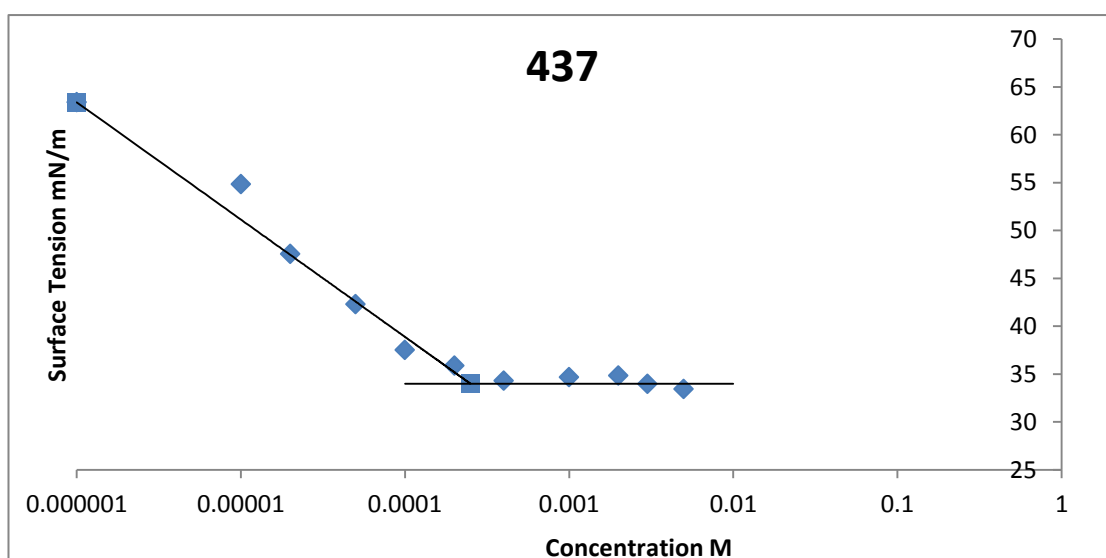
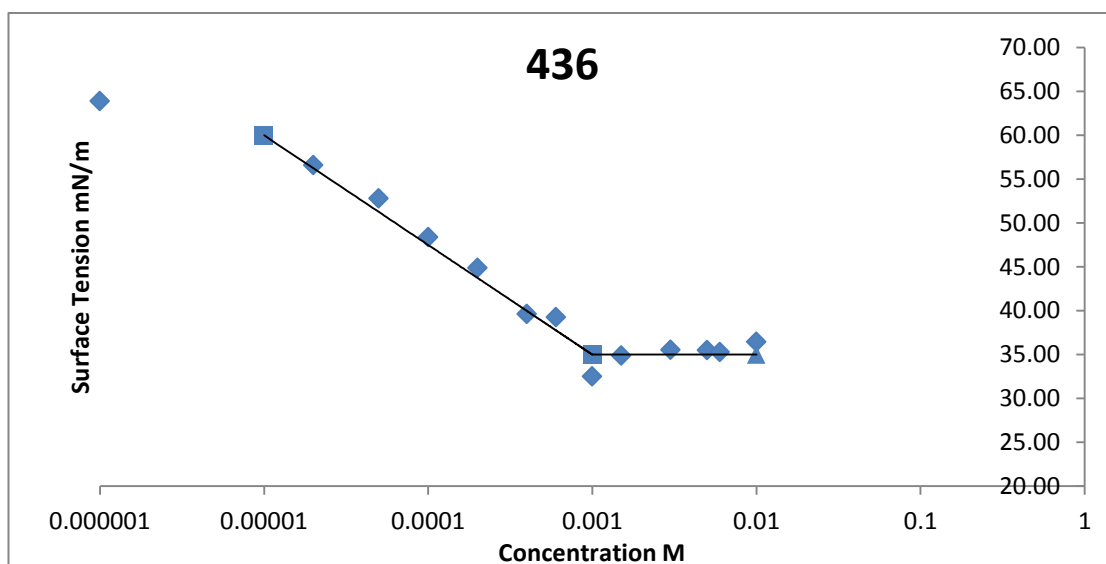
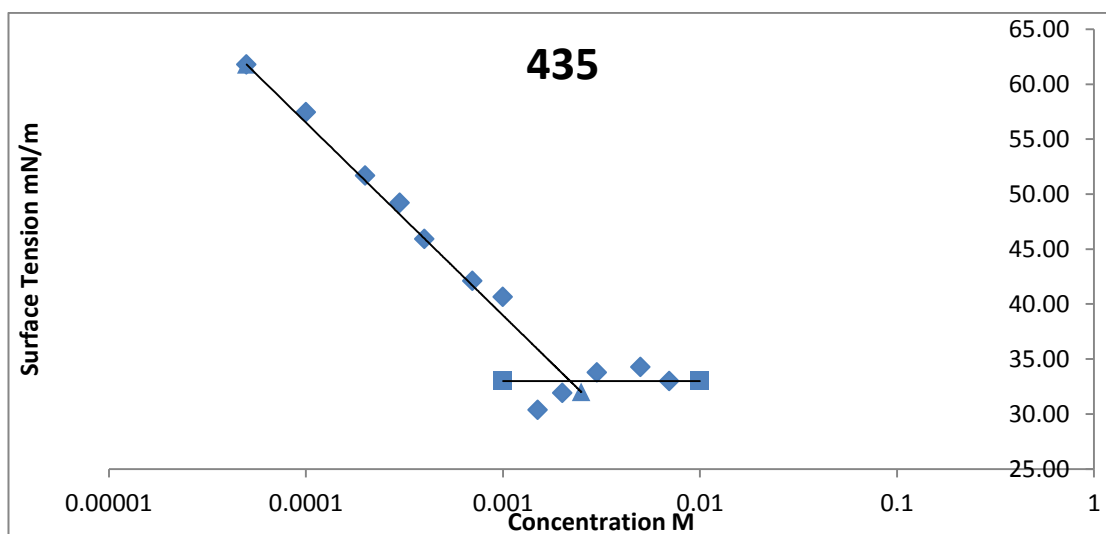
### Conductivity curves for bolaform cholinium surfactants (450-452)



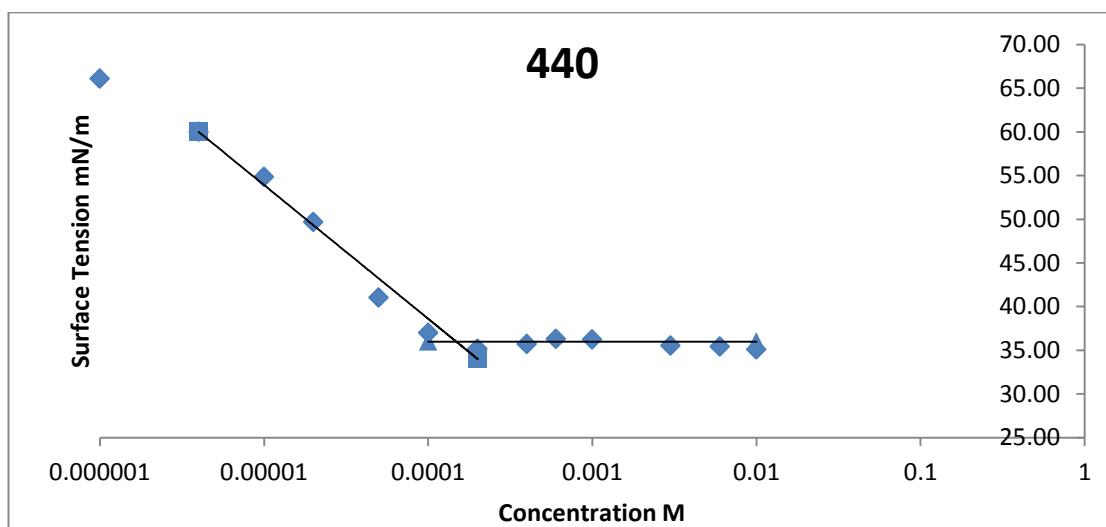
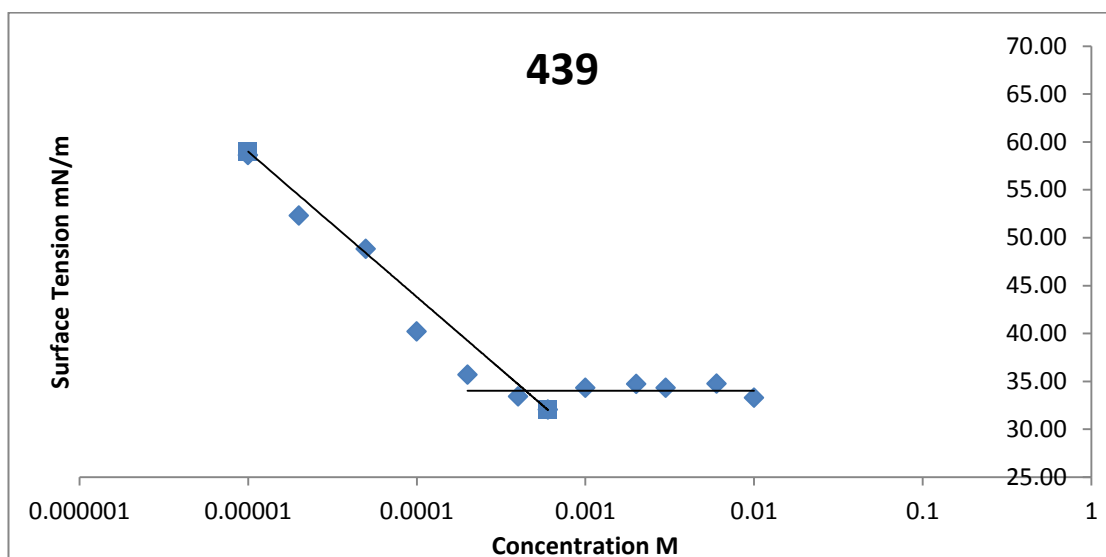
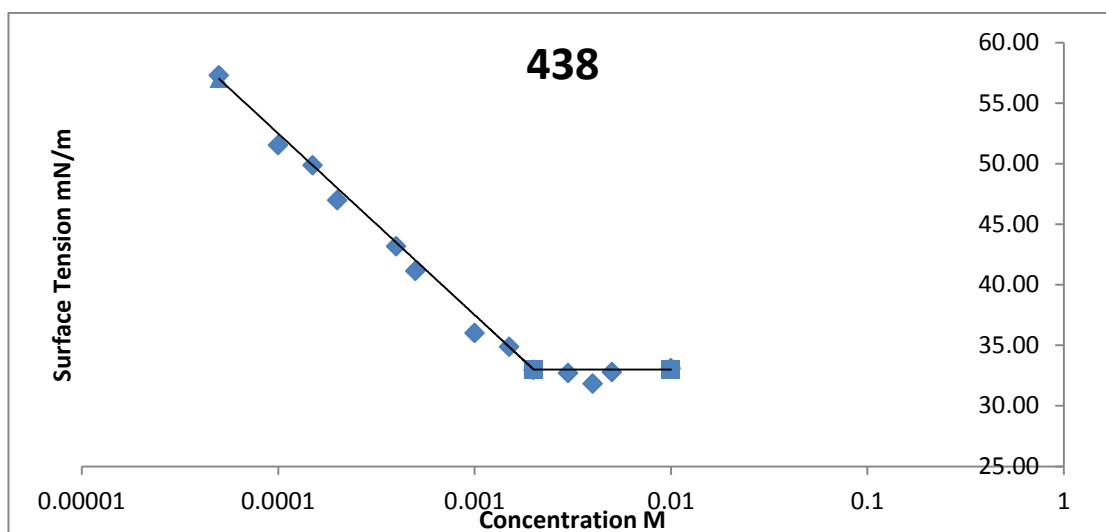
### Tensiometry curves for linear alkyl pyridinium surfactants (432-434)



### Tensiometry curves for linear alkyl imidazolium surfactants (435-437)

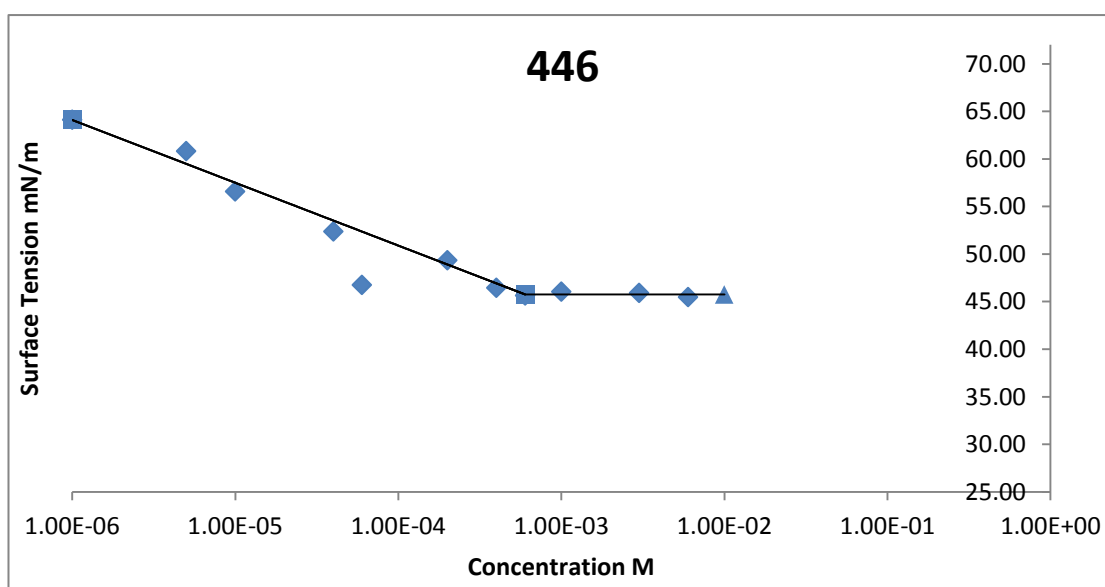
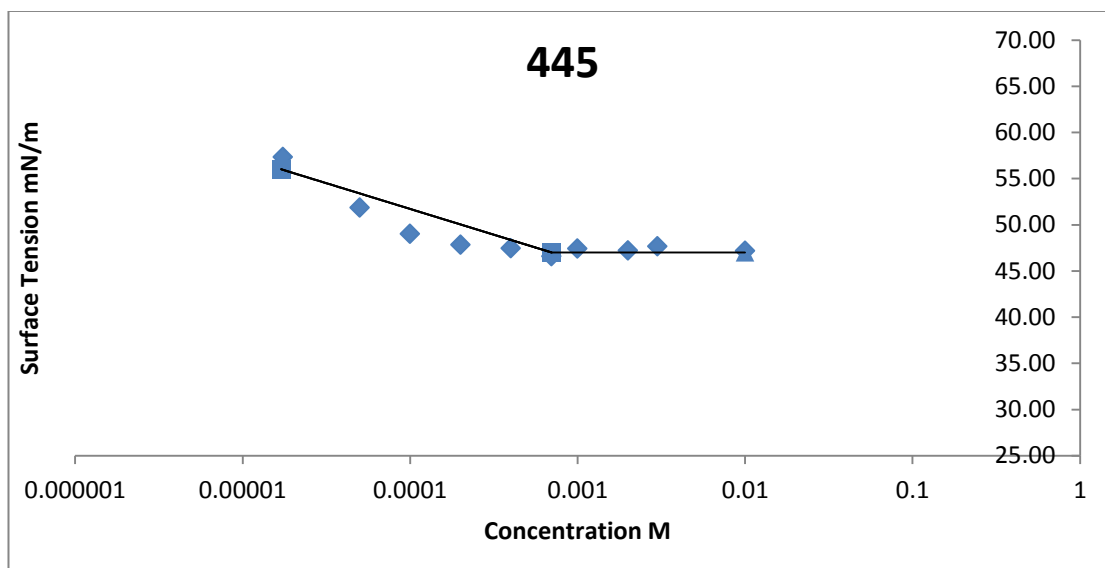
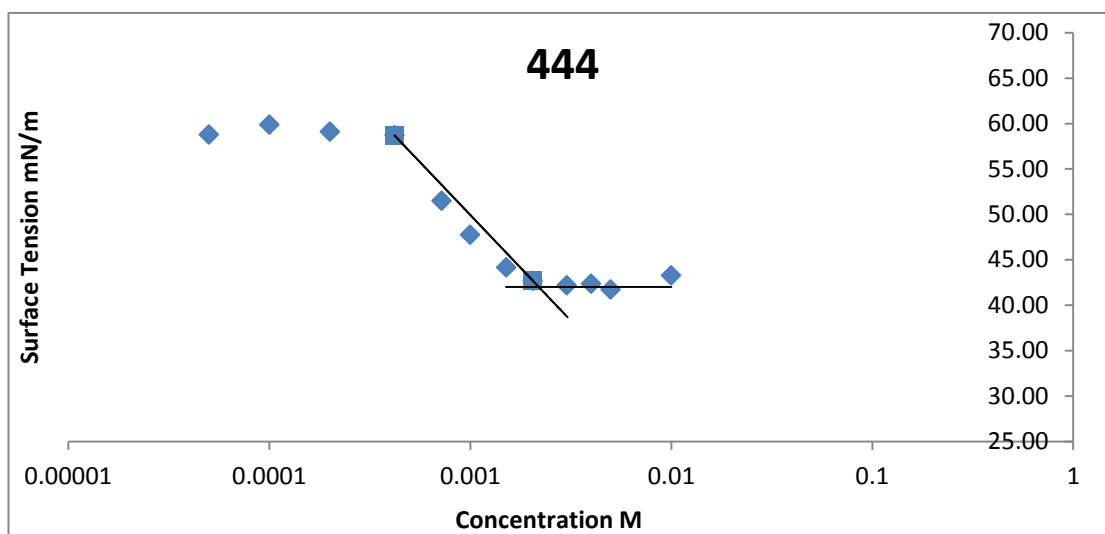


### Tensiometry curves for linear alkyl cholinium surfactants (438-440)

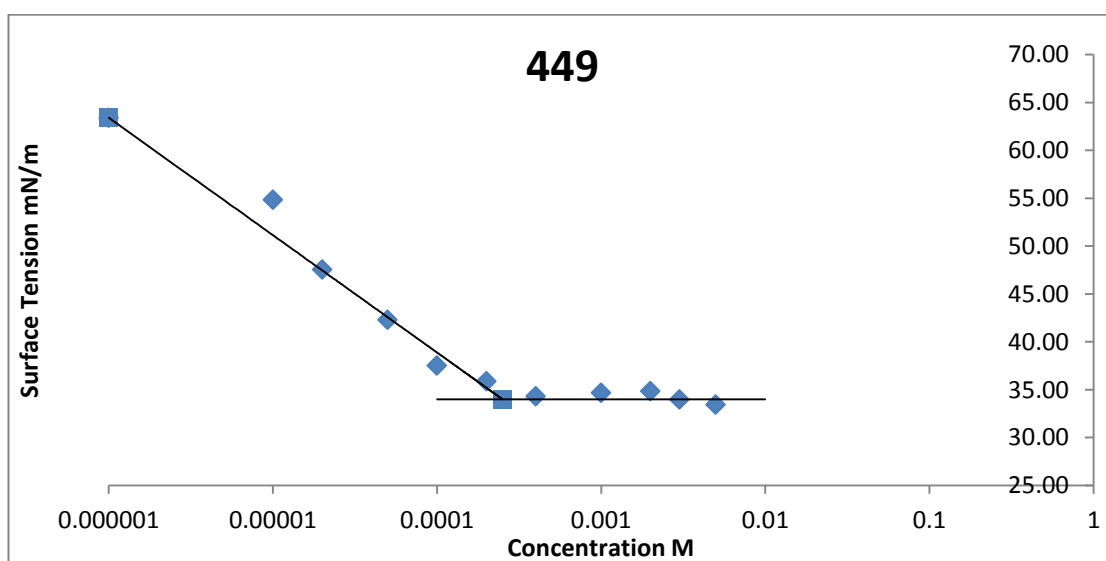
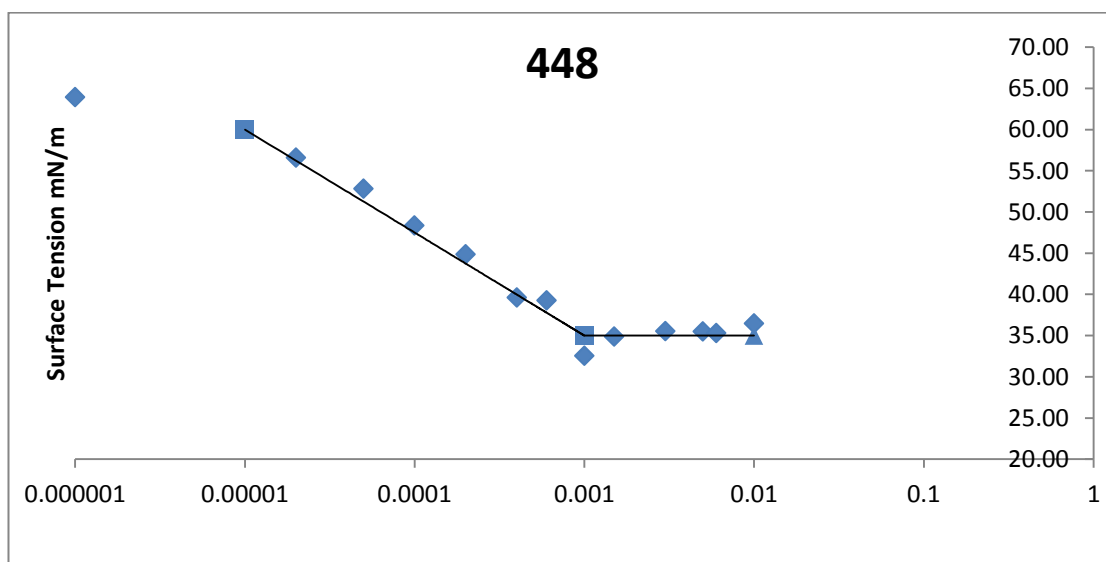
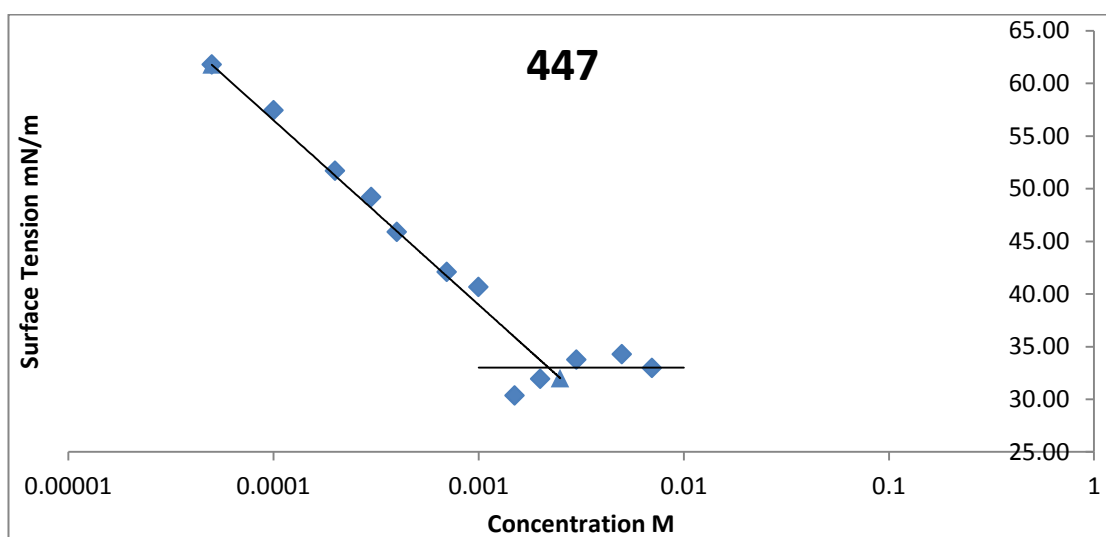




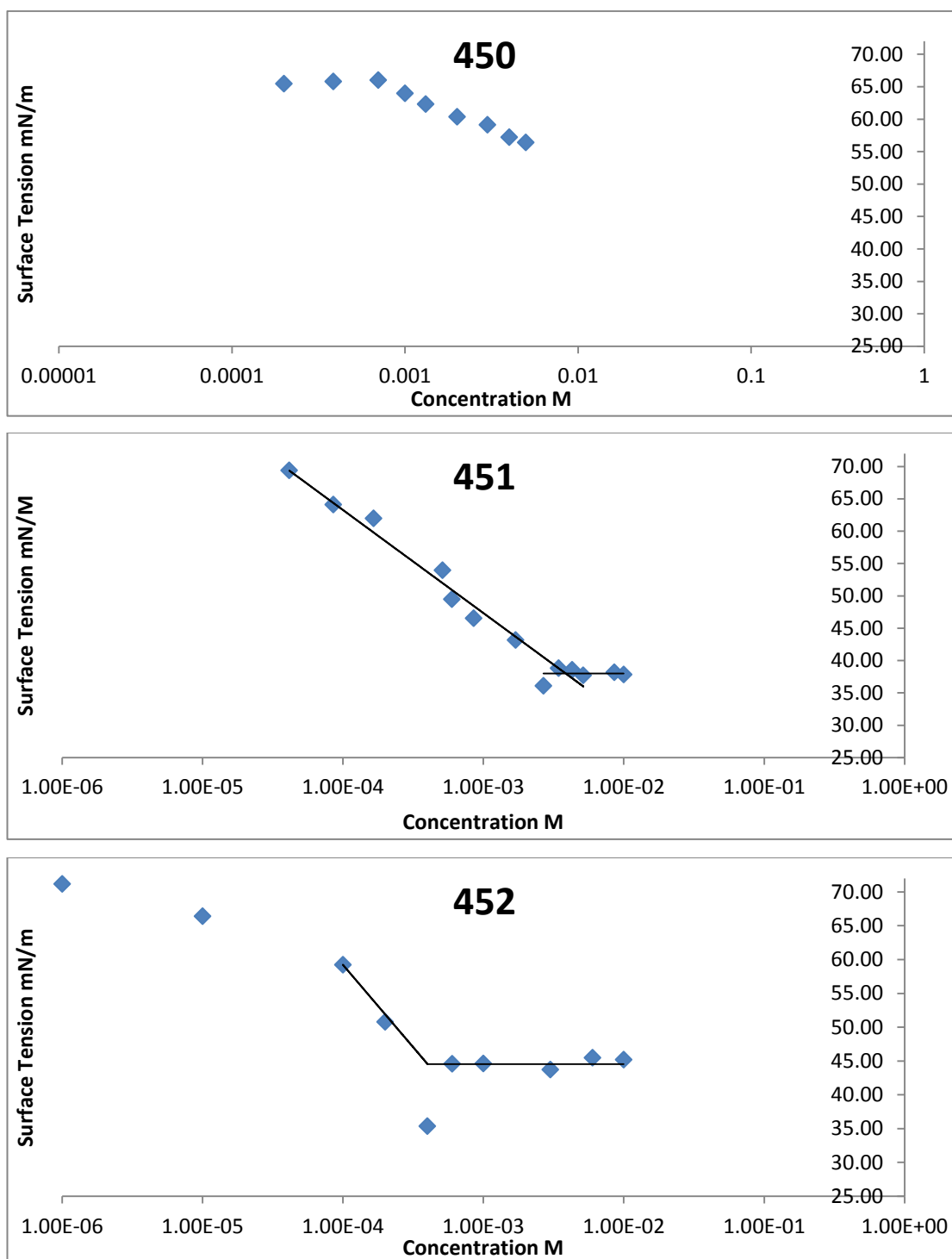
### Tensiometry curves for bolaform pyridinium surfactants (444-446)



## Tensiometry curves for bolaform imidazolium surfactants (447-449)

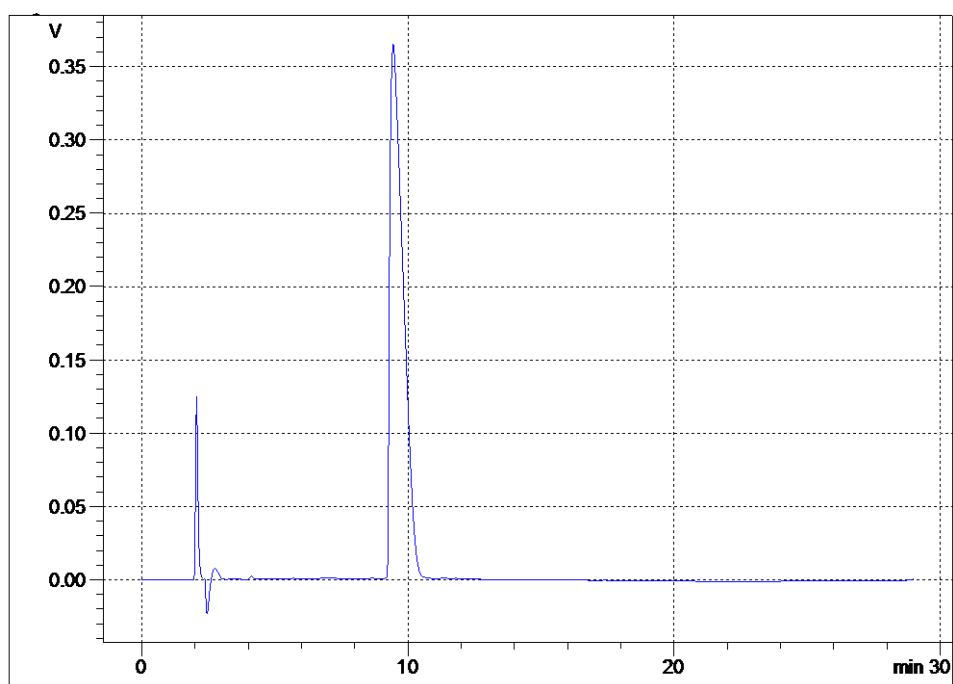


### Tensiometry curves for bolaform cholinium surfactants (450-452)

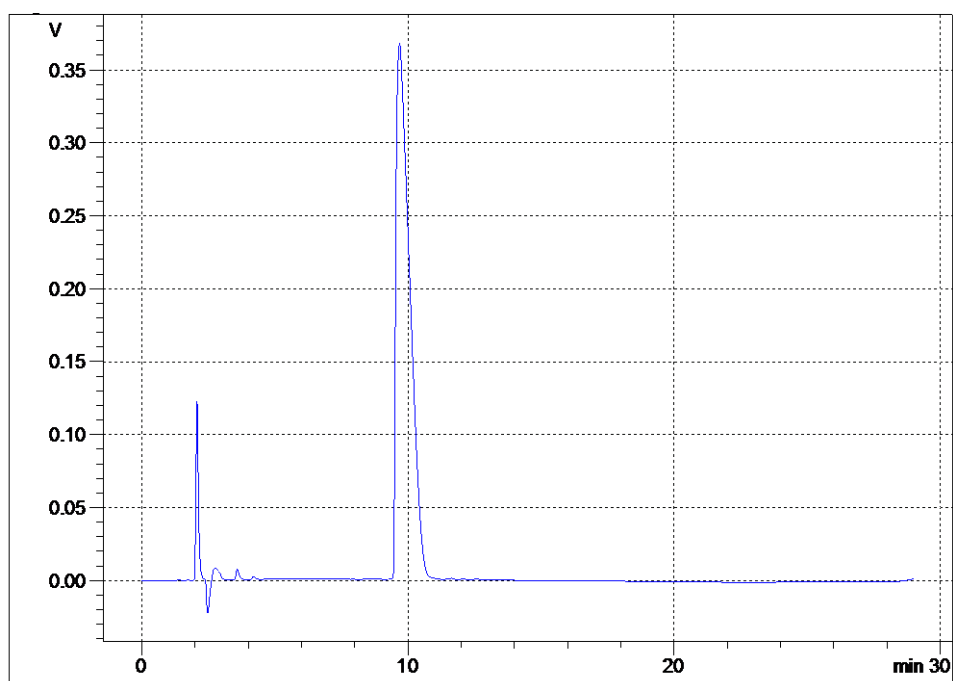


**HPLC/UV Traces for aqueous stability study for ILs (433, 436, 439).**

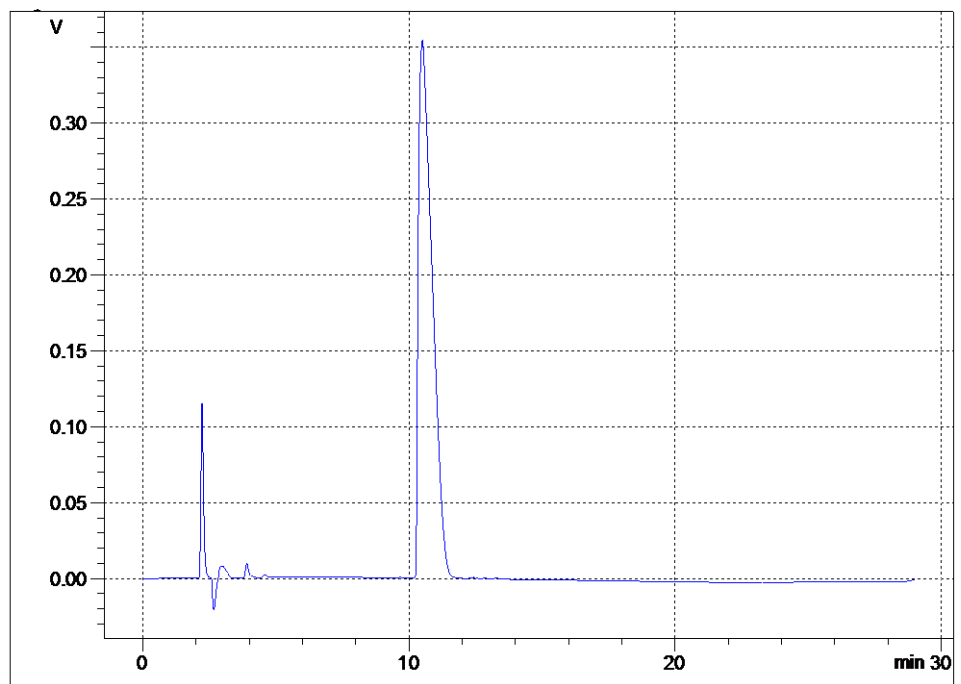
**Conditions: pH 7, 50 °C**



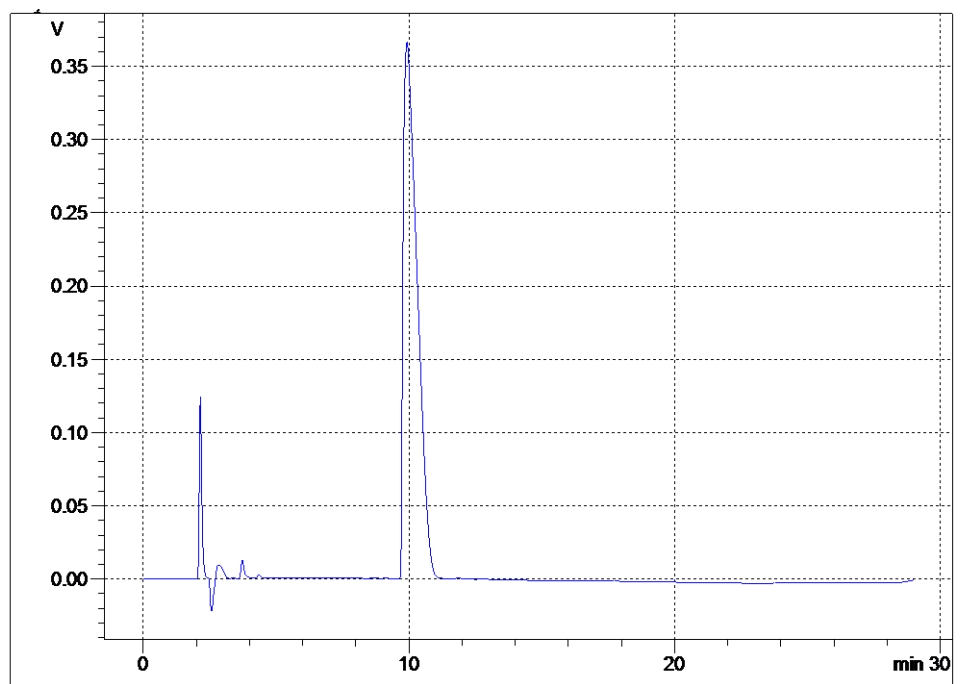
IL (433), t = 0 h



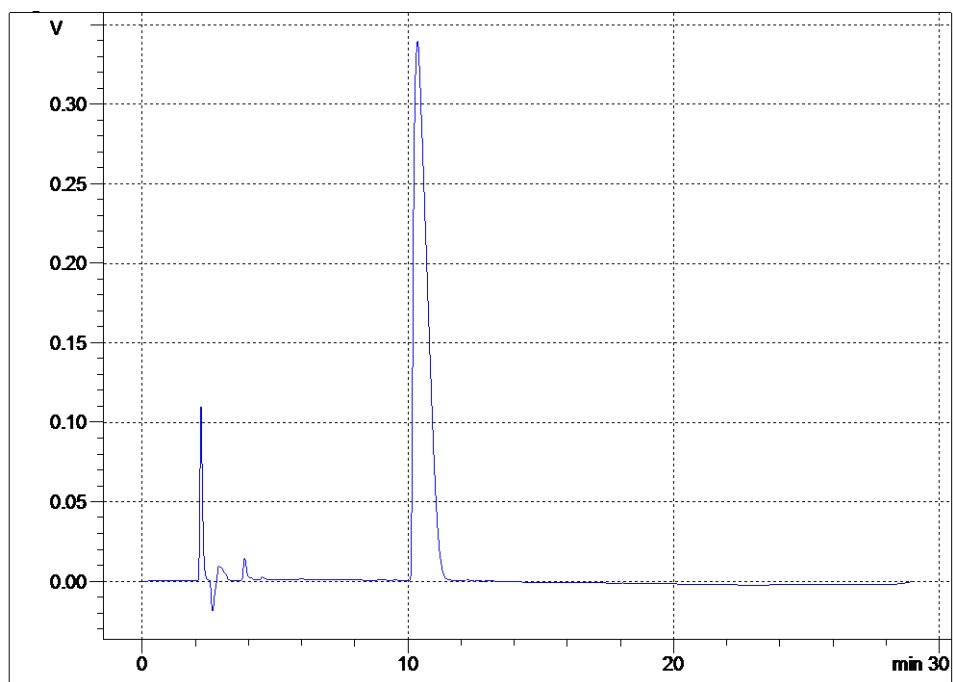
IL (433), t = 24 h



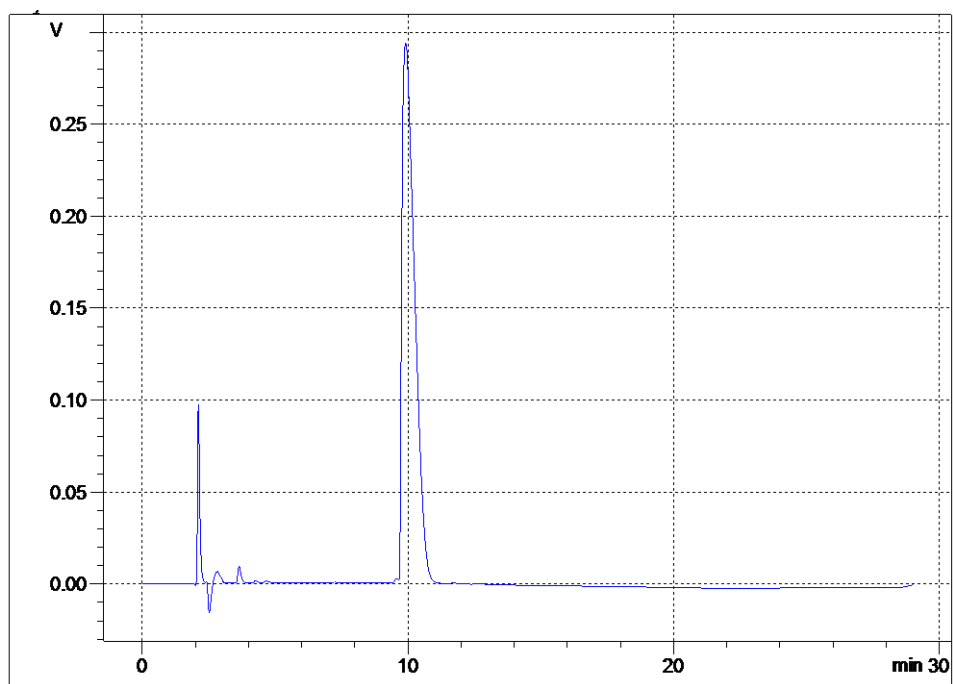
IL (433), t = 48 h



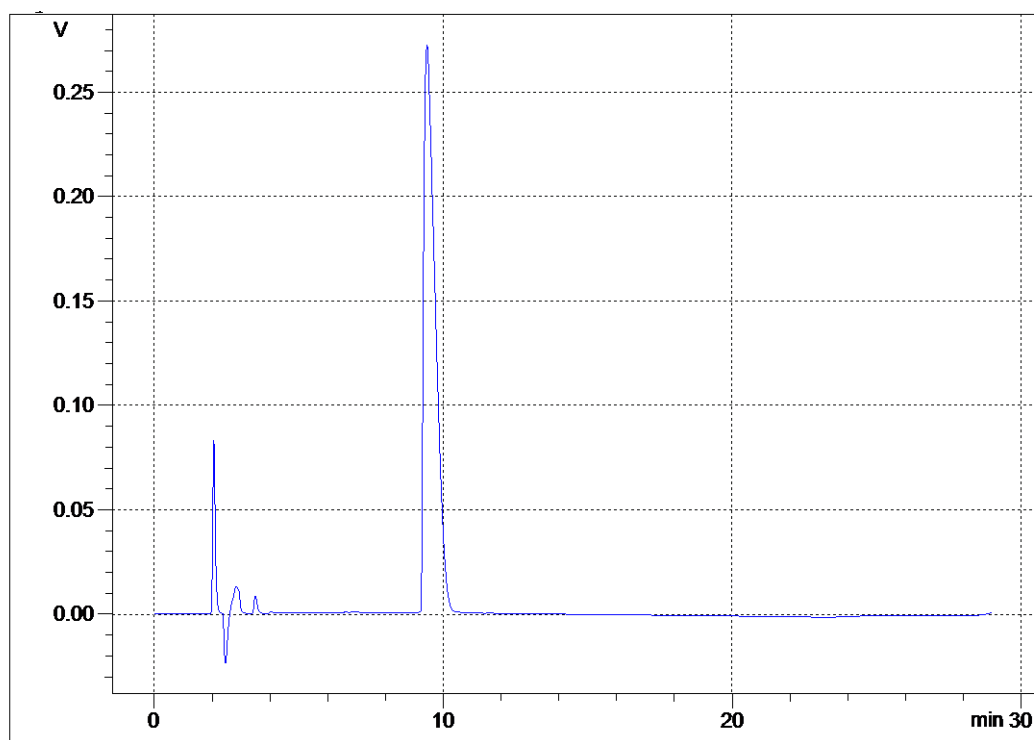
IL (433), t = 72 h



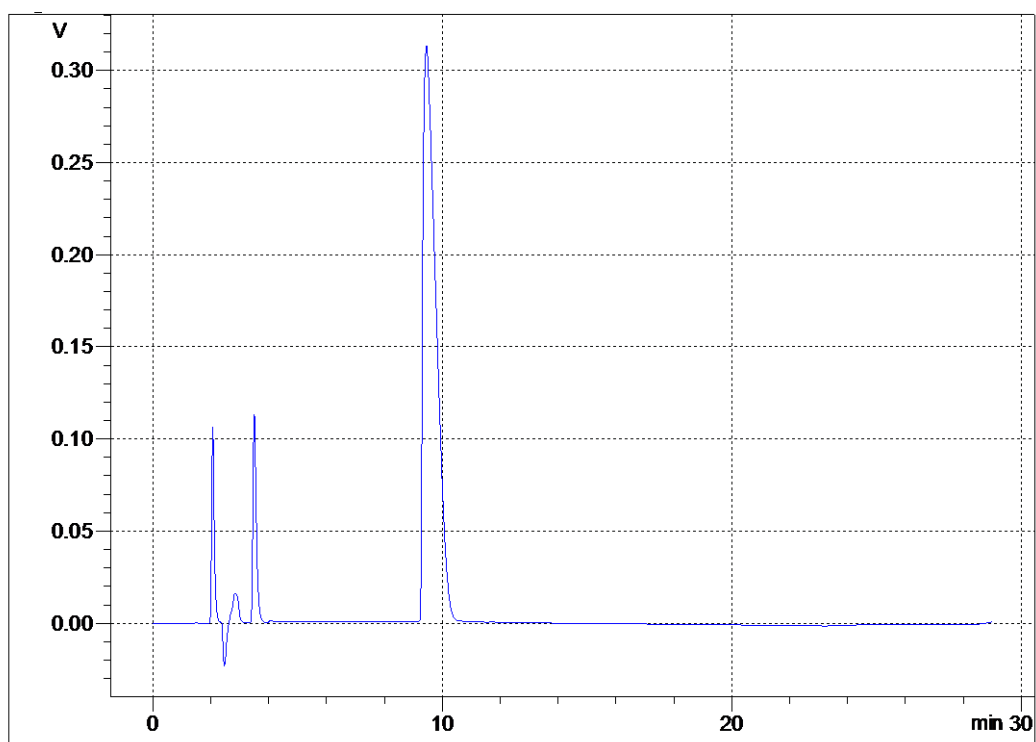
IL (433), t = 96 h



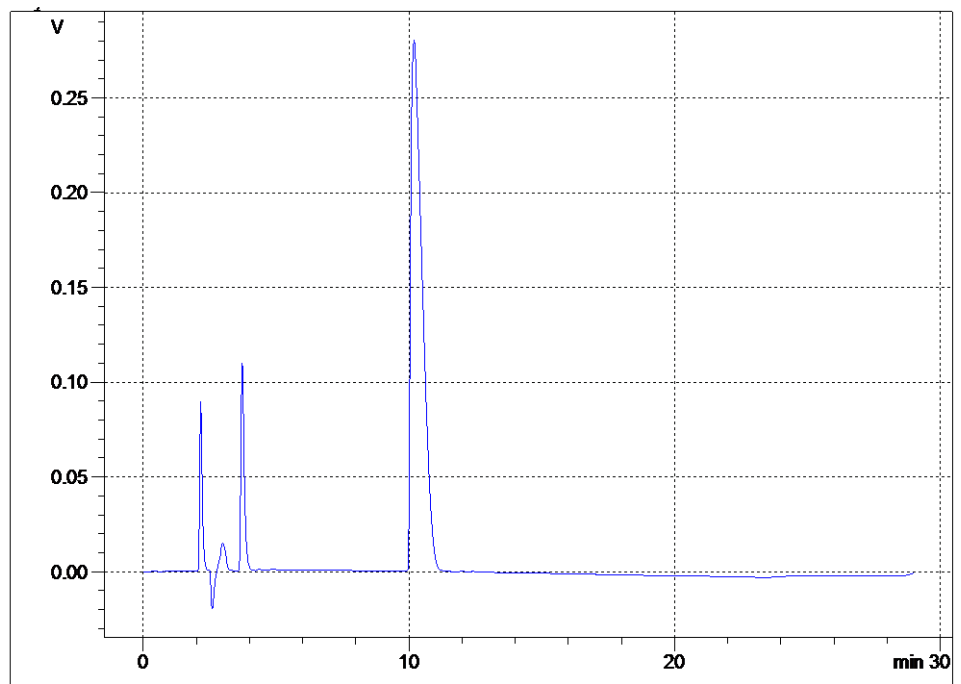
IL (433), t = 168 h



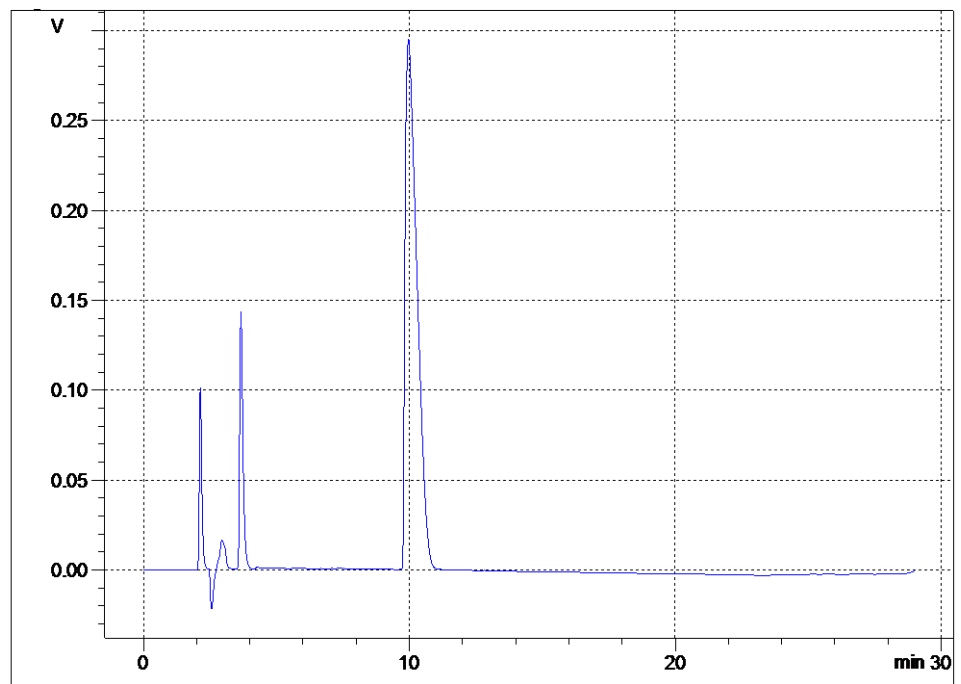
IL (436), t = 0 h



IL (436), t = 24 h

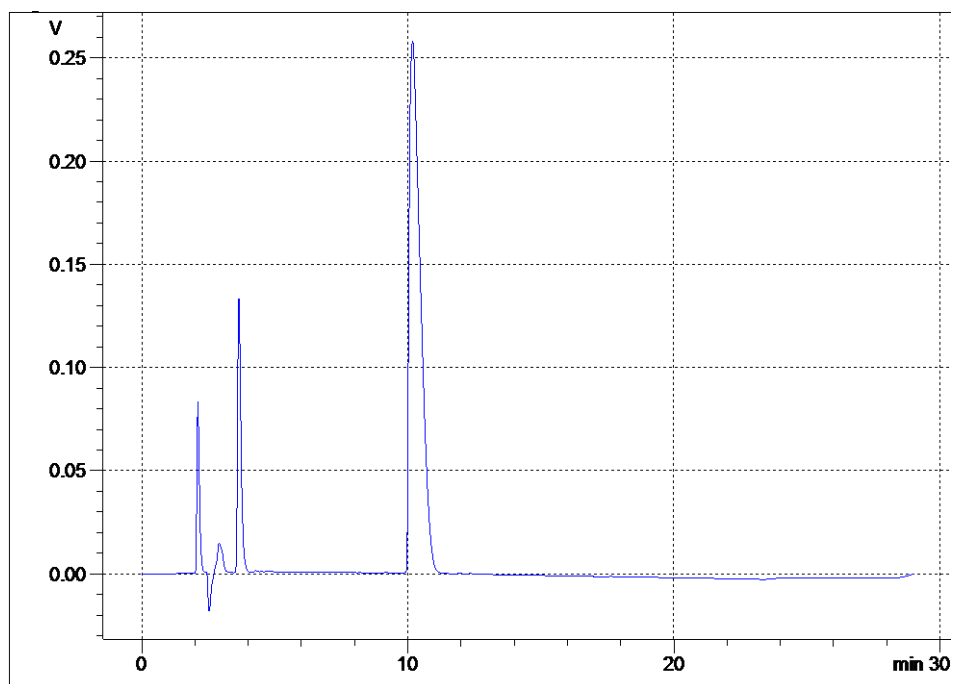


IL (436), t = 48 h

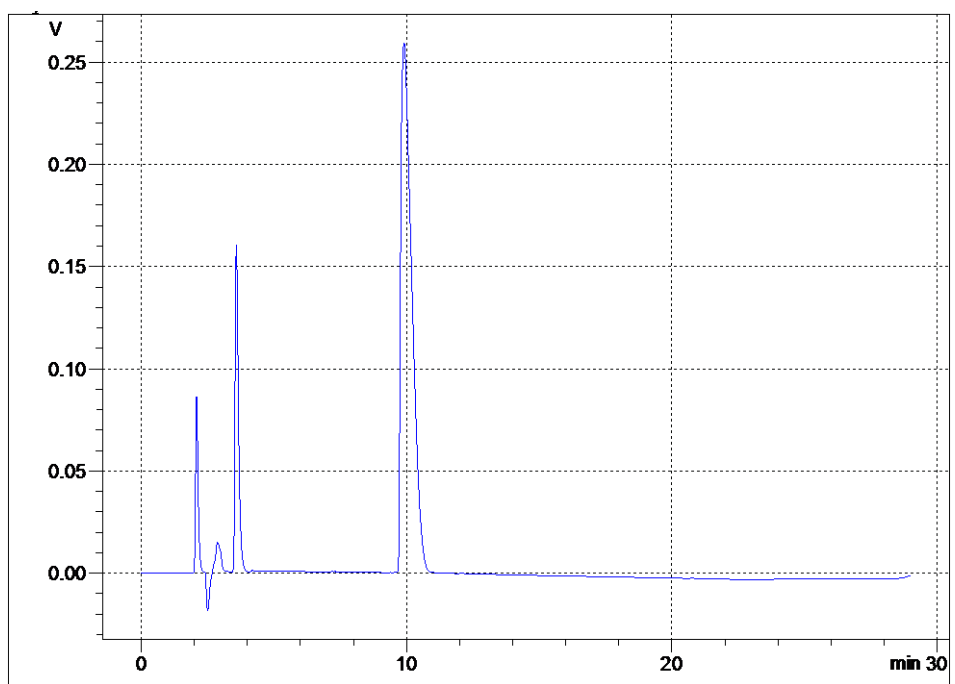


IL (436), t = 72 h

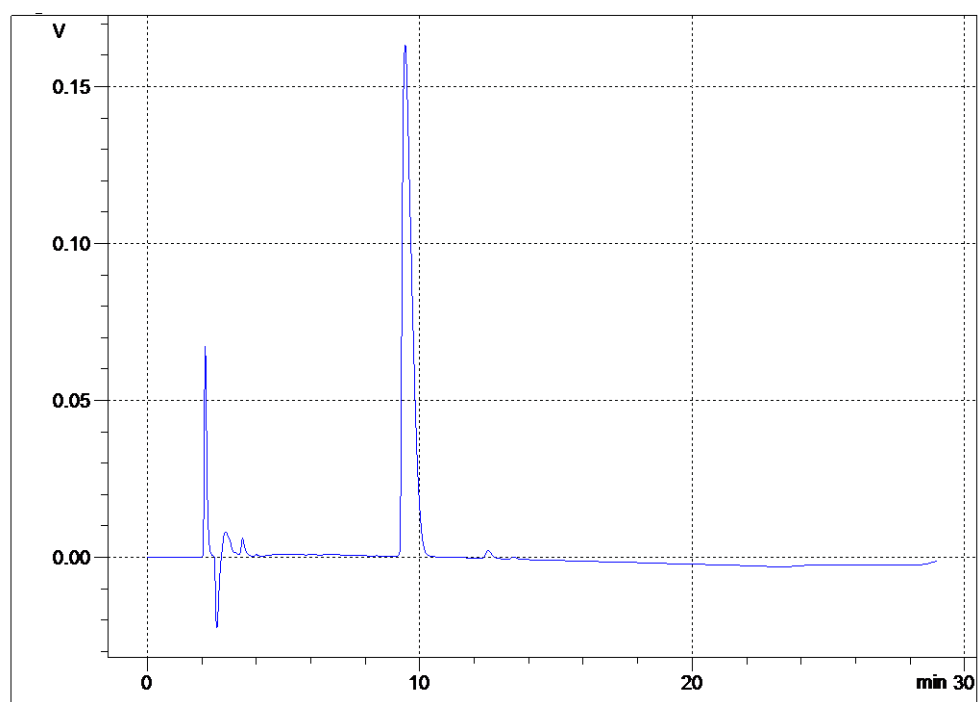




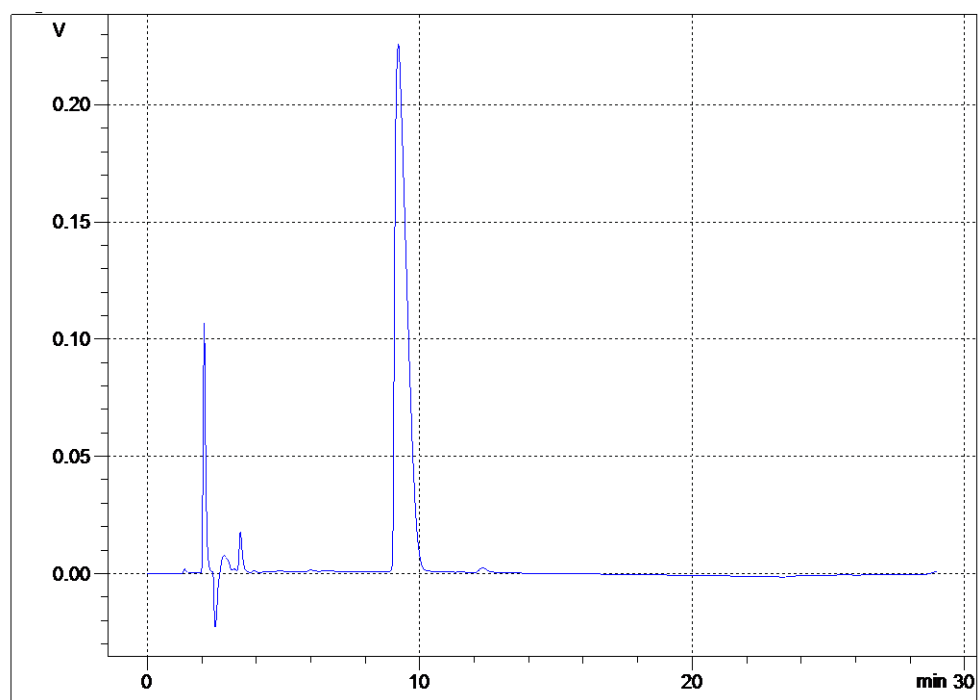
IL (436), t = 96 h



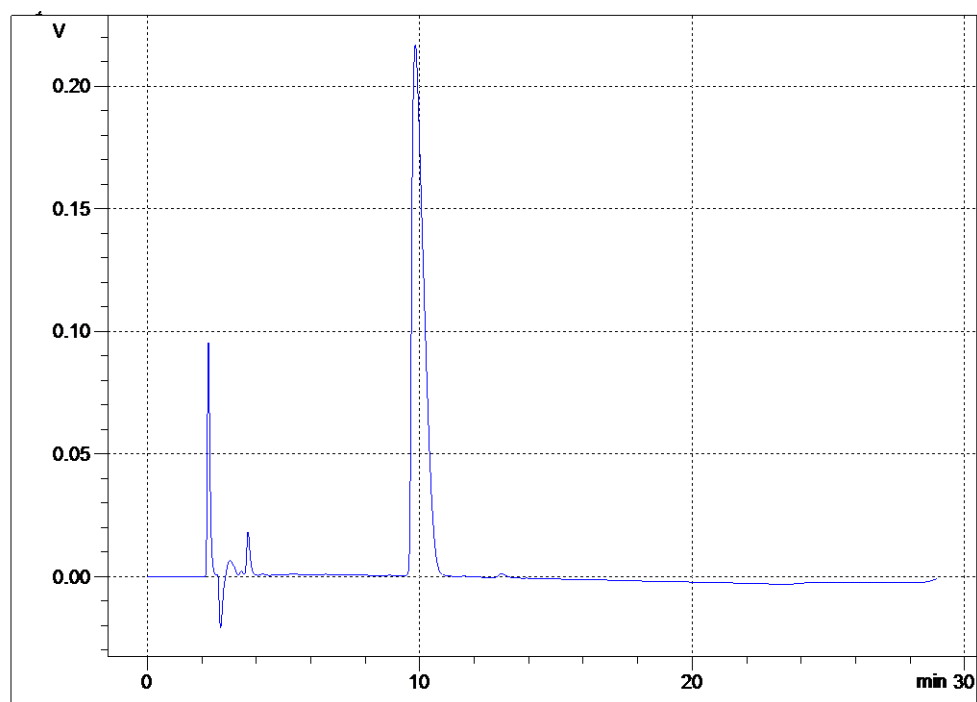
IL (436), t = 168 h



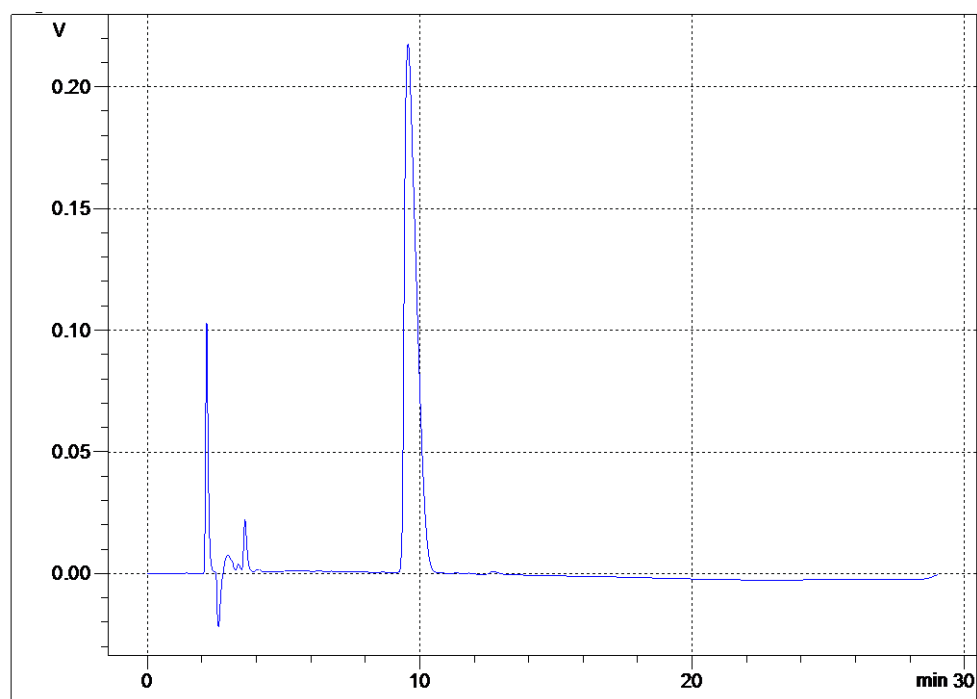
IL (439), t = 0 h



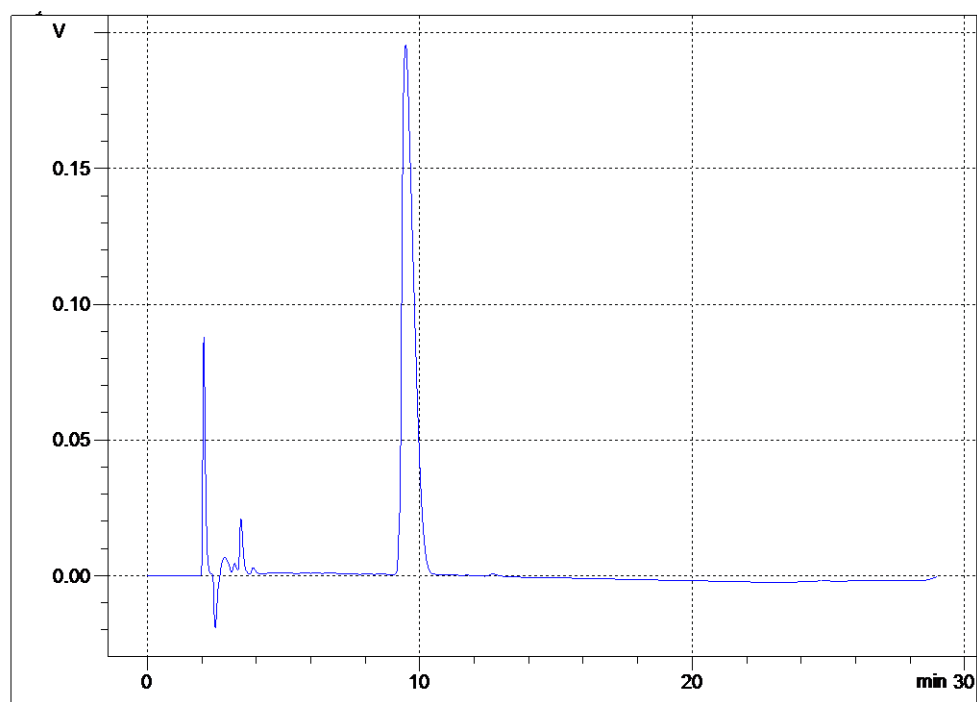
IL (439), t = 24 h



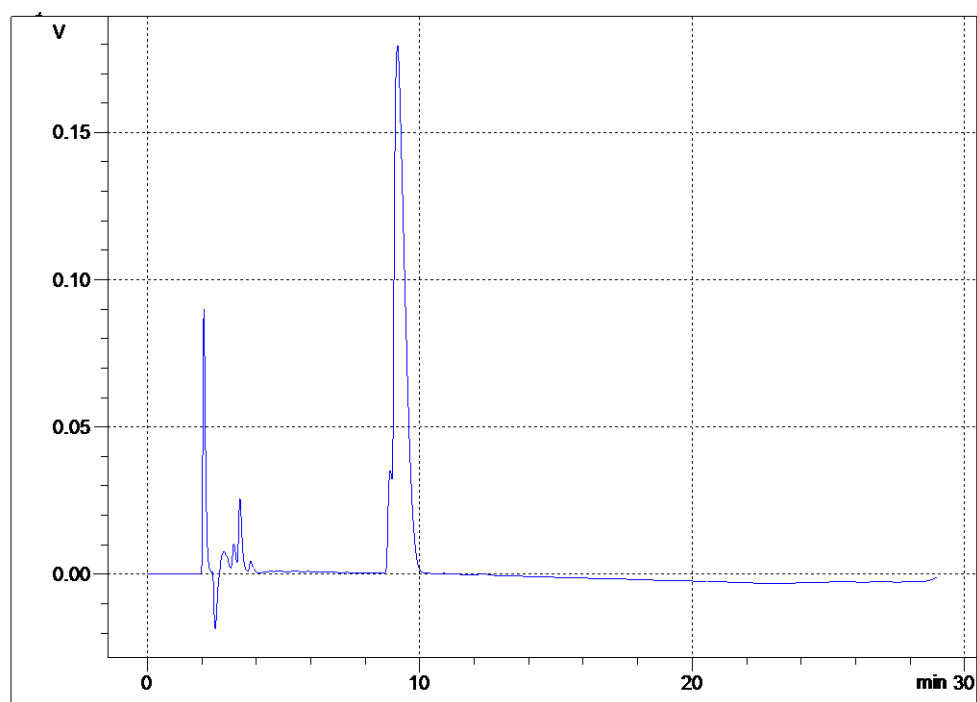
IL (439), t = 48 h



IL (439), t = 72 h



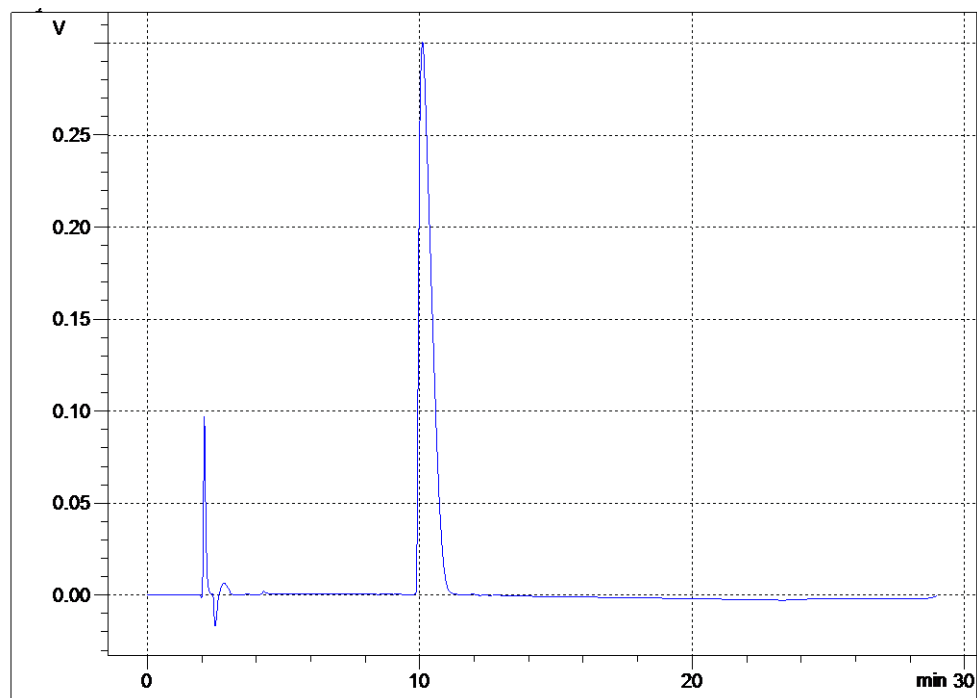
IL (439), t = 96 h



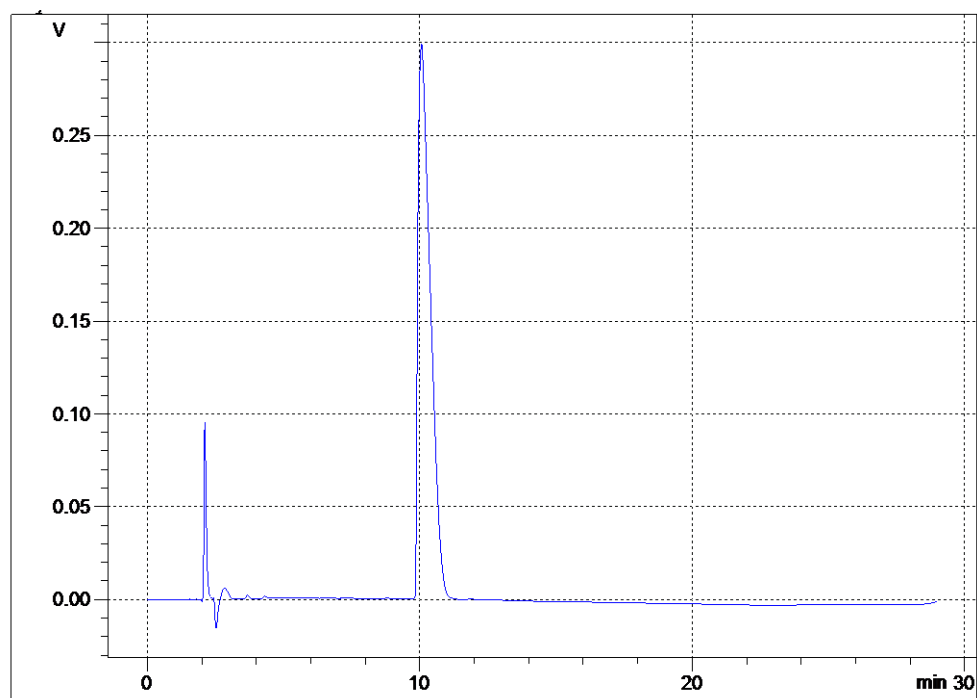
IL (439), t = 168 h

**HPLC/UV Traces for aqueous stability study for ILs (433, 436, 439).**

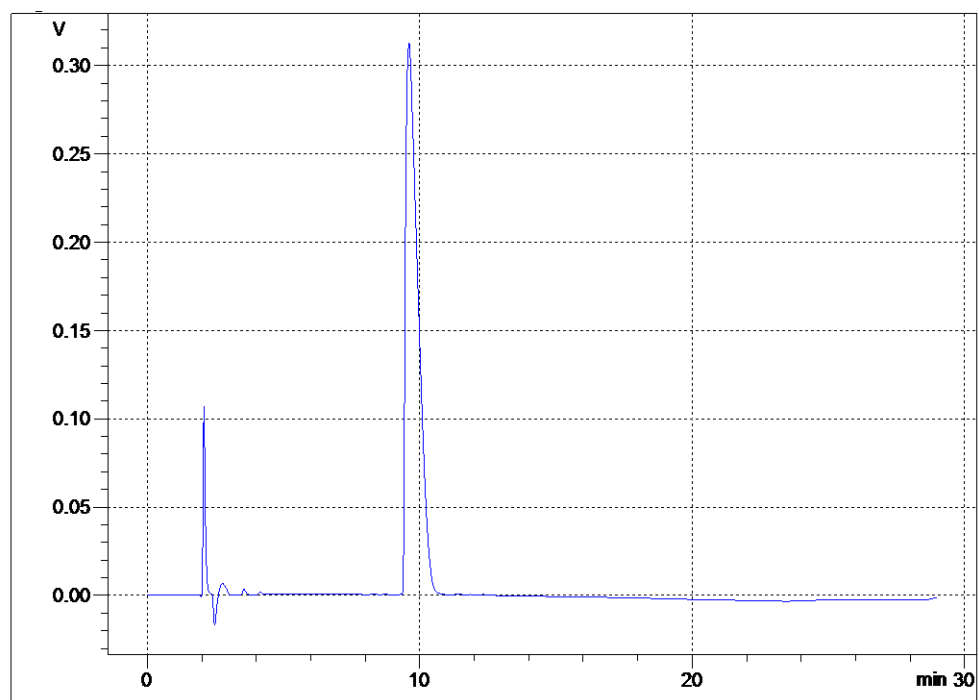
**Conditions: pH 2, 25 °C**



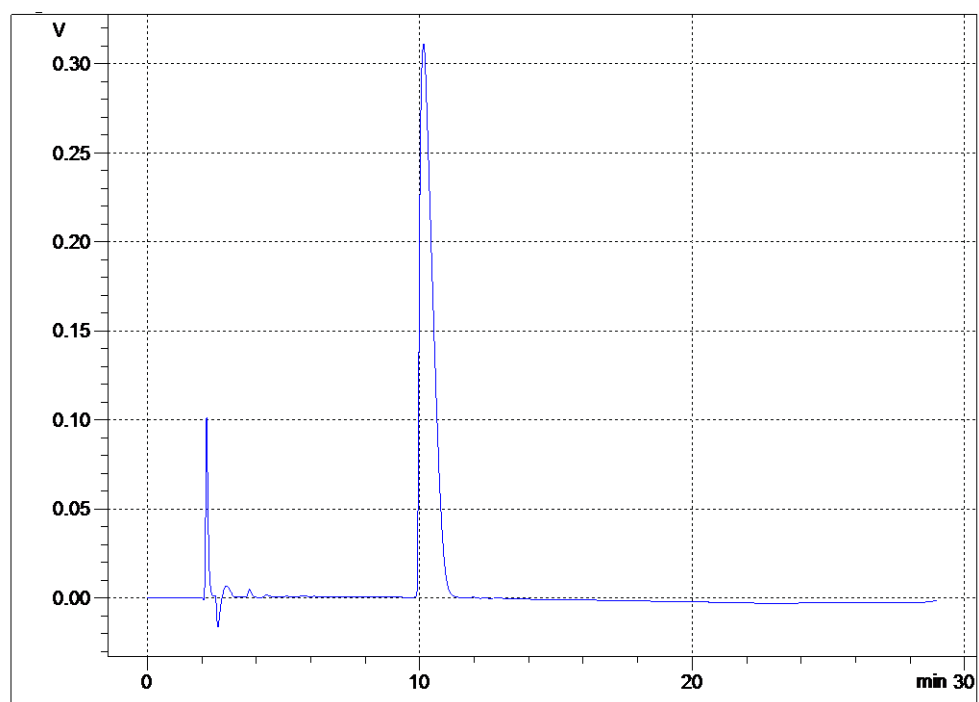
IL (433), t = 0 h



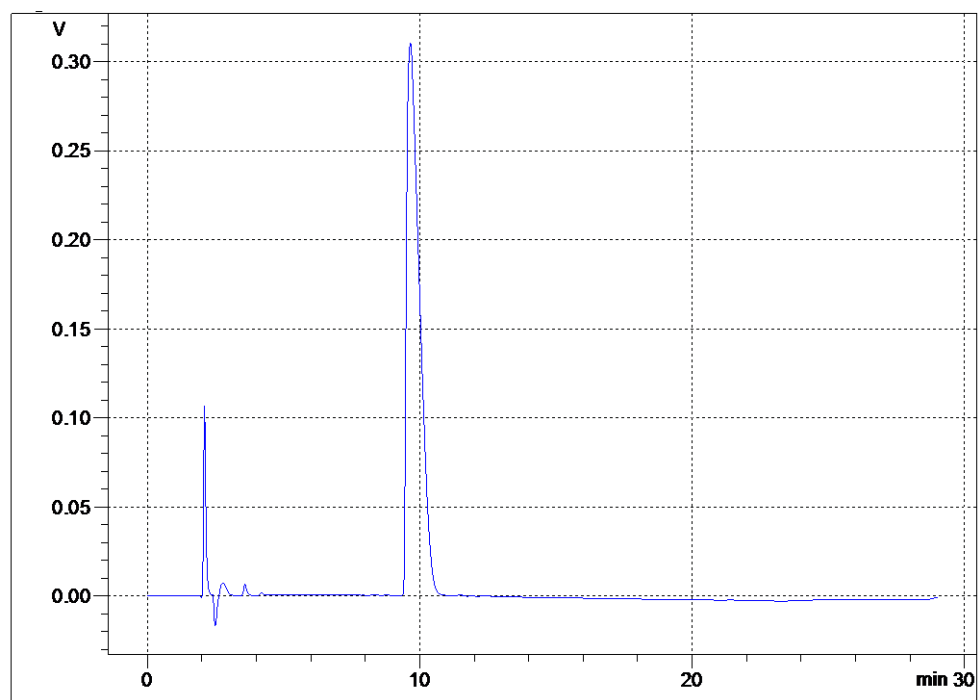
IL (433), t = 24 h



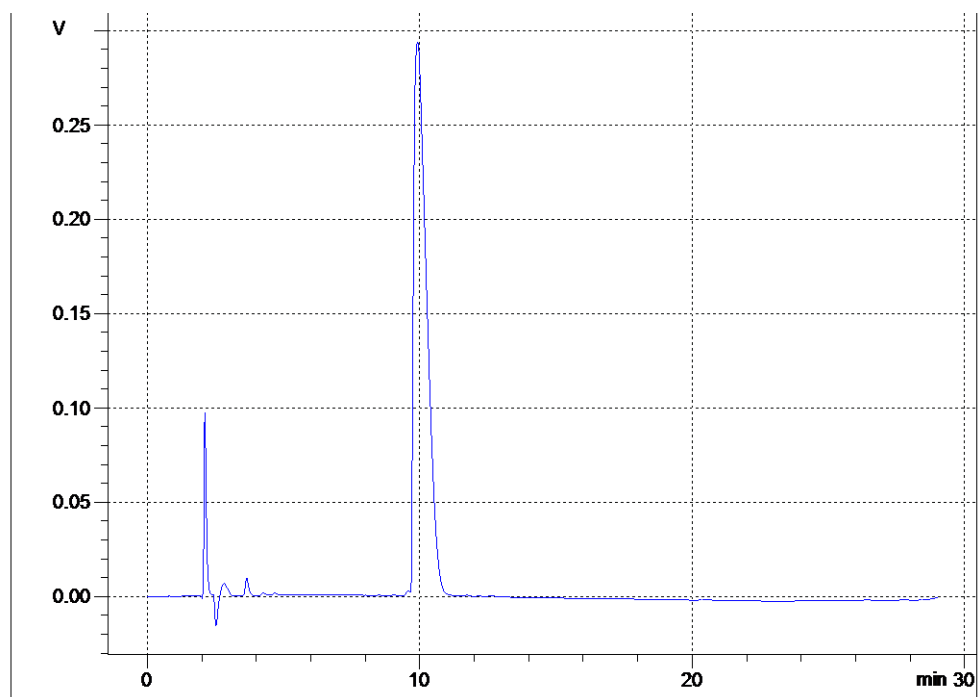
IL (433), t = 48 h



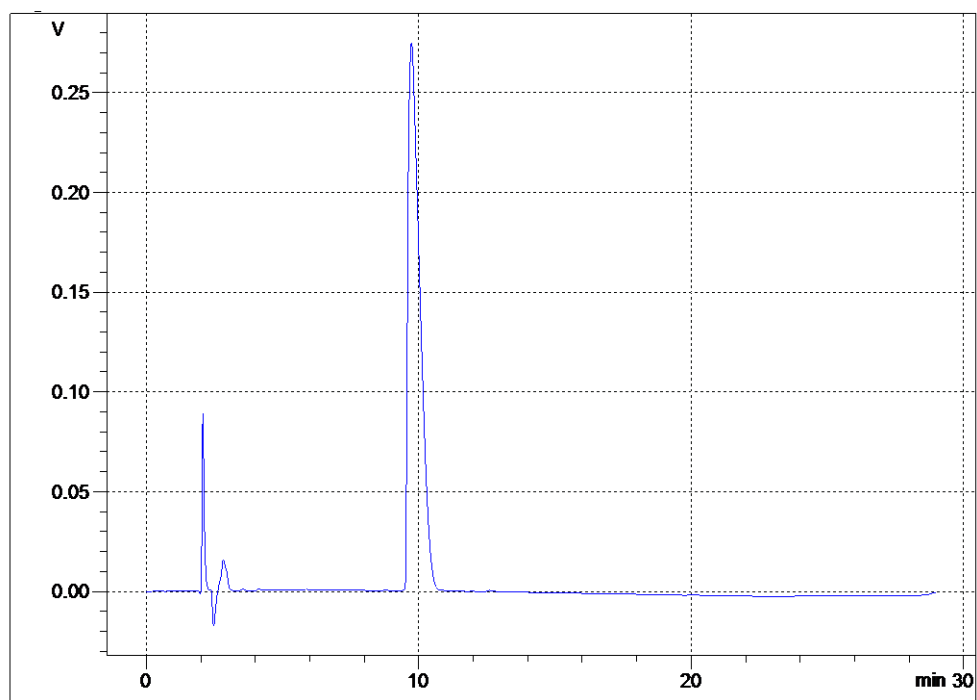
IL (433), t = 72 h



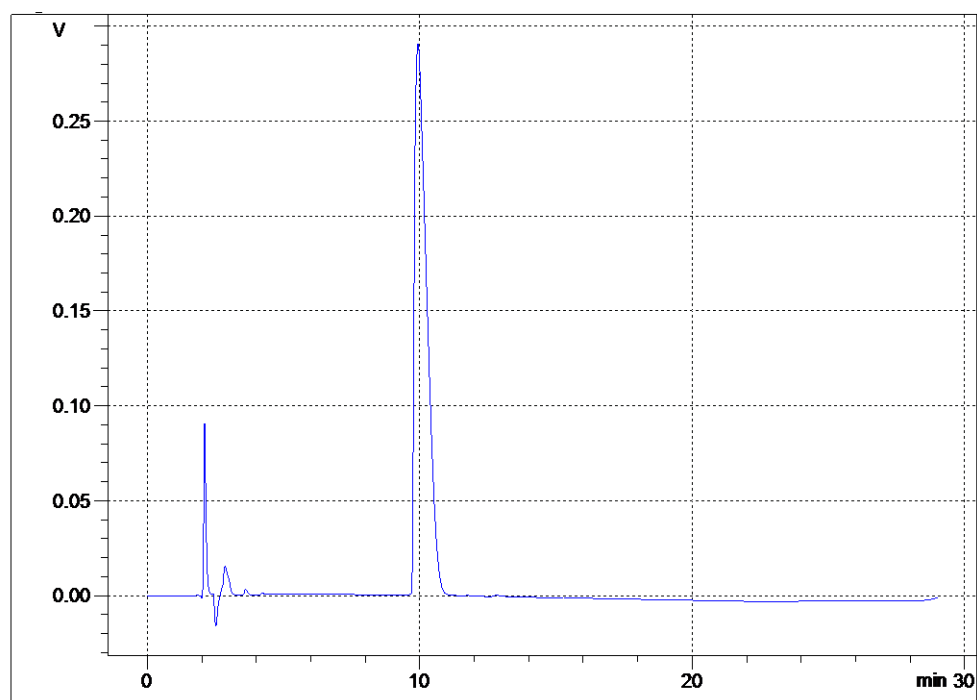
IL (433), t = 96 h



IL (433), t = 168 h

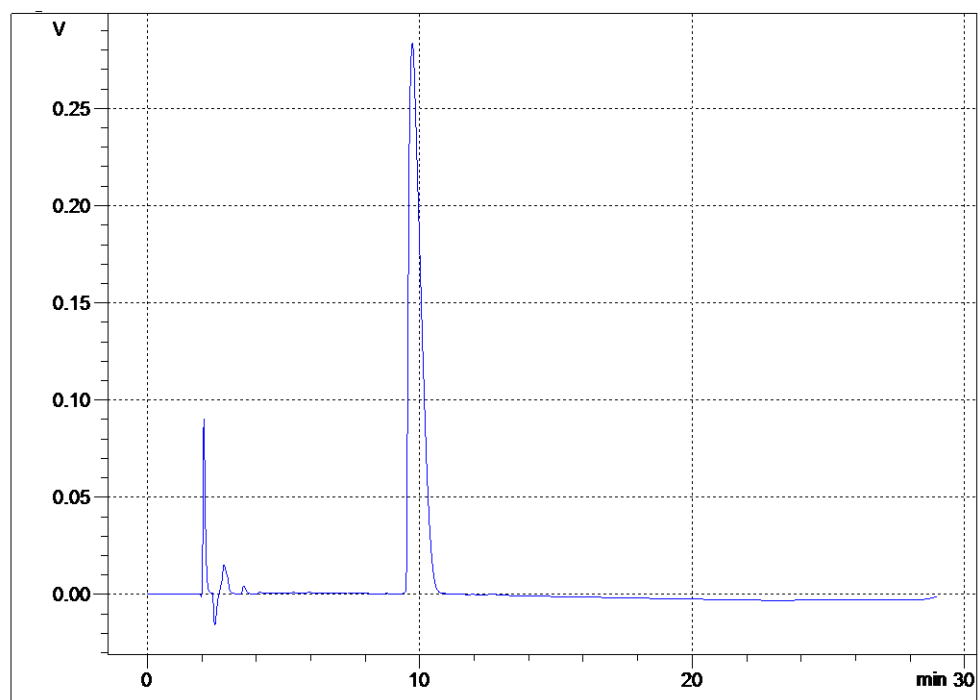


IL (436), t = 0 h

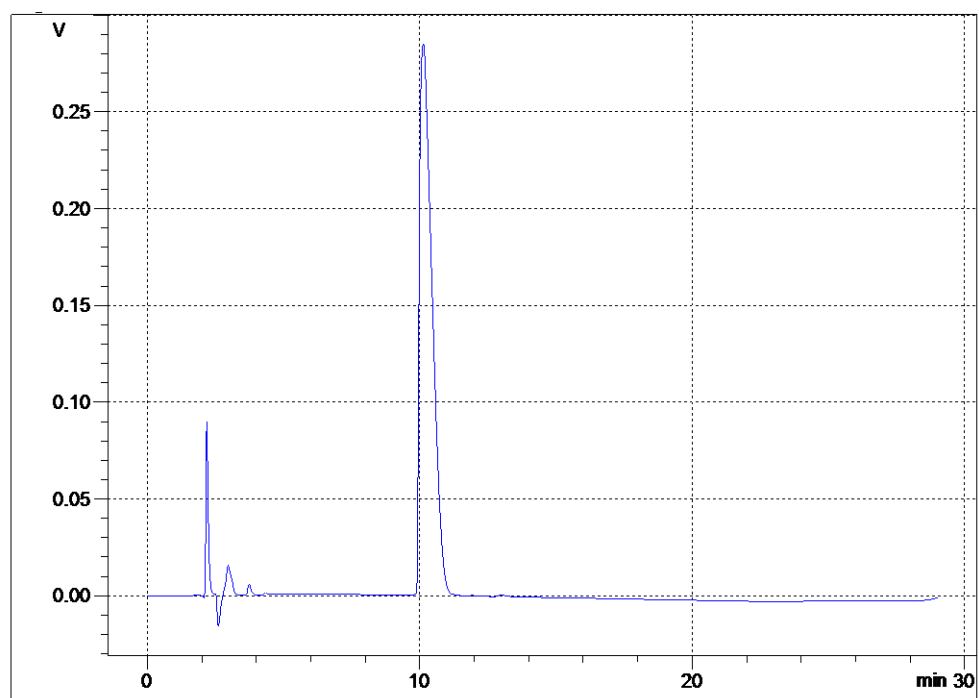


IL (436), t = 24 h

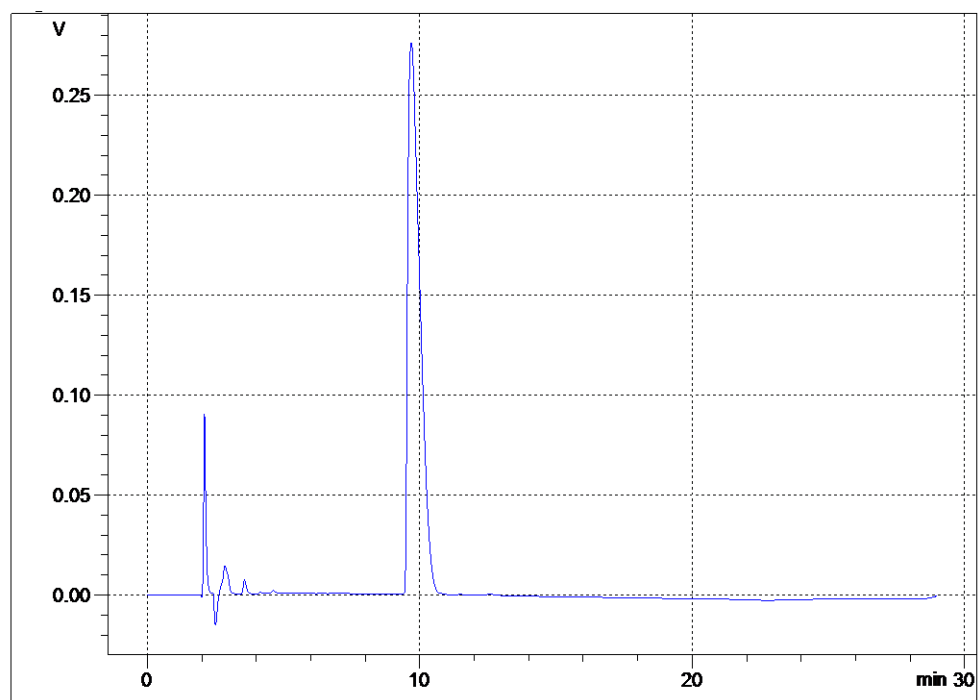




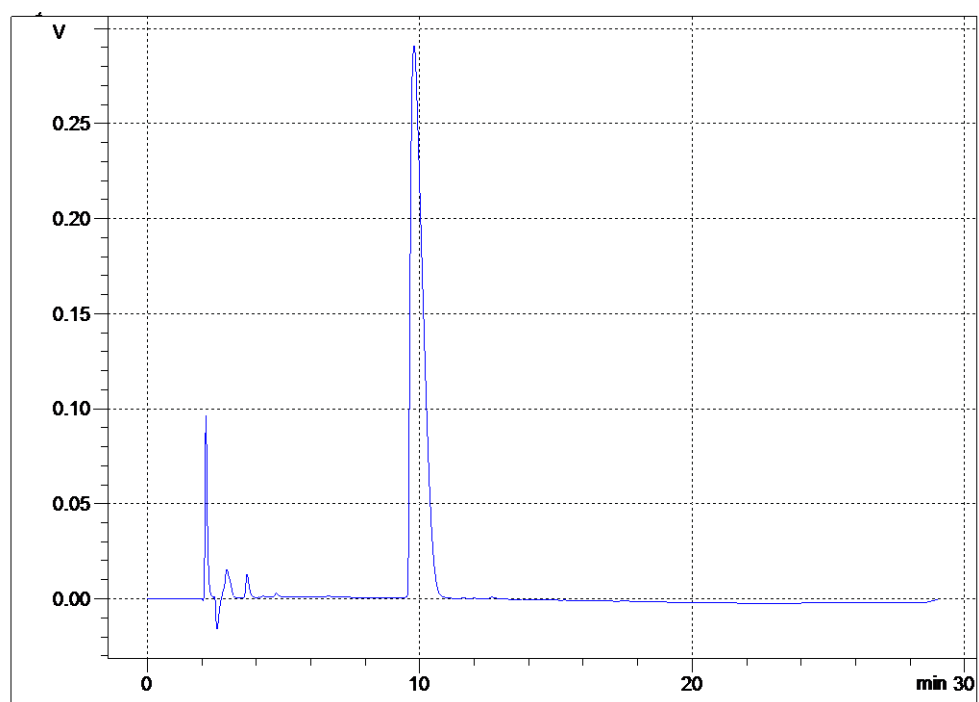
IL (436), t = 48 h



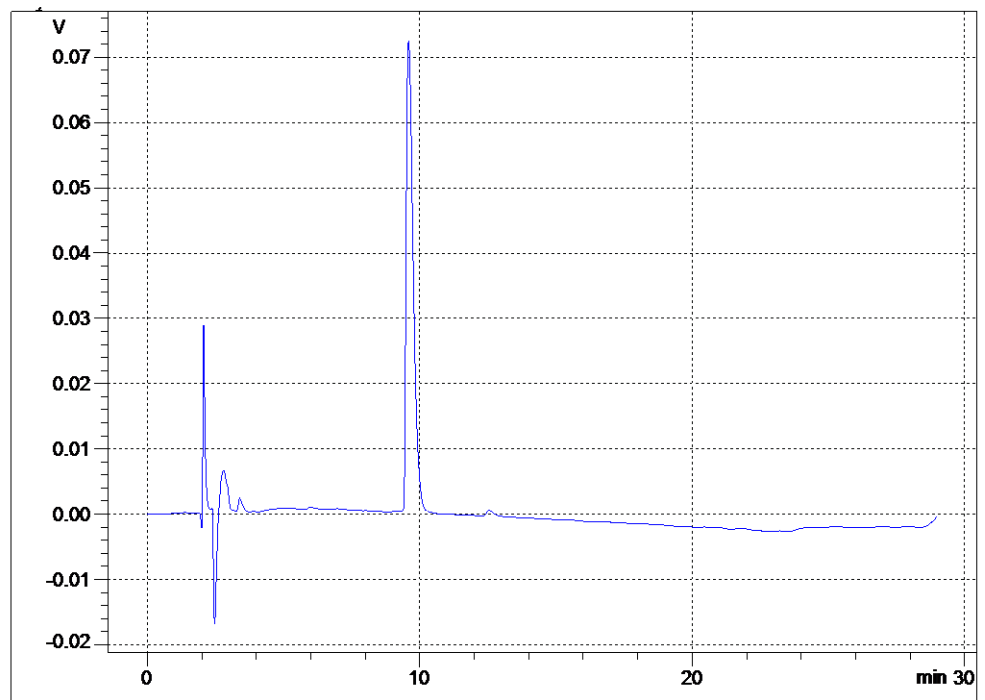
IL (436), t = 72 h



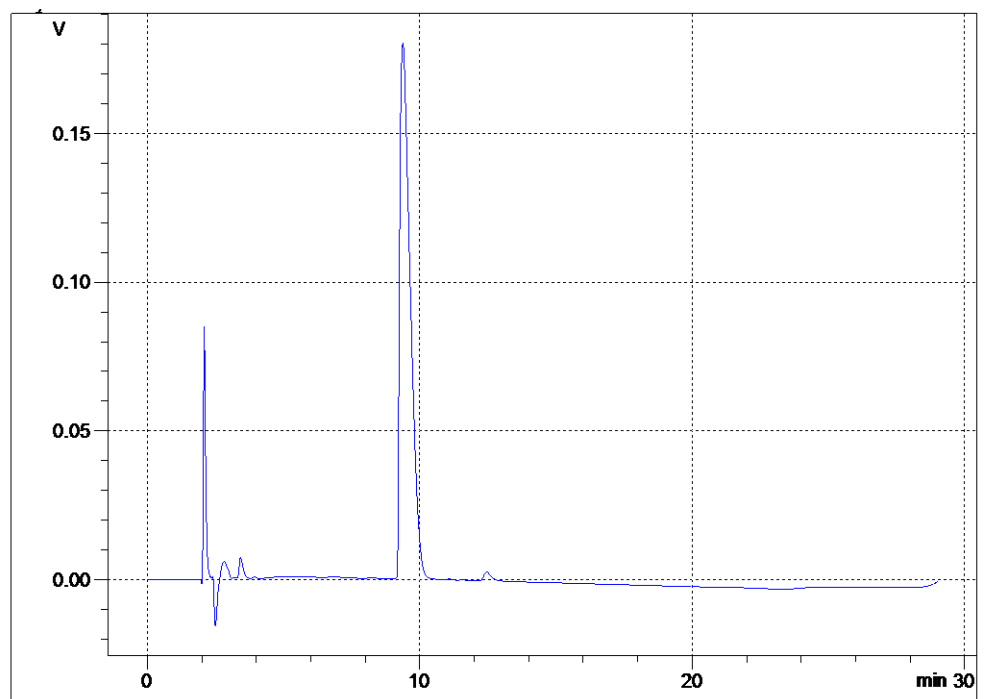
IL (436), t = 96 h



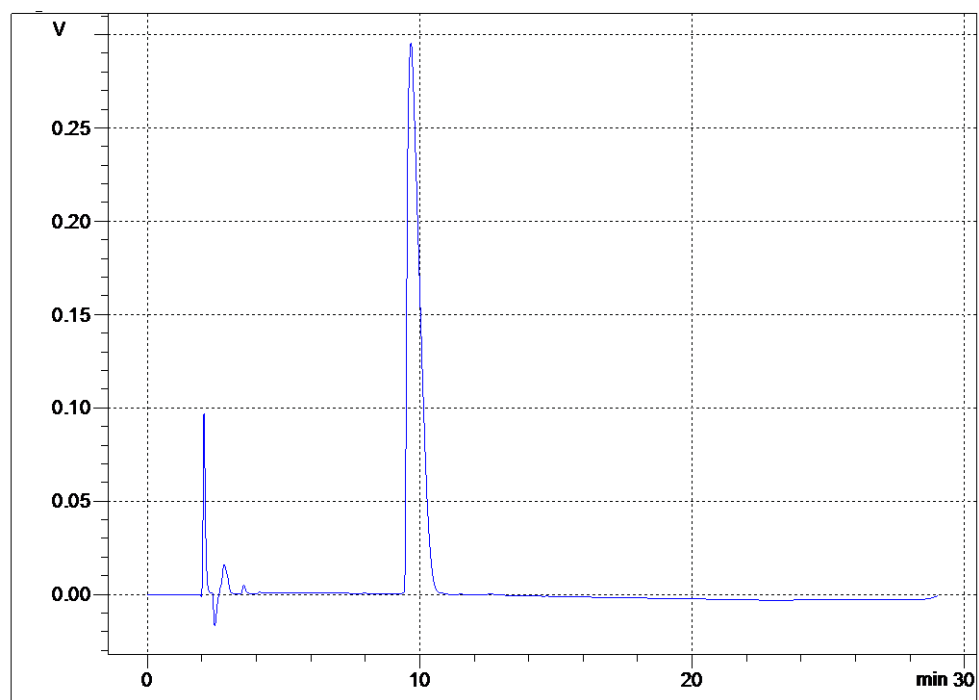
IL (436), t = 168 h



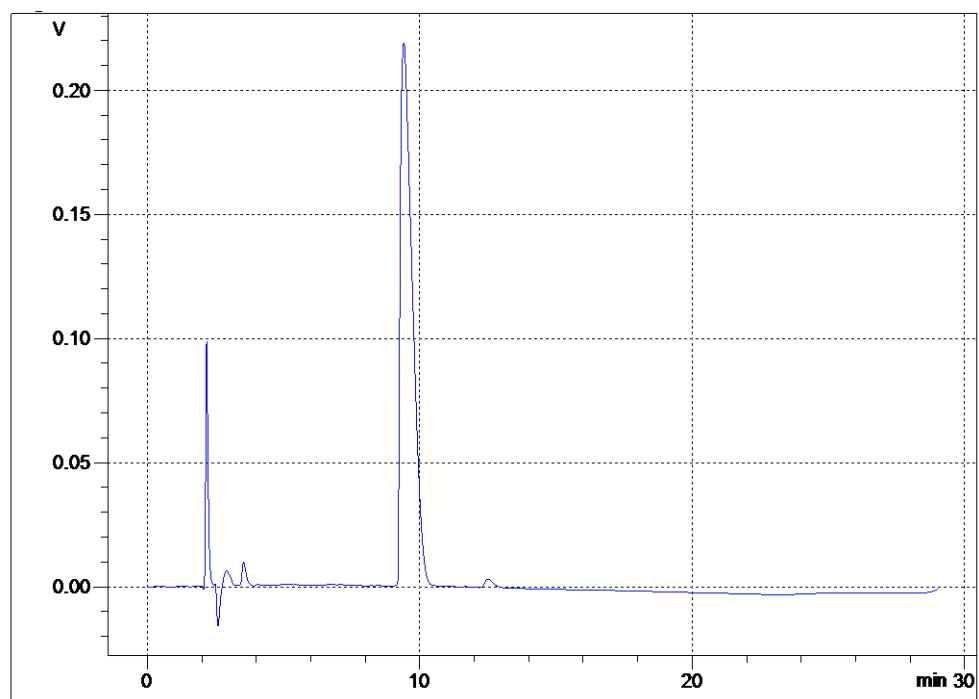
IL (439), t = 0 h



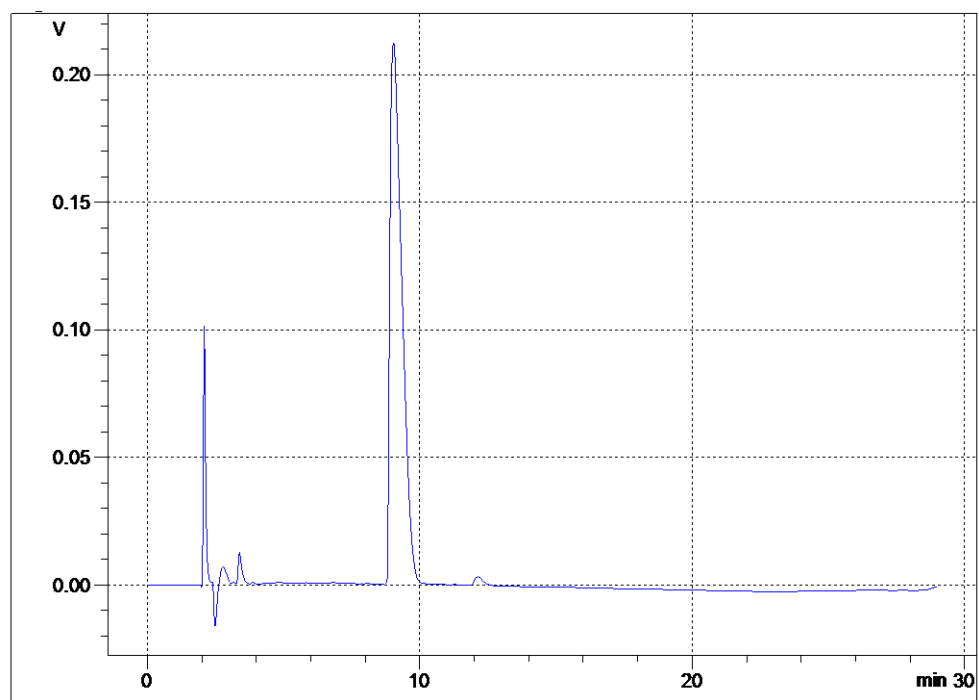
IL (439), t = 24 h



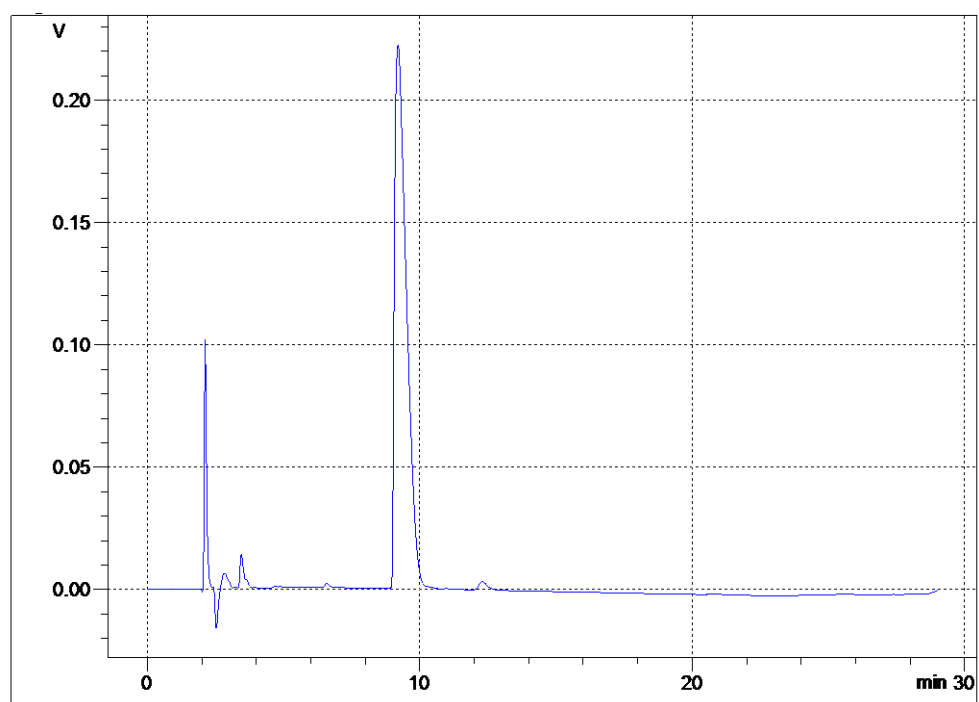
IL (439),  $t = 48$  h



IL (439),  $t = 72$  h



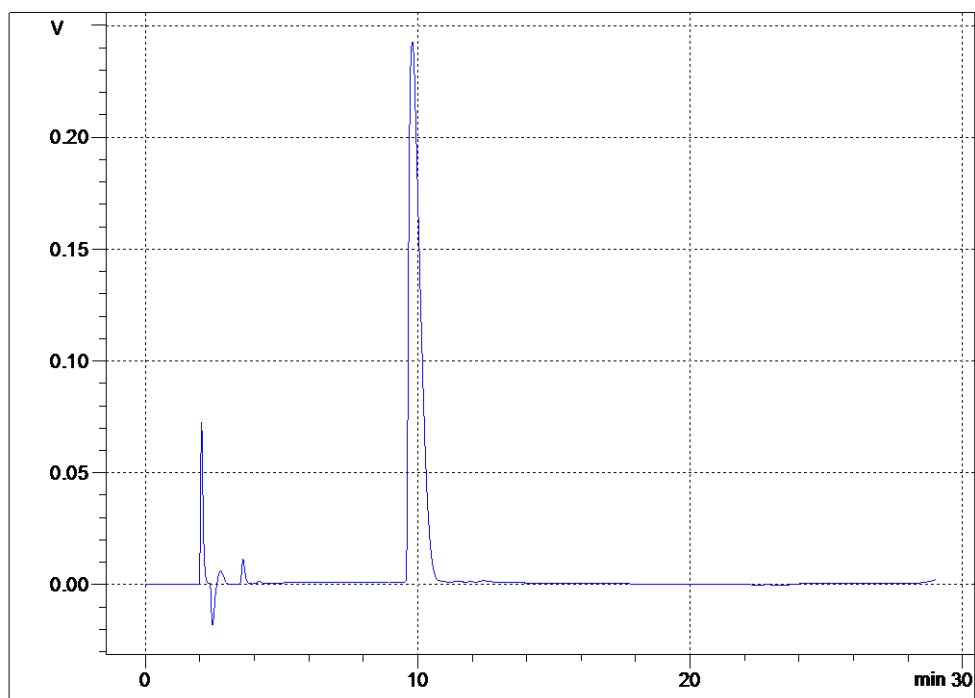
IL (439), t = 96 h



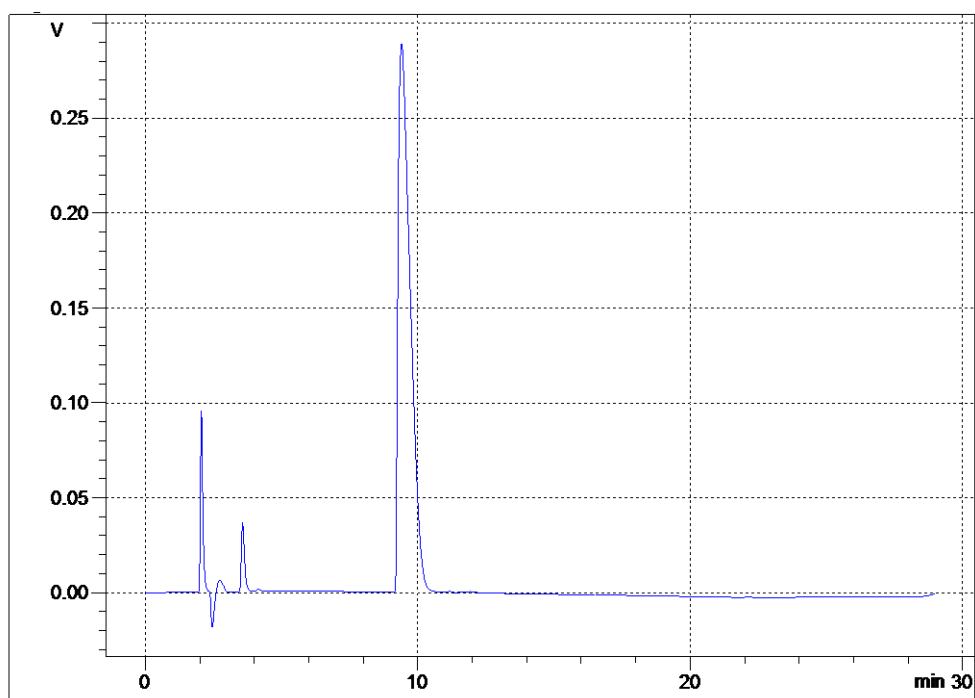
IL (439), t = 168 h

**HPLC/UV Traces for aqueous stability study for ILs (433, 436, 439).**

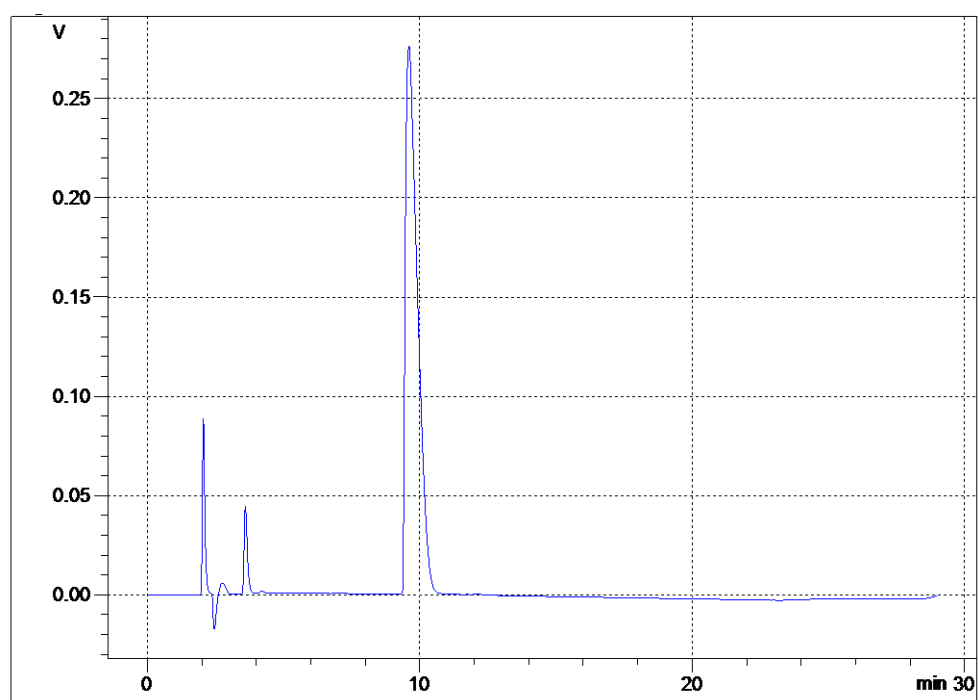
**Conditions: pH 10, 25 °C**



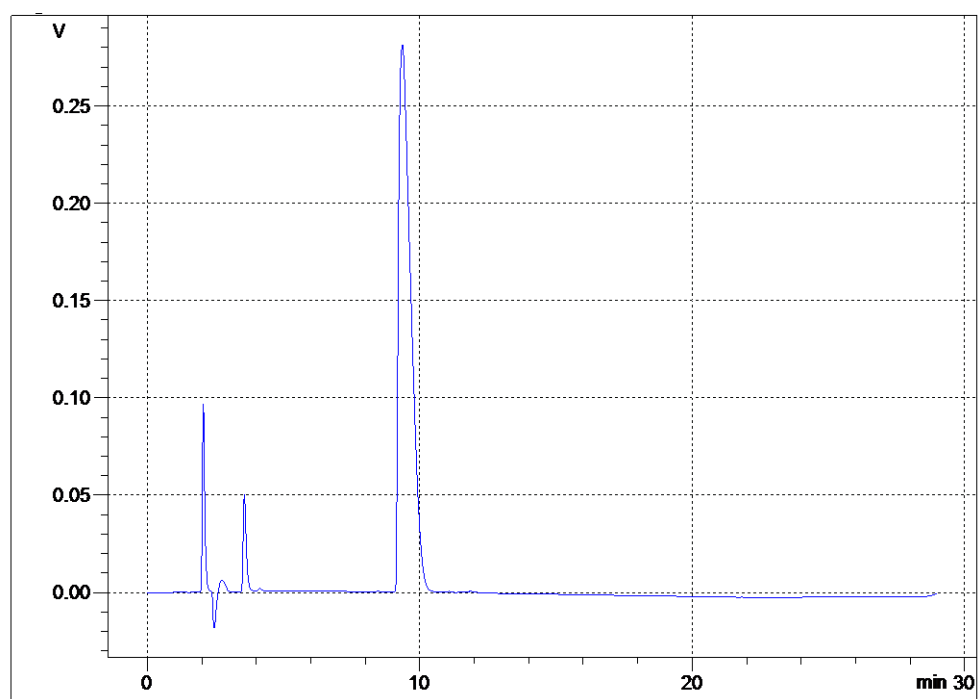
IL (433), t = 0 h



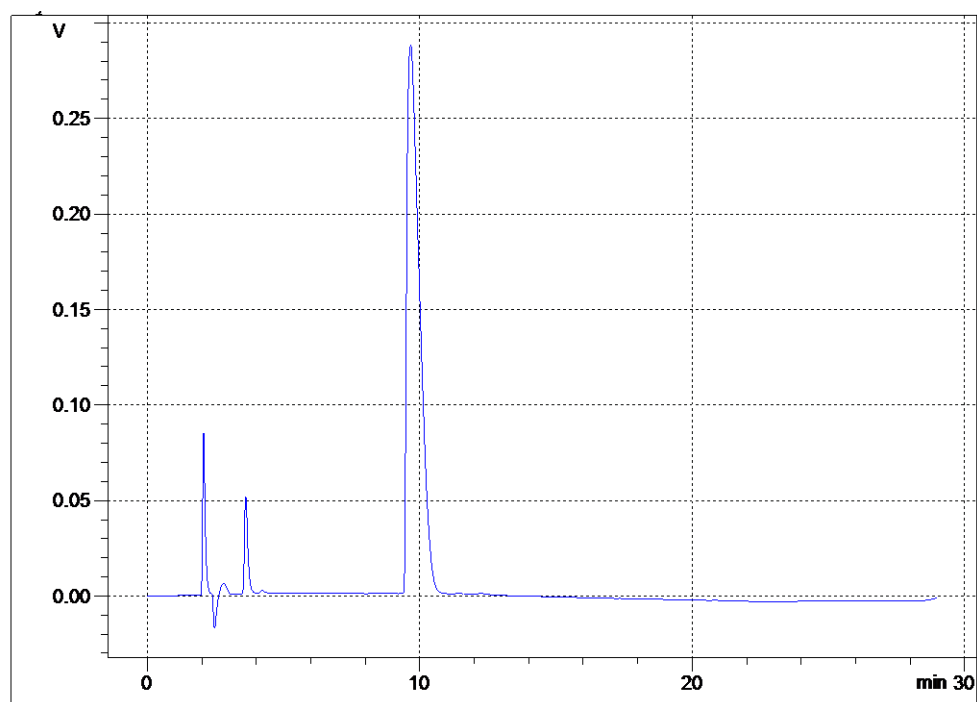
IL (433), t = 24 h



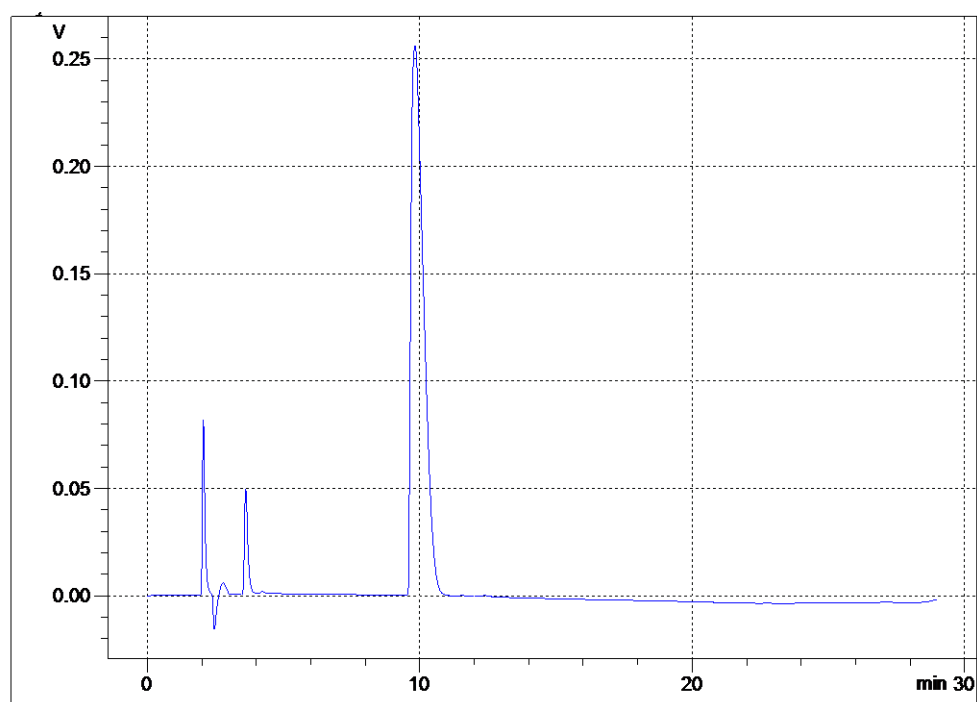
IL (433), t = 48 h



IL (433), t = 72 h

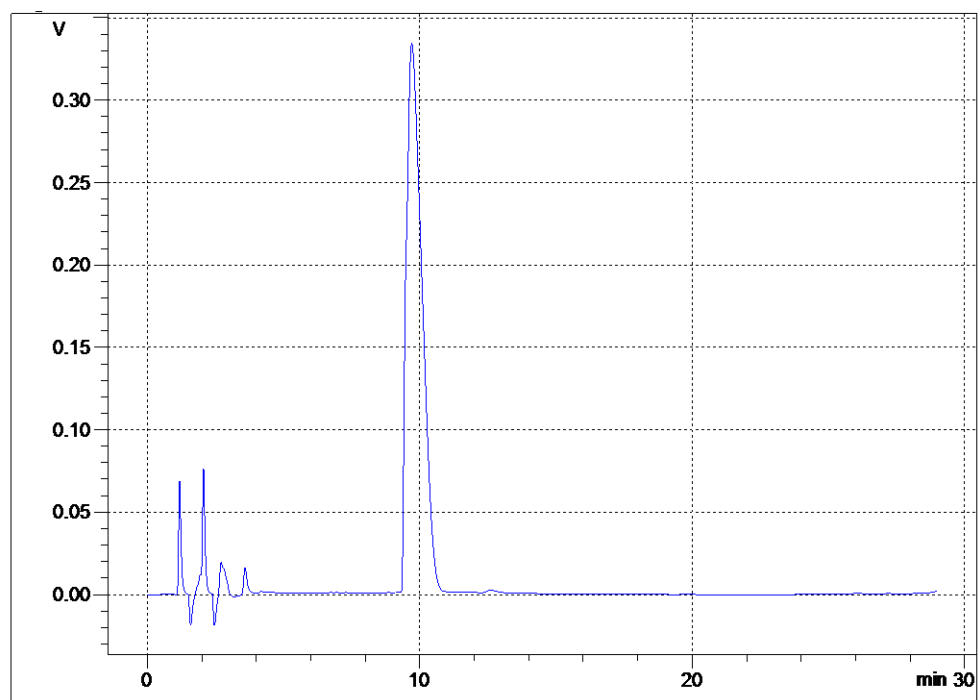


IL (433), t = 96 h

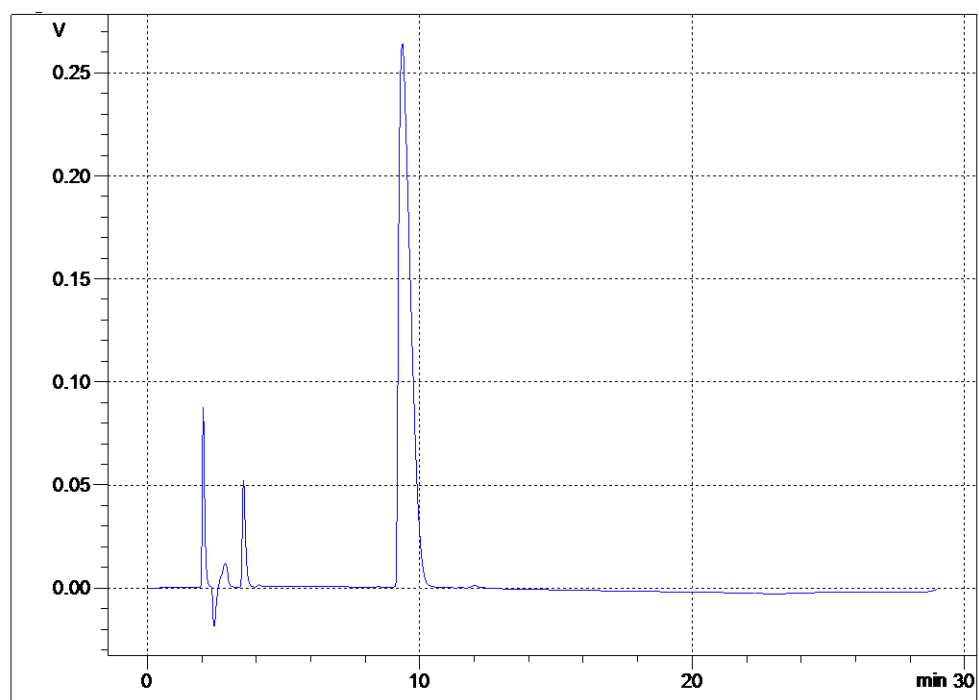


IL (433), t = 168 h

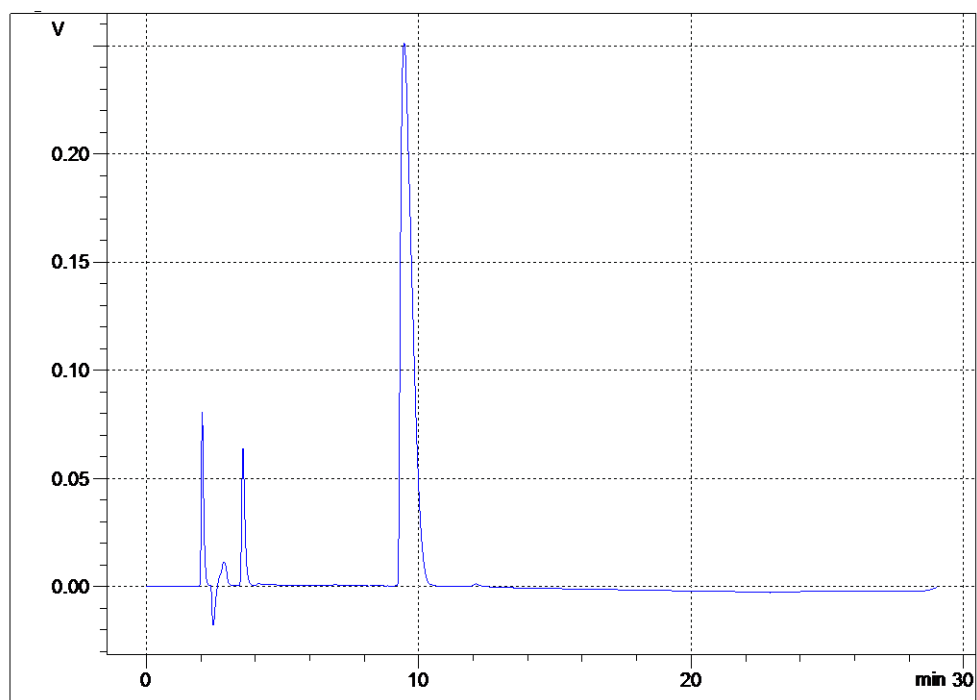




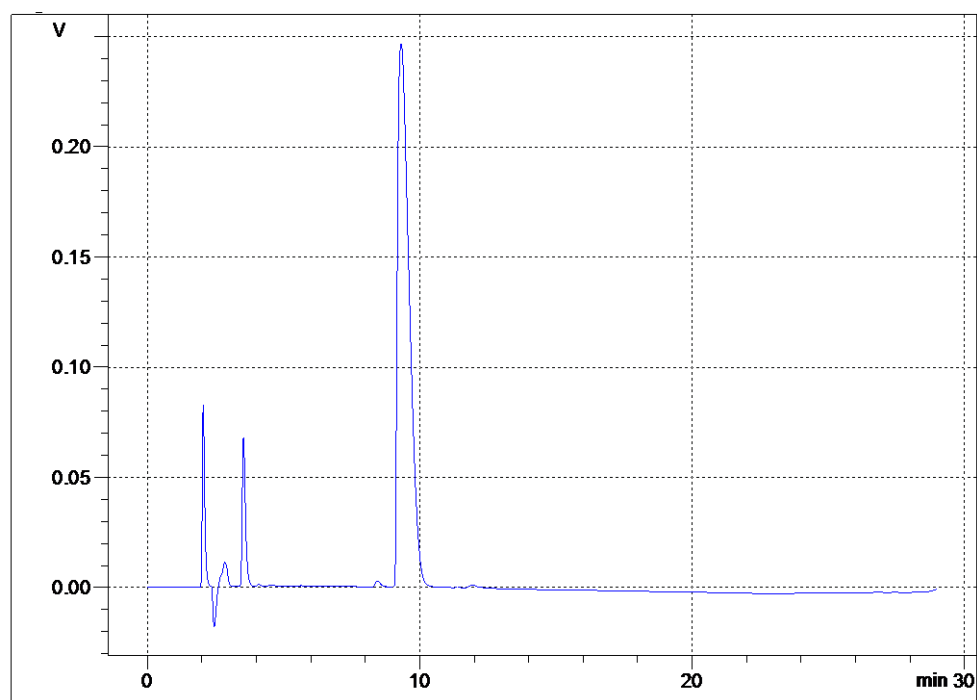
IL (436), t = 0 h



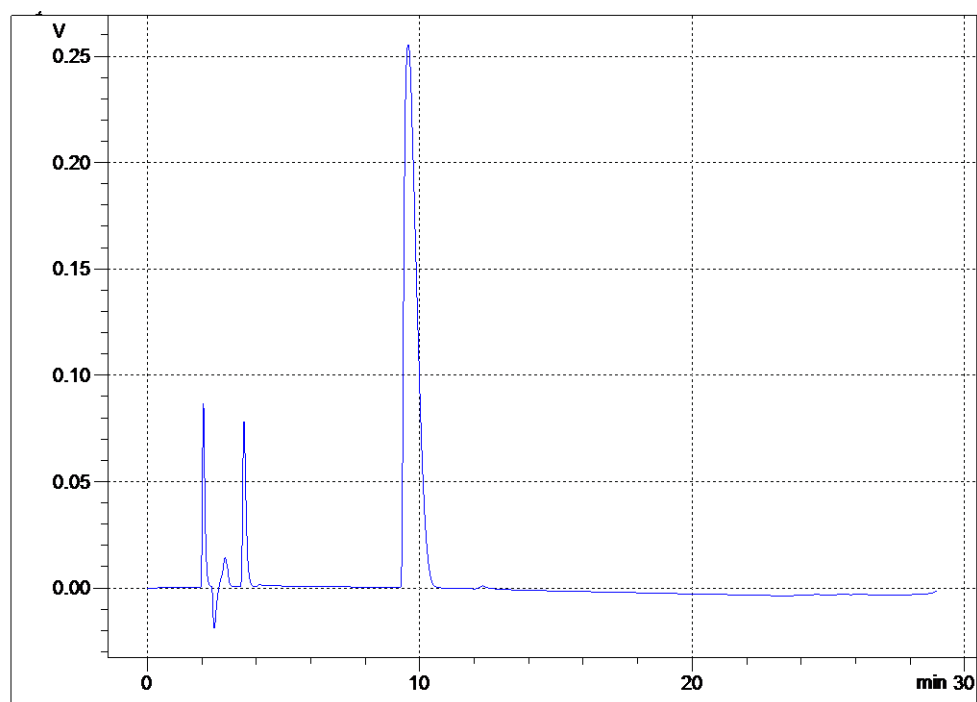
IL (436), t = 24 h



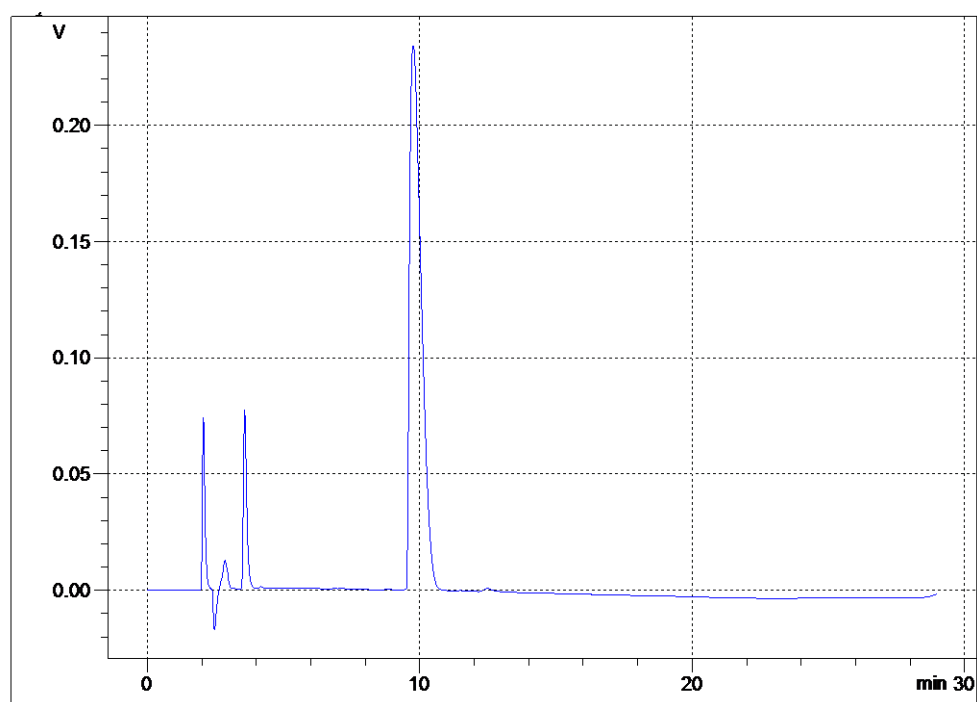
IL (436), t = 48 h



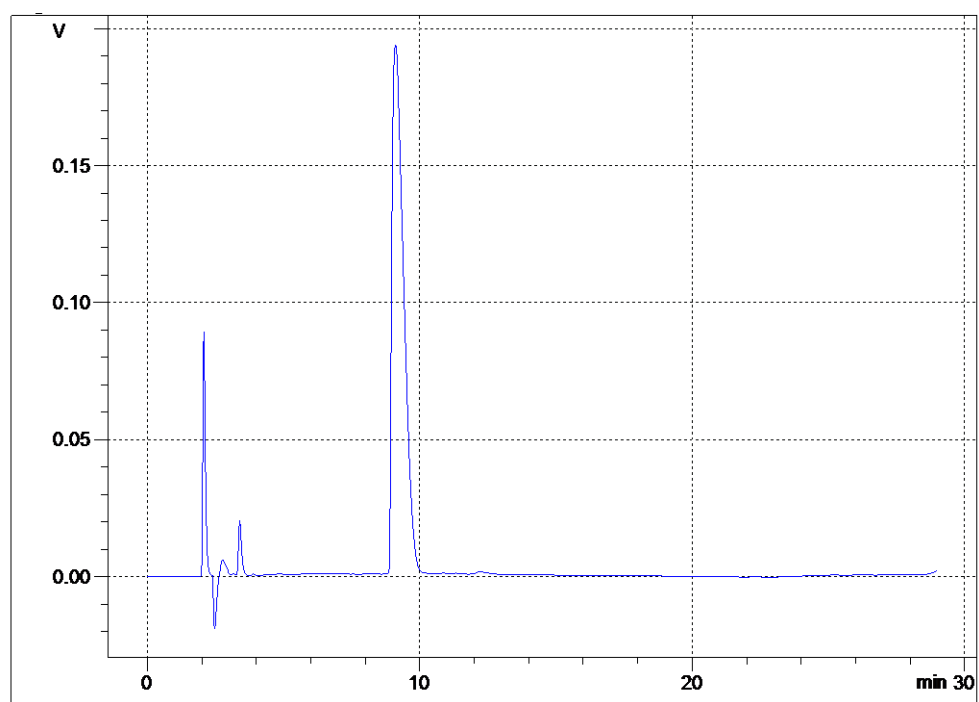
IL (436), t = 72 h



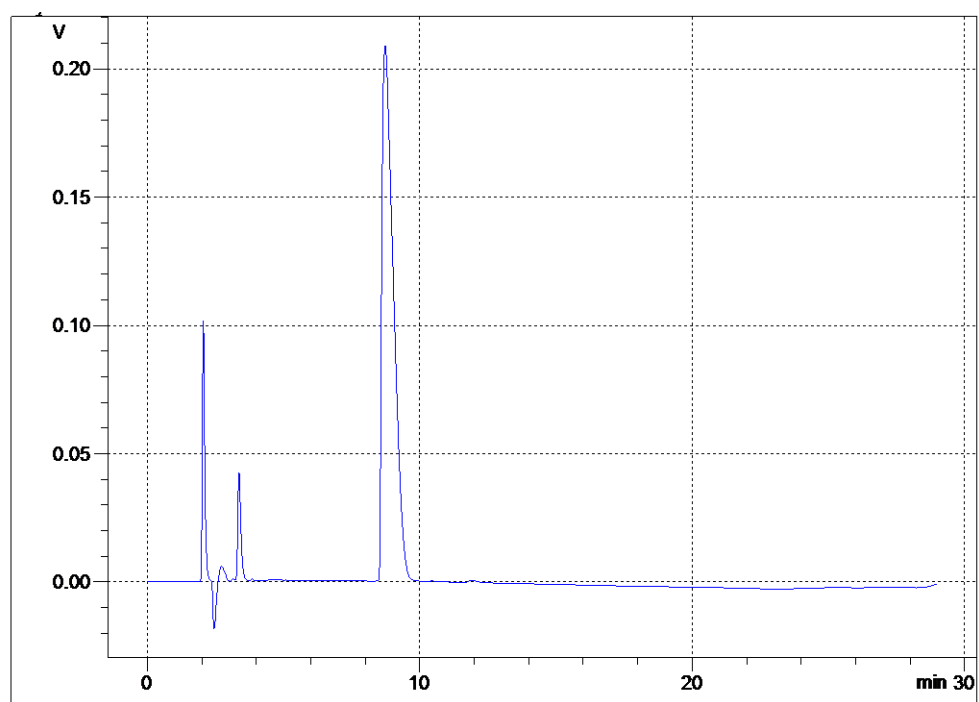
IL (436), t = 96 h



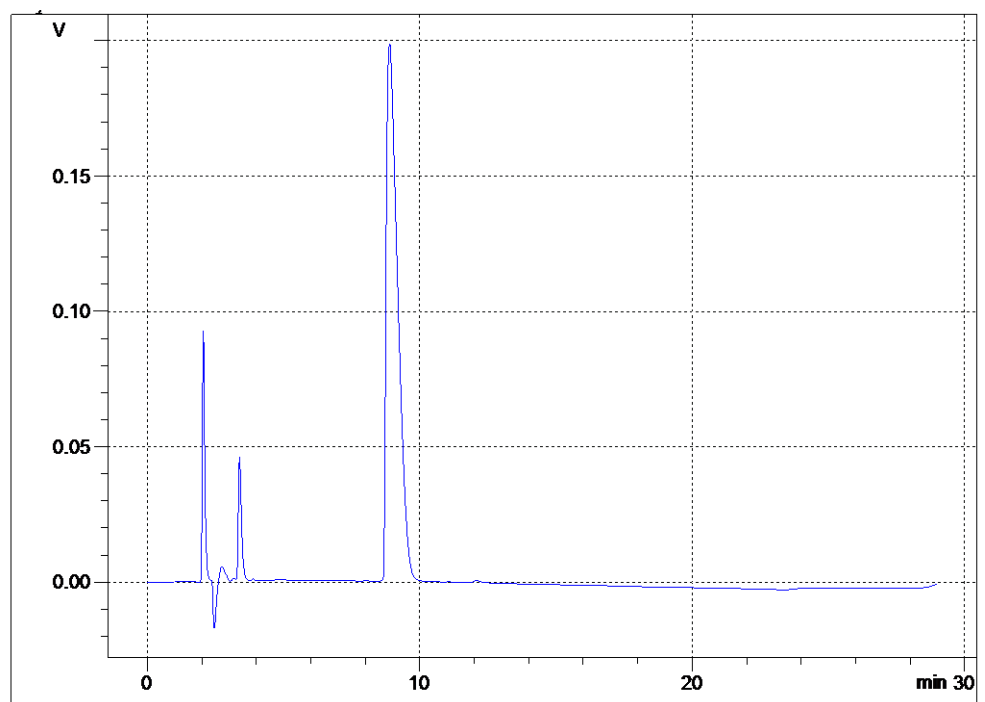
IL (436), t = 168 h



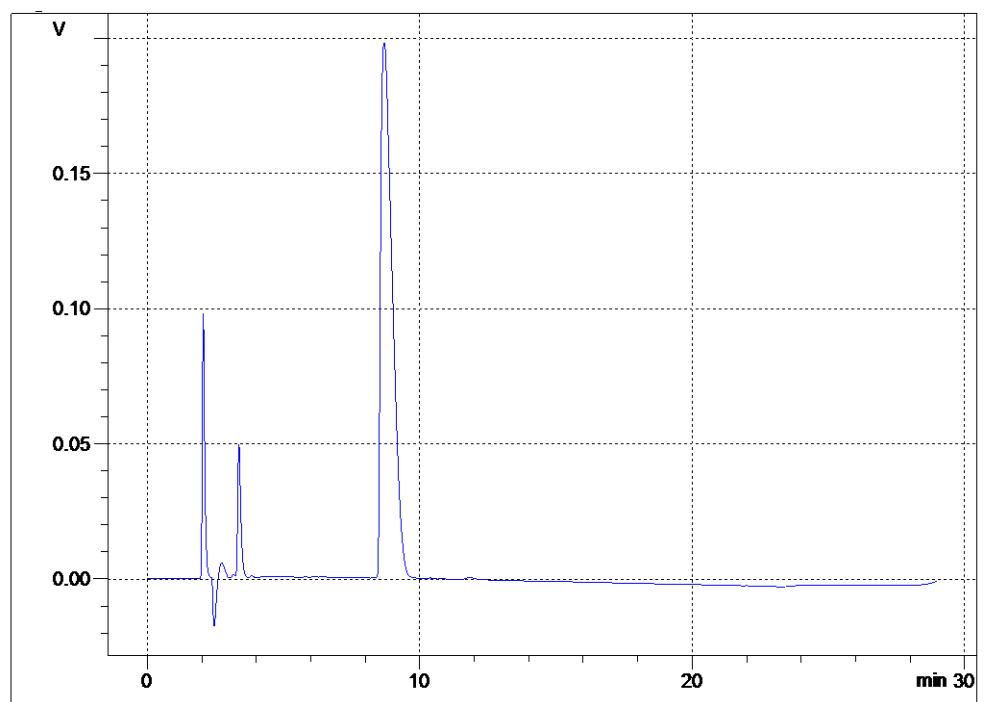
IL (439), t = 0 h



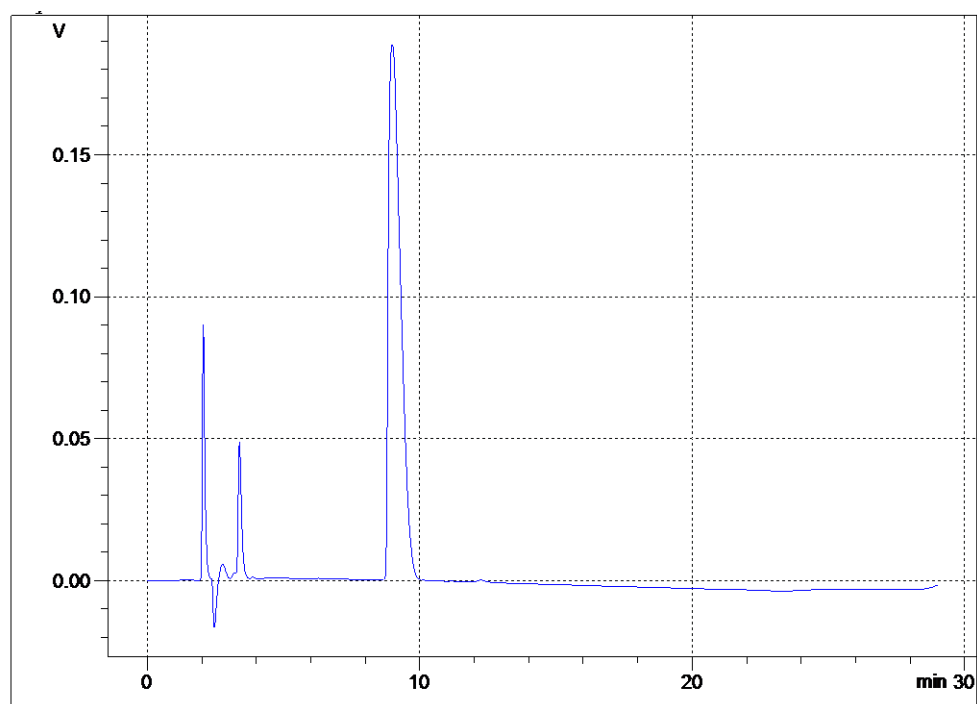
IL (439), t = 24 h



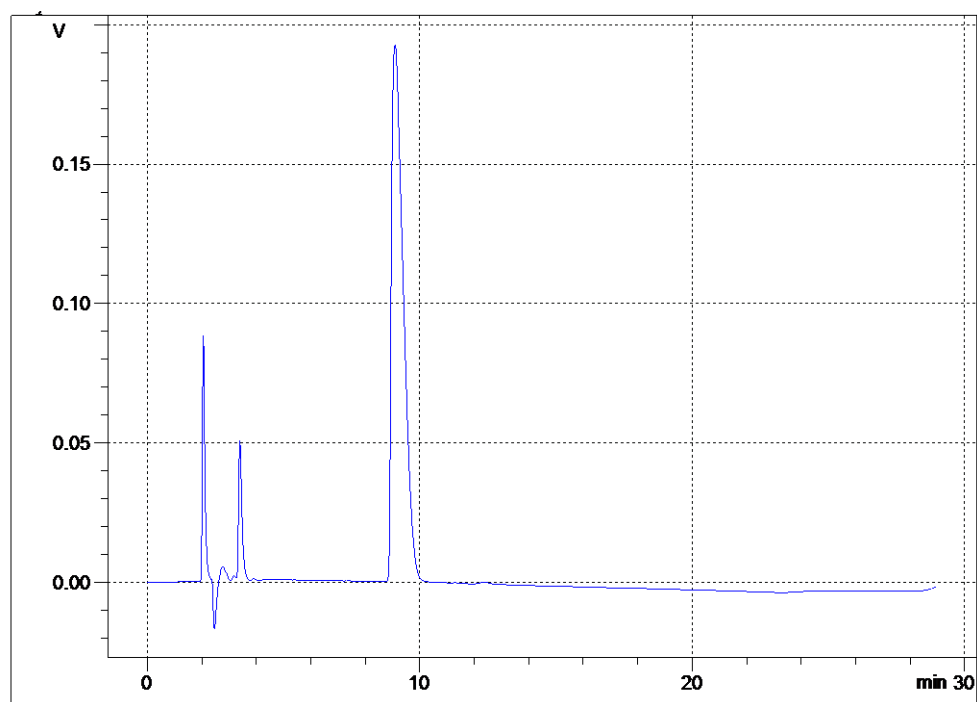
IL (439), t = 48 h



IL (439), t = 72 h



IL (439), t = 96 h



IL (439), t = 168 h